10th Anniversary International Conference on

Physics and Mechanics of New Materials and Their Applications

PHENMA 2021 2022

DIVNOMORSK, KRASNODAR REGION, RUSSIA, MAY 23-27, 2022

phenma2021.sfedu.ru


9 785927 541331

Don State Technical University
Southern Federal University
National Kaohsiung University of Science and Technology

10th Anniversary International Conference on "Physics and Mechanics of New Materials and Their Applications" (PHENMA 2021–2022)

Divnomorsk, Russia, May 23–27, 2022

http://phenma2021.sfedu.ru/

Abstracts & Schedule

Rostov-on-Don
Southern Federal University Press
2022

UDC 53:531/534(063)

10th Anniversary International Conference on “Physics and Mechanics of New Materials and Their Applications” (PHENMA 2021–2022, Divnomorsk, Russia, May 23–27, 2022) : Abstracts and Schedule / I. A. Parinov, A. N. Soloviev, S.-H. Chang (Eds.) ; Southern Federal University. – Rostov-on-Don ; Taganrog : Southern Federal University Press, 2022. – 378 p.

ISBN 978-5-9275-4133-1

The success of the Russian-Taiwanese Symposium “Physics and Mechanics of New Materials and Their Applications”, PMNM-2012 (Russia, 2012), 2013 International Symposium “Physics and Mechanics of New Materials and Underwater Applications”, PHENMA-2013 (Taiwan, 2013), 2014 International Symposium “Physics and Mechanics of New Materials and Underwater Applications”, PHENMA-2014 (Thailand, 2014), 2015 International Conference “Physics and Mechanics of New Materials and Their Applications”, PHENMA-2015 (Russia, 2015), 2016 International Conference “Physics and Mechanics of New Materials and Their Applications”, PHENMA-2016 (Indonesia, 2016), 2017 International Conference “Physics and Mechanics of New Materials and Their Applications”, PHENMA-2017 (India, 2017), 2018 International Conference “Physics and Mechanics of New Materials and Their Applications”, PHENMA-2018 (South Korea, 2018), 2019 International Conference “Physics and Mechanics of New Materials and Their Applications”, PHENMA-2019 (Vietnam, 2019) and 2020 International Conference “Physics and Mechanics of New Materials and Their Applications”, PHENMA-2020, (Japan, 2021) predefined objectives and scientific directions of the 10th Anniversary International Conference on “Physics and Mechanics of New Materials and Their Applications” (PHENMA 2021 – 2022, Divnomorsk, Russia, May 23 – 27, 2022).

The following PHENMA abstracts cover five scientific directions: (i) processing techniques of new materials, (ii) physics of new materials, (iii) mechanics of new materials, (iv) applications of new materials, and (v) industry and management. These are present by scientists from 18 countries, demonstrating strong scientific collaboration, formed for last decade.

The book was supported financially by the grant No. 21-19-00423 of the Russian Science Foundation in the Southern Federal University.

Published in author’s edition.

UDC 53:531/534(063)

ISBN 978-5-9275-4133-1

Sponsored by

Rostov Regional Administration, Russia

Ministry of Education and Science of the Russian Federation, Russia

Российский научный фонд

Russian Science Foundation

РФФИ

Russian Foundation for Basic Research, Russia

South Scientific Center of Russian Academy of Science, Russia

科 技 部

Ministry of Science and Technology

Ministry of Science and Technology of Taiwan, Taiwan

JSMS Kyushu Branch

The Society of Materials Science, Japan Kyushu Branch, Japan

公益財団法人 北九州観光コンベンション協会
Kitakyushu Convention & Visitors Association

Kitakyushu Convention & Visitors Association, Japan

The Korean Society for Composite Materials, South Korea

National Foundation for Science & Technology Development, Vietnam

Vietnam Association of Science Editing (VASE), Vietnam

Vietnam Union of Science and Technology Associations (VUSTA), Vietnam

New Century Education Foundation, Taiwan

Ocean & Underwater Technology Association, Taiwan

Unity Opto Technology Co., Taiwan

Fair Well Fishery Co., Taiwan

Woen Jinn Harbor Engineering Co., Taiwan

Lorom Group, Taiwan

Longwell Co., Taiwan

Kyutech
Kyushu Institute of Technology
Kyushu Institute of Technology, Japan

Korea Maritime and Ocean University, South Korea

Hanoi University of Science and Technology, Vietnam

Vietnam Maritime University, Vietnam

Vinh Long University of Technology Education, Vietnam

Hanoi University of Industry, Vietnam

Vietnamese-German University, Vietnam

Ho Chi Minh City University of Agriculture and Forestry, Vietnam

Research Institute of Agriculture Machinery, Vietnam

University of 17 Agustus 1945 Surabaya, Indonesia

Perkumpulan Ahli dan Dosen Republik Indonesia

University of Maarif Hasyim Latif, Sidoarjo, Indonesia

PDPM Indian Institute of Information Technology, Design and Manufacturing, India

South Russian Regional Centre for Preparation and Implementation of International Projects, Ltd., Russia

Organizing Committee

Conference Chairs

A. N. Soloviev (Don State Technical University, Russia)
I. A. Parinov (Southern Federal University, Russia)
S.-H. Chang (National Kaohsiung University of Science and Technology, Taiwan, ROC)

Advisory Chairs

A. N. Beskopylny (Don State Technical University, Russia)
C.-K. Chou (New Century Education Foundation, Taiwan, ROC)
T. Duc-Quy (Hanoi University of Industry, Vietnam)
V. K. Gupta (PDPM-Indian Institute of Information Technology, Design and Manufacturing Jabalpur, India)
L. Hai-An (Ministry of Education and Training, Vietnam)
M. Hatta (University of 45 Surabaya, Indonesia)
N. Hay (Nong Lam University, Ho Chi Minh City, Vietnam)
I.-C. Huang (Fair Well Fishery Group, Taiwan, ROC)
C. Hung- Phi (Vinh Long University of Technology Education, Vietnam)
S. Jain (PDPM Indian Institute of Information Technology, Design and Manufacturing, Jabalpur, India)
M. A. Jani (University of 17 Agustus 1945 Surabaya, Indonesia)
Y.-H. Kim (Korea Maritime and Ocean University, South Korea)
V. I. Kolesnikov (Rostov State Transport University, Russia)
K. Kolmetz (International Association of Certified Professional Engineers, USA)
Yu. F. Lachuga (Russian Academy of Sciences, Russia)
G. G. Matishov (South Scientific Center of Russian Academy of Sciences, Russia)
B. Ch. Meskhi (Don State Technical University, Russia)
N.-A. Noda (Kyushu Institute of Technology, Japan)
M. Nugroho (University of 17 Agustus 1945 Surabaya, Indonesia)
A. Ojha (PDPM Indian Institute of Information Technology, Design and Manufacturing, Jabalpur, India)
D. Pham-Xuan (Vietnam Maritime University, Vietnam)
P. Seshu (Indian Institute of Technology Dharwad, India)

I. K. Shevchenko (Southern Federal University, Russia)
B. Tien-Long (Vietnam Association for Science Editing – VASE, Vietnam)
D. Van-Phong (Hanoi University of Science and Technology, Vietnam)
P. Van-Song (Vietnamese-German University, Vietnam)
D. Vu-Minh (Vietnam Union of Science and Technology, Vietnam)
D.-S. Wu (National Chung Hsing University, Taiwan, ROC)
P. Xuan-Duong (Vietnam Maritime University, Vietnam)
C.-Y. Yang (National Kaohsiung University of Science and Technology, Taiwan, ROC)

Conference Co-Chairs

L. Anh-Tuan (Hanoi University of Science and Technology, VASE, Vietnam)
L.-K. Chien (National Taiwan Ocean University, Taiwan, ROC)
N. Duc-Toan (Hanoi University of Science and Technology, VASE, Vietnam)
A. Fatoni, R (Perkumpulan Ahli dan Dosen Republik Indonesia)
R. Hastijanti (University of 17 Agustus 1945 Surabaya, Indonesia)
K. Hasyim (University of Darul Ulum, Jombang, Indonesia)
H.-C. Huang (National Kaohsiung University of Science and Technology, Taiwan, ROC)
V. V. Kalinchuk (South Scientific Center of Russian Academy of Sciences, Russia)
P.K. Kankar (Indian Institute of Technology Indore, India)
M. I. Karyakin (Southern Federal University, Russia)
Y. H. Kim (Korea Maritime and Ocean University, South Korea)
C.-T. Lin (National Kaohsiung University of Science and Technology, Taiwan, ROC)
M. B. Manuilov (Southern Federal University, Russia)
A. V. Metelitsa (Southern Federal University, Russia)
V. I. Minkin (Southern Federal University, Russia)
A. V. Mozgovoi (Don State Technical University, Russia)
E.L. Mukhanov (Southern Federal University, Russia)
Nurmawati (University of 45 Surabaya, Indonesia)
I. Prasetyawan (Lloyd Register Asia, Malaysia)
M. A. Rahim (University of 17 Agustus 1945 Surabaya, Indonesia)
D. V. Rudoy (Don State Technical University, Russia)
Sajiyo (University of 17 Agustus 1945 Surabaya, Indonesia)
T.-T. Shih (National Kaohsiung University of Science and Technology, Taiwan, ROC)
S. V. Shvedova (Don State Technical University, Russia)
A. I. Sukhinov (Don State Technical University, Russia)
H. Trung-Hai (Hanoi University of Science and Technology, Vietnam)

T. Van- Nghia (Ministry of Science and Technology, Vietnam)
I. A. Verbenko (Southern Federal University, Russia)
W. Widiasih (University of 17 Agustus 1945 Surabaya, Indonesia)
J.-K. Wu (National Kaohsiung University of Science and Technology, Taiwan, ROC)
M.-C. Wu (National Tsing Hua University, Taiwan, ROC)

Secretariats

V. A. Chebanenko (South Scientific Center of Russian Academy of Sciences, Russia)
A. V. Cherpakov (Southern Federal University, Russia)
N. I. Glushko (Don State Technical University, Russia)
V. V. Kotov (Don State Technical University, Russia)
D. A. Nizhnik (Don State Technical University, Russia)
A.V. Olshevskaya (Don State Technical University, Russia)
E. P. Putri (University of 17 Agustus 1945 Surabaya, Indonesia)
I. A. Serebryanaya (Don State Technical University, Russia)
A. A. Solovieva (Don State Technical University, Russia)
H.-W. Tin (National Kaohsiung University of Science and Technology, Taiwan, ROC)
C. E. Vassilchenko (Southern Federal University, Russia)

Scientific Program Committee

O. A. Ageev (Southern Federal University, Russia)
S. M. Aizikovich (Don State Technical University, Russia)
B. Anh- Hoa (Hanoi University of Science and Technology, Vietnam)
N. Anh-Tu (Hanoi University of Industry, Vietnam)
M.Z. Ansari (PDPM Indian Institute of Information Technology, Design and Manufacturing Jabalpur, India)
R. G. Atram (Institute of Science, Nagpur, India)
B. M. Bahirwar (Gurunanak College of Science, Ballarpur, India)
Y.-Y. Bu (National University of Tainan, Taiwan, ROC)
J.-C. Chen (Vanung University, Taiwan, ROC)
R.-B. Chen (National Kaohsiung University of Science and Technology, Taiwan, ROC)
C.-L. Chiu (National Kaohsiung University of Science and Technology, Taiwan, ROC)
K.-K. Chong (National Kaohsiung University of Science and Technology, Taiwan, ROC)
L. Cong-Nho (Vietnam Maritime University, Vietnam)

D. Dinh-Phuong (Institute of Materials Sciences, Vietnam Academy of Science and Technology, Vietnam)
N. Dinh-Tung (Research Institute of Agricultural Machinery, RIAM, Vietnam)
Y.-C. Fang (National Kaohsiung University of Science and Technology, Taiwan, ROC)
J.-J. Ho (National Taiwan Ocean University, Taiwan, ROC)
H. Hong-Hai (Hanoi University of Science and Technology, Vietnam)
G. Hotta (National Institute of Technology, Ariake College, Japan)
Y.-Z. Hsieh (National Taiwan Ocean University, Taiwan, ROC)
C.-L. Huang (National Kaohsiung University of Science and Technology, Taiwan, ROC)
J.-H. Go (Korea Maritime and Ocean University, South Korea)
B. S. Jagdale (Science and Commerce College, India)
F.-S. Juang (National Formosa University, Taiwan, ROC)
A. Khalatkar (G H Raisoni College of Engineering Nagpur, India)
E. V. Kirillova (RheinMain University of Applied Sciences, Germany)
P. Koinkar (Tokushima University, Japan)
S. B. Kondawar (R.T.M. Nagpur University, Nagpur, India)
G. Kusnanto (University of 17 Agustus 1945 Surabaya, Indonesia)
Kuswanto (University of Darul Ulum, Jombang, Indonesia)
C.-Y. Lee (National Kaohsiung University of Science and Technology, Taiwan, ROC)
J. J.-Y. Lee (National Kaohsiung University of Science and Technology, Taiwan, ROC)
J.-W. Lee (Korea Institute of Industrial Technology, South Korea)
T.-F. Lee (National Kaohsiung University of Science and Technology, Taiwan, ROC)
P.-H. Lei (National Formosa University, Taiwan, ROC)
C.-F. Lin (National Taiwan Ocean University, Taiwan, ROC)
C.-H. Lin (National Kaohsiung University of Science and Technology, Taiwan, ROC)
C.-Y. Liu (National Kaohsiung University of Science and Technology, Taiwan, ROC)
A. D. Lukyanov (Don State Technical University, Russia)
H. Long (Hanoi University of Science and Technology, VASE, Vietnam)
T. R. Mahale (Science and Commerce College, India)
A. A. Matrosov (Don State Technical University, Russia)
I. P. Miroshnichenko (Don State Technical University, Russia)
M. A. More (S.P. Pune University, Pune, India)
S. Mukherjee (PDPM-Indian Institute of Information Technology, Design and Manufacturing Jabalpur, India)
R.-I. Murakami (National Taiwan University of Science and Technology,

Taiwan, ROC)
M. Nafi (University of 17 Agustus 1945 Surabaya, Indonesia)
A. N. Nakagaito (Tokushima University, Japan)
Y. Nakamura (Kagoshima University, Japan)
D. V. Nandanwar (Shri M. M. College of Science, Nagpur, India)
A. V. Nasedkin (Southern Federal University, Russia)
N. Ngoc-Trung (Hanoi University of Science and Technology, Vietnam)
K. Oda (Oita University, Japan)
A. E. Panich (Southern Federal University, Russia)
C.-W. Park (Korea Maritime and Ocean University, South Korea)
S.-J. Park (Korea Maritime and Ocean University, South Korea)
S.D. Patel (PDPM-Indian Institute of Information Technology, Design and Manufacturing, India)
A. V. Patil (L.V.H. College, India)
J.-H. Pee (Ministry of Trade, Industry and Energy, South Korea)
N. Phong-Dien (Hanoi University of Science and Technology, Vietnam)
D. A. Pozharskii (Don State Technical University, Russia)
O. O. Polushkin (Don State Technical University, Russia)
J. N. Ramteke (Shri M. M. College of Science, Nagpur, India)
L. A. Reznichenko (Southern Federal University, Russia)
F. Rodli (University of Maarif Hasyim Latif, Sidoarjo, Indonesia)
H. Sakamoto (Doshisha University, Japan)
V. Sangawar (Institute of Science, India)
H. Seputro (University of 17 Agustus 1945 Surabaya, Indonesia)
T. Sheorey (PDPM-Indian Institute of Information Technology, Design and Manufacturing, India)
S. N. Shevtsov (South Scientific Center of Russian Academy of Sciences, Russia)
M.-C. Shihg (National University of Kaohsiung, Taiwan, ROC)
D.-H. Shin (Korean Air Tech Center, South Korea)
B. V. Sobol (Don State Technical University, Russia)
T.-J. Su (National Kaohsiung University of Science and Technology, Taiwan, ROC)
M. A. Sumbatyan (Southern Federal University, Russia)
J. C. Sun (Dalian Maritime University, China)
R. Sunder (BiSS (P) Ltd, India)
Y. Takase (Kyushu Institute of Technology, Japan)
V. Toan-Thang (Hanoi University of Science and Technology, Vietnam)
V. Yu. Topolov (Southern Federal University, Russia)
B. Trung-Thanh (Hung Yen University of Technology and Education, Vietnam)
T. Trung Thanh (Vietnamese-German University, Vietnam)

TABLE OF ABSTRACTS

PREFACE

The success of the Russian-Taiwanese Symposium "Physics and Mechanics of New Materials and Their Applications", PMNM-2012 (Russia, 2012), 2013 International Symposium "Physics and Mechanics of New Materials and Underwater Applications", PHENMA 2013 (Taiwan, 2013), 2014 International Symposium "Physics and Mechanics of New Materials and Underwater Applications", PHENMA 2014 (Thailand, 2014), 2015 International Conference "Physics and Mechanics of New Materials and Their Applications", PHENMA 2015 (Russia, 2015), 2016 International Conference "Physics and Mechanics of New Materials and Their Applications", PHENMA 2016 (Indonesia, 2016), 2017 International Conference "Physics and Mechanics of New Materials and Their Applications", PHENMA 2017 (India, 2017) and 2018 International Conference "Physics and Mechanics of New Materials and Their Applications", PHENMA 2018 (South Korea, 2018), 2019 International Conference "Physics and Mechanics of New Materials and Their Applications", PHENMA-2019 (Vietnam, 2019) and 2020 International Conference "Physics and Mechanics of New Materials and Their Applications", PHENMA-2020, (Japan, 2021) predefined objectives and scientific directions of the 10th Anniversary International Conference on "Physics and Mechanics of New Materials and Their Applications" (PHENMA 2021 – 2022, Divnomorsk, Russia, May 23 – 27, 2022).

A significant interest to the PHENMA-2020 has led to the great sponsor support from Ministry of Education and Science of the Russian Federation, Russia; Russian Science Foundation; Russian Foundation for Basic Research; Ministry of Science and Technology of Taiwan; The Society of Materials Science, Kyushu Branch, Japan; Kitakyushu Convention & Visitors Association, Japan; The Korean Society for Composite Materials, South Korea; National Foundation for Science & Technology Development (Vietnam); Vietnam Union of Science and Technology Associations (VUSTA); Vietnam Association of Science Editing (VASE); South Scientific Center of the Russian Academy of Science; New Century Education Foundation (Taiwan); Ocean & Underwater Technology Association (Taiwan); Unity Opto Technology Co. (Taiwan); Fair Well Fishery Co. (Taiwan); Woen Jinn Harbor Engineering Co. (Taiwan); Lorom Group (Taiwan); Longwell Co. (Taiwan); Kyushu Institute of Technology, Japan Korea Maritime and Ocean University; Hanoi University of Science and Technology (Vietnam); Vietnam Maritime University; Vinh Long University of Technology Education (Vietnam); Hanoi University of Industry; Vietnamese-German University (Vietnam); Ho Chi Minh City University of Agriculture and Forestry (Vietnam); Research Institute of Agriculture Machinery (Vietnam); University of 17 Agustus 1945 Surabaya (Indonesia); Perkumpulan Ahli dan Dosen Republik Indonesia; University of Maarif Hasyim Latif, Sidoarjo (Indonesia); PDPM Indian Institute of Information Technology, Design and Manufacturing (India); South Russian Regional Centre for Preparation and Implementation of International Projects, Ltd.

The following PHENMA abstracts cover five scientific directions: (i) processing techniques of new materials, (ii) physics of new materials, (iii) mechanics of new materials, (iv) applications of new materials, and (v) industry and management. These are present by scientists from 17 countries, demonstrating strong scientific collaboration, formed for last years.

Conference Chairs,
Prof. Arkady N. Soloviev, Prof. Ivan A. Parinov, Prof. Shun-Hsyung Chang

The Way to Success: PHENMA for the Last Decade

Ivan A. Parinov[1]*, Shun-Hsyung Chang[2]*

[1]I.I. Vorovich Institute of Mathematics, Mechanics and Computer Sciences, Southern Federal University, Rostov on Don, Russia
[2]National Kaohsiung University of Science and Technology, Kaohsiung, Taiwan

[1]parinov_ia@mail.ru; [2]stephenshchang@me.com

Russian-Taiwanese Symposium "Physics and Mechanics of New Materials and Their Applications" (PMNM-2012), 4-6 June, 2012, Rostov-on-Don, Russia, http://pmnm.math.rsu.ru
2013 International Symposium on "Physics and Mechanics of New Materials and Underwater Applications" (PHENMA-2013), 5-8 June, 2013, Kaohsiung, Taiwan, http://phenma.math.sfedu.ru
2014 International Symposium on "Physics and Mechanics of New Materials and Underwater Applications" (PHENMA-2014), 27-29 March, 2014, Khon Kaen, Thailand, http://phenma2014.math.sfedu.ru
2015 International Conference on "Physics and Mechanics of New Materials and Their Applications" (PHENMA-2015), 19-22 May, 2015, Azov, Russia), devoted to 100-th anniversary of the Southern Federal University, http://phenma2015.math.sfedu.ru
2016 International Conference on "Physics and Mechanics of New Materials and Their Applications" (PHENMA-2016), 19-22 July, 2016, Surabaya, Indonesia, http://phenma2016.math.sfedu.ru
2017 International Conference on "Physics and Mechanics of New Materials and Their Applications" (PHENMA-2017), Jabalpur, India, October 14-16, 2017, http://phenma2017.math.sfedu.ru/; https://www.facebook.com/PHENMA2017/
2018 International Conference on "Physics and Mechanics of New Materials and Their Applications" (PHENMA-2018), Busan, South Korea, August 9-11, 2018, http://phenma2018.math.sfedu.ru/; https://www.facebook.com/PHENMA2018/
2019 International Conference on "Physics and Mechanics of New Materials and Their Applications" (PHENMA-2019), Hanoi, Vietnam, November 7-10, 2019, http://phenma2019.math.sfedu.ru/; https://www.facebook.com/PHENMA2019/
2020 International Conference on "Physics and Mechanics of New Materials and Their Applications" (PHENMA-2020), Kitakyushu, Japan, March 26-29, 2021, https://phenma2020.sfedu.ru//; https://www.facebook.com/PHENMA2020/
10th Anniversary International Conference on "Physics and Mechanics of New Materials and Their Applications" (PHENMA-2021-22), Divnomorsk, Russia, May 23-27, 2022, https://phenma2021.sfedu.ru/; https://www.facebook.com/PHENMA2021/


PMNM-2012

PHENMA-2014


PHENMA-2015

PHENMA-2013


PHENMA-2016


PHENMA-2017


PHENMA-2018

PHENMA-2019


PHENMA-2020 (online/offline)

Dynamics of presented abstracts, full-text papers and participating countries: more 2200 abstracts, about 900 full-text papers and about 50 participating countries

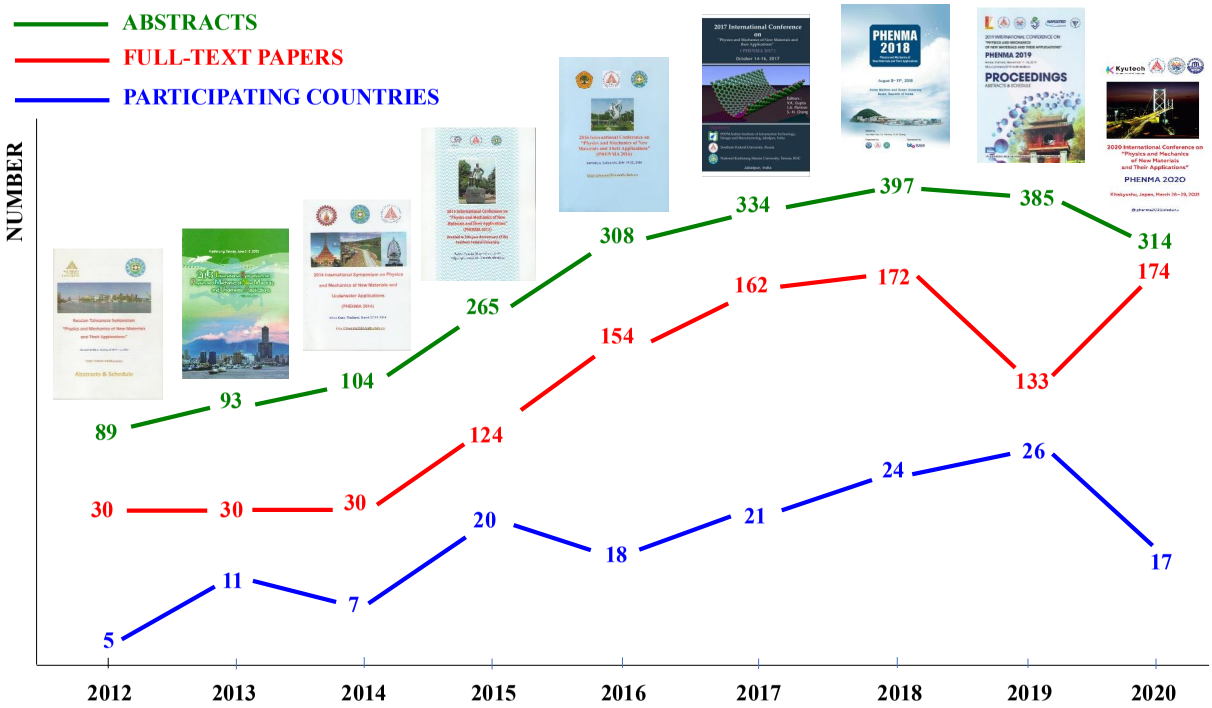

PMNM-2012 (Rostov-on-Don, Russia)

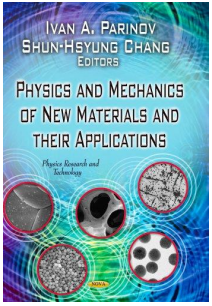

PHENMA-2013 (Kaohsiung, Taiwan)

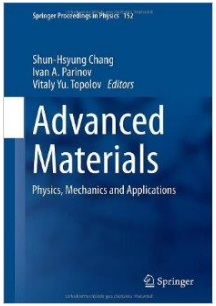

PHENMA-2014 (Khon-Kaen, Tailand)

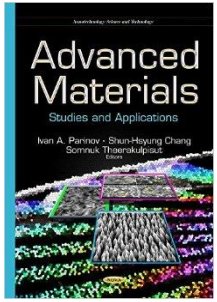

PHENMA-2015 (Azov, Russia)

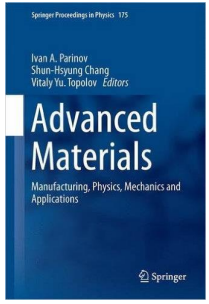

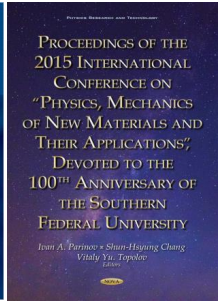

PHENMA-2016 (Surabaya, Indonesia)

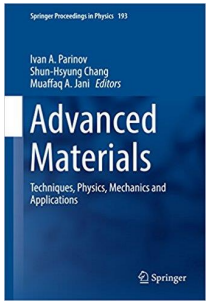

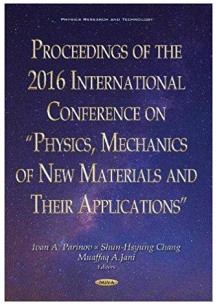

PHENMA-2017 (Jabalpur, India)

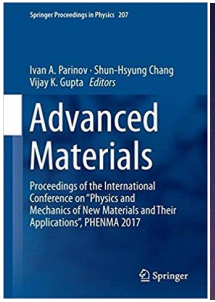

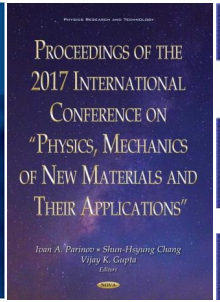

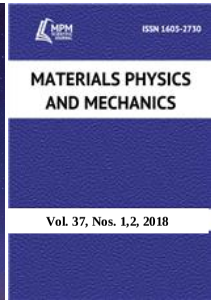

PHENMA-2018 (Busan, South Korea)

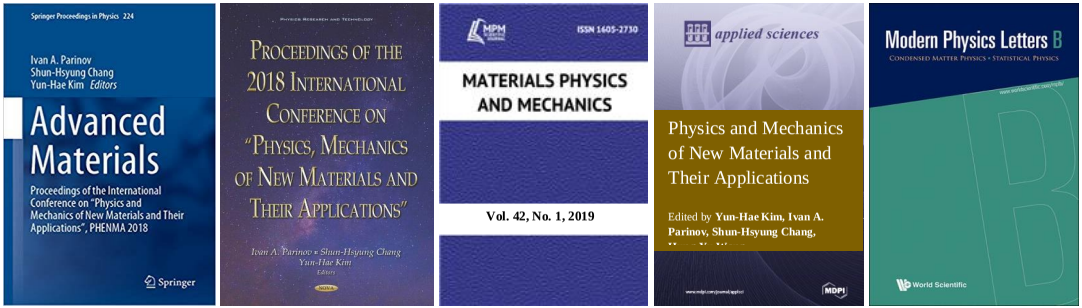

PHENMA-2019 (Hanoi, Vietnam)

PHENMA-2020 (Kitakyushu, Japan)

PARTICIPATING COUNTRIES

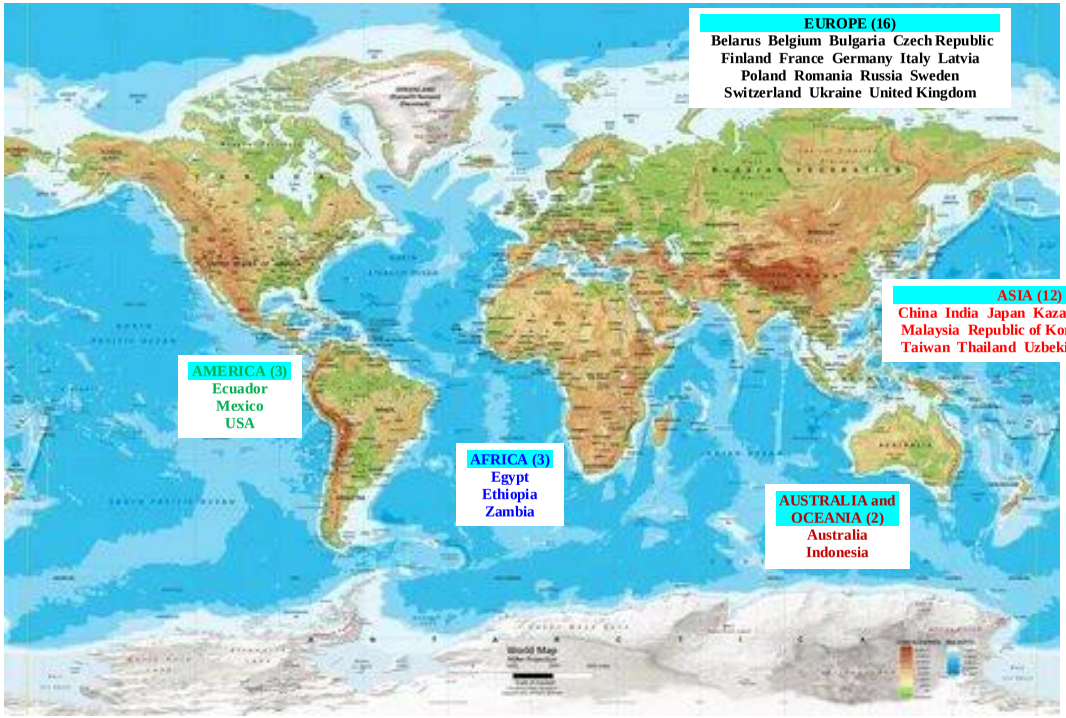

ABSTRACTS

Numerical Design and Modeling of Artificial Grass for Wireless Communication in Remote Areas

Abhay M. Khalatkar[1], Rakesh Kumar Haldkar[2]*, Ivan A Parinov[2]

[1]Mechanical Engineering Department, G H Raisoni College of Engineering, Nagpur, India.
[2]I. I. Vorovich Mathematics, Mechanics and Computer Sciences Institute, Southern Federal University, 344090, Rostov-on-Don, Russia

*rakeshhaldkar@gmail.com

In a remote area, there are many problems related to the electrical energy for wireless communication. The energy consumption of wireless microdevices is very low. A small amount of power is required for the microdevices. Wind flow is easily available in remote areas, and wind energy is converted into useful energy. In this work, a mechanism is proposed to convert wind energy to electrical energy with the help of the microfiber composite (MFC) and sets of various shapes of artificial grass. The deflection is obtained from the wind, and the bending mode of the piezoelectric is considered for this conversion. The amount of energy that can be extracted from such a type of artificial grass depends on its design parameters, such as length, width, tip mass, and shape are analyzed. The MFC energy harvester consists of a polypropylene beam, a polypropylene proof mass, and a microfiber composite patch. The MFC patch is attached to a polypropylene beam and the proof mass is attached at the top of the free end. The finite element analysis, as well as the analytical simulation of the MFC power harvester, has been performed using COMSOL Multiphysics to analyze and enhance the electrical properties in turns of charge output through geometrical analysis and mechanical properties of MFC material.

Acknowledgments. The equipments of SFedU and GHRCE Nagpur India were used. The authors acknowledge the support by Southern Federal University, grant No. VnGr-07/2020-04-IM (Ministry of Science and Higher Education of Russia).

Systematic Investigation of Dielectric Characteristics of $BaFe_{1/2}Sn_{1/2}O_{3-\delta}$ Ceramic

Abhinav Yadav[1]*, E. A. Bikyashev[2], S. P. Kubrin[1], N. V. Ter-Oganessian[1], I. P. Raevski[1]

[1]Institute of Physics, Southern Federal University, Rostov-on-Don, 344090, Russia
[2]Faculty of Chemistry, Southern Federal University, Rostov-on-Don, 344090, Russia

*abhinavyadav.ism@gmail.com

Lead-free barium ferrostannate $BaFe_{1/2}Sn_{1/2}O_{3-\delta}$ (BFSO) ceramics were prepared by conventional hydrothermal chemical synthesis followed by sintering at 1300 ºC for 3 – 10 h in air. Structural analysis of the material has been done using X-ray diffractometer at room temperature. X-ray diffraction (XRD) patterns revealed the single-phase perovskite structure with cubic symmetry. Room temperature microstructural analysis has been done by scanning electron microscopy (SEM) and it revealed that grains are distributed homogeneously throughout the surface. The high density and small porosity of the sample are also confirmed by the microstructural study of the sample. The dielectric analysis has been done for 50 – 450 K temperature range over a frequency window 600 Hz – 1 MHz. It was found out that prepared sample exhibits giant dielectric response with comparatively low losses. The BFSO ceramic suggests temperature dependent strong dispersion at low frequency in its dielectric behavior. The dielectric analysis reveals that orientational and interfacial polarization are present in BFSO sample. The activation energy value of conductivity-temperature dependence suggests that the single ionized oxygen vacancy is responsible for the conduction. The impedance analysis of BFSO sample revealed negative temperature coefficient resistance (NTCR) behavior for both grain's bulk and grain-boundaries. The results of impedance analysis also suggest that space charge polarization plays important role at low frequency region over all the measured temperature region. The modulus study suggests the non-Debye characteristics of the material and its strong dependence on frequency irrespective of temperature. The obtained results of BFSO ceramic analysis over a wide temperature and frequency ranges suggest that BFSO is a suitable lead-free candidate to use in semiconductor devices, oxide solid fuel cells and frequency dependent dielectrics prospective for practical applications.
Acknowledgement. This work was financially supported by the Russian Science Foundation, grant No. 19-12-00205.

Frequency Dependences of Complex Electromechanical Characteristics of PZT-type Porous Piezoceramics

P.A. Abramov*, M.G. Konstantinova, N.A. Shvetsova, D. I. Makarev, A.N. Rybyanets

Southern Federal University, Rostov-on-Don, 344090, Russia

*pav3l.abramov@yandex.ru

In this report, a comprehensive study of the frequency dependences of complex electromechanical characteristics for porous piezoceramics based on PZT-type composition

was carried out. Ferroelectrically "soft" PZT-type piezoelectric ceramics of the composition $Pb_{0.95}Sr_{0.05}Ti_{0.47}Zr_{0.53}O_3$ + 1% Nb_2O_5 with different relative porosity in the range of 0 – 50 % and average pore size of 10 – 30 μm were chosen as the object of the study. Experimental samples of porous piezoceramics were obtained using a modified method of pore former burning-out. The measurements of the complex dielectric, piezoelectric, and elastic parameters of the samples and their frequency dependences in the frequency range up to 10 MHz were obtained using impedance analyzer Agilent 4294A (Agilent Technologies, USA) and the software PRAP. Dispersion characteristics of complex dielectric, piezoelectric and electromechanical parameters for samples with porosity in the relative porosity range 0 – 50 % were measured and analyzed. As a result of experimental studies, regions of elastic, piezoelectric and electromechanical dispersion, characterized by anomalies in the frequency dependences of the real and imaginary parts of the complex constants of porous piezoelectric ceramics were revealed. It was found that the main microstructural features of porous piezoceramics that define the character of frequency dependences of complex electromechanical parameters of porous piezoelectric ceramics are branched 3D piezoceramics frame and quasi-rod piezoceramics structure. It was found out that ferroelectrically “hard” porous piezoceramics are characterized by unique combination of complex electromechanical parameters that makes them prospective materials for different technical applications.

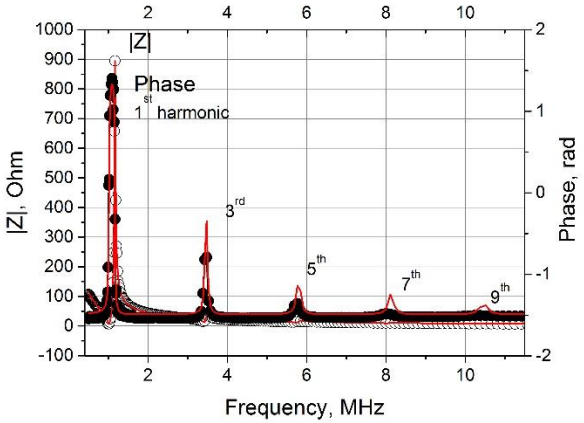

Fig. 1. Impedance spectra for the fundamental and higher-order resonances of the thickness extensional mode of PZT-type piezoceramic disks with diameter of 26.3 mm and thickness of 1.3 mm, polarized in thickness direction

Acknowledgement. The study was financially supported by the Ministry of Science and Higher Education of the Russian Federation (Project No. 0852-2020-0032 (BAS0110/20-3-08IF)).

Harmonious Linearization of Hysteresis Characteristic of an Electroelastic Actuator for Nanomechatronics Systems

S. M. Afonin

National Research University of Electronic Technology
(Moscow Institute of Electronic Technology MIET) Moscow, Russia

eduems@mail.ru

An electroelastic actuator on the piezoelectric or electrostriction effect is applied in nanotechnology, nanobiology, biomechanics and adaptive optics for the precision matching in nanomechatronics systems [1 – 8]. We used the harmonic linearization of hysteresis characteristic of an electroelastic actuator for the analysis and calculation of nanomechatronics systems. The piezo actuator works on the basis of the inverse piezoelectric effect due to its deformation, when the electric field strength is applied. To increase the range of movement of the piezo actuator to tens of micrometers, the multilayer piezo actuator is applied. The piezo actuator is used in nanomechatronics systems for nanodisplacement in adaptive optics, nanotechnology, scanning microscopy, nanobiomechanics, multicomponent telescopes [9 – 16]. The coefficients of harmonious linearization for the basic loop characteristic are determined by the metod of the theory of nonlinear automatic systems [17 – 19]. On the characteristic of electroelastic actuator deformation from the electric field strength, the initial curve is observed, on which the vertices of the basic hysteresis cycles lie. The basic hysteresis loops have a symmetric change in the electric field strength relative to zero, and partial cycles have an asymmetric change in the strength relative to zero. We recieved expressions for the hysteresis basic and local loops of an electroelastic actuator. We obtained the coefficients of harmonic linearization for the basic loop characteristic of an electroelastic actuator of nano mechatronics systems. Basic and local loops for hysteresis characteristics of an electroelastic actuator are proposed. Expression is determined for the generalized frequency transfer function of a nonlinear link with a hysteresis characteristic in the form of the basic hysteresis cycle of an electroelastic actuator.

References

[1] Schultz J., Ueda J., Asada H. *Cellular Actuators*. Butterworth-Heinemann Publisher, Oxford. 1–382, 2017.

[2] Uchino K. *Piezoelectric Actuator and Ultrasonic Motors*. Kluwer Academic Publishers, Boston. 1–350, 1997.

[3] *Physical Acoustics: Principles and Methods. Part A. Methods and Devices*, W. Mason (Ed.), Academic Press, New York. **1**, 1–515, 1964.

[4] Afonin S.M. Chapter 9 in *Piezoelectrics and Nanomaterials: Fundamentals, Developments and Applications*. I. A. Parinov (Ed.), Nova Science Publisher, New York. 225 – 242, 2015.

[5] Afonin S. M. // *Journal of Computer and Systems Sciences International*. Springer, New York, **44**(2), 266 – 272, 2005.

[6] Afonin S. M. // *Doklady Physics*. Springer, New York, **53**(3), 137–143, 2008.

[7] Afonin S. M. // *Russian Engineering Research*. Springer, New York, **35**(2), 89 – 93, 2015.

[8] Afonin S. M. // *Mechanics of Solids*. Springer, New York, **44**(6), 935 – 950, 2009.

[9] Afonin S. M. // *Doklady Mathematics*. Springer, New York, **74**(3), 943 – 948, 2006.

[10] Afonin S. M. // *Actuators*. MDPI, Basel, **7**(1), 1 – 9, 2018.

[11] Afonin S. M. // *Actuators*. MDPI, Basel, **8**(3), 1 – 14, 2019.
[12] Afonin S. M. // *Applied System Innovation*. MDPI, Basel, **3**(4), 1 – 7, 2020.
[13] Afonin S. M. // *Applied System Innovation*. MDPI, Basel, **4**(3), 1 – 11, 2021.
[14] Afonin S. M. // *Transactions on Networks and Communications*. Society for Science and Education, United Kingdom, **7**(3), 11 – 21, 2019.
[15] Afonin S. M. // *Transactions on machine learning and artificial intelligence*. Society for Science and Education, United Kingdom, **8**(4), 23 – 33, 2020.
[16] Afonin S. M. // *European Journal of Applied Sciences*. Society for Science and Education, United Kingdom, **9**(3), 26 – 36, 2021.
[17] Naumov B. N. *Theory of Nonlinear Automatic Systems*. *Frequency Methods*. Nauka, Moscow, 1 – 544, 1972 (In Russian).
[18] Besekersky V.A., Popov E.P. *Theory of Automatic Control Systems*. Profession. SPb, 1 – 752, 2003 (In Russian).
[19] Kim D. P. *Automatic Control Theory. Multidimensional, Nonlinear, Nptimal and Adaptive Systems*. Fizmatlit. Moscow, **2**, 1 – 440, 2007 (In Russian).

A New Design of the Surface Drive of the Screw Pump for the Extraction of High-viscosity Oil

Yu. A. Akopyan, S. O. Kireev, A. R. Lebedev, M. V. Korchagina*

Don State Technical University, Rostov-on-Don, Russia

*ms.korchaginamv@mail.ru

The equipment of wells with screw pump installations and their incorrect selection leads often to exceeding the maximum permissible depression on the formation, reducing the dynamic level of fluid in the well and releasing free gas into the annulus, the formation of depression funnels, increasing the water content of the extracted reservoir fluid [1 – 4]. The report is devoted to the modernization of the surface drive of the screw pump for the extraction of high-viscosity oil. The aim of the work is to increase the technical and economic indicators of the surface drive design by expanding its control range. The report proposes a promising design of the surface drive of a screw pump. The proposed surface drive of a submersible pumping unit is equipped with a gear insert kinematically connected to a gearbox made in the form of a two-stage gear mechanism, including driving, middle and driven gears of different diameters, sequentially engaged with each other. In this case, the shaft of the middle wheel is made with two connecting ends, and the intermediate shaft of the gearbox is equipped with one connecting end, derived respectively from the module and gearbox housings, which are equipped with attachment points at the outlets of the connecting ends. This allows the motor to be connected to any of the connecting ends of the shafts of the gearbox insert, which is connected to the drive or intermediate shaft of the gearbox. The driving, middle and driven wheels of the module are made with consistently increasing diameters in unequal proportions. This design allows one to obtain fourteen values of the gear ratios of the drive, and, consequently, the same number of control stages of the screw pump drive. The selection of the gear ratios of the pump drive was carried out and the design calculation of the main components of the reduction insert was carried out. A comparative analysis of the flow diagrams of a screw pump with a drive of the standard and proposed design is carried out. A 3D model of a reduction insert in CAD has been created. The strength calculation of the

housing of the reduction insert by the finite element method is performed. Possible sources of economic efficiency of this study are identified. The results obtained can be used in the oil industry for the extraction of hard-to-recover, high-viscosity oil, as well as oil with a high content of abrasive particles, when using a screw pump with a surface drive.

References

[1] Efimov A. V., Kireev S. O., Korchagina M. V. Efficiency is the only criterion for choosing the type of center drive // *MATEC Web Conference*, 2018, https://www.scopus.com/inward/record.url?eid=2-s2.0-85056505757&partnerID=40&md5=87323ec409e48c8452dc4ba556272c27

[2] Lemeshko M. A., Molev M. D., Iliev A. G. Adaptive drive of a technological machine with two working movements of the executive body // *MATEC Web Conference*, 2018, https://www.scopus.com/inward/record.url?eid=2-s2.0-85056496678&partnerID=40&md5=6c7ae5b1b86cf1f820b1c4e4a10b90f3

[3] Kaderov K. K., Kireev S. O., Korchagina M. V., Osipuk A. Yu. Improved seals in pipelines and high-pressure hoses // *Russian Engineering Research*, **38**(3), 241 – 243, 2018. https://doi.org/10.3103/S1068798X18030061

[4] Kaderov K., Kireev S., Korchagina M., Lebedev A. Determination of technological parameters and tools for flanging holes from sheet blanks // *E3S Web Conference*, **164**, 14019, 2020.

Advanced Methods for the Microstructure Control of Pt-based Catalysts to Increase Their Activity

A.A. Alekseenko[1]*, S.V. Belenov[1], E.A. Moguchikh[1], A.C. Pavlets[1], K.O. Paperj[1], M.V. Danilenko[1], E.N. Gribov[2], Yu.A. Bayan[1], E.L. Kozhokar[1]

[1]Southern Federal University, Rostov-on-Don, Russia;
[2]Boreskov Institute of Catalysis SB RAS, 5, Lavrentiev Ave., Novosibirsk, 630090, Russia

*an-an-alekseenko@yandex.ru

Low-temperature proton-exchange membrane fuel cells are an important part of the rapidly developing hydrogen energy industry. Almost all commercially produced PEMFC uses a catalyst that provides current-forming reactions (electroreduction of oxygen, electrooxidation of hydrogen and methanol). Pt-containing materials are the best electrocatalysts for proton exchange membrane fuel cells. Their widespread commercial use requires a reduction in the precious metal content while maintaining the activity and stability of the catalyst. This research is carried out in several directions: (I) Development of new methods for the Pt/C catalysts synthesis characterized by a uniform distribution of platinum nanoparticles on the surface of a carbon support and a narrow dispersion in particle size [1]. The authors of [2] confirmed the hypothesis that catalysts containing small-sized nanoparticles, uniformly distributed over the surface of a carbon support, can be both more active and more stable than catalysts based on larger particles, but with a lower uniformity of size and spatial distribution. (II) Development of a synthesis method for obtaining new catalysts with a special structure of bimetallic nanoparticles, which exhibit increased activity in ORR [3, 4]. (III) Doping of the carbon support in order to increase the stability of catalysts based on it in long-term stress

testing [5]. (IV) Development of new approaches to the certification of structural and electrochemical characteristics of catalysts [2].

Acknowledgement. The authors are grateful to the scientific consultant, Prof., DrSc. Guterman V.E. This research was supported by the Russian Science Foundation (project No 21-79-00258).

References

[1] Paperzh K.O., Alekseenko A.A., Safronenko O.A. et al. // *Colloid and Interface Science Communications*, **45**, 100517, 2021.
[2] Paperzh K.O., Alekseenko A.A., Safronenko O.A. et al. // *Beilstein J. Nanotechnol*., **12**, 593, 2021.
[3] Pavlets A.S., Alekseenko A.A., Tabachkova N.Y. et al. // *Int. J. Hydrogen Energy*, **46**, 5355, 2021.
[4] Kirakosyan S.A., Alekseenko A.A., Guterman V.E. // *Russian Journal of Electrochemistry*, **55**, 1258–1268, 2019.
[5] Moguchikh E.A., Paperzh K.O., Alekseenko A.A. et al. // *J. Applied Electrochem*., **52**, 231–246, 2022.

Production of Commercial Electrocatalysts for Low Temperature Fuel Cells

D. V. Alekseenko[1,2]*, S. V. Belenov[1,2], K. O. Paperj[1,2], I. A. Gerasimova[1]

[1]Laboratory of Nanostructural Materials for Electrochemical Power Engineering, Southern Federal University, Rostov-on-Don, Russia
[2]PROMETHEUS R&D Ltd., Rostov-on-Don, Russia

*dvalekseenko@sfedu.ru

Carbon-supported platinum (Pt/C) catalysts are widely used in low temperature fuel cells. The actual problem of such catalysts, connected with a reducing the content of precious platinum, while maintaining high activity and stability, is solved both by selecting the optimal carbon carrier and by controlling the size, shape, size and spatial distribution of platinum nanoparticles. In this report, we present the results of joint studies of Pt/C electrocatalysts obtained at R&D LLC PROMETEY (Russia) and studied at the Laboratory of Nanostructured Materials for Electrochemical Energy Engineering of the Southern Federal University. It was established that the electrocatalysts of the PM_X series (where X = 20 – 60 and corresponds to Pt-loading, % wt.) demonstrate the highest ORR activity among the Pt/C materials studied. Figure 1a shows a TEM photograph of fragments of the PM20 and PM40 electrocatalysts surface, indicating a small size of Pt NPs. For the PM20 material, the average size of platinum nanoparticles is 2.2 ± 0.2 nm. For the PM40 material, the average size of platinum nanoparticles is 3.0 ± 0.2 nm. Due to the strong anchoring and small size of NPs, the PM series catalysts exhibit higher electrochemically active surface area (ESA) during accelerated voltammetric stress testing (Fig. 1b) and, as a result, higher durability and mass activity in ORR compared to other studied.

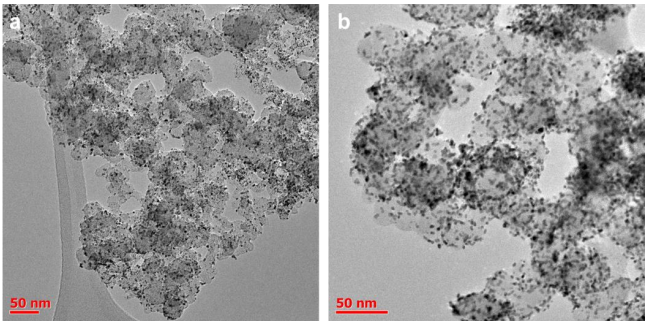

Fig. 1. TEM photograph of the PM20 (a) and PM40 (b) electrocatalysts surface fragments

Acknowledgement. This research was financially supported by the Ministry of Science and Higher Education of the Russian Federation (State assignment in the field of scientific activity No. 0852-2020-0019).

Modeling the Hysteresis Response of Ferroelectric Ceramics Subjected to High and Low Intensity Electric and Mechanical Fields

Alexander Skaliukh

I.I. Vorovich Institute of Mathematics, Mechanics and Computer Sciences, Southern Federal University, Rostov on Don, Russia

Skaliukh@gmail.com

The widespread use of piezoelectric ceramics in industry, diagnostics, medicine, and everyday life appliances put forward the problem of creating reliable mathematical models describing the behavior of polycrystalline ferroelectric materials in weak and strong electric and mechanical fields. The use of finite element programs imposes on the polarization models the requirements of simplicity, universality, and minimality of the stored information. An important feature of modeling is the satisfactory agreement between the calculated and experimental data in both strong and weak fields. To meet these requirements, within the framework of quasi-static processes, a mathematical model was developed for describe irreversible processes. Based on the one-dimensional Giles – Atherton model, a generalization was obtained to the case of three dimensions. The section of accounting reversible components has been supplemented and revised. The bloc of external loads has undergone a radical change. It provides a simultaneous action of both the electric field vector and the mechanical stress tensor for the most general case, when none direction of the principal axes of the stress tensor not coincides with the direction of the electric field vector. In the process of modeling, the functional dependences of the physical constants of material on the residual parameters were used. Generalized limiting dependences of polarization and strain are obtained for the three-dimensional case. The geometric relationships between the polarization vector and the strain tensor are established, which are necessary for describing the electromechanical response.

Energy balance relations are derived and hysteresis operators are obtained in the form of equations in differentials. As a result, the model makes it possible: (i) to calculate the residual polarization fields; (ii) to determine the principal axes and principal values of the permanent deformation tensor; (iii) to find the physical characteristics of non uniformly polarized and deformed ceramics as a locally anisotropic body, including a partial polarization; (iii) to determine dielectric and deformation hysteresis loops for any type of mechanical and electrical load. The tuning of the model for a specific type of ceramic material is carried out by selecting the parameters of the model by comparing the experimental and calculated hysteresis curves in a continuous metric. The developed model can be included in finite element programs; it allows storing information only about the residual polarization vector and the residual strain tensor at each finite element.

Acknowledgements. This work was supported by the Russian Science Foundation (project No. 21-19-00423) in the Southern Federal University.

Research of the Electrophysical Properties of Materials Based on Arrays of Nanorods with the Compositions ZnO (Sn) and ZnO (Au)

Alexandra Ivanishcheva[1]*, Irina Gulyaeva[1], Khabibulla Abdullin[2], Victor Petrov[1]

[1]Southern Federal University, Research and Education and Centre "Microsystem Technics and Multisensor Monitoring Systems", Taganrog, 347922, Russia
[2]Al Farabi Kazakh National University, National Nanotechnology Laboratory of Open Type, Almaty, 050040, Kazakhstan

*a.starnikova@mail.ru

In this work, the electrophysical properties of a material based on synthesized arrays of ZnO-nanorods grown by the hydrothermal method on a quartz substrate were investigated [1]. The formed ZnO-nanorods with a predominantly vertical orientation had an average transverse size of about 40 – 60 nm and a length of 500 – 800 nm. Gold (Au) nanoclusters were formed on top of the obtained ZnO-nanorods by vacuum thermal deposition, and tin (Sn) nanoclusters were formed on another sample. Au and Sn metal nanoparticles were deposited on top of ZnO-nanorods uniformly and had an average transverse size for a ZnO (Au) sample of 4 – 6 nm, and for a ZnO (Sn) sample, the size of Sn metal particles ranged from 5 to 28 nm. Investigations of the electrophysical properties of the obtained film samples were carried out on a hardware-software measuring setup, which makes it possible to measure the dependences of resistance on temperature, activation energy, and potential barrier [2]. The calculation of the activation energy of conductivity (E_a) was carried out on the basis of the expression of the Arrhenius equation: $1/R = (1/R_0)\exp(-E_a/kT)$, where E_a is the activation energy of conductivity, k is the Boltzmann constant, $1/R_0$ is a preexponential constant for temperature ranges in which a linear decrease in resistance is observed (from about 44 to 150 °C). The temperature range of 44 – 150 °C for the material, based on ZnO (Sn) nanorods, E_a was 0.25 eV, and for the material based on ZnO (Au) nanorods, it was 0.23 eV. To measure the potential energy barrier (φ_b) of the obtained samples, the method of thermally stimulated conductivity measurements was applied. In this method, the conductivity is measured as a function of the time after a sharp change in the sample temperature with a sharp temperature switch from the maximum to 200, 220 and 240 °C. The potential barrier values (φ_b) for the ZnO (Sn) and ZnO (Au) samples were 0.43 and 0.37 eV, respectively. Thus, the activation energy of the

conductivity of a ZnO (Sn)-based structure is slightly higher than that of a ZnO (Au)-based structure. This indicates that the mechanism of gas sensitivity of structures based on ZnO nanorods may differ from the mechanism of sensitivity of samples based on SnO_2 – ZnO films previously obtained by solid-phase pyrolysis, in which the values of the activation energy of conductivity decrease from 0.78 eV to 0.6 eV with an increase in the content of SnO_2.

Acknowledgement

The work was carried out with the financial support of the RFBR grant No. 20-07-00653_ A.

Reference

[1] Petrov V. V., Starnikova A. P, Varzarev Y. N., Abdullin K. A., Makarenko D. P. Gas sensitive properties of ZnO nanorods formed on silicon and glass substrates // *IOP Conf. Ser. Mater. Sci. Eng*., **703**, 012038, 2019.

[2] Petrov V. V., Sysoev V. V., Starnikova A. P., Volkova M. G., Kalazhokov Z. Kh, Storozhenko V. Yu, Khubezhov S. A., Bayan E. M. // *Chemosensors*, **9**, 124, 2021.

Peculiarities of the Dependences of the Dielectric Properties of Solid Solutions of Multicomponent Systems on the Electronegativity of the Cations Included in Their Composition

K. P. Andryushin[1]*, S. I. Dudkina[1], L. A. Shilkina[1], S. Sahoo[1,2], M. O. Moysa[1], I. N. Andryushina[1], I. A. Verbenko[1], L. A. Reznichenko[1]

[1]Southern Federal University, Research Institute of Physics, Rostov-on-Don, Russia
[2] University Siksha 'O' Anusandhan, Odisha, India

*kpandryushin@gmail.com

The report considers the features of the dependences of the dielectric properties of solid solutions of a number of multicomponent systems based on the lead titanate-zirconate on the electronegativity of their constituent cations. Solid solutions (SSs) of 3- and 4-component systems of the form $PbZrO_3 - PbTiO_3 - \sum_n (PbB'_{1-\beta}B''_{\beta}O_3)_n$ (n = 1, 2; B' = Nb/W; B'' = Ni, Mg, Co, Zn, Mn, Cd) were chosen as objects of the study. The dependences between the electrophysical parameters of the SSs of some multicomponent systems based on the lead titanate-zirconate and the crystal chemical characteristics of the cations B', B'' were previously established in [1]. They showed that the ferrohardness of the SSs (resistance of the domain structure to external influences) is directly dependent on the electronegativity (EN) of the B'' elements in the corresponding oxidation states, that is on the degree of B–O bond covalence. The relative permittivity of the polarized samples, $\varepsilon_{33}^{T}/\varepsilon_0$, in the solid solutions of the systems under consideration should decrease with an increase in the effective electronegativity (taking into account the fraction of elements in different valence states) in the series Mg → Cd → Co → Zn → Ni → Mn, that is in the order of the increasing degree of the bond covalence. However, the solid solutions with Ni^{2+} and Cd^{2+} do not satisfy the established regularity: the first show the highest values, the second demonstrates the lowest. The correspondence of the dependence on the electronegativity of the cations B'' ($EN_{B''}$) occurs with a significant decrease (by ~ 25%) in EN_{Ni2+} and an increase (by ~ 20%) in EN_{Cd2+}. Thus, in the solid solutions of the multicomponent systems, Ni^{2+} exhibits a significantly lower, and Cd^{2+}, higher electronegativity. The possible mechanisms of the observed are considered, namely, the mechanism of a decrease in the amount of Ni^{2+} in regular octahedral positions of the structure

of the solid solutions and the redistribution of Cd^{2+} over *A*- and *B*-positions, which is allowed by its size, which satisfies the stability conditions for a perovskite-type structure.

Acknowledgement. This work was supported by the Ministry of Science and Higher Education of the Russian Federation (State task in the field of scientific activity, scientific project No. (0852-2020-0032)/(BAZ0110/20-3-07IF).

Reference

[1] Fesenko E. G., Danziger A. Ya., Razumovskaya O. N. *New Piezoceramic Materials*. Rostov-on-Don: Rostov State University Press, 156, 1983 (in Russian).

Structure, Microstructure and Electrophysical Properties of Solid Solutions of a Three-component System of the Form $(1 - x)Pb(Ti_{0.5}Zr_{0.5})O_3 - xCdNb_2O_6$

K.P. Andryushin[1]*, L.A. Shilkina[1], A.V. Nagaenko[2], S. Sahoo[1], I.N. Andryushina[1], L.A. Reznichenko[1]

[1]Research Institute of Physics, Southern Federal University, 194, Stachki, Ave., Rostov-on-Don, 344090, Russia
[2]Institute of High Technology and Piezo Technic, Southern Federal University, 10, Milchakov Str., Rostov-on-Don, 344090, Russia

*kpandryushin@gmail.com

Ceramic solid solutions (SSs) based on the lead zirconate-titanate (PZT) system are still practically no alternative components for various areas of piezoelectric instrumentation. Various research groups are actively working to improve their properties by moving to more complex, multicomponent systems. In this regard, the development, creation and study of PZT-compositions with a third non-structural component seems to be relevant. The objects of the study were the SSs of the three-component system $(1 - x)Pb(Ti_{0.5}Zr_{0.5})O_3 - xCdNb_2O_6$ with $x = 0.025 - 0.100$, $\Delta x = 0.025$. X-ray diffraction shows that in the specified system in the range $0.025 \le x \le 0.100$, SSs are formed, the tetragonal symmetry of which is preserved, as in the basic system, but in the range $0.075 \le x \le 0.10$ clusters with lower symmetry appear. A very small amount of ZrO_2 is contained in all samples, except for SSs with $x = 0.100$. It is shown that with an increase in *x*, the diffraction pattern degrades: for all values of *x*, the diffraction peaks are a superposition of several peaks. It should be noted that the only condition preventing the formation of substitutional solutions in the system has not isostructural nature of the extreme components (perovskite – columbite). Other conditions, such as the difference in ionic radii and the difference in electronegativities of interchangeable elements, correspond to the rules of isomorphism. The grain landscape is represented by crystallites, the size, shape and nature of the packing of which change depending on the quantitative ratios of the components in the system. When the latter is enriched with cadmium niobate, the average grain size, $\overline{D}$, decreases almost threefold with $CdNb_2O_6$ variation in the range $0.025 \le x \le 0.100$. In this case, the nature of the dependence $\overline{D}$ (x) is nonmonotonic with a rapid change in $\overline{D}$ in the range $0.025 < x \le 0.050$, a gradually decreasing grinding rate $\overline{D}$ in the range $0.050 < x \le 0.075$ and a slow decrease in the transformation rate $\overline{D}$ at $0.075 < x \le 0.100$. It was found that an increase in the $CdNb_2O_6$ content to $x < 0.075$ does not cause any significant changes in the dielectric properties. The piezoelectric characteristics of the samples under study change

on average by ~ 60%. The most significant fluctuations of quantities are subject to elastic constants, namely, Q_M increases by ~ 2.5 times, while Y_{11}^E and V_1^E change by ~ 80%. The work provides a scientific interpretation of the results obtained.

Acknowledgement. The study was carried out with the financial support of the Ministry of Science and Higher Education of the Russian Federation (State task in the field of scientific activity, scientific project No. (0852-2020-0032)/(BAZ0110/20-3-07IF). The equipment of the Center of Research Institute of Physics SFedU, "High-Tech" SFedU was used.

On Design Considerations of In-Pipe Inspection Robot

Ankit Nayak

School of Automation, Banasthali Vidyapith University, Rajasthan, India

ankitnayak@banasthali.in

One of the objectives of robots is to remove human intervention from the hazards work environment, like to explore inaccessible workplaces. Pipelines also come under the categorization of the inaccessible workplace, due to its small space, the complex path having bend, joints and toxic gases, which might be harmful for human intervention. With an increase in automation in oil and gas transportation the demands of in-pipe inspection robots are increasing. The primary focus of such robots is the inspection of pipelines used for fuel or water transportation. Several robots have been developed in the past few decades and the gap of universal and sustainable design is still present. However, several designs have been proposed recently but the pipeline industry is not accepting them as a universal design for their use, and it is due to their design constraints. A comprehensive study related to the design of in-pipe inspection robot is required to move further towards the proposal of a new design. This paper is presenting a comprehensive review of different mechanisms and their capability of in-pipe inspection robots. It is also discussing the design considerations and constraints of different in pipe inspection robots, which have been proposed and reported in the literature.

Utilization of Industry 4.0 by City Farmers, Indonesia

Annisa Purnamasari

Department of Industrial Engineering, Universitas 17 Agustus 1945 Surabaya, Indonesia
Jl. Semolowaru No.45, Surabaya, Jawa Timur 60118, Indonesia

annisapurnamasari2806@gmail.com

Urban farmers are farmers who have experienced improvement and progress in terms of thought, knowledge, and ways to develop the field. The city's own farmers aim for farmers to continue to have an improvement in the industrial 4.0 era and not fall behind. The activities that have been carried out by previous people in planting and earning a plant have made young people reluctant to continue these activities. The activity in question only makes the minds of today's young people tired. The branding of a farming activity makes the work of farmers no longer in demand and over time it becomes lost. It is important to introduce farming methods

using the machines and tools that have been provided and an introduction to using the Internet on using farmers to change the mindset of today's young people, so that young people continue to preserve agriculture by continuing to develop, not eliminate. Utilizing social media to eliminate bad thoughts and provide constructive information about today's agriculture, especially in the industrial 4.0 era. In addition, the importance of digital marketing in marketing agricultural products in order to get feedback that is in accordance with the results of hard work and product results. The use of digital marketing is also very important so that many people know the agricultural products produced and make it easier for outsiders to place orders for these agricultural products.

Comparative Analysis of the Efficiency of Scalar and Vector-scalar Antennas for Onboard Receiving Systems

Artem M. Kharakhashyan

Department of Applied Mathematics, Don State Technical University, Rostov-on-Don, Russia

artemharahashyan@mail.ru

Nowadays, in order to achieve greater efficiency of hydroacoustic receiving systems that ensure the detection of low-noise objects and provide for stable underwater communication, an approach based on an increasingly complete extraction of information contained in the acoustic field is being intensively studied. This is usually accomplished by using vector-scalar antennas that can measure acoustical pressure and vibrational velocity of the particles of the medium simultaneously. The most common of them are stationary, towed and onboard. The noise component that makes the largest contribution to the resulting noise field differs for each type of the antennas. For stationary systems, the greatest noise source corresponds to the noise of the sea surface and the water column, for towed ones due to the flow-induced turbulent noise, and for onboard systems because of the structural interference, which is produced by vibrations of the frame and hull elements of the carrier structure. The purpose of this paper is the analysis of the detection characteristics of a target signal and the accuracy of determining the location of its source during the operation of the onboard receiving system in the presence of a background structural noise. The research is carried out using computer modeling and experimental data processing for a set of detection methods: P-method, based on pressure measurements processing; PV-method, employing both pressure and particle velocity; and W-method, using power flux components. Experimental characteristics of the structural noise are presented for the scalar and vector components of the acoustic field, as well as for the power flux. Based on the results of the calculations, a comprehensive comparison of the performance characteristics of scalar and vector-scalar antennas is carried out according to the following set of the considered criteria: the signal-to-noise ratio at the output of the receiving system, the probability of correct detection and false alarms, and the accuracy of the target coordinates assessment, namely the root-mean-square error and the target azimuth bias. Analysis of the results shows that the intensity of the structural noise for the power flux components is much lower than the noise intensity for the scalar and vector components. Variance values for the power flux components are lower than for scalar and vector ones even at small averaging times, and decrease faster depending on the averaging time. This factor is significant in further research and development of the detection algorithms, and it also explains the significant

advantage in detection probability for vector-scalar antennas in comparison with scalar ones. It is shown that the best detection characteristics for all the considered criteria are obtained for the method that employs a vector-scalar antenna and uses power flux components of the acoustic field in the data processing. The worst performance for all the considered criteria is observed for the method that uses only the scalar component of the acoustic field and is limited to acoustical pressure measurement. It is also important to note that when the direction of arrival of a signal from the target is close to the fore-and-aft aspects of the carrier, the P-method in most of the considered situations was not able to detect the signal at all, while the W-method has provided for target signal detection with a high probability. Thus, it can be concluded that vector-scalar antennas that allow for processing power flux components of an acoustical signals are promising and can be used to develop on-board receiving systems that achieve greater target detection probability.

Investigation of the Radio-absorbing Properties of Solid Solutions (xPbTiO$_3$ – yPbZrO$_3$ – zPbNb$_{2/3}$Mg$_{1/3}$O$_3$) – 0.02PbGeO$_3$ in the Microwave Range

P. A. Astafev[1]*, A. A. Pavelko[1], Y. M. Noykin[2]

[1] Research Institute of Physics, Southern Federal University, 194, Stachki Ave., Rostov-on-Don, 344090, Russia
[2] Department of Physics, Southern Federal University, 105/42 Bolshaya Sadovaya Str., Rostov-on-Don, 344006, Russia

*l.6.e.9.w.4.a.9.p@yandex.ru

Active studies of the electrodynamic properties of bulk ferroelectric materials in the microwave range have been carried out for more than two decades. Many prospects for their applications in radio engineering have been discovered, from varistors and varicaps, to filters and phase shifters. At present, the range of materials used in real microwave devices is often limited to compositions based on $BaTiO_3$ and $PbTiO_3$. The technology for the synthesis of such compositions is well developed, and materials based on them have acceptable characteristics. The development of synthesis and research methods makes it possible to obtain new promising materials and to refine the properties of previously known materials. Therefore, investigations in this area remain relevant to this day. In this research, we study the dependence of the electrodynamic characteristics of the 0.98 (xPbTiO$_3$ – yPbZrO$_3$ – zPbNb$_{2/3}$Mg$_{1/3}$O$_3$) – 0.02PbGeO$_3$ quaternary system on the composition. A wide selection of samples with various compositions along various sections of the Gibbs triangle is used as the objects of study. The samples are examined by the microstrip method in the frequency range from 10 MHz to 20 GHz. For each section, the dependences of direct and reverse electromagnetic losses on the composition were obtained. The total energy dissipated by the samples is calculated. Correlations were found in the dependences of the absorption energy on the composition. This is due to the relationship between dielectric constant and composition. Correlation relationships are nonlinear, which is associated with the dispersion of the dielectric constant in the studied range. The studies performed only characterize samples of a given shape, from a given material and within the scope of the chosen method. The technique used does not provide complete information on the properties of the material, but makes it possible to assess

the characteristics, and helps in the selection of compositions and forms for subsequent, more accurate studies. To refine the results, it is necessary to resort to various methods of mathematical modeling.

Acknowledgement. The study was carried out with the financial support of the Ministry of Science and Higher Education of the Russian Federation (State task in the field of scientific activity, scientific project No. 0852-2020-0032/BAZ0110/20-3-07IF).

Resistive Switching Reproducibility Investigation of Titanium Oxide Nanostructures Obtained by Local Anodic Oxidation

V. I. Avilov, L. G. Zhavoronkov*, V. A. Smirnov

Southern Federal University, Institute of Nanotechnology, Electronics and Electronic Equipment Engineering, Taganrog, Russia

*zhavoronkov@sfedu.ru

Memristor structures are one of the promising elements of nanoelectronics that can find their application in RRAM elements for large data processing systems, as well as in the manufacture of neuromorphic artificial intelligence devices. These structures can switch between a state with high (HRS) and low (LRS) resistance, have a high switching speed between states, low power consumption and can be used in non-volatile systems. In addition, memristor structures based on electrochemical titanium oxide have a large ratio of resistances in the HRS and LRS states and a long time of their preservation, low switching energy, and also do not require an additional electroforming operation. Thus, the task of studying the reproducibility of resistive switching of titanium oxide nanostructures obtained by local anodic oxidation is an urgent area of research. To conduct experimental studies of resistive switching of titanium oxide nanostructures, probe nanolithography was performed at the Ntegra nanolab (NT-MDT, Russia) by local anodic oxidation of titanium film. Then, for 1000 cycles, the voltage characteristics were measured at one point of the nanostructure, when a voltage loop was applied in the range ± 7 V.

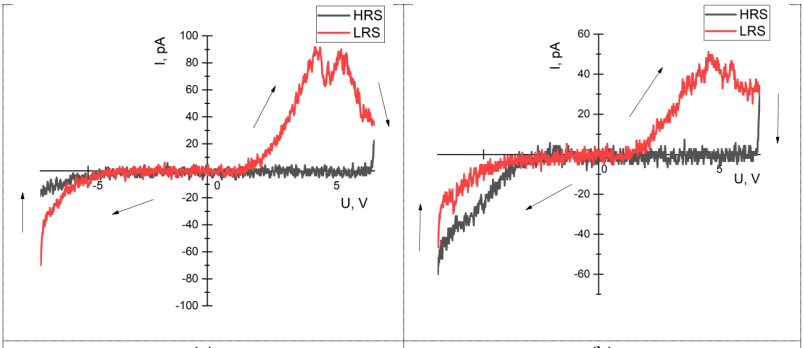

Fig. 1. Volt-ampere characteristic: (a) 1st cycle, (b) 1000th cycle

Analysis of the data obtained showed that at a voltage of 5 V during 1 cycle, the current through the structure in the LRS state was 71.8 pA, and 1.9 pA in the HRS state, the ratio of resistances in the LRS and HRS state is 37.8. For 1000 cycles, at a voltage of 5 V, the current in the LRS state was 46.6 pA, and 0.45 pA in the HRS state, the ratio of resistances in the LRS and HRS state is 103.5. The obtained results can be used in the development of technological processes for the formation of nanoelectronics elements and neuromorphic devices.

Acknowledgement. This work was supported by RFBR according to the research project No. 19-29-03041 mk, and by grant of the President of the Russian Federation No. MK-767.2020.8.

Droplet epitaxial formation of small-sized InAs nanostructures with a low surface density using two-stage As-exposure

S. V. Balakirev*, D. V. Kirichenko, N. E. Chernenko, N. A. Shandyba, M. M. Eremenko, O. A. Ageev, M. S. Solodovnik

Southern Federal University, Department of Nanotechnologies and Microsystems, Taganrog, Russia

*sbalakirev@sfedu.ru

Rapid development of nanophotonic devices and various quantum applications requires improvement of semiconductor technology, including droplet epitaxial growth of III-V nanostructures [1], which have advantageous optical and electronic properties. To control relative distances between quantum objects and exclude their mutual influence, a low surface density of nanostructures below 1×10^8 cm^{-2} must be achieved. In this report, we demonstrate that low-density InAs/GaAs nanostructures with an optically suitable size (~25 nm) can be obtained using two-stage exposure of In-droplets to the As-flux. Droplets obtained after deposition of 1.0 and 1.5 monolayers (ML) of indium (1-ML and 1.5-ML droplets) were exposed to an As_4 flux evaluated as a relative value P/P_0 (where P_0 is a background pressure) under different conditions. We observe that 1-ML droplets have low stability under the influence of the As-flux implying that they rapidly decay in the result of diffusion of atoms out of droplets. 1.5-ML droplets were found to increase in an average diameter from 65 to 98 nm but they show better resistance to As-vapor [2]. An increase of P/P_0 from 1 to 2.9 leads to a reduction of the droplet diameter from 98 to 18 nm and ring formation around original droplets. An increase of the As-pressure P/P_0 from 4 to 10 causes droplet etching of the surface with the formation of arrays of holes, which become deeper with increasing As-flux. To discuss a possibility of achieving fixation of the original droplet parameters, we also study the temperature effect on nanostructure parameters after the high-flux As-exposure ($P/P_0 = 714$). A decrease in the temperature (at which the exposure was carried out) down to 200 °C does not enable better control over characteristics of nanostructures. Appearance of monolayer disks is typical for As-exposure at $T = 300$ °C and 400 °C. In the latter case, an average disk diameter decreases, which may be due to the formation of stable bonds of surface atoms with the underlying epitaxial layer. A transition to $T = 500$ °C leads to the transformation of droplets into crystal nanostructures. The arrays have a large variation in size, which decreases with increasing time t between the beginning of As-supply and substrate heating up to 500 °C. Using two-stage exposure in an ultra-low As-flux and then during high-temperature irradiation, we achieve reproducible formation of arrays of small-size (25 nm) nanostructures with a low surface density (3×10^8 cm^{-2}) and a low variance in size (4%).

Acknowledgement*. This work was supported by the Russian Science Foundation Grant No. 19-79-10099.*

References

[1] Balakirev S.V., Solodovnik M.S., Eremenko M.M., Chernenko N.E., Ageev O.A. // *Nanotechnol.*, **31**, 485604, 2020.
[2] Balakirev S.V., Chernenko N.E., Eremenko M.M., Ageev O.A., Solodovnik M.S. // *Nanomaterials*, **11**, 1184, 2021.

Mechanical, Chemical and Microgeometrical Properties of Magnetron Sputtered TiN Thin Film

R. A. Bardakova, A. A. Kotova, E. V. Sadyrin, A. L. Nikolaev, I. O. Kharchevnikov, I. Yu Zabiyaka, S. M. Aizikovich*

Don State Technical University, 1 Gagarin Square, Rostov-on-Don, 344000, Russia

*saizikovich@gmail.com

A study of the mechanical properties of a thin titanium nitride (TiN) film deposited using the magnetron sputtering method on a Si (100) surface has been carried out. To create the coating under consideration, we used the method of magnetron sputtering of particles onto a silicon substrate using a VSM100 unit (Aktan Vacuum, Russia). The deposition took place in the mode with a stable power of 600 W, deposition type DC. The microgeometrical characteristics of the film surface were studied using an AFM Nanoeducator (NT-MDT, Russia) equipped with a tungsten probe in the semi-contact mode. The average values of the average roughness Ra and the maximum roughness height Rt were 17 ± 2 nm and 127 ± 35 nm, respectively. The probe movement speed was 7 μm/s, the estimated scanning time was 40 min. The film thickness and its chemical composition were determined using a Crossbeam 340 SEM (Carl Zeiss, Germany). For the present study, an Everhart-Thornley secondary electron emission detector was used at an accelerating voltage of 2 kV. The microgeometrical characteristics of the film surface (average roughness, maximum roughness height) were determined from the results of atomic force microscopy. The chemical composition of the film and its thickness were estimated using scanning electron microscopy. Thus, the thickness was 734.7 nm. The chemical composition investigated via energy-dispersive X-ray spectroscopy testified to the high quality of the deposition. The values of indentation hardness and reduced Young's modulus were evaluated using nanoindentation in a course of a series of experiments with increasing indentation load. A Nanotest 600 Platform 3 nanoindentation unit (Micro Materials, UK) with a Berkovich diamond indenter was used. The maximum indentation force, increasing from experiment to experiment, was set: from 1.5 to 29 mN. The indentation time into the TiN thin film was set to 30 s, the holding period of indenter at maximum load was 30 s, then the indenter was unloaded for 30 s. Starting from the indentation depth of about 120 nm, a characteristic “step” (also called “pop-in”) appears on the loading branches of the diagrams, indicating plastic processes in the coating. The plots of mechanical properties reveal a rather complex behavior. At small indentation depths (up to 180 nm), underestimated values of mechanical properties are observed due to the influence of surface microgeometry on the process of indenter penetration. Peak values of mechanical properties (a reduced Young's

modulus of 256.38 ± 12.79 GPa, a hardness of 21.3 ± 1.64 GPa) were found at depths of h_{max} = 209.26 ± 6.49 nm, presumably these values are close to the real values of the TiN coating. Taking Poisson's ratio of TiN for ν = 0.23 the presumable value of the Young's modulus of the film can be restored E = 312.75 ± 12.25 GPa.

Acknowledgement. This work was supported by the Russian Science Foundation grant 22-49-08014.

Study of the Physical Properties of Multiferroic $(1 - x)CoFe_2O_4 - xPbTiO_3$ System

Bashir Abdulvakhidov*[1], Zhengyou Li[2]

[1]*Dagestan State University, 43-a, Gadgiev Str., Makhachkala, 367000, Russia*
[2]*Southern Federal University, 178/24, Sladkov Str., Rostov-on-Don, 344090, Russia*

*babdulvakhidov@mail.ru

In this work, a multiferroic $(1 - x)CoFe_2O_4 - xPbTiO_3$ system was synthesized by the conventional solid-phase reaction method. Using a synergistic application of X-ray structure analysis, scanning electron microscopy (SEM) and energy-dispersive X-ray analysis (EDX), we found that the joint solid-phase sintering of the inverse spinel $CoFe_2O_4$ and the ferroelectric $PbTiO_3$ is often accompanied by the formation of additional phases: lead hexaferrite and solid solutions. These phases are not in small amounts, for example, for the sample x = 0.3, the hexaferrite accounts for 60.7%. These additional phases often affect the physical properties of this multiferroic $(1 - x)CoFe_2O_4 - xPbTiO_3$ system. For example, we observed the dielectric saturation polarization of $0.5CoFe_2O_4 - 0.5PbTiO_3$ is higher than the pure lead hexaferrite and lead titanate detailed in the literature. A concentration range ($0.3 \leq x \leq 0.7$) was found, within this range has the characteristics of a saturated ferroelectric hysteresis loop. These heterophase also affect their dielectric properties, activation energies, Raman spectra, FTIR spectroscopy and bandgaps. Magnetic coercive force (H_c), remanent magnetization (M_r), were obtained from the magnetic hysteresis loops, and saturation magnetization (M_s), and exchange field (H_R), and anisotropy field (H_A) were obtained by the law of approach to saturation magnetization.

Optimization of the Synthesis Conditions of N-doped TiO_2 Nanoparticles Wastewater Treatment

E.M. Bayan[1]*, L. E. Pustovaya[2], Yu. A. Bayan[1], T. G. Lupeiko[1]

[1]*Southern Federal University, Faculty of Chemistry, Rostov-on-Don, 344090, Russia*
[2]*Don State Technical University, Rostov-on-Don, 344000, Russia*

*ekbayan@sfedu.ru

The pollution of the aquatic environment in the 21st century has acquired a global scale. The most promising are photocatalytic methods of wastewater treatment, in which titanium dioxide

is most often used as a photocatalyst, since it is effective in purification processes, chemically inert and cheap. An active study of the properties of this material has led to the need to modify it to shift the absorption region to the visible part of the spectrum. N-doped TiO_2 is one of the promising materials. Most often, the low-temperature sol-gel method is used to obtain N-TiO_2. Previous studies have shown that amorphous titanium dioxide has low photocatalytic properties; therefore, it must be heat treated to obtain crystalline powders. The choice of the synthesis path determines the final properties of the material. Therefore, the purpose of this work was to determine the optimal conditions for the synthesis of N-doped TiO_2 nanoparticles, which can be used as a photocatalyst in wastewater purification from organic pollutants. In this work, this material was obtained by three methods of heat treatment: low-temperature, high-temperature, and hydrothermal synthesis. Synthesis was carried out using titanium (IV) chloride $TiCl_4$ and thiourea as precursors. The **N-doped TiO_2** samples were characterized by X-ray diffraction (XRD), differential thermal analysis (DTA) and thermogravimetric analysis (TGA) and transmission electron microscopy (TEM). Optimum calcination temperatures are determined by TGA/DTA. XRD has shown that the introduction of nitrogen makes it possible to stabilize the catalytically active anatase modification of titanium (IV) oxide up to 800 °C. TEM micrographs showed differences in the surface morphologies of the samples, obtained by different methods: materials, obtained by the hydrothermal method, have a boat-like shape; nanoparticles, obtained by low temperature and high temperature are spherical. The average crystallite sizes of various samples were 8 – 35 nm. It was found that an increase in the heat treatment temperature leads to an increase in the particle size during crystallization. The particle size is practically independent of the amount of nitrogen introduced. The photocatalytic activity (PCA) of the obtained samples was studied using the photodegradation reaction of a model organic pollutant, methylene blue. All synthesized materials showed higher photocatalytic activity than the commercial sample Degussa P25. The introduction of nitrogen into the material increases the PCA in visible light. It was found that the sample obtained by low-temperature sol-gel synthesis, both in the visible and UV regions, exhibits the maximum photocatalytic activity.

Synthesis Methods of High-performance Electrocatalysts with a Low Platinum Content

Yu. A. Bayan*, A. A. Alekseenko

Southern Federal University, Faculty of Chemistry, Rostov-on-Don, 344090, Russia

*bayan@sfedu.ru

Nowadays the problem of finding new highly efficient energy sources remains relevant. One of the alternative sources is low-temperature fuel cells. Such devices must contain a platinum-containing catalyst. Various requirements are put forward for electrocatalysts that characterize their properties. There are various methods for the synthesis of Pt/C catalysts, in which reducing agents or process conditions may vary. It is known that the amount of deposited platinum particles and (structural and morphological) characteristics of the material depend on the selected reducing agent, as well as on various conditions of the process: the pH of the system, the volume of reagents added, temperature, holding time and other parameters. In this study, two of the most common liquid-phase methods of obtaining materials were investigated.

Materials were obtained in the synthesis of which sodium borohydride (samples Y-1, Y-3) and formaldehyde (samples Y-2, Y-14, Y-15, Y-16) were used as reducing agents. The Vulcan XC-72 was selected as the carbon support for these materials. Via gravimetric analysis, it was found that the mass fraction of platinum in the obtained materials Y-1, Y-3 does not exceed 5 % (theoretical loading of 20 %). It was determined that it is impossible to obtain high-quality materials with this method without losing expensive platinum. The materials that were synthesized using formaldehyde as a reducing agent are characterized by an average size of platinum crystallites from 2 to 7.5 nm and a mass fraction from 17 to 20 %. The formaldehyde synthesis method was chosen as the main method for obtaining catalysts in further works. Porous carbon materials are used as support for platinum-containing electrocatalysts. The support used in the described experiment, Vulcan XC-72 carbon black, is one of the most widely used in the synthesis of Pt/C materials. However, the search for other carbon supports and modification of Vulcan XC-72 to obtain catalysts with better structural and morphological characteristics remains an urgent task. So, at the second stage of the study, we obtained materials based on various carbon carriers: Vulcan XC-72 treated with nitric acid; Vulcan XC-72 treated with sodium persulfate; Vulcan-XC-72R; C-TOB-S-75; Vulcan XC-72 aged in an oven with N in an argon atmosphere; Vulcan XC-72 aged in an oven with N in an argon atmosphere, pretreated with nitric acid. Further investigation of the obtained materials will be associated with the study of the nanoparticles size, their spatial distribution over the surface of the support, and electrochemical characteristics.

Acknowledgement. This research was financially supported by the Russian Science Foundation, grant 21-79-00258.

Inverse Problem for a Layer Weakened by a Cylindrical Cavity

O. A. Belyak

Rostov State Transport University, Rostov-on-Don, Russia

belyak.o.a@gmail.com

The paper considers the inverse problem of reconstructing a cylindrical cavity of small circular cross-section in a heterogeneous layer. A multiphase medium within the concept of effective homogeneity is considered as an equivalent homogeneous orthotropic medium [1]. First, the direct problem of oscillations of a layer weakened by a cylindrical cavity was studied in a two-dimensional formulation. The steady-state regime of layer oscillations under the action of a load applied at the upper boundary of the layer is considered. The solution is implemented by the method of boundary integral equations and by an asymptotic method. The system of boundary integral equations is obtained along the boundary of the guiding cylindrical cavity. Asymptotic analysis established the structure of the wave field on the contour of the defect and the structure of the wave field on the boundary of a semi-infinite medium. The wave field at the upper boundary of the layer consists of two terms [2]. The first of them is the wave field generated by the oscillation source in the layer without a defect. The second term is the field scattered by the defect. The wave field is presented as an expansion in terms of normal modes, with uniform and inhomogeneous modes taken into account. This approach made it possible to establish that information about the defect is contained in the amplitudes and phases of the scattered field. The structure of the scattered field amplitudes is established. When solving

inverse problems, this information was used. The resolving equations in the inverse problem are formulated on the basis of a system of boundary integral equations. As input information, wave fields were used, which were obtained in the framework of frequency and position soundings. We considered the frequency ranges outside the thickness resonances, in which one or two traveling waves propagated. The probing points were located to the left and to the right of the source of vibrations with a circular frequency ω. The combination of such probing methods made it possible to obtain a unique solution to inverse problems, excluding phantom solutions. In the case of antiplane vibrations, formulae are obtained for determining the characteristics of a small defect. The results of computational experiments were presented. The boundaries of the region of correct operation of the asymptotic approach were established.

Acknowledgments. The publication was carried out as part of the implementation of the grant of JSC "Russian Railways" for the development of scientific and pedagogical schools in the field of railway transport. The author is grateful to Prof. Vatulyan A.O. for attention to the work.

References

[1] Kolesnikov V.I., Belyak O.A. *Mathematical Models and Experimental Studies are the Basis for the Design of Heterogeneous Antifriction Materials*. Moscow: Fizmatlit, 216, 2021.
[2] Vatulyan A.O., Belyak O.A. // *Acoustical Physics*, **3**(66), 235–241, 2020.

Calculation of the Activation Energy of Conductivity for Cobalt Oxide Films

V. V. Bespoludin*, V. V. Polyakov, Yu. N. Varzarev

Institute of Nanotechnology, Electronics and Electronic Equipment Engineering, Southern Federal University, Taganrog, Russia

*vladislaw.bespoludin@yandex.ru

Cobalt oxide films are interesting as a sensing element in gas sensors. This is due to the fact that cobalt oxide has a good response to a large number of industrial gases, selectivity and long-term use. The aim of this work is to determine the activation energy of conductivity for cobalt oxide films. Cobalt films were formed on a pre-cleaned sitall substrate by vacuum thermal evaporation. After that, the obtained cobalt films for the formation of cobalt oxide films were subjected to rapid thermal annealing (RTA) by halogen lamps in the air at temperatures of 500 °C, 600 °C and 700 °C [1, 2]. Cobalt metal contacts were deposited on the surface of cobalt oxide films by vacuum thermal evaporation to measure the electrical parameters of the samples. Resistance measurements in the temperature range from room temperature to 400 °C were carried out using a universal voltmeter B7-78/1. There are two main types of cobalt oxide, Co_3O_4 and CoO. Both semiconductors have *p*-type conductivity due to the presence of defects. The change in the resistance of the samples during heating from room temperature to 400 °C was measured. At room temperature, the resistance of cobalt oxide films formed by RTA at 500 °C, 600 °C and 700 °C was 12.4 MΩ, 83.3 MΩ and 9.04 MΩ, respectively. At a temperature of 400 °C, the resistance of the samples annealed at a temperature of 500 °C, 600 °C, and 700 °C was 84.36 kΩ, 220 kΩ, and 83.23 kΩ, respectively. The values of the activation energy of conductivity (E_a) were calculated by Arrhenius equation [3, 4]: $\sigma = \sigma_o \exp(-E_a/kT)$, where σ is the conductivity at temperature T, σ_o is a constant, k is

the Boltzmann constant, T is the absolute temperature (K) and E_a is the activation energy of conductivity. Figure 1 shows the dependence of the conductivity of cobalt oxide films annealed at temperatures of 500 °C, 600 °C and 700 °C on $1/T$ in the temperature range from room temperature to 400 °C. The calculation results of the activation energy of conductivity are presented in Table 1. From the results, it can be seen that the activation energy of conductivity increases with increasing heating temperature. It can be explained by an increase in the energy of electrons in the result of thermal heating and their throwing to higher zones of the acceptor level. In addition, the cobalt oxide film formed at 600 °C shows the highest values of E_a in almost the entire temperature range. This sample is also characterized by the highest resistivity in comparison with samples, obtained at temperatures of 500 °C and 700 °C. Based on the obtained calculations of the activation energy of conductivity, it can be concluded that the activation energy of conductivity of cobalt oxide films depends significantly on the heating temperature, as well as on the resistivity of the cobalt oxide films.

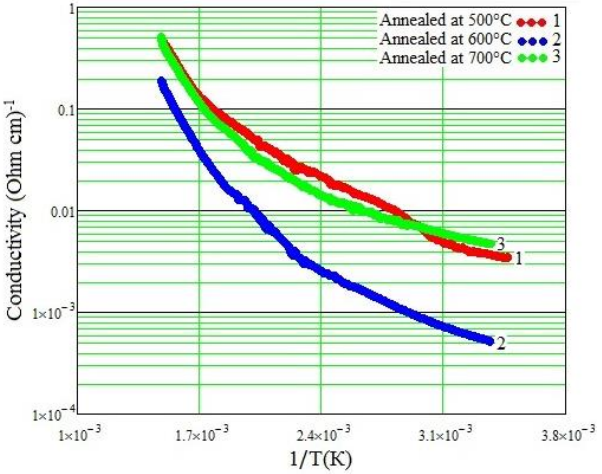

Fig. 1. Dependence of the conductivity on the heating temperature in the range from room temperature to 400 °C

Table. 1. Influence of heating temperature on the activation energy of the conductivity of cobalt oxide films

Cobalt oxide film	E_a in the temperature range from room temperature to 100 °C	E_a in the temperature range from 100°C to 150°C	E_a in the temperature range from 150°C to 200°C	E_a in the temperature range from 200°C to 250°C	E_a in the temperature range from 250°C to 300°C	E_a in the temperature range from 300°C to 350°C	E_a in the temperature range from 350°C to 400°C	Average value of E_a in the temperature range from room temperature to 400°C
RTA at 500°C	0.147 eV	0.162 eV	0.194 eV	0.251 eV	0.264 eV	0.432 eV	0.562 eV	0.251 eV
RTA at 600°C	0.127 eV	0.165 eV	0.316 eV	0.351 eV	0.410 eV	0.555 eV	0.679 eV	0.323 eV
RTA at 700°C	0.084 eV	0.130 eV	0.145 eV	0.283 eV	0.295 eV	0.487 eV	0.660 eV	0.255 eV

For example, a cobalt oxide film, formed by RTA at 600 °C and having a higher resistivity, has a higher average activation energy of conductivity than cobalt oxide films having a lower resistivity. It can also be added that in the temperature range from room temperature to 400 °C there is no intrinsic conductivity for cobalt oxide films because the band gap for Co_3O_4 is 1.4 – 1.8 eV, whereas the band gap for CoO is 2.2 – 2.8 eV [5]. Thus, it can be concluded that, in this temperature range, only acceptor conductivity is observed for cobalt oxide films.

References

[1] Bespoludin V. V., Polyakov V. V., Petrov V. V., Nesterenko A. V., Vakulov Z. E. // *IOP Conference Series: Materials Science and Engineering*, **1035**, 012006, 2021.

[2] Petrov V. V., Polyakov V. V., Varzarev Yu. N., Bespoludin V. V., Bayan E. M. In: International Conference on "Physics and Mechanics of New Materials and Their Applications" (PHENMA 2020), Kitakyushu, Japan, March 26–29, 2021, 213 – 214.

[3] Patil V., Pawar S., Chougule M., Raut B., Ramesh M., Sen S. // *J. Sens. & Trans*. **128**, 100 – 114, 2011.

[4] Bhargava R., Khan S., Ahmad N., Ansari M. M. N. // *AIP Conf. Proc*., **1953**, 030034, 2018.

[5] Balouria V., Kumar A., Samanta S., Bhattacharya S., Singh A., Debnath A. K., Mahajan A., Bedi R. K., Aswal D. K., Gupta S. K. // *AIP Conf. Proc*., **1451**, 289, 2012.

Influence of Rapid Thermal Annealing on Surface Roughness and Thickness of Cobalt Films

V. V. Bespoludin*, V. V. Polyakov, Yu. N. Varzarev

Institute of Nanotechnology, Electronics and Electronic Equipment Engineering, Southern Federal University, Taganrog, Russia

*vladislaw.bespoludin@yandex.ru

In this work, we studied the dependence of the surface roughness and thickness of cobalt films on the temperature of rapid thermal annealing (RTA). Cobalt films were formed on a pre-cleaned sitall substrate by vacuum thermal evaporation (UVN-72). The thickness of these films was 310 nm. After that, the obtained cobalt films were subjected to RTA by halogen lamps in air for the formation of cobalt oxide films. RTA was carried out at temperatures from 400 to 1000 °C with a step of 100 °C. Earlier, it was found that RTA at temperatures from 600 to 1000 °C allows one to form the phase of cobalt oxide (Co_3O_4) from metallic cobalt [1, 2]. The roughness of the surface of cobalt films without annealing and with RTA annealing was investigated by the AFM method using the Ntegra Vita nanolaboratory (NT MDT, Moscow), see Fig. 1(a). The thickness of the cobalt films was measured by the MII-4 microinterferometer depending on the annealing temperature, see Fig. 1(b). Figure 1(a) shows that with an increase in the annealing temperature from 400 to 1000 °C, the roughness of the film surface increases, with the exception of the sample annealed at a temperature of 900 °C. For this sample, the surface roughness was 18.2 nm. At an annealing temperature of 400 °C, the thickness of the cobalt film decreases from 310 to 210 nm, which can be explained by the compaction of the film and an increase in the roughness of the film surface without oxidation. A further increase in the temperature of the RTA leads to an increase in the thickness of the film, which is associated with the diffusion of oxygen into the depth of the film through the previously formed oxide film on the surface. This leads to loosening of the film and the growth

of the oxide and thereby to an increase in surface roughness. According to the results of the XRD study, the annealing temperature of 500 °C is not enough for the formation of the cobalt oxide phase. At a temperature of 500 °C, only insignificant oxidation of the cobalt film is possible. At an annealing temperature of 600 °C, the cobalt oxide phase (Co_3O_4) is formed [2, 3]. With a further increase in temperature, the growth of the film in thickness passes into the saturation stage, which is associated with the complete oxidation of the film to the entire thickness. Based on these results, it can be seen that the use of RTA can significantly change the surface roughness of the cobalt film, as well as significantly change the thickness of the cobalt film. Thus, at an annealing temperature of 1000 °C, the roughness of the cobalt oxide film is 26.55 nm, and its thickness is 584 nm, whereas the roughness of the metallic cobalt film without annealing is 2.316 nm, and its thickness is 310 nm.

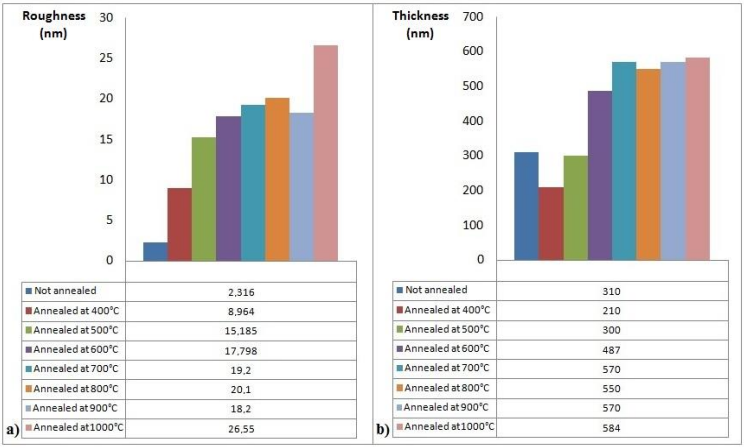

Fig. 1. (a) Influence of RTA temperature on the surface roughness and (b) thickness of cobalt films

References

[1] Bespoludin V. V., Polyakov V. V., Petrov V. V., Nesterenko A. V., Vakulov Z. E. // *IOP Conference Series: Materials Science and Engineering*, **1035**, 012006, 2021.

[2] Petrov V. V., Polyakov V. V., Varzarev Yu. N., Bespoludin V. V., Bayan E. M. In: International Conference on "Physics and Mechanics of New Materials and Their Applications" (PHENMA 2020), Kitakyushu, Japan, March 26 – 29, 2021, 213 – 214.

[3] Bespoludin V. V., Starnikova A. P., Varzarev Yu. N., Bayan E. M., Polyakov V. V., Petrov V. V. // *NanoOstrava 2021, 7th Nanomaterials and Nanotechnology Meeting Nanotechnology Centre*, CEET, VŠB, Technical University of Ostrava, Czech Republic, May 17 – 20, 2021, 57.

Design and Principle of Operation of the Pneumatic Wedge Gripper

A. V. Bil*, D. V. Karabanov, S. O. Kireev, M. V. Korchagina

Don State Technical University, Rostov-on-Don, Russia

*avbill@mail.ru

SPO (descent and lifting operations) is a labor-intensive, as well as a noticeably long part of the drilling process. They account for up to 40% of the total time spent on the construction of the well. Automation and mechanization of these drilling operations is the most effective means of improving their organization. To perform all operations, the drilling rig is equipped with a set of mechanisms and tools for grabbing, lifting, holding the rotor of the drill or casing string on the weight or on the table when screwing and unscrewing pipes extracted from the well or lowered into it [1]. Pneumatic wedge grippers are designed to hold the drill string during descent and lifting operations and the casing string when fixing the well. Moreover, wedge grips hold the column directly behind the cylindrical surface of the pipe [2]. When lowering the wedges, their working elements-dies with notches come into contact with the pipe surface and when lowering the pipe column for a certain distance, its jamming and retention occurs. Thus, the principle of operation of the wedge gripper is the same as that used in column heads. The only difference is that the column heads provide a permanent suspension of the casing strings, and in the rotor, the capture of the drill string is temporary, periodically carried out only when lifting or lowering the pipes. The pneumatic wedge gripper is interlocked by the rotor drive in such a way that when the wedge gripper is raised, the possibility of rotation of the rotor table is excluded. During the operation of the grippers on the well, it is necessary to fulfill certain conditions, including such as maintenance after the end of each well, the establishment of basic operating conditions under which reliable operation is ensured within the specified loads (matching the size of the wedges (dies) to the size of the gripped pipes; simultaneous replacement of the dies for all wedges (in the amount of 4 pieces) for all the gripping wedges; inspection of the equipment: the toothed surface of the dies must be smooth, the absence of burrs, cracks, dents, potholes on the working surfaces of the wedges, dies, housing inserts is checked; ensuring the lubrication and cleaning process of the support surfaces of the wedges and inserts in accordance with the lubrication map; the rotation of the wedges in the hinge joints must be free, without jamming; checking the smoothness and freedom of lifting and lowering the wedges; checking the absence of damage to the pipe in the places of its capture by wedges; the landing of the pipe column on the wedges should be carried out only after the complete stop of the column, compliance with the actual loads, which should not exceed 320 tons in accordance with the technical characteristics [3].

References

[1] Severinchik N. A. *Machinery and Equipment for Drilling Wells*. Nedra, Moscow, 1986 (In Russian).

[2] Danielyan A. A. *Drilling Machine and Mechanisms*. GOSO-PERISTAT, State scientific-technical publishing house of the oil and mining and fuel literature, Moscow, 1956 (In Russian).

[3] Kostin I. I. *Oil Machinery and Equipment*. STATE OPTTEKHIZDAT, State Scientific and Technical Publishing House of Oil and Mining and Fuel Literature, Moscow, 1963 (In Russian).

Research Tension and Deformations in the Elastic Element of the Universal Spherical Preventer Seal

A. V. Bil, M. V. Korchagina*, S. O. Kireev, V. N. Stepanov

Don State Technical University, Rostov-on-Don, Russia

*ms.korchaginamv@mail.ru

One of the most important units that ensure the efficient and safe operation of the drilling rig is anti-blowout equipment (air defense). The universal spherical preventer is used during well drilling and is intended for sealing the mouth during drilling operations both in the presence of drill pipes and drilling tools, and without it. The reliability of the preventer depends on the greatest extent of the rubber-metal seal. Various designs of seals are known to have certain advantages and disadvantages [1]. The main problems of existing structures are high metal consumption, significant weight and low reliability of seals, when working on a complete well closure. In order to optimize the design of sealing elements, studies on the nature of stress distribution and the stages of deformation of the elastic element of the seal are relevant [2, 3]. This report presents studies of the stress-strain state of seals with various shapes of reinforcing metal segments [4], concentrically distributed over the volume of a massive rubber matrix, compressing the columns of casing and drill tubes, and also considers the deformation and stress of the seal in the absence of drilling tools. The research is carried out using numerical methods on full-scale models in applied CAD packages. In the course of the study, data were obtained on the ratio of the volumes of rubber and metal parts of the seal to the diameter of the conditional passage. The nature of stresses arising in reinforcing segments of various shapes, as well as the direction and degree of shaping of the rubber matrix at various degrees of compression (casing pipe, drill pipe, complete closure of the well) are considered. The greatest values of the contact force and contact pressure in the contact zones with the lid and pipe are calculated. The obtained values can be used to calculate the structural elements of the improved and newly designed seals of universal annular spherical preventers. Determination of the main parameters of their operation: the required stroke of the piston, pressure in the hydraulic control system, friction forces arising during the operation of the unit.

References

[1] Gulyants G. M. *Blowout Equipment of Wells Resistant to Hydrogen Sulfide*. Moscow: Nedra, 348, 1991 (In Russian).

[2] Kireev S. O., Korchagina M. V., Kaderov H. K., Efimov A. V. Upgraded design of a ring rotating preventer with a piston braking device // *Advanced Technologies and Systems of Mechanical Engineering*, **1**(64), 37 – 42 2019. (In Russian).

[3] Bangaev S. S., Saidov M. A., Perekrestov A. P. Development of the universal preventer sealer design // *Bulletin of AGTU. Serie: Marine Engineering and Technology*, **1**, 126 – 128, 2009 (In Russian).

[4] Kireev S. O., Korchagina M. V., Artemova M. D. The study of the design and functioning of the sealing element of the ring preventer // *Young Researcher of Don*, **3**(24), 7 – 11, 2020 (In Russian).

Identification of Prestress in Round Inhomogeneous Solid and Annular Plates for the Timoshenko's Theory

I. V. Bogachev

Southern Federal University, Rostov-on-Don, Russian Federation

bogachev89@yandex.ru

Modelling of new inhomogeneous materials, in particular, functionally graded materials (FGMs), taking into account the presence of characteristic prestress (PS) fields in them, is a one of most important directions of modern science. Such materials are widely used in the modern high-tech industry, in particular, in instrument making, aviation and space industries, and the production of components for nuclear reactors. A distinctive feature of these materials is that their mechanical properties and PS are functions of spatial coordinates and can vary significantly over the volume of the body. The reasons for the gradient of the characteristics of such materials can be inhomogeneities in the structure of the chemical composition, microstructure, or atomic order arising from the peculiarities of their manufacture. The nature of the occurrence of PS in them is most often technological temperature treatments followed by cooling, used in the production of FGMs. Operational problems arising from the use of FGMs can affect the strength characteristics, in particular, fragility and susceptibility to extreme operating conditions, caused by the possible development of defects and residual stress concentrators. Another problem is the need to verify that the values of mechanical properties correspond to those specified at the design stage. In this regard, the inverse problems of identifying the characteristics of such materials, both mechanical properties and PS, are of particular importance, both for checking these materials at the manufacturing stage and for current operational monitoring. For identification, it is necessary to develop new diagnostic non-destructive techniques that meet the requirements for speed, accuracy, and ease of practical implementation. These requirements are met by the acoustic sensing method, which has proven itself in other identification problems. This method makes it possible to determine the necessary parameters by analyzing the acoustic response when measuring dynamic characteristics. In this report we present modeling of round solid and annular inhomogeneous prestressed plates within the framework of the Timoshenko hypotheses. Using the general linearized statement of the problem on vibrations of a prestressed body, a general form of expressions for bending moments and shear forces of the Timoshenko plate having prestress is obtained, with the help of which the equations of bending vibrations are derived. New inverse problems of prestress identification are studied based on the analysis of the acoustic response by applying a probing load. To solve the inverse problems, a special projection approach is used, based on the constructed weak statements of problems, which makes it possible to determine the desired characteristics in given classes of functions. For both cases of solid and annular plates, we estimate the sensitivity of the amplitude-frequency characteristics, the values of which are used as additional data in the inverse problems, to a change in the prestress level; the most favorable frequency ranges of identification were revealed. The solution of inverse problems is illustrated by a series of computational experiments on reconstructing prestress of various levels and distribution patterns within the plates.

Acknowledgement. Research was financially supported by Southern Federal University, grant No. VnGr-07/2020-04-IM (Ministry of Science and Higher Education of the Russian Federation).

Modeling of Solid and Holed 2D FGM Plates with Prestress

I. V. Bogachev, R. D. Nedin

Southern Federal University, Rostov-on-Don, Russian Federation

bogachev89@yandex.ru

Functionally graded materials are new inhomogeneous materials, the change in structure and properties of which throughout the volume is continuous and can be described by smooth functions. At the same time, the main advantage of these materials is that the laws of change in the properties of these materials can be accurately designed in advance, taking into account the specifics of the area of their use. This is of great interest in a variety of fields, including aerospace engineering, nuclear power, sensor manufacturing, biomedical implants, optoelectronic devices, and energy absorption systems. In the case when the properties of FGMs depend on one coordinate, in the modern literature such FGMs are denoted 1D (one-dimensional inhomogeneity), the dependence of properties on two and three coordinates, respectively, is denoted as 2D and 3D. At the same time, for various plate structures, in particular, rectangular, the most common case is precisely 2D FGM. FGMs manufacturing technologies, in particular, based on 3D printing, make it possible to create objects of complex geometry without using classical technologies, including casting, which requires additional production of molds. However, due to the fact that temperature and other preliminary influences are used in the manufacture of FGMs, they are often characterized by the presence of prestress (PS) fields. Modeling of 2D FGMs plates, for which both the mechanical properties and the PS are functions of two coordinates, is currently rather poorly studied, but its development is necessary for constructing the theoretical foundations for solving problems of identifying these characteristics. This work is devoted to modeling the vibrations of solid and perforated 2D FGMs plates taking into account the inhomogeneous field of prestress. The properties of the plate and the components of the preliminary state in the considered plate formulation were functions of two coordinates. On the basis of a general linearized formulation of the problem of vibrations of a pre-stressed-deformed body, the problem of steady-state planar vibrations of the considered plates is presented. A weak formulation of the problem is also given, with the use of which a finite element scheme for solving the direct problem of calculating the vibrations of plates is constructed. Numerical solutions of boundary value problems were implemented using the finite element method in the FreeFem++ software. To increase the accuracy for perforated plates, a local refinement of finite element meshes was used. It was believed that the prestresses arose in the result of the combined action on the plates, the PS fields were calculated in the result of solving the corresponding auxiliary problems of statics, also implemented in the FreeFem++ software. An extensive analysis of the solution of direct problems on the calculation of plate vibrations, amplitude-frequency characteristics, stress-strain state has been carried out. The influence of the factors of the PS level, its distribution in the plates, the area and the location of the holes on the dynamic characteristics of the plates was evaluated in order to identify the optimal loading modes and frequency ranges for constructing an approach to their identification. The results obtained can become the basis for the development of new methods for identifying two-dimensional distributions of material parameters and PS state in plates.

Acknowledgement. The work was supported by the Russian Science Foundation (project code 18-71-10045, https://rscf.ru/project/18-71-10045/).

Structure and Dielectric Characteristics of Ternary Ceramics $(1 - x - y)BiFeO_3 - xPbFe_{0.5}Nb_{0.5}O_3 - yPbTiO_3$

N. A. Boldyrev*, E. I. Sitalo

Research Institute of Physics, Southern Federal University, 344090, Rostov-on-Don, Russia

*nboldyrev@sfedu.ru

Unalloyed samples of solid solutions of the ternary system $(1 - x - y)BiFeO_3 - xPbFe_{0.5}Nb_{0.5}O_3 - yPbTiO_3$ ($x = 0.60$, $0.075 \le y \le 0.175$, $\Delta y = 0.025$) were prepared by the solid-phase reactions technique with following sintering using conventional ceramic technology. Using X-ray studies, it was found that these objects have a tetragonal crystal structure. X-ray diffraction studies at various temperatures showed a rather complex evolution of the phase composition with increasing T, including the formation of planes of crystallographic shear and the appearance of sinusoidal modulation of the crystal structure of the studied objects. Phase states diagrams for researched section have been determined. The diffuse phase transition, which corresponds to the first maximum in the $\varepsilon'/\varepsilon_0(T)$ dependence, occurs in the range (360 – 430) K (Fig. 1). The second maximum at the $\varepsilon'/\varepsilon_0(T)$ dependence is associated with the effects of Maxwell-Wagner polarization and relaxation of charge carriers at the grain boundaries in the temperature region (500 – 630) K. High piezoelectric response (~ 351 pC/N) was observed in the sample with $y = 0.15$.

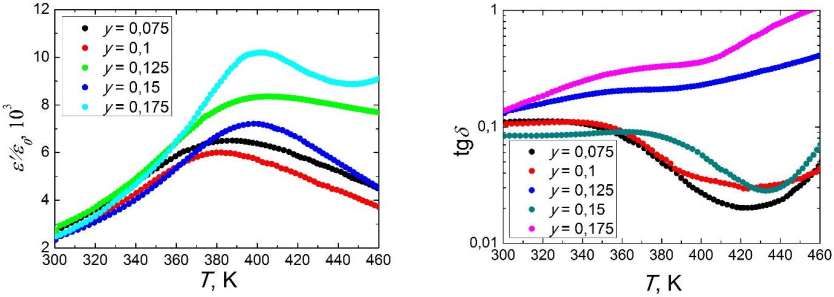

Fig. 1. Dependences $\varepsilon'/\varepsilon_0(T)$, $\mathrm{tg}\delta(T)$ in the temperature range (300 K – 460 K) at the $f = 50$ kHz

Acknowledgement. The study was carried out with the financial support of the Ministry of Science and Higher Education of the Russian Federation (State task in the field of scientific activity, scientific project No. 0852-2020-0032), (BAZ0110/20-3-07IF). This work was performed using the equipment of the Center for Collective Use "Electromagnetic, Electromechanical and Thermal Properties of Solids", Research Institute of Physics, Southern Federal University.

New Relativistic Equation for Statistical Operator

Boris V. Bondarev

Moscow Aviation Institute, Moscow, Russia

bondarev.b@mail.ru

In quantum physics, the main tool is the statistical operator $\hat{\varrho}$. However, a covariant quantum equation for this operator has not yet been written.
Let us write a new equation for a free particle [1 – 3]:

$$\mathrm{i}\hbar\,\partial\hat{\varrho}/\partial t = 1/(2m)\,[\hat{\boldsymbol{p}}^2\hat{\varrho}] + \mathrm{i}\gamma/\hbar\{[\hat{\boldsymbol{r}}[\hat{\boldsymbol{r}}\hat{\varrho}]] - \mathrm{i}\hbar\,\beta/(2\,m)[\hat{\boldsymbol{r}}\,[\hat{\boldsymbol{p}}\hat{\varrho}]_+]\},$$

here γ is an attenuation coefficient. This is a non-relativistic equation.
We write down the momentum and kinetic energy operators of a relativistic particle:

$$\hat{\boldsymbol{p}}_{\mathrm{relativ}} = \hat{\lambda}\hat{\boldsymbol{p}}\,, \qquad \hat{E}_{\mathrm{relativ}} = \hat{\lambda}mc^2,$$

where

$$\hat{\boldsymbol{p}} = m\hat{\boldsymbol{v}}, \qquad \hat{\lambda} = (1 - \hat{v}^2/c^2)^{-1/2}.$$

Using the formula $\hat{\boldsymbol{p}} = m\hat{\boldsymbol{v}}$, we express the velocity operator $\hat{\boldsymbol{v}}$ of the particle in terms of the momentum operator: $\hat{\boldsymbol{v}} = \hat{\boldsymbol{p}}/m$. Thus, we get:

$$\lambda(\hat{p}) = \{1 - \hat{p}^2/(m^2\,c^2)\,\}^{-1/2}.$$

Therefore, we will have a covariant quantum equation for the statistical operator of a free particle [4]

$$\mathrm{i}\hbar\,\partial\hat{\varrho}/\partial t = mc^2[\lambda(\hat{p})\hat{\varrho}] - \mathrm{i}\gamma/\hbar\{[\hat{\boldsymbol{r}}[\hat{\boldsymbol{r}}\hat{\varrho}]] + \mathrm{i}\hbar\,\beta/(2\,m)[\hat{\boldsymbol{r}}[\lambda(\hat{p})\hat{\boldsymbol{p}}\hat{\varrho}]_+]\}.$$

If we decompose the function $\lambda(\hat{p})$ into a Taylor series, we will have

$$\mathrm{i}\hbar\,\partial\hat{\varrho}/\partial t \cong [\hat{p}^2/(2\,m) - 3/(4\,m^3\,c^2)\hat{p}^4,\,\hat{\varrho}] - \mathrm{i}\gamma/\hbar\{[\hat{\boldsymbol{r}}[\hat{\boldsymbol{r}}\hat{\varrho}]] + \\ + \mathrm{i}\hbar\,\beta/(2\,m)[\hat{\boldsymbol{r}}\,[\{1 + \hat{p}^2/(2m^2\,c^2)\}\hat{\boldsymbol{p}}\,\hat{\varrho}]_+]\}.$$

Now we write down a covariant quantum equation for the statistical operator of the hydrogen atom. There are two particles in this atom. This is an electron and a proton, which carry electric charges −e and +e. Therefore, they have a potential energy:

$$U_{ep}(\boldsymbol{r}_e - \boldsymbol{r}_p) = -\,\mathrm{e}^2/|\boldsymbol{r}_e - \boldsymbol{r}_p|,$$

where $\boldsymbol{r}_e$ and $\boldsymbol{r}_p$ are the radius-vectors of the electron and proton.
The Hamiltonian of the atom will be equal to

$$\hat{H} = \hat{\boldsymbol{p}}_e^2/(2m_e) + \hat{\boldsymbol{p}}_p^2/(2m_p) + U_{ep}(\boldsymbol{r}_e - \boldsymbol{r}_p),$$

where $\hat{\boldsymbol{p}}_e$ and $\hat{\boldsymbol{p}}_p$ are the electron and proton pulses, m_e and m_p are their masses.
We take the dissipative operators equal to

$$\mathrm{i}\hbar\hat{D} = -\,\mathrm{i}\gamma/\hbar\{[\boldsymbol{r}_e - \boldsymbol{r}_p[(\boldsymbol{r}_e - \boldsymbol{r}_p)\hat{\varrho}]] + \mathrm{i}\hbar\,\beta/(2\,m_e)[\boldsymbol{r}_e - \boldsymbol{r}_p[(\hat{\boldsymbol{p}}_e - \hat{\boldsymbol{p}}_p)\hat{\varrho}]_+].$$

Now we will write a non-relativistic equation:

$$\mathrm{i}\hbar\,\partial\hat{\varrho}/\partial t = [\hat{H}\hat{\varrho}] + \mathrm{i}\hbar\hat{D}.$$

In relativistic physics, the formulas are known:

$$\hat{\boldsymbol{p}}^{(e)}_{\mathrm{relativ}} = \hat{\lambda}_e\,\hat{\boldsymbol{p}}_e\,, \qquad \hat{E}^{(e)}_{\mathrm{relativ}} = \hat{\lambda}_e\,m_e c^2,$$

where

$$\hat{\lambda}_e = \lambda(\hat{\boldsymbol{p}}_e/m_e) = \{1 - \hat{\boldsymbol{p}}_e^2/(m_e^2\,c^2)\}^{-1/2}$$

for an electron;

$$\hat{\boldsymbol{p}}^{(p)}_{\mathrm{relativ}} = \hat{\lambda}_{\boldsymbol{p}}\,\hat{\boldsymbol{p}}_{\boldsymbol{p}}\,, \qquad \hat{E}^{(p)}_{\mathrm{relativ}} = \hat{\lambda}_{\boldsymbol{p}}\,m_{\boldsymbol{p}}c^2,$$

where

$$\hat{\lambda}_{\boldsymbol{p}} = \lambda(\hat{\boldsymbol{p}}_{\boldsymbol{p}}/m_{\boldsymbol{p}}) = \{1 - \hat{\boldsymbol{p}}_{\boldsymbol{p}}^2/(m_{\boldsymbol{p}}^2\, c^2)\}^{-1/2}$$

for the proton.

Now we will write down a covariant quantum equation for the statistical operator of the hydrogen atom [4]:

$$\mathrm{i}\hbar\, \partial\hat{\varrho}/\partial t = [\lambda(\hat{\boldsymbol{p}}_e/m_e)m_e c^2 + \lambda(\hat{\boldsymbol{p}}_{\boldsymbol{p}}/m_{\boldsymbol{p}})m_{\boldsymbol{p}}\, c^2 + U_{ep}(\boldsymbol{r}_e - \boldsymbol{r}_p),\ \hat{\varrho}] -$$
$$- \mathrm{i}\gamma/\hbar\{[(\boldsymbol{r}_e - \boldsymbol{r}_p)[(\boldsymbol{r}_e - \boldsymbol{r}_p)\hat{\varrho}]] + \mathrm{i}\hbar\,\beta/(2\,m_e)[(\boldsymbol{r}_e - \boldsymbol{r}_p)\cdot$$
$$\cdot\,[\lambda(\hat{\boldsymbol{p}}_e/m_e)\,\hat{\boldsymbol{p}}_e - \lambda(\hat{\boldsymbol{p}}_{\boldsymbol{p}}/m_{\boldsymbol{p}})\,\hat{\boldsymbol{p}}_{\boldsymbol{p}}, \hat{\varrho}]_+]\,.$$

Spin manifests itself only when a term that describes the influence of spin appears in the equation for the operator $\hat{\varrho}$:

$$-\,\mu_{\mathrm{B}}[\hat{\sigma}\hat{\mathcal{H}}\hat{\varrho}]\,,$$

where $\mu_{\mathrm{B}} = \mathrm{e}\hbar/(2m)$ is the Bohr magneton, $\sigma = \pm\,1/2$ is the electron spin, $\mathcal{H} = \mathcal{H}(t, \boldsymbol{r})$ is the modulus of the magnetic field strength.

References

[1] Lindblad G. On the generators of quantum dynamical semigroups // *Commun. Math. Phys*., **48**, 119 – 130, 1976.

[2] Bondarev B.V. Quantum Markovian master equation for a system of identical particles interacting with a heat reservoir // *Physica A*, **176**(2), 366 – 386, 1991.

[3] Bondarev B.V. *Density Matrix Theories in Quantum Physics*. Bentham, 393, 2020.

[4] Bondarev B.V. *My Scientific Articles*, Book 4, Moscow: Sputnik+, 69, 2021.

Statistical Operator and Density Matrix for Gamma-quant and Deuterium

Boris V. Bondarev

Moscow Aviation Institute, Moscow, Russia

bondarev.b@mail.ru

In this report, we study the problem of how the statistical operator $\hat{\varrho}$ can be used to describe the nuclear reaction of the death of deuterium *D* when it is irradiated with a γ-quantum:

$$\gamma + D \to p + n,$$

as a result, deuterium decays into a proton *p* and a neutron *n*. A gamma-ray quantum having a frequency ω is identified with that part of the light wave that is carried in space at the speed of light *c* and occupies the volume $V = SL$ of a cylinder with an area *S* and a length $L \sim 1/k$, where *k* is the modulus of the wave vector $\boldsymbol{k}$, and directed along this vector. In quantum physics, a photon is considered as a wave particle having energy $\varepsilon = \hbar\,\omega$ and momentum $\boldsymbol{p} = \hbar\,\boldsymbol{k}$, where $k = \omega/c$.

In classical physics, the electromagnetic field is described by the vectors of electric $\boldsymbol{E} = \boldsymbol{E}(t, \boldsymbol{r})$ and magnetic $\boldsymbol{H} = \boldsymbol{H}(t, \boldsymbol{r})$ fields. A gamma-ray quantum is a part of a plane wave:

$$E_x = 0\,,\ \ E_y = E_0\cos(\omega\, t - k\, x)\,,\ \ \ E_z = 0\,;$$
$$H_x = 0\,,\ \ H_y = 0,\ \ H_z = H_{\mathrm{o}}\cos(\omega\, t - k\, x)\,,$$

and the energy of the gamma-ray quantum $\varepsilon = \hbar\,\omega$ and its momentum $\boldsymbol{p} = \hbar\,\boldsymbol{k}$ will be equal to the wave energy:

$$W = 1/2\ \int(\varepsilon_0\,\boldsymbol{E}^2 + \mu_0\,\boldsymbol{H}^2)\mathrm{d}V = \varepsilon_0 SLE_0^2\cos^2(\omega t - kx)$$

and the energy $W^{(S)}$, which is transferred by radiation through the area *S* during the time $\tau = L/c$. This energy will be equal to

$$W^{(S)} = S\int_0^t S_x \mathrm{d}t,$$

where S_x is the projection of the Umov – Poiting vector $\boldsymbol{S} = [\boldsymbol{EH}]$, the projections of which on the coordinate axis will be equal to

$$S_x = \sqrt{\varepsilon_0/\mu_0}\, E_0^2 \cos^2(\omega t - kx), \qquad S_y = 0\,, \quad S_z = 0\,.$$

Deuterium consists of a proton and a neutron. To write down the equation for it, we need to know their potential energy $\widehat{U}(\hat{\boldsymbol{r}})$. It was hypothesized that the proton and neutron have a nucleon charge κ, and their energy is equal to

$$\widehat{U}(\hat{\boldsymbol{r}}) = U(\boldsymbol{r}_p - \boldsymbol{r}_n) = -\kappa^2/|\,\boldsymbol{r}_p - \boldsymbol{r}_n|\,,$$

where $\boldsymbol{r}_p$ and $\boldsymbol{r}_n$ are the radius-vectors of the proton and neutron. Thus, we can write the equation [1 – 4]:

$$\mathrm{i}\hbar\,\partial\hat{\varrho}/\partial t = 1/(2m)[(\hat{\boldsymbol{p}}_c^2 + \hat{\boldsymbol{p}}^2)\hat{\varrho}] + [\widehat{U}(\hat{\boldsymbol{r}})\hat{\varrho}] + \alpha/(2m)[\hat{\boldsymbol{r}}[\hat{\boldsymbol{p}}\,\hat{\varrho}]_+].$$

The solution of this equation is equal to $\hat{\varrho} = \hat{\varrho}^{(D)}\hat{\varrho}^{(c)}$, where $\hat{\varrho}^{(D)}$ is the operator of the deuterium at rest:

$$\mathrm{i}\hbar\,\partial\hat{\varrho}^{(D)}/\partial t = 1/(2m)\,[\hat{\boldsymbol{p}}^2\hat{\varrho}^{(D)}] + [\widehat{U}(\hat{\boldsymbol{r}})\,\hat{\varrho}^{(D)}] + \alpha/(2m)[\hat{\boldsymbol{r}}\,[\hat{\boldsymbol{p}}\,\hat{\varrho}^{(D)}]_+].$$

and the operator $\hat{\varrho}^{(c)}$ describes the motion of the center of mass:

$$\mathrm{i}\hbar\,\partial\hat{\varrho}^{(c)}/\partial t = 1/(2m)[\hat{\boldsymbol{p}}_c^2\,\hat{\varrho}^{(c)}].$$

Now we need to write down the equations:

$$\mathrm{i}\hbar\,\partial\hat{\varrho}^{(c)}/\partial t = 1/(2m)[\hat{\boldsymbol{p}}_c^2\,\hat{\varrho}^{(c)}] + [\widehat{W}^{(S)}\,\hat{\varrho}^{(c)}],$$

$$\mathrm{i}\hbar\,\partial\hat{\varrho}^{(D)}/\partial t = 1/(2m)[\hat{\boldsymbol{p}}^2\hat{\varrho}^{(D)}] + [\widehat{U}(\hat{\boldsymbol{r}}) + \widehat{W},\ \hat{\varrho}^{(D)}] + \alpha/(2m)[\hat{\boldsymbol{r}}[\hat{\boldsymbol{p}}\,\hat{\varrho}^{(D)}]_+].$$

The first equation describes the motion of the center of mass under the action of a light wave along the *x*-axis, and the second equation describes the change in the state of deuterium under the action of a wave in which the vector $\boldsymbol{E}$ is directed along the *y*-axis.

Now we will calculate the average values of the coordinates $\langle\hat{\boldsymbol{r}}\rangle$ and the momentum $\langle\hat{\boldsymbol{p}}\rangle$, which by definition are equal:

$$\langle\hat{\boldsymbol{r}}\rangle = \mathrm{Tr}(\hat{\boldsymbol{r}}\hat{\varrho}), \quad \langle\hat{\boldsymbol{p}}\rangle = \mathrm{Tr}(\hat{\boldsymbol{p}}\hat{\varrho}),$$

and the change of these values over time will be obtained by the formulas:

$$\mathrm{d}\langle\hat{\boldsymbol{r}}\rangle/\mathrm{d}t = \mathrm{Tr}\,(\hat{\boldsymbol{r}}\,\partial\hat{\varrho}/\partial t), \qquad \partial\langle\hat{\boldsymbol{p}}\rangle/\partial t = \mathrm{Tr}(\hat{\boldsymbol{p}}\,\partial\hat{\varrho}/\partial t).$$

It turned out that the equation for $\hat{\varrho}^{(c)}$ gives the value of the deuterium velocity after irradiation with its gamma quantum, which will be equal to

$$v_x(\tau) = c/2\{\,\omega\tau + 1/2\sin(\,2\,\omega\tau)\}, \qquad v_y(\tau) = v_z(\tau) = 0.$$

Under the action of a gamma-ray quantum, the energy of which does not coincide with the decay energies of deuterium: $\hbar\,\boldsymbol{\omega} \neq \boldsymbol{E_0}$, it receives the velocity:

$$v_y(\tau) = v_0\exp\{\Omega^2\,A/(2\omega)[\cos(2\omega\tau + \alpha) - \cos\,\alpha]\},$$

$$v_x(\tau) = 0, \qquad v_z(\tau) = 0,$$

where

$$A = c\omega[1 - v(\tau)/c\,]/\sqrt{\{(\Omega^2 - \,4\omega^2)^2 \,+\, (4a\omega)^2\}}\,.$$

When the condition $\hbar\omega = E_0$ is fulfilled, deuterium decays into a proton and a neutron. The projections of the decay product velocities have the form

$$v_{1y}(\tau) = v_0\exp\{\Omega^2\,A/(2\omega)[\cos(2\omega\tau + \alpha) - \cos\,\alpha]\,\},$$

$$v_{2y}(\tau) = -\,v_{1y}(\tau).$$

References

[1] Lindblad G. On the generators of quantum dynamical semigroups // *Commun. Math. Phys*., **48**, 119 – 130, 1976.

[2] Bondarev B.V. Quantum Markovian master equation for a system of identical particles interacting with a heat reservoir // *Physica A*, **176**(2), 366 – 386, 1991.

[3] Bondarev B.V. *Density Matrix Theories in Quantum Physics*. Bentham, 393, 2020.

[4] Bondarev B.V. *My Scientific Articles*, Book 4, Moscow: Sputnik+, 69, 2021.

Reconstruction of the Shape of Obstacles Located in Two-dimensional Acoustic and Elastic Media According to the Characteristics of Scattered Short Longitudinal Waves

N.V. Boyev

I. I. Vorovich Mathematics, Mechanics and Computer Science Institute, Southern Federal University, Rostov-on-Don, Russia

nvboev@sfedu.ru

An algorithm for reconstructing the shape of nonconvex solid obstacles in two-dimensional acoustic and elastic media, as well as cavity defects in an elastic material in the ray approximation, is presented. We consider simply connected domains of obstacles with a non-smooth boundary contour of positive curvature, which has a finite number of corner points, the opening angle of which is greater than a straight line. When an obstacle is irradiated with short longitudinal waves in an echo mode at an arbitrary angle, there is always at least one point of specular reflection lying on one of the convex parts of the convex shell of the boundary contour. In the general case, the diffraction pattern in the vicinity of the convex parts of the boundary located inside the convex hull is more complicated. However, the above assumptions mean that for a given angle of the incident wave, there is one point of simple single reflection lying on one of the arcs located inside the convex shell of the defect contour. The considered reconstruction algorithm is as follows. We will assume that for circular irradiation of the boundary in the echo mode, the time of arrival of the reflected pulse and the real amplitude of the reflected longitudinal wave are known. Knowledge of the time of arrival of the pulse completely determines the convex hull of the object boundary, since in this case the support function becomes known, which determines the distance from a certain selected center inside the region to the tangent to the convex boundary at a point with a normal parallel to the direction of incidence of the wave. In this case, the convex hull of the defect contour is the envelope of the family of these tangents, the Cartesian coordinates of which are written out by the well-known methods of differential geometry. After the convex hull has been built, to determine the internal arcs of the boundary, it is necessary to draw the square of the complex amplitude of the reflected wave. At the intervals of variation of the angle of irradiation in the visibility zones of the inner convex parts, there is a superposition of waves. In this case, the amplitude of the reflected wave is represented by the sum of two terms and its intensity, expressed through the support function, does not depend on the distance between the obstacle and the observation point. The amplitude intensity, equal to the square of the modulus of the amplitude, contains the sum of two radii of curvature at the corresponding points of back reflection and a rapidly oscillating term depending on the wave number of the longitudinal wave. To restore the internal arcs, the natural equation of the curve is used and the coordinates of its points in the Cartesian coordinate system are written out through integrals over the length of the curve. The operation of integration in the obtained formulae, if a function known from the experiment is substituted in them, provides filtering of the low-frequency component. Numerical experiments have shown that this natural filtering way provides a more accurate reconstruction than many other known methods. An example of reconstruction of a contour from the considered class in the form of intersecting circles is given. However, the accuracy

of the reconstruction of the proposed method is wider than in the class of contours described in this work. This is also confirmed by the example of reconstructing the contours of areas in the form of a union of two touching circles and a smooth contour in the form of a three-petalled rose. It was found that the accuracy of reconstruction improves with increasing frequency.

Effect of High-Power Electromagnetic Pulses and Dielectric Barrier Discharge in Air on Structural, Physicochemical and Technological Properties of Eudialyte

I. Zh. Bunin*, V. A. Chanturiya, M. V. Ryazantseva

Academician Melnikov Institute of Comprehensive Exploitation of Mineral Resources — IPKON, Russian Academy of Sciences, Moscow, Russia

*bunin_i@mail.ru

Eudialyte is a rock and ore-forming mineral of lujaurites and uvites with its content in these rocks up to 20 – 30%, which ensures high concentratibility of eudialyte ores by gravitational-magnetic separation with eudialyte recovery to concentrate up to 75 – 80%. The eudialyte-group minerals are readily soluble in mineral inorganic acids; however, the recovery of zirconium does not exceed 75 – 77% during acid leaching. To reduce the loss of Zr and other rare elements, it is recommended to decompose the eudialyte concentrate for obtaining sol at the initial stage and/or use mechanical, physicochemical and energy effects on mineral raw materials as preparatory operations before the leaching of concentrates and eudialyte flotation. The use of energy-saving high-voltage electric discharge technologies in the processing of rebellious minerals allows achieving effective separation of mineral complexes (liberation) and creating optimal conditions to enhance the contrast of the physicochemical and flotation properties of minerals and subsequent separation during flotation due to the appearance of hydrophobic and hydrophilic nanoformations on their surface [1, 2]. This work aims at studying and analyzing the mechanisms of exposure to high-power nanosecond electromagnetic pulses (HPEMPs) and dielectric barrier discharges (DBDs) in air under standard conditions (atmosphere pressure) on surface morphology, microhardness, physicochemical properties, adsorbability and floatability of eudialyte $Na_{15}Ca_6(Fe^{2+}, Mn^{2+})_3Zr_3[Si_{25}O_{73}](O, OH, H2O)_3(OH, Cl)_2$ and eudialyte concentrate from the Lovozero deposit (Russia) in order to increase the efficiency of flotation concentration of complex eudialyte ores. The research methods were the Fourier-transform infrared spectroscopy, electron microscopy, microhardness testing, flow potential determination and other techniques. The results obtained testify to the effectiveness of high-power electromagnetic pulses and a dielectric barrier discharge for a directed change in the physicochemical properties and floatability of eudialyte. In all experiments, a decrease in the negative zeta-potential of eudialyte leads to an increase in adsorbability of anionic collector and, as a consequence, an increase in the eudialyte recovery to concentrate. In the result of preliminary short-term electromagnetic pulse treatment and the use of sodium oleate at a consumption of 1000 g/t during flotation, the recovery of eudialyte concentrate to the flotation froth increased by 15% and amounted to 57 – 63%, and at a consumption of 2000 g/t it increased by 4% and amounted to 84%. The rational parameters of electromagnetic pulse treatment are developed and recommended: HPEMP ($\tau \sim 4 – 10$ ns is the pulse duration, $U \sim$

25 kV is the pulse amplitude, $E \sim 10^7$ V·m^{-1} is the electric field intensity) and DBDs (duration of pulse-initiating charges ~10 μs, $\tau_{front} \sim 200 - 300$ ns, $U \sim 20$ kV). The advantages of short-term ($t_{treat} = 10 - 50$ s) energy deposition toward enhanced efficiency of complex eudialyte-bearing ore flotation are justified experimentally.

Acknowledgments. This work was supported by the Ministry of Science and Higher Education of the Russian Federation, project No. 13.1902.21.0018, agreement No. 075-15-2020-802.

References

[1] Chanturiya V. A. // *Gornyi Zhurnal (Mining J.)*, **11** (2017).
[2] Bunin I. Zh., Ryazantseva M. V., Samusev A. L., Khabarova I. A. // *Mining J.*, **11** (2017).

Influence of Additives of Technogenic Raw Materials on the Properties of Heat-insulating Materials

N. I. Buravchuk[1]*, O. V. Guryanova[1]*, E. P. Putri[2]**

[1]Institute of Mathematics, Mechanics and Computer Science named after I.I. Vorovich Southern Federal University, Rostov-on-Don, Russia
[2]Department of Industrial Engineering, University of 17 Agustus 1945 Surabaya, Indonesia

*burav44@mail.ru, **guryanovaolga@mail.ru

The priority direction in the production of building materials is the development of new technologies for obtaining high-quality, competitive materials based on man-made industrial waste, allowing not only to reduce the cost of production, but also to save natural resources. In the Rostov region, a significant amount of waste from the extraction, enrichment and combustion of solid fuels is concentrated. Most of these wastes, according to the results of scientific research [1, 2] and practical experience, are valuable technogenic raw materials and can be successfully used in the manufacture of building materials of a wide range. The purpose of this work is to substantiate the possibility of using rocks of mine dumps, ash-and-slag waste in the technology of heat-insulating materials. There is some experience in the use of heat electric station (HES) ash in the production of aerated concrete. The use of burnt rocks in aerated concrete technology is less common. However, due to the burnt mine rocks, it is possible to significantly expand the raw material base for the further development of the production of products from aerated concrete and other heat-insulating materials. Mine rocks are thermally affected in dumps during long-term self-firing. Ash-and-slag waste is formed during the combustion of coal in boilers. Ashes from thermal power plants and burnt rocks have some peculiarities. These man-made materials are capable of exhibiting physicochemical and latent hydraulic activity. The activity of burnt mine rocks and ash-and-slag waste is due to the presence of several active components in them. The presence of these components is associated with a violation of the crystal lattice of clay minerals under thermal influences and the appearance of a certain energy potential in thermally altered products. Burnt rocks exhibit the properties of active clay. The most active component of ash-and-slag is vitrified substance and glass phase. The activity of the ashes is mainly associated with the presence of the glass phase. On local areas of the surface, there are active centers that make a certain contribution to the binding of calcium hydroxide. Such particles actively interact with calcium hydroxide released during cement hydrolysis. In this case, a significant quantity of cementitious

substances is formed. The use of burnt rocks and ash-and-slag materials in the technology of aerated concrete technology is promising instead of sand. The specificity of the formation of this technogenic raw material contributes to the formation of particles with a macro- and microporous structure. The sources of pore formation are the processes of dehydration of clay minerals and the dissociation of particles of limestone, gypsum and organic matter. In the result of appearance of the gaseous phase, the melt swells and the porous structure is fixed upon cooling. Unlike quartz sand, they are more reactive. Due to the porosity of the particles, they have a lower bulk density. These properties make it possible to use ash and burnt mine rocks in the non-autoclave method of producing aerated concrete more efficiently than sand. The specific surface area of ash-and-slag waste and burnt mine rocks used as a silica component for the preparation of aerated autoclave-free concrete must be at least 200 m^2/kg. Aerated concrete, based on dry ash with a density from 700 to 1100 kg/m^3, has the following strength: 3.6 – 7.5 MPa in compression; 2.0 – 4.1 MPa in bending; 0.54 – 1.12 MPa in tension. Burner-type aerated concrete has the following strength: 2.2 – 3.8 MPa in compression; 1.2 – 2.1 MPa in bending; 0.33 – 0.57 MPa in tension. Aerated concrete with a density from 500 to 900 kg/m^3 can be obtained with materials from burnt rocks. Drying shrinkage for aerated concrete varied from 0.04 to 2.5 mm/m, for aerated concrete from burnt rock it did not exceed 2.0 mm/m; frost resistance was at least 25 cycles of alternating freezing and thawing; thermal conductivity was within 0.15 – 0.23 W/(m·°C); water absorption was 41.7 – 56.0 %. The raw material base for the production of lightweight aggregates, as well as materials for heat-insulating backfill, are burnt or burnt-out mine rocks with a highly porous structure and a bulk density of less than 100 kg/m^3. Aggregates from burnt rocks are comparable in bulk density to artificial porous aggregates. Strength grade of the recommended aggregates for heat-insulating backfill is 200; 400; 600, water absorption is 0.5 – 4.0 %, porosity is 3 – 12 %.

Table 1. Results of comparative tests for thermal conductivity of materials for bulk thermal insulation

Material	Density (ρ), kg/m^3	Thermal conductivity coefficient (λ), W/(m°·C)
Expanded clay		
sample No. 1	586	0.142
sample No. 2	590	0.146
sample No. 3	612	0.152
sample No. 4	610	0.150
sample No. 5	578	0.148
Crushed stone-sand mixture from burnt rocks		
sample No. 1	885	0.161
sample No. 2	897	0.170
sample No. 3	923	0.172
sample No. 4	932	0.175
sample No. 5	951	0.181
sample No. 6	664	0.154
sample No. 7	668	0.157
sample No. 8	661	0.152
sample No. 9	670	0.158
sample No. 10	676	0.164

Comparative tests of crushed stone fraction from burnt rocks and expanded clay for thermal conductivity are shown in Table 1. Ash and slag waste and burnt mine rocks can become a raw material base for obtaining expanded granular thermal insulation materials with a density below 300 kg/m^3. Gas generators, cullet and liquid glass are additionally introduced into the composition of the charge for molding granules. Expanded of granules on ash-and-slag waste occurs at a temperature of 860 – 880 °C and on burnt rock occurs at a temperature of 930 – 950 °C, holding at a swelling temperature of 10 minutes. The production of such material takes place according to the principle of thermal shock. With the rapid firing of granules, the processes of gas evolution and melting coincide, and a porous structure is formed. Such material can be used quite widely. Figure 1 shows samples of heat-insulating materials from technogenic raw materials, namely burnt rocks of mine dumps and ash-and-slag materials.

Fig. 1. Laboratory samples of heat-insulating materials from technogenic raw materials

References

[1] Buravchuk N. I., Rutkov K. I. *Processing and Use of Waste from Mining and Combustion of Coal*. Rostov-on-Don: North Caucasian Scientific Center of the Higher School Press, 224, 1997 (In Russian).

[2] Buravchuk N. I., Budnitsky V. M., Brazhnikov V. F., Melent'ev S. A. *Resource Saving in the Technology of Binders and Concretes*. Rostov-on-Don: North Caucasian Scientific Center of the Higher School Press, 176, 1999 (In Russian).

Use of Technogenic Raw Materials in the Technology of Ceramic Materials and Products

N. I. Buravchuk[1]*, O. V. Guryanova[1], E. P. Putri[2]**

[1] I.I. Vorovich Institute of Mathematics, Mechanics and Computer Science, Southern Federal University, Rostov-on-Don, Russia
[2]Department of Industrial Engineering, University of 17 Agustus 1945 Surabaya, Indonesia

*nburavchuk@sfedu.ru, **oguranova@sfedu.ru

Pottery is the oldest of all man-made building materials. The ceramic art of each country reflects the era in which peoples live and create. Ceramic products have an almost unlimited

service life. Such products as wall bricks, ceramic tiles, facade and facing tiles, art ceramics, refractories, etc. are architecturally more expressive and durable in color, texture, shape. Buildings made of ceramic materials are perceived as prestigious, the aesthetic appeal of which persists over time. The exceptional richness of the aesthetic possibilities of ceramics has ensured its wide application in almost all structural elements of buildings and structures, including roofing materials, external and internal cladding, in the chemical and metallurgical industry, namely acid-resistant and refractory materials, in electronics and radio engineering, in art and household products for various purposes. The ceramic industry is developing, creating and filling new niches in a changing environment. The production of ceramic materials is one of the most material-intensive sectors of the national economy. In ceramics technology, an important point is a selection of raw materials, the quality of which directly affects the properties of the finished product [1]. There is a wide range of ceramic products on the building materials market. Products with high consumer properties at a relatively low cost can win the competition. The solution of these two tasks: improving the quality and reducing costs for the production of ceramic products will be facilitated by the use of technogenic raw materials as corrective additives to natural substandard raw materials. In this regard, the use of industrial waste in the technology of ceramic products is of particular relevance. Mine rocks and ash and slag waste are used as corrective additives to regulate the technological properties of low-grade clay raw materials in order to bring it to the required level [2, 3]. The technical and economic interest, that this type of technogenic raw materials arouses, is linked: (i) with the huge reserves of mine rocks and ash and slag waste in all coal-mining regions, (ii) with the aggravated ecological situation near mine waste heaps and ash dumps, (iii) with the search for new mineral raw materials, equal in quality and properties to traditional ones, but more accessible and cheaper. In this work, the possibility of using burnt rocks of mine dumps and ash-and-slag materials in the technology of ceramic products for various purposes was investigated. The object of study of this work was clay raw materials of Russia: loams of the Oktyabrsky and Sukho-Chaltyrsky deposits and refractory clay of the Fedorovsky deposit. Loams are classified as medium-plastic raw materials, and refractory clay is classified as highly plastic raw materials. The preparation of clay raw materials was carried out by dry and wet methods, depending on the products being manufactured. Technogenic raw materials are represented by burnt rocks of the mine dump Petrovsky and ash-and-slag materials of the Novocherkasskaya TRES. Technogenic raw materials are the products of thermal impact on coal-bearing rocks and mineral components of coals. The conditions for the formation of these materials are different. Burnt rocks are formed during prolonged self-burning of coal-bearing rocks, which occurs in waste heaps, namely cone-shaped dumps near coal mines at temperatures of 600 – 1000 °C. According to the lithological composition of the rock mass, the dump of the mine. Petrovsky is clayey. The material composition of the dump is represented by mudstone-siltstone, sandy-clayey, weakly sandy rocks. There are carbonaceous and clayey shales, sandstones. The composition of the clay component is hydromica with an admixture of kaolinite and chlorite. Ash-and-slag waste is a product of coal combustion in boiler furnaces at temperatures above 1000 °C, up to 1700 °C. In terms of chemical, granulometric and phase-mineralogical composition, these wastes are largely identical to natural mineral raw materials. Ash and burnt rocks contain the main groups of substances: crystalline, amorphous and organic. The amorphous component of the ash is represented by the glass phase and amorphous clay substance, that is metakaolinite, amorphous silica and alumina. The preparation of technogenic raw materials included drying to a moisture content of 2 – 3 %, crushing, fractionation to a given granulometric composition. Finely ground burnt rocks and fly ash were also used in the compositions of charges for ceramic products. Finely dispersed materials have been used in batch compositions for tiles and roof tiles. The

compositions of the charge for facing ceramic bricks, ceramic tiles, roof tile, refractory products were developed. The technology for the production of prototypes included the preparation of a charge by mixing the components, molding the samples by a semi-dry or plastic method, drying and firing the samples, testing the physical and mechanical properties. Burnt rocks of mine dumps and ash-and-slag materials in the compositions of ceramic masses were a lean, burn-out additive, a melting and structure-forming element. A clay component was used as a binder. The main advantages of using burnt rocks and ash-and-slag waste in the technology of ceramic masses include the effect of reducing the sensitivity of raw materials to drying, expanding the sintering interval, eliminating the formation of stresses in the structure of the material, increasing the brand strength, frost resistance of finished products, reducing shrinkage and rejects. The efficiency of using burnt rocks and ash-and-slag materials in the manufacture of thin-walled ceramic products is associated with their dispersion. The finely ground fraction of the additive is evenly mixed with the finely dispersed clay and is an effective weakening agent. The binding and sintering part of the mass becomes clay, emaciated by one or another amount of dust-like fraction. If this finely dispersed fraction is sufficient, then the lean clay in drying and firing has moderate volumetric changes that do not lead to a violation of the forming structure of the shard. With a decrease in the amount of a fine fraction, the degree of depletion of the binder clay decreases and the likelihood of the appearance of structural defects and disruption of its continuity increases. Good formability of masses with finely dispersed additives ensures the correct shape and dimensional accuracy of products. This allows them to be used in the manufacture of shaped products, which are subject to stringent requirements in terms of correct shape and dimensional accuracy, as well as increased density. Figure 1 shows samples of pilot batches of ceramic products, in the manufacture of which burned rocks of mine dumps and ash-and-slag materials were used. The use of the investigated technogenic raw materials in the technology of ceramic products provides high indicators of their quality. So, the strength grade can reach values from M200 up to M600, and M300 at bending, frost resistance does not lower than the F300 brand, fire resistance is 1380 – 1670 °C, water absorption is 0.2 – 3.9 %. With the emergence of crushing and screening complexes for processing and preparing rocks for use at mine dumps, construction industry enterprises will have the opportunity to more widely use this raw material in the production of ceramic materials and products. When using technogenic raw materials, it is equally important to reduce the load on the environment during the disposal of solid waste.

Fig. 1. Prototypes of ceramic products from technogenic raw materials

Reference
[1] Augustinic A. I. *Ceramics*. Leningrad: Stroyizdat, 591, 1975 (In Russian).
[2] Rimkevich V. S., Pushkin A. A., Churushova O.V. // *Mining Information and Analytical Bulletin*, **6**, 250, 2015 (In Russian).
[3] Fedorova N. V., Shaforost D. A. // Heat Power Engineering, **1**, 53, 2015, (In Russian).

Modeling of Inhomogeneous Stress in the Embryonic Aorta of Danio Rerio and Study of its Role in the Production of Hematopoietic Stem Cells

D.V. Chalin*, I. Yu. Golushko

Research and Education Center "Materials", Don State Technical University, Rostov-on-Don, Russia

*chalin.d.v@mail.ru

Transplantation of hematopoietic stem cells (HSCs) is a promising technology that can cure such blood diseases as myeloma, lymphoma, leukemia, aplastic anemia, and myelodysplasia. The existing *in vitro* HSC production methods are far from being technologically proficient and are still with dangerous side-effects including the ones associated with transgenes. In the organism, the first HSCs are formed from the endothelial cells of the embryonic aorta via a complex process known as the endothelial-to-hematopoietic transition (EHT). This process was discovered in *Danio rerio* fish in 2010. Today we know that the main wave HSCs production occurs in a similar manner in embryos of all vertebrates. In the dorsal aorta (DA) of the *Danio rerio* embryo, the HSCs production process starts near 24 hours post fertilization (h.p.f.) and ends by 65 h.p.f. During this period, almost 50% of endothelial cells comprising walls of the DA transform into HSCs via EHT. The shape of the aorta undergoes significant changes: in the ventral region between 40 h.p.f. and 55 h.p.f., the initially straight cylindrical vessel with constant radius develops a characteristic pattern of thicker and thinner regions alternating along the axis of the vessel. During the same period, stem cell production rate reaches its peak. In the present work, we investigate the physical mechanisms that govern the shape evolution of *Danio rerio* embryonic aorta during the main wave of HSC production. We develop a coarse-grained DA model within the framework of the theory of elastic membranes. The proposed model also considers the anisotropic interaction with surrounding tissues, blood pressure, as well as inhomogeneous mechanical stress that occurs in the vessel due to the growth and collective migration of cells to the ventral region. Comparing the results of our numerical simulations with obtained micro images of the aorta, we show that the accumulation of mechanical stress in the ventral region leads to an instability, which results in the formation of the periodic pattern that persists throughout the main stage of HSC production. The proposed theoretical approach also suggests how mechanical forces (the considered stress in tissue and hydrostatic blood pressure) can provide different elastic responses in the dorsal and ventral regions of the aorta, and, therefore, lead to an effective difference in mechanical signals that control gene expression and contribute to the production of HSCs.

Acknowledgement. The work is supported by the Russian Science Foundation, grant No. 20-72-00164.

Modeling the Process of Indentation of Thin Composite Coatings

M. I. Chebakov*, S. A. Danilchenko

I. I. Vorovich Institute of Mathematics, Mechanics and Computer Sciences, Southern Federal University, Rostov-on-Don, Russia

*michebakov@yandex.ru

Modern surface engineering includes the processes of modifying the surface of products by applying various coatings. Typically, these surface structures are thin or ultra-thin. In this regard, the problem arises of determining their physical and mechanical properties. One of the methods widely used in the study of thin coatings and films is the indentation method. It consists in simultaneous measurement of indentation force and displacement of a specially shaped indenter to build a "load-unload" curve. The analysis of such a curve allows one to determine hardness, modulus of elasticity, creep, and other parameters. However, experimental determination of some characteristics, such as the yield strength, for such structures is quite time-consuming and sometimes impossible. In the present work, an attempt is made to quantify the yield strength of thin composite coatings by comparing the finite element model of indentation and experimental data. The simulation was carried out using the ANSYS software package. A planar axisymmetric problem for a homogeneous layer was considered. A cone with special parameters of cone angle and rounding angle at the apex was used as an indenter. Such an indenter has the same area and depth projection function as a standard Berkovich indenter. The resulting model allows plotting "load-unload" curves similar to the experimental ones. The coating material was a composite with a matrix based on Phenylon C-2 with various fillers. For each coating, an experiment was performed on a NanoTest 600 complex (Micro Materials Limited, UK). The obtained elastic characteristics of the composites were used as input parameters in the calculations. The initial value of the yield strength was taken as to 1/3 of the hardness value. Based on the comparison of the load-unload curves, the yield strength value was optimized in order to obtain the maximum coincidence of the curves. The simulation results showed that by adjusting the yield strength value, it is possible to achieve a good agreement between the simulation and experimental results.

Acknowledgment. Research was financially supported by the Southern Federal University, grant No. VnGr-07/2020-04-IM (Ministry of Science and Higher Education of the Russian Federation).

Contact Problem on the Interaction of a Stamp in the Form of a Rotation Paraboloid and a Poroelastic Layer Fixed on an Elastic Half-Space

M. I. Chebakov*, E. M. Kolosova**

I. I. Vorovich Institute of Mathematics, Mechanics and Computer Sciences, Southern Federal University, Rostov-on-Don, Russia

*michebakov@yandex.ru, **a_lena_ch@mail.ru

Porous materials are a sufficiently new class of materials with unique physical, mechanical,

acoustic, electrical and thermal properties. It is widely used in the space industry due to the optimal balance of weight and strength. The most important issue in the production of such materials is the control and assessment of their mechanical characteristics. There are various approaches to the study of such problems. One approach to modeling porous materials was developed by Cowin-Nunziato. This theory, called the theory of microdilation, was applied to the study of porous bodies with empty (unsaturated) pores. It uses linear elasticity theory with an additional kinematic variable that describes the properties of porosity change. Thus, deformation and porosity are related fields that have a common response to external loads applied to the body. In this report on the basis of the equations of the theory of poroelastic bodies by Cowin-Nunziato, the contact problem of the penetration of a rigid punch in the form of a rotation paraboloid into a poroelastic layer, fixed on an elastic half-space is considered. It is assumed that there is no friction in the contact zone. Using the Hankel integral transform, the problem is reduced to solving an integral equation for an unknown contact stress. The collocation method is used to solve the integral equation. The contact area and the values of contact stresses are found, and the deformation of the surface outside the punch is investigated. The relationship between the force, acting on the stamp, and its displacement is also investigated. A comparative analysis of the investigated quantities for various values of the poroelastic layer parameters and the elastic foundation is carried out. Numerical results are presented in the form of tables and plots.

Acknowledgement. The work is financially supported by the Southern Federal University, project No. VnGr-07/2020-04-IM (Ministry of Science and Higher Education of the Russian Federation).

Effect of High-Temperature Annealing on the Morphology of the FIB-Modified GaAs Surface

N. E. Chernenko*, D. V. Kirichenko, N. A. Shandyba, S. V. Balakirev, M. M. Eremenko, M. S. Solodovnik

Institute of Nanotechnologies, Electronics and Equipment Engineering, Southern Federal University, Taganrog, 347928, Russia

*nchernenko@sfedu.ru

Controlling the position, size, and shape of quantum dots, both single and in an array, is an urgent task for creating a promising element base for quantum communications (sources of single and entangled photons) and quantum computing (quantum registers based on quantum dots). One of the promising ways to control the self-organization processes is the pre-growth surface nanopatterning. In this paper we study effect of a combination of focused ion-beam (FIB) treatment modes of a GaAs surface and subsequent ultra-high vacuum annealing on the nanoholes formation on the FIB-modified GaAs surfaces. The FIB treatment of the GaAs surface was carried out using a NovaNanoLab 600 scanning electron microscope (SEM) equipped with an FIB system with a Ga^+ ion source. Then, the samples were annealed in the growth chamber of molecular beam epitaxy (MBE) system SemiTEq STE 35. The resulting samples were studied by SEM, AFM, and the Kelvin probe method (KP-AFM). The results of the studies showed that after annealing, nanoholes begin to form at the points of FIB-exposure. Nanohole's size, shape and faceting are determined by the number of beam passes (dose). The dependence of the nanohole size is nonmonotonic. Initially (up to 20 passes) both the diameter

and depth increase from 197 to 361 and from 75 to 160 nm, respectively. Then (starting from 40 passes) they decrease to 197 and 85 nm, respectively. The coefficient of asymmetry of the structures (the ratio of the lateral sizes in the [010] and [001] crystallographic directions) remains at the level of 0.9 over the entire range. One of the most important results of the work is that, as the dose increases, the shape of the nanoholes changes from a regular 4-sided prismatic, faceted (111) planes, to a regular rectangular, faceted by complex, which includes eight facets: four (111) and four (110) facets. In this case, the dispersion of characteristics also decreases. This opens broad prospects for using this method to obtain regular arrays of symmetric quantum dots.

Acknowledgements. The study was supported by Russian Science Foundation Grant No. 21-79-00310 at the Southern Federal University.

Construction of Algorithmization of the Problems for Identification of Objects in the Image

A. V. Cherpakov[1,2], N. Yu. Baturina[2], I. A. Parinov[1]

[1]Southern Federal University, Rostov-on-Don, Russia
[2]Don State Technical University, Rostov-on-Don, Russia

*alex837@yandex.ru

With arising the digital technologies in the field of digital image processing, analytical methods of image matching began to be used to restore the contours of three-dimensional objects. The image of an object is represented as a three-dimensional display array of the color palette and the coordinate area. The object has some points in the image with known coordinates, that have peak color values. Using simple enumeration algorithms, as well as elements of linear interpolation in the selected range in a certain area of image points, a set of points corresponding to extreme values is searched. Knowing these data, it is possible to solve the optimization problem. For this, it will be necessary to find the minimum of the error function by varying the object's center of mass matrix T and the object's rotation matrix R to find the boundaries of the object's shape. To analyze the classification of an object, a database of information features can be built. The basis of the base is a set of qualitative integral indicators that allow, by a minimum set of five characteristic features, to determine or classify the type of an object. Neural networks can be used as a tool for classifying an object in an image.

Acknowledgement. This research was funded by the grant from the Ministry of Science and Higher Education of Russia supported by the Southern Federal University, grant No. VnGr-07/2020-04-IM.

Design of the Elements of Vibration Diagnostics System

A. V. Cherpakov [1,2], K. G. Bukhanevich [1], V. E. Yakovlev[2], M.-Y. Yeh[3], C.-D Yang[3]

[1]Don State Technical University, Rostov-on-Don, Russia
[2]Southern Federal University, Rostov-on-Don, Russia
[3]Department of Microelectronics Engineering, National Kaohsiung University of Science and Technology, Kaohsiung, Taiwan (R.O.C.)

*alex837@yandex.ru

Vibration diagnostics is a method of diagnosing an object based on the analysis of vibration parameters generated by operating equipment or being a secondary vibration due to the structure of the object under study. The task of vibration diagnostics is troubleshooting and assessing the technical condition of the object under study. Vibration analysis implies the study of the functional dependence of the measured vibration parameters on time, frequency, spatial coordinates and serial number in a group of independent vibration measurements. Analysis in the time domain, together with analysis in the frequency domain (spectral vibration analysis, etc.) is the main analytical tool for vibration diagnostics. Vibration diagnostics examines the following parameters: (i) vibration velocity is the speed of movement of a point or system under the action of vibration; (ii) vibration displacement is the displacement of a point or system under the action of vibration; (iii) vibration acceleration is the acceleration of the movement of a point or system under the action of vibration.

Vibration diagnostics can be used as an element. Emergency protection systems are designed to automatically shut down equipment at the initial stage of an emergency. Their use allows minimizing the consequences of the accident and the volume of restoration work. Vibration in buildings and structures, in addition to the negative impact on human health, can have a serious impact on the condition of load-bearing and enclosing structures. Objects operated under conditions of vibration exposure undergo increased wear, which significantly reduces the service life of structures. In such cases, constant monitoring of the state of structural units and elements is required. As a hardware platform for vibration diagnostics, the choice consists of three microcontroller platforms: Arduino, ESP32 and STM32. Vibration analysis can be performed in 2 ways. The first is to use the NUCLEO-H743ZI2 debug board to take vibration measurements and perform analysis. In this case, it is necessary to connect a display to the board, and part of the processor time will be occupied by calculations and displaying the result, which will slightly reduce the accuracy of measurements, as the frequency of polling sensors will decrease. Send the second readings of the sensors to another device, on which vibration analysis will be performed. Communication can be organized in the following ways: (i) using built-in USB OTG FS micro-AB and data transfer via virtual COM port; (ii) using the built-in Ethernet RJ45 connector; (iii) connecting an esp8266 module or ESP32 series board for Wi-Fi transmission;(iv) connecting a radio module according to the nRF24L01 type. When comparing options, two favorites stand out. When using USB, the issue of supplying electricity is immediately closed and in the cases of wireless communication, a carrier of electricity is needed. Transmission via Wi-Fi, although it has a smaller radius and higher power consumption than that of radio modules, it compensates for the transfer rate of 150 Mb/s versus 2 Mb/s.

Acknowledgement. This research was funded by the grant from the Ministry of Science and Higher Education of Russia supported by Southern Federal University, grant No. VnGr-07/2020-04-IM.

Carrying out a Simulation of an Axial-type Piezoelectric Power Generator with an Active Base

A. V. Cherpakov[1,2]*, I. A. Parinov[1], R. K. Haldkar[1]

[1]*Southern Federal University, Rostov-on-Don, Russia*
[2]*Don State Technical University, Rostov-on-Don, Russia*

*alex837@yandex.ru

Within the framework of scientific research, a finite element model was developed using the ANSYS software. Experimental testing of a piezoelectric generator (PEG) with a proof mass and an active base was carried out. The active base is made in the form of cylindrical piezoelectric elements, located in the place, where the generator plate is fixed parallel to the generator axis. The axial piezoelectric transducer for converting mechanical energy into electrical energy contains a base plate in the form of a rigid beam structure made of an elastic material, on which piezoelectric bimorph elements are glued. One end of the beam structure is bolted to the base using fixing supports. From the other end, at the base, piezoelectric elements of a cylindrical type are fixed coaxially with the base bar through the L-shaped bar. An additional attached mass is located between the edge of the base, fixed with a bolt, and the piezoelectric elements. The paper [1] presents the results of modal and harmonic analysis of vibrations. In this case, energy generation in cylindrical piezoelectric elements occurred due to the transfer of compression forces to the piezoelectric element at the base of the PEG during excitation of structural vibrations. A technique for experimental analysis of vibrations is described, and a laboratory setup has been developed, which made it possible to obtain experimental results of the output characteristics of a piezoelectric generator under low-frequency loading, which differ from the finite element results within 5%.

Acknowledgement. The work was supported by the grant No. 21-19-00423 of the Russian Science Foundation in the Southern Federal University.

[1] Cherpakov A. V., Parinov I. A., Haldkar R. K. Parametric and Experimental Modeling of Axial-Type Piezoelectric Energy Generator with Active Base // *Applied Sciences*, **12**(3), 1700, 2022.

Algorithmization of the Process of Analyzing Vibration Signals in the Case of Multi-parameter Identification of the Properties of Linearly Extended Structures

A. V. Cherpakov[1,2]*, V. E. Yakovlev[2], Khamis Modar[1], J.-P. Wang[3]

[1]*Don State Technical University, Rostov-on-Don, Russia*
[2]*Southern Federal University, Rostov-on-Don, Russia*
[3]*Department of Naval Architecture Engineering, National Kaohsiung University of Science and Technology, Kaohsiung, Taiwan (R.O.C.)*

*alex837@yandex.ru

The use of means for identifying defective (ID) zones of linearly extended objects can be considered together with design elements of algorithms for multi-parameter identification of

properties (MIP). Various sections in a linear type bar structure may have prestressing elements. The proposed method of MIP and ID, based on the analysis of the shapes of various vibration modes (mode shape-based damage detection, MSBDD), is used in conjunction with the preliminary preparation of neural networks based on modeling in the ANSYS FE software and the use of boundary problems describing the longitudinal and transverse vibrations of the rod based on analytical models in the Matlab software [2]. The use of neural networks makes it possible to prepare in advance a static model for restoring the initial feature field based on the analysis of the collected data on the vibration parameters of the bar structure. Additional information for solving the problem of defect reconstruction is a set of natural frequencies and vibration modes of the structure under study. The refinement of the solution can be based on the use of analytical models in solving inverse coefficient problems, describing the propagation of waves in an inhomogeneous elastic body. At the same time, the analysis of vibration modes allows solving the problem at the first stage, after which an analytical or finite element model of a structure with defects is built, and the problem at the second stage is solved using direct calculations. The novelty of the algorithm lies in the fact that the ID procedure is divided into the following stages: (i) a preliminary model is assembled in the calculation software, variational parameters are determined in the form of deviations of certain values that determine the cross-section and properties in it; (ii) oscillations are simulated at determined impacts and data collection in the diagnosed locations of the structure; (iii) the construction of a neural network depending on the given values; (iv) the location of the defect is determined, and (v) the degree of damage is stated. These diagnostic elements are tested on analytical models.

Acknowledgement. The study was supported by the Russian Science Foundation grant No. 22-29-01259, https://rscf.ru/project/22-29-01259/.

References

[1] Soloviev A. N., Parinov I. A., Cherpakov A. V., Esipov Y. V. Experimental vibration diagnostics of the floor plate set of building construction. In: *Proceedings of the 2nd Annual International Conference on Material, Machines and Methods for Sustainable Development (MMMS2020)*, Lecture Notes in Mechanical Engineering, Banh Tien Long, Yun-Hae Kim, Kozo Ishizaki, Nguyen Duc Toan, Ivan A. Parinov, Ngoc Pi Vu., Springer Nature, Cham, Switzerland, 255 – 260, 2021.

[2] Cherpakov A. V., Soloviev A. N., Gricenko V. V., Goncharov O. U. Damages identification in the cantilever-based on the parameters of the natural oscillations // *Defense Science Journal*, **66**(1), 44 – 50, 2016.

DM-MIMO Based GFDM Advanced Underwater Image Transmission Scheme

Chin-Feng Lin[1]*, Yu-Chi Wei[1], Chai-Sheng Wen[1], Chan-Chung Wen[2], Shun-Hsyung Chang[3], Ivan A. Parinov[4], Sergey Shevtsov[5]

[1]*Department of Electrical Engineering, National Taiwan Ocean University, Taiwan, ROC*
[2]*Deaprtment of Shipping Technology, National Kaohsiung University of Science and Technology, Taiwan, ROC*
[3]*Deaprtment of Microelectronic Engineering, National Kaohsiung University of Science and Technology, Taiwan, ROC*
[4]*I. I. Vorovich Mathematics, Mechanics, and Computer Science Institute, Southern Federal University, Russia*
[5]*Head of Aircraft Systems and Technologies Lab at the South Center of Russian Academy of Science, Russia*

*lcf1024@mail.ntou.edu.tw

In the report, a 2×2 direct mapping (DM) multi-input multi-output (MIMO) based generalized frequency division multiplexing (GFDM)-low density parity check (LDPC) code underwater image transmission scheme (UITS) is proposed. The adaptive 4 *quadrature amplitude modulation*s (QAM) and 16 QAM modulations, are integrated into the proposed UITS (see Fig. 1). The performances of bit error rates (BERs) and peak signal-to-noise ratios (PSNRs) of the proposed UITS with perfect channel estimation (PCE) (0%) are explored. From these simulation results, we evaluate the performances of the proposed advanced UITS with a PCE (see Fig. 2).

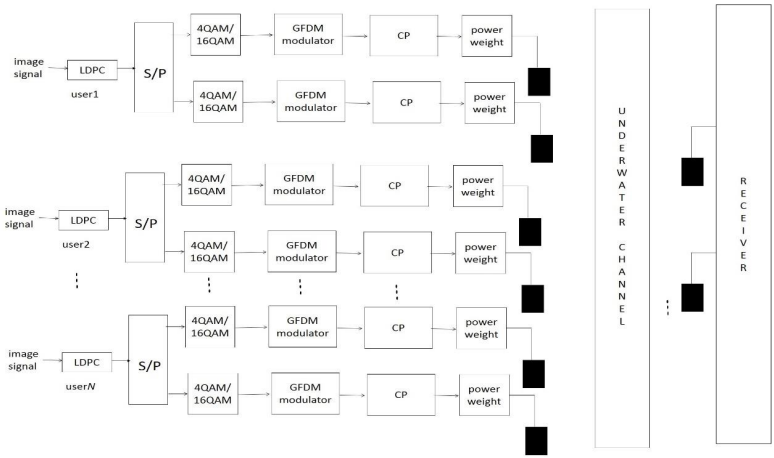

Fig. 1. Proposed DM MIMO based GFDM-LDPC advanced UITS

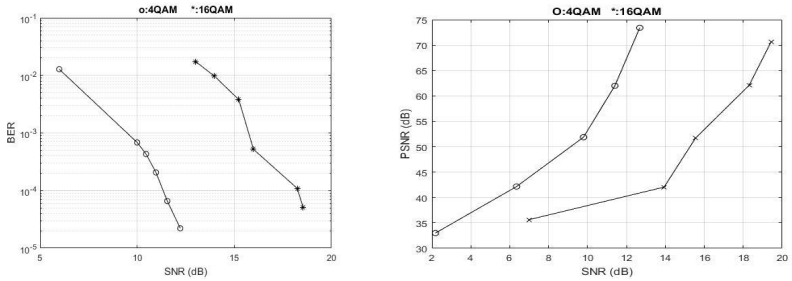

Fig. 2. (a) BER performance and (b) PSNR performance of the DM-MIMO GFDM-LDPC UITS with PCE

Acknowledgement. The authors acknowledge the support of the grant from The Ministry of Science and Technology of Taiwan, under contract No. MOST 109-2221-E-992-091.

Using Convolutional Neural Networks to Recognize Randomly Generated Images and Visualize the Results

Chin-Shiuh Shieh[1]*, Chin-Dar Tseng[1,2], Chen-Lin Kang[3]*****, Hsuan-Chih Hsu[3]******, Liyun Chang[4]*******, Chin-Hsueh Lin[1]***, Yu-Jie Huang[5]********, Tsair-Fwu Lee [1,2,6] ******

[1]Department of Electronics Engineering, National Kaohsiung University of Science and Technology, Kaohsiung, Taiwan, R.O.C.
[2]Medical Physics and Informatics Laboratory of Electronics Engineering, National Kaohsiung University of Science and Technology, Kaohsiung, Taiwan, R.O.C.
[3]Department of Hematology and Oncology, Kaohsiung Chang Gung Memorial Hospital and Chang Gung University College of Medicine, Kaohsiung, 83342, Taiwan, R.O.C.
[4]Departments of Medical Imaging and Radiological Sciences, I-Shou University, Kaohsiung 82445, Taiwan, R.O.C.
[5]Department of Radiation Oncology, Kaohsiung Chang Gung Memorial Hospital and Chang Gung University College of Medicine, Kaohsiung 83342, Taiwan, ROC
[6]Ph.D. program in Biomedical Engineering, Kaohsiung Medical University, Kaohsiung 80708, Taiwan, ROC

*csshieh@gmail.com; **1102405111@gm.kuas.edu.tw; ***cslin@nkust.edu.tw; ****tflee@nkust.edu.tw; *****k1074.kang@gmail.com; ******hsuan5@cgmh.org.tw; *******liyunc@isu.edu.tw; ********yujie1115@gmail.com

The Convolutional Neural Network (CNN) is a neural network architecture of a mapping function. Recently, it has shone in the fields of face recognition, image classification, and autonomous driving. Randomly generated bar pictures of different colors and different lengths are used for classification. The images are divided into number 1 (No. 1) and number 2 (No. 2), each with 1000 sheets. The number of bars in graph No. 1 is 1. The number of bars in graph

No. 2 is 2. This research is concerned with the numbers of bars in the graph. CNN is used to recognize randomly generated images and visualize the results. The research flowchart is shown in Fig. 1. After model training is completed, different epochs produce different accuracy and loss. The accuracy of training and testing is close to 100% when the epoch is 5. In addition, the loss in epochs is 5.0%. This result shows that the model is effective for the classification of this type of images. A 2 × 2 pooling operation can reduce the size of the original image to 25% without affecting the object. Through pooling, we reduced the number of image features to 25% and retained the original information. The extraction of the upper layer of the classification is shown in Fig. 2.

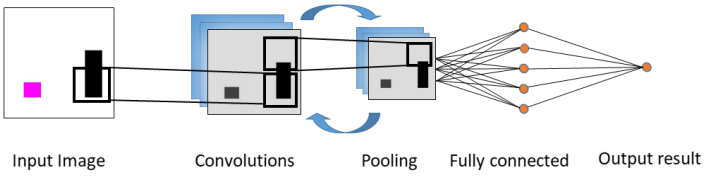

Fig. 1. CNN image classification flowchart。

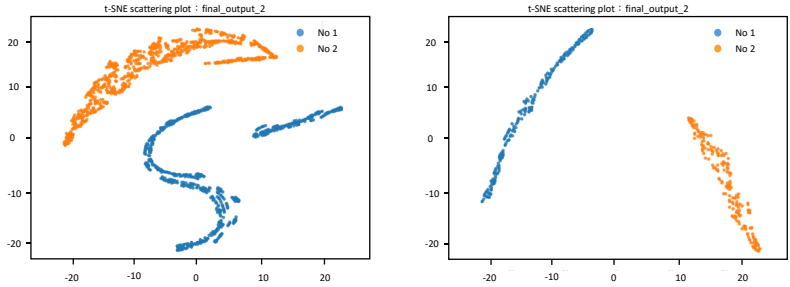

(a) (b)

Fig. 2. Extraction of the upper layer of the classification: (a) train, (b) test

The most obvious benefit of this is that it can reduce the number of pixels and calculations that the neural network needs to process, and increase the training speed of the model. In future research, the results of the CNN classification model pre-trained by others will be used for feature extraction of the picture. In more in-depth research in the future, for example, the texture, direction, and style of graphics can be changed.

Expertise of Prestressed Floor Slabs

Daniil V. Bezhanov

Don State Technical University, Rostov-on-Don, Russia

daniilbezanov345@gmail.com

Reinforced concrete, compared to other building materials, appeared relatively recently and

almost simultaneously in Europe and America and is widely used in construction. Ceilings of prestressed slabs are used in high-rise construction to build apartment houses, industrial buildings, etc., with a span length from 8 to 13 m. The practicability of their use is conditioned by the insufficient loading ability and the length of the span of slabs with unstressed reinforcement. The slabs can be up to 3 m wide and from 80 to 120 mm thick. Technical inspection of the slabs gives full information on the state of design and existing defects. Timely examination of the floor slab can prevent it from collapse. Modern ultrasonic devices are used for the examination to measure the parameters of the cracks that have occurred. Concrete strength can be quickly measured with impact pulse, elastic rebound, and shear rebound instruments. Concrete strength testing of reinforced concrete structures is an integral part of slab testing. Increased operating loads require additional calculations, analytical studies with subsequent reinforcement. The final document of the experts' work contains a description of all the defects identified during the examination, the nature of the destructive processes is explained, the forecast of the situation is built, the allowable loads are calculated. Early diagnosis of defects allows one to detect design flaws or errors in the device technology in time. Inspection of floors before the reconstruction or repair gives the opportunity to objectively assess the current technical condition of the structures. Based on the results of the inspection, a design decision is made to repair or completely replace the floor slabs.

Features of the Structure and Physical Properties of Composite-like Ceramics Based on Sodium Potassium Niobate

A. O. Denisova[1,2], Yu. V. Kabirov[1], S. E. Filippov[3], A. G. Rudskaya[1]*

[1]Department of Physics, Southern Federal University, 344090, Rostov-on-Don, Russia
[2]I. I. Vorovich Institute of Mathematics, Mechanics and Computer Science, Southern Federal University, 344090, Rostov-on-Don, Russia
[3]Scientific Design and Technological Bureau «Piezopribor» (NCTB «Piezopribor»)

*agrudskaya@sfedu.ru

In recent years, there has been an active search for environmentally friendly lead-free ceramics that can compete with the well-known, widespread and highly demanded ceramics based on lead zirconate-titanate (PZT). One of the currently popular lead-free ceramic compositions is potassium-sodium niobate $K_{1-x}Na_xNbO_3$ (KNN) ceramic. KNN solid solutions have become a significant representative of lead-free piezoelectric materials with environmentally friendly properties, good piezoelectric performance and high Curie temperature. In our study, the multicomponent composition $0.965(K_{0.48}Na_{0.52})(Nb_{0.96}Sb_{0.04})O_3 - 0.035(Bi_{0.5}Na_{0.5})(Zr_{0.85}Hf_{0.15})O_3$ (KNNS-BNZH) is considered. KNNS-BNZH piezoelectric ceramics are manufactured using the conventional solid phase reaction method. According to the chemical formula, Bi_2O_3, Nb_2O_5, Sb_2O_3, ZrO_2, HfO_2 oxides, Na_2CO_3 and K_2CO_3 carbonates were used for the preparation of these ceramics, with a chemical purity of more than 99 %. To obtain a homogeneous mixture, the reagents were mixed in a mortar with the addition of alcohol for 1 hour. Then the dried mixture was pressed into disks of 10 mm in diameter and 1.5 mm height under a pressure of 2 – 3 MPa. The KNNS-BNZH composition was synthesized for 6 hours at a temperature of 1123 K. Next, the sample was subjected to repressing and the repeated synthesis at a temperature of 1343 K for 6 hours. Using the XRD

method, the structure and phase composition of the synthesized samples were refined. By selecting various additives, it was possible to increase the size of the coherent scattering regions of the studied composition. The following additives were used: tungsten oxide WO_3, quartz SiO_2, germanium oxide GeO_2, zinc oxide ZnO, potassium carbonate $BaCO_3$, nickel nitrate $NiNO_3$. The presence of the additional phases, in addition to KNNS-BNZH, with the perovskite structure, demonstrates the composite nature of our compositions. Similarities of structural types and behaviour of the structures in the presence of the external influences (electric fields, pressure) suggest that lead-free ceramics have a high potential for improvement. The samples, due to glass-forming additives in the concentrations of 1 – 2 mass %, have good ceramic qualities, namely hardness and density. Moreover, when developing new composite-like compositions based on KNN, we used the concept of non-ergodicity of the materials exhibiting interesting properties in the low-symmetry phases [2]. In contrast to [3], our preliminary studies have shown that the values of the thick piezoelectric modulus d_{33} in the synthesized compositions are about 30 pC/N, and the value of the Curie temperature is about 673 K.

Acknowledgement. Research was financially supported by the Southern Federal University, grant No. VnGr-07/2020-04-IM (Ministry of Science and Higher Education of the Russian Federation).

Reference

[1] Takenaka T., Maruyama K.-I., Sakata K. // *Japanese Journal of Applied Physics.* **30**, 2236, 1991.

[2] A.Yu Zakharov. Theoretical foundations of physical materials science. Statistical thermodynamics of model systems. 2016. 256 p.

[3] L. Qiao. G.Li, H. Tao et. al., *Ceram. Internat*. **46**, 5641 (2020).

Features of the Electronic Structure of Some MeOx/MWCNTs

V. O. Dmitriev*, M. Khalil, A. P. Budnik, E. S. Bogoslavskaya, V. A. Shmatko, G. E. Yalovega

Faculty of Physics, Southern Federal University, Rostov-on-Don, Russia

*vdmitriev@sfedu.ru

The study of the electronic structure of composites based on carbon nanotubes and transition metal oxides is important since they can provide unique physical and chemical properties that make them suitable for many applications, including catalysts, sensors, and supercapacitors. The aim of this work was to study the electronic structure of nanocomposite materials based on transition metal oxides (Cu, Ni) and multi-walled carbon nanotubes (MWCNTs) by XANES spectroscopy and optical spectroscopy in the UV and visible range. The X-ray absorption spectra of CuOx/MWCNTs have features associated with the interaction of CuOx with nanotubes and also changes in the local structure. Because of formation CuOx/CNT nanocomposite, the change in oxidation state and phase composition of CuOx nanoparticles were observed. In contrast to pure nanoparticle, significant increase of CuO phase and reduction of Cu_2O phase were observed [1]. The X-ray absorption data indicate the formation of new chemical bonds in the carbon nanotubes in the result of NiOx/MWCNTs nanocomposite formation, associated with chemical interaction between the NiOx and the nanotubes. The analysis of the Ni K-edge XANES spectrum showed that chemical state of Ni

in the composite compound is 2+ and there is Ni with different oxygen surroundings in the composite [2]. The optical absorption spectra of the studied samples were measured. The spectral profile of different samples was compared. It was found that the functionalization of MWCNTs by transition metal oxide nanoparticles has a weak effect on the absorption spectrum profiles. At the same time, the introduction of metal oxide nanoparticles can lead to a modification of the surface of the nanotubes, which, in turn, leads to a change in the band gap energy.

References

[1] Shmatko V., Yalovega G., Barbashova A., Kuriganova A., Bogoslavskaya E., Smirnova N. // *Key Engineering Materials*. **683**, 215 – 220, 2016.

[2] Shmatko V., Leontyeva D., Nevzorova N., Smirnova N., Brzhezinskaya M., Yalovega G. // *Journal of Electron Spectroscopy and Related Phenomena*. **220**, 76 – 80, 2017.

Production of Vanadium Dioxide Thin Films by Pulsed Laser Deposition

V.G. Dneprovski*, E.M. Kaidashev

Laboratory of Nanomaterials, I. I. Vorovich Mathematics, Mechanics and Computer Science Institute, Southern Federal University, Rostov-on-Don, Russia

*valdnepr@ya.ru

This report is devoted to a review and analysis of works aimed at obtaining thin films of vanadium dioxide by pulsed laser deposition. In this year, a large review of studies on the preparation, properties, and application of nanostructures and films of vanadium dioxide was published [1]. However, very little attention is paid to the laser deposition there, despite the fact, that the use of this method makes it possible to obtain sufficiently high-quality films of vanadium dioxide. Therefore, we consider, just, this method. The sharp changes in the structural, electrical, and optical properties accompanying the phase transition of vanadium dioxide (VO_2) make it a promising material for the wide range of thin film applications in electronics, photonics, and plasmonics. Vanadium dioxide (VO_2) undergoes the metal-insulator transition (MIT) at 68 °C, after which its conductivity changes by several orders of magnitude. In this case, a second-order phase transition occurs in VO_2 from the low-temperature monoclinic dielectric phase to the high-temperature octahedral metallic phase (rutile). This transition can be caused thermally, mechanically, electrically, or optically. The MIT transition occurs especially quickly ($\Delta t < 100$ fs) at the optical exposure. MIT in VO_2 has been used in particular for various microwave/terahertz applications (i.e. tunable filters and modulators), steep tilt transistors, antennas, photoelectronic devices, sensors, and opens a door to the development of the next generation of memory devices. Thin VO_2 films withstand a significantly higher number of switching cycles than the single crystal samples. In this work, we consider the parameters of pulsed laser deposition of vanadium dioxide, which lasers and substrates are used, and the main properties of condensed thin films. In particular, KrF pulsed excimer laser with wavelength $\lambda = 248$ nm, pulse width of 25 ns, and repetition rate ranging from 3 Hz up to 25 Hz [2], Ti: sapphire laser (central wavelength of 800 nm), Nd: glass laser ($\lambda = 527$ nm, $\tau = 250$ fs) and TiO_2, glass, Si/SiO_2, sapphire (0001), r-sapphire, silicon (100) substrates etc. were used. The targets for deposition, for example, were the metal vanadium, pressed powder of V_2O_5, V_2O_3 or VO_2. The deposition was usually carried out in the oxygen atmosphere.

Acknowledgements. This work was financially supported by the Internal Grant of Southern Federal University VnGr-07/2020-06-MM.

Reference

[1] Zhang Y., Xiong W., Chen W., Zheng Y. // *Nanomaterials*, **11**(338), 1 – 48, 2021.
[2] Hamaoui G., Horny N., Gomez-Heredia, C. L. et al. // *Scientific Reports*, **9**(8728), 2019. https://doi.org/10.1038/s41598-019-45436-0

Features of Processing Information from Surface Acoustic Wave Sensor

V. G. Dneprovski, G. Ya. Karapetian*, I. A. Parinov

I. I. Vorovich Mathematics, Mechanics and Computer Science Institute, Southern Federal University, Rostov-on-Don, Russia

*jorichkaka@yandex.ru

Surface acoustic wave (SAW) sensors are increasingly used in the automated systems for remote wireless monitoring of the physical parameters of various structures, vehicles and other objects. This is due to their reliability, miniature size, high manufacturability, temperature stability, relatively low cost and the ability to work in the passive wireless mode [1, 2]. When the passive wireless SAW sensors are using, the single frequency reader is used to detect acoustic fields based on a membrane capacitor. The main element of the sensor is the SAW delay line, which includes the receiving and reflective interdigital transducers (IDTs). The reflective IDT is loaded on an impedance (in our case, the membrane capacitor), the value of which depends on the measured physical magnitude, in particular, on the parameters of low-frequency oscillations. Under the influence of the acoustic field, the sensor membrane begins to vibrate, which leads to a change in its capacitance, and, consequently, to a change in the SAW reflection coefficient from the IDT, to which the membrane capacitor is connected. This leads to a change in the time of the parameter S11 of the sensor antenna, as well as to a change in the parameter S11 of the reader, which receives the signal from the sensor antenna. Then the amplitude of the signal, received by the reader, begins to change in accordance with the change in acoustic fields, that act on the membrane capacitor. For example, if the sound wave is monochromatic, then the on output of the reader will be a sine wave. Using the calibrated sound source, we can create a calibration curve from which we can determine the amplitude of the signal acting on the membrane capacitor. With such reader, to process information from the sensor, Fourier transform programs of the received signal are used, which makes it possible to determine the frequencies of the harmonic components of the received acoustic signal, as well as their amplitudes. The algorithms have also been developed that make it possible to determine the distance between the sensor and the reader by the amplitude of the received signal, using data from the reference channel and calibration curves, which are taken at the different distances between them. The reader operating at the one frequency makes it possible to simplify the mathematical processing of the signal as much as possible, since at its output a signal is obtained, that corresponds to the emitted signal.

Acknowledgements. This work was financially supported by the Grant No. 19-08-00365 of the Russian Foundation for Basic Research and the Internal Grant of Southern Federal University VnGr-07/2020-06-MM.

Reference
[1] Bagdasaryan A. S., Bagdasarian S. A. // *Electronics (Science, Technology, Business)*. **2**(00142), 96 – 102, 2015.
[2] Dneprovski V. G., Karapetyan G. Y., Parinov I. A. *Surface Acoustic Wave Devices*. Nova Science Publishers, New York, 178, 2016.

Applications of Fractional Calculus to Fluid Motion Problems

Yu. E. Drobotov

Southern Federal University, Rostov-on-Don, Russia

yu.e.drobotov@yandex.ru

The motion of viscous fluid substances is described by the Navier-Stokes equations carried out from the equation of continuum dynamics and the incompressibility equation considered in the case of isothermal motion. In the research presented, the stream function approach is applied to a plane problem, previously used, for example, in studies [1, 2] in the context of a problem on a fluid motion in a channel of constant width. Let v_x, v_y denote the velocities of the liquid's particles and ν stand for kinematic viscosity. After certain transformations, the Navier-Stokes equations can be reduced to the equation:

$$\frac{\partial}{\partial t}\Delta\psi+\frac{\partial\psi}{\partial y}\frac{\partial}{\partial x}\Delta\psi-\frac{\partial\psi}{\partial x}\frac{\partial}{\partial y}\Delta\psi-\nu\Delta\Delta\psi=0, \qquad (1)$$

where the stream function ψ is introduced with the relations:

$$v_x=\frac{\partial\psi}{\partial y},\quad v_y=-\frac{\partial\psi}{\partial x}.$$

This report provides a solution to equation (1) carried out by applying specific properties of the Riesz potentials. On the other hand, hypersingular integrals are known to provide an extension of partial differential operators, since any homogeneous partial differential operator with constant coefficients may be represented as a hypersingular-type operator [3, p. 505]. Together with potential-type operators, they form the Riesz fractional integrodifferentiation terminology that is used here to investigate the solutions of (1) and their properties.

Acknowledgement. The research was financially supported by Southern Federal University, grant No. VnGr/2020-04-IM (Ministry of Science and Higher Education of the Russian Federation).

References

[1] Sumbatyan M. A., Abramov V. V. // *Izvestiya Vuzov. Severo-Kavkazskii Region. Natural Science*. 2014. *No. 1*, 42–46.
[2] Sumbatyan M. A., Piskunov A. S. // *Izvestiya Vuzov. Severo-Kavkazskii Region. Natural Science*. 2018. *No. 1*, 43–48.
[3] Samko S. G., Kilbas A. A., Marichev O. I. *Fractional Integrals and Derivatives. Theory and Applications.* Gordon and Breach Science Publishers, 1993.

Integral Equations with Semi-Axial Riesz Potential in Grand Lebesgue Spaces

Yu. E. Drobotov

Southern Federal University, Rostov-on-Don, Russia

yu.e.drobotov@yandex.ru

The Riesz potential on the half-axis defined as the integral operator:

$$I_0^\alpha f = \frac{1}{2\Gamma(\alpha)\cos(\alpha\pi/2)}\int_0^\infty \frac{f(t)}{|t-x|^{1-\alpha}}\,dt, \quad x>0,$$

is known as the most important operators in fractional calculus, arising as an analogy with those known from mathematical physics [1, p. 213]. Due to the equation [1, p. 221]:

$$I_0^\alpha = \left[2\cos(\alpha\pi/2)\right]^{-1}\left(I_{0+}^\alpha + I_-^\alpha\right),$$

it is related to the right-sided Liouville fractional integral I_-^α as

$$I_{0+}^\alpha f(x) = \frac{1}{\Gamma(\alpha)}\int_0^x \frac{f(t)}{(x-t)^{1-\alpha}}\,dt, \quad I_-^\alpha f(x) = \frac{1}{\Gamma(\alpha)}\int_x^\infty \frac{f(t)}{(t-x)^{1-\alpha}}\,dt, \quad 0<x<\infty,$$

that appear to deliver the realization of an integral on a fractal [2, p. 25]. In this report, a generalization of I_0^α is considered in the form of the integral operator:

$$J_0^\alpha f(x) = x^{-\alpha} I_0^\alpha f(x)$$

with the homogeneous kernel $k(x,t) = x^{-\alpha}|x-t|^{\alpha-1}$. The acting of J_0^α is studied in the grand Lebesgue spaces [3]:

$$L^{p),\theta}(\Omega) := \left\{ f : \|f\|_{p),\theta} := \sup\left(\varepsilon^\theta \int_\Omega |f(x)|^{p-\varepsilon}\,dx\right)^{\frac{1}{p-\varepsilon}} < \infty \right\}, \quad \theta>0, \quad 1<p<\infty,$$

and the theoretical results of [4] are applied to investigate the solutions of the corresponding integral equations. Due to their strong relation to mathematical modeling of solids with non-classical material structure, the obtained results are interest for applications in mechanics and physics of new materials.

Acknowledgement. The study was financially supported by Grant No. 21-19-00423 of the Russian Science Foundation in the Southern Federal University.

References

[1] Samko S. G., Kilbas A. A., Marichev O. I. *Fractional Integrals and Derivatives. Theory and Applications*. Gordon and Breach Science Publishers, 1993

[2] Tarasov V. E. *Fractional Dynamics*. *Applications of Fractional Calculus to Dynamics of Particles, Fields and Media*. Springer, 2010

[3] Umarkhadzhiev S. M. Generalization of a notion of grand Lebesgue space // *Russian Math. (Izv. VUZov)*, **58**(4), 35–43, 2014.

[4] Drobotov Yu. E., Umarkhadzhiev S. M. Riesz potential with homogeneous kernel in grand Lebesgue spaces on semi-axis // *Herald of the Academy of Sciences of the Chechen Republic*, **38**(1), 18 – 25, 2018.

On Analytical Approaches in Mathematical Modelling of Ferroelectric Switching Kinetics in Injection Mode

Yu. E. Drobotov[1,2]

[1]*Southern Federal University, Rostov-on-Don, Russia*
[2]*North-Caucasus Center for Mathematical Research of the Vladikavkaz Scientific Centre of the Russian Academy of Sciences, Vladikavkaz, Russia*

yu.e.drobotov@yandex.ru

Ferroelectrics make up a class of dielectrics with spontaneous polarization, the dipole moment of which can be reoriented by inducing an external electric field. The process of switching polarization in such materials is the result of the formation of self-similar structures, resulting in the self-similar structure of domains and the fractality of electrical responses. A mathematical model for switching the polarization of a ferroelectric under electron irradiation, considering fractality, was proposed in [1] and then developed in [2], which reported the results of its computational implementation within the framework of the hybrid fractal-stochastic approach.

The proposed model includes an initial value problem for the equation of a domain's boundary:

$$\frac{d^{\alpha}u}{dt^{\alpha}} = f\big(t, u(t)\big), \quad u(t_0) = u_0, \tag{2}$$

where $u(t)$ is the desired distance function, $t \in [t_0, T]$, $t_0 \geq 0$. The order of the differential operator is assumed to be fractional: $0 < \alpha < 1$, which is intended to reflect the fractality of the domain's boundary dynamics. Depending on the type of initial condition, two definitions of fractional derivative are used: Riemann – Liouville and Caputo, connected by certain expressions. This report aims to propose analytical approaches to the study of problem (1), developed in two directions: the application of the spectral theory of operators and the application of fractional analysis in non-standard functional spaces. The first method goes back to the paper [3] and is used for considering Wu as the right side of the equation, where W is an operator, that meets specific conditions. It is shown that in this case the exact solution of problem (1) can be written in the form of a series, the coefficients of which are calculated from the system of root vectors of the operator in the right part. The second method uses the representation of the desired function by a fractional integral in both the case of a constant and variable order of integration. In the second case, for generalized Hölder spaces, the following representation takes place [4]:

$$D_{t_0+}^{\alpha(\cdot)}\, I_{t_0+}^{\alpha(\cdot)}\varphi(t) = \varphi(t) + \int_{t_0}^{t} k(t, t-\tau)\, \varphi(\tau)\, d\tau, \quad u = I_{t_0+}^{\alpha(\cdot)}\varphi,$$

which makes it possible to consider the original equation as a Fredholm equation of the II kind, where the kernel $k(\cdot)$ is explicitly expressed.

Acknowledgement. The research was financially supported by Southern Federal University, grant No. VnGr-07/2020-04-IM (Ministry of Science and Higher Education of the Russian Federation).

References

[1] Maslovskaya A. G., Barabash T. K. // *Ferroelectrics*, **442**, 18 – 26, 2013.
[2] Moroz L. I., Maslovskaya A. G. // *Mathem. Mod*., **31**(9), 131 – 144, 2019 (In Russian).

[3] Lidskii V. B. Summability of series in terms of the principal vectors of non-selfadjoint operators // *Tr. Mosk. Mat. Obs.*, **11**, 3 – 35, 1962 (In Russian).
[4] Vakulov B. G., Kochurov E. S., Samko N. G. // *Russian Mathematics* (*Izvestiya VUZ. Matematika*), **55**(6), 20 – 28, 2011.

On the Stress State of Details with Projections of Complex Shape

Yu. E. Drobotov

Southern Federal University, Rostov-on-Don, Russia

yu.e.drobotov@yandex.ru

In this report, the Airy stress function, and the values of normal and tangent stresses due to pure stretching of a rod with two symmetric hyperbolic notches are considered. The classical result of Heinz Neuber [1, 2] is extended for an isometric curvilinear coordinate system in the form of

$$x(u,v)=\sinh(u)\varphi(v),\qquad y(u,v)=-\cosh(u)\varphi'(v),\qquad \varphi(v)=\begin{cases}\alpha\cos(v-v_0)+\beta\sin(v-v_0), & v\ge 0;\\ \alpha\cos(v+v_0)-\beta\sin(v+v_0), & v<0,\end{cases}$$

where $v_0>0$, and the coordinates used by Neuber are included as a particular case.

To calculate stresses due to pure stretching, the stress function:

$$F=\Phi_0+x\Phi_1,$$

$$\Phi_0=A(yv-xu)+B\cosh u\cos v,\quad \Phi_1=Au,$$

is reconsidered for this generalized coordinate system. The results obtained are particularly useful when designing methods for reducing a three-dimensional problem of stress concentration in complex-shaped elastic bodies to more accessible two-dimensional ones. The method of local approximations (MLA) is an example of such an approach [3]. For MLA, the combination of two-dimensional problems is applied. The one is on deflections in a cantilever plate under concentrated or distributed loading, while the other is on stress concentration in a rod with two deep symmetric hyperbolic notches. MLA is applied not only for theoretical studies in solid mechanics but also for sustainable design of details with loaded projections, providing the possibilities of varying the calculated section of a projection.

Acknowledgement. Research was financially supported by Southern Federal University, grant No. VnGr-07/2020-04-IM (Ministry of Science and Higher Education of the Russian Federation).

References

[1] Neuber H. Zur Theorie der Kerbwirkung bei Biegung und Schub // *Ing. Arch.* **5**, 238–244 (1934) doi:10.1007/BF02110709
[2] Neuber H. *Kerbspannungslehre. Theorie der Spannungskonzentration Genaue Berechnung der Festigkeit*. Springer-Verlag Berlin Heidelberg, 2001, doi: 10.1007/978-3-642-56793-3
[3] Zhuravlev G. A., Drobotov Y. E. About determination of stress concentration in bodies of a Complex Shape // *AMM*, **404**, 350-356, 2013, doi:10.4028/www.scientific.net/amm.404.350

The Spherical Fractional Poisson Equation and the Characteristics of Conditioning

Yu. E. Drobotov[1,2]*, D. S. Baraeva[1]

[1]Southern Federal University, Rostov-on-Don, Russia
[2]North-Caucasus Center for Mathematical Research of the Vladikavkaz Scientific Centre of the Russian Academy of Sciences, Vladikavkaz, Russia

*yu.e.drobotov@yandex.ru

Let $S^n := \{x \in \mathbb{R}^{n+1} : |x| = 1\}$ is a hypersphere centered at the zero point of the Euclidean space $\mathbb{R}^{n+1}$, whose elements are multidimensional vectors with real coordinates. In this report, the following equation is considered:

$$\delta^{\alpha/2} f = g, \quad f, g : S^n \to \mathbb{R}, \tag{3}$$

where $\delta^{\alpha/2}$, $0 < \mathrm{Re}\alpha < 2$, is understood as the power of the Laplace-Beltrami operator:

$$\delta f(x') = |x|^2 \, \Delta f(x/|x|), \quad \Delta f(x) = \frac{\partial^2 f}{\partial x_1^2} + \ldots + \frac{\partial^2 f}{\partial x_{n+1}^2}, \quad x' := \frac{x}{|x|}.$$

The latter can be expressed as the composition $\delta^{\alpha/2} f(x') = P \; (I^{\alpha,\nu})^{-1} f(x')$, where P is a spherical convolution operator with the known Fourier – Laplace multiplier, $(I^{\alpha,\nu})^{-1}$ is the inverse operator for the spherical Riesz potential:

$$I^{\alpha,\nu} f(x') = \frac{1}{\gamma_n(\alpha)} \int\limits_{S^n} \frac{f(\sigma)}{|x' - \sigma|^{n-\alpha}} \ln^{\nu} \frac{\sqrt{2}}{|x' - \sigma|} \, d\sigma, \quad \nu = \begin{cases} 0, & \alpha \neq n + 2k, \\ 1, & \alpha = n + 2k, \end{cases} \quad k \in \mathbb{N}_0,$$

And $\gamma_n(\alpha)$ is a normalizing constant. The research presented aims to bring the results of the papers [1, 2] on the structure of $(I^{\alpha,\nu})^{-1}$ to representing the solutions of (1) in various cases. Moreover, the methods for considering the conditioning of Equation (1) are described, based on the concept of generalized Hölder spaces and the results on acting of $I^{\alpha,\nu}$ on them [2, 3].

Acknowledgement. The research was financially supported by Southern Federal University, grant No. VnGr-07/2020-04-IM (Ministry of Science and Higher Education of the Russian Federation).

References

[1] Pavlov P. M., Samko S. G. Description of spaces $L_p^{\alpha}(S_{n-1})$ in terms of spherical hypersingular integrals // *Dokl. Akad. Nauk SSSR*, **276**(3), 546 – 550, 1984.

[2] Vakulov B. G., Drobotov Yu. E. In *Recent Applications of Financial Risk Modelling and Portfolio Management.* Hershey, PA, IGI Global, 275 – 296, 2021.

[3] Vakulov B. G. An operator of potential type on a sphere in generalized Hölder classes // *Russian Math. (Iz. VUZ)*, **30**(11), 90 – 94, 1986.

Hypersingular Integral Equations with Specific Characteristics and Their Applications

Yu. E. Drobotov*, K. A. Egiazaryan

Southern Federal University, Rostov-on-Don, Russia

*yu.e.drobotov@yandex.ru

In this study, a hypersingular integral equation is considered, written in its operator form as

$$\left(c_\alpha I + D_\theta^\alpha\right) A f = g, \quad 0 < \operatorname{Re}\alpha < 1, \tag{4}$$

where c_α is a real constant, I is the identity operator: $I f = f$, and D_θ^α is a hypersingular integral with a special characteristic $\theta(\cdot)$, generally defined as [1, 2]:

$$\left(D_\theta^\alpha f\right)(x) = \frac{1}{\gamma(n,-\alpha)} \int_{\mathrm{R}^n} \frac{f(y) - f(x)}{|x-y|^{n+\alpha}} \theta(x,y)\, dy$$

with the function f bounded at infinity and locally differentiable. In the equation (1), the operator A is considered as a parameter defined in the context of the current problem statement. Equations similar to (1) arise in the context of various problems in mathematical physics [3]. Thus, the superdiffusion process is known to be described by equation [4]:

$$\frac{\partial \rho}{\partial t} = -D(-\Delta)^{\alpha/2} \rho(x,t), \quad \alpha, D > 0,$$

where the fractional order of the Laplace operator is defined by a hypersingular integral with constant characteristic. Considering its stationary statement leads to a special case of equation (1), which makes the corresponding research of interest within this problem. The presented research aims at determining the kernels of the integral operator A, for which the solutions of the equations considered can be represented in terms of Riesz potential-type operators. Related physical interpretations are discussed, motivated mostly by applications of the fractional Poisson equation to processes in fractal media.

Acknowledgement. The research was financially supported by Southern Federal University, grant No. VnGr/2020-04-IM (Ministry of Science and Higher Education of the Russian Federation).

References

[1] Samko S.G. *Hypersingular Integrals and Their Applications*. Taylor & Francis, 2002.

[2] Samko S. G., Kilbas A. A., Marichev O. I. *Fractional Integrals and Derivatives: Theory and Applications*. Philadelphia, PA: Gordon and Breach Science Publishers, 1993.

[3] Tarasov V. E. *Fractional Dynamics: Applications of Fractional Calculus to the Dynamics of Particles, Fields and Media.* Berlin, Germany: Springer, 2010.

[4] Zolotarev V.M., Uchaikin V.V., Saenko, V.V. *Superdiffusion and Stable Laws* // *J. Exp. Theor. Phys*. **88**, 780–787, 1999, https://doi.org/10.1134/1.558856

On Numerical and Analytical Approaches to the Problem on the Stress-Strain State of a Cantilever Plate

Yu. E. Drobotov[1,2]*, R. K. Haldkar[1]

[1]Southern Federal University, Rostov-on-Don, Russia
[2]North-Caucasus Center for Mathematical Research of the Vladikavkaz Scientific Centre of the Russian Academy of Sciences, Vladikavkaz, Russia

*yu.e.drobotov@yandex.ru

One of the relevant problems in various fields of technology is the stress-strain state of a cantilever plate bended by a transverse load [1]. It is stated in both engineering calculations and in the creation of new methods for researching stresses in bodies of complex shape [2]. At the same time, the main difficulty in calculating cantilever plates is in complicated systems of partial differential equations which do not have a solution in a closed form. In this report, emphasis is placed on the approaches proposed within the framework of two theories: Kirchhoff's classical theory of thin plates and the Reissner refined theory for plates of finite thickness. Within the framework of the first of them, exact solutions to the problem of displacement and force factors are considered, for example, in [3, 4]. Within the framework of both theories, variations of the numerical-analytical solution [5] are considered, as well as numerical solutions, using the finite element method. The report presents an overview of specific solutions and ways of their implementation, both with the studying of their applicability and accuracy. The results of the presented mathematical models are vitrificated by comparing with the finite element method models carried out in ANSYS.

Acknowledgement. The research was financially supported by Southern Federal University, grant No. VnGr-07/2020-04-IM (Ministry of Science and Higher Education of the Russian Federation).

References

[1] Khalatkar A. M., Gupta V. K., Haldkar R. K. Study of effect of geometry parameters on piezoelectric cantilever by modal and harmonic analysis // *Advanced Materials Research.* **383 – 390**, 6689 – 6694, 2012.

[2] Zhuravlev G. A., Drobotov Yu. E. About Determination of Stress Concentration in Bodies of a Complex Shape // *Applied Mechanics and Materials. Engineering Decisions for Manufacturing Systems.* **404**, 350 – 356, 2013.

[3] Jaramillo T. J. Deflections and moments due to a concentrated load on a cantilevered plate of infinite length // *Journal of Applied Mechanics*. **17**(1), 67 – 72, 1950.

[4] Valov G. M. // *Tr. Conf. Teor. Plastin i Obolochek*, Kazan University, Kazan, 60 – 65, 1961 (In Russian).

[5] Sukhoterin M. V. Rectangular cantilever plate bending with regard to transverse shear deformation // *VESTNIK of Samara University. Aerospace and Mechanical Engineering.* **7**(1), 174 – 180, 2008, doi: 10.18287/2541-7533-2008-0-1(14)-174-180, (In Russian).

On Generating the Solutions of Poisson-Type Equations in the Generalized Hölder Spaces

Yu. E. Drobotov[1,2]*, A. S. Piskunov[1]

[1]Southern Federal University, Rostov-on-Don, Russia
[2]North-Caucasus Center for Mathematical Research of the Vladikavkaz Scientific Centre of the Russian Academy of Sciences, Vladikavkaz, Russia

*yu.e.drobotov@yandex.ru

In this study, the smoothness properties of potential type operators are considered. The paper reviews specific results on such operators in the generalized Hölder spaces, providing relevant terminology for formalizing the local smoothness of a reflection on a hypersphere, and due to the stereographic projection on the compactification of a hyperplane. Theoretical results establishing the characteristics of the function spaces are implemented in Julia and Python software with estimation of the performance of algorithms considered. As these integral operators form the basis of the Riesz fractional integro-differentiation used in mathematical modelling of complex structured media [1], the results on them are of interest for mechanics and material science. It is demonstrated that the acting of such operators on the generalized Hölder spaces, both weighted and non-weighted, can be studied with two different approaches. The first one is based on the concept of the Fourier–Laplace multiplier, while another one supposes sophisticated estimating the continuity modulus of the operator. The first way allows for considering the integral operators as spherical convolutions with specific kernels, and their images are calculated here in the case when a function is expanded into a series through spherical harmonics. The paper presents methods for computing the Fourier–Laplace multiplers and their estimation, which makes it possible not to include complicated transforms into consideration. As an example, the implementation of powered Laplacian through potential-type operators is considered, and the solutions of Poisson-type equations in the Hölder spaces are discussed [2]. For applications in practical problems, coefficient estimations are applied and their relation to the precision of the computation is considered [3, 4].

Acknowledgement. The study was financially supported by the Grant No. 21-19-00423 of the Russian Science Foundation in the southern Federal University.

References

[1] Tarasov V. E. *Fractional Dynamics. Applications of Fractional Calculus to Dynamics of Particles, Fields and Media*. Springer, 2010

[2] Vakulov B. G., Drobotov Yu. E. In: *Recent Applications of Financial Risk Modelling and Portfolio Management*, IGI Global, Hershey, PA, T. Škrinjarić, M. Čižmešija, B. Christiansen (Eds.), 275—296, 2021.

[3] Samko S. G., Kilbas A. A., Marichev O. I. *Fractional Integrals and Derivatives. Theory and Applications*. Gordon and Breach Science Publishers, 1993

[4] Drobotov Yu. E., Andreeva T. M. In: *Proceedings of the 2020 International Conference on "Physics, Mechanics of New Materials and Their Applications"*, Nova Science Publishers, New York, Ivan A. Parinov, Shun-Hsyung Chang, Yun-Hae Kim, Nao-Aki Noda (Eds.), 63–71, 2021.

On Smoothness of the Riesz Potential Type Operator with a Power-Logarithmic Kernel

Yu. E. Drobotov*, B. G. Vakulov

Southern Federal University, Rostov-on-Don, Russia

*yu.e.drobotov@yandex.ru

A fractional Riesz integro-differentiation is known to implement the fractional powers of the Laplace operator as integral operators of two kinds: the Riesz potentials I^α and hypersingular integrals D^α [1, p. 483]:

$$(-\Delta)^{\alpha/2} f = \begin{cases} I^\alpha f, & \operatorname{Re}\alpha > 0, \\ D^{-\alpha} f, & \operatorname{Re}\alpha < 0, \end{cases} \quad \Delta = \frac{\partial^2}{\partial x_1^2} + \ldots + \frac{\partial^2}{\partial x_n^2}.$$

The Riesz potential for all α, $\operatorname{Re}\alpha > 0$, is defined as the convolution [2, p. 492]:

$$I^\alpha f = \int_{\mathrm{R}^n} k_\alpha(x-y) f(y)\, dy,$$

where the Riesz kernel $k_\alpha(x)$ is considered in the form of

$$k_\alpha(x) = \frac{1}{\gamma_n(\alpha)} \begin{cases} |x|^{\alpha-n}, & \alpha - n \neq 0, 2, 4, 6, \ldots, \\ |x|^{\alpha-n} \ln\dfrac{1}{|x|}, & \alpha - n = 0, 2, 4, 6, \ldots \end{cases}$$

In the present report, a generalization of I^α is studied on a sphere $\mathrm{S}^{n-1} \subset \mathrm{R}^n$ in the form of

$$\left(K^{\alpha,\nu} f\right)(x) = \int_{S^{n-1}} \frac{f(\sigma)}{|x-\sigma|^{n-1-\alpha}} \ln^\nu \frac{r}{|x-\sigma|}\, d\sigma, \ \nu \in \mathrm{R}, \ x \in \mathrm{S}^{n-1},$$

where $\mathrm{S}^{n-1} := \left\{x \in \mathrm{R}^n : |x| = 1\right\}$. The integral operator $K^{\alpha,\nu}$ is called the Riesz potential type operator with a power-logarithmic kernel, and here its smoothness is studied, being understood in terms of the generalized Hölder spaces. For specific values of ν, the inverse operator is calculated, and these results, including [2] and those on its boundedness [3], are used to investigate the properties of related equations. The results obtained are discussed for possibilities of use in mathematical modeling of mechanical objects with complex material properties.

Acknowledgement. The study was financially supported by the Grant No. 21-19-00423 of the Russian Science Foundation in the Southern Federal University.

References

[1] Samko S. G., Kilbas A. A., Marichev O. I. *Fractional Integrals and Derivatives. Theory and Applications*. Gordon and Breach Science Publishers, 1993

[2] Vakulov B. G., Drobotov Yu. E. In: *Recent Applications of Financial Risk Modelling and Portfolio Management.* T. Škrinjarić, M. Čižmešija, B. Christiansen (Eds.). IGI Global, 275, 2021, http://doi:10.4018/978-1-7998-5083-0.ch014

[3] Vakulov B. G., Drobotov Yu. E. In: I. A. Parinov, S.-H. Chang, Y.-H. Kim, N.-A. Noda (Eds.) *Physics and Mechanics of New Materials and Their Applications. PHENMA 2020. Springer Proceedings in Materials*, Springer, Cham, **10**, 147-159, 2021, https://doi.org/10.1007/978-3-030-76481-4_13

On Vibrations of Two Inhomogeneous Elastic Objects

V. V. Dudarev*, R. M. Mnukhin

Department of Theory of Elasticity, I.I. Vorovich Institute of Mathematics, Mechanics and Computer Sciences, Southern Federal University, Rostov-on-Don, Russia

*dudarev_vv@mail.ru

Nowadays materials with continuously varying physical properties are increasingly being applied. They are characterized by increased crack resistance compared to conventional layered composites. The production of objects with given variable characteristics is a complex process and includes several technological stages. Therefore, one of the important applied problems is the certification of finished products properties. The most popular method for identifying solid characteristics is the acoustic method. In the present study, within the framework of the linear elasticity, the problems of steady vibrations of an inhomogeneous hollow elastic cylinder and a plate are considered. Assume that the material properties are described by continuous functions in two spatial coordinates. Solutions for both problems were obtained numerically using the FEM implemented in the FlexPDE package. One of the advantages of this package is the ability to set the laws for variable properties explicitly. On the basis of the obtained numerical solutions, the influence of the inhomogeneity laws on the amplitude-frequency characteristics, natural frequencies, free oscillations modes, and displacement fields is studied. The analysis of the results showed the possibility of using the data obtained to determine the variable material properties. Some methods and approaches for the implementation of the identification procedure are proposed.

Acknowledgement. The research was supported by Russian Science Foundation at the Southern Federal University (project No. 18-71-10045), https://rscf.ru/en/project/18-71-10045/.

Choice of the Optimal Technological Procedures for the Manufacture of Modified Bismuth Ferrite

S. I. Dudkina[1]*, S. V. Khasbulatov[2], L. A. Shilkina[1], I. A. Verbenko[1], L. A. Reznichenko[1]

[1]Research Institute of Physics, Southern Federal University, Rostov-on-Don, Russia
[2]Chechen State University, Grozny, Russia

*s.i.dudkina@yandex.ru

Among the materials that are most promising for meeting the modern requirements of the technical and technological development of the world community, multiferroics stand out, which are a wide class of media with a combination of ferroelectric, ferromagnetic and ferroelastic properties. This determines new areas of their application in devices based on mutual control of magnetic and electric fields: magnetic field sensors, information recording/reading devices, in spintronics and others. The most popular among others is bismuth ferrite, $BiFeO_3$, as it does not contain toxic elements and has high temperatures of

electrical (Curie temperature, T_C, ~ 1083 K) and magnetic (Néel temperature, T_N, 643 K) ordering [1]. However, technological difficulties in the production of bismuth ferrite ceramics limit its widespread use in practice. The aim of this work is to select the optimal technological procedures for the production of $BiFeO_3$ modified with rare earth elements (REE) in a wide range of their concentrations. The following compositions were considered: $Bi_{1-x}REE_xFeO_3$ (*REE* = La, Pr, Nd, Sm, Eu, Gd, Tb, Dy, Ho, Er, Tm, Yb, Lu; x = 0.00 – 0.50, Δx = 0.025, 0.05, 0.10). The samples were obtained by two-stage solid-phase synthesis from high-purity oxides, followed by sintering using conventional ceramic technology. The optimal technological procedures for the manufacture of the solid solutions ceramics were selected on a series of samples by varying the multiplicity, temperatures and durations of synthesis and sintering with X-ray control of each stage of the technological process. The optimal conditions for the phase formation of high-density, strong, unalloyed (or with a small content of ballast phases) ceramics of the specified composition, obtained by the described method, were determined on the basis of a comprehensive (using various experimental techniques) study of their structure, grain structure, and dielectric properties. The influence of size effects (ionic radii of *REE*s) on the form of phase diagrams of $BiFeO_3$/*REE* systems, structural nonstoichiometry of the solid solutions, polycrystallinity of the ceramics and their macroresponses has been established.

Acknowledgement. The study was carried out with the financial support of the Ministry of Science and Higher Education of the Russian Federation (State task in the field of scientific activity, scientific project No. (0852-2020-0032)/(BAZ0110/20-3-07IF).

[1] Smolenskiy G.A., Chupis I.E. Ferromagnets // *Uspekhi Fizicheskikh Nauk*, **137**(7), 415-448, 1982.

Problems of the Anionic Impurities in Niobate Ferroelectric Materials

S. I. Dudkina*, L. A. Shilkina, E. V. Glazunova, I. A. Verbenko, L. A. Reznichenko

Research Institute of Physics, Southern Federal University, Rostov-on-Don, Russia

*s.i.dudkina@yandex.ru

Actively engaged in the development of the ferroelectric materials based on the alkali metal niobates, the technology of their manufacture in large blocks, we made sure that when using different batches of Nb_2O_5 that meet the current State Standards, but differ in impurity composition, it is not possible to achieve reproducibility of the properties of the ceramics. The spread in the values of the electrophysical characteristics sometimes reaches several tens and even hundreds of the percent. In some cases, ceramics cannot be obtained at all due to their spontaneous destruction. All this testifies to the dependence of the physical properties of the alkali metal niobates on the characteristics of the applied Nb_2O_5. An analysis of the bibliographic and original data on the cationic modification of the alkali metal niobates showed that, as a rule, they improve the quality of the alkali metal niobates. The influence of the anionic impurities, namely F, S, P remains unknown. Among them, a fluorine impurity can be harmful to the alkali metal niobates, forming the most aggressive compounds to Nb-containing oxides – low-melting salts of alkali metal fluorides, as well as complex F-containing niobates such as LiNbOF, $NaNbO_3F$, Li_3NbO_4F [1]. The presence of the impurity phases and the associated fluctuations of the composition determine the corresponding changes in the kinetics of the solid-phase sintering of the solid solutions (from solid-phase to

liquid-phase), the nature of the recrystallization (from continuous to discontinuous secondary one), grain growth conditions (from isotropic the solid phase to anisotropic, when the resulting liquid phase acts as an active solvent, causing the crystallization of large grains from the melt), their final form (from equiaxed to ideomorphic) and packing (from dense to loose). Crystallizing in the form of small single crystals, ideomorphic grains form numerous interlayers in the bulk of the samples, contributing to the formation of a composite-like state: "single crystal – ceramic". Insufficient intergranular connectivity of such particles softens the samples, favoring spontaneous destruction of the ceramics during the sintering. The deterioration of the ceramic properties leads to the suppression of the piezoactivity of the solid solutions. The report considers rational technological methods that neutralize the effects of the presence of fluorine associated with the introduction of mechanoactivating procedures at different stages of the technological process.

Acknowledgement. The study was carried out with the financial support of the Ministry of Science and Higher Education of the Russian Federation (State task in the field of scientific activity, scientific project No. (0852-2020-0032)/(BAZ0110/20-3-07IF).

Reference

[1] Agulyansky A.I., Bessonova V.A., Kuznetsov V.Ya., Kalinnikov V.T. Interaction of niobium dioxide fluoride with lithium carbonate // *Journal of Inorganic Chemistry*, **29**, 1066 – 1068, 1984.

Natural Radioactivity and Outdoor Dose Assessment from Soil Samples at Sin Quyen Copper Mine, Lao Cai Province

Dung Nguyen Van*, Anh Vu Thi Lan, Cuc Nguyen Thi

[1]*Faculty of Environment, Hanoi University of Mining and Geology*

*nguyenvandung@humg.edu.vn

The results determined the activity of natural radionuclides in 55 soil samples taken from the Sin Quyen copper mine area, Lao Cai province. The activities of natural radionuclides ^{226}Ra, ^{232}Th and ^{40}K in soil samples were analyzed by low background gamma spectrometer with HpGe probe. The average activity results of natural radionuclides: ^{226}Ra, ^{232}Th and ^{40}K were 157.1 ± 11.5 Bq·kg^{-1}, respectively; 183.8 ± 14.3 Bq·kg^{-1} and 423.2 ± 19.3 Bq·kg^{-1}. The average activity of ^{226}Ra and ^{232}Th in this region is higher than the world average. Meanwhile, ^{40}K activity is roughly equivalent to the world average. The mean annual effective external dose (E_{eff}) and radium equivalent equilibrium (Ra_{eq}) are 0.39 ± 0.03 mSv·year^{-1} and 379.8 ± 24.4 Bq·kg^{-1}, respectively.

Novel Ferro-piezoceramic Material to Composites with Improved Hydrostatic Parameters

L. A. Dykina[1], P. A. Borzov[1], V. Yu. Topolov[2], V. V. Svirsky[1]

[1]Scientific Design & Technology Institute 'Piezopribor', Institute of High Technologies and Piezotechnics, Southern Federal University, 344090, Rostov-on-Don, Russia
[2]Department of Physics, Southern Federal University, 344090, Rostov-on-Don, Russia

*vutopolov@sfedu.ru

One of the tasks being solved on manufacturing a piezo-composite consists in a choice of a monolithic ferro-piezoceramic (FPC) matrix. Our study is concerned with a novel FPC that is based on lead zirconate-titanate and suitable for this matrix function. The novel FPC is characterised by large values of the longitudinal (d_{33} and g_{33}) and hydrostatic piezoelectric coefficients $d_h = d_{33} + 2d_{31}$ and $g_h = g_{33} + 2g_{31}$ as well as by a reduced acoustic impedance Z_a as compared to compositions (Table 1) being widely used in hydroacoustic applications.

Table. 1. Electrophysical parameters of FPCs at room temperature

FPC	$\varepsilon_{33}^T/\varepsilon_0$	d_{33}, pC/ N	d_h, pC/ N	g_{33}, mV·m/ N	g_h, mV·m/ N	Z_a, MRayl
Novel FPC	970	333	79	39.1	8.7	21.1
ZTS-36 [1]	655	221	43	38.0	7.2	25.3
ZTS-19 [1]	1770	377	81	24.1	5.3	22.9

The value of the longitudinal piezoelectric coefficient d_{33} of the studied novel FPC (see Table) complies with most highly sensitive FPC compositions, and this indicates an applicability of the novel FPC in general-purpose electromechanical transducers. Moreover, when manufacturing piezo-composites, including those with porous structures, an anisotropy of the piezoelectric coefficients d_{3j} increases [2], and the hydrostatic piezoelectric coefficient $d_h = d_{33} - 2|d_{31}|$ is restricted by the upper bound (d_{33}). As a consequence, the large d_{33} value of the monolithic FPC is a prerequisite for achieving the large hydrostatic parameters of the piezo-composite based thereon. Experimental studies on the novel FPC show that the large value of d_h leads to the large value of g_h, and the hydrostatic piezoelectric coefficient g_h serves as one of the most important characteristics of electronic-acoustic transducers that operate in a hydrostatic reception mode. Achieving large values of g_h (ca. 1.7 times larger than g_h of the ZTS-19 FPC) is caused by a decrease of the relative dielectric permittivity $\varepsilon_{33}^T/\varepsilon_0$ of the studied FPC, see Table 1. It should be also taken into account that the large hydrostatic piezoelectric coefficient d_h of the manufactured FPC exceeds d_h of the ZTS-36 FPC by ca. 1.8 times, see Table. The set of the properties of the studied novel FPC enables one to recommend it as a component of piezo-composites with various connectivities. To date, of great interest are porous piezo-composites that are applied in hydroacoustic systems due to the large hydrostatic parameters. In deep-sea applications, important characteristics are the mechanical strength of piezo-composites and stability of their sensitivity at various pressures [3]. Initial characteristics of the novel FPC indicate a possibility of achieving high hydrostatic sensitivity even at low porosities of the samples, and this circumstance will allow for expanding a range of operating pressures for final products. It should be noted that the acoustic impedance Z_a of the novel FPC is smaller than Z_a of the majority of the known FPCs. This leads to a better acoustic matching to a water medium and to decreasing losses of a radiation intensity of

transducers. Thus, based on the shown characteristics, one can conclude that the novel FPC is of interest for use in hydroacoustic transducers, as a piezo-active component of composites.

References

[1] Gorish A. V., Dudkevich V. P., Kupriyanov M. F., Panich A. E., Turik A. V. *Piezoelectric Device-Making.* **1**. *Physics of Ferroelectric Ceramics.* Moscow, Radiotekhnika, 1999 (In Russian).

[2] Filippov S. E., Vorontsov A. A., Brill O. E. et al. // *Funct. Mater. Lett*. **7,** 1450029, 2014.

[3] Panich A. A., Skrylev A. V., Dolya V. K. et al. // *Proc. XIVth All-Russian Conference "Applied Technologies of Hydroacoustics and Hydrophysics"*, St-Petersburg, 470 – 473, 2018 (In Russian).

Customs Construction and Technical Expertise of Commercial Wood

I. O. Egorochkina*, E. Yu. Bespaly, K. S. Desyatnikov

Don State Technical University, Rostov-on-Don, Russia

*arin77@bk.ru

Russia is the largest country-producer of materials and structures made of industrial commercial wood [1]. The turnover of commercial timber is constantly growing and expanding, representing a huge potential for economic development. Offenders of trade and customs transactions often use the techniques of imitation, falsification on a qualitative and quantitative basis for the implementation of criminal intentions in order to extract illegal profits [2]. The development of a methodology and program for the examination of timber will make it possible to identify the structure and properties of the samples under study, classify and encode information, prevent the declaration of timber from valuable wood species that are subject to a certain duty, excluding forgery (replacement) for low-grade, substandard timber, which is undoubtedly a measure to protect the economic interests of the state. The purpose of the research is to develop a technological cycle of customs construction and technical examination of timber. A general cycle of customs examination has been developed, which includes the following stages:

(I) The stage of commodity assessment of timber samples selected for the purposes of the examination, including the determination of the geometric dimensions, mass, density, roughness, moisture content of the samples in dry and natural conditions. The assessment of properties is carried out by measuring methods according to standard methods using modern means of technical diagnostics.

(II) The stage of qualimetric assessment, which includes an assessment of the indicators of the weight of individual properties, their ranking depending on the purpose of timber. For building structures and furniture lumber, the physical and mechanical properties (density, moisture) will be priority for finishing materials (veneer, parquet board, interior products), in particular, texture, color, shine, etc. Assessment of properties is carried out by expert organoleptic methods.

(III) The stage of economic assessment, including classification in accordance with the All-Russian Product Classification code, Harmonized System Codes and the calculation of the commercial, customs value of timber.

(IV) The stage of preparation of an expert opinion, allowing to identify the timber under study and establish their value and environmental safety.

The value of the research work is to develop a methodology for identifying timber samples to prevent the risk of economic damage due to the replacement of valuable timber with inappropriate analogs.

References

[1] Krivokochenko L. V. Opportunities and prospects for the development of Russian export of sawn timber to China and India // *Russian Foreign Economic Bulletin*, **7**, 58 – 65, 2020. DOI: 10.24411/2072-8042-2020-00071 (In Russian).

[2] Egorochkina I. O., Khalyusheva, O. N. Features of the examination of the quality of timber from valuable species of wood // *Collection of Abstracts of the International Conference*. Makeevka: DONNASA", 33, 2019 (In Russian).

Use of Crushed Brick for the Production of Ceramic Concrete

I. O. Egorochkina*, I. A. Serebryanaya, A. A. Osipova, P. A. Poboev

Don State Technical University, Rostov-on-Don, Russia

*arin77@bk.ru

As a result of the implementation of state programs for the demolition of emergency buildings in various regions of Russia, a large amount of technogenic raw materials in the form of brick and concrete scrap has been accumulated, which can be reused in construction production. This problem is especially relevant for areas where there is no natural gravel and rocks suitable for the production of crushed stone, and such areas make up almost a third of the territory of Russia. As the foreign and domestic experience shows, with an integrated approach to solving the problem of using technogenic raw materials, it is possible to develop a technology for the production of a new type of building material [1]. Brick buildings of the 1960 – 70s make up more than 50% of those planned for demolition. The use of brick fighting in the manufacture of wall products is one of the urgent tasks of resource conservation [2]. An integrated approach will expand the raw material base of building materials and improve environmental safety in the region. The purpose of our research work is to study the properties of ceramic aggregates, structure and properties of ceramic concrete based on them. It was found that the grains of crushed brickwork, consisting of crushed bricks and masonry mortar, have a similar structure and strength values, so there is no need to separate them. However, due to the high porosity of the ceramic aggregate, concrete mixtures are characterized by increased water demand, and concretes by increased shrinkage deformations, which reduces the strength and durability of the finished wall blocks. To solve the problem, the technology for preparing concrete mixtures has been improved. The technological cycle consists of the following stages: (i) intensive mixing of brick aggregates in a mixer in order to separate loosely fixed particles of masonry mortar from the surface of large grains; (ii) introduction of polyvinyl acetate emulsion into the concrete mixture with 2/3 of the mixing water followed by mixing in order to increase the adhesion of the cement-sand stone with grains of coarse aggregate; (iii) introduction of an organosilicon polymer and 1/3 of mixing water into the concrete mixture in order to form polysilicic acids in the mixture; (iv) introduction them into cement and sand mixer and final mixing. A complex additive including an organosilicon polymer and polyvinyl acetate contributes to an increase in concrete strength and a decrease in its open porosity, as evidenced by a decrease in the amount of water absorption of the resulting concrete by 35 – 40 %. The

use of a complex additive and a two-stage scheme for preparing concrete mixtures made it possible to obtain concrete of class up to B25 with improved thermal performance.

References

[1] Mirjana Malešev, Vlastimir Radonjanin, Snežana Marinković. Recycled Concrete as Aggregate for Structural Concrete Production // *Sustainability*, **2**, 1204 – 1225, 2010.

[2] Egorochkina I. O. // News South-Ural State University: Building and Architecture, **3**, 49 – 53, 2014.

Construction Technical Expertise of Reused Aggregates

I. O. Egorochkina*, E. A. Shlyakhova, D. S. Glushkov, I. Yu. Yurchenko

Don State Technical University, Rostov-on-Don, Russia

*arin77@bk.ru

The formation of the market of dismantling and demolition of buildings and structures creates prerequisites for the development of a promising area of business – recycling [1]. The product of demolition of building structures is a valuable raw material, namely rebar, coarse and fine aggregate for concrete, dusty aggregate [2]. Crushed concrete aggregate is a non-standard material and special methods should be developed for its evaluation, but at the same time, since this construction material is used for the preparation of concrete structures for mass construction, this type of aggregate should meet the requirements for concrete materials. The use of secondary aggregates will be possible if standard tests confirm its identity with natural aggregates. The purpose of the research work is a construction-technical expertise of aggregate from crushed concrete to assess the possibility of replacing natural crushed stone in concrete for the manufacture of ordinary concrete and reinforced concrete structures of prefabricated construction. The Table 1 shows a fragment of the program of construction-technical expertise of aggregate from crushed concrete:

Table 1

Cycle	Composition of expert procedures
Preparation stage	Selection of the expert group. Formulation of the task. Information support of work of experts. Studying of normative documents. Sampling.
Visual quality assessment	Assessment of the condition of the object by organoleptic methods.
Instrumental laboratory examinations	Determination of quality indicators (grain composition); content (dust and clay particles, clay in clumps, grains of weak rocks, lamellar and needle forms, crushed grains); determination (density; grade of strength, frost resistance, water absorption, environmental class of crushed stone).
Comparative expertise	Assessment of compliance of quality indicators of secondary aggregates and concretes based on them with the requirements of standards
Conclusion	Analysis of the results of expert evaluation, discussion of the results, preparation of the expert report.

The developed expert methodology for assessing the quality of aggregates made from crushed concrete will take into account the structural and physicochemical features, the effect on the

properties of concretes based on them, predict and manage the formation of a high level of quality and safety of concretes based on them.

References

[1] Shlyakhova E. A., Egorochkina I. O., Serebryanaya I. A., Matrosov A. A. // *Materials Science Forum*, **931**, 618 – 623, 2018. DOI:10.4028/www.scientific.net/MSF.931.618

[2] Egorochkina I. O., Serebryanaya I. A., Sukiasyan A. A. // Inzhenernyj Vestnik Dona, **9**(69), 237 – 245, 2020, URL: ivdon.ru/magazine/archive/n9y2020/6601

Strengthening of the Foundation Bases in Urban Development Conditions

I. O. Egorochkina*, E. A. Shlyakhova, O. A. Mikhailov, P. R. Kurasanov

Don State Technical University, Rostov-on-Don, Russia

*arin77@bk.ru

At present, in all countries of the world there is a persistent tendency towards urban growth and an increase in building density. Territories favorable for development have already been practically used, therefore, the process of modern urban construction is increasingly taking place in unfavorable geotechnical conditions. Foundations and their soil bases are among the most important and critical elements of buildings and structures that determine the fulfillment of this condition. Construction and reconstruction of foundations is a complex of construction work, which is often complicated by the presence of unfavorable geomorphological, engineering-geological, hydrogeological and mining-geological conditions. During the operation of buildings and structures, the properties of soil foundations and the hydrogeological regime of the territory often deteriorate, which necessitates their strengthening [1]. Common methods of strengthening soil foundations are surface and deep compaction and consolidation of soil with binders, but in recent years, new, more rational combined methods of improving the building properties of a soil massif, combining the advantages of two or more technologies for transforming soil properties, have become more widespread. So, soil compaction and consolidation are shared, as well as vibration and vibration pressure [2]. In this work, a combined method of strengthening the foundations of buildings and structures is considered, namely the method of high-pressure cementation, in which the fixing solution is fed into the soil under high pressure, which provides soil rupture in a certain zone of the massif with the formation of voids in the form of cavities, gaps and cracks, followed by filling the voids with a fixing mixture based on cement and aggregates from crushed concrete [3]. When the fixing mixture is supplied under pressure, additional compaction of the surrounding soil occurs. After the mixture hardens in the borehole and cracks in the soil, a spatial body of increased strength is formed. The advantages of the high-pressure cementation method are: the absence of dynamic effects on the soil; high strength and water resistance of the fixed base; the possibility of carrying out work in the winter period above and below the groundwater level; the use of inexpensive and non-scarce materials. The advantages of the considered method include a wide area of use: strengthening the soil foundations of buildings and structures; conservation of dumps of highly toxic, radioactive and other wastes without their development; straightening in this way the banks of high-rise buildings and structures. The main disadvantage of the high-pressure cementation method is the insufficient volume of recommendations for the selection of technological process parameters, which determines the relevance and goals of our further research.

References
[1] Egorochkina I. O., Serebryanay I. A., Shlyakhova E. A. Monitoring the condition of structures of an existing building near new construction. In: *Physics and Mechanics of New Materials and Their Applications. Abstracts & Schedule*. Kitakyushu, Japan, 99 – 100, 2021.
[2] Serebryanaya I. A., Egorochkina I. O., Shlyakhova E. A. Integrated construction and technical structural analysis of the industrial buildings. In: IOP Conference Series: Materials Science and Engineering. Construction and Architecture: Theory and Practice of Innovative Development CATPID-2020, 022071, 2020.
[3] Egorochkina I. O., Shlyakhova E. A., Cherpakov A. V., Parinov I. A., Liu Y. M. Optimization of the composition of the repair mixture based on non-shrinking and expanding cements. In: *Physics and Mechanics of New Materials and Their Applications. Abstracts & Schedule*. - Kitakyushu, Japan, 103 – 104, 2021.

Customs Expertise of Dry Building Mixtures

I. O. Egorochkina*, A. A. Tron, A. A. Yurkina, O. V. Chubatova

Don State Technical University, Rostov-on-Don, Russia

*arin77@bk.ru

Today, dry building mixtures for carrying out repair and restoration works and caring for monuments, as a rule, multicomponent compositions based on cement, are widely represented on the market of building materials. During the customs registration of such goods, there are problems of customs identification. Unscrupulous violators of customs legislation often attempt to import expensive restoration compositions under the guise of ordinary mineral binders. Unfair declaration complicates customs registration, distorts the customs value and import duties in the direction of understatement and poses a threat to the economic security of the country [1]. In the cases of detection (suspicion) of facts of customs offenses, customs officials have the right to initiate a customs identification examination, which is a comprehensive study and, as a rule, includes types of examinations: (i) documentation (analysis of shipping documentation); (ii) classification; (iii) technological (identification of raw materials and finished products during processing in the customs territory), the main stages of which are considered in [2]; (iv) commodity science (establishing the belonging of goods to a certain group, class). Customs identification is carried out by specialists of customs laboratories, in some cases, involving experts in the field of special knowledge of the object under study. In the research work, an algorithm for a comprehensive customs examination of restoration dry mixes has been developed, which includes the following stages: (i) study and analysis of shipping documents, labeling, inspection of packaging for violation of integrity, replacement of contents or the presence of hidden attachments; (ii) selection of identification criteria, namely the main properties of the product; (iii) sampling for testing; (iv) separate and comparative tests using express methods and laboratory tests, including conducting mineralogical and petrographic studies. Conducting a comprehensive customs examination will allow unambiguously identifying restoration multicomponent compositions for the purpose of reliable customs clearance.

References
[1] Egorochkina I. O. *Customs Expertise Textbook*. Rostov-on-Don.: Rostov State Building University Press, 2009 (In Russian).
[2] Shlyakhova E.A., Serebryanaya I.A., Egorochkina I.O. Compositions Based on Expansion Additive for the Repair of Reinforced Concrete Structures // *IOP Conference Series: Materials Science and Engineering, XVI International Scientific-Technical Conference "Dynamics of Technical Systems" (DTS-2020)*, **1029**, 2021, 012047, doi:10.1088/1757-899X/1029/1/012047.

Customs Tracological Expertise of Motor Vehicles

I. O. Egorochkina*, R. E. Zatona, E. S. Tsygankova

Don State Technical University, Rostov-on-Don, Russia

*arin77@bk.ru

A huge number of vehicles are imported into Russia [1]. The purpose of the custom expertise is to determine the technical parameters of the vehicle, clearly establish the location of the markings, the content of the marking, the principle of application, anomalies in the vehicle's marking for the purpose of identification for subsequent customs clearance. Trasological expertise of vehicle is part of a comprehensive customs formalities [2]. Features, sequence and content of the customs trasological expertise of the vehicle are presented in Table 1.

Table 1. Content of the custom expertise of the vehicle

Step	Contents	Substantive content
Previous step	Custom expertise of vehicles	Inspection, registration of detained vehicles, examination of documentation. Inspection of vehicles by criminal investigation officers. Study of the requirements of national and industry standards for labeling vehicles and their units.
Primary step	Definition of general identification parameters	Product name, brand name, trade name, country of manufacture, manufacturing company, month, year of manufacture, environmental class. General technical data: type, category, wheel arrangement, type of transmission, weight, color of body (cabin). Technical information of the engine: model, number, type, capacity, displacement. Accordance to the information declared in the declaration.
	Analysis of marking labels	Establishment of marking locations. Structure and content of markings. Principle of marking (micro milling, micro engraving, "punching by dots"). Identification of anomalies in markings.
	Comparative studies	Finding differences in identifying indicators and evaluating them. Determining matches in the identifying indicators and estimating them.
Final step	Documenting the results of the expertise	Customs classification and coding. Valuation. Drawing up an expert report, completing the customs formalities (registration).

Traceological expertise of vehicles with the issuance of an expert opinion is extremely important for making an informed decision on the passage of goods through the customs border.

References

[1] Nagaitsev A. A. *Study of the Markings of Passenger Cars of Foreign Production*. Moscow: BINOM, 258, 1999 (In Russian).

[2] Egorochkina I. O. *Customs Expertise Textbook*. Rostov-on-Don: Rostov State Building University Press, 2009 (In Russian).

Study of the Initial Annealing of FIB-treated Silicon

M. M. Eremenko*, S. V. Balakirev, N.E. Chernenko, N. A. Shandyba, M. S. Solodovnik, O. A. Ageev

Southern Federal University, Institute of Nanotechnologies, Electronics, and Electronic Equipment Engineering, Taganrog, 347922, Russia

*eryomenko@sfedu.ru

Recently, interest has increased in possible solutions for the integration of A3B5 structures on Si. However, achieving the desired low-defect and, as a result, high-performance structures remain a difficult task. To date, a large number of techniques are used to reduce more defects during the monolithic integration of A_3B_5 on Si. However, studies of the initial stage are still crucially important for understanding the processes of formation of further grown layers, and will also make it possible to obtain regimes with the lowest density of defects, most of which are assumed to be localized in the lower layers. In this work, we studied the effect of initial annealing on the modified areas of silicon. Silicon substrates were modified with a focused ion beam (Ga^+) at various accelerating voltages and beam passes. Accelerating voltages varied from 5 kV to 30 kV, and number of passes were 1, 5, 30 and 200. Annealing was carried out at temperature equal to 800 °C. A decrease in the accelerating voltage from 30 kV down to 5 kV led to the disappearance of Ga droplets in almost all ranges of the considered modifications and temperatures, except for 200 beam passes at a temperature of 800 °C. We believe that this is due to the intense evaporation of the material from the surface, which does not lie deeply, and this process is more advantageous when modifying the surface with beams with a low accelerating voltage and annealing at high temperatures. On the other hand, with an increase in the accelerating voltage on the surface of the modified areas, the implanted material emerges on the surface already from 5 beam passes. We explain its presence by the fact that at a high accelerating voltage, the depth of the material is high and the material gradually comes out to the surface and does not have time to completely desorb from the surface during annealing. However, it should be noted that during processing with an accelerating voltage of 30 kV and 200 beam passes, holes were left on the surface of the modified areas, without the presence of droplets of implanted Ga. The presence of such holes is apparently caused by a large deformation of the Si surface during processing by focused ion beams. In the future, it is planned to study these samples using Raman spectroscopy to confirm or disprove our theories.

Acknowledgement. This work was supported by the Russian Science Foundation (grant No. 20-69-46076).

Simulation of Ultrasonic Probing by Inclined Non-contact Transducers

O. A. Ermolenko, E. V. Glushkov*, N. V. Glushkova

Institute for Mathematics, Mechanics, and Informatics, Kuban State University, Krasnodar, 350040, Russia

*evg@math.kubsu.ru

The air-coupled or submerged transducers are increasingly used in the structural health monitoring (SHM) of safety-critical engineering constructions such as aircraft, pipelines, nuclear storages, etc. They are easy to operate, allowing for inspection of large areas with both bulk and guided waves (GWs). Optimization of the contactless ultrasonic technologies assumes the choice of better parameters for the wave excitation, for example, the angle of source inclination depending on the frequency, distance to the surface, and the ratio between the material properties of the sample and acoustic environment. This requires mathematical and computer models to adequately simulate the wave generation and propagation in the coupled system "source – acoustic medium – elastic plate". For this purpose, we have been developing analytically based computer models providing fast numerical study. The models are based on the integral and asymptotic representations through Green's functions of the corresponding boundary-value problems. If the emitter is parallel to the sample surface, the solution can be derived in the close form of inverse Fourier transform path integrals. The far-field asymptotics of the reflected and transmitted acoustic waves are derived from these integrals by the stationary phase method. The GWs generated in the plate by the incident acoustic beam are obtained as the residues from the integrand's real and nearly real poles. With a tilted transducer, a closed-form solution is also possible, but it is too cumbersome. Therefore, we simulate it as a superposition of point sources distributed over the radiating element area and use the already obtained explicit representations for the wave fields generated by each. This approach retains the advantages of analytical solution, essentially decreasing computational expenses compared to the mesh-based finite element simulation and providing physically clear insight into the wave structure (e.g., source energy distribution among the excited wave modes). The developed computer model is validated against the finite element simulation (Comsol Multiphysics 5.6). Numerical examples illustrating the dependence of GW amplitudes on the source inclination are presented, and the search for optimal parameters (sweet spots) for the excitation of selected modes is discussed.

Acknowledgement. The work is supported by the State Assignment of the Russian Ministry of Science and Higher Education, Project FZEN-2020-0017.

Development Strategy of MSMEs Based on Creative Economy in Indonesia

Erni Puspanantasari Putri

Department of Industrial Engineering, Universitas 17 Agustus 1945 Surabaya, Indonesia

erniputri@untag-sby.ac.id

Micro, small and medium enterprises (MSMEs) have a social function as a safeguard for the national economy. MSMEs are needed low-income people to carry out creative economic activities. At present, the MSME creative economy sector faces various challenges in developing its business, including (i) complexity of entering the global market, (ii) limited production capacity, (iii) production machine capacity is not standardized, (iv) complexity in accessing market information, and (v) inadequate capacity to explore export markets. Various strategies need to be applied to overcome the problems of creative economy SMEs. Thus, MSMEs can carry out their functions as the backbone of the national economy and the spearhead of the economic cycle in Indonesia. The development of creative economy MSMEs requires a variety of strategies. These strategies are as follows: (i) intensive provision for MSME actors, (ii) creation of a creative economy roadmap with comprehensive programs, (iii) training for creative economy MSME actors, (iv) legal protection for creative economy products, and (v) the existence of investors to accelerate the realization of creative economy MSME activities.

Development Strategy of the Local Village Economy in Indonesia

Erni Puspanantasari Putri

Department of Industrial Engineering Universitas 17 Agustus 1945 Surabaya, Indonesia

erniputri@untag-sby.ac.id

Local economic development is very important to encourage national economic growth activities. The driving wheel of the local economy can contribute to the improvement of the national economy to face global challenges. The local economy that continues to develop will generate added value and income, especially for people who are unable to bridge income inequality. Local economic development plays an important role in supporting the implementation of sustainable development goals. Village economic development is a process that makes the village economy independent. Thus, the village community will be able to develop well and the village government can become a driver of the village economy. The main purpose of village economic development is to foster a village economic environment that allows the community to have an active, healthy, and long life. Indicators of village economic development, as such: adequate village infrastructure, good public facilities, access to information, quality of human resources, and local community income. Several strategies for village economic development in Indonesia are as follows: (i) building comparative advantages of villages, (ii) building globally competitive villages, (iii) increasing village independence, (iv) building village economic institutions, and (v) development of local potential.

Performance Evaluation Using Input-oriented Envelopment DEA Method: A Case Study of Micro and Small Industry in Indonesia

Erni Puspanantasari Putri*, Zainal Arief, Istantyo Yuwono

Department of Industrial Engineering Universitas 17 Agustus 1945 Surabaya, Indonesia

*erniputri@untag-sby.ac.id

Performance evaluation is necessary for the company's business to operate effectively in a changing business environment. Therefore, this function is necessary for the survival of the company. Performance evaluation is defined as the process required to measure actions on the basis of qualifications and performance. The role of micro and small industries (MSIs) in economic growth in Indonesia is considered important because MSIs are able to absorb labor and contribute to the gross domestic product (GDP). MSIs are faced with several problems that hinder their business development. Therefore, we need an effort to encourage and empower MSIs to a better level. Performance evaluation is an effort to determine the effectiveness of the MSIs. The effectiveness of the MSIs can be used as a reference to improve the fluctuating MSIs' business performance as a result of competitive business competition. Thus, MSIs can develop their business activities even better in the future. The purpose of this research is as an effort to encourage and empower micro and small industries to a better level through the performance evaluation of MSIs. Performance evaluation is an effort to determine the effectiveness of the MSIs. The method used in this research is the Input-Oriented DEA Envelopment Model. Data envelopment analysis (DEA) is a linear programming method that deals with measuring performance in an integrated model. The DEA model uses a linear programming formula that is oriented to minimize input while the output condition remains at the current level. The results of the efficiency analysis for micro and small industries identified 9 efficient DMUs and 25 inefficient DMUs. The percentages for each of these conditions are efficient DMUs (26%) and inefficient DMUs (74%).

Heat Exchange of Main Gas Pipelines with the Environment

A. A. Fomenko[1], D. D. Fugarov[2]*, Abugharbi Ali Thamer Khalil[2], D. A. Volkov[2]

[1]M. I. Platov South-Russian State Polytechnic University (NPI), Novocherkassk, Russia
[2]Don State Technical University, Rostov-on-Don, Russia

*ddf_1@mail.ru

The temperature regime of the gas pipeline affects the pressure and throughput [1]. When choosing the operating modes of compressor stations, it is necessary to take into account not only the capabilities of the gas cooling systems after compression, but also the temperature distribution in the sections of the gas pipeline between neighboring stations [2]. The distribution of temperature when calculating heat transfer between pipelines and the environment depends on many factors, including seasonal fluctuations in air and soil temperature, accompanied by a change in the aggregate state, a change in moist soil, and a change in the temperature of the pipeline surface [3]. The movement of a perfect gas through

a pipeline under conditions of heat exchange with the environment is described by a system of equations, including the law of conservation of specific energy, continuity equation, and the equation of state of the gas [4]. The equation, describing the temperature distribution along the length of the gas pipeline, which is due to heat transfer to the environment has the form:

$$\frac{T(x)-T_{oc}}{T_H-T_{oc}}=\exp\left(-\frac{\pi DkL}{MC_p}\cdot\frac{x}{L}\right),$$

where T_{oc} is the ambient temperature; C_p is the average isobaric heat capacity of the gas; k is a heat transfer coefficient. It is possible to obtain the temperature at the end of the gas pipeline section from this equation at $x = L$ [5].

References

[1] Poluyan A. Yu., Purchina O. A., Fugarov D. D., Golovanov A. A., Smirnova O. V. Solution of task on the minimum cost data flow based on bionic algorithm // *Journal of Physics: Conference Series*. International Conference "Information Technologies in Business and Industry", Mathematical Simulation and Computer Data Analysis, **2**, 032056, 2019.

[2] Fugarov D. D., Purchina O. A., Poluyan A. Y., Gerasimenko A. N., Rasteryaev N. V. Magnetodielectric ac measuring transducer for automation systems in oil refineries // *Journal of Physics: Conference Series*. International Conference "Information Technologies in Business and Industry", 062020, 2019.

[3] Onyshko D., Fugarov D., Purchina O., Poluyan A., Rasteryaev N., Skakunova T. Synchronization system in wireless sensor networks of oil and gas complex // *E3S Web of Conferences. Topical Problems of Green Architecture, Civil and Environmental Engineering, TPACEE 2019*, 03030, 2020.

[4] Poluyan A. Yu., Purchina O. A., Fugarov D. D., Gerasimenko E. Yu., Skakunova T. P. Application of bionic and immune algorithms for the solution of ambiguous problems of transportation routing // *Journal of Physics: Conference Series*. International Conference "Information Technologies in Business and Industry", Mathematical Simulation and Computer Data Analysis, **2**, 032057, 2019.

[5] Gerasimenko Y., Gerasimenko A., Fugarov D., Purchina O., Poluyan A. Mathematical modeling and synthesis of an electrical equivalent circuit of an electrochemical device // *Advances in Intelligent Systems and Computing*, **1259**, 471 – 480, 2021.

Temperature Modes of Operation of Main Gas Pipelines

A. A. Fomenko [1], D. D. Fugarov[2]* , V. A. Brazhnikov[2], I. D. Abrosimov[2]

[1]M. I. Platov South-Russian State Polytechnic University (NPI), Novocherkassk, Russia
[2]Don State Technical University, Rostov-on-Don, Russia

*ddf_1@mail.ru

The operation mode of the main gas pipeline is determined by the joint operation of compressor stations, as well as linear sections. The output parameters of the previous section are considered the input parameters of the subsequent one [1]. When gas is compressed in gas-pumping apparatuses, the gas temperature increases, which at the output of centrifugal blowers can reach 70 °C. This technological procedure is used when transporting hydrocarbon gases through trunk pipelines, pumping them into oil and gas bearing structures in order to maintain reservoir pressure, during filling of underground gas storage facilities, and also during

transportation of liquefied gases [2]. The main sources of hazards during the operation of compressor units are: (i) increased gas pressure; (ii) increasing the temperature of the compressed gas; (iii) reciprocating and rotational movement of working bodies; (iv) the possibility of liquefying individual components of compressible gas mixtures; (v) the presence of flammable and toxic substances in the compression volume [3]. Compression of gas at compressor stations leads to an increase in its temperature at the output of the station. The numerical value of this temperature is determined by its initial value at the input of the compressor station and the degree of gas compression [4]. Excessively high gas temperature at the output of the station, on the one hand, can lead to the destruction of the insulating coating of the pipeline, and on the other hand, to a decrease in the supply of process gas and an increase in energy consumption for its compression (due to an increase in its high consumption) [5].

References

[1] Onyshko D., Fugarov D., Purchina O., Poluyan A., Rasteryaev N., Skakunova T. Synchronization system in wireless sensor networks of oil and gas complex // *E3S Web of Conferences. Topical Problems of Green Architecture, Civil and Environmental Engineering, TPACEE 2019*, 03030, 2020.

[2] Poluyan A. Yu., Purchina O. A., Fugarov D. D., Golovanov A. A., Smirnova O. V. Solution of task on the minimum cost data flow based on bionic algorithm // *Journal of Physics: Conference Series*. International Conference "Information Technologies in Business and Industry", Mathematical Simulation and Computer Data Analysis, **2**, 032056, 2019.

[3] Fugarov D. D., Purchina O. A., Poluyan A. Y., Gerasimenko A. N., Rasteryaev N. V. Magnetodielectric ac measuring transducer for automation systems in oil refineries *// Journal of Physics: Conference Series*. International Conference "Information Technologies in Business and Industry", 062020, 2019.

[4] Poluyan A. Yu., Purchina O. A., Fugarov D. D., Gerasimenko E. Yu., Skakunova T. P. Application of bionic and immune algorithms for the solution of ambiguous problems of transportation routing // *Journal of Physics: Conference Series*. International Conference "Information Technologies in Business and Industry", Mathematical Simulation and Computer Data Analysis, **2**, 032057, 2019.

[5] Gerasimenko Y., Gerasimenko A., Fugarov D., Purchina O., Poluyan A. Mathematical modeling and synthesis of an electrical equivalent circuit of an electrochemical device // *Advances in Intelligent Systems and Computing*, **1259**, 471 – 480, 2021.

Theoretical Estimation of Porosity and Fluid Saturation by Ultrasound Methods Based on Surface Waves

S. I. Fomenko[1]*, R. B. Jana[2], M. V. Golub[1]

[1]Institute for Mathematics, Mechanics and Informatics, Kuban State University, Krasnodar, Russia
[2]Digital Agriculture Laboratory, Skolkovo Institute of Science and Technology, Moscow, Russia

*sfom@yandex.ru

Many environmental studies – from agriculture and forestry to flood prediction and natural resources conservation, as well as studies on fundamental stability of buildings and other structures, require a deep understanding of soil processes and sub-surface water flow

dynamics. Estimation of the moisture level (water saturation), as well as soil porosity, is important for forecasting and, accordingly, improving of yields. The goals of this investigation are parametric analysis of porosity on phase velocities of surface waves and estimation of effective parameters of the poroelastic fluid-saturated medium based on the solution of the inverse problem. For the theoretical study of elastic wave propagation in fluid-saturated media with pores, the Biot-Frenkel equations, generalizing the Lame equations of the classical linear theory of elasticity to the case of two-phase media, are used. It is well known that the mutual oscillations of the elastic skeleton and pore fluid result on change of the velocities of longitudinal (P1), shear (S) body waves as well as the occurrence of the additional slow longitudinal wave (P2). The microstructure is also manifested in wave effects connected with the presence of boundaries. Firstly, the laws (coefficients) of refraction and reflection of body wave incident on the interface of two-phase media change, and, therefore, characteristics of surface and channel waves propagating along extensive boundaries change. Secondly, additional surface waves manifest due to the porosity and fluid saturation that is discussed in details, too. The influence of the porosity and fluid saturation on the phase velocities of surface waves is discussed in details. The solution of inverse problem for the effective parameters of poroelastic medium, based on the minimisation of the discrepancy between the experimental measured and simulated phase velocities, is discussed, too.

Acknowledgement. The authors are grateful to the support of the Russian Science Foundation and the Krasnodar Regional Administration (Project proposal No 22-21-20053).

Mathematical Modelling of Electrolyte Concentration Field in the Controlled Electrochemical Resistance

D. D. Fugarov*, E. Yu. Gerasimenko, O. A. Purchina, Shuvailat Mohammed Yasin Joudah

Don State Technical University, Rostov-on-Don, Russia

*ddf_1@mail.ru

The aim of the study is mathematical modeling of the concentration field of an electrolyte in a controlled electrochemical resistance. All processes occurring in the object are considered isothermal, electric fields in all fragments of electrochemical resistance are potential, plane-parallel [1]. All physical and chemical parameters of the object's materials are constant values. The kinetics of all electrode processes in the object of study is controlled by the diffusion stage in the electrolyte [2]. As a research method, the operator method of Laplace and Fourier decomposition is used to obtain an analytical description of the concentration field of the electrolyte [3]. In the course of the study, a mathematical model of the concentration field of the electrolyte was obtained with a uniform distribution of the current density [4]. An analytical expression is obtained that allows one to construct the surface of the change in the concentration of the electrolyte in the controlled electrochemical resistance. The concentration profiles of the electrolyte at different temperatures and the time dependences of changes in the concentration of the electrolyte are calculated [5].

References

[1] Gerasimenko Y., Gerasimenko A., Fugarov D., Purchina O., Poluyan A. Mathematical modeling and synthesis of an electrical equivalent circuit of an electrochemical device // *Advances in Intelligent Systems and Computing*, **1259**, 471 – 480, 2021.

[2] Onyshko D., Fugarov D., Purchina O., Poluyan A., Rasteryaev N., Skakunova T. Synchronization system in wireless sensor networks of oil and gas complex // *E3S Web of Conferences. Topical Problems of Green Architecture, Civil and Environmental Engineering, TPACEE 2019*, 03030, 2020.
[3] Poluyan A. Yu., Purchina O. A., Fugarov D. D., Golovanov A. A., Smirnova O. V. Solution of task on the minimum cost data flow based on bionic algorithm // *Journal of Physics: Conference Series*. International Conference "Information Technologies in Business and Industry", Mathematical Simulation and Computer Data Analysis, **2**, 032056, 2019.
[4] Fugarov D. D., Purchina O. A., Poluyan A. Y., Gerasimenko A. N., Rasteryaev N. V. Magnetodielectric ac measuring transducer for automation systems in oil refineries *// Journal of Physics: Conference Series*. International Conference "Information Technologies in Business and Industry", 062020, 2019.
[5] Poluyan A. Yu., Purchina O. A., Fugarov D. D., Gerasimenko E. Yu., Skakunova T. P. Application of bionic and immune algorithms for the solution of ambiguous problems of transportation routing // *Journal of Physics: Conference Series*. International Conference "Information Technologies in Business and Industry", Mathematical Simulation and Computer Data Analysis, **2**, 032057, 2019.

An Analysis of The Effect of Pressure Load and Particle Size (Mesh 200 – 350) on Mechanical Properties of Polypropylene Reinforced Coal Ash (Bottom Ash) Composite

Gatut Prijo Utomo, Supardi Ismail*, I Made Kastiawan, Bimo Aji Setyawan, Nizar Rowandi

Mechanical Engineering, University of 17 Agustus 1945 Surabaya, Indonesia

*supardis@gmail.com

Plastic is gradually shifting glass, wood and metal, while coal bottom ash is a relatively cheap material that tends to be free, because it includes factory waste from coal combustion which is usually piled up unused in the ash disposal area of the factory. From the explanation above, an analysis will be carried out on how to increase the strength of the plastic composite material (thermoplastic) with coal bottom ash reinforcement in order to inhibit the deformation of the molecular bonds in the plastic. The present study employed an experimental study, starting with the process of making composite materials with a ratio of 90% polypropylene as a matrix and 10% coal bottom ash with particle size of 200 – 350 (mesh). First, the polypropylene is heated at a temperature of 170 °C. Once it melts completely, the coal bottom ash is added and stirred at 20 rpm for 30 minutes. Following this, the castings are poured into the mold (die), and added with a compressive load with a jack of 15, 25, and 35 kgf/cm^2 for 5 minutes. The composite material was then adjusted to the shape of ASTM D-638 for tensile testing, and ASTM D-790 for bending test to determine its mechanical properties. Morphological analysis was also carried out with SEM photos to show the microstructure of the composite. The study collected the data about the effect of pressure and particle size of coal bottom ash on the mechanical properties of the polypropylene matrix composite material. It is expected that this research can be used as a reference on similar research for the development of polymer composite technology.

Planar Multitip Field Emission Cell Based on Graphene Films on Silicon Carbide

G. D. Gavrishchakin, I. L. Jityaev*, G. A. Malakhov, A. I. Kovalets, A. M. Svetlichnyi

Southern Federal University, Institute of Nanotechnologies, Electronics, and Equipment Engineering, Taganrog, 347922 Russia

*izhityaev@sfedu.ru

Blade field emission cathodes and multiemitter structures make it possible to increase the current density in comparison with single tip emitters. However, in this case, the phenomena of local amplification of the electric field on the emitting surface, overheating of the cathode sections and changes in the cathode shape can occur [1]. Therefore, it is necessary to take into account the processes affecting the stability of the emission and the durability of the field emission cathode when developing field emission structures with a high current density. Modeling the distribution of the electric field in the interelectrode gap makes it possible to predict emission processes and optimize the structure of the field emission cell to increase the uniformity of the field on the emitting surface. The aim of this work is to theoretically study a planar nanoscale field emission cell containing a multipoint cathode based on graphene films on silicon carbide. The use of graphene films on silicon carbide is explained by their high mechanical strength, thermal conductivity, and electrical conductivity. The simulation of the distribution of the electric field strength in the interelectrode space of the field emission cell was carried out. The influence of the distance between the tips, the interelectrode distance and the change in the height of the tips of the cathode on the uniformity of the electric field strength at the emitting surface of the tips is investigated. The interelectrode distance was varied from 10 to 100 nm, the distance between the tips was from 110 to 200 nm, the height of the cathode tips was changed according to the Gaussian law by changing the coefficient σ from 10^3 to 10^4. The dependences of the electric field strength at the emitting surface on the parameters of the field emission cell were obtained from the simulation results. The simulation results showed the presence of a local increase in the electric field strength at the edge tips of the field emission cathode. The theoretical dependences made it possible to determine the distance between the tips, the interelectrode distance and the value of the coefficient σ, at which an increased uniformity of the electric field was observed at the emitting surface of each tip of a planar cathode. The minimum distance between the tips in the matrix was from 160 to 200 nm, and the minimum value of the coefficient σ was from 7×10^3 to 10^4, at which the field strength is uniform in the considered range of the interelectrode distance.

References

[1] Jityaev I. L., et al. // *J. Vac. Sci. Technol. B*, **37**, 012201, 2019.

Temperatures of Ferroelectric, Magnetic and Rotational Phase Transitions of Binary Perovskite Structure Oxides and Fluorides

G. A. Geguzina[1]*, I. G. Popova[2]

[1]*Southern Federal University, Research Institute of Physics, Rostov-on-Don, Russia*
[2]*Don State Technical University, Department of Physics, Rostov-on-Don, Russia*

*geguzina@sfedu.ru

The ferro-, antiferroelectric, magnetic and rotational phase transitions of known binary perovskite structure oxides (PSO) ABO_3 and fluorites (PSF) ABF_3 have been considered. The correlations between their phase transition's temperature values, on the one hand, and the interatomic bond $A - X$ (X = O or F) strain values, on the other hand, have been constructed. It has been established that the known binary PSO and binary PSF with different nature of phase transition (PT) caused of a lot of their composition and structure factors, are conditioned, among another, by the interatomic bond A – O strain in their structure (see Fig. 1).

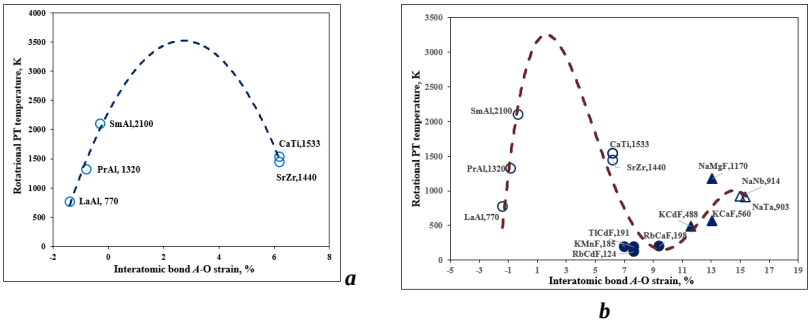

Fig. 1. Correlations between δ_{AO} (*a*) and δ_{AO} for PSO and δ_{AF} for PSF (*b*) and their rotational PTs temperatures, where symbols "O_3" in the chemical formulae ending are not indicated for PSO, but symbols "F" without "…$_3$" are indicated in contrast for PSF.

As effect of the structural PT's symmetry O_h^1 of preceding phase reduces abruptly into a lower symmetry and, as rule, transforms to any of its subgroups. Ferroelectrics and their solid solutions (SS) are basic of the active functional materials for electronics and their PTs temperatures values play an important role. In this connection understanding why a compound is ferro- or antiferroelectric or undergoes rotational PTs and what its temperature can depend on is of great theoretical interest as well as has a practical implication for directed research into new compounds and materials with the certain structure and properties? Is there a common feature of the binary PSO and PSF structure that can determine their PT's nature and temperature Tc values to classify their PTs? The theory of ferroelectricity tries different concepts and parameters for this role. They are used to construct some qualitative and quantitative correlations between the PT's nature and their temperature values and those parameters. Some of them can been determined only experimentally, others – both experimentally and calculated *a'priori*. Why are ferroelectric PTs not observed for PSFs while there are no symmetric constraints for it? Can polar phases appear for those fluorites? Why do

similar rotational PTs take places for both PSO and PSF? The aim of this work is to answer the above and other questions using the strains of the interatomic bonds *A*-O, δ_{AO}, and *A*-F, δ_{AF}, calculated using the perovskite structure quasi-elastic model proposed by Sakhnenko V. P. with co-authors and to construct some correlations between these parameters and PT's temperatures.

Acknowledgement. The study was financially supported by the Ministry of Science and Higher Education of the Russian Federation [State task in the field of scientific activity, scientific project No. 0852-2020-0032 (BAS0110/20-3-08IF)].

Change Areas of Different Phase Transitions Temperatures of Binary Perovskites with Change in Their Interatomic Bond Strains

G. A. Geguzina[1]*, I. G. Popova[2], A. A. Panich[3]

[1]*Southern Federal University, Research Institute of Physics, Rostov-on-Don, Russia,*
[2]*Don State Technical University, Department of Physics, Rostov-on-Don, Russia*
[3]*Southern Federal University, Institute of High Technology and Piezotechnics, Rostov-on-Don, Russia*

*geguzina@sfedu.ru

Perovskite structure binary oxides ABO_3, possessing the consecutive phase transitions (PTs): ferro- (FE) or antiferroelectric (AFE) at Curie temperature T_C, and ferro- (FM), antiferro- (AFM) at Neel temperature T_N, which can be called multiferroics (MFs), and also classical ferro- and antiferroelectrics without any magnetic PTs are considered.

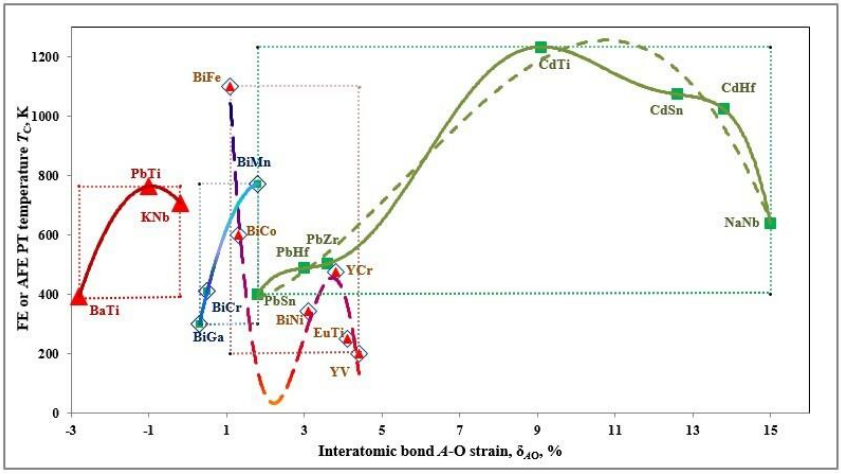

Fig. 1. Rectangular change in T_C areas for FE and AFE PTs of binary perovskites and MFs with a change in their interatomic bond *A*-O strains, and the corresponding dependences $T_C(\delta_{AO})$.

The goal is to find out to what extent the areas of change in their interatomic bonds *A*-O strains, δ_{AO}, are separated from each other together with their different nature PT's temperatures and their differences, or how much they overlap with each other by constructing these areas using the calculated values of δ_{AO}. Previously, we studied all of these characteristics for different perovskite categories or separately, or together. At the same time, we found out what and how the temperatures T_C, T_N and their differences $T_C - T_N$ of considered binary perovskites depend on. It is noticed that ternary MFs with FE PTs occupy the δ_{AO} ranges: δ_{AO} = 0.1 – 1.4 %, where T_C = 203 – 385 K, and T_N = 11 – 213 K, that is less than those observed for the binary MFs with FE PTs: δ_{AO} = 1.1 – 4.4%, where T_C = 200 – 1100 K (Fig. 1) and T_N = 4.2 – 643 K. For example, the PTs temperature variation areas of classical binary ferroelectric and antiferroelectrics with their interatomic *A*-O bond strains change are clearly separated from each other, in contrast to MFs with FE and AFE PTs areas, which intersect with each other partially, as well as with the classical AFE oxides area. In these cases, the ranges of differences $T_C - T_N$ in the same δ_{AO} ranges are as follows: $T_C - T_N$ = 50 – 214 K for ternary MFs, and for binary MFs, it is much wider: 43 – 452 K. However, binary MFs with AFE Ps are clearly distinguished from classic AFE oxides.

Acknowledgement. The study was financially supported by the Ministry of Science and Higher Education of the Russian Federation [State task in the field of scientific activity, scientific project No. 0852-2020-0032 (BAS0110/20-3-08IF)].

The Effect of Mechanical Activation on the Microstructure and Dielectric Properties of a Multicomponent System Based on Alkali Metals Niobates

E. V. Glazunova[a]*, L. A. Shilkina[a], A. V. Nagaenko[b], I. A. Verbenko[a], L. A. Reznichenko[a]

[a]*Research Institute of Physics, Southern Federal University, Rostov-on-Don, 344090, Russia*
[b] *Institute of High Technology and Piezo Technic, Southern Federal University, Rostov-on-Don, Russia*

*kate93g@mail.ru

The interest in the search for and development of bases for lead-free ferropiezoelectric materials has not decreased for several decades. One of the most popular materials for the construction of lead-free multi-component systems is sodium potassium niobate (KNN). The works aimed at increasing the combination of mechanical quality factor and piezoactivity are particularly relevant [1]. Despite on the great interest in these compositions, their preparation complicated by the critical dependence of the properties of lead-free ceramics on their thermodynamic history [2, 3]. Therefore, many works study the effect of mechanical activation (MA) on the synthesis and properties of solid solutions based on KNN [2]. Thus, the purpose of this work was to study the effect of MA on the particle size distribution and properties of solid solution $Li_aK_bNa_cNb_dTa_mSb_nO_3$ modified ($BiFeO_3$ + $CuNb_2O_6$). The raw materials were $NaHCO_3$ (99%), $KHCO_3$ (98%), Li_2CO_3 (98%), Nb_2O_5 (98%), Ta_2O_5 (99%), Sb_2O_5 (99%), Fe_2O_3 (98%), Bi_2O_3 (99%), and preliminarily synthesized $CuNb_2O_6$. The solid solutions were synthesized by the solid-phase method in two stages at T_1 = 1000 °C, T_2 = 1100 °C for 6 h, followed by sintering according to the conventional ceramic technology T_{sint} = 1195 °C for two hours. MA was carried out in an AGO-2 planetary mill in an alcohol medium using ZrO_2

grinding balls for 5 – 20 min. (drum rotation speed 1800 rpm). It established that when using MA, it is possible to reduce the inhomogeneity of the granulometric composition. The average size of crystallites reduced for a short MA time (5 min). The use of MA led to an increase in the values of the permittivity, as well as to a qualitative change in the thermal-frequency behavior of the dielectric properties of solid solutions was established.

Acknowledgement. The study was carried out with the financial support of the Ministry of Science and Higher Education of the Russian Federation, State task in the field of scientific activity, scientific project No (0852-2020-0032)/(BAZ0110/20-3-07IF) using the equipment of the Collective Use Center "Electromagnetic, Electromechanical and Thermal Properties of Solids" of the Research Institute of Physics.

References

[1] Andryushin K. P., Pavlenko A. V., Verbenko I. A., Turik A. V., Dudkina S. I., Reznichenko L. A. Lead-free ferroelectric materials with a wide range of mechanical quality factors, dielectric and piezoelectric activity // Structures from Composite Materials. **2**, 53 – 59, 2011.

[2] Beltrami R., Mercadelli E., Baldisserri C., Galassi C., Braghin F., Lecis N. Synthesis of KNN powders: Scaling effect of the milling step // *Powder Technology*. **375**, 101 – 108, 2020.

[3] Zhang Ya., Zhai J., Xue Sh. Effect of three step sintering on piezoelectric properties of KNN-based lead-free ceramics // *Chemical Physics Letters*. **758**, 137906, 2020.

The Phase Formation and Properties of Solid Solutions in the $(1-x)BiFeO_3-(x/2)PbFe_{1/2}Nb_{1/2}O_3-(x/2)PbFe_{2/3}W_{1/3}O_3$ System

E.V. Glazunova*, L. A. Shilkina, A. V. Nagaenko, I. A. Verbenko, L. A. Reznichenko

Research Institute of Physics, Southern Federal University, Rostov-on-Don, 344090, Russia

*kate93g@mail.ru

Presently, one of the most intensively studied areas of materials science is multiferroics (materials with a combination of electrical, magnetic, and elastic ordering). They are attracting attention due to their wide range of possible applications. Bismuth ferrite (BFO), as well as ferroniobate (PFN) and lead ferrotungstate (PFW), are representatives of this class of materials and are currently considered as the basis for the creation of magnetoelectric devices. However, the widespread application of these materials in the industry is limited by several factors. Thus, it is well-known the preparation of BFO in a single-phase state is difficult due to its location at the boundary of stability perovskite compounds. Moreover, the presence of ions of variable valence (Fe^{2+}/Fe^{3+}) and oxygen vacancies in these compounds leads to the high electrical conductivity of objects. Despite on this, the creating of solid solutions based on the above compounds allows one to stabilize the perovskite structure and improve the properties of materials. Thus, the study of regularities of phase formation, microstructure formation and dielectric responses of ceramics of the system $(1-x)BiFeO_3-(x/2)PbFe_{1/2}Nb_{1/2}O_3-(x/2)PbFe_{2/3}W_{1/3}O_3$ is relevant. The solid solutions of the $(1-x)BiFeO_3-(x/2)PbFe_{1/2}Nb_{1/2}O_3-(x/2)PbFe_{2/3}W_{1/3}O_3$ ($0.05 \le x \le 0.50$, $\Delta x = 0.05$) system were the subjects of this study. The solid solutions were prepared using a two-stage solid-state synthesis at T_1 = 800 °C, T_2 = 850 °C; $\tau_1 = \tau_2$ = 10 h, including mechanoactivation. The sintering was carried out using conventional ceramic technology at T_{sint} = 870 – 890 °C, τ = 2 h. X-ray diffraction demonstrated that a series of phase transitions appear in the system under study at room

temperature: the objects have a rhombohedral crystal structure at $0.05 \leq x \leq 0.30$, a transition from the rhombohedral to the cubic phase through the pseudocubic phase occurs at $0.30 \leq x \leq 0.40$, and the objects have a cubic crystal structure at $x \geq 0.40$. Analysis of the microstructure demonstrated that sintering occurs in the presence of a liquid phase, and there is also a correlation between X-ray and microstructural data. The transition to the cubic phase leads to compaction of the microstructure and increasing its homogeneity. The study of the dielectric characteristics demonstrated that the objects under study exhibit relaxor behavior associated with the Maxwell-Wagner polarization caused by the accumulation of oxygen vacancies in the structure due to a change in the oxidation state of ions with variable valence. The anomaly on the dependences of dielectric characteristics was found at $0.30 \leq x < 0.50$, in region of $T = 550 – 570$ °C, depending on the composition, which can be associated with structural changes. The obtained data is advisable to use in the development of new materials based on multiferroics.

Acknowledgement. The study was carried out with the financial support of the Ministry of Science and Higher Education of the Russian Federation, State task in the field of scientific activity, scientific project No. (0852-2020-0032)/(BAZ0110/20-3-07IF), using the equipment of the Collective Use Center "Electromagnetic, Electromechanical and Thermal Properties of Solids" of the Research Institute of Physics.

Prospects of the Vector Scalar Arrays Usage for Underwater Communications

G. M. Glebova, G. A. Zhbankov, O. A. Maltseva*

Institute for Physics, Southern Federal University, Rostov-on-Don, Russia

*oamaltseva@sfedu.ru

In underwater communication, the acoustic method of sending and receiving messages is the most common method. Underwater communications are known to be difficult due to factors such as multipath, limited bandwidth and severe signal attenuation, especially over long distances. The most realistic way to increase the reliability of communication is the use of towed arrays for receiving. Vector scalar receiving systems (VSRSs) are a relatively new type of hydroacoustic systems for various purposes. Signal detection algorithms based on VSRSs for onboard systems and systems operating against the background of sea noise have shown their significant advantage over scalar ones. This advantage is due to the power flow signal processing. Towed receiving systems are usually used for underwater communications. Since the main source of interference in such arrays is considered to be the noise generated by the towing vehicle itself (a ship or a submarine), it is necessary to know the experimental characteristics of the hydrodynamic noise (HN) of the towing vehicle. This paper presents an experimental study of such noises. In the experiment, an array was used in which the vector component was calculated as a pressure gradient, using two spaced hydrophones. The receiving array had an aperture of 10 m, the operating range was from 0.02 to 2 kHz. Towing was carried out by a surface vessel at a depth of 10 m with a cable length of 50 m. Analysis of the spectral, correlation and statistical characteristics of the HN for all components of the acoustic field required for signal processing in the proposed detection algorithms using scalar, vector components and power flux revealed a number of features that distinguish the characteristics of the HN from the noise, generated by the disturbed sea surface. Due to the

small-scale structure of the turbulent flow, the signal on two closely spaced sensors is not correlated even when the distance between them is much less than the wavelength. As a consequence, the noise power at the vector component is twice as high as the noise power at the scalar sensor, while for sea noise the noise power at the vector receivers is four times less than at the scalar sensors. This fact was confirmed by an analysis of the spatial correlation characteristics of the HN: (i) in the entire operating frequency range, all components of the acoustic field at the array aperture are not correlated, while for sea noise, the correlation radius is at least half the wavelength; (ii) as a consequence, the noise power on the vector component is two times higher than the noise power on the scalar sensor, and for sea noise, the noise power on vector receivers is 3 – 4 times less than on scalar sensors; (iii) the power flux has a Laplace distribution, and the variance of the flux component decreases much faster than the variance of the scalar and vector components of the field. The statistical characteristics for the power flux of the HN are similar to the characteristics of sea noise and interference in the direct vicinity of the ship. This shows that the creation of vector scalar towed arrays is one of the promising ways that contribute to an increase in the quality and range of underwater communications.

Software Module Drawing and Report Generation Based on the Results of Two-Dimensional Rod Metal Structure Strength Validation

S. G. Glushko[1], Yu. Yu. Shatilov[1], A. V. Cherpakov[1,2]

[1]Don State Technical University, Rostov-on-Don, Russia
[2]Southern Federal University, Rostov-on-Don, Russia

glsege98@gmail.com

Rod structures are widespread in construction due to a number of advantages, such as economy, versatility, freedom of design shapes and sizes.

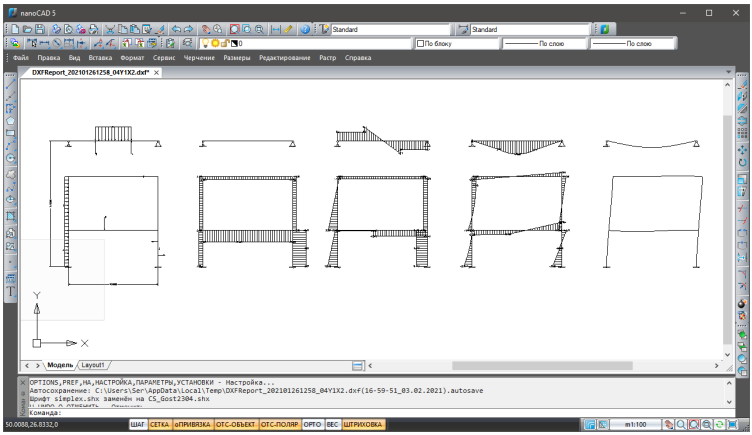

Fig. 1. Plot drawing of a bar and a statically indeterminate frame

Due to these characteristics of rod structures, their modeling and calculation are urgent tasks in the design of building structures. Automatic solution of these problems leads to an increase in design efficiency and calculation accuracy and lower costs. This report presents a software module that generates output documents of a web application for calculating rod metal structures. The software is developed in C# on the .NET platform using the Spire.Doc and netDxf plug-in libraries. The module generates AutoCAD-compatible drawings and text reports in accordance with Russian standard SP 16.13330. The internal forces in the structure are preliminarily calculated using the finite element method 0. Information output for each section is carried out in accordance with the requirements for a specific type of section and structural element. Figure 1 shows an example DXF drawing opened with nanoCAD. The possibility of automated generation of reports allows more efficient use of the computing complex in production, which makes it a useful instrument for design engineers.

Acknowledgement. The study was supported by the Russian Science Foundation grant No. 22-29-01259, https://rscf.ru/project/22-29-01259/.

Reference

[1] Glushko S. G., Shatilov Yu. Yu. // *Engineering Journal of Don*, **76**(4), 97 – 104, 2021.

Detection of Osteoporosis Diagnostic Signs in Quantitative Ultrasound Bone Inspection

E. V. Glushkov[1]*, N. V. Glushkova[1], O. A. Ermolenko[1], A. Tatarinov[2]

[1]Institute for Mathematics, Mechanics, and Informatics, Kuban State University, Krasnodar, 350040, Russia
[2]Riga Technical University, Riga, LV-1048, Latvia

*evg@math.kubsu.ru

Being non-radiative, non-invasive, and relatively cheap, Quantitative Ultrasound (QUS) is a promising tool for assessing the quality of bone tissue. Uncovering the regularities of guided wave (GW) propagation depending on the bone thickness, porosity, and effective elastic moduli (degree of mineralization), as well as accounting for the presence of surrounding soft tissues, can provide hidden signs of osteoporosis to improve its diagnostics [1, 2]. Our report aims to present and discuss the results of experimental measurements and analytically based computer simulation of ultrasound GWs, generated in samples (phantoms), mimicking real bones to identify such signs predicting osteoporosis. To focus on the influence of porosity and soft covering, bi-layer phantoms (gelatin/PMMA) with regular sets of holes drilled to the half-thickness of the PMMA plate have been of prime concern. Frequency B-scans and time-frequency patterns obtained using discrete Fourier transform and windowed wavelets are analyzed. Promising results are obtained with the matrix pencil method (MPM) [3], allowing wavenumber estimation of the excited GWs, including their imaginary parts, that is the attenuation decrements depending on the porosity level. Analytically based computer simulation provides a deeper insight into the influence of bone structure on the GW characteristics. The computer models are based on explicit integral and asymptotic representations via the waveguide's Green matrix. In addition to the case study, these models are used to assess effective elastic moduli and thicknesses using the experimentally obtained GW characteristics, similar to those implemented in the case of fiber-reinforced [4] and nano-wared [5] composite structures. Extraction of the effects of mode repulsion, zero group

velocity (ZGV), and thickness resonances from the measured data to use them as diagnostic signs and the influence of soft covering on their distinguishing are also discussed.

References

[1] Moilanen P., et al. // *Ultrasound in Med. Biol*., **32**, 709 – 719, 2006
[2] Tatarinov A., et al. // *Ultrasonics*, **54**, 1162, 2014
[3] Chang C. Y., Yuan F. G. // *Ultrasonics*, **89**, 143 – 154, 2018
[4] Eremin A. A., et al. // *Comp. Struct*., **125**, 449 – 458, 2015
[5] Glushkov E., et al. // *Appl. Sci*., **8**, 2319, 2018

Multi-layered Acoustic/Elastic Metamaterials with Arrays of Strip-like Cracks: Modelling and Manufacturing

M.V. Golub[1]*, S.I. Fomenko[1], O.V. Doroshenko[1], I. Moroz[2], E. Okoneshnikova[1], Y. Wang[3], C. Zhang[3]

[1]Institute for Mathematics, Mechanics and Informatics, Kuban State University, Krasnodar, Russia
[2]Membrane Institute, Kuban State University, Krasnodar, Russia
[2]Chair of Structural Mechanics, Department of Civil Engineering, University of Siegen, Siegen, Germany

*m_golub@inbox.ru

Nowadays composite materials and smart structures are used extensively in the aerospace industry, mechanical and civil engineering, and many high-performance facilities due to their enhanced properties. In recent years, a novel class of composites, the so-called phononic crystals and acoustic/elastic metamaterials (AMMs), providing several unusual properties has been receiving special attention in the scientific community. AMMs are composites periodically engineered to have special properties arising from the composition of two or several material components. For the wave propagation analysis, efficient and accurate mathematical models and numerical simulation tools should be developed for fast parametric studies at the development stage or the implementation in real electromechanical devices and systems. In particular, they should take into account the coupled mechanical and electrical fields, complex shapes of sensors as well as wave-fields scattered by inhomogeneities located at the surfaces or inside the structures. In this study, the boundary integral equation method is employed to simulate periodic arrays of cracks and electrodes in layered AMMs, where sub-layers are periodically arranged. Also, the frequency-domain spectral element method (FDSEM) and a hybrid approach based on the semi-analytical BIEM and the FDSEM are employed to simulate the elastic wave propagation in multi-layered AMMs with a finite number of inhomogeneities and a network of piezoelectric transducers mounted on their surface. The proposed method incorporates the advantages of the BIEM, which is efficient to model the wave propagation in elastic, piezoelectric, dielectric elastomer or functionally graded waveguides with electrodes and cracks, and the FDSEM, which is convenient for the discretization of the surface-mounted components (such as piezoelectric actuators or sensors, stiffeners, T-joints, etc.). The results of numerical analysis (reflection/transmission coefficients, band-gaps and pass-band formation) are demonstrated. The manufacturing of the proposed configurations of AMMs is also discussed, and some examples of the structures based on the proposed AMMs are demonstrated. Possible applications of these AMMs as wave filters or converters are discussed.

Zero-Point Energy of Compressed Rare-Gas Crystals in the Model of Deformable Atoms

Ie. Ie. Gorbenko[1]*, E. A. Pilipenko[2], I. A. Verbenko[3], E. V. Glazunova[3]

[1]Lugansk State Pedagogical University, Lugansk, Ukraine
[2]Donetsk A. A. Galkin Physics and Technology Institute, Donetsk, Ukraine
[3]Research Institute of Physics, Southern Federal University, Rostov-on-Don, Russia

*e_g81@mail.ru

Rare-gas crystals (RGCs) (He is the exception) form the *fcc*-structure with one atom in the unit cell. They are the simplest molecular crystals that are confined by comparatively weak Van-der-Waals forces. As a result, RGCs are frequently used as standard test objects in many theoretical studies. The dynamic matrix of rare-gas crystals was constructed by us on the basis of an *ab-initio* short-range repulsive potential, taking into account the three-body interaction and deformation of electron shells of dipole-type atoms within the pair and three-body approximations. *Ab-initio* calculations of the zero-point energies for compressed rare-gas crystals are performed at two mean-value points (the values of which are determined by the Chadi-Cohen method) in a wide pressure range. The numerical analysis showed the contribution to the zero-point energy from dipole-type electron shell deformation within the pair and three-body approximation increases with an increase in pressure (compression). In this case, the relative contributions from three-body forces due to the electron shell overlapping are small and only slightly increase with an increase pressure for Kr and Xe. Unfortunately, we know experimental data on the zero-point energy E_{zp} for Ne, Ar, and Kr only at $p = 0$. Our calculated E_{zp} value in model that takes into account three-body forces due to the electron shell overlapping and electron shell deformation for dipole-type atoms within the pair and three-body approximations is 79.185 K. The experimental zero-point energy for Ne is $E_{zp} = 78.5$ K. The discrepancy of our calculation result compared to the experimental value is $\gamma = 1.4$ %. The experimental zero-point energy is $E_{zp} = 86.1 \pm 2.5$ K for Ar (the discrepancy is $\gamma = 11.95$ %) and $E_{zp} = 67.4 \pm 3$ K for Kr (the discrepancy is $\gamma = 7.77$ %). The worst consistency between our and experimental E_{zp} values is for Ar; although, it should be taken into account that the experimental error is 3 % for Ar and 4 % for Kr. Thus, our results of calculating E_{zp} with allowance for three-body forces and deformation of dipole-type atomic electron shells within the pair and three-body approximations are in satisfactory agreement with the experiment data.

Acknowledgement. The work was funded by the Ministry of Science and Higher Education of the Russian Federation, State task in the field of scientific activity, scientific project No. (0852-2020-0032)/(BAZ0110/20-3-07IF). The equipment of the Center of Research Institute of Physics SFedU was used.

Research of the Photoconductivity Characteristics of ZnO – SnO_2 Sol-gel Thin Films

I. A. Gulyaeva[1]*, A. V. Nesterenko[1], A. V. Petrov[2], V. V. Petrov[1]

[1]Southern Federal University, Institute of Nanotechnologies, Electronics, and Equipment Engineering, Taganrog, Russia
[2]Municipal Autonomous Educational Institution Lyceum No. 4 (TMGL), Taganrog, Russia.

*iten@sfedu.ru

In this work, we studied the photoconductivity parameters of thin ZnO – SnO_2 films formed by the sol-gel method on opaque substrates. Nanocomposite ZnO – SnO_2 films were deposited on polycor substrates with a Zn:Sn molar ratio of 0:100, 1:99, 0.5:95.5, 5:95, 50:50 and annealed at a temperature of 550 °C. The film thickness was 150 – 200 nm. Over the films, by thermal vacuum evaporation through a mask, interdigital contact V-Ni metallization was deposited and a planar photoresistor with an initial "dark" resistance R_0 was formed. The electrophysical and gas sensitive properties of these films were studied in [1]. In this work, we studied the direct change in photoconductivity under the action of light from an LED with a peak wavelength of 470 nm, which forms an illumination level of 525 lux on the sample. The measurements showed that the ultraviolet component was absent in this case. Radiation parameters were measured using a CENTER 532 ultraviolet radiation intensity meter (China) and a CENTER 530 light meter (China). Measurements were carried out until the beginning of the "flattening" of dependencies. In this case, a change in the photoconductivity was observed for all the films under study. Subsequently, the time constant of the generation of charge carriers under the action of light was calculated. Studies have shown that pure tin dioxide has the longest time constant for the generation of charge carriers of 87 s. Zinc oxide additions of 0.5 % and 5 % to tin oxide sharply reduce the time constant to 17 – 19 s. At the same time, with the addition of 1 % zinc oxide, an increase in the time constant to 43 s is observed. The fastest response time of 9 s is found in a sample with a Sn:Zn ratio of 50:50. This behavior of the photoconductivity parameters is associated with the nanocomposite structure of the film material, and lower values of the time constant are associated with a higher concentration of charge carrier generation centers at the ZnO – SnO_2 interface at a Sn:Zn ratio of 50:50. It can also be noted that the response kinetics for all the films was similar, which indicates the same generation mechanisms, namely the recombination of charge carriers in the sol – gel SnO_2 films with the addition of ZnO. Thus, the photoconductivity kinetics of thin ZnO – SnO_2 films, formed by the sol-gel method, was measured and the time constant of charge carrier generation was calculated. The calculations showed that the time constant has a minimum value of 9 s for ZnO – SnO_2 films with a Zn:Sn ratio of 50:50.

Acknowledgement. The study was supported by the Russian Science Foundation grant No. 22-29-00621, https://rscf.ru/en/project/22-29-00621/ at the Southern Federal University.

Reference

[1]. Starnikova A. P., Gulyaeva I. A., Storozhenko V. Yu., Volkova M. G., Bayan E. M., Petrov V. V. Study of the electrophysical and gas-sensitive properties of thin ZnO – SnO_2 films formed by the sol-gel method // *Journal of Physics: Conference Series*, **2103**, 012132, 2021.

Design and Optimization of a Compliant Mechanism for Vibration-Assisted Drilling

Hai-Thanh Nguyen, Van-Khien Nguyen, Huy-Tuan Pham, Quang-Khoa Dang*, Son-Minh Pham

Faculty of Mechanical Engineering, Ho Chi Minh City University of Technology and Education, Ho Chi Minh City Vietnam

*khoadq@hcmute.edu.vn

Compliant Mechanisms (CMs) are the external force-based dynamic and variable mechanisms based on the elastic deformation of materials with advantages such as compactness, high accuracy, ease of fabrication, and application in many different fields [1]. In this work, a case study of using flexible hinges in drilling applications for a non-resonant vibration-assisted drilling application is proposed. The geometric design of the mechanism was optimized using finite element analysis (FEA) based on NSGA-II optimization procedure, aiming to maximize the natural frequencies. The optimization procedure is programmed in MATLAB whereas the ANSYS Mechanical ADPL-code is embedded to support and enhance the calculation process. Finite element analysis was performed to verify for the accuracy of the design model. The analysis shows that the discrepancy between the optimization results and the FEA results is 1.7% for the displacement and 0.6% for the dynamic frequency of the designed mechanism. Finally, the structure, using the optimal parameters, will be fabricated and performed the system performance testing. The developed mechanism (Fig. 1) includes outer and inner base. The outer base will be located on the machining base and linked to the inner base via flexible hinges. Guiding shaft and sliding bearings will guild the inner base therefore only vertical movement remain on it which will be actuated by piezoelectric actuators.

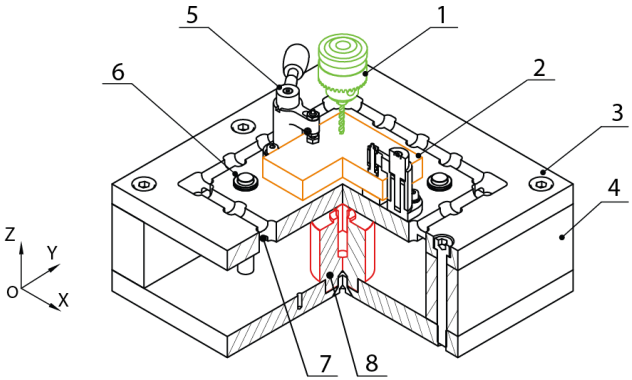

Fig. 1. Structure of VADrill system: drill machine (1), workpiece (2), outer base (3), support (4), clamp workpiece (5), slide bearing (6), flexible hinge (7), piezoelectric actuator (8)

Acknowledgement. This work was supported by the Ho Chi Minh City University of Technology and Education and the project grant No. B2021-SPK-02 funded by the Ministry of Education and Training and hosted by Ho Chi Minh City University of Technology and Education, Vietnam.

References

[1] Nguyen K.H., Nguyen V.K., Pham H.T. Dang Q.K., Hoang T. K., Pham S. M., In: *2020 Physics and Mechanics of New Materials and Their Applications*, 332 – 338, 2020.
[2] Dang Q.K., Chang P.L., Dang T.N., Weng F., Uan J.Y., Wang D.A. // *Journal of Materials Processing Technology*, **266**, 208 – 216, 2019.
[3] Nguyen V.K., Pham H.H., Pham H.T. // *Modern Environmental Science and Engineering*, **4**(5), 469 – 475, 2018.
[5]. Wang D.A., Chuang W.Y., Hsu K., Pham H.T. // *Ultrasonics*, **51**, 148 – 156, 2011.

Design, Modeling, and Comparison of Energy Generators with Dual-Mode Piezoelectric Material

R. K. Haldkar[1]*, I. A. Parinov[1], A.V. Cherpakov[1,2], O. V. Shilyaeva[2]

[1]Southern Federal University, Rostov-on-Don, Russia
[2]Don State Technical University, Rostov-on-Don, Russia

*rakeshhaldkar@gmail.com

In this report, a new design of an energy generator with d_{31} piezo-patches and d_{33} piezo-cylinders is analysed and compared. Based on the generic coupled technique, this work is focused on a coupled piezoelectric-permanent magnet-electromagnetic energy harvesting technique that converts energy using an extended cantilever beam design. The permanent magnet is attached at the free end, and it also works as a proof mass. The electromagnet is used to generate impulse and reactive forces. The force causes a deflection to the permanent magnet. Numerical simulations were carried out to calculate their natural frequencies and output voltages. The different positions of the piezo-patches and piezo-cylinders are analysed and the output characteristics are compared. Software ANSYS is used for the numerical solutions.

Acknowledgments. The equipment's of SFedU was used. The authors acknowledge the support by Southern Federal University, grant No. VnGr-07/2020-04-IM (Ministry of Science and Higher Education of Russia).

Study on Biochar Amendment in Food Waste Composting Process to Reduce Odorous Emissions

Hsueh Chen Shen[1], Ching Ti Yeh[2], Chin Ko Yeh[2], Ming Hong Zheng[3], Chitsan Lin[3]*

[1]Ph.D. Program in Maritime Science and Technology, College of Maritime, National Kaohsiung University of Science and Technology, Kaohsiung 81157, Taiwan (R.O.C.)
[2]Department of Marine Engineering, National Kaohsiung University of Science and Technology, Kaohsiung 81157, Taiwan (R.O.C.)
[3]Department of Marine Environmental Engineering, National Kaohsiung University of Science and Technology, Kaohsiung 81157, Taiwan (R.O.C.)

*ctlin@nkust.edu.tw

According to United Nations statistics, about 1.3 billion tons of food are thrown away annually worldwide. In Taiwan, according to statistics from the Environmental Protection Agency (Taiwan EPA) in 2018, more than 590,000 metric tons of food waste was recycled nationwide. In 2020, Taiwan EPA reported the daily recovery averaged at 1,447 metric tons is an increase of 6 % compared to that of 1,365 metric tons in 2019. Therefore, a diversified food waste resourcing and reuse scheme is in demand. Food waste composting can significantly reduce the amount of municipal solid waste to reduce the burden of the incinerator. The finished compost product is high-quality organic fertilizer, and it is the best soil conditioner to maintain fertilities. However, the successful food waste composting operation is seriously hindered by the emissions of malodorous gases. In order to reduce the odorous gases production and to preserve the nutrients, the amendment of various proportions of biochar was employed in this study to optimize the food waste composting processes. Adding biochar can increase the starting pH of initial compost mixture that may benefit to the thriving of bacteria at the initial stage of composting. Compost porosity can also be increased by adding biochar; thus, aerobic composting environment is favored. Biochar is also known rich in adsorption capacity, therefore, reduction in odorous gases emission is well anticipated. Finally, our results have demonstrated that adding different proportions of biochar can effectively adsorb NH_3 and H_2S and other odorous substances. The removal efficiency of odor substances reached 99 % by adding 5 % of washed biochar, which achieves the best effect of odor reduction. Therefore, adding biochar, particularly washed biochar, is suggested for future food waste composting processes.

Registration of Magnetic Particles in a Biological Medium with Using Magnetometers

L.P. Ichkitidze[1,2]*, M.V. Belodedov[3], A.Yu. Gerasimenko[1,2], D.V. Telyshev[1,2], S.V. Selishchev[1]

[1]Institute of Biomedical Systems of National Research University of Electronic Technology, MIET, Zelenograd, Moscow, Russia
[2]Scientific and Technological Park of Biomedicine of I.M. Sechenov First Moscow State Medical University, I.M. Sechenov University, Moscow, Russia
[3]*Bauman Moscow State Technical University, Russia*

*ichkitidze@bms.zone

Methods for non-invasive registration of magnetic nanoparticles in aqueous suspension (biological environment model) are considered. A simple analytical formula has been obtained for calculating the maximum distance l from the magnetic field sensor to the object under study, relating this distance to the parameters of magnetic particles and the threshold magnetic sensitivity δB of the sensor. Magnetic measurements of aqueous suspensions containing superparamagnetic nanoparticles of iron oxide (linear dimensions $\leq$ 30 nm) with a concentration of 1 – 5 wt. % [1]. The measured and calculated values l are compared for different values of residual magnetization. In the case when magnetic nanoparticles acquired magnetization in the Earth's magnetic field, they were recorded at a distance of $l \leq 23$ mm from the magnetic field sensor having $\delta B = 10$ nT. The estimate of the same distance, obtained by the proposed formula, was $l \approx 9$ mm. In another case, in a constant magnetic field of 100 mT, magnetic nanoparticles acquired a residual magnetization of 1.8 – 2.0 A·m^2/kg, and the measured and calculated distances (50 and 48 mm) practically coincided. It is shown that for some types of commercial magnetic nanoparticles with high remanent magnetization (> 50 A·m^2/kg), this distance can be $\leq$ 200 mm, that is they can be registered at a great depth of their occurrence in the human body. It is noted that at low concentrations of $\leq 10^{-5}$ wt. % of magnetic nanoparticles, they can only be controlled using magnetometers containing magnetically sensitive elements having ultra-low $\leq$ 10 fT, in particular SQUIDs [2], combined magnetic field sensors and nanostructured combined magnetic field sensors [3, 4]. Thus, experimental studies have shown: (i) using a magnetometer, it is possible to non-invasively control magnetic nanoparticles in an aqueous suspension; it is possible to estimate their concentration and residual magnetization, as well as the distance of their location to the magnetically sensitive element of the magnetometer, that is assess the depth of their occurrence in the biological environment; (ii) satisfactory correlations of calculated and experimental data on registration of magnetic nanoparticles were obtained. Apparently, non-invasive control of magnetic nanoparticles loaded with various drugs and antibodies will be in demand in theranostics. For example, knowing the magnetic parameters and the concentration of magnetic nanoparticles in the biological environment, one can adequately select the parameters of a remagnetizing alternating magnetic field for effective hyperthermia of cancer or, based on data on changes in the concentration of magnetic nanoparticles, evaluate the effectiveness of osteoarthritis therapy [5, 6].

Acknowledgement. The research was funded by the Ministry of Science and Higher Education of the Russian Federation under the grant No. 075-15-2021-596 (Sechenov University).

References

[1] https:/sileks.com/

[2] http://www.supracon.com/files/online/SQUIDSensoren/ms
[3] Pannetier M., Fermon C., Le Goff G., Simola J., Kerr E. // *Science*, **304**(5677), 1648 – 1650, 2004.
[4] Ichkitidze L. P., Selishchev S. V., Potapov D. A., et al. // *AIP Conf. Proceed.*, **2140**, 020028, 2019.
[5] Dallet L., Stanicki D., Voisin P., Miraux S., Ribot E. // *Scientific Reports*, **11**, 3286, 2021.
[6] Gambaro F. M., Ummarino A., Andón F. T., at el. // *Int. J. Mol. Sci.*, **22**(17), 9137, 2021.

The Role of Magnetic Particles and Nanoparticles in Cancer Hyperthermia

L. P. Ichkitidze[1,2], G. Yu. Galechian[1], A. Yu. Gerasimenko[1,2], D. V. Telyshev[1,2]

[1]Institute of Biomedical Systems of National Research University of Electronic Technology, MIET, Zelenograd, Moscow, Russia
[2]Scientific and Technological Park of Biomedicine of I.M. Sechenov First Moscow State Medical University, I.M. Sechenov University, Moscow, Russia

*ichkitidze@bms.zone

Magnetic hyperthermia is a new treatment method in which irreversible thermal ablation of a pathological target is performed. This occurs due to the generation of heat and an increase in the local temperature of the dispersion with magnetic nanoparticles (MNPs). As a result, the viability of cancer tissue cells is significantly reduced in the temperature range of 41– 46 °C, while healthy cells can survive. We analyzed literature sources in which MNPs based on iron oxides with different physical parameters were used for cancer hyperthermia. In particular, they were spherical superparamagnetic nanoparticles (SPION) with iron oxide γ-Fe_2O_3 SPION with an average diameter of $d \sim 11$ nm and a saturation magnetization of $M \sim 4$ emu/g [1], as well as Fe_3O_4 SPION particles ($d \sim 5$ nm) with a value of $M \sim 20 – 25$ emu/g [2]. In the *in-vitro* mode during hyperthermia, in the case of large sizes of Fe_3O_4 MNPs ($d \geq 20$ nm) and low $M \sim 10$ emu/g, the tissue temperature increased by $\Delta T \sim 0.7$ °C, and at large $M \sim 70$ emu/g the tissue additionally warmed up by $\Delta T \sim 2.0$ °C [3]. For Fe_3O_4 magnetic nanoparticles with diameters in the range of 30 – 80 nm, the maximum efficiency was obtained at a level of ~ 0.9 kW of allocated power per 1 g of magnetic nanoparticles [4]. It is noted in many works that the heating efficiency depends on many factors, and the main ones are: the magnetic energy stored in the magnetic nanoparticles, the parameters of the alternating magnetic field, and the dosage of the magnetic nanoparticles. The shape of the magnetic particles is also important. For example, in rod-like nanoparticles ($d \sim 100$ nm), due to their magnetic anisotropy, the value of M is much higher than in spherical magnetic nanoparticles. In this regard, it can be assumed that bacterial magnetosomes and carbon nanotubes with MNPs will also be promising for cancer hyperthermia. In general, hyperthermia using magnetic particles is a complex technique that depends on numerous parameters, therefore its effectiveness in the treatment of cancer has not yet been optimized. However, at present, hyperthermia for the treatment of cancer has moved from laboratory research to clinical trials.

Acknowledgement. The research was funded by the Ministry of Science and Higher Education of the Russian Federation under the grant No. 075-15-2021-596 (Sechenov University).

References

[1] Burinaru T. A., et al. // *IOP Conf. Ser.: Mater. Sci. Eng*., **485**, 012005, 2019.

[2] Gutierrez F. V., et al. // *Nanomaterials*, **11**, 2197, 2021.
[3] Yu L., et al. // Scientific Reports, **4**, 7216, 2014.
[4] Simeonidis K., et al. // *ACS Appl. Nano Mater*., **3**, 4465 − 4476, 2020.

Thin Film Superconducting Magnetic Field Concentrator

L. P. Ichkitidze[1,2]*, A. Yu. Lysenko[1]

[1]Institute of Biomedical Systems of National Research University of Electronic Technology, MIET, Zelenograd, Moscow, Russia
[2]Scientific and Technological Park of Biomedicine of I.M. Sechenov First Moscow State Medical University, I.M. Sechenov University, Moscow, Russia

*ichkitidze@bms.zone

Most magnetic field sensors (MFSs) have high resolution, that is low threshold sensitivity: $\delta B_0 \leq 1$ nT, achieved through the use of superconducting film magnetic field concentrators (MFCs). They decrease in the MFSs, in which various structures can serve as magnetosensitive elements (MSEs), such as Josephson junctions, Hall sensors, sensors based on spintronic effects, etc. [1 – 4]. In this work, we study a planar structure (see Fig. 1), in which the MFCs and MSEs are on the same plane and do not intersect with each other. The above structure had the following parameters. Figure 1*a*, *b*: receiving rings 1 – 2 mm outer diameter, 0.8 mm ring width; 2 – substrate; 3 – active bands (ABs), 30 μm wide; 4 – MCE having a width of 10 μm; 5 – the width w_a of the gap between the AB and MSE varied in the range 0.2 – 5 μm; $(0,0)$ is the coordinate system; (x_0, y_0) are the coordinates of the AB. All elements deposited on the substrate have the same thickness of 20 nm. Figure 1*c*, *d* and *e*: parallel sections in the AB are located uniformly across the width, unevenly far from the MSE and close to the MSE, respectively.

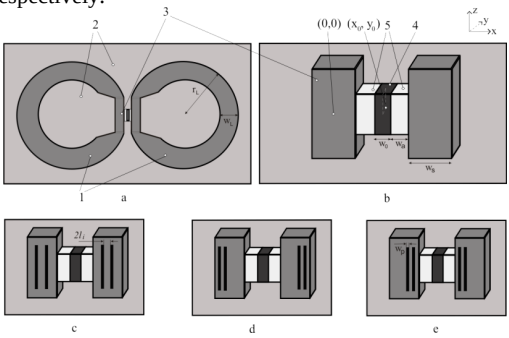

Fig. 1

The concentration factor F of the magnetic field is defined as the ratio of the average magnetic field at the MSE to the value of the external registered field B_0. It has been established that the MFC made from a film of a low-temperature superconducting material (LTSC, the penetration depth of the magnetic field is $\lambda \sim$ 50 nm) concentrates the magnetic field on the MCE, which has a degree of inhomogeneity of more than 20% in the range $B_0 \leq 1$ μT. MFC from a film of high-temperature superconducting material (HTSC, $\lambda \sim$ 1000 nm) concentrates the magnetic field on the MSE, which has a degree of inhomogeneity of less than 10%. It is shown that parallel cuts with coinciding widths increases the value several times, especially strongly for the case shown in Fig. 1*c*. In this case, for LTSC films, higher values

of F are realized as compared to HTSC films. The results obtained will improve the efficiency of existing magnetic field sensors in the form of a decrease in their threshold sensitivity, which will also make it possible to reduce the size of the receiving antenna and, accordingly, register magnetic particles with smaller sizes.

Acknowledgement. The research was funded by the Ministry of Science and Higher Education of the Russian Federation under the grant agreement No. 075-15-2021-596 (Sechenov University).

References

[1] Robbes D. // *Sensors and Actuators A: Physical*, **129**(1), 86 – 93, 2006.
[2] Pannetier-Lecoeur M., Parkkonen L., Sergeeva-Chollet N., et al. // *Appl. Phys. Lett*., **98**(15), 153705, 2011.
[3] Ichkitidze L. P. Superconducting film sensor of weak magnetic field with magnetic flux transformer // *Patent RU No. 2289870, 20.12.2006* (In Russian)
[4] Ichkitidze L. P., Mironyuk A. N. // *Physica C*., **472**(1), 57 – 59, 2012.

Films of Biological Nanomaterials as a Prototype of a Tactile Sensor

L. P. Ichkitidze[1,2]*, V. A. Petukhov[1], N. A. Demidenko[1], E. P. Kitsyuk[3], A. Y. Gerasimenko[1,2], D. V. Telyshev[1,2]

[1]Institute of Biomedical Systems of National Research University of Electronic Technology, MIET, Zelenograd, Moscow, Russia
[2]Scientific and Technological Park of Biomedicine of I.M. Sechenov First Moscow State Medical University, Sechenov University, Moscow, Russia
[3]*Scientific-Manufacturing Complex "Technological Centre", Zelenograd, Moscow, Russia*

*ichkitidze@bms.zone

The most sensitive mechanical receptors are found on the tips of the tongue and fingers. Their tactile sensitivity is in the range of 2 – 5 mg/mm^2 (20 – 50 Pa) with resolutions: spatial ~ 1 mm, temporal 700 Hz [1]. Various tactile sensors are currently being actively developed to approach these limits. Biological nanomaterials containing carbon nanotubes, upon deformation, acquire the properties of a tensoresistive effect. We studied the change in resistance R/R_0 from the bending angle θ of the film of biological nanomaterials and the possibility of their use as a prototype of a tactile sensor. Here R_0 is the resistance in the absence of deformation, R is the resistance in the presence of deformation. Films with a size of (0.05 – 0.5 μm) × (2 – 5 mm) × (10 – 20 mm) of bovine serum albumin (BSA) or microcrystalline cellulose (MCC), containing multi-walled carbon nanotubes (MWCNTs), served as a sensitive element to deformation. An aqueous dispersion of a composite nanomaterial was applied on flexible polyethylene terephthalate (PET) substrates with thicknesses of d_0 ~ 30 μm, 60 μm and paper ~ 60 μm. PET substrates at d_0 ~ 30 μm had weights of ~ 4 – 4.8 mg. Deformation and measurements of physical parameters were carried out automatically, the data were saved in a computer. Films with a thickness of d ~ 0.1 μm showed an optical transparency of ~ 80% and a high resistance of ~ 1 MΩ. Thin films (d < 0.2 μm) exhibited the properties of a bipolar strain sensor [2]; when bending in the form of a concavity, the resistance decreases, and when bending in the form of a bulge, the resistance increases. The bending strain sensitivity was determined as $S_\theta = (R/R_0 - 1)/\Delta\theta$, where $\Delta\theta$ is the change in the bending angle θ. Highest $S_\theta \approx$ 1.5%/deg was realized in a film made of MCC/MWCNTs nanomaterial with a thickness of d

~ 0.1 μm. The recalculation of the force coming to the bending area corresponded to 2 – 6 mg/mm^2 (20 – 60 Pa). These values are in the same order as the tactile sensitivity of human fingers. Apparently, an increase in the accuracy of measuring the film resistance (error ≤ 0.1%) will make it possible to record a detectable pressure ≤ 10 Pa. The films studied by us from composite nanomaterial BSA/MWCNTs and MCC/MWCNTs contain a small amount of carbon nanotubes (≤ 0.1%), have a high degree of biocompatibility, can be applied directly to the surface of human skin and be a prototype of a tactile sensor.

Acknowledgement. This work was financed by the Ministry of Science and Higher Education of the Russian Federation within the framework of state support for the creation and development of World-Class Research Centers "Digital Biodesign and Personalized Healthcare" No. 075-15-2020-926.

References

[1] Salim A., Lim S. // *Sensors*, **17**, 2593, 2017.

[2] Ichkitidze L.P., et al. Bipolar Strain Sensor Based on a Biocompatible Nanomaterial // *Patent RU No. 2662060, 23.07.2018* (In Russian).

Effect of Annealing Temperature on the Formation of Thin Nanocomposite Films of Co_3O_4 – ZnO

I. O. Ignatieva[1]*, I. A. Gulyaeva[2], V. V. Petrov[2], E. M. Bayan[1]

[1]Southern Federal University, Faculty of Chemistry, Rostov-on-Don, Russia
[2]Southern Federal University, Institute of Nanotechnologies, Electronics, and Equipment Engineering, Taganrog, Russia

*iignateva@sfedu.ru

Nanostructured film materials based on zinc oxide doped with various additives are of great interest in different fields of industry. The ability to use them as solar cells, gas-sensitive sensors, lasers, and LEDs in the UV-region of the spectrum is due to the availability of materials, as well as unique physical and chemical properties. The main purpose of this study was to investigate the effect of calcination temperature on the formation of thin nanocomposite films. During the two-stage synthesis by solid-phase pyrolysis, materials of zinc oxide containing 10 mol % Co_3O_4 were obtained according to the previously described method [1]. Zinc acetate dihydrate, cobalt (II) acetate tetrahydrate and organic acid were used as starting compounds. During the first stage, zinc and cobalt salts were melted in organic acid. The resulting mixture was further ground to a finely dispersed state, and an intermediate product was obtained. During the second stage, the intermediate product was dissolved in a non-polar solvent 1,4-dioxane. Then, the resulting solution was applied three times to the pre-prepared glass substrates. All substrates were calcined for 2 hours at 600, 700 and 800 °C. Nanostructured film materials were examined by XRD (diffractometer Thermo ARL, Switzerland) in CuKα radiation and scanning electron microscopy methods (SEM, scanning electron microscope Nova Nanolab 600). According to the results of X-ray phase analysis, it was found that the obtained materials are two-phase, because all the peaks of the final product are matched either with Co_3O_4 or ZnO. Moreover, the peak intensities of the hexagonal ZnO phase are much stronger than the peak intensities of Co_3O_4 phase. The particle sizes were calculated using the Scherrer formula. With an increase in the annealing temperature, the

particle size decreases and is about 23, 29, and 41 nm for films calcined at 600, 700, and 800°C, respectively. Thin nanocomposite films of Co_3O_4 – ZnO were obtained by solid-phase pyrolysis. The annealing temperature had a significant impact on the quality of film materials. Further study of the optical and electrophysical properties of the obtained composites is a promising direction in modern chemistry.

Acknowledgement. The study was supported by the Russian Science Foundation grant No. 22-29-00621 at the Southern Federal University.

References

[1] Petrov V. V. et al. // Synthesis, characterization and gas sensing study of ZnO – SnO_2 nanocomposite thin films // *Chemosensors*, 9(6), 124, 2021.

About the Monitoring of the Medium Stratification by the Parameters of the Surface Waves

Igor Andjikovich[1]*, Alexey Konovalov[1], Irina Michailova[1], Andrey Sedov[2], Artyom Turchin[1]**

[1]I. I. Vorovich Mathematics, Mechanics and Computer Sciences Institute, Southern Federal University, 344090, Rostov-on-Don, Russia
[2]M. I. Platov South-Russian State Polytechnic University, Novocherkassk, 346428, Russia

*ocean_8@mail.ru; **asedov@mail.com

The problem of non-destructive testing of the stress-strain state (SSS) of structures and the presence of defects in various mechanical objects is urgent, which determines the need to create new methods for monitoring the "serviceability" of complex structures to improve their reliable operation and prevent emergencies. In connection with the modern development of technology for the production of new materials and increased requirements for the characteristics of parts and assemblies, it becomes necessary to create simple and effective methods of continuous control (continuous monitoring) of the state of the object. The method of monitoring the state of an object, namely the presence of internal stresses, the occurrence and development of defects by analyzing the features of surface vibrations assumes the presence of a large number of control points in various nodes and structural elements. The vast majority of such systems use accelerometers. However, in some cases, the use of accelerometers is impractical and often impossible. Especially when it comes to monitoring the integral parameters of the controlled object. In such cases, it is advisable to use strain gauges that allow obtaining "integral information" about the state of the object. Of considerable interest are miniature ferroelectric film sensors of the generator type with a low intrinsic mass, a wide range of operating frequencies at relatively low cost. They are created using thin-film technology and represent a thin ferroelectric film deposited on a metal foil. Thus, an object was created that combines the high piezoelectric characteristics of ceramics with the high strength of the metal to mechanical stress. These sensors have shown high efficiency when used in systems for monitoring the state of bar structures. In this paper, we propose a system for monitoring the stress state of a structure based on the use of thin-film ferroelectric sensors. The object of observation is the wave field on the surface of a square metal rod, which is acted upon by a force applied at its center. The surface wave field is created by a pulse source located at one of the ends of the rod. Studies have shown that small changes

in the load lead to a significant change in the surface wave field, both in amplitude and in phase characteristics. The complex nature of the change in the parameters of the wave process does not allow sufficient control of their relationship with the deformation of the object. To establish a clearer connection between the wave field and the loading of the object, a bispectral method is used, which converts the signal coming from the sensor in the form of an amplitude-time diagram to a specific point in the two-dimensional space of recognition features. The studies carried out have shown a high sensitivity of a thin-film sensor compared to an accelerometer.

Acknowledgement. Research was financially supported by Southern Federal University, grant No. VnGr-07/2020-04-IM (Ministry of Science and Higher Education of the Russian Federation).

On the Problem of Monitoring the Safe Operation of Pipeline Transport

Igor Andjikovich[1]*, Valery Kalinchuk[2], Irina Michailova[2], Alexey Konovalov[2]**

[1]*I. I. Vorovich Mathematics, Mechanics and Computer Sciences Institute, Southern Federal University, Rostov-on-Don, Russia*
[2]*Southern Scientific Center of Russian Academy of Sciences, Rostov-on-Don, Russia*

***ocean_8@mail.ru; ****vkalin415@mail.ru

The problem of developing simple and effective methods for monitoring the state and resource capacity of pipeline transport based on low-frequency continuous monitoring is one of the most urgent in the reliability assurance system operation and prevention of emergencies, prevention and elimination of undesirable consequences of technological disasters. In this regard, the technique for registering the state of a product or structure by analyzing surface vibrations is a simple and effective method that allows one to obtain integral information about the state of the controlled object. The method of registering the state of the product by analyzing surface vibrations assumes the presence of a large number of control points in various nodes and structural elements. In this study, we propose a system for monitoring the occurrence and development of internal defects in a pipe, based on the use of miniature ferroelectric accelerometers. The object of monitoring is the wave field on the surface of a circular pipe. The surface wave field is created by a pulsed source located at one of the ends of the pipe. The complex of experimental studies carried out showed that small changes in the position of the defect on the inner surface of the pipe lead to certain changes in the wave field, both in amplitude and in phase characteristics. The complex nature of the change in the parameters of the wave process does not allow sufficient control of their relationship with the deformation of the object through the use of traditional methods of processing the recorded signal such as correlation, autocorrelation, cross-correlation, etc. In this work, to establish a clearer connection between the wave field and the state of the controlled object, the bispectral method is used, which converts the signal coming from the sensor in the form of an amplitude-time diagram to a specific point in the space of recognition features. This approach makes it possible to represent possible changes in the controlled object to geometric objects in the recognition space. The experiment showed that the most convenient and at the same time sufficient in terms of information content form for the implementation of such an approach is the presentation of information in the form of a two-dimensional image. The studies carried out have shown the high sensitivity of the proposed approach to changes of various nature.

Acknowledgement. This work was carried out within the framework of the implementation of the state assignment of the Southern Scientific Center of the Russian Academy of Sciences, state registration number 01201354242 with partial financial support from the Russian Foundation for Basic Research, project 19-48-230042.

Restoring the Time History of Non-stationary Loading Acting on a Cylindrical Isotropic Elastic Rod

L. A. Igumnov*, I. P. Markov

National Research Lobachevsky State University of Nizhny Novgorod

*igumnov@mech.unn.ru

Problem of the identification of time history of external loadings applied to structural elements has important practical significance. Since in the many instances direct measurements of loads is difficult or impossible, this class of problems is often considered in the framework of inverse problems of mechanics. Among other methods, the frequency domain approaches, e.g. [1, 2], are used to tackle such problems. In this work, using an original combined approach, we solve a problem of estimating the time dependence of external load with known geometrical distribution on the boundary of an isotropic elastic solid. Time domain structural response of the solid directly measured at some point by some other means serves as an input data. At the first step, we formulate an accompanying direct problem in the Laplace domain, where load with known time history is applied at exactly the same boundary area as the load in question. This accompanying problem is then solved with Laplace domain Boundary Element Method. After the solution is obtained the load in question firstly restored in Laplace domain and after that can be inverted to the time domain using some method for numerical inversion of Laplace transform or used to obtain structural responses in Laplace domain at other points of the solid. The described original technique is expanded to address the issue with effective sampling strategy for Laplace domain boundary element solution of the accompanying problem. The present approach is used to determine the time history of impact loading acting on a base of a long cylindrical metallic bar.

Acknowledgement. The work was financially supported by the Strategic Academic Leadership Program "Priority 2030" (internal number H-496-99_2021-2023).

References

[1] Boukria Z., Perrotin P., Bennani A. Experimental impact force location and identification using inverse problems: Application for a circular plate // *International Journal of Mechanics*, **5**(1), 48 – 55, 2011.

[2] Gombi S. L., Ramakrishna D. S. A solution to the inverse problem of impact force determination from structural responses // *International Journal of Engineering and Innovative Technology*, **1**(3), 192 – 196, 2012.

Analysis of the Driving and Dependence Power of the Barriers to Implement ERPII in Manufacturing Organizations

Inayat Ullah[1], Rakesh Kumar Haldkar[2]*, Ivan A Parinov[2]

[1]Department of Mechanical Engineering, G H Raisoni College of Engineering, Nagpur, Maharashtra, India
[2]I. I. Vorovich Mathematics, Mechanics and Computer Sciences Institute, Southern Federal University, Rostov-on-Don, 344090, Russia

*rakeshhaldkar@gmail.com

The purpose of this study is to analyse potential barriers that could impede Indian manufacturing organizations to implement Enterprise Resource Planning II (ERPII). This paper uses interpretive structural modelling (ISM) to establish relationships between the barriers and MICMAC analysis to determine the driving and dependence power of barriers. A group of industry and academic experts was contacted to develop the contextual relationship among the barriers and to construct the structural model. The findings of the study are useful in identifying and categorising the significant barriers, as well as revealing the direct and indirect effects of each barrier on ERPII implementation. The findings will aid practitioners and policymakers in developing a thorough understanding of the ERPII implementation process and the barriers to its implementation.
Acknowledgments. The equipment's of SFedU and GHRCE Nagpur India were used. The authors acknowledge the support by Southern Federal University, grant No. VnGr-07/2020-04-IM (Ministry of Science and Higher Education of Russia).

Prioritizing the Barriers to the Adoption of Cyber-physical Systems in Manufacturing SMEs Using Fuzzy AHP

Inayat Ullah[1], Rakesh Kumar Haldkar[2]*, Ivan A Parinov[2]

[1]Department of Mechanical Engineering, G H Raisoni College of Engineering, Nagpur, Maharashtra, India
[2]I. I. Vorovich Mathematics, Mechanics and Computer Sciences Institute, Southern Federal University, Rostov-on-Don, 344090, Russia

*rakeshhaldkar@gmail.com

In the near future, cyber-physical systems and the Internet of Things will be ubiquitous. These technologies will be deeply integrated with manufacturing strategies, processes, and systems to assist manufacturing firms in carrying out routine operations while achieving the organizational objectives. However, to realise this vision, several barriers and obstacles need to be conquered. Therefore, the aim of this research is to identify and prioritize the barriers to the adoption of cyber-physical systems in manufacturing SMEs. To this end, the study employs a two-phase approach. In the first phase, an exhaustive literature review has been conducted to identify the barriers and categorize them into different groups. In the second phase, the barriers are ranked using the fuzzy analytical hierarchy process (AHP) technique.

Further, the robustness of the findings has been evaluated by performing sensitivity analysis. The findings of this study offer a roadmap that could be helpful to the practitioners in deciding how to proceed towards the adoption of cyber-physical systems.

***Acknowledgments*.** The equipment's of SFedU and GHRCE Nagpur India were used. The authors acknowledge the support by Southern Federal University, grant No. VnGr-07/2020-04-IM (Ministry of Science and Higher Education of Russia).

Nanoscale Materials for Gas Sensors Based on MOS Transistors

Irina Gulyaeva*, Victor Petrov

Southern Federal University, Research and Education and Centre "Microsystem Technics and Multisensor Monitoring Systems", Taganrog, 347922, Russia

*iten@sfedu.ru

Gas detectors are widely used in all areas of human activity, especially in production, at nuclear power plants, etc. The area of their application is continuously expanding. The semiconductor sensors are most promising and widely used, since, in addition to their small size, they are easy to manufacture and fit well with subsequent electronic devices. If these sensors are incorporated into integrated circuits, it can take the development of gas sensors to a higher level. To do this, it is necessary to research and use new materials, the properties of which can be changed over a wide range and their parameters must be reproduced when repeating technological processes. In [1], a gas sensor based on a 2D FET transistor is reported, consisting of several layers of black phosphorus (BP), boron nitride (BN) and molybdenum disulfide (MoS_2) as the upper gate, dielectric layer, and conductive channel, respectively. In this device configuration, the BP top gate with good gas adsorption capacity serves as a sensitive material, while the MoS_2 conductive channel is isolated from the environment by a coating of the BN dielectric layer. The authors experimentally demonstrated that the proposed 2D FET material not only achieved a detection limit of 3.3 ppb to NO_2 but was also capable of differentiating oxidizing and reducing gases. In [2], the authors report on a toxic gas detection system based on amorphous indium-gallium-zinc oxide (IGZO). The microsystem contains an IGZO thin film transistor (TFT) as a sensing element and exhibits high selectivity and sensitivity to low concentrations of nitrogen dioxide (NO_2), 100 ppb. In both cases, the control potential of the sensor sensitivity equal to 15 – 25 V was applied to the gate. In order to reduce this potential and increase the sensitivity of the sensor, nanocomposite oxide films with their own surface potential can be used. To study the surface potential by solid-phase low-temperature pyrolysis, thin nanocomposite ZnO – SnO_2 films with a ratio of 0 : 100; 0.5 : 99.5; 1 : 99; and 5 : 95 were synthesized [3]. The study of the surface potential was carried out by scanning probe microscopy using the Kelvin method (SKPM). The Kelvin Probe method is based on a two-pass technique. In the first pass, the surface relief of the sample is determined, and in the second pass, this relief is tracked when passing over the sample at a certain height to determine the surface electric potential. During the second pass, the oscillations of the cantilever are excited not mechanically, but electrically by applying a bias voltage to the probe, and the surface potential is recorded. Studies have shown that the surface potential of ZnO – SnO_2 nanocomposite films was rather high in the range 0.01 – 1 V, depending on the film composition. Thus, depending on the composition of the material components, it is possible to form films with a higher or lower surface potential, which in MOS structures can strongly affect the value of the gas sensitivity to the analyzed gas.

Acknowledgement. The work was carried out with the financial support of the RFBR grant №. 20-07-00653_ A.

References

[1] Sigang S., Ruixue H., Enxiu W., Quanning L., Xuejiao C., Wenlan G., Chonglin S., Xiaodong H., Daihua Z., Jing L. Highly sensitive gas sensor based on two-dimensional material field effect transistor // *Nanotechnology*, **29**, 435502, 2018.

[2] Vijjapu Mani T., Surya Sandeep G., Yuvaraja S., Zhang X., Alshareef Husam N., Salama Khaled N. Fully integrated indium gallium zinc oxide NO_2 gas detector // *ACS Sensors*, **5**(4), 984 – 993, 2020.

[3] Petrov V. V., Sysoev V. V., Starnikova A. P., Volkova M. G., Kalazhokov Z. Kh., Storozhenko V. Yu., Khubezhov S. A., Bayan E. M. Synthesis, characterization, and gas sensing study of znosno2 nanocomposite thin films // *Chemosensors*, **9**, 124, 2021.

The Influence of Mechanical Activation on the Structure and Physical Properties of $PbZr_{0.7}Ti_{0.3}O_3$

Ivan Dmitrenko[1]*, Kamaludin Abdulvakhidov[1], Li Zhengyou[1], Marina Sirota[1], Irina Mardasova[2], Marina Vitchenko[2]

[1]Southern Federal University, 178/24, Sladkov Str., Rostov-on-Don, 344090, Russia
[2]Don State Technical University, 1, Gagarin Sq., Rostov-on-Don, 344000, Russia

*vanekdmitrenko@gmail.com

Lead zirconate titanate $Pb(Zr_{1-x}Ti_x)O_3$, known as PZT, is one of the most popular materials in every modern **fi**eld of electronics based on its versatile functionalities [1]. Because of its high electromechanical coupling, PZT shows strong piezoelectric e**ff**ect, high ferroelectricity, pyroelectricity and dielectric response. Based on these properties, the PZT-based materials are used in applications like miniaturized tunable capacitors, transducers, actuators. The aim of this work was studying of possibility of managing the physical properties of piezoelectric ceramics on the basis of $PbZr_{0.7}Ti_{0.3}O_3$ solid solutions by changing of concentration and type of structural defects by mechanical activation of synthesized powder with using of Bridgman anvils.

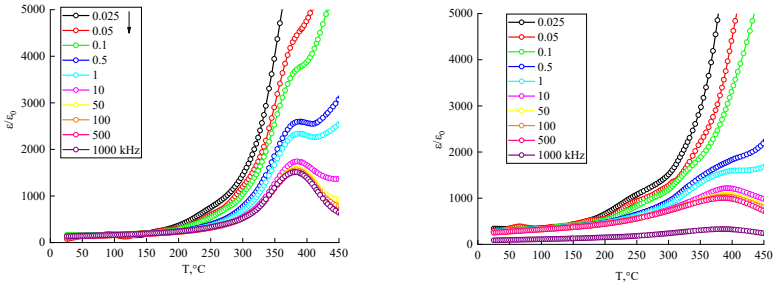

Fig. 1. Temperature dependence of dielectric permittivity of the reference (a) and activated (b) samples for different frequencies of the applied electric field

The PbO, TiO_2 and ZrO_2 metal oxides were used to obtain $PbZr_{0.7}Ti_{0.3}O_3$ by "columbite" method. Mechanical activation between the Bridgman anvils in the pressure range from 80 to 320 MPa was applied to synthesized samples. Depending on the applied pressure, the activated material ends up in various metastable states, which leads to changes in both the structure and physical properties of the material. In this report, the relationship between the pressure and the change in the lattice parameters of the synthesized samples was studied by XRD method. Dielectric characteristics were investigated at various frequencies (25Hz – 1MHz). The maximum value of temperature, T_m of the dielectric permittivity changes nonmonotonically with an increase in applied pressure (see Fig. 1). Moreover, the IR spectra and magnetic properties of the compositions at room temperature were studied. A shift in the absorption bands of the IR spectra were found. The pressure dependences of the band gap E_g were determined by optical absorption spectroscopy.

Reference

[1] Abdulvakhidov K. G., *et al.* Influence of mechanical activation on the dielectric and dynamic properties and structural parameters of the solid solution of $Pb(Zr_{0.56}Ti_{0.44})O_3$ // *Mater. Res. Express*, **5**, 115029, 2018

Mold Core DSLR Camera Tool Mark Analysis According to the Surface Roughness of the Aspherical Lens

Jeong Wan Kim[1,a], Tae Gyu Kim[2,b]

[1]Department of Nano Fusion Technology, Pusan National University, Busan 627-706, Korea
[2]Department of Nanomechatronics Engineering, Pusan National University, Busan 627-706, Korea

[a]baramkjw@gmail.com; [b]tgkim@pusan.ac.kr

Aspheric glass lenses used in optical and electronic devices are manufactured by the compression molding method of the mold, and mold technology is very important. In this study, the improvement of surface roughness by tool marks on the mold core surface according to DTM grinding was studied. Cemented carbide with high hardness and excellent thermal properties was manufactured as a mold, and the mold surface is subjected to a process of removing fine scratches or oval tool marks remaining by DTM grinding machine processing or subsequent polishing process depending on the shape of the aspherical lens. For DSLR camera lenses, the performance level of the bokeh captured in the photo is determined depending on whether the tool mark is removed from the mold. The mold was precisely machined with a resolution of 0.1 μm with a DTM grinding machine, and the processing and dimension correction were repeated 10 times to improve the shape precision of the aspherical lens. The processed mold core was hand-polished according with diamond-paste particle sizes of 3, 1, 1/2 and 1/4 μm, and lubricant SPR-O was mixed. The surfaces of two samples, the mold core subjected to the subsequent polishing process and the mold core subjected to pure DTM grinding without the subsequent polishing process, were analyzed. Also, a ta-DLC thin film with excellent releasability was deposited on the mold surface to a thickness of 100 nm. A compression molding process was performed by inserting an aspherical lens raw material into two types of mold cores depending on the presence or absence of a subsequent polishing process. For molding conditions, the maximum temperature (UT-Max) of the upper mold core was set to 600 °C, the lower mold core maximum temperature (LT-Max) was set to 610 °C,

and the cylinder pressure was set to 300 MPa. The shape error of the real coefficient value of the aspherical glass lens transferred through compression molding was confirmed through the FTS measuring machine. In the result of FTS measurement, the PV and ACC before polishing were at the maximum of 2.5 μm and 1.4 μm, respectively, but the PV and ACC after polishing were at the maximum of 1.3 μm and 1.0 μm, suggesting that the shape error of the mold core was improved. The surface roughness of the aspherical lens of the two mold cores was measured by AFM, and it was found that RMS was improved to 2.206 and 1.005 nm, respectively, before and after polishing. In the result of photographing performance by assembling, the aspherical lenses of the two mold cores directly into the imaging optical system, it was found that the performance level of the bokeh was clearly differentiated according to the process before and after polishing, so that the performance level of the bokeh was distinguishable with the naked eye. In addition, in the result of measuring the resolution with the MTF measurement system, the aspheric lens PV and ACC showed that the central resolution peak was reduced by about 5% after the polishing process.

Study on the Growth of Gallium Oxide Thin Films Using Diamond Buffer Layer Grown by the Hot Filament-CVD

Ji-Yeon Seo[1,4,a], Min-Su Kim[2], Sung-ho Cho[3,4], Yun-Ji Shin[4], Seong-Min Jeong[4], Si-Young Bae[4,b], Tae-Gyu Kim[2,c]

[1]Department of Nano Fusion Technology, Pusan National University, Busan, Korea
[2]Department of Nanomechatronics Engineering, Pusan National University, Busan, Korea
[3]Department of Materials Science and Engineering, Pusan National University, Korea
[4]Energy and Environmental Division, Korea Institute of Ceramic Engineering and Technology, Jinju, Korea

[a]sjy0833@naver.com, [b]sybae@kicet.re.kr, [c]tgkim@pusan.ac.kr

Gallium oxide is in the spotlight as a next-generation power semiconductor material due to its excellent properties with a wide band gap and high breakdown field [1]. However, the thermal conductivity of gallium oxide is 22.5 W/m·K for beta gallium oxide (010), which is low compared to other power semiconductor materials. If single crystal diamond (thermal conductivity 2500 W/m·K) with very good thermal conductivity is used, the thermal properties of gallium oxide can be dramatically improved [2]. CVD diamond growth methods include high-frequency plasma chemical vapor deposition and microwave plasma chemical vapor deposition. Among them, the hot filament chemical vapor deposition method is a method of applying heat to the filament without using plasma, so it is easy to expand the deposition area and has economic advantages. In this experiment, a CVD diamond heat dissipation layer was formed by controlling the concentration of hydrogen as a carrier gas and methane as a source gas, filament voltage, pressure in the reaction chamber, gas flow rate, and thin film growth time using a hot filament chemical vapor deposition apparatus. After that, a gallium oxide layer was grown on the diamond/silicon substrate using an atomization chemical vapor deposition apparatus, and the experiment was carried out by setting a variable to a growth temperature of 400 – 550 °C to observe the thin film formation. To confirm the formation of the diamond heat dissipation layer, Raman analysis was performed to observe the *D*-peak (1333 cm^{-1}) and the *G*-peak (1580 cm^{-1}), and the crystal structure of the diamond heat

dissipation layer was (111) through XRD 2-theta scan. In addition, the thickness of each layer of the gallium oxide/diamond structure and the state of the interface were observed through SEM, and it was confirmed that the diamond heat dissipation layer was about 3.2 – 3.6 μm and the gallium oxide thin film was about 1 – 1.5 μm. Then, to study how the thermal properties of each thin film had an effect on the gallium oxide/diamond epitaxial structure, thermal conductivity was measured using the TDTR method and samples were prepared. To measure the thermal conductivity of the diamond heat dissipation layer using the TDTR method [3], thin films with a thickness of about 1.8 μm and 3.5 μm were measured, and an Au-layer, which is a heat reflective layer, was deposited on it with about 0.4 μm. As a result, the thermal conductivity of the diamond heat dissipation layer was confirmed to be 142 W/m·K and 163 W/m·K. Thermal conductivity measurements of gallium oxide/diamond/silicon structures require additional research. Since thermal properties are one of the important research fields in the semiconductor, aerospace industry, and next-generation material development, the possibility of application of next-generation power semiconductor materials is expected by improving the thermal properties of gallium oxide.

References

[1] Nemanich R. J., Carlisle J. A., Hirata A., Haenen K. // *MRS Bull*. **39**, 490, 2014.
[2] Inyushkin A.V., Taldenkov A.N., Ralchenko V.G., Bolshakov A.P., Koliadin A.V., Katrusha A.N. // P*hys. Rev. B* **97**, 144305, 2018.
[3] Jiang P., Qian X., Yang R. // *Journal of Applied Physics* **124**, 161103, 2018.

A Meso-scale Tensile Model for Woven Fabrics Based on Timoshenko Beam Theory

Jichong Wang, Xiongqi Peng*

School of Materials Science and Engineering, Shanghai Jiao Tong University, Shanghai 200030, China

*wangjichong@sjtu.edu.cn

Woven fabrics are widely used as reinforcement in composite materials. The yarn weave architectures highly influence the mechanical response of woven fabrics. To provide an accurate prediction of woven fabrics under tension, a mesoscale model is developed in this study. The model takes into account yarn properties, yarn weaving pattern and interactions between yarns. Each yarn in fabric is modeled as a Timoshenko beam with a weaving shape modeled by a parabolic function. The yarn shape evolution and mechanical response of undulated yarn under tension are computed based on the Castigliano's second theorem. The maximum stress failure criterion is used to establish damage onset by introducing random yarn strength. The damage variable is introduced to characterize the progressive failure behavior of woven fabric. The model is demonstrated on woven jute fabrics. Analytical and numerical analysis are carried out and show good prediction in macroscopic tensile response of woven jute fabric with progressive failure. The model provides a quantitative understanding between yarn geometrical parameters and the expected material response and makes it helpful for designing woven structural composites with high performance.

Influence of Ternary Intermetallic Inclusions on the Mechanical Properties of Aluminum Alloys in Al-Ti-Zn System

D. A. Kalganov*, V. V. Kaminskii

Advanced Data Transfer Systems Institute, ITMO University, Saint-Petersburg, Russia

*kalganov@itmo.ru

In this work, aluminum alloys with inclusions of Al-Ti-Zn ternary intermetallic compounds were studied. The distribution of these phases in samples after hot extrusion has been obtained. The amplitude dependences of internal friction and Young's modulus were obtained for a frequency of about 100 kHz by the piezoelectric resonator method. Aluminum alloys ASD-1 hardened by inclusions of $Al_{11}Ti_4Zn$ and $Al_{66}Ti_{25}Zn_9$ phases was studied. Samples were obtained in several stages: synthesis of the Al_3Ti intermetallic compound by SHS in vacuum, mechanical alloying using zinc powder, addition of aluminum D16 to the alloy, and thermoplastic processing of the prepared mixtures by hot extrusion. Both intermetallic compounds showed a microscale hardening effect in the original aluminum alloys. Particles of the $Al_{11}Ti_4Zn$ intermetallic compound have a greater effect on the hardness of the matrix. This hardening is realized by means of the wrapping mechanism (Orowan mechanism). This conclusion was confirmed by the amplitude dependences of internal friction. The harder intermetallic compound ($Al_{11}Ti_4Zn$) introduces more stress into the matrix, thereby creating more barriers to the movement of dislocations. Dynamic tests also showed a hardening effect in both samples with the addition of intermetallic inclusions.

Investigations of Magnesium Alloys Containing LPSO Phase by Composite Oscillator Method

D.A. Kalganov[1]*, V.V. Kaminskii[1], A.E. Romanov[1], E. Abe[2], Y. Kawamura[3]

[1]Advanced Data Transfer Systems Institute, ITMO University, Saint-Petersburg, Russia
[2]Research Center for Structural Materials, National Institute for Materials Science, Tsukuba, Japan
[3]Magnesium Research Center, Kumamoto University, Kumamoto, Japan

*kalganov@itmo.ru

The advantages and prospects for the use of magnesium-based materials are due to their low density and high strength. In comparison with alloys of other light metals, they can significantly reduce the weight and dimensions of products (against aluminum alloys) or provide economic advantages and safety of their use (against beryllides). Obtained by traditional methods, magnesium alloys have low plasticity and can be destroyed during processing or operation. However, for some of them, methods are known that make it possible to form an ordered periodic structure (LPSO), changing the mechanism of stress relaxation and significantly improving mechanical properties. The search for such materials and the study of the origin and interaction of defects in them is an important scientific problem. The alloys obtained by the method of rapid crystallization and subsequent hot extrusion in the Mg-Zn-Y

system for the content of zinc from 0.2 to 6 and yttrium from 0.6 to 9 atomic percent have been studied. The density of the samples varied in the range of 1.768 – 2.320 g/cm^3. The volume fraction of the LPSO-phase was determined by X-ray diffraction (Dron-8, Cuk$_\alpha$) and scanning electron microscopy (Tescan Vega 3). Microhardness was determined by the Vickers method with a load of 200 gf and an exposure of 60 s. The corresponding values varied in the ranges of 8.5 – 12.5 gf/cm² and 7.0 – 2.0 gf/cm² when measured in the direction of extrusion and normal to it, respectively. The effective modulus of elasticity, measured by the compound piezoelectric resonator method, increased with the content of the LPSO-phase from 44.3 GPa to 53.8 GPa.

Advantages of the Novikov Transmission on the Slow-speed Stage of the Cylindrical Gearbox Transmission

D. V. Karabanov*, V. V. Zaitsev, S. O. Kireev, M. V. Korchagina

Don State Technical University of Rostov-on-Don

*carabanov12@gmail.com

Novikov's gearing is widely used in high-loaded drives (drilling rigs, crane production, mining equipment) due to its high contact strength of the teeth, relatively involute. This advantage applies mainly to cases, where gears are manufactured with low tooth hardness (up to 350 HB), where the contact strength plays a decisive role. The basis for an active study of the load capacity of Novikov gears and their introduction into production was the Resolution of the Council of Ministers of the USSR of January 18, 1960 No. 53 "On the specialization of the production of normalized gearboxes", according to which it was necessary to organize the production of cylindrical gearboxes with an axial distance of up to 250 mm at the Izhevsk Gear Plant and ensure their production up to 180 thousand pieces per year [1]. Based on the results of the tests, the following main conclusions were made. Gears with post-pole engagement of Novikov (OLZ) with the initial contour according to the temporary all-Union normal with heat treatment of gear shafts "improvement" with the hardness of the teeth HB 270 – 300 and HB 230 – 260 wheels transmit loads to continuous operation by 1.5 times, and with Novikov pre-post-pole gearing (DLZ) with the original contour "Ural-2N" by 2.0 times larger than similar gears with involute gearing. Based on V. I. Korotkin's calculations, it can be concluded that the load capacity of Novikov's gears in terms of contact strength is significantly higher than that of involute gears with any hardness of the tooth surfaces and the degree of accuracy of the compared analogues. The load capacity of high-precision uncorrected Novikov and involute gears of the same module in bending strength is comparable with a slight advantage in the latter. Starting from the 8th degree of accuracy and coarser, the advantage passes to Novikov transmissions, which is confirmed by long-term bench tests [2]. Thus, having understood the history of the Novikov transmission and all its nuances, it can be concluded that the use of this transmission at the slow-speed stage of the rocking machine gearbox will significantly reduce the mass dimensions of the drive itself, which will reduce the cost of materials and transportation. SO, the complexity and high cost of the tool can be leveled in large series.

References

[1] Yakovlev A.S. Once again to the question of the effectiveness of the use of gears with Novikov gearing // *Reducers and Drives*, **1, 2** (08), 48 – 55, 2007 (In Russian).

[2] Korotkin V. I. On the preferred spheres of application of Novikov and involute gears // *Bulletin of NTU "KhPI"*, **23** (1195), 82 – 87, 2016 (In Russian).

Optical Properties of $Sr_{0.5}Ba_{0.5}Nb_2O_6$ Films Grown on a MgO (110) Substrate

S. V. Kara-Murza[1]*, N. V. Korchikova[1], A. G. Silcheva[1], Yu. V. Tekhtelev[1], R. G. Chizhov[1], K. M. Zhidel[2], A. V. Pavlenko[2,3]

[1]*Lugansk State Pedagogical University, Lugansk, 91000,* Ukraine
[2]*Research Institute of Physics, Southern Federal University, Rostov-on-Don, Russia*
[3]*Federal Research Center The Southern Scientific Centre of the Russian Academy of Sciences, Rostov-on-Don, Russia*

*skaramurza@gmail.com

Solid solutions of ferroelectrics $Sr_xBa_{1-x}Nb_2O_6$ (SBN) in the form of nanoscale films are of interest from both applied and fundamental points of view. Earlier, we presented the results of optical studies of heteroepitaxial films of barium-strontium niobates of various thicknesses on single-crystal substrates Al_2O_3(0001) and MgO(001). This report is devoted to the research of the SBN-50 film deposited by RF cathode sputtering of a ceramic target of stoichiometric composition in an oxygen atmosphere on single-crystal substrates of MgO orientation (110); the sputtering time was 60 minutes. By means of X-ray diffraction analysis, it was found that under the deposition modes used, the SBN-50 film crystallizes in such a way that the direction [410] is perpendicular to the plane of the substrate. In this case, the crystallographic *Z*-axis (direction of the optical *c*-axis) of the film lies in the plane of its surface. This orientation of the film made it possible by using spectrophotometry at normal incidence of partially polarized light in different planes of incidence of the beam to determine the refractive indices n_o and n_e, as well as their dispersion. The transmission spectra were measured at room temperature in the wavelength range of 300 – 800 nm using a Shimadzu UV-50 spectrophotometer. The analysis of interference extrema made it possible to calculate the values of the refractive indices at the corresponding points of the spectra. The theoretical curve was interpolated using the Sellmeier formula; the root-mean-square deviation of the experimental points from the theoretical curve did not exceed 2%. The Table 1 shows the obtained values n_o and n_e depending on the wavelength of electromagnetic radiation.

Table 1

n	λ, nm						
	400	450	500	550	600	650	700
n_o	2.52	2.44	2.38	2.34	2.32	2.30	2.28
n_e	2.45	2.37	2.33	2.30	2.29	2.26	2.25

In order to determine the exact value of the film thickness and study the nature of the surface, ellipsometric measurements were carried out using a multi-angle reflective ellipsometer at a wavelength of a helium-neon laser of 632.8 nm. The plane of incidence of the beam, intersecting the crystallographic axis of the film material, was used for a two-layer model of

the surface, including a substrate, a base transparent layer with a thickness d_0 with a refractive index n_e, and a damaged layer with effective parameters d_{ef} and n_{ef}. Based on the results of ellipsometric measurements, the following values of the optical parameters of the film were obtained: $n_e = 2{,}28$, $d_0 = 418$ nm, n_{ef} = 1.42, d_{ef} = 10 nm. There is no boundary film-substrate layer. The value of the effective refractive index of the damaged layer n_{ef} = 1.42 corresponds to the volumetric filling factor of the damaged layer with the film material q = 0.47.

SAW Dual Channel Current Sensor with FeNi Film

G. Ya. Karapetyan*, M. E. Kutepov, E. M. Kaidashev

Laboratory of Nanomaterials, Southern Federal University,
Rostov-on-Don, Russia

*gkarapetyan@sfedu.ru

In [1], the magnetic field surface acoustic wave (SAW) sensors on the basis of changes of inductance in the gap in magnetic core, located around the current bar, and also on the basis of changes in the capacitance of varicaps under the voltage induced in the coil wound on this magnetic core are described. Such sensors must necessarily have a magnetic circuit for their operation, which significantly increases the weight and dimensions of the sensor, as well as complicates its installation. Dual channel designs of passive wireless SAW current sensors (Fig. 1) with a sensitive element in the form of a FeNi film or based on them are proposed and considered. Sensors with such films have a high sensitivity (the velocity of the SAW changes 1/30000, when the current changes by 1 A) and therefore do not need magnetic cores and can be installed directly on the conductive busbar [2 – 5].

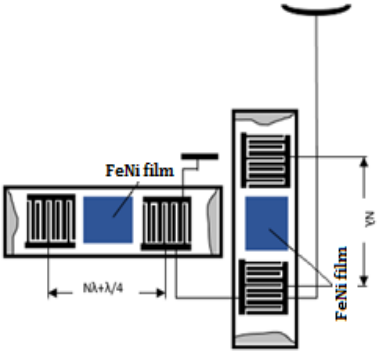

Fig. 1. Design of two-channel sensor with mutually perpendicular channels

References

[1] Kislitsyn V. O., Kalinin V. A., Karapetyan G. Ya., Kataev V. F., Ermolaeva N. V. Sensitive Elements of Passive Wireless Sensors on Surface Acoustic Waves for Measuring Current in

Three-Phase Circuits // News National Research Nuclear University (MEPI), **9**(2), 177 – 183, 2020 (In Russian).
[2] Jie Tong, Yang Wang, Shiyue Wang, Wen Wang, Yana Jia, Xinlu Liu. Development of a Magnetostrictive FeNi Coated Surface Acoustic Wave Current Sensor // *Appl. Sci*., **7**, 755, 2017, doi:10.3390/app7080755
[3] Morgan D., *Surface Acoustic Wave Filters with Applications to Electronic Communications and Signal Processing*. Academic Press, 2007.
[4] Mistyukov V., Volodin P., Kapitanov V., Single-chip implementation of the FFT algorithm on Xilinx FPGA // *Components and Technologies*, **2**, 2000 (In Russian).
[5] Bodong Li Nedime, Pelin M. H., Salem Ioanna Giouroudi, Jurgen Kosel, Integration of thin film giant magnetoimpedance sensor and surface acoustic wave transponder // *Journal of Applied Physics*, **111**, 07E514, 2012.

Creation and Research of the SAW Transducer with a Single-phase Grid and a Piezoelectric Zinc Oxide Film

G. Ya. Karapetyan*, M. E. Kutepov, A. L. Nikolaev, E. M. Kaidashev

Laboratory of Nanomaterials, Southern Federal University, Rostov-on-Don, Russia

*gkarapetyan@sfedu.ru

A method for obtaining a new type of surface acoustic waves (SAWs) transducer operating at double frequency with a single-phase closed-loop lattice and a piezoelectric zinc oxide film is developed and experimentally investigated (Fig. 1). A method for calculating such a converter has been developed, its equivalent circuit has been compiled, taking into account propagation losses, losses in the metal film and the inductance of the connecting wires. When the frequency is doubled, the SAWs attenuation per unit length increases [1 – 5].

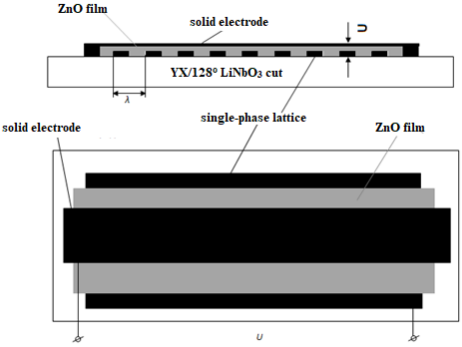

Fig. 1. New type of SAWs transducer with a single-phase grid and a piezoelectric zinc oxide film on YX/128° $LiNbO_3$ cut

References
[1] Wixforth A., Kotthaus J. P., Weimann G. Quantum oscillations in the surface acoustic-wave attenuation caused by a two-dimensional electron system // *Phys. Rev. Lett*. **56**, 2104, 1986.
[2] RU 2 602 392, MPK-2006.01 N03N 9/64, V82V1/00, 20.11.2016.
[3] Kino G. S., Wages R. S. Theory interdigital couplers on nonpiezoelectric substrates // *J. Appl. Phys*. **44**, 1480 – 1488, 1973.
[4] Morgan D. *Surface Acoustic Wave Filters with Applications to Electronic Communications and Signal Processing*. Academic Press, Elsevier, 2007.
[5] *5-th International Conference Interaction of Radiation with Solids*. October 6-9, 2003, Minsk, Betam, 288, 2003.

Microprofiling of Silicon Wafers by Plasma-Chemical Methods

I. O. Kessler*, V. S. Klimin

Institute of Nanotechnologies, Electronics, and Electronic Equipment Engineering, Southern Federal University, Taganrog, Russia

*kessler@sfedu.ru

Currently, plasma-chemical etching is widely used in modifications of substrate surfaces [1 – 3]. This technological process, in comparison with similar ones, gives a high quality of micro- and nanostructures. The present work is aimed at studying the dependence of the accelerating voltage of the ion beam on the local modification of the surface and the height of the structures during plasma chemical treatment, as well as the effect of the processing time on the angle of inclination of the walls of the structure. The studies used silicon substrates with a local modification of the 5×5 μm^2 regions by a focused beam of Ga^+ ions at the number of beam passes N-50, with a dose of 12.5 pC/mm^2, and an ion beam current of 10 pA, at an accelerating voltage from 10 to 30 keV. Plasma-chemical treatment of samples with modified regions was carried out in a fluorine-containing plasma under the following conditions: the flow of fluorinated gas N_{SF6} is 15 cm^3/min, the flow of N_{Ar} is 100 cm^3/min, the pressure in the reactor is 2 Pa, the power of the inductively coupled plasma source W_{ICP} is 250 W, the power of the capacitive plasma source W_{CP} is 25 W, the bias voltage U_{BV} is 16 V, the processing time varied from 15 to 180 seconds. As a result, the dependence of the height of the structures on the accelerating voltage of the ion beam and the dependence of the angle of inclination of the wall of the structure on the processing time and on the height of the structures were obtained.

Acknowledgement. This work was supported by the Grant of the Russian Science Foundation No. 20-69-46076. The results were obtained using the equipment of the Research and Education Center "Nanotechnologies" of the Southern Federal University.

Reference
[1] Klimin V. S., Rezvan A. A., Ageev O. A. Research of using plasma methods for formation field emitters based on carbon nanoscale structures // *J. of Phys: Conference Series*. **1124**, 071020, 2018.
[2] Giannuzzi L. A., Stevie F. A. *Introduction to Focused Ion Beams: Instrumentation, Theory, Techniques and Practice*. New York: Springer, 357, 2004.
[3] Bhushan B. *Springer Handbook of Nanotechnology*, 3rd ed., Bharat Bhushan (Ed.) New York: Springer, 1964, 2010.

Design and Optimization of a 2-DOF Compliant Mechanism for Vibration-Assisted Milling

Khac-Huy-Nguyen[1,2], Huy-Tuan Pham[2]*, Van-Khien Nguyen[2,3]

[1]Ly Tu Trong College of Ho Chi Minh City, Vietnam
[2]Ho Chi Minh City University of Technology and Education, Vietnam
[3]Nam Sai Gon Polytechnic College, Vietnam

*phtuan@hcmute.edu.vn

Vibration assisted machining (VAM) is a hybrid machining method that combines small amplitude vibration into either the conventional or non-conventional subtractive machining approaches to enhance the cutting performance and efficiency.

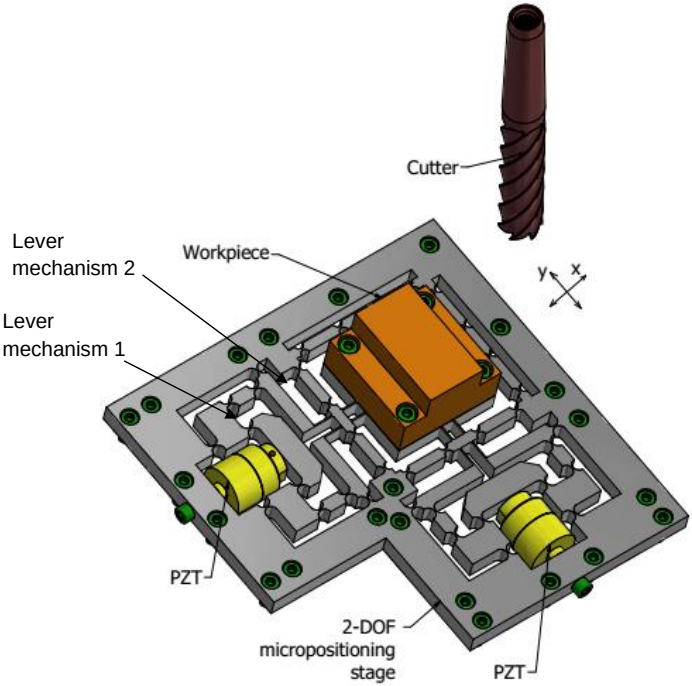

Fig. 2. 3D model of the 2-DOF vibration-assisted milling mechanism.

This report proposes a new 2-DOF XY vibration compliant stage using flexural hinges and leaf springs for a vibration-assisted milling application. The design uses a symmetrical two-stage lever mechanism to transfer and amplify vibrations from piezo-actuators. In the design process, the Taguchi method and finite element analysis are used to evaluate the influence of each design variable on the design optimization problem. The objectives of the design are to

maximize the first-order natural frequency and minimize the parasitic motion while maintaining the equivalent stress under the allowable limit. Optimization results show machining stability in the frequency range from 1,000 to 1,900 Hz, which would be preferable for various vibration-assisted milling applications. Figure 1 illustrates the schematic of the 2-DOF vibration-assisted milling mechanism. Vibration from the PZT actuator is amplified and transferred to the central table by symmetrical two-stage compliant lever mechanisms. Semi-circular flexural hinges and leaf springs are used to design the mechanism. During the machining process, the integrated vibration will intermittently separate the tool from the workpiece to reduce the cutting force and processing temperature. Consequently, this machining method can fabricate hard materials and the lifetime of the tool can also be enhanced as well.

Trunk Pipeline Laying Technology

A. R. Kharitonov[1], D. D. Fugarov[2]*, M. I. Kazmenko[2], Ajel Mohaimen Abbas Ajel[2]

[1]M. I. Platov South-Russian State Polytechnic University (NPI), Novocherkassk, Russia
[2]Don State Technical University, Rostov-on-Don, Russia

*ddf_1@mail.ru

The laying of pipelines is carried out single or in parallel with other existing or projected main pipelines in a technical corridor [1]. The technical corridor of main pipelines is understood as a system of parallel pipelines along one route, intended for the transportation of oil or gas. In some cases, with a feasibility study and the condition of ensuring the reliability of the operation of pipelines, joint laying of oil pipelines (oil product pipelines) and gas pipelines in the same technical corridor is allowed. The maximum permissible (total) volumes of transportation of products within one technical corridor and the distance between these corridors are determined in accordance with building codes and regulations approved in the prescribed manner [2]. It is not allowed to lay main pipelines through the territories of settlements, industrial and agricultural enterprises, airfields, railway stations, sea and river ports, wharves and other similar facilities [3]. To ensure normal operating conditions and exclude the possibility of damage to main pipelines and their facilities, protective zones are established around them, the size of which and the procedure for production in these zones of agricultural and other work are regulated by the rules for the protection of main pipelines [4]. Pipelines and their structures should be designed taking into account the maximum industrialization of construction and installation, while the decisions taken in the project should ensure uninterrupted and safe operation of pipelines [5].

References

[1] Gerasimenko Y., Gerasimenko A., Fugarov D., Purchina O., Poluyan A. Mathematical modeling and synthesis of an electrical equivalent circuit of an electrochemical device // *Advances in Intelligent Systems and Computing*, **1259**, 471 – 480, 2021.

[2] Onyshko D., Fugarov D., Purchina O., Poluyan A., Rasteryaev N., Skakunova T. Synchronization system in wireless sensor networks of oil and gas complex // *E3S Web of Conferences. Topical Problems of Green Architecture, Civil and Environmental Engineering, TPACEE 2019*, 03030, 2020.

[3] Poluyan A. Yu., Purchina O. A., Fugarov D. D., Golovanov A. A., Smirnova O. V. Solution of task on the minimum cost data flow based on bionic algorithm // *Journal of Physics: Conference Series*. International Conference "Information Technologies in Business and Industry", Mathematical Simulation and Computer Data Analysis, **2**, 032056, 2019.
[4] Fugarov D. D., Purchina O. A., Poluyan A. Y., Gerasimenko A. N., Rasteryaev N. V. Magnetodielectric ac measuring transducer for automation systems in oil refineries *// Journal of Physics: Conference Series*. International Conference "Information Technologies in Business and Industry", 062020, 2019.
[5] Poluyan A. Yu., Purchina O. A., Fugarov D. D., Gerasimenko E. Yu., Skakunova T. P. Application of bionic and immune algorithms for the solution of ambiguous problems of transportation routing // *Journal of Physics: Conference Series*. International Conference "Information Technologies in Business and Industry", Mathematical Simulation and Computer Data Analysis, **2**, 032057, 2019.

Pipes for the Construction of Trunk Pipelines

A. R. Kharitonov[1], D. D. Fugarov[2]*, A. A. Kompaniets[2], Alchganbe Ahmed Abed Tuama[2]

[1]M. I. Platov South-Russian State Polytechnic University (NPI), Novocherkassk, Russia
[2]Don State Technical University, Rostov-on-Don, Russia

*ddf_1@mail.ru

The material for pipes of main pipelines is steel [1]. According to the manufacturing method, pipes for main pipelines are divided into seamless, electric longitudinal seam and welded with a spiral seam [2]. Pipes with a diameter of up to 500 mm inclusive are made of calm and semi-calm carbon and low-alloy steels [3]. Pipes up to 1020 mm in diameter are made of calm and semi-calm low-alloy steels [4]. In the manufacture of pipes with a diameter of up to 1420 mm, low-alloy steels are used in a thermally or thermomechanically hardened state. The welded joint of pipes must be of equal strength to the base metal [5]. In this case, the curvature of the pipes should not be more than 1.5 mm per 1 m of length, and the total curvature should not be more than 0.2% of the length of the pipe. The length of the pipes supplied by the plant should be in the range of 10.5 – 11.6 m. As a material for pipes with a diameter of 1020 mm and more, sheet and coil steels are used, which have passed 100% inspection by physical non-destructive methods (ultrasound with subsequent decoding of defective places by X-ray transmission).

References

[1] Fugarov D. D., Purchina O. A., Poluyan A. Y., Gerasimenko A. N., Rasteryaev N. V. Magnetodielectric ac measuring transducer for automation systems in oil refineries *// Journal of Physics: Conference Series*. International Conference "Information Technologies in Business and Industry", 062020, 2019.
[2] Gerasimenko Y., Gerasimenko A., Fugarov D., Purchina O., Poluyan A. Mathematical modeling and synthesis of an electrical equivalent circuit of an electrochemical device // *Advances in Intelligent Systems and Computing*, **1259**, 471 – 480, 2021.
[3] Onyshko D., Fugarov D., Purchina O., Poluyan A., Rasteryaev N., Skakunova T. Synchronization system in wireless sensor networks of oil and gas complex // *E3S Web of*

Conferences. Topical Problems of Green Architecture, Civil and Environmental Engineering, TPACEE 2019, 03030, 2020.
[4] Poluyan A. Yu., Purchina O. A., Fugarov D. D., Golovanov A. A., Smirnova O. V. Solution of task on the minimum cost data flow based on bionic algorithm // *Journal of Physics: Conference Series*. International Conference "Information Technologies in Business and Industry", Mathematical Simulation and Computer Data Analysis, **2**, 032056, 2019.
[5] Poluyan A. Yu., Purchina O. A., Fugarov D. D., Gerasimenko E. Yu., Skakunova T. P. Application of bionic and immune algorithms for the solution of ambiguous problems of transportation routing // *Journal of Physics: Conference Series*. International Conference "Information Technologies in Business and Industry", Mathematical Simulation and Computer Data Analysis, **2**, 032057, 2019.

AFM Study of FIB Induced Holes on GaAs Surface

D. V. Kirichenko*, N. E. Chernenko, N. A. Shandyba, M. M. Eremenko, S. V. Balakirev, M. S. Solodovnik

Institute of Nanotechnologies, Electronics and Equipment Engineering, Southern Federal University, Taganrog 347922, Russia

*dankir@sfedu.ru

Controlling the parameters of quantum-dimensional structures, including quantum dots is of great importance for the development of electronic and photonic devices. One of the promising ways to control the quantum dots parameters is the use of modified substrates. The use of focused ion beams (FIBs) for these tasks has a number of advantages, including a high precision of the technique and wide possibilities for creating topologies. The aim of this work is to study the effect of the mode of ion beam treatment on the characteristics of the hole arrays on the GaAs surface, which can act as the centers of the future quantum dot nucleation. The surface modification was carried out with the following FIBs parameters: accelerating voltage was 30 kV, current was 1 pA, number of passes was 5 – 300. Analysis of morphology at the exposure points was carried out by atomic force microscopy. The analysis of the surface potential was carried out by Kelvin-Probe force microscopy. We compared such parameters of obtained holes arrays as depth, diameter at the substrate level and at the half-depth level. With an increase in the number of passes from 5 to 300, the depth at the hole increased from 15.1 to 69.7 nm. At the same time, the hole diameter at the level of the surface and half of the depth varied within 154 – 197 nm and 42 – 56 nm, respectively. It follows that the aspect ratio increases with the number of passes. KPFM showed the largest change in surface potential at 120 passes. Small bursts of surface potential were also detected in the holes obtained at 40 and 300 beam passes. Potential changes were not recorded in surface holes with a lesser degree of FIB treatment. Changes in the surface potential can be associated with the occurrence of imperfections of the crystal structure in the near-surface region. Thus, it was shown that with an increase in the number of FIB passes, not only the depth of the hole increases, but also their aspect ratio. Analysis of the distribution of the surface potential showed that with an increase in the degree of FIB treatment of the GaAs substrate, the degree of crystal structure imperfections in the obtained holes increases.

Acknowledgement. This work was supported by the Ministry of Science and Higher Education of the Russian Federation; the state task in the field of scientific activity No. 0852-2020-0015.

The Ferroelectric Properties Features of $Sr_{0.5}Ba_{0.5}Nb_2O_6$ Thin Films Grown on $Ba_{0.2}Sr_{0.8}TiO_3$/Si(001)

D. A. Kiselev[1], A. V. Pavlenko[2,3]*, S. P. Zinchenko[3], Ya. Yu. Matyash[3], M. A. Klyuchnikov[2], L. I. Kiseleva[3]

[1]National University of Science and Technology "MISIS", 4, Leninskiy Ave., Moscow, 119049, Russia
[2]Research Institute of Physics of the Southern Federal University, 194, Stachki Ave., Rostov-on-Don, 344090, Russia
[3]Federal Research Center Southern Scientific Center of the Russian Academy of Sciences, 41, Chekhov Ave, Rostov-on-Don, 344006, Russia

*antvpr@mail.ru

Heterostructures based on ferroelectrics and semiconductors receive much attention, which is associated with the prospects of their application in non-volatile memory (FeRAM) and MEMS elements. This report presents a study results of the ferroelectric characteristics of a multilayer SBN-50/BST-20/Si(001) heterostructure using dielectric spectroscopy and scanning probe microscopy (SPM). The heterostructures were fabricated by RF cathode sputtering of the corresponding ceramic targets. Figure 1 shows images of the topography and piezoelectric responses (vertical and lateral) of the unpolarized region of the SBN-50 film. It is shown that the SBN-50 films with a thickness are characterized by a low surface roughness (less than 6 nm), the average size of ferroelectric domains is ~ 93 nm.

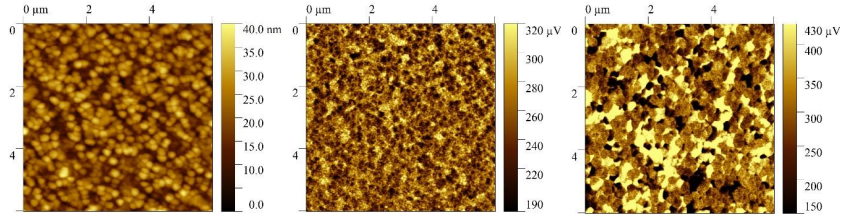

Fig. 1. Surface topography (*a*), vertical (*b*) and lateral (*c*) pictures of the piezoelectric response of the SBN-50 film

An analysis of the experimental results showed that, after synthesis, in *c*-oriented SBN-50 films, a polydomain structure is formed, which, on the one hand, is characterized by the spontaneous polarization, arising during the synthesis of the film and directed from its surface to the substrate, and, on the other hand, by the predominance of the horizontal component of the polarization vector in comparison with vertical. The revealed regularities were reflected in the study of the dielectric characteristics of capacitor structures based on SBN-50/BST-20/Si(001) before the field effect, the capacitance of the investigated heterostructure is ~ 10 pF, which indicates that the surface of the Si (*p*-type) substrate is in the mode impoverishment. The reasons for the revealed regularities are discussed, taking into account the specifics of the domain structure, which was reflected in the analysis of the effects of aging.

Acknowledgement. The work was carried out as part of the state assignment of the South Scientific Center of the Russian Academy of Sciences (theme of state registration No. 01201354247). PFM studies were performed at the Center for Shared Use "Material Science and Metallurgy" at the National University of Science and Technology «MISiS» and were supported by the Ministry of Science and Higher Education of the Russian Federation (Project No. 075-15-2021 -696) and as part of the State Assignment (basic research, Project No. 0718-2020-0031).

Production of Graphene-like Films by Atomic Layer Etching

V. S. Klimin[1], J. V. Morozova[1]*, Z. E. Vakulov[2]

[1]Department of Nanotechnology and Microsystems, Southern Federal University, Taganrog 347922, Russia
[2]Federal Research Center Southern Scientific Center of the Russian Academy of Sciences., Rostov-on-Don, 344006, Russia

*ulamrzv@gmail.com

This report presents a study on the production of graphene-like films by atomic layer etching (AST) [1]. AST is a cyclic self-limited process that consists in the removal of thin layers of material. Currently, this technology is considered by the semiconductor industry as an alternative to continuous etching, as well as an existing analogue of atomic layer deposition [2, 3]. A graphene-like film was formed on a silicon carbyl substrate. The substrate underwent preliminary chemical cleaning. At the first stage, a pointed structure was created by the method of focused ion beam (FIB). According to the simulation results, it became known that gallium ions under these modes of formation by the FIB method are located at a depth of 5 – 10 atomic layers. Defective atomic surface layers were removed by layer-by-layer plasmochemical two-stage etching. On the formed nanoscale defect-free silicon carbide structures, a graphene coating was formed by plasma chemical etching in a fluoride low-temperature discharge inductively coupled plasma (ICP) by removing silicon atoms from the silicon carbide lattice. As a result, a structure with a depth of 900 nm, a height of 860 nm and a minimum structure size of 280 nm was formed. This structure can be used as a sensitive element of a gas sensor due to increased selectivity to such gas molecules as NH_3, CO, NO_2, and H_2O vapors.

Acknowledgement. The reported study was funded by the Russian Foundation for Basic Research, project No. 19-38-60052. The results were obtained using the equipment of the Research and Education Center "Nanotechnologies" of the Southern Federal University.

References

[1] Kanarik K. J., Tan S., Gottscho R. A., Atomic Layer Etching: Rethinking the Art of Etch // *J. Phys. Chem. Lett*. **9**, 4814 − 4821, 2018.

[2] Min K. S., Kang S. H., Kim J. K., Jhon Y. I., Jhon M. S., Yeom G. Y., Atomic layer etching of Al_2O_3, using BCl_3/Ar for the interface passivation layer of III–V MOS devices // *Microelectronic Engineering*, **110**, 457 – 460, 2013.

[3] Klimin V. S., Rezvan A. A., Morozova J. V., Critical pressure during the formation of carbon nanotubes by the method of plasma chemical vapor deposition // *J. Phys.: Conf. Ser*., **1410**, 2019.

Thermo-mechanical Model for Film Laser Annealing on Substrate

Yu. V. Klunnikova[1]*, M. V. Anikeev[1,2], U. Nackenhorst[3]

[1]Southern Federal University, Taganrog, Russia
[2]Fraunhofer SIT, Darmstadt, Germany
[3]Gottfried Wilhelm Leibniz University Hannover, Germany

*jklunnikova@rambler.ru

The possibility of obtaining thin films on dielectric and semiconductor substrates is very important for the design of functional devices such as photoelectric converters or sensitive elements of gas sensors. Application of laser radiation for obtaining thin films on substrate surface increases performance of gas element production, provides stability of film parameters and increased oxide quality. The main benefits of gas sensor development on sapphire substrate with TiO_2 film are: lowering of working temperature, high selectivity to detectable gases, and increased stability in time. The mismatch of the lattice parameters and the thermal expansion properties between thin film layers and substrate materials is the main cause of cross-layer defect development and stress generation. Thermoelastic stresses in a thin film often hamper its performance. Therefore, to increase the quality of thin films and minimize their defects, it is important to be able to control the stress formation in thin film. We have simulated TiO_2 thin films obtaining on sapphire substrates and conducted the experiments. The laser annealing is carried out using the radiation of a pulsed solid-state Nd:YAG laser with a wavelength of 1064 nm. The materials properties, cracks and fracture risk were considered. We develop a three-dimensional model of stresses distribution in film-substrate structure in ANSYS and analyze the emergence of stresses and other defects in film-substrate structure. The films properties were investigated with atomic force microscopy method, scanning electron microscopy, and X-ray phase analysis. We have found out that the temperature on TiO_2 film (thickness of 5 μm) surface is about 500 – 600 °C at an average laser radiation power of 30 W, which is a prerequisite for the growth of films on the substrate surface. It corresponds to the level of thermoelastic stresses (lesser than material elastic limit) such that the cracks formation is not expected. The morphology of the film structure can be varied by changing the laser power and temperature, which allows one to reallocate defects in the structure and improve the quality of the films for their using in microelectronics and thin film optics. Higher scan speed leads to lower temperatures and higher thermal gradient during the material heating and cooling. The film thickness and substrate thickness play the key role in cracks and defects formation in films. The studies showed that cracks on the surface can be formed in thicker films. Thus, the thickness ratio of TiO_2 film/substrate, laser power and laser scan speed are one of the crucial conditions to obtain the most uniform film for their application in microelectronics.

Acknowledgement. This work was supported by the Ministry of Science and Higher Education of the Russian Federation and the German Academic Exchange Service (DAAD) within the framework of the joint program “Mikhail Lomonosov”.

Transient and Emergency Processes in Main Oil Pipelines

D. E. Kochegarov, D. D. Fugarov*, A. A. Brosalin, P. P. Solomakhin

Don State Technical University, Rostov-on-Don, Russia

*ddf_1@mail.ru

The main danger in accidents at oil trunk (OT) pipelines is oil emissions, which, getting into the environment, pollute it [1]. One of the main factors determining the scale of pollution and fire and explosion hazard is the amount of oil leaked from the oil refinery. This value depends on a number of factors: technological parameters of the pipeline (diameter, pressure); operating regulations for OT; relief (profile) of the route; the nature of the destruction (size and shape of defective holes) of the pipeline; promptness of actions to prevent and localize the accident [2]. Obviously, when analyzing and assessing the consequences of accidents at the OT, it is necessary to correctly take into account the above factors. Unfortunately, in recent years, there has been a tendency towards simplified and often erroneous modeling of situations in OT [3]. The proposed method is based on the numerical solution of a nonstationary system of one-dimensional equations of hydrodynamics for a weakly compressible isothermal medium [4]. The approach under consideration is fully consistent with the points of methodological documents and can be used: (i) at the design stage of the oil pump in order to substantiate the protection systems against overpressure and minimize emissions, for example, due to the optimal placement of valves on the route; (ii) to analyze the consequences of accidents that have already occurred and determine the damage caused; (iii) for the analysis of the risk of oil and gas, for example, in order to develop measures to eliminate and localize emergency situations, to justify design solutions that compensate for deviations from the current requirements, when justifying the minimum safe distances [5].

References

[1] Fugarov D. D., Purchina O. A., Poluyan A. Y., Gerasimenko A. N., Rasteryaev N. V. Magnetodielectric ac measuring transducer for automation systems in oil refineries *// Journal of Physics: Conference Series*. International Conference "Information Technologies in Business and Industry", 062020, 2019.

[2] Onyshko D., Fugarov D., Purchina O., Poluyan A., Rasteryaev N., Skakunova T. Synchronization system in wireless sensor networks of oil and gas complex // *E3S Web of Conferences. Topical Problems of Green Architecture, Civil and Environmental Engineering, TPACEE 2019*, 03030, 2020.

[3] Poluyan A. Yu., Purchina O. A., Fugarov D. D., Gerasimenko E. Yu., Skakunova T. P. Application of bionic and immune algorithms for the solution of ambiguous problems of transportation routing // *Journal of Physics: Conference Series*. International Conference "Information Technologies in Business and Industry", Mathematical Simulation and Computer Data Analysis, **2**, 032057, 2019.

[4] Gerasimenko Y., Gerasimenko A., Fugarov D., Purchina O., Poluyan A. Mathematical modeling and synthesis of an electrical equivalent circuit of an electrochemical device // *Advances in Intelligent Systems and Computing*, **1259**, 471 – 480, 2021.

[5] Poluyan A. Yu., Purchina O. A., Fugarov D. D., Golovanov A. A., Smirnova O. V. Solution of task on the minimum cost data flow based on bionic algorithm // *Journal of Physics: Conference Series*. International Conference "Information Technologies in Business and Industry", Mathematical Simulation and Computer Data Analysis, **2**, 032056, 2019.

Investigation of Carbon Dioxide Absorption by Microalgae in the Aerosol State

Yu. B. Kohanov[1], Yu. E. Drobotov[2]*

[1]Don State Technical University, Rostov-on-Don, Russia
[2]Southern Federal University, Rostov-on-Don, Russia

*yu.e.drobotov@yandex.ru

Currently, there are various models for the absorption of carbon dioxide CO_2 by microalgae (MA), for example, Chlorella vulgaris, which are in a liquid state and in a certain volume: a circular cylinder, parallelepiped, container of arbitrary shape [1, 2]. This modeling can accurately predict how much CO_2 is consumed by a given quantity of microalgae when filling the volume with carbon dioxide due to aeration and/or mixing of the entire volume of culture liquid. In this report, it is stated that when microalgae are transferred from liquid: MA + H_2O + MA, to aerosol: MA + CO_2 + MA, state the absorption capacity of a given quantity of microalgae increases. This hypothesis is based on the fact that the concentration of carbon dioxide entering the aerosol is equal to the concentration in the air, while in the case of using a liquid solution, its absorption capacity is limited by the solubility of carbon in the liquid. Furthermore, the distance between MA cells in the aerosol state significantly exceeds their transverse diameter, while they are surrounded by CO_2 molecules, which negates the effect of shielding neighboring microalgae cells. To prove this hypothesis, the authors used full-scale tests and mathematical modeling. The latter is performed under various assumptions about the nature of the diffusion process, being based on a non-classical diffusion equation with a Riesz fractional derivative, for the study of which the Riesz fractional integro-differentiation is used [3, 4].

Acknowledgement. The research was financially supported by Southern Federal University, grant No. VnGr-07/2020-04-IM (Ministry of Science and Higher Education of the Russian Federation).

References

[1] *Probiotics in food: health and nutritional properties and guidelines for evaluation, Food and Agriculture Organization of the United Nations*: World Health Organization, Rome, 2006

[2] Aureli P., et al., Probiotics and health: An Evidence-Based Review // Pharmacological Research, **63**(5), 366–376 (2011), doi: 10.1016/j.phrs.2011.02.006.

[3] Samko S. G. *Hypersingular Integrals and Their Applications*. London and New York: Taylor & Francis, 2002

[4] Samko S. G., Kilbas A. A., Marichev O. I. *Fractional Integrals and Derivatives. Theory and Applications*. Gordon and Breach Science Publishers, 1993

Study of the Mechanical Properties of Composites Modified with Nanosized Additives

V. I. Kolesnikov, O. A. Belyak*, T. V. Suvorova, D. S. Manturov

Rostov State Transport University, Rostov-on-Don, Russia

*belyak.o.a@gmail.com

The paper presents studies of the mechanical characteristics of composite materials with matrices of the structural material phenylone C-2, epoxy-diane resin. Spinel TiN, Al_2O_3 was used as nanoadditives. Laboratory experimental studies of the mechanical properties of such nanocomposites were carried out on the NanoTest 600 setup by the nanoindentation method. In the result of laboratory experiments, "load – depth of immersion" diagrams were constructed, which are analogous to the "stress – strain" diagram in traditional macrotests on a tensile testing machine. The mechanical characteristics of composites for different volume fractions of applied nanosized additives were studied based on a finite element model in the ANSYS software. The static contact problem of penetration of a conical indenter into a multiphase medium is considered. A multiphase heterogeneous medium within the concept of effective homogeneity is considered as an equivalent homogeneous isotropic medium [1]. Diagrams "load – depth of implementation" were constructed, which were obtained in numerical experiments. Comparison of experimental and numerical diagrams made it possible to verify the proposed model and study relaxation processes in composites. Important conclusions have been made. The use of the considered nanosized additives contributes to the suppression of relaxation processes in composites [2]. The value of energy dissipation, which is due to internal friction in the material under study, was estimated for a composite with nanoadditives. The energy absorbed and dissipated by the sample in one loading-unloading cycle during nanoindentation is proportional to the area of the hysteresis loop. Irreversible losses of mechanical energy in one cycle are due to the presence of internal friction in a viscoelastic medium, the indicator of which is the so-called mechanical loss tangent. For the composites under consideration with such nanosized additives, the formation of interfacial regions due to the presence of good interfacial adhesion is observed. In this regard, a significant improvement in the mechanical properties of composite materials with a small proportion of additives is observed. Mechanical properties (hardness, Young's modulus) increase compared to the original matrix.

Acknowledgement

This study was supported by the Russian Science Foundation (project No. 20-08-00614), grant of the Rostov State Transport University.

References

[1] Kolesnikov V. I., Belyak O. A. *Mathematical Models and Experimental Studies are the Basis for the Design of Heterogeneous Antifriction Materials*. Moscow: Fizmatlit, 216, 2021.

[2] Smirnov S. V., Veretennikova I. A., Fomin V. M., Filippov A. A., Brusentseva T. A. Studying the viscoelastic properties of an epoxy resin strengthened with silicon dioxide nanoparticles by instrumented microindentation // *Mechanics of Composite Materials*. **55**(3), 337 – 347, 2019.

Finite Element Modeling of Highly Porous Materials Composed of Regular Gibson-Ashby Cells of Various Configurations

A. S. Kornievsky*, A. V. Nasedkin**

I. I. Vorovich Institute of Mathematics, Mechanics and Computer Sciences, Southern Federal University, 344090, Rostov-on-Don, Russia

*alexandr5koren@gmail.com, **nasedkin@math.sfedu.ru

Recently, there have been a lot of papers devoted to the study of highly porous materials. The increased interest of highly porous materials is associated with both the development of methods for the production of these structures from plastics or metals, and their mechanical advantages in some areas. For example, foam, cellular or honeycomb structures have relatively high rigidity and low thermal conductivity at low density. There are various mathematical approaches that describe the behavior of cellular materials, but the method based on the Gibson-Ashby cell is the most generally accepted and popular today. This model is determined by a fairly simple frame structure and describes the relationship between stiffness moduli and porosity. Numerical studies, in which the cell shape depends only on the porosity value, have been carried out. In this report, we consider regular lattices composed of Gibson-Ashby cells, in which not only porosity but also geometric characteristics can change, namely the dimensions of the edges and the inner frame of the cell. Algorithms for building models, generating finite element lattices, and numerically solving of the homogenization problem in the software package ANSYS have also been developed. The formulation of six boundary-value problems with displacement boundary conditions (three problems of stretching along the axes and three shear problems) is given. These problems allow us to find a complete set of effective stiffness moduli. Numerical experiments for a relative cell, which was considered earlier in other works, showed that the Gibson-Ashby analytical model accurately describes the effective properties of the material at a porosity of more than 70 %. These results were obtained in the researches of various authors, including the paper [1]. In the current study, the calculations were carried out at a fixed porosity and at various edge thickness values. The presented results demonstrate that the effective moduli of highly porous structures composed of Gibson-Ashby cells depend not only on porosity, but also on the geometric configuration. It has been found that the lattice stiffness increases as the thickness of the Gibson-Ashby cell struts increases at the same porosity. Anisotropic properties of Gibson-Ashby cell regular lattices were also determined by the Zener ratio.

Acknowledgement. This research was funded by the RFBR, project number 20-31-90057.

Reference

[1] Kornievsky A. S., Nasedkin A. V. Comparison of foam models from regular and irregular arrays of Gibson-Ashby's open-cells // *Bulletin of PNRPU. Mechanics*, **3**, 70 – 83, 2021.

Review of the Extended Concept of Numerical Modeling of Trunk Pipeline Networks

A. A. Korolenko, D. D. Fugarov*, V. V. Aseev, Albelame Amir Basim Kadim

Don State Technical University, Rostov-on-Don, Russia

*ddf_1@mail.ru

The extended concept of numerical modeling of trunk pipeline networks was developed and scientifically substantiated by V. E. Seleznev [1]. Initially, this concept was considered as a set of interrelated and mutually agreed propositions, formulated in the form of key rules and detailed recommendations for the use of high-precision numerical modeling to solve production problems of pipeline transport at all stages of its life cycle [2]. A promising form of practical use of such modeling is the technology of high-precision computer modeling (THPCM) of the life cycles of trunk pipeline networks [3]. The term "life cycle" should be understood as the period of time from the moment the need arises to create a system to the moment of its disposal [4]. Thus, the use of the technology of high-precision computer modeling of the life cycles of trunk pipelines networks is necessary already at the stages of the production of pipes and tubular parts, the design of pipeline systems and verification of the design decisions. The basis for the construction of a specific THPCM is a specially formed group of developed or selected methods of computer modeling [5]. It should provide a high-precision numerical analysis of the full range of states and processes in pipeline systems, corresponding to the complex of production tasks that this THPCM solves.

References

[1] Poluyan A. Yu., Purchina O. A., Fugarov D. D., Gerasimenko E. Yu., Skakunova T. P. Application of bionic and immune algorithms for the solution of ambiguous problems of transportation routing // *Journal of Physics: Conference Series*. International Conference "Information Technologies in Business and Industry", Mathematical Simulation and Computer Data Analysis, **2**, 032057, 2019.

[2] Fugarov D. D., Purchina O. A., Poluyan A. Y., Gerasimenko A. N., Rasteryaev N. V. Magnetodielectric ac measuring transducer for automation systems in oil refineries *// Journal of Physics: Conference Series*. International Conference "Information Technologies in Business and Industry", 062020, 2019.

[3] Gerasimenko Y., Gerasimenko A., Fugarov D., Purchina O., Poluyan A. Mathematical modeling and synthesis of an electrical equivalent circuit of an electrochemical device // *Advances in Intelligent Systems and Computing*, **1259**, 471 – 480, 2021.

[4] Onyshko D., Fugarov D., Purchina O., Poluyan A., Rasteryaev N., Skakunova T. Synchronization system in wireless sensor networks of oil and gas complex // *E3S Web of Conferences. Topical Problems of Green Architecture, Civil and Environmental Engineering, TPACEE 2019*, 03030, 2020.

[5] Poluyan A. Yu., Purchina O. A., Fugarov D. D., Golovanov A. A., Smirnova O. V. Solution of task on the minimum cost data flow based on bionic algorithm // *Journal of Physics: Conference Series*. International Conference "Information Technologies in Business and Industry", Mathematical Simulation and Computer Data Analysis, **2**, 032056, 2019.

A New Approach to Assessing and Improving the Load-bearing Capacity of Novikov Gears

V. I. Korotkin*, E. M. Kolosova

I. I. Vorovich Southern Federal University, Institute of Mathematics, Mechanics and Computer Science

*vkorotkin@sfedu.ru

The use of Novikov gearing with teeth of different hardness for various purposes is considered. For gearboxes of general machine-building application, the options of transmissions with hardened teeth are offered, for which a special basic profile is developed, which is part of the Russian State Standard. A fundamental approach to solving the problem of determining the main parameters for calculating the strength of these gears, consisting of two stages, is presented: (i) determination of both the main bending, contact stresses and stiffness of the teeth, and the phase, taking into account the coefficients of influence of the ends of the gear rim; (ii) modeling of the process of real multi-pair engagement with finding criterial stress in dangerous areas of the teeth that determine the load-bearing capacity and service life of the gearbox. By implementing this approach, generalized results of solving the spatial problem of the stress-strain state of the teeth at any position of the contact pad along their length are obtained and the way of obtaining partial forces at the contact sites and criterial stress are indicated. An engineering method for calculating the strength of Novikov gearing is proposed, on the basis of which gearboxes of general mechanical engineering with high-hard Novikov gears of relatively low degrees of accuracy are created. This made it possible to replace high-precision expensive involute gearing on the strained output stages of the gearboxes with less time-consuming in the manufacture hardened Novikov gearing of coarser degrees of accuracy and reduce the specific gravity of the gearbox by 1.5 times compared to the involute analogues. Preliminary calculations of the created promising hardened high-precision Novikov gearing are given and their significant advantage in comparison with involute analogues is shown. First, the developed modified Novikov gears with longitudinal modification of the working surfaces of thermally improved teeth of drive gearboxes of widely used for oil pumping units are described. On the example of one of the models of the gearbox, it is shown that the use of the proposed longitudinal modification of the working surfaces of the teeth in combination with an increase in the gear module provides a significant impact on reducing contact and bending stresses, increasing the load-bearing capacity and service life of the gearbox compared to the serial version produced by the domestic industry. The achieved effect at different stages of the gearbox reduces the stresses of the teeth from 1.75 to 2.54 times, increases the load-bearing capacity of the gearbox from 2.81 to 4.1 times, and increases the service life of the gearbox by an order of magnitude.

Acknowledgement. The work is financially supported by the Southern Federal University, project No. VnGr-07/2020-04-IM (Ministry of Science and Higher Education of the Russian Federation).

Mastering the Optimal Elements of Automotive Service in Evaluating Work Efficiency

E. E. Kosenko[1], A. V. Gladkiy[1], A. V. Cherpakov[1,2]*, C.-Y. Jenny Lee[3], C.-C. Yang[3]

[1]Don State Technical University, Rostov-on-Don, Russia
[2]Southern Federal University, Rostov-on-Don, Russia
[3]Department of Microelectronics Engineering, National Kaohsiung University of Science and Technology, Kaohsiung, Taiwan (R.O.C.)

*alex837@yandex.ru

The reliability of technical systems is one of the important indicators in the design of a car service [1]. This is especially true for the production of automotive equipment. A modern car is a complex system equipped with an on-board computer that allows real-time tracking of failures and possible pre-failure states. One of the important conditions for the efficient operation of modern automotive technology is the high-quality and timely maintenance [2]. Modern technical service is an interconnected system, the main purpose of which is to maintain the performance of automotive equipment. New automotive equipment coming into operation invariably needs constant monitoring and high-quality warranty service. It is the warranty policy of the enterprise that determines both the quality of the manufactured products and the possibility of attracting additional customers to purchase the manufactured equipment. In particular, a dealership providing a guarantee to a consumer of automotive equipment can offer other, but no less favorable conditions than a factory warranty, thereby expanding the circle of loyal customers. The methods used in evaluating the effectiveness of the warranty service are based on standard software products and the individual policy of the manufacturer, which consists in assessing the following indicators: (i) the number (percentage of the total number) of claims returned for revision due to violation of the requirements for their execution and presentation; (ii) the number (percentage of the total number) of rejected reclamation acts; (iii) presence of violations of the rules and requirements of KAMAZ PJSC, detected during on-site audits of the service center. The second important point in improving the efficiency of the service center is the well-functioning work of the spare parts service. The relationship of spare parts service and warranty service largely determines the terms of repair of automotive equipment, eliminates possible shortcomings of new cars made by manufacturers and allows expanding the base of loyal customers by improving the quality of customer service. Optimization of the work of the spare parts warehouse requires compliance with the following indicators: (i) mandatory maintenance of vehicles at the dealership; (ii) development of an algorithm for the storage of spare parts in a dealer center; (iii) optimization of cost and probability of meeting the demand for spare parts; (iv) development of informative relationship with the warranty service; (v) development of appropriate methods and software products to track demand and calculate the likelihood of complaints. Moreover, when developing methods to improve the efficiency of the car service, it is necessary to take into account the experience of world car brands, in which the warranty system and the spare parts supply system have already been debugged.

Acknowledgement. This research was funded by the grant from the Ministry of Science and Higher Education of Russia, supported by the Southern Federal University, grant No. VnGr-07/2020-04-IM.

References
[1] Kosenko E. E., Alekhin V. S. Analysis of methods for assessing the reliability of machines // *Proc. Int. Sci. Techn. Conf. "Transport and Transport-Technological Systems"*, 260 – 263, 2017 (In Russian).
[2] Kosenko E. E., Cherpakov A. V., Kosenko V. V., Nedoluzhko A. I. Methods for assessing the operational reliability of vehicles // ***Engineering Journal of Don***, **3**(46), 33, 2017 (In Russian).

Conducting Research on the Effect of Temperature on the Strengthening Properties of Building Steels

E. E. Kosenko[1], V. V. Kosenko[1], A. V. Cherpakov[1,2]*, S.-H. Chang[3]

[1]Don State Technical University, Rostov-on-Don, Russia
[2]Southern Federal University, Rostov-on-Don, Russia
[3]Department of Microelectronics Engineering, National Kaohsiung University of Science and Technology, Kaohsiung, Taiwan (R.O.C.)

*alex837@yandex.ru

A technique for determining the strength characteristics of reinforcing steels A240 and A500S, exposed to various temperature factors, has been developed [1]. Samples of building steels were loaded with uniaxial tension. The rods were hardened to a certain level. As a criterion, the proportion of the viscous component in the fracture of the samples after impact fracture was used, and the proportion of the viscous component of 70 % – 75 % was set as extreme values. An analysis of the experiments carried out allows one to draw the following conclusion. Unhardened reinforcement A240 has an almost 100 % ductile character at 20 °C in fracture. However, at –10 °C, the proportion of the viscous component drops to a critical 70 %. Hardened reinforcement A240 by 10 % above $\sigma_{t.av.}$ even at 20 °C already loses 20 % of the fraction of viscous component, and it exhausts the viscous properties at –5 °C. The reinforcement, hardened to $1.2\sigma_{t.av.}$, demonstrates at any temperature a brittle fracture. The conducted studies have shown a high tendency of steel A240 to brittle fracture. This tendency was clearly observed both with a decrease in temperature and with hardening of the samples by uniaxial tension. Such a behavior of steel A240 samples determines the scope of its application in non-critical structural elements not subject to deformations. The study of the strength potential of thermomechanically hardened steel A500S showed its greater resistance to thermal and mechanical stress. The use of steel A500S is possible at low temperatures not lower than –50 °C.

Acknowledgement. This research was funded by the grant VnGr-07/2020-04-IM, supported by Southern Federal University (Ministry of Science and Higher Education of Russian Federation).

Reference

[1] Vernezi N. L., Kosenko E. E., Kosenko V. V., Demchenko D. B., Cherpakov A. V. Research of strength capabilities of building steels under temperature effects // *Journal of Physics: Conference Series*, **2131**(2), 022019, 2021.

Development of a Service System for Universal Containers for Transportation

E. E. Kosenko[1], S. A. Zakharov[1], A. V. Cherpakov[1,2], S.-H. Chang[3], C.-F. Lin[4]

[1]Don State Technical University, Rostov-on-Don, Russia
[2]Southern Federal University, Rostov-on-Don, Russia
[3]Department of Microelectronics Engineering, National Kaohsiung University of Science and Technology, Kaohsiung, Taiwan (R.O.C.)
[4]Department of Electrical Engineering, National Taiwan Ocean University, Taiwan (R.O.C.)

*alex837@yandex.ru

The relevance of the issues of transportation of municipal solid waste (MSW) has not raised questions for many years. The constant growth of the population in cities [1], the difficulties with the disposal of solid waste and recycling are the tasks that need to be addressed in the near future. When solving technical issues related to the development of various devices, it is necessary to solve the following tasks: (i) development of automated places for temporary storage of solid waste; (ii) development of technical devices, which will be based on the technology of a smart container, designed for transporting solid waste; (iii) development of appropriate sanitary standards that allow organizing at the legislative level a system for the removal of solid waste for subsequent disposal at waste processing plants; (iv) development of a service system to monitor the technical condition of containers and carry out maintenance. The basis for the development of the service area and the recovery of containers for the transportation of MSW should take into account the type of container, the material from which the supporting elements are made. Such devices must meet modern safety requirements and provide the necessary functionality with minimal time spent on moving the container, operating the towing device, providing the possibility of assessing the technical condition, etc. An important element of the functioning of the solid waste disposal system is the development of an appropriate regulatory framework and a modern complex for managing the system for moving vehicles with containers. As temporary storage and sorting points, the development of terminals is required, the use of which is possible not only for the restoration of containers, but also for the storage of already restored containers, their sanitization, and preventive measures related to monitoring their current state. As the analysis of literary sources shows, the most common material for the manufacture of containers is steel with a thickness from 1.25 to 3 mm. The connection of the elements of the container is carried out by well-known methods, by means of welding. The operating conditions of containers determine the advised loaded zones, and the main task of the repair zone is to carry out diagnostic operations in order to control these zones. As diagnostic methods, it is planned to use scanning devices and an organoleptic method. The site for maintenance and restoration of containers must be equipped with specialized equipment that allows turning, milling, drilling and welding. The design of such lines requires the use of various approaches related to ensuring their reliability [2]. After the repair, it is required to control the welded joints, as well as the organization of a site for the restoration of the paintwork, the application of which should take into account the impact of aggressive environments.

Acknowledgement. This research was funded by the grant from the Ministry of Science and Higher Education of Russia supported by Southern Federal University, grant No. VnGr-07/2020-04-IM.

References
[1] Skudina A. A., Zagutin D. S., Bakhteev O. A., Kosenko E. E., Morozov D. S., Osipov I. Yu. Methodology for accounting for passenger flows and transport mobility of the population in the Rostov-on-Don city // ***Engineering Journal of Don*. 2**(53), 25, 2019 (In Russian).
[2] Kasyanov V. E., Teplyakova S. V., Demchenko D. B., Kosenko E. E., Khvan R. V. Reliability management of technical systems // *Truck*. **3**, 7 – 10, 2020 (In Russian).

On the Solutions of a Multidimensional Differential Equation in the sense of Riesz Fractional Calculus and Their Applications

G. S. Kostetskaya[1], Yu. E. Drobotov[1,2]*

[1]Southern Federal University, Rostov-on-Don, Russia
[2]North-Caucasus Center for Mathematical Research of the Vladikavkaz Scientific Centre of the Russian Academy of Sciences, Vladikavkaz Russia

*yu. e. drobotov@yandex. ru

Let R^n is the Euclidean space of multidimensional vectors with real coordinates. It is known that the class of hypersingular integrals D_{Ω}^{α} with a homogeneous characteristic $\Omega(\cdot)$ contains all homogeneous differential operators [1, p. 114; 2, p. 527]:

$$P_m(D) := \sum_{|j|=m} c_j \frac{\partial^m}{\partial x_1^{j_1} \ldots \partial x_n^{j_n}}, \quad |j| = j_1 + \ldots + j_n, \quad c_j \in \mathrm{R}^1.$$

Consequently, a large number of equations of mathematical physics can be reduced to the form of a hypersingular differential equation in the sense of Riesz differentiation:

$$D_{\Omega}^{\alpha} \varphi(x) = f(x), \quad x \in \mathrm{R}^n, \tag{1}$$

It is also clear that Equation (1) itself is of interest in the context of the creation of new mathematical models of complex physical processes.
The present paper raises the question of the fundamental solution of equation (1) in the case of more general conditions on $\Omega(\cdot)$ a function, based on its smoothness characteristics. Thus, a function $\varphi_{\alpha}(x)$, $x \in \mathrm{R}^n$ is found, satisfying the equation:

$$D_{\Omega}^{\alpha} \varphi_{\alpha}(x) = \delta(x), \tag{2}$$

where $\delta(x)$ is the Dirac delta-function. Equation (2) is understood in the sense of generalized functions over the Lizorkin class [2, p. 487]:

$$\lim_{\varepsilon \to 0} \left(D_{\Omega,\varepsilon}^{\alpha} \varphi_{\alpha}, \varphi \right) = (\delta, \varphi), \quad \varphi \in \Phi,$$

where $D_{\Omega,\varepsilon}^{\alpha}$ is the truncated hypersingular integral [1, p. 122], and Φ is a subspace of Schwartz space whose elements are orthogonal to polynomials [2, p. 487]. The resulting fundamental solution is then used in application to some problems of mathematical physics, providing Equation (1).
Acknowledgement. The research was financially supported by Southern Federal University, grant No. VnGr/2020-04-IM (Ministry of Science and Higher Education of the Russian Federation).

References
[1] Samko S. G. *Hypersingular integrals and their applications*. Taylor & Francis, 2002.
[2] Samko S. G., Kilbas A. A., Marichev O. I. *Fractional Integrals and Derivatives. Theory and Applications*. Gordon and Breach Science Publishers, 1993.

Solving and Applying a Multidimensional Integral Equation of the First Kind with the Riesz Potential Type Operator Featured by a Difference Characteristic

G. S. Kostetskaya[1], Yu. E. Drobotov[1,2]

[1]Southern Federal University, Rostov-on-Don, Russia
[2]North-Caucasus Center for Mathematical Research of the Vladikavkaz Scientific Centre of the Russian Academy of Sciences, Vladikavkaz, Russia

[2]yu.e.drobotov@yandex.ru

Let R^n is a Euclidean space of multidimensional vectors with real coordinates. In this report, a regularization and a numerical method for solving the following integral equation of the first kind are discussed:

$$K_c^\alpha \varphi(x) = f(x), \quad \varphi \in L^p(\mathrm{R}^n), \quad f \in I^\alpha(\mathrm{R}^n), \quad 1 < p < \frac{n}{\alpha}, \tag{1}$$

where K_c^α is the integral operator of the Riesz potential type with the difference characteristic:

$$K_c^\alpha \varphi(x) = \int_{\mathrm{R}^n} \frac{c(x-t)\varphi(t)}{|x-t|^{n-\alpha}}\, dt, \quad 0 < \alpha < n,$$

By L^p, $1 \le p \le \infty$, the classic space of p-integrable functions is denoted, while

$$I^\alpha(L^p) := \left\{ f : \quad f = I^\alpha \varphi, \quad \varphi \in L^p(\mathrm{R}^n) \right\}, \quad \|f\|_{I^\alpha(L^p)} = \|\varphi\|_{L^p(\mathrm{R}^n)},$$

$$I^\alpha \varphi(x) := \int_{\mathrm{R}^n} k_\alpha(x-t)\varphi(t)\, dt, \quad k_\alpha(x) = \frac{1}{\gamma_n(\alpha)} \begin{cases} |x|^{\alpha-n}, & \alpha - n \ne 0, 2, 4, \ldots, \\ |x|^{\alpha-n} \ln|x|, & \alpha - n = 0, 2, 4, \ldots, \end{cases}$$

is the space of Riesz potentials [1, p. 39]. The numerical multiplier $\gamma_n(\alpha)$ is selected in such a way as to provide the following for Fourier images [2, p. 490]:

$$\widehat{k_\alpha}(x) = |x|^{-\alpha}, \quad \alpha > 0.$$

The paper demonstrates the conditions under which Equation (1) is reduced to the form:

$$\varphi(x) + A\varphi(x) = g(x), \quad g(x) = R f(x), \tag{2}$$

where A and R are the integral operators computed in the framework of the study. The presented work reports the algorithm for solving the equation of the second kind (2) and its software implementation.

Acknowledgement. The research was financially supported by Southern Federal University, grant No. VnGr/2020-04-IM (Ministry of Science and Higher Education of the Russian Federation).

References
[1] Samko S. G. *Hypersingular Integrals and Their Applications*. Taylor & Francis, 2002.

[2] Samko S. G., Kilbas A. A., Marichev O. I. *Fractional Integrals and Derivatives. Theory and Applications*. Gordon and Breach Science Publishers, 1993.

On an Integrodifferential Equation and Its Solutions in Terms of the Riesz Potential Type Operator with a Difference Characteristic

G. S. Kostetskaya, Yu. E. Drobotov*, B. G. Vakulov

Southern Federal University, Rostov-on-Don, Russia

*****yu.e.drobotov@yandex.ru

Let R^n denotes the Euclidean space of real vectors, and K_c^α is the Riesz potential type operator

$$K_c^\alpha f(x) = \int_{\mathrm{R}^n} \frac{c(x-t) f(t)}{|x-t|^{n-\alpha}} dt, \quad 0 < \alpha < n, \tag{1}$$

where the function $c(x-t)$, called a characteristic, is bounded. In this report, the characteristic is assumed to have discontinuity of homogeneous function type:

$$c(t) = b(|t|)\theta(t/|t|).$$

Then, if $b(r)$ and $\theta(\sigma)$ are smooth enough with respect to the radial variable $r = |x|$ and the angle variable $\sigma = x/|x|$, the integral operator (1) may be inversed in the form of a convolution:

$$\left(K_c^\alpha\right)^{-1} f = D_\Omega^\alpha f + \mu_\alpha * f, \tag{2}$$

where $\mu_\alpha(x)$ is integrable, D_Ω^α is the hypersingular integral with the characteristics $\Omega(\cdot)$:

$$\left(D_\Omega^\alpha f\right)(x) = \frac{1}{d_{n,l}(\alpha)} \int_{\mathrm{R}^n} \frac{\left(\Delta_t^l f\right)(x)}{|t|^{n+\alpha}} \Omega(t) dt, \quad 0 < \alpha < l, \tag{3}$$

and specific conditions hold [1]. In the relation (3), $\left(\Delta_t^l f\right)(x)$ is a finite difference of the function f centered at the point x, having the order l and the step t; $d_{n,l}(\alpha)$ is the normalizing constant such that $D_\Omega^\alpha = (-\Delta)^{\alpha/2}$, if $\Omega \equiv 1$. In fact, hypersingular integrals can be considered as a natural generalization of partial differential operators to the case of non-integer orders [2], which brings new possibilities to handle sophisticated problems in physics and engineering.

In the report presented, the solutions of the equation related to operator (2) are studied, and the ways in which the results obtained may be applied are discussed.

Acknowledgement. The research was financially supported by Southern Federal University, grant No. VnGr/2020-04-IM (Ministry of Science and Higher Education of the Russian Federation).

References

[1] Vakulov B. G., Kostetskaya G. S., Drobotov Y. E. Riesz Potential in Generalized Hölder Spaces. In: *Fractal Approaches for Modeling Financial Assets and Predicting Crises*, I.

Nekrasova, O. Karnaukhova, B. Christiansen (Ed.), IGI Global, 249 – 273, 2018. http://doi:10.4018/978-1-5225-3767-0.ch013
[2] Samko S. G. *Hypersingular Integrals and Their Applications*. Taylor & Francis, 2002.

Nanoscale Field Emission Cell with a Blade-type Cathode

A. I. Kovalets*, I. L. Jityaev, G. D. Gavrishchakin, G. A. Malakhov, A. M. Svetlichnyi**

Southern Federal University, Institute of Nanotechnologies, Electronics, and Equipment Engineering, Taganrog, 347922, Russia

*kovalec@sfedu.ru, ******izhityaev@sfedu.ru

Development and research of nanoscale field emission cathodes is a promising area of nanoelectronics. However, it is necessary to solve several problems associated with lowering the threshold voltage, optimizing the nanoscale structure of the field emitter, and using cathode materials that meet the requirements for the stability and durability of the cathode. The use of carbon nanomaterials is advisable, since they are characterized by high electrical and thermal conductivity, as well as high resistance to ion bombardment. In this study, a vertical-type nanoscale field-emission cell is considered. The design is based on a blade SiC cathode with multilayer graphene films on the surface. Blade emitters allow an increase in the emission current density due to the larger surface area compared to pointed cathodes. The disadvantage of blade field emission cathodes is the destruction of the edge sections of the emitter. This is due to a local increase in the electric field strength and overheating of the cathode material [1]. The aim of the work is to optimize a field emission cell with a blade-shaped cathode and to increase the uniformity of the electric field strength on the emitting surface. The report presents a theoretical study of the electric field strength distribution in the interelectrode space of a cell with a blade-shaped cathode. The influence of the anode length on the distribution of the electric field strength at the emitting surface of the blade cathode was evaluated. The simulation results made it possible to reveal that the length of the homogeneous section of the field near the emitting surface is maximum in the considered range of cell parameters and is about 850 nm, when the anode length is ~ 97% of the cathode length (1000 nm). At the same time, local enhancements of the electric field strength at the corners of the field emission cathode were present in the plots. The field strengths at the corners of the emitter are 18% higher than those in the central region. It is possible to increase the uniformity of the field strength on the emitting surface by decreasing the anode length to a value of ~ 89% or less than the cathode length. In this case, the electric field strength at the corners of the blade does not exceed the value in the flat section by more than 0.5%, and the length of the homogeneous section is ~ 625 nm. Thus, it has been shown that reducing the length of the anode as compared to the length of the blade-shaped cathode is an effective way to increase the one-sidedness of the electric field at the emitting surface.

References

[1] Jityaev I. L., et al. // *J. Vac. Sci. Technol. B*, **37**, 012201, 2019.

Stereoselectivity of Acetylene Catalytic Hydrochlorination over Supported Palladium Chloride Complexes

T. V. Krasnyakova[1]*, S. A. Yurchilo[1], D. V. Nikitenko[1], I. O. Krasniakova[2], K. D. Kobets[1], I. A. Verbenko[3], S. A. Mitchenko[1]

[1]*Institute of Physical Organic and Coal Chemistry, Donetsk, Ukraine*
[2] *Southern Federal University, The Department of Physics, Rostov-on-Don, Russia*
[3]*Research Institute of Physics, Southern Federal University, Rostov-on-Don, Russia*

*ktv_list.ru

Polyvinyl chloride is one of the modern materials that are widely used commercially. It is characterized by wear resistance, mechanical strength, rigidity, lightness, dielectric and thermal insulation properties, resistance to corrosion and chemical attack, weather and temperature changes, lack of toxicity, high biocompatibility, etc. Such a unique combination of properties makes this material indispensable in construction and automotive industries, in the production of a wide range of medical products, sports equipment, etc. The monomer of this demanded plastic is vinyl chloride, about a third of which is industrially produced by the acetylene method. The industrial process for the acetylene hydrochlorination uses readily sublimated mercuric chloride deposited on activated carbon as a catalyst, and is accompanied by toxic emissions of mercury into the environment. Currently, there is no environmentally benign replacement for the industrial $HgCl_2$/C catalyst capable of providing the required process efficiency. This stimulates the search for alternative catalysts for the acetylene hydrochlorination. Purposeful development of new catalytic systems is impossible without the reaction mechanism understanding. A practical tool for establishing the mechanism of catalytic acetylene hydrochlorination is the method of isotopically labeled reagents, which makes it possible to reveal the stereoselectivity of the reaction and its rate-determining step. Using this method, we showed that products of both *anti*- and *syn*-addition of DCl to the triple bond in C_2H_2 are formed over carbon-supported palladium catalysts $PdCl_2$/C and $(NH_4)_2PdCl_4$/C. In addition, the reaction is accompanied by vinyl chloride isomerization: *trans*-H**D**C=CH**Cl** is transformed into *cis*-H**D**C=CH**Cl**. The activation energy of the *anti*-attachment pathway is lower than that for the formation of a *syn*-product: *trans*-vinyl chloride is predominantly released at low temperatures whereas at increasing temperature, the proportion of *cis*-vinyl chloride rises. The results of a study of the catalytic acetylene hydrochlorination in the systems with $PdCl_2$/C and $(NH_4)_2PdCl_4$/C will be reported. The main attention will be paid to the nature of the active sites of heterogeneous catalysts responsible for the formation of *anti*- and *syn*-addition products.

Acknowledgement. The study was carried out with the financial support of the Ministry of Science and Higher Education of the Russian Federation, State task in the field of scientific activity, scientific project No (0852-2020-0032)/(BAZ0110/20-3-07IF).

Parametric Transformation of Fractal Structures

G. M. Kravchenko[1], L. I. Pudanova[1], A. V. Cherpakov[1,2]*, I. A. Parinov[2]

[1]Don State Technical University, Rostov-on-Don
[2]Southern Federal University, Rostov-on-Don

*alex837@yandex.ru

The issues of implementing unique design solutions using parametric fractal algorithms are considered. The statement is substantiated that natural forms must be used in the design of unique buildings and structures. Fractal geometry allows the development of new biomorphic structures applicable in information design. The evolution of the shaping of flat and volumetric fractal structures is studied. The structures were modeled using specially developed algorithms, including those simulating the Koch fractals. The deterministic approach allows one to control the process of evolution. On the basis of the study, it was found that the obtained fractal structures of older generations are light without loss of stability. Recommendations are given for the use of fractal and parametric structures for solving a wide range of engineering problems: from the creation of load-bearing structures to the development of a road transport network of an urban environment. The introduction of innovative technologies, such as 3D printing, in conjunction with the new paradigm of parametric shaping, allows one to obtain architecturally and structurally more optimized and highly efficient designs. The result is the solution of structural and spatial problems in architecture, aesthetic improvement of the designed objects.
Acknowledgement. This research was funded by the grant No. VnGr-07/2020-04-IM from the Southern Federal University (Ministry of Science and Higher Education of Russian Federation).

Modeling an Acoustic Signal from Sources of Various Shapes with an Optoacoustic Effect in a Liquid

D. A. Kravchuk[1]*, I. B. Starchenko[2]**

[1]Southern Federal University, Taganrog, 347922, Russia
[2]OOO "Parametrica", Taganrog, 347922, Russia

*kravchukda@sfedu.ru; **ibstarchenko@gmail.com

The mechanisms of laser sound generation are different, and their relative contributions strongly depend on the density of the released energy. This effect is based on the thermal expansion of the part of the medium, where the light has been absorbed [1, 2]. The presence of microparticles in the liquid layer significantly changes the nature of sound generation due to the "deferred" release of heat from the particles into the liquid. The optoacoustic contribution of individual particles immersed in a non-absorbing liquid was investigated theoretically in the case of pulsed laser excitation [2]. The shapes of acoustic signals were calculated. When an acoustic pulse formed by a cylinder was formed in a liquid layer, a bipolar signal was formed with a rise amplitude equal to the duration of the laser action and a

relaxation zone, while the total duration of the signal was 550 μs. The calculations performed allow a more complex modeling process, when micron-sized sources may be present in a liquid cylindrical source, which will make it possible to evaluate the change in the signal depending on the number and size of these sources [3, 4]. The results obtained complement the studies carried out in the modeling of the optoacoustic signal for detecting infections in the blood and establishing the level of oxygen saturation, for flow cytometry [5 – 7].

References

[1] Gusev V. E. Karabutov F. A. *Laser Optoacoustics*. Moscow: Nauka, 304, 1991 (In Russian).

[2] Diebold G. J., Westervel P. J. The photoacoustic effect generated by a spherical droplet in a fluid // *J. Acoust. Soc. Am*., **84**(6), 2245 – 2251, 1988.

[3] Kravchuk D. A.Modeling the recovery of the optoacoustic image of oxygenated erythrocytes // *Applied Physics*, **2**, 73, 2021 (In Russian).

[4] Kravchuk D. A., Starchenko I. B. Reconstruction of the Optical Acoustic Signal for Visualization of Biological Tissues. In: P*hysics and Mechanics of New Materials and Their Applications - Proceedings of the International Conference PHENMA 2021*, Ivan A. Parinov, Shun-Hsyung Chang, Yun-Hae Kim, Nao-Aki Noda (Eds.) Springer Proceedings in Materials. Springer Nature, Cham, **10**, 473 – 479, 2021.

[5] Starchenko I. B., Kravchuk D. A., Kirichenko I. A. An optoacoustic laser cytometer prototype // *Biomedical Engineering*, **51**(5), 308 – 312, 2018.

[6] Kravchuk D. A. Mathematical model of detection of intra-erythrocyte pathologies using optoacoustic method // *Biomedical Photonics*, **7**(3), 36 – 42, 2018.

[7] Kravchuk D. A., Starchenko I. B., Orda-Zhigulina D. V., Voronina K. A. Research of optoacoustic signals on red blood cell models in a fluid with contrasting nanoagents // *Acoustic Journal*, **67**, 345 – 348, 2021 (In Russian).

The Results of Calculations of Visualization of Biological Tissues Based on the Optoacoustic Effect

D. A. Kravchuk[1]*, I. B. Starchenko[2]**

[1]Southern Federal University, Taganrog, 347922, Russia
[2]OOO "Parametrica", Taganrog, 347922, Russia

*kravchukda@sfedu.ru; **ibstarchenko@gmail.com

Currently, optoacoustic imaging is a new imaging technique in biomedicine [1 – 3]. The use of reconstruction for layered media is gradually attracting more and more attention [4]. We use a general extension method and pre-migration to construct an optoacoustic image. The proposed method transfers the positions of the transducer in advance to the corresponding position of the virtual scan, thereby forming a reconstruction that satisfies the assumptions about the homogeneity of the medium [4]. It is shown that it is efficient to combine the pre-migration method with all classical reconstruction algorithms. Due to calculations over a wide frequency range, the pre-migration operation is computationally efficient [5]. In addition, pre-migrations in polar and Cartesian coordinates can be used for tomography and microscopy applications, respectively. Forms of acoustic signals are calculated, during formation The method of preliminary migration is used to solve the problem of reconstructing an optoacoustic

image in inhomogeneous layered media. Moreover, direct wave propagation data are simulated by the Matlab 2017 k-wave program on a PC with a GeForce 1060 GPU [6 – 8].

References

[1] Bychkov A. S., Zarubin V. P., Karabutov A. A., et al., On the use of an optoacoustic and laser ultrasonic imaging system for assessing peripheral intravenous access // *Photoacoustics*, **5**, 10 – 16, 2017.

[2] Bychkov A. S., Cherepetskaya E. B., Karabutov A. A., Makarov V. A. Improvement of Image Spatial Resolution in Optoacoustic Tomography with the Use of a Confocal Array // *Acoustical Physics*. **64**(1), 77 – 82, 2018.

[3] Starchenko I. B., Kravchuk D. A., Kirichenko I. A. An optoacoustic laser cytometer prototype // *Biomedical Engineering*, **51**(5), 308 – 312, 2018.

[4] Estrada H. C., Huang X., Rebling J., Zwack M., Gottschalk S., Razansky D., Virtual craniotomy for high-resolution optoacoustic brain microscopy // *Scientific Reports*, **8**(1), 1459 – 1459, 2018.

[5] Kravchuk D. A Modeling the recovery of the optoacoustic image of oxygenated erythrocytes// *Applied Physics*. (2), 73, 2021 (In Russian).

[6] Kravchuk D. A., Starchenko I. B. Reconstruction of the Optical Acoustic Signal for Visualization of Biological Tissues. In: P*hysics and Mechanics of New Materials and Their Applications - Proceedings of the International Conference PHENMA 2021*, Ivan A. Parinov, Shun-Hsyung Chang, Yun-Hae Kim, Nao-Aki Noda (Eds.) Springer Proceedings in Materials. Springer Nature, Cham, **10**, 473 – 479, 2021.

[7] Kravchuk D. A., Starchenko I. B., Orda-Zhigulina D. V., Voronina K. A. Study of Optoacoustic Signals Using Models of Erythrocytes in a Liquid with Contrast Nanoagents // *Acoustical Physics*, **67**(3), 336 – 339, 2021.

[8] Kravchuk D. A. Application of the optoacoustic effect to measure glucose concentration // *Applied Physics*, (6), 63 – 66, 2021 (In Russian).

Development of Fused Filament Fabrication Based Additive Manufacturing Setup to Fabricate Flexible Part with Ethylene-Vinyl Acetate Material

Krishnanand[2], Ankit Nayak[1]*, Mohammad Taufik[2]

[1]Banasthali Vidyapith, Rajasthan, 304022, India
[2]Maulana Azad National Institute of Technology, Bhopal, 462003, India

*ankitnayak42@yahoo.in

Additive manufacturing (AM) is widely used for part fabricating from thermoplastic materials and metals. Fused filament fabrication (FFF) is one of the popular methods of AM, which is used to fabricate parts from thermoplastic materials. In FFF, the material in filament form is supplied to the extruder. Extruders heat up the filament up to the temperature so that the material can reach up to a semi-molten phase. The nozzle deposits the material on the build platform in a layered manner to fabricate the part. For filament-based extrusion, the filament must have enough column strength that it can feed in the extruder without its buckling. So that it can produce the required pressure in the extruder to deposit material from the nozzle on the build platform. Filament extrusion of Ethylene-Vinyl Acetate (EVA) is not possible due to its

low column strength. EVA filament may get buckled while it is feeding in the extruder. This article presents the development of FFF based AM machine and its software for pellet-based extrusion of the EVA material. The developed AM machine can directly process the pellets to fabricate the flexible parts using EVA material.

Mössbauer Studies of Magnetic Phase Transitions in Lead-free Multiferroic $BiFeO_3 - AFe_{1/2}B_{1/2}O_3$ (A = Ca, Sr; B = Nb, Sb) Solid Solutions

S. P. Kubrin[1], A. V. Pushkarev[2], N. M. Olekhnovich[2], Yu. V. Radyush[2], S. I. Raevskaya[1], V. V. Titov[1], M. A. Evstigneeva[1], I. G. Sheptun[1], I. N. Zakharchenko[1], M. A. Malitskaya[1], I. P. Raevski[1]*

[1]Physics Research Institute and Faculty of Physics, Southern Federal University, Rostov-on-Don, 344090, Russia
*[2]Scientific-Practical Materials Research Centre of NAS of Belarus, Minsk, **220072,** Belarus*

*igorraevsky@gmail.com

Compositional dependences of magnetic phase transition temperature, T_M, for lead-free perovskite solid solutions of $BiFeO_3$ (BFO) with the highly-ordered complex perovskite $SrFe_{1/2}Sb_{1/2}O_3$ (SFS) and its disordered counterparts $CaFe_{1/2}Nb_{1/2}O_3$ (CFN) and $SrFe_{1/2}Nb_{1/2}O_3$ (SFN) were studied using Mössbauer spectroscopy. Ceramic samples of BFO – SFS were obtained using high-pressure synthesis at 4 – 6 GPa and those of BFO – AFN (A = Ca, Sr) by usual synthesis at atmospheric pressure. Neither XRD nor Mössbauer studies detected the presence of the long-range ordering in the compositions studied except BFO – SFS compositions with x = 0.9 and 1. It was established previously [1] that in solid solutions of BFO with the highly-ordered complex perovskite $PbFe_{1/2}Sb_{1/2}O_3$ (PFS) concentration dependence of the magnetic phase transition temperature T_N is close to the theoretical $T_N(x)$ dependence [2], calculated for the case of the ordered distribution of Fe^{3+} and non-magnetic Sb^{5+} ions in the lattice. In contrast to this $T_N(x)$ dependences for $BiFeO_3 - x$SFS, $BiFeO_3 - x$SrFN and $BiFeO_3 - x$CaFN solid solution compositions with $x < 0.6$ were found to be close to the $T_N(x)$ dependence for $BiFeO_3$ solid solution with disordered perovskite $PbFe_{1/2}Nb_{1/2}O_3$ (PFN) plotted using the results of the magnetization and Mössbauer studies [1, 2]. It is worth noting that for the latter system experimental T_N values are somewhat lower than those calculated for the case of the disordered distribution of Fe^{3+} and non-magnetic B^{5+} ions in the lattice [2]. This ordering is likely to be a short-range and local and thus not detectable by the XRD. However, for compositions with $x > 0.6$ the $T_N(x)$ dependences show an abrupt drop down to $T_N \approx 50$ K. For all the three solid solution systems studied, these drops in the $T_N(x)$ curves are located in the $x \approx 0.65 - 0.75$ range, that is close to the percolation threshold for Bi^{3+} ions in the A-sublattice. Thus, the results obtained seem to be an experimental evidence of the magnetic superexchange between Fe^{3+} ions in $BiFeO_3$ via the empty 6p-states of Bi ions theoretically predicted by De Sousa et al. [3].

Aknowledgement. This study was supported by the Russian Foundation for Basic Research (Grant 20-52-00045) and Belarusian Republican Foundation for Fundamental Researches (Grant T20R-169).

References
[1] Raevski I. P., Kubrin S. P., Gusev A. A., Pushkarev A. V., Olekhnovich N. M., Radyush Y. V., Raevskaya S. I., Titov V. V., Permiakov A. Yu., Malitskaya M. A. // *Ferroelectrics*, **576**, 29 – 39, 2021.
[2] Smolenskii G. A., Yudin V. M. // *Sov. Phys.-Solid St*. **6**, 2936 – 2942, 1965.
[3] de Sousa R., Allen M., Cazayous M. // *Phys. Rev. Lett*. **110**, 267202, 2013.

Mössbauer and Dielectric Studies of $Bi_{1-x}Nd_xFe_{0.5}Cr_{0.5}O_3$ Solid Solutions Fabricated by a High-pressure Synthesis

S. P. Kubrin[1], A. V. Pushkarev[2], N. M. Olekhnovich[2], Yu. V. Radyush[2], S. I. Raevskaya[1], V.V. Titov[1], M. A. Malitskaya[1], P.A. Shishkina[1], I. P. Raevski[1]*

[1]Physics Research Institute and Faculty of Physics, Southern Federal University, Rostov-on-Don, Russia
[2]Scientific-Practical Materials Research Centre of NAS of Belarus, Minsk, Belarus

*igorraevsky@gmail.com

Multiferroics are the materials that possess two or more order parameters, for example ferroelectric and magnetic, attract huge attention due to the possibility of cross-control of their magnetic and electrical properties. The most widely studied perovskite is $BiFeO_3$, in which the temperatures of both ferroelectric and magnetic phase transitions significantly exceed room temperature. One of the main disadvantages of the most widely studied perovskite multiferroic $BiFeO_3$ is that it is an antiferromagnetic. On the basis of first-principal calculations, the possibility of obtaining ferromagnetic properties in $BiFe_{0.5}Cr_{0.5}O_3$ composition was predicted [1]. However, several works failed to find neither ferro- nor ferrimagnetic properties in ceramics, fabricated by a high-pressure synthesis (it is the only known method to obtain the perovskite modification of $BiFe_{0.5}Cr_{0.5}O_3$) [2]. $Bi_{1-x}Nd_xFe_{0.5}Cr_{0.5}O_3$ (x = 0.05, 0.2, 0.4, 0.6, 0.8) compositions studied were obtained by both usual and high-pressure (T_S = 1300 – 1400 °C, P = 4 GPa) synthesis. Samples, obtained by usual solid-state synthesis at atmospheric pressure, contained besides perovskite phase also some parasitic phases, mainly γ-phase of Bi_2O_3 (sylenite phase). In contrast to this the samples, obtained by high-pressure synthesis, consisted of pure perovskite phase. X-ray diffraction studies have shown that in such samples the morphotropic region between R3m and Pbam phases lies in the x = 0.1 – 0.2 compositional range, that is approximately at the same x-values as in other $Bi_{1-x}Nd_xFe_{1-y}Cr_yO_3$ systems. Thorough studies of Mössbauer spectra, measured at 15 K have shown that in $Bi_{1-x}Nd_xFe_{0.5}Cr_{0.5}O_3$ compositions a severe clustering of Fe and Cr ions takes place. As a result, the volume of the sample is almost completely filled with clusters, either enriched or depleted in Cr-ions. This clusterisation seems to be the main origin of the absence of ferro-nor ferrimagnetic properties in $BiFe_{0.5}Cr_{0.5}O_3$ as well as the similarity of concentration dependences of Neel temperature in solid solutions, where Fe-ions are replaced by paramagnetic ones [4, 5]. The temperature dependences of tgδ and both the real ε' and imaginary ε'' parts of the complex permittivity ε^* of $Bi_{1-x}Nd_xFe_{0.5}Cr_{0.5}O_3$ compositions were studied in a wide range of temperatures (15 – 450 K) and frequencies (100 Hz – 1 MHz) using an E7-20 impedance meter. Measurements at higher temperatures were not carried out because of the fast increase of conductivity and the danger of transformation of the metastable

perovskite phase, obtained by synthesis under high pressure into other phases stable at atmospheric pressure. While the tg$\delta(T)$ and $\varepsilon''(T)$ curves show several maxima, the temperature of which increase with the measuring frequency, the anomalies at the $\varepsilon'(T)$ curves have the step-like form and the low-frequency values of ε' are very large. Such behavior is typical, for example, for materials with the relaxation of the Maxwell – Wagner type. Conductivity activation energy (0.44 eV) corresponding to grain boundaries appears to be is substantially larger than activation energies of tgδ and ε'' (0.13 eV) which confirms the supposition of the relaxation of the Maxwell – Wagner type.

Acknowledgement. This study was partially supported by RFBR (project 20-52-00045 Bel_a) and by the Belarussian Republican Foundation for Fundamental Researches (project T20R-169).

Methodological Principles for Predicting the Thermophysical Properties of Ion-plasma Coatings

O. V. Kudryakov[1]*, V. I. Kolesnikov[2], V. N. Varavka[1], L. P. Aref'eva[1], E. S. Novikov[2], A. I. Voropaev[2]**

[1]Don State Technical University, Rostov-on-Don, Russia
[2]Rostov State Transport University, Rostov-on-Don, Russia

*kudryakov@mail.ru, **varavkavn@gmail.com

Currently, many scientific centers around the world are conducting intensive research on methods for modifying a metal surface and obtaining coatings with optimization of deposition technology, using digital synthesis software methods to predict the composition, structural parameters and functional properties of the deposited material. In addressing this ambitious challenge with regard to, for example, thermal barrier coatings (TBCs), which are applied to turbine blades of gas turbine engines in order to reduce thermal load, one of the key obstacles remains the lack of methods for predicting the thermophysical data of a thin modified surface layer or coating. One of the important conditions in the field of designing heat-shielding coatings is to ensure their low thermal conductivity, which, in turn, significantly depends on the microstructure and its characteristics such as volume, configuration and distribution of pores and secondary phases in the coating, matrix texture, structure of the substrate-coating interface, etc. In this regard, the main goal of the work was to create a calculation and experimental technique for determining the thermal conductivity of coatings. Its distinguishing features are: (i) a clear formulation of the basic physical principles of the model based on measuring the contact potential difference (CPD), calculating the Fermi level energy and calculating the thermal conductivity of a single-phase coating matrix from these data; (ii) instrumental determination of the characteristics of the microstructure, elemental and phase composition of the coating; (iii) correction of the value of thermal conductivity of the coating matrix, taking into account the morphology of the coating structure, their phase composition and porosity. To test the calculation method, we used the blades of an experimental high-speed gas turbine locomotive engine made of heat-resistant precipitation-hardening cast chromium-nickel alloy *Inconel 713LC*. Using vacuum ion-plasma technology, an experimental multiphase coating of the Nb-Ti-Al system with a small presence of Cr and Si and a thickness of about 80 μm was deposited on the blades. Due to the large thickness of the coating, arc deposition was carried out in a forced mode simultaneously from three cathode units with the

magnetic separation turned off. As a result, a coating with a complex morphology was formed, namely with porosity, elemental and phase composition variable in depth. A complex of fine metal-physical studies made it possible to take into account these structural features to the maximum extent in the calculation procedure. Calculating the thermal conductivity of the base metal of *Inconel 713LC* blades gives a result of 14.34 W/m·K. This value corresponds with satisfactory accuracy to the reference data, where the range of experimental values of 11.2 – 14.5 W/m·K is given for this alloy (for the corresponding temperature range of 25 – 800 °C). When calculating the thermal conductivity of the Nb-Ti-Al coating, a value of 4.76 W/m·K was obtained, corresponding to the level of thermal conductivity of ceramic materials. This result characterizes the Nb-Ti-Al coating as a thermal barrier coating that fully meets its functional purpose. Thus, as the main result of the work, it should be noted the creation and testing of the calculation and experimental technique for predicting and modeling the thermophysical properties of materials and coatings, taking into account their structural and phase features. The obtained values of the thermal conductivity of the base metal and the experimental coating of the Nb-Ti-Al system also indicate the expediency of using the CPD measurement technique in the process of predicting thermal conductivity.

Acknowledgement. The work was supported by the Russian Science Foundation (grant No. 21-79-30007).

Effect of B–Cation Ordering on the Phase Transition Temperature in $PbYb_{1/2}Nb_{1/2}O_3$ and $PbIn_{1/2}Nb_{1/2}O_3$

Yu. A. Kuprina*, A. A. Makarenko

Research Institute of Physics, Southern Federal University, Rostov-on-Don, Russia

*kyprins@rambler.ru

Double perovskites of $AB^1{}_{1/2}B^2{}_{1/2}O_3$ compositions have been actively studied over the past decade, since controlling the degree of ordering in the *B*-sublattice makes it possible to obtain objects of the same composition, but with different ferroelectric properties. Using the example of indoniobate and ytterboniobate, it was possible to show how a change in the degree of ordering in a *B*-sublattice changes the properties of ceramics from ferroelectric (antiferrelectric) with complete ordering of *B*-cations, to relaxor (with disordering of the corresponding sublattice). In double perovskites of type $AB^1{}_{1/2}B^2{}_{1/2}O_3$, there is an ordering in the *B*-sublattice, otherwise, the system $PbB^{3+}B^{5+}O_3$ can be considered as two sublattices PbB_1O_3 and PbB_2O_3, which can be in relation to each other as in an unordered state (then each elementary cell of a perovskite can have any neighbor, that is, the system will be in an unordered state, and in the volume of the crystal the parameter of the elementary lattice will be the average parameter of the entire set of elementary cells). However, there are states in which cations B^{3+} and B^{5+} are distributed in the volume of the crystal in such a way that they form an independent sublattice. This condition leads to changes in the properties of the samples. There are a number of double perovskites that can be both in a state of disorder and an ordered state, and the ferroelectric state of the system depends on the degree of order. It was shown [1] that in the $PbIn_{1/2}Nb_{1/2}O_3$ system, when the degree of order *s* changes from 0.6 to 0, both the temperature of the maximum dielectric susceptibility and its magnitude change. With complete disordering in the *B*-sublattice, a change in the dielectric susceptibility

characteristic of relaxor systems was observed, such as a shift in the maximum of the dielectric permittivity depending on the frequency of the applied field. In the absence of ordering in the *B*-sublattice for both $PbYb_{1/2}Nb_{1/2}O_3$ and $PbIn_{1/2}Nb_{1/2}O_3$ [2], the samples retain an elementary cell in a wide temperature range and a structural phase transition is not observed. The ordering temperature of $PbIn_{1/2}Nb_{1/2}O_3$ is 2325 K, but by varying synthesis methods it can be obtained in an unordered state in the form of a single crystal [2]. Obtaining monocrystal samples made it possible to observe the displacements of cations in *A*-sites and in sublattices depending on the presence of ordering In and Nb from the ferroelectric state with complete ordering of In and Nb ions to the manifestation of relaxor properties, when measuring the permittivity [2].

References

[1] Raevski, I. P., Kuprina Yu. A., Zakharchenko I. N., Gusev A. A., Isupov V. P., Bunina O. A. et al. Structural and dielectric studies of $PbYb_{1/2}Nb_{1/2}O_3$ ceramics with the differing degree of the long-range compositional ordering fabricated by mechanoactivation. In: *Advanced Materials: Proceedings of the International Conference on "physics and Mechanics of New Materials and Their Applications", PHENMA 2017*. Springer Nature, I. A. Parinov, S.-H. Chang, V. K. Gupta (eds.), **207**, 209 – 224, 2018.

[2] Kenji Ohwada, Shinya Tsukada et al. Effect of *B*-site randomness on the antiferroelectric/relaxor nature of the ground state: Diffuse and inelastic X-ray scattering study of $Pb(In_{1/2}Nb_{1/2})O_3$ // Physical Review B **98**, 054106, 2018.

Embedding Epitaxial VO_2 Film with Quality Metal-Insulator Transition to SAW Devices

M. E. Kutepov*[1], G. Ya. Karapetyan[1], T. A. Minasyan[1], V. E. Kaydashev[1], I. V. Lisnevskaya[2], K. G. Abdulvakhidov[3], E. M. Kaidashev[1]

[1]I. I. Vorovich Mathematics, Mechanics and Computer Science Institute, Laboratory of Nanomaterials Southern Federal University, 200/1 Stachki Ave., Rostov-on-Don, 344090, Russia

[2]Department of Chemistry, Southern Federal University, 7, Zorge St., Rostov-on-Don, 344090, Russia

[3]Smart Materials Research Institute, Southern Federal University, 178/24, Sladkov St., Rostov-on-Don, 344090, Russia

*kutepov.max@yandex.ru

We have implemented a concept of the "impedance loaded surface acoustic waves (SAWs) sensor" [1, 2] to embed a high quality epitaxial VO_2 film to SAWs devices. The VO_2 sensor, being the external load outside the acoustic channel, influences on the radio frequency (RF) signal reflection of interdigital transducer (IDT) or SAWs transfer to another channel, but not attenuating SAWs, which is beneficiary for wireless applications. Electrical characteristics alteration induced by phase transition in VO_2 film were optimized by varying oxygen ambient pressure, growth temperature and substrate type to meet requirements for embedding of a sensor to SAWs device. Best epitaxial VO_2 films grown by our pulsed laser deposition protocol show great switching characteristics with resistance altered from ~0.8 MΩ to ~100 Ω and narrow $R(T)$ hysteresis loop. We have characterized two SAWs devices, in which VO_2 sensing element is connected to input receiving-transmitting IDT, or to intermediate SAWs splitting IDT, in which the response is altered more than 3 times or more than twice

correspondingly upon phase transition in VO_2. Moreover, a 50° SAW phase shift is observed for SAW transmitted through the coupler. Additionally, the proposed devices were shown to operate as near infrared (IR) photodetectors/optically controlled RF splitters, which are prospective building blocks for smart wireless applications.

References

[1] Karapetyan G. Ya., Kaydashev V. E., Zhilin D. A., Kutepov M. E., Minasyan T. A., Kaidashev E. M. A surface acoustic wave impedance-loaded high sensitivity sensor with wide dynamic range for ultraviolet light detection // *Sensors and Actuators A*, **296**, 70 – 78, 2019.

[2] Karapetyan G. Ya., Kaydashev V., Kutepov M., Minasyan T., Kalinin V., Kislitsyn V., Kaidashev E., Passive wireless UV SAW sensor // *Applied Physics A*, **126**, 793, 2020.

A Novel Method for Determining Thermal Conductivity Coefficient, Thermal Diffusion Coefficient and Specific Heat Capacity of Moist Material

Le Quang Huy[a], Tran Van Phu[b], Pham Van Kien[c], Nguyen Hay[d,*]

[a]*Cao Thang Technical College, Ho Chi Minh City, 700000, Vietnam*
[b]*Phenikaa University, Hanoi, 100000, Vietnam*
[c]*Van Lang University, Ho Chi Minh City, 700000, Vietnam*
[d]*Nong Lam University, Ho Chi Minh City, 700000, Vietnam*

*ng.hay@hcmuaf.edu.vn

The study conducts the research on establishing mathematical model for drying process, in which the temperature field and moisture content are also determined. In which, the thermal conductivity equation, single-valued conditions, boundary conditions and thermal physics parameters of moist materials are determined. In this study, a novel method is proposed to simultaneously determine the thermal conductivity coefficient, thermal diffusion coefficient and specific heat capacity of moist materials by numerical analysis, and based on approximate roots of the thermal conductivity equation with symmetric boundary conditions of second type when Fourier is small enough. The formulas are established for determining the thermal conductivity coefficient, thermal diffusion coefficient and specific heat capacity of moist materials, in which: (i) thermal conductivity coefficient, $\lambda = \frac{4qL\left(t_{tb}(\tau)-t_0\right)}{\pi\left(t_1(\tau)-t_0\right)^2}$; (ii) thermal diffusion coefficient, $a = \frac{4L^2\left(t_{tb}(\tau)-t_0\right)^2}{\pi\tau\left(t_1(\tau)-t_0\right)^2}$; (iii) specific heat capacity, $C = \frac{q.\tau}{L.\left(t_{tb}-t_0\right).\rho}$.

Based on this result, the drying experiments were conducted using rice (ω = 12%, t = 29 °C) and pollen (ω = 30%, t = 21 °C) as the materials to detect the error and evaluate the reliability of the method proposed. In comparison to the results of the Rahman study, the method error for thermal conductivity coefficient of rice is 7.8%, and for thermal diffusion coefficient is 7.7%. In comparison to the results of the Monika study, the method error for thermal conductivity coefficient of pollen is 1.05%, and for thermal diffusion coefficient is 4.9%. The comparison results showed that the error of the method proposed is acceptable, which is helpful for the dryer design.

Non-stoichiometric PMN: Structure and Properties

A. R. Lebedinskaya

Southern Federal University, 344090, Rostov-on-Don, Russia

*lebed1989@rambler.ru

Ferroelectrics-relaxors are objects of great interest of researchers all over the world due to their unique properties [1, 2]. Due to these properties relaxors are perspective materials for using in areas of electronic engineering and energy storage [3]. One of the reasons for the appearance of relaxor properties is the presence of disorder, caused by the composition. Relaxors are characterized by cationic disorder at the nanoscale, which leads to random fields and local phase fluctuations. Among oxide perovskites of complex composition $A_3(B'B''_2)O_9$, lead magnoniobate $PbMg_{1/3}Nb_{2/3}O_3$ (PMN), which is still a traditionally model object for studying relaxor properties. Classical PMN has a cubic perovskite structure, but disorder in the *B*-site occupation by Nb^{5+} and Mg^{2+} results in the strongly distorted local structure. Despite intensive studies of relaxors the atomistic mechanism of the relaxor phenomenon is not well understood [3, 4]. The aim of this work was to obtain and study the structure and properties of ferroelectric ceramic samples of non-stoichometric lead magnoniobate. Samples of non-stoichiometric lead magnoniobate were obtained by solid-phase synthesis from a mixture of PbO, MgO, and Nb_2O_5 oxides, selected in the appropriate proportions, corresponding to the demanded compositions of $Pb(Mg_{1-y}Nb_y)O_{3-z}$ with $y = 0.25; 0.50; 0.75$ and $z = 0; 0.25$. The X-ray diffraction patterns of the initial precursors obtained by the solid-state methods for each composition of nonstoichiometric PMN-based solid state samples, taken at temperatures from 20 °C to 450 °C, are the typical X-ray diffraction profiles for the X-ray ceramic samples [5]. In the paraelectric phase, the arrangement of atoms in the PMN is described by the space group Pm3m. It was found that the cubic perovskite cell in PMN does not undergo distortion over the entire investigated temperature range from 20 °C to 450 °C. The obtained temperature dependences of the dielectric constant of the samples under study were used to estimate the size of the regions of chemical ordering in the *B*-sublattice. The possible structural models corresponding to the results, obtained in the study of non-stoichometric lead magnoniobate, are discussed in this work.

References

[1] Vakhrushev S. B., Kvjatkovskiy B. E., Naberezhnov A. A., Okuneva N. M., Tolerverg B. P. // *Ferroelectrics*, **90,** 173, 1989.

[2] Cowley R. A., Gvasaliya S. N., Lushnikov S. G., Roessli B., Rotaru G. M. // *Advances in Physics*, **60**(2), 229, 2011.

[3] Pandya S., Wilbur J., Kim J., Gao R., Dasgupta A., Dames C., Martin L. W. // *Nature Materials*, **17**(5), 432 – 438, 2018.

[4] Lebedinskaya A. R., Kasparova N. G., *Advanced Materials, Advanced Materials - Proceedings of the International Conference on "Physics and Mechanics of New Materials and Their Applications", PHENMA 2018*, Springer Proceedings in Physics, Ivan A. Parinov, Shun-Hsyung Chang, Yun-Hae Kim (Eds.). Springer Nature, Cham, Switzerland, **224**, 267 – 276, 2019.

[5] A.R. Lebedinskaya, A.G. Rudskaya, *IOP Conf. Series: Materials Science and Engineering*, **100**, 012061 (2020).

Influence of Synthesis Conditions of Lead Magnoniobate on its Structure and Properties

A. R. Lebedinskaya*, A. G. Rudskaya

Southern Federal University, 344090, Rostov-on-Don, Russia

*lebed1989@rambler.ru

This work continues our series of studies on the structural features of the ferroelectric relaxors [1, 2]. Relaxor ferroelectrics with the general chemical formula $Pb(B'B'')O_3$ and with a perovskite structure have attracted a great deal of scientific attention because they exhibit a range of unique physical properties. It was found that only lead magnoniobate $PbMg_{1/3}Nb_{2/3}O_3$ (PMN) with a perovskite structure has unique relaxor properties, but not with a pyrochlore structure [3, 4]. Therefore, the main purpose of this work was to determine the conditions for obtaining samples of non-stoichometric PMN with a perovskite structure and then to investigate its physical properties. To solve the set tasks, a number of non-stoichiometric samples were synthesized by solid-phase synthesis of samples of lead magnoniobate with general chemical formula $(1 - x)PbMg_{1/3}Nb_{2/3}O_3 - xPbMg_{1/2}Nb_{1/2}O_{2.5}$ in the concentration range of x from 0 to 1 with a step of $\Delta x = 0.1$ at firing temperatures equal 870, 880 and 890 °C. X-ray diffraction profiles obtained of synthesized samples on a DRON-3M X-ray diffractometer (using Co_{K_α} radiation with Bragg-Brentano focusing). The X-ray diffraction profiles of all samples were processed using the PowerCell computer program. For compositions $(1 - x)PbMg_{1/3}Nb_{2/3}O_3 - xPbMg_{1/2}Nb_{1/2}O_{2.5}$ with x = 0.1, 0.2,…, 0.9 phase concentrations are determined perovskite and pyrochlore structure of PMN, as well as small amounts of lead and niobium oxides. For the composition $0.3PbMg_{1/3}Nb_{2/3}O_3 - 0.7PbMg_{1/2}Nb_{1/2}O_{2.5}$ the concentrations of the perovskite and pyrochlore PMN phases are determined, and also a small amount of magnesium oxide. Reflections, present on X-ray diffraction patterns, corresponding to the extreme compositions $(1 - x)PbMg_{1/3}Nb_{2/3}O_3 - xPbMg_{1/2}Nb_{1/2}O_{2.5}$, are characteristic of the perovskite and pyrochlore PMN phases, while also for lead oxide. It was found that as the parameter x increases, slight decrease in the volume of perovskite cells from $V = 66.35$ Å^3 at $x = 0$ to $V = 66.21$ Å^3 at $x = 1$ indicates the formation of a solid solution $(1 - x)PbMg_{1/3}Nb_{2/3}O_3 - xPbMg_{1/2}Nb_{1/2}O_{2.5}$. Noted, that the relative intensity of the peaks of all reflections does not change from changes in concentration x at all firing temperatures.

References

[1] Lebedinskaya A. R., Kasparova N. G., *Advanced Materials, Advanced Materials - Proceedings of the International Conference on "Physics and Mechanics of New Materials and Their Applications", PHENMA 2018*, Springer Proceedings in Physics, Ivan A. Parinov, Shun-Hsyung Chang, Yun-Hae Kim (Eds.). Springer Nature, Cham, Switzerland, **224**, 267 – 276, 2019.

[2] A.R. Lebedinskaya, A.G. Rudskaya, *IOP Conf. Series: Materials Science and Engineering*, **100**, 012061 (2020).

[3] Pandya S., Wilbur J., Kim J., Gao R., Dasgupta A., Dames C., Martin L. W. // *Nature Materials*, **17**(5), 432 – 438, 2018.

[4] Bokov A. A., Rodriguez B. J., Zhao X., Ko J.-H., Jesse S., Long X., Qu W., Kim T. H., Budai J. D., Morozovska A. N., Kojima S. // *Z. Kristallogr.*, **226**, 99 – 107, 2011.

The Influence of the Lattice Defects on the Magnetic and Dielectric Behavior in $YbMn_{1-x}Fe_xO_3$

Li Zhengyou*[1], Kamaludin Abdulvakhidov[1], Alexander Soldatov[1], Ivan Dmitrenko[1], Marina Sirota[1], Irina Mardasova[2], Marina Vitchenko[2], Elizaveta Vinokurova[3]

[1]Southern Federal University, 178/24, Sladkov Str., Rostov-on-Don, 344090, Russia
[2]Don State Technical University, 1, Gagarin Sq., Rostov-on-Don, 344000, Russia
[3]Premium Consulting, 16, Bld. 2, Pestovskiy Alleyway, Moscow, 109462, Russia

*chl@sfedu.ru

Ytterbium iron perovskites ($YbFeO_3$) and ytterbium perovskite manganites ($YbMnO_3$), have attracted considerable attention for their potential using as materials for magnetic field sensors and magneto-optical data storage devices. Rare-earth ferrites with the general formula $RFeO_3$ (R = Dy – Yb) have generally orthorhombic structure, and the hexagonal phase of $YbFeO_3$ has been successfully synthesized in the form of thin-film at a specific temperature [1]. $ErMnO_3$ undergoes a phase transition from hexagonal to orthorhombic structure at 20.2 GPa [2]. However, the phase transitions in $YbMnO_3$ under pressure have not been adequately studied. Moreover, the influence of the concentration of the lattice defects, caused by the high-pressure torsion (HPT) in the phase transition, on the magnetic and dielectric behavior of $YbMn_{1-x}Fe_xO_3$ is still poorly understood. In this work, we investigated the phase transition of $YbMn_{0.3}Fe_{0.7}O_3$ at relatively small pressures (less than 1 GPa) and shear deformation using rotating Bridgman anvils. The relationship between the HPT pressure and the change of the lattice parameters of these synthesized samples was built. The dielectric characteristics were studied at various frequencies (1 kHz – 1 MHz) and temperatures (77 K – 773 K) by the dielectric spectroscopy method. The pressure dependencies of bandgap E_g on the pressures were determined by the optical absorption spectroscopy method. The influence of pressure on the Fourier-transform infrared spectroscopy (FTIR), magnetic and ferroelectric dielectric hysteresis loops were analyzed. The frequency-dependent magnetoresistive responses were studied at various frequencies (1 kHz – 1 MHz) and temperatures (77 K – 773 K).

References

[1] Rai R. C., Horvatits C., Mckenna D., Du Hart J. Structural studies and physical properties of hexagonal-$YbFeO_3$ thin films // *AIP Adv.* **9**, 015019, 2019.
[2] Lin C., Liu J., Li X., Li Y., Chu S., Xiong L., Li R. Phase transformation in hexagonal $ErMnO_3$ under high pressure // *J. Appl. Phys.* **112**, 113512, 2012.

The Influence of the Lattice Defects on the Physical Properties of $Yb_3Fe_5O_{12}$ Iron Garnet

Li Zhengyou*[1], Kamaludin Abdulvakhidov[1], Alexander Soldatov[1], Ivan Dmitrenko[1], Marina Sirota[1], Irina Mardasova[2], Marina Vitchenko[2], Elizaveta Vinokurova[3]

[1]Southern Federal University, 178/24, Sladkov Str., Rostov-on-Don, 344090, Russia
[2]Don State Technical University, 1, Gagarin Sq., Rostov-on-Don, 344000, Russia
[3]Premium Consulting, 16, Bld. 2, Pestovskiy Alleyway, Moscow, 109462, Russia

*chl@sfedu.ru

Ytterbium iron garnet (YbIG) has properties similar to other rare-earth garnets, which could be used in various microwave, acoustic, and optical devices. However, YbIG has not been well studied, and there are only a few published results on its properties. In this work, YbIG was synthesized by the solid-phase reaction method and mechanically activated by the high-pressure torsion (HPT) method in Bridgman anvils in the pressure range from 50 MPa to 1 GPa. The lower anvil was rotated at the speed of 6 revolutions per hour (rph). Using a synergistic application of X-ray diffraction analysis (XRD), scanning electron microscope (SEM), and energy-dispersive X-ray analysis (EDX), we revealed that the unit cell parameters, particle sizes, and the crystalline sizes of mechanically activated samples are varying with the pressure. In the result of a change in the concentration of the lattice defects in mechanically activated samples, various metastable phases were formed. We also found that the recrystallization process occurred at a pressure of about 380 MPa, and the amorphous phase begins to increase significantly when the pressure exceeds 500 MPa. The dielectric characteristics were investigated at various frequencies (1 kHz – 1 MHz) and temperatures (77 K – 773 K) by the dielectric spectroscopy method, and the dependencies of bandgap E_g on the pressures were determined by the optical absorption spectroscopy method. The influence of pressure on the Fourier-transform infrared spectroscopy (FTIR), magnetic and ferroelectric dielectric hysteresis loops were analyzed. The frequency-dependent magnetoresistive responses were studied at various frequencies (1 kHz – 1 MHz) and temperatures (77 K – 773 K). These studies were a proceeding of previous studies [1] in a deeper and broader range.

References

[1] Abdulvakhidov K., Soldatov A., Dmitrenko I., Li Z., Kallaev S., Omarov, Z. The influence of the structural defects on the physical properties of $Er_3Fe_5O_{12}$ ferrite-garnet // *Results Phys.* **22**, 103905, 2021, https://doi.org/https://doi.org/10.1016/j.rinp.2021.103905.

Influence of Structural Defects and Crystallite Size on Physical Properties of $YbFeO_3$

Li Zhengyou[1], Kamaludin Abdulvakhidov*[1], Pavel Plyaka[2], Marina Sirota[1], Marina Vitchenko[3], Irina Mardasova[3], Elza Ubushaeva[4]

[1]Southern Federal University, 178/24, Sladkov Str., Rostov-on-Don, 344090, Russia
[2]Southern Scientific Center of the Russian Academy of Sciences, 41, Chekhov Ave, Rostov-on-Don, 344006, Russia
[3]Don State Technical University, 1, Gagarin Sq., Rostov-on-Don, 344000, Russia
[4]Moscow Aviation Institute, 4, Volokolamskoe shosse, Moscow, 125993, Russia

*phys.kam@mail.ru

The perovskite-structured orthoferrite $YbFeO_3$ is an antiferromagnetic phase at room temperature and high temperature, and can be used as smart devices, gas detection sensors, oxygen-permeable membranes, and oxidation or reduction active catalysts due to its unique properties. Therefore, it has attracted extensive attention of researchers in recent years. Another thing that has attracted the attention of researchers is mechanical activation, which is one of the ways to control the physical properties of materials without changing their stoichiometry. Mechanical activation using a Bridgman anvil is a relatively clean method compared to using planetary ball mills and other dispersants. This paper was the first time to study the effects of structural defects and crystallite size on the physical properties of $YbFeO_3$. $YbFeO_3$ was synthesized using conventional solid-phase synthesis reaction method, with structural defects and size controlled by mechanical activation in the Bridgman anvil. The pressure range was from 100 MPa to 1.4 GPa. Several methods such as SEM, XRD, UV-vis, VSM, EPR were used to analyze the physical properties of reference and mechanically activated samples. The size of coherent scattering regions (D) and magnitude of microstrain ($\Delta d/d$) were determined by the full-profile Rietveld method using the Fullprof software package. The dislocation density was calculated from the size D. Since mechanical activation is a process of mechanical action with the relaxation of mechanical energy through various channels, the crystal lattice should undergo significant distortion and enter a metastable state. By analyzing the dependence of the magnetic hysteresis loop on the crystallite size D, we found the critical crystallite size of $YbFeO_3$, at which the coercive force H_c has a maximum value. The changes in g-factor of nanoscale crystallites were found to be correlated with the parameters of the magnetic hysteresis loop.

Complex Electromechanical Characteristics and Microstructure Features of Porous Piezoceramics

M. A. Lugovaya*, N. A. Shvetsova, E. I. Petrova, I. A. Shvetsov, M. A. Marakhovsky, O. E. Bryl, A. N. Rybyanets

Southern Federal University, 344090, Rostov-on-Don, Russia

*lugovaya_maria@mail.ru

In this paper, a comprehensive study of microstructure/properties interrelation for porous piezoceramics based on PZT-type composition was carried out. Ferroelectrically "soft" PZT-

type piezoelectric ceramics of the composition $Pb_{0.95}Sr_{0.05}Ti_{0.47}Zr_{0.53}O_3$ + 1% Nb_2O_5 with different relative porosity in the range of 0 – 50 % and average pore size of 10 – 30 μm were chosen as the object of the study. Experimental samples of porous piezoceramics were obtained using a modified method of pore former burning-out. Microstructural studies were performed on polished and chipped surfaces of porous piezoceramics samples using the scanning electron microscopes (JEOL JSM-6390LA and TM-100, Hitachi). The measurements of the dielectric, piezoelectric, and electromechanical parameters of the samples were carried out at the radial and thickness modes of oscillations of piezoceramic discs in accordance with the IEEE Standard, as well as using the method of analysis of resonance spectra (PRAP). Porosity dependencies of dielectric, elastic, piezoelectric and electromechanical coefficients of the porous ceramics in the relative porosity range 0 – 50 % were measured and analyzed. In the result of SEM microstructure analysis, it was found that at any connectivity type (3-0, 3-3) and porosity up to 50 % the real structures of porous piezoceramics were close to the matrix medium structure with continuous coral-like piezoceramic skeleton. It was revealed that the following microstructural features of porous piezoceramics define the dielectric, piezoelectric and electromechanical properties of porous piezoelectric ceramics: branched flexible three-dimensional piezoceramics skeleton and quasi-rod piezoceramics structure in the direction of residual polarization of porous piezoceramics. Changes in the mechanical and electrical boundary conditions on the branched coral-like microstructure, as well as inhomogeneous polarization of the piezoceramic skeleton also play a significant role in the formation of electromechanical properties of porous piezoelectric ceramics. It was found that porous piezoceramics similarly to 1-3 type composites are characterized by increased values of k_t and d_{33}, and reduced values of d_{31}, k_p, compared to dense piezoceramics, that makes them perspective materials for different ultrasonic applications in medical diagnostics and therapy, nondestructive testing, and active piezoelectric membranes for reverse osmosis, ultra- and microfiltration processes. It was revealed that the microstructural features of porous piezoceramics define the character of the porosity dependences of the dielectric, piezoelectric and electromechanical properties of porous piezoelectric ceramics. In conclusion, the relationship between microstructure and properties, as well as technological aspects of industrial production and new applications of porous piezoceramics for medical ultrasound diagnostics and therapy, non-destructive testing and piezoelectrically active membranes for reverse osmosis, ultra- and microfiltration processes are discussed.

Acknowledgement. The study was financially supported by the Ministry of Science and Higher Education of the Russian Federation (Scientific project No. 0852-2020

New Opportunities of Thermodynamic Calculations in Studying Phase Systems

T.G. Lupeiko, D.V. Chirkova*, A.N. Soloviev

Southern Federal University, Rostov-on-Don, Russia

*sdanamail@list.ru

Using the example of ternary reciprocal systems (TRS) with exchange interaction in melts, a new thermodynamic platform has been developed and successfully tested. Instead of the

traditional enthalpies and entropies, it is based on two energy characteristics expressed in *RT* units, one of which belongs to exchange interaction in melts ($\Delta G/RT$), and the second characteristic describes the transition of the corresponding solid phase into the liquid state ($\Delta Z_{AX}/RT$). Using new thermodynamic parameters, the primary equations for symmetric isotherms of solubility of TRS phases were obtained. In particular, for the solubility isotherms of salt *AX* in the TRS melts, this equation has the form:

$$\ln xy + \frac{\Delta G}{RT}(1-x)(1-y) - \frac{\Delta Z_{AX}}{RT} = 0 \qquad (1)$$

where *x* and *y* are equivalent fraction of ions A^+ and X^- in the equilibrium melt, respectively. On the basis of these equations, we have derived for the first time the quantitative criteria for the existence of a homogeneous melt (complete phase solubility) of a fuel assembly and the conditions for the existence of equilibria of melts with their solid phases. More than that, we obtained conditions of limited solubility (stratification) in fuel assembly melts, as well as a number of other breakthrough results. It is concluded that, in comparison with the traditional thermodynamic approach, the platform of new variables is much more effective when applied to the analysis of phase equilibria of fuel assemblies. It can be recommended for the analysis of other phase systems as well as complicated physico-chemical process of solubility in general.

On the Study of Eigen-vibrations of Orthotropic Topographic Waveguides

Lyubov I. Parinova

I. I. Vorovich Institute of Mathematics, Mechanics and Computer Science, Southern Federal University, 8a, Milchakov Street, Rostov-on-Don, 344090, Russia

parinovali@mail.ru

The regularities of elastic wave propagation in topographic waveguides, are widely used in flaw detection, aircraft industry, seismology and space industry. Using the method of non-destructive testing in welding and soldering structures, the resulting defects are detected. Taking into account the peculiarities of the behavior of edge bending waves, compact devices are being created to monitor the state of the cutting tool. Topographic waveguides made of elastic materials can be used as delay lines, and can also be used as filters to suppress false signals. In previous studies [1 – 6], based on the hypotheses of plates of variable stiffness of the Kirchhoff type [1 – 4] and the Timoshenko type [5, 6], using the variational principle of Hamilton-Ostrogradsky, semi-analytical methods were developed for constructing dispersion dependences for wave modes, propagating in elastic orthotropic topographic waveguides with different types of cross-sections. In [1], oscillations of an infinite orthotropic wedge-shaped waveguide were studied. Using the developed method, the relative phase velocities of the first two modes are found. For an isotropic material, a comparison was made with similar results obtained from the well-known geometric-acoustic theory. An orthotropic topographic waveguide limited in height with a triangular cross-section was studied in [2]. In [3], the dispersion properties of orthotropic topographic waveguides limited in height were studied depending on the geometry of the cross-section. The dispersion sets obtained are compared with the results of [2]. In [4], oscillations of a semi-infinite plate waveguide were studied and

compared with the results obtained for the Konenkov flexural wave. In [5], for a Timoshenko-type model, vibrations of a topographic waveguide limited in height with a triangular cross-section were studied. In [6], a topographic waveguide with a cross-section in the form of an isosceles trapezoid was studied, and the functional, constructed for a Timoshenko-type model, was compared with the functional, constructed for a Kirchhoff-type model, and described in [3]. A comparison was also made for models of the Timoshenko type and the Kirchhoff type. In [7], the features of wave processes in topographic waveguides with rheological properties were studied. A problem is formulated in operator form for a topographic orthotropic waveguide with an arbitrary cross-section, limited in height. The constructed dispersion curves for a viscoelastic waveguide are compared with similar curves, constructed for an elastic waveguide. In the present study, using the finite element method, the oscillation features of isotropic and orthotropic height-limited topographic waveguides with a triangular cross-section are studied. The cut-off frequencies obtained by the semi-analytical method are compared with similar results, obtained using the FlexPDE finite element package.

***Acknowledgements*.** This study was funded by RFBR, project No. 19-31-90079. The author expresses gratitude to Prof. A. O. Vatulyan for his constant attention to the work.

References

[1] Vatulyan A. O., Parinova L. I. Study of Wedge Waves in Orthotropic // *Vestnik DGTU*, **5** (4(26)), 491 – 499, 2005 (In Russian).

[2] Vatulyan A. O., Parinova L. I. On the Elastic Waves Propagating Along the Edge of the Wedge with Small Opening Angle. In: *Advanced Materials - Techniques, Physics, Mechanics and Applications*, Springer Proceeding in Physics, Ivan A. Parinov, Shun-Hsyung Chang, Muaffaq A. Jani (Eds.). Heidelberg, New York, Dordrecht, London: Springer Cham. **193**, 309 – 319, 2017.

[3] Vatulyan A. O., Parinova L. I. On The Study of Dispersion Properties of Topographic Waveguides // *News of Universities North-Caucasus Region. Natural Sciences*. **3**, 10 – 17, 2018. (In Russian)

[4] Parinova L. I. On the Wave Propagating Along the Plate-like Waveguide. In: *Advanced Materials Proceedings of the International Conference on "Physics and Mechanics of New Materials and Their Applications", PHENMA 2018*, Springer Proceeding in Physics. Ivan A. Parinov, Shun-Hsyung Chang, Yun-Hae Kim, **224**, 487 – 494, 2019.

[5] Vatulyan A., Parinova L. On the Use of Models of the Timoshenko Type in the Analysis of Wave Processes in Wedge-Shaped Waveguides. In: *Advanced Materials – Proceedings of the International Conference on "Physics and Mechanics of New Materials and Their Applications", PHENMA 2019*, Springer Proceedings in Materials, Ivan A. Parinov, Shun-Hsyung Chang, Banh Tien Long (Eds.). Springer Nature, Cham, Switzerland, **6**, 383 – 389, 2020.

[6] Vatulyan A. O., Parinova L. I. A Study of Wave Processes in Elastic Topographic Waveguides // *Acoustical Physics*, **67**(2), 101 – 107, 2021.

[7] Vatulyan A. O., Parinova L. I. On Wave Processes in Viscoelastic Topographic Waveguides // *Mechanics of Solids*, **57**(2), 50 – 60, 2022.

Triode-type Field Emission Cell with a Nanoscale Pointed Cathode

G. A. Malakhov, I. L. Jityaev*, A. I. Kovalets, G. D. Gavrishchakin, A. M. Svetlichnyi

Southern Federal University, Institute of Nanotechnologies, Electronics, and Equipment Engineering, Taganrog, 347922, Russia

*izhityaev@sfedu.ru

Important tasks in the development of field emission structures are the reduction of the geometric dimensions of the field emission cell, the reduction of the power consumption, the choice of materials that ensure the durability of the cathode and emission stability. Recently, increased interest has been observed in field emission nanostructures based on graphene films. Therefore, the aim of this work is to study a triode type field emission cell with a graphene-based cathode on silicon carbide and a nickel control grid separated from the cathode by a silicon dioxide dielectric layer. Theoretical studies of design parameters make it possible to optimize the shape of the cell and take into account possible destabilizing factors [1]. The influence of the design parameters of the cell on the distribution of the electric field strength in the interelectrode space was estimated and the following series of studies were performed:
(i) the influence of the SiO_2 thickness in the range of 10 – 100 nm and the voltage on the control grid in the range from –5 to +5 V on the distribution of the electric field strength in the interelectrode space at fixed values of the interelectrode distance;
(ii) the influence of the interelectrode distance in the range of 10 – 100 nm and voltage in the range from –5 to +5 V at the control electrode on the distribution of the electric field in the interelectrode space at a fixed SiO_2 thickness;
(iii) the influence of the height of the SiO_2 layer and the control grid in the range of 900 – 990 nm and the voltage in the range from –5 to +5 V at the control electrode on the distribution of the electric field in the interelectrode space at fixed values of SiO_2 thickness and interelectrode distance.
The dependences of the electric field strength on the design parameters of the triode-type field emission cell were obtained on the basis of the simulation results. The obtained dependences made it possible to determine the design parameters of the field emission cell at which the maximum values of the electric field strength are reached at the top of the field emission cathode. It was revealed that the minimum allowable dielectric thickness to ensure the absence of electrical breakdown is 50 nm. A decrease in the interelectrode gap leads to an increase in the electric field strength by 37 – 160 % for a fixed dielectric thickness of 50 nm. A change in the potential of the control electrode from –1 to +5 V and an increase in its height from 900 to 990 nm leads to an increase in the electric field strength by 6 – 32 %.

References

[1] Jityaev I. L., et al. // *J. Vac. Sci. Technol. B*, **37**, 012201, 2019.

The Electromagnetic Field Localization Method in the Topology of a Microwave Double Ring Split Resonator

I. V. Malyshev*, E. V. Nikolayev, A. A. Fedotov

Southern Federal University, Taganrog, Russia

*ivmalyshev@sfedu.ru

Based on the electrodynamic analysis of the double ring split resonator topology, the filling of the resonator internal space with electromagnetic power is revealed. The picture of the electromagnetic field level distribution is shown in Fig. 1*a*. The propagation of electromagnetic power must be localized under study in the structure volume. The optimal solution lies in the location placement of the metallized polygon inside the resonator [1]. The width of the gap between the inner polygon and the resonator ring is chosen according to orientation of the region width with the maximum level of electromagnetic power in the inner resonator region. This size corresponds to a value equal to half of the ring width. The image of the resulting topology is shown in Fig. 1*b*. In the result of further research, it was found that the location of radio-electronic path elements or microwave path elements is possible at the polygon place, because they do not influence on the resonator transfer characteristic. Application the sampling in the polygon location area allows us to use the internal space for placing other microwave structures or for interlayer transitions, which may be relevant, when modeling such structures in a multilayer microwave printed circuit board. The considered topology change does not shift the resonant frequency of the structure. In the transmission characteristics, one can detect an increase in the attenuation coefficient by 0.8 %.

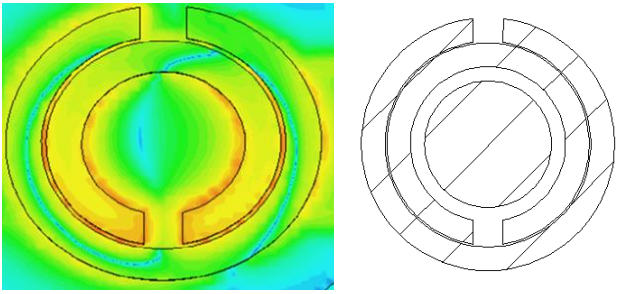

(a) (b)

Fig. 1. Results of ring resonator simulation: (a) distribution of electromagnetic power in the ring resonator, (b) proposed option for shielding of the resonator inner region

Reference

[1] Malyshev I. V., Nikolayev E. V. Frequency selection in conducting lines using cascade connections of ring concentric split resonant structures // *Successes of Applied Physics*. **7**(6), 601 – 605, 2019 (In Russian).

Analysis of Chiral Substrates Properties Containing Spiral Inclusions

I. V. Malyshev*, N. V. Parshina

Southern Federal University, Taganrog, Russia

*ivmalyshev@sfedu.ru

The most of investigators and designers, dialed with circuit boards for strip and coplanar transmission lines, show interest in developing of microwave and EHF transmission lines passive nodes [1]. When the substrate is represented as a chiral medium containing a uniformly distributed equal number of single-pass left- and right-helical elements (so-called modified Tellegen elements [2]), which are made of thin-wire metal spiral spring elements consisting of *N* turns with radius *R*, located at a distance *h* from each other, one can consider the theory of elements, set with next parameters: *l* is the length of the spiral in the expanded state, *r* is the radius of the wire [1, 2]. Maxwell's equations for such medium are determined by the known relations: $\vec{D} = \varepsilon_0 \varepsilon \vec{E} \mp i\chi_a \vec{H}$, $\vec{B} = \mu_0 \mu \vec{H} \pm i\chi_a \vec{E}$, where ε_0 and μ_0 are the electric and magnetic permeability of the vacuum; $\chi_a = \chi\sqrt{\varepsilon_0 \mu_0}$ is the absolute chirality index; the sign of plus corresponds to left-screw, and the sign of minus corresponds to right-screw spiral inclusions. The chirality coefficient unites the chiral properties in the form of a constant, having the linearly dependence on the frequency and conductivity of the entire substrate [1 – 3]. It is known that, when metamaterials are represented as a set of chiral elements distributed in a homogeneous container with a medium, the material Maxwell-Garnett relations take place [1], which have the form:

$$\frac{\varepsilon - \varepsilon_s}{\varepsilon + 2\varepsilon_s} = n\frac{\varepsilon_r - \varepsilon_s}{\varepsilon_r + 2\varepsilon_s}, \qquad \varepsilon_s(\omega) = \varepsilon_r + \frac{{\beta_0}^2}{{\omega_0}^2 + \omega^2}, \quad \chi(\omega) = A\frac{{\beta_0}^2 \omega}{c({\omega_0}^2 + \omega^2)}, \tag{1}$$

where: ε_r, ε_s and ε are the relative permeabilities of the container, the Tellegen element, and the medium, respectively, β_0 is a parameter associated with internal processes in the medium; *c* is the speed of light; *A* is a parameter proportional to the value of $(R/r^2)Nhl$, n is the concentration of spirals in the container. It follows to: $\chi = \frac{A\omega}{cn}\frac{(\varepsilon_r + 2\varepsilon_s)(\varepsilon_s - \varepsilon)}{(\varepsilon + 2\varepsilon_s)}$, which get possibility to associate three important parameters *F*, *n* and χ, which, with the total permittivity parameter $\varepsilon_\Sigma = \varepsilon_r + \varepsilon_s + \varepsilon$, determines the main properties of this structure. The results of the calculations are given in Figs.1 and 2 for frequencies of UHF range *F* (20 – 30 GHz), for three values of the concentration *n* ($n_1 = 10^{11}$ m^{-3}, $n_2 = 10^{12}$ m^{-3}, $n_3 = 10^{13}$ m^{-3}). These dependences are convenient for calculating the chirality coefficient and for solving electrodynamic problems related to determining of the parameters of chiral inclusions.

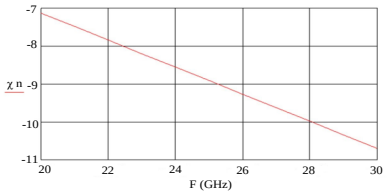

Fig. 1. Dependence of the (χn) parameter on the frequency *F*

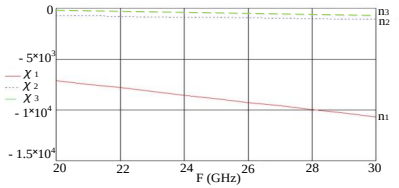

Fig. 2. Dependence of χ parameter on the frequency *F* for three values of the concentration *n*

Reference
[1] Osipov O. V., Karalkin M. V., Dementyev A.V. The use of Maxwell-Garnett and Bruggeman models for describing the heterogeneity of a chiral metamaterial based on gammadions // *Infocommunication Technologies*, **18**(4), 391 – 402, 2020 (In Russian).
[2] Malyshev I. V., Parshina N. V., Chervyakov G. G. Propagation of EMV in biisotropic media with a uniform distribution of the concentration of dispersed particles // *Special Technique*, **1**, 41 – 43, 2015(In Russian).
[3] Malyshev I. V., Parshina N. V., Osadchy E. N. Determination of electrophysical parameters of spiral inclusions in a dielectric medium to ensure chiral properties // *Engineering Bulletin of the Don*. **12**, 2020 (In Russian).
http://www.ivdon.ru/ru/magazine/archive/n12y2020/6713

Behavior of Bulk Semiconductor Structures and Superlattices Output Parameters under the Influence of Strong External Constant and Alternating Electric Fields

I. V. Malyshev*, N. V. Parshina, O. A. Goncharova

Southern Federal University, Taganrog, Russia

*ivmalyshev@sfedu.ru

It is known [1] that the mobility of charge carriers in III–V type semiconductors will determine the conductivity of the entire structure. When using the phenomenological approach to the description of kinetic processes, the mobility is determined on the basis of the quasi-momentum and energy conservation equations, which can be represented as an equation for the average drift of charge carriers: $dp/dt = eE - p/\tau$ (where e is the electron charge, E is the electric field strength, p is the average drift quasi-momentum, τ is the average quasi-momentum relaxation time) and their heating equations: $dW/dt = eEp/m - -(W-W_0)/\tau_e$ (where τ_e is the average energy relaxation time, m is the effective mass of electrons, W is the bottom of the conduction band, T_0 = 300 K is the temperature of the medium, k is the Boltzmann constant). In this case, the dependence of the effective mass of electrons on their kinetic energy is determined by the dispersion law. After representing the dependence: $1/m = f(W)$ in the form of a Taylor series expansion and limiting it to two members of this series: $1/m = 1/m_0(1 - p_m(W-W_0)/W_0$ and using the stationary case $dW/dt = 0$ we can get the components for the constant: $\frac{W_{00}-W_0}{W_0} = \frac{x^2}{p_m(1+x^2)}$ (where $x = \frac{E_0}{E_t} = \sqrt{\frac{p_m e^2 \tau\tau_э E_0^2}{m_0 W_0}}$ is the dimensionless strength of the constant electric field, $E_t = \frac{m_0 W_0}{p_m e^2 \tau\tau_э}$ is the strength of the threshold field of the Gunn effect) and the variable component $W_{\sim}$. Taking into account the above relations, the expression for the current density can be written in a dimensionless form: $X = \frac{j_{\sim}}{enE_{\sim}\mu_{пл}} = \frac{\mu_{ал}+j\mu_{rл}}{\mu_{пл}} = \frac{1}{1+jxy}\left(1 - \frac{x^2(2-jxy)}{(1+x^2)+jy}\right)$ (where μ_{al} and μ_{rl} are the low-signal volumetric active and reactive high-frequency mobilities [2]). Therefore, it is possible to find the components of the volumetric conductivity of the structure in the form: x = var (0.5 – 2.5). The numbering of the curves corresponds to different values of the external field strength: 1 – x = 1; 2 – x = 1.2; 3 – x = 1; 4 – x = 1.6; 5 – x = 1.8; 6 – x = 2.5 (see Figs. 1, 2).

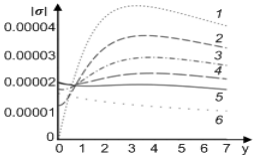

Fig. 1. Frequency response of the normalized volumetric signal conductivity

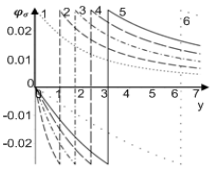

Fig. 2. PFC of the normalized low-signal conductivity

From the obtained graphs, it is possible to determine the required values of the constant field strength, which provides the required mode of operation of devices at given frequencies.

Reference

[1] Malyshev I. V., Osadchiy E. N., Fil K. A. Methods for taking into account the energy dependence of the effective mass of hot carriers in the volume of $A^{III}B^{V}$ semiconductors for various cases of dispersion // *Engineering Bulletin of the Don*, 4, 2017, ivdon.ru/magazine/archive/n4y2017/4396 (In Russian).

[2] Malyshev I. V., Fil K. A., Parshina N. V. Nonlinearity of the diffusion coefficient of hot carriers in the bulk of a semiconductor under the action of electric and magnetic fields // *News of Universities. Physics*. 6, 3 – 6, 2017 (In Russian).

Using Sequential Cascade Combining of Double Ring Split Resonators to Control the Frequency Notch Filters Response

I.V. Malyshev*, N.V. Parshina, E. V. Nikolaev

Southern Federal University, Taganrog, Russia

*ivmalyshev@sfedu.ru

Currently, research is being actively carried out on the use of double ring split resonators (DRSRs) for the formation of notch filters in the microwave frequency range. Such resonators make it possible to obtain a high-quality filter with smaller linear overall parameters in comparison with a bandpass filter (Fig. 1) [1]. The results presented in this report were the studies of three types of notch filters, based on the DRSR. Experimental studies of the filter gain, obtained in the result of measurements on a vector network analyzer, are shown in Fig. 2. A filter, based on a single DRSR, gives a suppression value of about 12 dB. Filters are made by their cascade placement (Fig. 1).

(a) (b)

Fig. 1. Printed circuit boards of notch filters: (a) filter based on single resonator; (b) filter based on three resonators.

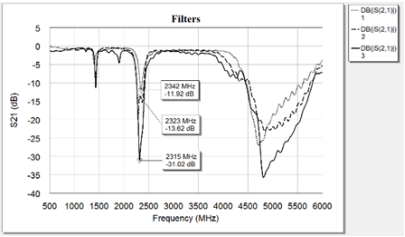

Fig. 2. Microwave power transmission coefficient of filters, based on 1st, 2nd, and 3th DRSR types.

The three-stage arrangement of the resonators increases the suppression ratio at the resonant frequency up to 30 dB.Similar elements with DRSR are structures for coplanar, strip and similar transmission lines. An increase in the number of pairs of split ring resonators makes it possible to increase the transmission coefficient (S21) by several times. The parameters of the modeled and fabricated working layouts of structures with several DRSRs can be adjusted by finely adjusting the overall parameters, that is also a practical convenience, when creating specific microwave devices [2].

Reference

[1] Malyshev I. V., Nikolaev E. V. A New Method to Control Filtration Properties of the Dielectric Materials with a Concentric Cut Rings Structures // 2018 International Conference on "Physics and Mechanics of New Materials and Their Applications" (PHENMA 2018) August 9 – 11th, 2018, Busan, Republic of Korea, 230 – 231, 2018.

[2] Malyshev I. V., Nikolayev E. V. A method for creating band-blocking elements based on concentric split rings in the band transmission lines of the microwave and HF bands // *Proc. 28 Int. Conf. "Microwave Equipment and Telecommunication Technologies"*, 9 – 15.09.2018, Krim, Russia, 876 – 883, 2018.

Technological Aspects of Optimization of Ferroelectric Ceramics Designed for Extreme Conditions

M. A. Marakhovskiy*, A. E. Panich, V. A. Marakhovskiy

Scientific Design and Technological Bureau "Piezopribor" Southern Federal University, 10, Milchakov St., Rostov-on-Don, 344090, Russia

*marmisha@mail.com

Among the wide range of ferroelectric materials, a special place is occupied by materials designed to work in extreme conditions. Such ferroelectric materials are characterized by the stability of electrophysical parameters under the influence of high temperatures and pressures. Strict operational requirements are imposed on converters used in aviation and space technology, energy, oil and gas complexes and others. The main properties of ferroelectric ceramics are formed at the sintering being the most important technological stage of production. The sintering process consists in the nucleation of grains and the formation of a ceramic frame responsible for the mechanical properties directly related to the dielectric characteristics of ceramics (since the piezoelectric effect is an electromechanical transformation). The aim of the work was to study the influence of manufacturing methods

and technological parameters on the functional characteristics of ferroelectric ceramics designed to work in extreme conditions. A material based on the $Bi_{0.75}Ti_{0.24}Na_{0.01}$ system with relatively high values of the piezomodule d_{33}, resistant to high temperatures (up to 500 °C) and uniaxial mechanical compression (up to 1500 kg/cm^2) was selected as the model object of the study [1]. In addition to the conventional method of sintering in a chamber furnace at atmospheric pressure, there are more effective methods of consolidated sintering of ceramic materials, namely hot pressing and spark plasma sintering. Both sintering methods reduce the final sintering temperature and form a dense homogeneous ceramic structure. Recently, special attention has been paid to the spark plasma sintering (SPS) method, which allows not only to reduce the final sintering temperature, but also to significantly shorten the duration of the sintering process, used for sintering powder materials (technical, structural and ferroelectric ceramics). The SPS method provides the formation of fine-grained, close to the monophase structure of ceramics, compared with conventional sintering at atmospheric pressure. In this work, three sintering methods were used: the conventional method using a chamber furnace, the hot-pressing method and SPS. The quality of sintered ferroelectric ceramics $Bi_{0.75}Ti_{0.24}Na_{0.01}$ was evaluated based on the results of scanning electron microscopy, experimental density values and electrophysical parameters. The study showed that the sintering of ceramics by hot pressing and SPS increases the density values by 14% and 20%, respectively, with a decrease in sintering temperatures by 160 – 200 °C. At the same time, the microstructure of ceramic elements obtained by consolidated sintering significantly differed from the microstructure of elements, obtained in a chamber furnace. Despite the homogeneous fine-grained and defect-free architecture of ceramic frames with increased density indicators, the values of the piezoelectric modulus (d_{33}) and the relative permittivity ($\varepsilon^T_{33}/\varepsilon_0$) were the same. However, a significant reduction in temperatures and sintering durations by 50 times (!) significantly decreases energy consumption in the manufacture of ceramic elements and reduce their cost. Thus, the methods of consolidated sintering considered in this work are promising methods for producing not only ferroelectric ceramics based on the $Bi_{0.75}Ti_{0.24}Na_{0.01}$ system, but also previously studied PCR-8, BST, PMN-PT and other compositions [2 – 4].

Acknowledgement. The research was performed by using the equipment of the CCP "High Technologies".

References

[1] Vusevker Yu. A., Feinrider D. E., Panich A. E., Gorish A. V., Zlotnikov V. A. Piezoelectric ceramic material // *Russian Patent on invention* dated by 10.20.1999 (application No. 2139840, 26.01.1998) (In Russian).

[2] Marakhovsky M. A., Panich A. A., Talanov M. V., Marakhovskiy V. A. Study of the influence of technological factors on improving the efficiency of ferroelectrically hard piezoceramic material PCR-8 // *Ferroelectrics*, **560**(1), 1–6, 2020.

[3] Marakhovsky M. A., Panich A. A., Marakhovskiy V. A. Investigation of the characteristics of ferroceramics of barium-strontium titanate obtained by spark plasma sintering. // *INTERMATIC-2018*, Moscow, **2**, 430, 2018.

[4] Marakhovsky M. A., Panich A. A. Obtaining piezoceramics of the PMN-PT system by spark sintering // *News of the SFU. Technical Sciences*. **2**, 42, 2017 (In Russian).

Boundary Element Analysis of Transient Deformation of a Poroelastic Half-space

I. P. Markov*, A. N. Petrov, A. V. Boev

National Research Lobachevsky State University of Nizhny Novgorod

*markov@mech.unn.ru

A direct boundary element approach for solving dynamic initial-boundary value problems of the three-dimensional linear theory of isotropic fully saturated poroelasticity is presented. The approach is based on the joint application of the Laplace transform and an original iterative algorithm for rational approximation of Laplace domain vector-valued functions [1]. The boundary element technique is based on the regularized Laplace domain boundary integral equations (BIEs) for displacements. A scheme based on a mixed approximation model is used. According to this scheme, the boundary surface of the region under consideration is approximated by quadratic elements, displacements are linear, tractions are approximated by constant elements. For spatial discretization, the collocation method is used. Iterative algorithm for rational approximation of Laplace domain vector-valued functions is used for adaptive sampling of the response functions over a given frequency range. It allows for computationally efficient (without oversampling) and accurate (without undersampling) representation of their main characteristics in the frequency domain. The described boundary element approach is used to solve dynamic problems of a suddenly applied load acting on a poroelastic half-space with various configurations: homogeneous, half-space containing a cavity, half-space with a slab rested on it, and a half-space with a tunnel.

Acknowledgement. The reported study was funded by RFBR, project number 20-08-00451.

Reference

[1] Markov I.P., Petrov A.N., Boev A.V. An Iterative Technique for Rational Approximation of Laplace Domain Vector-Valued Functions // *Advanced Structured Materials*, **155**, 337 – 356, 2022.

The Study of the Effect of Chromium on the Semiconductor Properties of Pyrolyzed Polyacrylonitrile by Quantum Chemistry Methods

Marta M. Avilova[1]*, Natalia V. Zolotareva[2], Olga V. Popova[3]

[1]Southern Federal University, Taganrog, Russia
[2]Astrakhan State University, Astrakhan, Russia
[3]Don State Technical University, Rostov-on-Don, Russia

*m.avir89@yandex.ru, mavilova@sfedu.ru

Polyconjugated polyacrylonitrile (pPAN) is widely used in gas sensors as a sensitive element of a resistive type in gas sensors. It is known that this material has a significant advantage among electrically conductive analogs due to its gas sensitivity at low (room) temperature [1 – 5]. However, to assess the effect of molecules and atoms by metals of *d*-, *f*-groups on the pPAN matrix and to study the structural and electronic properties, it is more promising to study the structure of Me-pPAN by multilevel quantum mechanical calculations. At present, the

methods of quantum chemistry is the only method for studying the structures and properties of materials, which makes it possible to study the possibility of the occurrence of chemical reactions and the products of their formation without financial costs and laboratory experiments. In addition, the successful use of the implementation of quantum chemical calculations is due to the speed of obtaining the necessary data. As part of the implementation of multi-level quantum mechanical calculations using basis sets (PM7, RHF/6-31G, DFT/cc-PVDZ), the structural and electronic properties of the "pPAN – Cr_2O_3" cluster model were evaluated. The frequency of stretching vibrations for pPAN was calculated, the optimal interatomic distances and the Mulliken distribution of point charges on atoms in the initial molecules and in the cluster model were calculated, as well as the volume parameters and the values of the HOMO-LUMO EHL gap for Cr_2O_3. In the process of optimizing pPAN by the DFT/cc-PVDZ method, the characteristic vibration frequencies of individual functional groups (1700 – 1600 cm^{-1}) were determined, which correspond to the ν(C=N)calc vibrations, weak deformation vibrations in the range of 1470 – 1410 cm^{-1} belong to H–C–H, stretching vibrations ν(C–H)calc in the region of 3000 – 2960 cm^{-1} are also identified. Additionally, it was established that the introduction of a Cr_2O_3 molecule into the pPAN structure leads to an increase in the contact surface area and to a redistribution of point charges, which confirms the results presented in [7, 8].

References

[1] Karbownik I., Fiedot M., Rac O., Suchorska-Woźniak P., Rybicki T., Teterycz H. // *Polymer*, **75**, 97 – 108, 2015, https://doi.org/10.1016/j.polymer.2015.08.015.

[2] Wang W., Zheng Y., Jin X., Sun Y., Lu B., Wang H., Fang J., Shao H., Lin T. // *Nano Energy*, **56**, 588 – 594, 2019, https://doi.org/10.1016/j.nanoen.2018.11.082.

[3] Logothetidis S. // *J. Mater. Sci. Eng. B*, **152**, 96 – 104, 2008, https://doi.org/10.1016/j.mseb.2008.06.009.

[4] Efimov M. N., Sosenkin V. E., Volfkovich Yu. M., Vasilev A. A., Muratov D. G., Baskakov S. A., Efimov O. N., Karpacheva G. P. // *Electrochem. Commun*., **96**, 98 – 102, 2018. https://doi.org/10.1016/j.elecom.2018.10.016.

[5] Chen L., Zuo Y., Zhang Y., Gao Y. // *Mater. Lett*., **215**, 268 – 271, 2008. https://doi.org/10.1016/j.matlet.2017.12.119.

[6] Petrov V. V., Semenistaya T. V. *Metal-containing Polyacrylonitrile: Composition, Structure, Properties*. Taganrog: SFedU Press, 169, 2015 (In Russian).

[7] Eremin V. S., Bronstein L. M., Dyachkova V. P., Mirzoeva E. Sh., Loginova T. P., Valetsky P. M., Voishchev V. S. // *Vysokomol. Soedin*., **35**(4), 450 – 454, 1993 (In Russian).

[8] Solodovnikov S. P., Bronstein L. M., Loginova T. P., Mirzoeva E. Sh., Lependin O. L., Valetsky P. M. // *Vysokomol. Soedin*., **35**(1), 26 – 29, 1993 (In Russian).

Modelling of Stress-Strain State of Marine Infrastructure Support Element

A. A. Matrosov*, R. A. Bardakova, A. A. Kotova

Don State Technical University, 1, Gagarin Sq., Rostov-on-Don, 344010, Russia

*amatrosov@donstu.ru

The use of modern high-performance computer systems allows solving quite complex problems in modal analysis, calculating the stress-strain state of building structures and

determining their bearing capacity. The work considers supports of shallow water (diving depth up to 50 m) production complexes of offshore oil and gas structures. The support in question is used for its functional purpose to store the obtained oil product and is a hollow concrete cylinder tapering upwards, coated for protective purposes from the outside and from the inside with a layer of metal. The problem is considered as an axisymmetric problem in a linear statement. Lower end of column is rigidly embedded in base, located at sea bottom. At the upper end there are above-deck structures, modeled by the attached mass. During its operation, the support can experience complex rather heterogeneous loads: the effect of wind on the surface of the support; the effect of wind on the above-deck structures, reduced to additional force applied to the upper part of the support; impact of waves on the upper part of the support; the effect of the bottom currents on the part of the column under water; fluctuations of support base caused by earthquakes, hydrostatic pressure of oil stored inside the column. For offshore oil and gas production facilities located in the northern seas, additional bulk action of ice on the surface part of the support is possible. All these loads have a constant deterministic component. However, at the same time, they can all have, in addition to the deterministic, also a stochastic component. The work builds a mathematical model of such a support. In the software complex of finite-element analysis ANSYS, there are built finite-element model of support, performed analysis of own oscillation frequencies [1, 2], calculated stresses and deformations occurring in support over its entire height depending on applied loads [3 – 5]. Calculations are performed both for averaged values of deterministic loads acting on the support, and taking into account stochastic components. The contribution of the latter to the emerging stress-strain state is evaluated.

References

[1] Bardakova R. A., Kotova A. A., Matrosov A. A. // *Intelligent Technologies and Mathematical Modeling Challenges (IT&MMC-20)*, 2020 (In Russian).

[2] Kotova A. A., Bardakova R. A., Matrosov A. A. // *Physical and mathematical modeling of systems (PMMS-2020)*, 2021 (In Russian).

[3] Kislyakov E. A., Matrosov A. A. // *Innovative technologies in science and education (ITSE-2018)*, 2018 (In Russsian).

[4] Kislyakov E. A., Matrosov A. A. // *Intelligent Technologies and Mathematical Modeling Challenges (IT&MMC-18)*, 2018 (In Russian).

[5] Kislyakov E. A., Matrosov A. A. // *Physics and Mechanics of New Materials and Their Applications (PHENMA 2018)*, 2018.

Effects of Piezoactuator on Fish Reproductive Cells During the Equilibrium Stage

A. A. Matrosov*, D. A. Nizhnik, A. N. Soloviev

Don State Technical University, Rostov-on-Don, 344010, Russia

*amatrosov@donstu.ru

The solution to the important problem of preserving and restoring populations of valuable fish species is to create a cryobank of reproductive cells. However, in order to create it, it is necessary to effectively protect the cells from damage during cryo-freezing. To date, the most relevant method of protection is the use of a cryoprotectant at the equilibration stage. Reproductive cells placed in the cryoprotector represent a certain suspension. Exposing this suspension to an acoustic field with specially selected parameters allows the cryoprotectant to

penetrate the cell more quickly, which leads to an increase in the survival rate of reproductive cells. In this report, we build a mathematical model of acoustic impact by a piezoactuator on the cryoprotector, which contains fish reproductive cells [1 – 3]. Within the framework of continuum mechanics, the equations of linear elasticity theory; equations of linear electroelasticity theory; equations of motion of liquid and gaseous media in the acoustic approximation are used. To these equations, the corresponding boundary conditions for mechanical and electric fields are added. The suspension is in a standard glass laboratory low graduated beaker B-1-50 XC and simulated by a homogeneous liquid medium with some averaged parameters. Acoustic waves are excited by a piezoactuator glued externally to the bottom of the beaker at the center. A circular plate of piezo-ceramics, pre-polarized to the thickness, is used as a piezoactuator. Electrodes of negligibly small thickness are placed on its front surfaces. The piezoactuator causes bending oscillations of the bottom of the beaker, which leads to effective excitation of the acoustic field in the suspension. The geometrical model of the considered problem and the corresponding finite-element mesh are constructed in the program complex of the freely distributed (free software) finite-element analysis software ACELAN. The modal analysis is performed and the dependence of the natural frequencies of resonance, antiresonance, and electromechanical coupling coefficient on the piezoelement radius is found. The piezoelement radius at which resonance occurs at the first bending mode of oscillations is determined. Analysis of the velocity and pressure field in the acoustic medium shows that at the resonance frequency the phenomenon of stirring of suspension inside the occupied volume is also observed. This phenomenon contributes to intensive penetration of the cryoprotectant inside the reproductive cells and ensures their protection from damage during cryo-freezing.

Acknowledgements: This research was supported by the Russian Foundation for Basic Research grant No. 21-16-00118.

References

[1] Matrosov A. A., Nizhnik D. A., Soloviev A.N. Simulation of Impact of Acoustic Field Produced by Piezoactuator on Biological Fluid with Cryoprotector // *Mathematical Modeling, Inverse Problems and Big Data*, 2021 (In Russian).

[2] Matrosov A. A., Nizhnik D.A., Ponomareva E. N., Soloviev A. N., Chebanenko V. A. Modeling of Impact of Acoustic Field on Biological Fluid with Cryoprotector // *Modern Problems in Modeling Materials for Mechanical, Medical, and Biological Applications* (MPMM&A-2021), 2021 (In Russian).

[3] Matrosov A. A., Nizhnik D. A., Soloviev A. N. Mathematical modeling of acoustic impact during equilibration // *Actual Problems of Engineering, Technology and Education*, 2022 (In Russian).

Mathematical Modeling of Full-Scale Tests of Ceramic Bricks

A. A. Matrosov[1]*, I. A. Serebryanaya[1], D. S. Serebryanaya[2], D. A. Nizhnik[1]

[1]*Don State Technical University, Rostov-on-Don, 344010, Russia*
[2]*South-Russian Institute of Management - Branch of the Russian Academy of National Economy and Public Administration, Rostov-on-Don, 344002, Russia*

*amatrosov@donstu.ru

The basis of the forecast of the load capacity of the designed construction structure is the correct determination of the strength indicators of the used construction materials. When

designing masonry, these indicators are established on the basis of compression and bending tests. The methods of such tests are regulated by state standards. During the tests, it is assumed that the samples should be in a uniaxial stress-strain state. However, triaxial compression is practiced due to a number of reasons, among which the presence of contact friction forces between the sample and the plate of the test press. In addition, the support face of ceramic bricks always has some deviations from flatness. This does not ensure uniformity of load distribution on the entire support surface [1, 2]. In this regard, in preparing the samples for testing, the surfaces are pre-aligned. As an alignment method, according to the standard, grinding must be used. Such grinding is not only a very time consuming and unsafe method, but also leads to a systematic error during testing. Moreover, the friction forces between the contact surfaces of the body and the metal plates of the press must be taken into account. This coefficient of friction depends significantly on the method of brick surface alignment. In the work, a finite element model of the tested ceramic brick was built, the corresponding boundary conditions were set [3]. The numerical experiment was performed in the software complex of finite element analysis ANSYS using eight-node three-dimensional finite elements. In addition, a number of field trials were carried out. Based on the results of field and numerical experiments, it was found [4, 5] that the method of preliminary alignment significantly affects the value of the coefficient of friction between the supporting surface of the brick and the press plate. This in turn affects the value of the friction force, which leads to the appearance of a complex three-dimensional stress-strain state and significantly affects the deformation conditions of the samples. Ultimately, this leads to a distortion of the test results. In order to reduce this effect and achieve uniaxial compression, it seems appropriate to further adjust the standard test method.

References

[1] Poryadina N. A., Serebryanay I. A., Matrosov A. A., Nizhnik D. A. // *Construction and Architecture-2017*, 2017 (In Russian).
[2] Lukinova N. A., Matrosov A. A., Nizhnik D. A., Serebryanay I. A., Terekhina Yu. V. // *Innovative Technologies in Science and Education (ITSE-2017)*, 2017 (In Russian).
[3] Lukinova N. A., Matrosov A. A., Nizhnik D. A., Serebryanay I. A., Terekhina Yu. V. // *Physics and Mechanics of New Materials and Their Applications (PHENMA 2017)*, 2017.
[4] Matrosov A. A., Serebryanay I. A., Lukinova N. A., Nizhnik D. A., Terekhina Yu. V. // *Physics and Mechanics of New Materials and Their Applications (PHENMA 2018)*, 2018.
[5] Poryadina N. A., Serebryanay I. A. // *Innovative Technologies in Science and Education (ITSE-2018)*, 2018 (In Russian).

Features of the Choice of Construction Materials for Downhole Equipment

K. P. Matsneva*, M. V. Korchagina, S. O. Kireev

Don State Technical University, Rostov-on-Don, Russia

*kristinamatsneva99@gmail.com

In oilfield engineering, steel, as well as non-ferrous metals and cast iron, are mainly used as structural materials for the manufacture of equipment in the fields [1]. Designers in the development of parts are faced with the problem of choosing a material, since the work of tools, machines, apparatus and structures used in the oil and petrochemical and gas industries

are in different conditions, the selection of materials makes it necessary to look for criteria for a rational choice, and in some cases create new ones. types of alloys and non-metallic materials in relation to the working conditions. When choosing, it must be taken into account that the parts work under static, cyclic and shock loads, at low and high temperatures, in contact with various media, for example, for oil production in Siberia, it is necessary to choose a material taking into account not only heavy loads, but also take into account the effect of low temperatures at which metals exhibit a loss of plasticity and toughness and an increased tendency to brittle fracture. Operational requirements are of paramount importance in the selection of materials. To ensure operability, the material must have high structural strength. Structural strength is a combination of mechanical properties that ensure reliable and long-term operation of a material under operating conditions. The most widespread in the oilfield machine building are steels, which for the manufacture of certain products are classified according to grades and strength groups [2]. Strength group is determined by mechanical characteristics, higher strength is achieved by varying the chemical composition of steel or by heat treatment [3]. A significant part of the equipment for drilling and operating wells is made up of metal pipes. These include kelly, steel, drill collar, casing and tubing. Let us consider the importance of the correct choice of material using the example of the choice of material for oil country tubular goods. Special drilling, casing and tubing pipes supplied according to GOST or international standards are used in drilling and operation of wells. The analysis of compliance of strength groups according to Russian and international standards has been carried out. In recent years, many Russian standards have been brought into conformity with international ISO and American API standards, the classification of strength groups according to these standards differs from that used in Russia. The operating conditions of downhole equipment, including drilling, production and production strings, are significantly difficult: high axial loads, cyclic tensile-compressive stresses, torsion, as well as abrasive and corrosive environments impose special responsibility on the selection of materials for oil country tubular goods, it is necessary to strictly observe values of ultimate loads by strength groups recommended by the standards.

References

[1] Pokrepin B. V. *Oil and Gas Production Operator: Textbook*. Volgograd: Publishing House Doam "In-Folio", 448, 2011 (In Russian).

[2] Bukhalenko E. I., Bukhalenko V. E. Equipment and Tools for Well Repair. Moscow: Nedra, 1991 (In Russian).

[3] *Oil and Gas Field Equipment*. V.N. Ivanovsky (Ed.). Moscow: Centrlitneftegaz, 720, 2006 (In Russian).

Temperature Measurement of Instantaneous Explosive Flames

Min-Gyu Jeon[1,*], Gyeong-Rae Cho[1], Jeong-Woong Hong[2], Deog-Hee Doh[1]

[1]Division of Mechanical Engineering, Korea Maritime and Ocean University, Busan, 49112, Republic of Korea
[2]Division of Refrigeration & Air-conditioning Engineering, Korea Maritime and Ocean University, Busan, 49112, Republic of Korea

*jeon85@kmou.ac.kr

High-temperature and high-pressure processes are required to produce high-quality materials such as metal smelting. In particular, precise control of the gas used during this process is

required. There are several methods to measure the state information of gas. Thermocouples are widely used for temperature measurement. On the other side, the tunable diode laser absorption spectroscopy (TDLAS) technique can simultaneously measure the temperature and concentration of the target gas. Hard to measure the information of gas that changes rapidly within tens of microseconds like an explosion phenomenon. This study, suggests a method of measuring the temperature of the flame generated during the explosion process. In this case, a real-time temperature measurement method TDLD, using the characteristics of the photodiode, was applied. The important factors in the measurement of the explosion process are pressure and temperature terms. The temperature was corrected by considering real-time pressure in addition to the existing optical measurement method. The temperatures obtained using the TDLD technique were evaluated relative to those obtained by the thermocouple and TDLAS methods.

Acknowledgments. This research was supported by Basic Science Research Program through the National Research Foundation of Korea (NRF) funded by the Ministry of Education (No. 2020R1I1A1A01052771). Further, this work was supported by the Technology Innovation Program (No. 20005750, Commercial Development of Combustion System Control Technology for Minimizing Pollutant with Multiple Analysis) funded by the Ministry of Trade, Industry & Energy (MOTIE, Republic of Korea).

Modeling of the Stress State in Layered Structural Materials with Isotropic and Transverse-isotropic Layers at Multi-pulse Probing Impact

I. P. Miroshnichenko[1]*, I. A. Parinov[2]

[1]Don State Technical University, Rostov-on-Don, Russia,
[2]Southern Federal University, Rostov-on-Don, Russia

*ipmir@rambler.ru

The emergence of new structural materials, namely, layered structural materials with isotropic and transverse-isotropic layers and their use in various machines and equipment leads to the need to develop new methods for analyzing the results of diagnosing their condition. This is most relevant for cases of the use of multiple probing effects in the process of diagnostics by acoustic active methods of non-destructive testing. The problem of recognizing the diagnostic results obtained in terms of identifying the compliance of typical internal defects also remains relevant. The stress state is modeled in typical layered structural materials with isotropic and transverse-isotropic layers under various variants of multi-pulse probing impact. In the simulation, mathematical models were used to determine the stress state in isotropic and transverse-isotropic layered plates and layered cylindrical shells, based on the application of the generalized method of scalarization of dynamic elastic fields in transverse-isotropic media [1]. The obtained results are intended for *a priori* and *a posteriori* analysis in the process of diagnostics by acoustic active methods of non-destructive testing of the state of layered structural materials with isotropic and transverse-isotropic layers under multi-pulse probing impact in mechanical engineering, shipbuilding, aircraft construction, etc.

Acknowledgement. The study was performed under partial support of the Russian Ministry of Education and Science and Russian Foundation for Basic Research (No. 19-08-00365).

Reference
[1] Sizov V. P., Miroshnichenko I. P. *Elastic Waves in Layered Anisotropic Structures*. LAP LAMBERT Academic Publishing, Saarbrucken, Germany, 270, 2012.

On the Modification of the Optical Interference Measuring Instrument for Determination of the Displacements of Control Object Surfaces

I. P. Miroshnichenko[1]*, I. A. Parinov[2]

[1]Don State Technical University, Rostov-on-Don, Russia
[2]Southern Federal University, Rostov-on-Don, Russia

*ipmir@rambler.ru

In [1, 2], optical interference devices are proposed for contactless measurements of the displacements of control object surfaces when diagnosing the state of structural materials by acoustic active methods of non-destructive testing and during experimental studies of the strength properties of power elements of various goods. These measuring instruments are developed on the basis of the method of illumination of the surface of the object of control by laser radiation (or the "luminous point" method) [3]. Their functional characteristics are sufficiently well studied in the process of conducting computational, theoretical and experimental studies, they have been tested and successfully applied to solving practical problems. A new design (modification) of measuring instruments has been developed [1, 2], which allowed expanding the functionality of known devices by providing the possibility of measuring spatial (linear and all angular components) displacements of the control object surface. The computational and theoretical modeling of the functional properties of the new measuring instrument was carried out, the results of which allowed us to confirm the achievement of the goals of its development. The obtained results are intended for use in the creation of new contactless optical interference measuring instruments for spatial displacements of control object surfaces.

Acknowledgement. The study was performed under partial support of the Russian Ministry of Education and Science and Russian Foundation for Basic Research (No. 19-08-00365).

Reference
[1] Miroshnichenko I. P., Parinov I. A., Rozhkov E. V. Optical Interferential Device for Measurements of Movements of Surfaces of Controlled Objects // *Russian Patent No. 2512697, 10 April 2014* (In Russian).
[2] Miroshnichenko I. P., Parinov I. A., Rozhkov E. V. Optical device for measuring the displacements of control object surfaces// *Russian Patent No. 2343402, 10 January 2009* (In Russian).
[3] Miroshnichenko I. P., Serkin A. G., Sizov V. P. Use of Point Radiation Source for Extension of Functionality of Displacement Meter // *Journal of Optical Technology*. **75**(7), 437, 2008.

Controlling Residual Stresses During the 3D-printing Process of a Thermo-viscoelastic Cylinder

Montaser Fekry ID

Department of Mechanics and Control Processes, Moscow Institute of Physics and Technology (National Research University), Moscow, Russia
Department of Mathematics, Faculty of Science, South Valley University, Qena, Egypt

mohamed.mf@phystech.edu, montaser.fekry@yahoo.com

The residual stresses that appear during the additive manufacturing process is one of the challenges this technology faces. This work is devoted to the study of some technical treatments that help reduce residual stress, one of which is non-homogeneous additional volumetric heating that can be achieved through the skin effect phenomena. The study focuses on a developed mathematical model for estimating the temperature and residual stress fields in thermo-viscoelastic cylindrical growing body, with analysis of the influence of the viscosity properties of the material and additional volumetric heating on reducing the residual stresses. The model of the process is carried out by recurrently solving a sequence of boundary value problems of full coupled thermoelasticity, that determine the thermoelastic response of the joints of the initial cylinder and the increasing number of attached layers. The initial data for each step is determined by the final values of the fields at the previous step, supplemented by the initial data for the attached layer. A closed-form solution is constructed for this problem and the temperature field on the growing surface is analyzed numerically for various accretion scenarios.

Gas-sensitive Graphene and its Application

J. V. Morozova*, V. S. Klimin

Department of Nanotechnology and Microsystems, Southern Federal University, Taganrog, 347922, Russia

*ulamrzv@gmail.com

This paper presents a study of an ionization sensor of gases with a sensitive element based on a graphene-like film. The formation of a graphene-like film includes two stages: the formation of a relief sensitive element by the method of focused ion beams and the formation of a graphene-like film by plasmochemical etching in fluoride plasma. Silicon carbide was used as the substrate material, when creating the sensing element of the gas ionization sensor. The SiC substrates were previously chemically cleaned. The method of focused ion beams was used to form the pointed structures. The formed nanoscale structure was placed in the reactor of a plasma chemical etching plant, where the remaining gallium ions were removed in several stages after treatment with focused ion beams, and then a graphene film was formed on the surface of the structures in a fluoride plasma atmosphere by removing silicon atoms from the silicon carbide lattice. At the second stage, a dielectric layer was applied to the attachment points of the upper contact by plasma chemical deposition; silicon oxide was used as a

dielectric [1, 2]. In the result of experimental studies, structures with a depth of 900 nm, a height of 860 nm and a minimum structure size of 280 nm were formed. The manufactured mock-up of the sensing element of the ionization gas sensor has a low sensitivity threshold due to ionization processes, which ensures energy efficiency. Such detector devices can be integrated into various multifunctional environmental monitoring systems and control environmental parameters of the environment [3].

Acknowledgement. This work was supported by the Russian Foundation for Basic Research Project No. 18-29-11019 mk. The results were obtained using the equipment of the Research and Education Center "Nanotechnologies" of the Southern Federal University

References

[1] Aderhold J., Davydov V. Yu., Fedler F., Klausing H., Mistele D., Rotter T., Semchinova O., Stemmer J., Graul J. // *J. Cryst. Growth*, **151**, 701, 2001.

[2] Strite S., Morkoc H. // *J. Vac. Sci. Technol. B*, **10**, 1237, 1992.

[3] Klimin V. S., Rezvan A. A., Ageev O. A. Research of using plasma methods for formation field emitters based on carbon nanoscale structures // *Journal of Physics: Conference Series*, **1124**(7), 071020, 2018.

Influence of the Modes of Forming Nanoscale Structures on the Surface of a Silicon Substrate by the Method of Focused Ion Beams

J. V. Morozova*, V. S. Klimin, B. R. Dominguez Encalada, I. N. Kotz

Department of Nanotechnology and Microsystems, Southern Federal University, Taganrog, 347922, Russia

*ulamrzv@gmail.com

This report presents a study of the modes of forming nanoscale structures on the surface of a silicon substrate by the method of focused ion beams. The regularities of the influence of the ion beam current, accelerating voltage and radiation dose on the morphology of the surface of nanoscale structures are determined. Due to the tendency to decrease the lateral dimensions of nanoelectronics and nanophotonics elements, the urgency of mastering new methods for local modification of the surface of substrates and structures with nanoscale resolution increases. One of the promising methods for the formation of nanoscale structures is the use of focused ion beams (FIBs), which is used for maskless etching, deposition, as well as surface modification in the formation of nanoscale structures in micro- and nanoelectronics technology [1]. The method is based on the interaction of accelerated ions with the substrate surface, in the result of which various processes occur on the surface and in the subsurface layer: ion implantation, formation of a disturbed layer, sputtering of the material, etc. The minimum diameter of the ion beam in the FIBs method can reach 7 nm, which opens up wide opportunities for using it to form nanoscale structures of nanoelectronics and nanophotonics elements [2]. As a result, it was investigated that due to the overlap of the etching areas of the FIBs and the broadening of the ion beams due to an increase in the density of the ion flux at high doses, an increase in roughness is observed. The results obtained can be used in the development of manufacturing technology for nanoelectronics and nanophotonics instrument structures [3].

Acknowledgement. This work was supported by the Russian Foundation for Basic Research, Project No. 20-69-46076. The results were obtained using the equipment of the Research and Education Center "Nanotechnologies" of the Southern Federal University

References

[1] Salvati E., Brandt L. R., Papadaki C., Zhang H., Mousavi S. M., Wermeille D., Korsunsky A. M. Nanoscale structural damage due to focused ion beam milling of silicon with Ga ions // *Mater. Lett*. **213**, 346 – 349, 2018.

[2] Wang Y.-C., Xie D.-G., Ning X.-H., Shan Z.-W. Thermal treatment-induced ductile-tobrittle transition of submicron-sized si pillars fabricated by focused ion beam // *Appl. Phys. Lett*. **106**(8), 081905, 2015.

[3] Klimin V. S., Rezvan A. A., Ageev O. A. Research of using plasma methods for formation field emitters based on carbon nanoscale structures // *Journal of Physics: Conference Series*, **1124**, 071020, 2018.

Interactive Editor for Finite Element Modelling in ACELAN-COMPOS Package

D. A. Moskalenko[1], P. A. Oganesyan[1], A. N. Soloviev[1,2]*, M.-Y. Yeh[3], C.-D Yang[4]

[1]Southern Federal University, Rostov-on-Don, Russia
[2]Don State Technical University, Rostov-on-Don, Russia
[3]Department of Microelectronics Engineering, National Kaohsiung University of Science and Technology, Kaohsiung, Taiwan (R.O.C.)
[4] Department of Microelectronics Engineering, National Kaohsiung University of Science and Technology, Kaohsiung, Taiwan (R.O.C.)

*solovievarc@gmail.com

The problem formulation for finite element (FE) models can be implanted in multiple ways. Packages usually rely on graphical user interfaces (GUIs) or scripting languages. While GUIs allow prototyping the geometry of model and visualize results, they usually lack the flexibility of scripting languages, including custom computational scenarios. The main purpose of ACELAN-COMPOS [1, 2] package is to solve series of boundary problems to estimate the effective material properties of the representative volume. The representative volume can be generated with different parameters and each combination of parameters requires new series of computation. Such tasks require both automation of parametrized numerical experiment and interactive visualization of the representative volumes. Some computational results obtained during the experiment can be used on the next step of the series. This set on requirements led us to development of new web application that relies on interactive editor with domain specific language (DSL) for modelling of composites and has distributed scalable back-end architecture. In this study we present approaches to build parametrized interactive FE models with specific type of caching that allow us to reduce time of numerical experiments. The structure of the application consists of three parts: client application that includes 2D and 3D visualization and text editor with syntax highlighting, webserver which stores sessions and cache, parses the input scripts, and distributed computational tasks between multiple computational nodes, and set of computational nodes responsible for solving different FE problems. Computational nodes have different specification for different tasks: CPU, GPU or

memory could be the most important for the problem, and web server select the most suitable node for a problem with the respect to current load of the node. This architecture allows one to perform series of experiments in parallel queues and balance the load on the computational nodes. Set of policies implemented on the server allows simultaneous access to the model for multi-user editing or viewing and sharing parts of models.

Acknowledgement. This research was supported by the RSF project No. 22-11-00302

References

[1] Kurbatova N. V., Nadolin D. K., Nasedkin A. V., Nasedkina A. A., Oganesyan P. A., Skaliukh A. S., Soloviev A. N. Models of Active Bulk Composites and New Opportunities of the ACELAN Finite Element Package. In: *Wave Dynamics and Composite Mechanics for Microstructured Materials and Metamaterials. Advanced Structured Materials*. M. A. Sumbatyan (Ed.). Springer, **59**, 133-157, 2017. DOI: 10.1007/978-981-10-3797-9_8

[2] Kudimova A. B., Nadolin D. K., Nasedkin A. V., Oganesyan P. A., Soloviev A. N. Finite element homogenization models of bulk mixed piezocomposites with granular elastic inclusions in ACELAN package // *Materials Physics and Mechanics*, **37**, 25 – 33, 2018.

Dielectric Spectroscopy of Solid Solutions Based on Sodium-Potassium-Cadmium Niobates in a Wide Range (10 – 1000 K) temperatures

M. O. Moysa*, K. P. Andryushin, S. P. Kubrin, A. V. Pavlenko, L. A. Reznichenko

Research Institute of Physics, Southern Federal University, Rostov-on-Don, Russia

*maksim.moysa@mail.ru

Earlier, in [1] we studied the dielectric spectra of solid solutions (SSs) of the $(1 - x - y)$ $NaNbO_3 - xKNbO_3 - yCdNb_2O_6$ system with $x = 0.05 - 0.20$, $y = 0.075$ in the temperature range 300 – 1000 K, and in [2] these studies were continued in the low-temperature 10 – 300 K region, with the object being SS with $x = 0.15$, $y = 0.025$. Taking into account the current interest of researchers in lead-free compositions and the possibilities of their use under critical conditions under the effects of ultra-low temperatures, in this work the concentration range of the components included in the SSs is expanded and a spectroscopic analysis of the dielectric properties of the SSs of this system in the field of "nitrogen" and "helium" temperatures is undertaken. At the same time, studies of the real, $\varepsilon'/\varepsilon_0$,, and imaginary, $\varepsilon''/\varepsilon_0$, parts of the relative complex permittivity depending on the frequency of the alternating electric field, *f*, were carried out on unpolarized samples in the temperature range 10 – 330 K using LCR-meter Wayne Kerr 6500 B. The samples were cooled using a CCS-150 closed-type helium refrigerated cryostat manufactured by Cryogenics. Temperature control was carried out using a LakeShore 331 temperature controller, which allows maintaining the set temperature with an accuracy of ± 0.01 K. During measurements, the samples were placed in the vacuum chamber of a cryostat, and the vacuum was created with a Boc Edwadrs turbomolecular pump. Figure 1 shows the dependences $\varepsilon'/\varepsilon_0(f,T)$, combined with the results obtained in [1]. It is clearly seen that, in addition to the extremum $\varepsilon'/\varepsilon_0$ at the Curie point, in the ferroelectric region below room temperature, at first (for small values of *x*) a small local maximum $\varepsilon'/\varepsilon_0$ is formed, which gradually (as the system is enriched with potassium niobate) is smeared and becomes to the inflection point at significant concentrations of $KNbO_3$. The nature of the emerging anomaly is clarified with the help of low-temperature X-ray experiments.

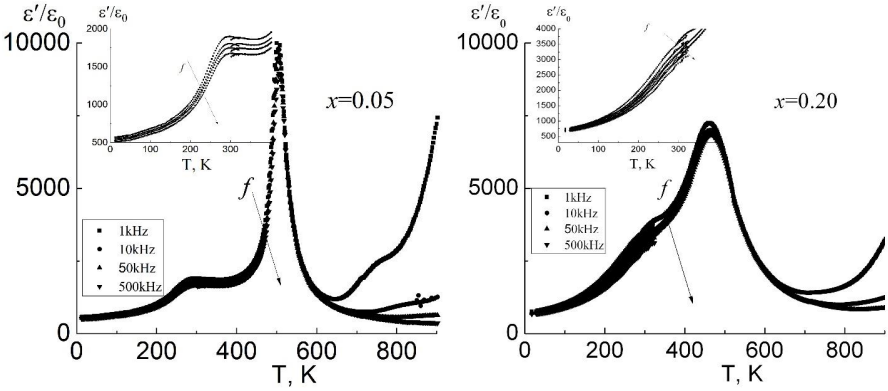

Fig. 1. Dependence $\varepsilon'/\varepsilon_0(T)$of TS samples of the system $(1-x-y)\ NaNbO_3 - xKNbO_3 - yCdNb_2O_6$ with $y = 0.075$, $x = 0.05$ and 0.20

Acknowledgement. The study was carried out with the financial support of the Ministry of Science and Higher Education of the Russian Federation (State task in the field of scientific activity, scientific project No. (0852-2020-0032)/(BAZ0110/20-3-07IF)).

References

[1] Moysa M. O., et al. // *Journal of Physics: Conference Series*, **1942**, 012027, 2021.
[2] Andryushin K. P., et al. *Materials*, **14**(14), 4009, 2021, DOI 10.3390/ma14144009

Numerical Simulation of Particle-filled Piezocomposite Using Tunable Random Representative Volume

A. V. Nasedkin[1]*, M. E. Nassar[1,2]**

[1]*Southern Federal University, Rostov-on-Don, Russia*
[2]*Faculty of Electronic Engineering, Menoufia University, Menouf, Egypt*

*nasedkin@math.sfedu.ru, **mohammed.alsayed75@el-eng.menofia.edu.eg

To improve the mechanical, electrical, and functional properties of porous piezoceramic compounds, A. Rybyanets et al. developed a new method for manufacturing piezocomposites by introducing different types of polymeric microgranules, which are filled or coated with metal-containing micro- or nanoparticles, into the ceramic matrix during the manufacturing process. With this approach, they produced a piezoceramic composite with superlattices of closed pores coated by metal nanoparticles, which is referred here to as the system with a metalized pore surface (SMPS). Computer simulation approaches for piezocomposites are required to obtain a prior estimate of the proportion of each component based on the needed equivalent characteristics. Since there are no constraints on geometry, material properties, number and size of phases in the piezocomposite, numerical inhomogeneity approaches, such as finite element analysis, appear to be a well-suited way to describe the behavior of these materials. The finite element homogenization approach predicts the equivalent properties of a

heterogeneous material by analyzing the constitutive mathematical relationships over a periodic/random representative volume element (RVE) using specific boundary conditions. Then, the homogenized properties are calculated from the finite element solution according to the law of energy conservation. Unlike periodic structures such as cellular solids, particle-filled compounds lack a basic repeating unit that properly reproduces the microstructure of the composite. In fact, the microstructure of these composites is a matrix with a specific volume ratio of irregularly distributed impurities. Here, we are interested in modeling the effect of potential fabrication inaccuracies on the composite's effective properties. For this purpose, we introduced the regularity coefficient into the relationship determining the inclusion's volume fraction and generated an RVE with cubic inclusions of different sizes randomly dispersed throughout the piezoceramic matrix. The hollow metal inclusions are designed as cubes filled with piezoelectric material with minimal elastic stiffness, piezoelectric coefficients, and very high dielectric permittivity coefficients. Finally, we explored the effects of changing the regularity coefficient on the equivalent properties of the composite. The results of this work confirm that there is a good agreement between the results obtained using the periodic RVE and those obtained using the random RVE. The effects of the regularity coefficient on the equivalent properties increase as the inclusion's volume fraction increases. The effective dielectric permittivity decreases as the regularity coefficient increases, increasing the effectiveness of the piezoelectric transducer in sensing applications. According to the findings, the volume fraction of the inclusions has a stronger impact on the electromechanical characteristics of SMPS compared to the regularity coefficient. The SMPS-based piezoelectric transducers are expected to perform well in piezoelectric motors and transverse piezoelectric sensors. The newly developed RVE in this work can be applied to model a wide range of composites with inclusions or pores of various sizes.

Acknowledgement. This research was done, in part, in the framework of the Government of the Russian Federation, contract number 075-15-2019-1928, and RFBR, project number 20-31-90102. M. E. Nassar is funded by a scholarship under the executive program between the Arab Republic of Egypt and the Russian Federation.

The Features of Microstructure of $SrFe_{2/3}W_{1/3}O_3$ Multiferroic Ceramics

A. V. Nazarenko*, G. V. Valov, A. V. Pavlenko

Federal Research Centre The Southern Scientific Centre of the Russian Academy of Sciences, Rostov-on-Don, 344006, Russia

*avnazarenko1@gmail.com

As it is known, the presence of impurity phases in ceramics, which are subsequently used as cathodes for the synthesis of thin films, can significantly affect the quality of the obtained materials. Therefore, the study of their granular structure, phase and elemental composition, the internal structure of crystallites using complementary methods (optical and electron microscopy) is relevant. One of the promising materials for the fabrication of thin films is the $SrFe_{2/3}W_{1/3}O_3$ (SFWO) compound, a ferrimagnet with high T_M and T_C values. The magnetic phase transition in SFWO occurs in the temperature range 380 – 400 K, while the ferroelectric phase transition occurs in 420 – 490 K. The report presents the results of studying the grain structure and internal structure of cleavage crystallites of single-phase (according to X-ray diffraction analysis) ceramics $SrFe_{2/3}W_{1/3}O_3$. The study was carried out using complementary

methods (optical and electron microscopy). It is noted that the cleavage proceeded mainly through the volume of ceramic crystallites, which indicates higher strength characteristics of grain boundaries compared to the grain volume. The grains are characterized by a prismatic habit, while their shape varies from quadrangle to hexagon. Ceramic has a very high density. An elemental analysis of the internal structure of the grain was carried out at a qualitative level, which showed that the composition is consistent with above formula. The spectrum of elements is well distinguishable with an acceptable natural background. An analysis of the crystallite sizes showed that grains of different sizes vary from 3 to ~18 μm. The average size is 9 – 11 microns. When considering the scatter of grains in size, a tendency for a symmetrical (normal) distribution was noted. which can be an important characteristic, when creating films based on SFWO. This kind of homogeneity can affect the mechanical properties (elasticity, surface tension, acoustic properties, etc.).

Acknowledgement. The work is performed as part of the project No 122020100294-9 of the SSC RAS State Order with the use of equipment of the Centers for Collective Use No. 501994.

Prestress Modelling and Sensitivity Analysis in 2D Problems for Elastic Inhomogeneous Cylinders

R. D. Nedin*, V. O. Yurov

Department of Elasticity Theory, I.I. Vorovich Institute of Mathematics, Mechanics and Computer Sciences, Southern Federal University,
8a, Milchakov Str., Rostov-on-Don, 344090, Russia
Vladikavkaz Scientific Center of Russian Academy of Sciences, Southern Mathematical Institute, 22, Markus Str., Vladikavkaz, 362027, Russia

*rdn90@bk.ru

As in the case of material inhomogeneity, there is a lack of studies in the literature, devoted to theoretical modeling and identification of a complex inhomogeneous prestress state in cylindrical bodies. This is mainly due to the complexity of the mathematical apparatus and computational difficulties that arise at the stage of setting and solving the accompanying inverse problems. In the literature, there is often an approach to solving problems of modeling and restoring a uniaxial prestress field in cylindrical structures, based on *a priori* information that these stresses are formed as a result of applying some mechanical loads. For a finite cylinder that is inhomogeneous in the radial and axial directions, a weak statement is formulated that takes into account the presence of prestress fields of an inhomogeneous structure. The prestress tensor is given by four nonzero components that are functions of the coordinates. Two techniques are proposed for specifying the prestress fields for a cylinder clamped by one end. The first one is based on the calculating of the prestress field as a finite element solution of the corresponding initial statics problem on the deformation of a cylinder under the action of some preload; for that, the cases of initial swelling by internal pressure, pre-twisting and pre-stretching are considered. The second way is based on the construction of analytical solutions for the ring in the case of swelling and twisting by the moments applied to the inner and outer boundaries, and also for the problem of stretching an infinite cylinder. A significant difference between the analytical and finite element solutions is observed in a fairly small neighborhood of the pinched end of the cylinder. The possibility of using

analytical solutions instead of numerical ones was demonstrated by analyzing the solutions in the vicinity of the clamped end and then analyzing the effect of prestress on the deformation characteristics of the cylinder. The calculated displacement fields in problems with analytical and numerical prestress differ insignificantly due to the conditions for fixing the cylinder. An influence of the three considered prestress types on the field of small superimposed displacements was analyzed; sensitivity analysis was carried out for three types of loading: (i) tensile load applied to the free end; (ii) swelling by internal pressure; torsion by a tangential load applied to the end. The computational experiments performed have shown that the highest sensitivity is observed mainly in the vicinity of the free edge. The inverse problem on the reconstruction of the intensities of the three considered prestress types is studied, when the additional data on the displacements field in the entire region is known. The system of linear equations for finding the inhomogeneous prestress amplitudes is built on the basis of weak statement equations. In the absence of noise in the input information, a sufficiently high accuracy of the inverse solution is observed.

Acknowledgement. This work is supported by the Russian Science Foundation, grant #18-71-10045, https://rscf.ru/project/18-71-10045/

Features of the Electronic Structure of Polyaniline and PANI/Cu, PANI/Zr Composites by X-ray and UV-VIS Spectroscopy

O. V. Nedoedkova*, V. Y. Lysenko, E. V. Pronina, V. A. Shmatko, G. E. Yalovega

Faculty of Physics, Southern Federal University, Rostov-on-Don, Russia

*nedoedkova@sfedu.ru

Materials, based on organic substances with high electrical conductivity, are used for electronic and nanoelectronic devices (field-effect transistors, organic solar cells with high efficiency, chemical sensors). One of such materials is polyaniline (PANI), to being the most common representative of the class of conducting polyconjugated polymers with their own conductivity. PANI is a polymer consisting of oxidized and reduced fragments. Depending on the degree of oxidation, there are three main forms of PANI: (i) the fully oxidized form of PANI, namely pernigraniline; (ii) the fully reduced form of PANI, namely leucoemeraldine; (iii) PANI with a ratio of oxidized and reduced fragments equal to 1:1, namely emeraldine. In addition, the conductive properties of polyaniline, which are based on its electronic structure, can be varied by modifying the polymer with various compounds, in particular metal salts. The atomic and electronic structure of various forms of polyaniline and composites based on it PANI/Cu and PANI/Zr has been studied by spectral methods: UV and visible spectroscopy, X-ray absorption spectroscopy. The samples for the study were obtained by the acid-free method followed by thermostating [1]. The presence of two bands on the UV-spectra corresponding to the amine and quinonimine forms allows us to conclude that polyaniline in the studied samples is in a partially oxidized state. Doping of polyaniline with copper dihydrochloride and zirconium oxide-dichloride leads to a shift in the absorption bands, which indicates a change in the shape of polyaniline in PANI/Cu. Analysis of changes in the optical spectra of PANI and PANI/Zr composites showed that pure PANI is in the form of an emeraldine base, PANI-Zr composites at temperature control temperatures of 30 °C and 90 °C have the same degree of oxidation. The study of the features of the atomic and electronic

structure of various forms of PANI and PANI/Zr was carried out on the basis of quantum chemical calculations using the electron density functional theory and theoretical modeling of X-ray absorption spectra beyond the carbon edge using the FDMNES software package. The calculation of the density of electronic states obtained by the chains of polyaniline forms showed that the smallest band gap is in emeraldine, and it is approximately equal to 0.4 eV, it is 1.8 eV in leucoemeraldine, and it is 0.9 eV in pernigraniline. All the values obtained correspond to semiconductors. Polyaniline is characterized by the presence of unoccupied states up to the Fermi level. In the course of geometric optimization of the PANI/Zr composite based on the quantum chemical calculations, using the electron density functional theory, structural models were obtained and theoretical calculations of absorption spectra were carried out for them. Based on the analysis of NEXAFS spectra, it was found that PANI is the part of the Pani/Zr nanocomposite in the form of an emeraldine salt. The presence of zirconium in the composite causes the protonation of emeraldine. Zirconium interacts with the polymer chain through nitrogen atoms, which indicates that positively charged imine groups predominate in the composite, obtained by the acid-free method.

Acknowledgement. This study was funded by the Ministry of Science and Education of Russia (Grant № 121100500084-2). The authors are grateful to Myasoedova T. N. for the samples of the study.

Reference

[1] Shmatko V. A., Myasoedova T. N., Yalovega G. E. Electronic structure of polyaniline modified with copper and zirconium salts // *Optics and Spectroscopy*, **5**, 617, 2020.

Characteristics of the Operating Mode of the Main Pipeline

I. V. Nemchenko, D. D. Fugarov*, P. P. Solomakhin,V. I. Kharabadzhakhov

Don State Technical University, Rostov-on-Don, Russia

ddf_1@mail.ru

The main characteristics that make it possible to perform technological calculation of the mode of the main pipeline are: pipeline performance, physical properties of the transported substance, soil temperature at the depth of the pipeline axis and air temperature [1]. Physical properties are required, when performing hydraulic and thermal calculations for a pipeline. For this purpose, the values of density, viscosity, specific heat and Joule-Thomson coefficient are required at various pressures and temperatures [2]. Gas viscosity characterizes the ability of a gas to resist the movement of one part of the gas relative to another. The magnitude of the force of internal friction between two moving layers is proportional to the area of contact of these layers and the change in the speed of movement in the direction perpendicular to the plane of contact of the layers [3]. The coefficient of proportionality between the force of internal friction and the product of the surface area by the change in the speed of movement is called the coefficient of dynamic viscosity [4]. For example, the viscosity of a gas depends on the pressure, temperature and composition of the gas. The compressibility factor shows the ratio of the real volume of the transported substance to the ideal volume. These characteristics are necessary, when creating complex mathematical models that allow calculating the technological modes of operation of pipelines [5].

References
[1] Gerasimenko Y., Gerasimenko A., Fugarov D., Purchina O., Poluyan A. Mathematical modeling and synthesis of an electrical equivalent circuit of an electrochemical device // *Advances in Intelligent Systems and Computing*, **1259**, 471 – 480, 2021.
[2] Fugarov D. D., Purchina O. A., Poluyan A. Y., Gerasimenko A. N., Rasteryaev N. V. Magnetodielectric ac measuring transducer for automation systems in oil refineries *// Journal of Physics: Conference Series*. International Conference "Information Technologies in Business and Industry", 062020, 2019.
[3] Onyshko D., Fugarov D., Purchina O., Poluyan A., Rasteryaev N., Skakunova T. Synchronization system in wireless sensor networks of oil and gas complex // *E3S Web of Conferences. Topical Problems of Green Architecture, Civil and Environmental Engineering, TPACEE 2019*, 03030, 2020.
[4] Poluyan A. Yu., Purchina O. A., Fugarov D. D., Gerasimenko E. Yu., Skakunova T. P. Application of bionic and immune algorithms for the solution of ambiguous problems of transportation routing // *Journal of Physics: Conference Series*. International Conference "Information Technologies in Business and Industry", Mathematical Simulation and Computer Data Analysis, **2**, 032057, 2019.
[5] Poluyan A. Yu., Purchina O. A., Fugarov D. D., Golovanov A. A., Smirnova O. V. Solution of task on the minimum cost data flow based on bionic algorithm // *Journal of Physics: Conference Series*. International Conference "Information Technologies in Business and Industry", Mathematical Simulation and Computer Data Analysis, **2**, 032056, 2019.

Study of Carbon Nanotubes for Harvesters of Energy

A. V. Nesterenko*, N. N. Rudyk, O. I. Il'in, V. V. Petrov

Southern Federal University, Institute of Nanotechnologies, Electronics, and Equipment Engineering, Taganrog, Russia

*vvpetrov@sfedu.ru

It is known that a person practically lives in the field of electromagnetic radiation, that is the so-called "scattered" energy surrounds his. One of the types of devices collecting scattered energy is "harvester" (from English "Harvester" - a combine, a machine for harvesting), allowing one to collect and accumulate scattered energy to subsequent transmission and used by other devices. On the other hand, a modern person uses numerous small-sized electronic devices in his daily life, which make it more comfortable life. Their disadvantage is the constant need for their recharging. The task that has actively become developed in the last two dozen years is to use energy harvesters for nutrition (or recharging) of gadgets. The same problem also relates to medical gadgets (hearing aids, pacemakers, etc.). Here, the use of energy harvesters can help reduce dimensions, product costs, as well as an increase in their service life. The main materials used to convert the mechanical energy of motion, oscillations, vibrations into electrical are piezo- and ferroelectrics, the most applicable of which is zinc oxide, lead zirconate, $Pb(Zr, Ti)O_3$, and niobate lithium. One of the serious problems in the development of harvesters of energy is the formation of ohmic and barrier contacts for removing the electrical signal. In some cases, it is proposed to use carbon nanotubes (CNTs) arrays, which can serve as highly elastic electrode materials of harvesting energy. CNTs

technology, the length of which exceeds several microns, is well known. However, for the harvesters of energy, using active material in the form of a film, it is necessary to have a CNTs length not higher than 1 μm. It is known that the length of the CNTs is affected by the thickness of the film of the catalytic material. In this work on the surface of oxidized silicon, a thin film of nickel (60 – 120 nm) was applied by the method of thermal vacuum evaporation (UVN-2M, Russia). The cultivation of CNTs was carried out by plasma chemical deposition from the gas phase (PECVD, Russia). Studies of the parameters of formed carbon nanostructures were carried out on the scanning electron microscope (Nova Nanolab 600, The Netherlands). Studies have shown that nanostructures have a shape of a cone that have a diameter of the base of 80 – 250 nm. The diameter of the vertex was 50 – 100 nm. The height of the nanostructures was within 400 – 600 nm.

Acknowledgement. Growing an array of CNTs and SEM measurements were financially supported by the Ministry of Science and Higher Education of the Russian Federation; the state task in the field of scientific activity (project No. FENW-2022-0001).

Setup for Studying the Photoconductivity of Thin Semiconductor Films and Heterostructures Formed on Opaque Substrates

A. V. Nesterenko*, Yu. N. Varzarev, V. V. Petrov

Southern Federal University, Institute of Nanotechnologies, Electronics, and Equipment Engineering, Taganrog, Russia

*vvpetrov@sfedu.ru

Recently, the properties of new semiconductor oxide materials and heterostructures based on them have been actively developed and studied for use in photosensitive sensors and photovoltaic devices. The optical properties of thin films of new materials, as a rule, are investigated by spectrophotometry. For this, thin films must be formed on transparent substrates, namely glass or quartz. However, in photosensitive sensors, these materials are applied to opaque substrates. In this case, the optical properties of the oxide material films deposited on transparent and opaque substrates may differ. On the other hand, the study of the photosensitive characteristics of thin oxide films directly during their formation allows one to reduce technological and financial costs. In order to study the parameters of the photoconductivity of thin semiconductor films and heterostructures, formed on opaque substrates, a setup was designed and manufactured. The work of the setup is based on measuring the kinetics of the photoconductivity of a resistive structure, based on the film under study, when it is irradiated with a LED with a given wavelength. Eight LEDs with a maximum radiation wavelength of 940, 660, 625, 525, 470, 400, 365 and 265 nm were chosen for the research. In addition, the design of the setup includes a pulsed constant voltage power supply AKIP-1101 (Russia), which makes it possible to regulate the energy characteristics of the radiation. To measure the characteristics of radiation, an ultraviolet radiation intensity meter CENTER 532 (China) and an illumination meter (luxmeter) CENTER 530 (China) are used. A sample of an oxide material film deposited on an opaque substrate is placed on a heating table, which provides heating of the film sample to 300 °C. Before the photoconductivity measurement process, contact metallization is formed over the film to create a photosensitive resistor. The electrical contact is provided by tungsten probes, and the photoconductivity is

monitored with a Tektronix DMM 4050 digital multimeter (China). Studies, carried out with samples of nanocomposite films of the SnO_2 – ZnO composition with a Sn:Zn molar ratio of 5:95, 50:50, and 95:5, the optical properties of which were investigated by us in [1], showed that the sample with Sn:Zn ratio equal to 50:50 had better properties, which is probably due to the higher concentration of SnO_2 – ZnO heterostructures in the film. This leads to a higher concentration of centers of generation - recombination of charge carriers and, accordingly, to lower lifetimes of charge carriers.

Acknowledgement. The research was supported by the grant No. 22-29-00621 of the Russian Science Foundation, https://rscf.ru/project/22-29-00621/ in the Southern Federal University.

References

[1] Bayan E. M., Petrov V. V., Volkova M. G., Storozhenko V. Yu., Chernyshev A.V. SnO_2 – ZnO nanocomposite thin films: The influence of structure, composition and crystallinity on optical and electrophysical properties // *Journal of Advanced Dielectrics*, **11**(4 – 5), 2160008, 2021.

Size-dependent Models of Thermoelastic Bending of a Layered and Functionally Graded Beams

S. A. Nesterov

Southern Mathematical Institute - branch of the VSC RAS, Vladikavkaz, Russia

1079@list.ru

In connection with the development of microelectronics and micro-electromechanical systems, much attention of scientists is drawn to the study of the stress-strain state of small-sized bodies. When calculating the mechanical behavior of small homogeneous beam structures, non-classical models of continuum mechanics are usually used, for example, the gradient theory of thermoelasticity, which takes into account scale effects. However, the bending of a layered and functionally graded microbeam, which occurred under the influence of a thermal load, has not been studied. In the work, in the framework of the beam theories of Bernoulli-Euler and Timoshenko, the scale effects that arise during thermoelastic bending of a layered and functionally graded microbeam are studied. Scale effects are taken into account using the one-parameter gradient theory of thermoelasticity. Equilibrium equations, boundary conditions and conjugation conditions are obtained by applying the Lagrange variational principle. Displacements and stresses are presented as the sum of solutions to the thermoelasticity problem in the classical formulation and gradient parts. The difference between the displacement distributions found on the basis of the solutions of the problem in the classical formulation and in the gradient formulation is shown. The influence of the mechanical and thermal gradient parameters, the conditions of fastening and loading, the thickness of the layers, as well as the laws of inhomogeneity on the magnitude of the beam deflection is studied. A comparison is made of the calculations, obtained in the result of applying the beam theories of Euler-Bernoulli and Timoshenko.

Acknowledgement. This work was supported by the Russian Science Foundation (project No. 22-11-00265).

Solution of the Inverse Problem of Thermoelasticity for an Inhomogeneous Hollow Cylinder by the Method of Algebraization

S. A. Nesterov

Southern Mathematical Institute - Branch of the VSC RAS, Vladikavkaz, Russia

1079@list.ru

To calculate the strength of structures under thermal power loading, it is necessary to solve problems associated with finding the stress-strain state. Such calculations are most often carried out for homogeneous materials. However, today more and more heterogeneous materials used are the layered composites and functionally graded materials (FGMs). In this case, the thermomechanical characteristics of inhomogeneous materials can be determined only on the basis of the apparatus of coefficient inverse problems (COPs). Currently, a lot of research has been carried out on the solution of the COPs of thermal conductivity and theory of elasticity. For some materials, it is necessary to take into account the field coupling and solve the COPs of thermoelasticity, which are currently poorly studied for inhomogeneous materials. Usually, the study of inverse problems is reduced to solving the corresponding extremal problems and applying the gradient method for minimizing the residual functional. COPs of thermoelasticity are nonlinear problems. To solve such problems, the author previously applied an iterative approach, at each stage of which the Fredholm integral equation of the first kind was solved. On the basis of an iterative approach, the inverse problems of thermoelasticity for a rod, layer, and cylinder are investigated. At the same time, alternative methods for solving the COPs are used, for example, the method of algebraization. This work is devoted to the application of the method of algebraization to solve the COPs for an inhomogeneous thermoelastic cylinder. Two types of cylinder loading are considered, namely thermal and mechanical ones. The thermomechanical characteristics of the cylinder are functions of the radial coordinate. Unknown thermomechanical characteristics are presented in the form of a polynomial, the coefficients of which must be determined. To solve the direct problem after applying the Laplace transform, the Galerkin method is used. The Maple software calculates the determinant of a system of algebraic equations. This determinant becomes equal to zero for some values of the Laplace transform parameter p. To find these values, we approximate the additional information, measured at the boundary of a cylinder at some points in time in the form of a linear combination of exponential functions. The exponents in the expansions are found by the Prony method. In the result of substitution of the values of p into the determinant, we obtain a system of nonlinear algebraic equations, the solution of which is sets of numbers. The criteria for selecting a suitable set are: (i) limited thermomechanical characteristics; (ii) the minimum value of the residual functional. The method of algebraization allows an identification with high accuracy only for monotonic functions, but with much less machine time than the iterative approach. For nonmonotonic functions, the solution obtained by the algebraization method can serve as an initial approximation in the iterative process.

Acknowledgement. This work was supported by the Southern Mathematical Institute, a Branch of the VSC RAS, Vladikavkaz.

Effect of Ultrasonic Vibration Parameters on Beam Geometry and Mechanical Properties of the SS304 Piping by an Orbital Welding

Ngoc-Thien Tran*, Pham Son Minh, Tran Minh The Uyen

Ho Chi Minh city University of Technology and Education, Viet Nam

*thientn@hcmute.edu.vn

The Ultrasonic Vibration Assisted Welding (UVAW) showed the effective solution to improve penetration, microstructure, and mechanical properties of the weld metal of SS304. Thus, the experiment was made on oscillation of the surface of SS304 tube by a piezo-actuator during the TIG orbital welding using metal filler. The TIG welding parameters were set for purpose of creating a full penetration and different ultrasonic vibration parameters (amplitude of voltage was 2 V, 4 V, 5 V; frequency was 400 Hz, 500 Hz, 600 Hz). The bead geometry, mechanical properties, and microstructure of tube welds were discussed in this report. The result illustrates that the finer and uniform microstructures of the weld zone are observed in samples that were assisted by the ultrasonic vibration (UV). The UV process has significantly affected the mechanical properties of tube welds. The highest tensile strength was 534 MPa at a voltage amplitude of 2 V and a frequency of 600 Hz, which is higher than for specimen without vibration (408 MPa). It is also found that the hardness slightly increases with the various frequency from 200 Hz to 600 Hz at a voltage amplitude of 2 V.

Evaluating the Efficiency of Organic Matter Treatment Using Vetiver Grass (*Vetiveria Zizanioides* L.) - A pilot-scale

Nguyen Minh Ky[1,3,*], Chitsan Lin[2,], Nguyen Duy Hieu[1], Nguyen Cong Manh[3], Nguyen Tuan Anh[3]**

[1]Ph.D. Program in Maritime Science and Technology, College of Maritime, National Kaohsiung University of Science and Technology, Kaohsiung, 81157, Taiwan
Department of Marine Environmental Engineering, National Kaohsiung University of Science and Technology, Kaohsiung 81157, Taiwan
[3]Faculty of Environment and Natural Resources, Nong Lam University, Ho Chi Minh Ciy 700000, Vietnam

*nmky@hcmuaf.edu.vn; **ctlin@nkust.edu.tw

Phytoremediation is widely considered a sustainable method to treat polluted water sources. However, choosing the right plants is the key factor of successful implementation. Thus, this study evaluates the efficiency of using Vetiver grass (*Vetiveria Zizanioides* L.) to treat organic matter such as BOD_5 and COD in the canal D, Binh Duong province, Vietnam. The major sources of wastewater are from the local residential and industrial areas in the canal catchment. A high concentration of organic matter has been observed in the water of canal D and were equal to 121±41 – 146±39 mg/L and 204±7 – 276±9 mg/L for BOD_5 and COD, respectively. For the experimental, pilot tanks (dimension: 1×1×1 m^3) designed based on constructed wetlands were built to culture the grass for five months, reaching stability and maturity.

Finally, water from the canal was led through the tanks with different loading levels of 500 mL/min/m^2 (T1), 1000 mL/min/m^2 (T2), and 1500 mL/min/m^2 (T3). Results show that the removal ratio of BOD_5 and COD is more than 90% and 80%, respectively. High removal efficiency can be explained by the great contribution of Vetiver grass within the tanks based on vertical flow characteristics. Also, the loading level is considered a significant factor ($p < 0.05$) affecting the treatment. Treated water that meets the Vietnam irrigation water standard can be reused for agricultural activities.

Building Process of Sewing Templates for Jacket of Garment Enterprises

Nguyễn Phương Linh*, Duong Thi Hoan

Hanoi Industrial Textile Garment University, Ha Noi, Viet Nam

*linh.bk0303@gmail.com

Clothing technology template is a special auxiliary clothing production tool, and it is a new mode of clothing production. Now the development of garment template technology is more and more extensive for many products; it is used for garment processing manufacturing process. Based on the theory of garment process template, this report introduces how to design and make the sewing template for jacket, a complex structure product. From the basic design principles, component composition and basic design steps of the template are analyzed from the structure of jacket prototype and process characteristics in order to provide beneficial reference for the template design process. The results of paper is going to solve the demand of garment enterprises for high-quality products, provides reference for the transformation and upgrading the designing templates process.

A Study on the Effect of the Grip Coefficient on the Slip Coefficient when Braking of the Tractor Semi-trailer on a Straight Road at a Speed of 80 km/h

Nguyen Thanh Tung[a], Luong Van Van[b]

Vinh Long University of Technology Education,
73, Nguyen Hue Street, Vinh Long City, Vietnam

[a]tungnt@vlute.edu.vn, [b]vanlv@vlute.edu.vn

When a vehicle is braked, slip coefficient occurs at the tireprint between the tire and the ground, which affects the braking efficiency and safety of the vehicle. The authors establish a dynamic model of the tractor semi-trailer and use Matlab-Simulink software to simulate the slip coefficient. The results show that, when a tractor semi-trailer is braked with the torque $M_B = 80\%M_{Bmax}$ on three types of roads with grip coefficient $\varphi_{xmax} = [0.8, 0.9, 1.0]$ at a speed of 80 km/h, the slip coefficient is less than 5 %, the tractor semi-trailer moves stably and safely. When a tractor semi-trailer is braked on three types of roads with grip coefficient $\varphi_{xmax} = [0.5, 0.6, 0.7]$ the slip coefficient is 100%, the tractor semi-trailer moves unstably and unsafely.

Fragrance Durability Depending on Compression of Knitted Fabric Bandage Coated by Microcapsule Contained Cinnamon Essential Oil

Nguyen Thi Tu Trinh, Chu Dieu Huong*

Hanoi University of Science and Technology, Hanoi, Vietnam

*huong.chudieu@hust.edu.vn

Fabric treated by natural essential oil was one of textile applications. Microencapsulation is the good method to keep the fragrance longer in fabrics. Because the odor is a psychophysical phenomenon so the evaluation of fragrance durability of fabric treated by natural essential oil was always the subject of many researches. At the same time, the quantitative determination of the fabric fragrance intensity is difficult and not always be agreement with odor characteristics, obtained by different testers. In this report we used the quantitative method to evaluate the fragrance intensity, which was related the remained oil quantity on knitted fabric treated by microcapsule loaded by cinnamon essential oil. The evaluation was based on the combination of the expert method and diluted solution method. The research had carried out on single jersey fabric which were knitted from the Ne 40/1 CVC yarn (60% cotton and 40% polyester), then treated by microcapsule containing cinnamon essential oil. The influence of the fabric using conditions such as applied pressure and the duration by using for fabric fragrance intensity had been investigated. The results showed that fabric fragrance intensity remained only about 30% after 60 minutes in used under applied pressure of 15 mmHg.

Investigation of the Creep Relaxation Behavior in Use of Single Jersey Fabric Depending on the Elastic Yarn Ratio

Nguyen Thi Tu Trinh, Chu Dieu Huong*

Hanoi University of Science and Technology, Hanoi, Vietnam

*huong.chudieu@hust.edu.vn

After a period of using garment products, some deformation appears due to external forces such as laundry, ironing or body movements affecting the aesthetic value. The phenomena are more severe in tight-fitting sportswear which require a high elasticity. Knitted fabrics which use the yarn combined elastic fibres in different proportions can promote elastic properties. This report investigated the creep relaxation behavior after 5 washing cycles to simulate the creep relaxation behavior of two groups of single jersey fabrics. The first fabrics were knitted from CVC yarn (60% Cotton, 40% Polyester) with four spandex setting levels: 100%, 50%, 33%, 25% of total stitches. The seconds were knitted from TC yarn (35% cotton, 65% PES) with four spandex feeding ratios: 100%, 75%, 66%, 50% of total stitches. The fabric stress was calculated by Laplace's law to find the suitable applied load for the study. The three-element viscoelastic model has been applied to build the equations, which simulated viscoelastic characteristics of the knitted fabrics. The results showed that the fabrics with more spandex yarn ratio had less total deformation and elastic deformation before and even after washing cycles. In the other hand the residual deformation increased while spandex yarn ratio

decreased. The equations simulated the fabric's creep relaxation behavior had been created depended on the fabric's elastic yarn ratio and the washing cycles.

Application of Silicon Carbide as a Functional Element in Nanoelectronics

V. V. Niftalieva*, V. S. Klimin

Institute of Nanotechnologies, Electronics, and Electronic Equipment Engineering, Southern Federal University, Taganrog, Russia

*niftalieva@sfedu.ru

Currently, graphene is a promising self-organizing material, which has a high carrier mobility and resistance to ionizing effects [1]. Thermal decomposition of the SiC surface is the main method for producing graphene films on the SiC surface [2]. The advantages of the method consist in low cost and the possibility of obtaining homogeneous nanocarbon films of a large area [3]. A significant drawback is that annealing is required at very high temperatures, which lead to the formation of high mechanical stresses. In this regard, it is important to study the use of a combination of focused ionic and plasma-chemical etching to obtain graphene films on SiC [4]. At the initial stage, the studies were carried out by the method of focused ion beams. A scanning electron microscope with an ion column NovaNanoLab 600 (FEI, Netherlands) was used, with the help of which templates for etching structures were formed, which were a torus with an outer diameter of 2 microns and an inner diameter from 600 to 800 nm. The ion beam current was 30 pA. The accelerating voltage was 30 keV. The structures were then etched onto a silicon carbide substrate. In this experiment, studies were carried out for the formation of carbon nanostructures on the surface. This technology can be used for the formation of modern vacuum microelectronic devices, as well as for the development of pressure and gas sensors.

Acknowledgement. This work was supported by the Russian Foundation for Basic Research Project No. 18-29-11019 mk. The results were obtained using the equipment of the Research and Education Center "Nanotechnologies" of the Southern Federal University.

References

[1] Klimin V. S., Rezvan A. A., Ageev O. A. Research of using plasma methods for formation field emitters based on carbon nanoscale structures // *Journal of Physics: Conference Series*, **1124**, 071020, 2018.

[2] Li J., Yan X., Gou G., Wang Z., Chen J. // *Phys. Chem. **Chem. Phys.*** **16**, 1850 – 1855, 2014.

[3] Chen J., Li J., Yang J., Yan X., Tay B.-K., Xue Q. // *Appl. Phys. Lett*. **99**, 173104, 2011.

[4] Klimin V. S., Solodovnik M. S., Lisitsyn S. A., Rezvan A. A., Balakirev S. V. // *Journal of Physics: Conference Series*, **1124**, 041024, 2018.

Fast Photodetector Based on Zinc Oxide Nanorods

A. L. Nikolaev

Don State Technical University, 1 Gagarin Square, 344000, Rostov-on-Don, Russia

*andreynicolaev@eurosites.ru

The structural, optical, and electrical properties of zinc oxide nanorod arrays, grown by carbothermal synthesis on oxidized Si (001) substrates, were studied. These rods served as the active element of the photodetector prototype. The prototype was made in several steps. First, a thin (~100 nm) ZnO film was deposited on the surface of oxidized silicon using pulsed laser deposition. Then, using a combination of direct and reverse photolithography methods, parallel ZnO strips were formed on the surface of the substrate with a length of about 4 mm, a width of 30 micrometers and a period of 30 micrometers. After that, using pulsed laser deposition, gold nanoparticles were deposited on the resulting system of strips, which acted as a catalyst for the growth of nanorods. Contacts to the resulting structure were made using silver paste. Studies using a scanning electron microscope showed that a dense network of misoriented nanorods grew in the space between the ZnO strips, while nanorods with a predominantly vertical orientation grew on the surface of the strips. The resulting nanorods had a relatively low concentration of point defects and had a high crystallinity. This was confirmed by studying X-ray spectra and photoluminescence spectra. The current-voltage characteristics of the prototype had a pronounced asymmetric diode nonlinearity. The photoresponse of the prototype was measured by exposure to a halogen lamp. Sections were cut out from the lamp spectrum using an MDR-2 monochromator, and the response was recorded at each wavelength segment from 300 to 800 nm with a step of 20 nm. To take into account the influence of intensity on the measurement results, the photoresponse of the prototype was normalized relative to the full spectrum of the used halogen lamp, obtained with a SOLAR TII monochromator-spectrograph. The obtained spectral intensity of the prototype showed predominantly ascending character from 300 to 800 nm with a pronounced peak in the interval from 340 to 380 nm. Next, a study of the time-resolved photoresponse of the prototype was carried out using a nanosecond laser. The prototype showed high sensitivity to optical radiation and a very fast response to single nanosecond laser pulses. To clarify and verify the reproducibility of the results obtained, a series of prototypes was made with various combinations of strips and rods, oxidized silicon, ZnO thin films and ZnO nanorods were studied. Various versions of silver contacts were also investigated, for example, deposited using a pulsed laser method. The obtained results explained the non-linear behavior of the current-voltage characteristics of the prototypes.

Acknowledgement. This work was supported by the Russian Foundation for Basic Research, project 20-07-00637 A.

Drop Precision Control on Distribution of Medical Equipment and Medicines Using UAV for Hard-to-reach Areas Affected by Disasters

Nuril Esti Khomariah*, Muaffaq Achmad Jani, Niken Adriaty Basyarach

Informatics Engineering Department, University of 17 Agustus 1945 Surabaya, Indonesia

*nuril@untag-sby.ac.id

Indonesia is one of the Asian countries that is most frequently affected by natural disasters such as volcanoes and tsunamis. Disaster areas always experience severe damage, especially in transportation infrastructure. This resulted in delays in the delivery of aid such as food and medicine. In this report, we propose the application of UAV technology, which has the main function to help drive the aid delivery process. Delivery is prioritized for areas that are difficult to reach using land routes and urgently needed items such as medical equipment and medicines. The UAV is equipped with various supporting sensors to be able to fly to the target location point and be able to drop the package in a safe condition. The UAV also equipped with live streaming video, where users can see the conditions around the UAV in real time when flying. The drop point control system uses the Fuzzy Logic method. The system will determine the release time of the package based on the input data, that is air speed and altitude sensors. The drop point precision test was carried out on 5 variations of flying height, such as 30 m, 40 m, 50 m, 60 m and 70 m. The results show that the flying height is 30 m, getting the smallest error, which is 11.48 m. While the largest error of 37.38 m was obtained when the UAV was flown at a height of 70 m.

Communication Channels of Telemetry Systems of Drilling Rigs

D. A. Onyshko[1], G. D. Dudkin[1] , D. D. Fugarov[2]*, R. V. Shapovalov[2]

[1]M. I. Platov South-Russian State Polytechnic University (NPI), Novocherkassk, Russia
[2]Don State Technical University, Rostov-on-Don, Russia

*ddf_1@mail.ru

The communication channel determines the design of telesystems, information content, reliability, usability, as well as the conditions for the passage of signals. It is the communication channel that is the main problem for telemetry systems while drilling due to the physical conditions of signal transmission [1]. The communication channels of telemetry systems for drilling rigs use hydraulic, electromagnetic, acoustic, electrically conductive and combined methods of information transmission. Each of these methods has its own advantages and disadvantages. The variety of drilling conditions, as well as economic feasibility, determine its area of application for each communication channel [2]. At present, an electrically conductive communication channel is widely used, since it does not require the expenditure of hydraulic energy and has high communication reliability, speed and noise immunity. The disadvantage of this type of connection is the presence of a cable in the drill string, which complicates the drilling process, and also increases the time spent on laying it and ensuring the cable is protected from mechanical damage [3]. The hydraulic

communication channel uses devices that create pressure pulses in the flow of drilling fluid. Such a communication channel has poor informational content due to the low speed of information transmission, as well as low noise immunity, consistency in the transmission of information [4]. The electromagnetic channel is based on electromagnetic waves that propagate between an isolated section of the drill string and the rock. On the surface of the earth, the signal is received as the potential difference from current spreading over the rock between the drill string and a receiving antenna installed in the ground at a certain distance from the drilling rig. The quality of communication in this case depends on the physical properties and the alternation of rock layers. The acoustic communication channel is based on sound vibrations that are transmitted in the borehole through the drilling fluid, drill string or surrounding rock. The complexity and variety of properties of the hydroacoustic channel in the borehole have led to its poor knowledge [5].

References

[1] Fugarov D. D., Purchina O. A., Kazimirov N. I., Onyshko D. A. Monitoring of normal operating modes of operative dc systems // *Physics and Mechanics of New Materials and Their Applications. Abstracts & Schedule. Kitakyushu, Japan*, 114 – 115, 2021.

[2] Purchina O. A., Poluyan A. Y., Fugarov D. D., Onyshko D. A. Parallel bioinspiral search for task solutions about extremal path // *Science Prospects*. **11**(98), 31 – 34, 2017.

[3] Fugarov D. D., Solomentsev K. Yu., Onyshko D. A., Purchina O. A. Identification of parameters of control objects in the oil and gas complex // *Science and Business: Ways of Development*, **3**(81), 20 – 23, 2018.

[4] Fugarov D. D., Purchina O. A., Vovchenko D. V., Onyshko D. A. Building base blocks of imitation simulation // *Physics and Mechanics of New Materials and Their Applications. Abstracts & Schedule. Kitakyushu, Japan*, 117 – 118, 2021.

[5] Onyshko D., Fugarov D., Purchina O., Poluyan A., Rasteryaev N., Skakunova T. Synchronization system in wireless sensor networks of oil and gas complex // *E3S Web of Conferences. Topical Problems of Green Architecture, Civil and Environmental Engineering, TPACEE 2019*, 03030, 2020.

Routing Algorithm for Sensor Network Nodes

D. A. Onyshko[1], S. A. Himishev[1], D. D. Fugarov[2]*, A. A. Brosalin[2]

[1]M. I. Platov South-Russian State Polytechnic University (NPI), Novocherkassk, Russia
[2]Don State Technical University, Rostov-on-Don, Russia

*ddf_1@mail.ru

Currently, communication networks with a heterogeneous topological structure, consisting of wired and wireless elements, are widely used [1]. Wireless and energy-saving technologies allow the creation of fundamentally new sensor networks [2]. They cover a wide range of frequencies, including real-time delivery and streaming of large amounts of data from one device to another. Wireless network elements often have a limited energy resource, since the nodes operate on batteries of chemical current sources. Therefore, the network has limited bandwidth and the probability of transmission errors increases [3]. In our case, it is very important that the sensor network works for a long time. In this case, data aggregation helps to reduce the amount of data transferred between the sensor nodes and the base station, and the chosen LEACH protocol is the solution to this problem. This is a hierarchical protocol in

which most of the nodes transmit data to the head elements of the clusters, which collect and compress data and then send it to the base station. This routing protocol provides power savings for the power supplies of the sensor nodes on the network, thus maintaining a long network life [4]. Each stage of the protocol corresponds to the clustering levels: the network is divided into groups (clusters) with head nodes (CH); head nodes are divided into their clusters. All operations in such a network are divided into rounds. In the initial phase for transmission, each time a master node is selected in the cluster. The choice is made independently by all nodes at the same time. Energy efficiency is a critical consideration, when using the wireless sensor network routing protocol. Efficiency, as well as energy balancing, significantly increases the service life of the elements of this network [5].

References

[1] Onyshko D., Fugarov D., Purchina O., Poluyan A., Rasteryaev N., Skakunova T. Synchronization system in wireless sensor networks of oil and gas complex // *E3S Web of Conferences. Topical Problems of Green Architecture, Civil and Environmental Engineering, TPACEE 2019*, 03030, 2020.

[2] Fugarov D. D., Solomentsev K. Yu., Onyshko D. A., Purchina O. A. Identification of parameters of control objects in the oil and gas complex // *Science and Business: Ways of Development*, **3**(81), 20 – 23, 2018.

[3] Purchina O. A., Poluyan A. Y., Fugarov D. D., Onyshko D. A. Parallel bioinspiral search for task solutions about extremal path // *Science Prospects*. **11**(98), 31 – 34, 2017.

[4] Fugarov D. D., Purchina O. A., Vovchenko D. V., Onyshko D. A. Building base blocks of imitation simulation // *Physics and Mechanics of New Materials and Their Applications. Abstracts & Schedule. Kitakyushu, Japan*, 117 – 118, 2021.

[5] Fugarov D. D., Purchina O. A., Kazimirov N. I., Onyshko D. A. Monitoring of normal operating modes of operative dc systems // *Physics and Mechanics of New Materials and Their Applications. Abstracts & Schedule. Kitakyushu, Japan*, 114 – 115, 2021.

Using the ZigBee Network Protocol to Build Monitoring Systems

D. A. Onyshko[1], I. A. Lomakin [1] , D. D. Fugarov[2]*, Yu. S. Chudnov[2]

[1]M. I. Platov South-Russian State Polytechnic University (NPI), Novocherkassk, Russia
[2]Don State Technical University, Rostov-on-Don, Russia

*ddf_1@mail.ru

Currently, a large number of industrial companies are introducing new IT technologies, with the help of which they increase the safety and efficiency of production processes [1]. To minimize the human factor, the most effective is the use of automated monitoring of parameters using wireless sensor network technologies. The main elements of the network are wireless sensors, which are infocommunication devices consisting of microcontrollers, memory modules, ADC and DAC, radio frequency modules, sensors, and batteries. The types of sensors used depend on the monitored parameters of the elements of the technological process [2]. The data processing of the sensor network is carried out at the control station, which is the operator's computer. The elements of the sensor network implement the exchange of information among themselves using their radio frequency modules. In the event that one or part of the sensor nodes go out of the network, for example, due to a loss of battery power, then the functioning of the network is ensured after its automatic reconfiguration. The design

of sensor systems is carried out on the basis of network protocols that take into account international standards in the field of infocommunication technologies [3]. One of the efficient network protocols that provide reliable data transfer for industrial automation sensor networks is the ZigBee protocol. The main advantages of the protocol are: (i) international standard IEEE 802.15.4; (ii) automatic configuration of routing for a network with a large number of devices (up to several thousand); (iii) self-healing in case of router failure; (iv) exchange security using AES128 data encryption; (v) long-term operation of self-powered sensors [4]. The system structure of ZigBee technology consists of three main components: a ZigBee coordinator, a router, and an end device. Each ZigBee network should consist of one coordinator, which acts as a bridge to the network. The coordinator acts as a center for receiving and storing important information during data transmission operations. The ZigBee router acts as an intermediary between the information hub and the end devices, which allows traffic or commands to travel through them to the end device [5].

References

[1] Purchina O. A., Poluyan A. Y., Fugarov D. D., Onyshko D. A. Parallel bioinspiral search for task solutions about extremal path // *Science Prospects*. **11**(98), 31 – 34, 2017.

[2] Fugarov D. D., Solomentsev K. Yu., Onyshko D. A., Purchina O. A. Identification of parameters of control objects in the oil and gas complex // *Science and Business: Ways of Development*, **3**(81), 20 – 23, 2018.

[3] Fugarov D. D., Purchina O. A., Vovchenko D. V., Onyshko D. A. Building base blocks of imitation simulation // *Physics and Mechanics of New Materials and Their Applications. Abstracts & Schedule. Kitakyushu, Japan*, 117 – 118, 2021.

[4] Onyshko D., Fugarov D., Purchina O., Poluyan A., Rasteryaev N., Skakunova T. Synchronization system in wireless sensor networks of oil and gas complex // *E3S Web of Conferences. Topical Problems of Green Architecture, Civil and Environmental Engineering, TPACEE 2019*, 03030, 2020.

[5] Fugarov D. D., Purchina O. A., Kazimirov N. I., Onyshko D. A. Monitoring of normal operating modes of operative dc systems // *Physics and Mechanics of New Materials and Their Applications. Abstracts & Schedule. Kitakyushu, Japan*, 114 – 115, 2021.

Designing a Composite Impedance Measurement System

D. A. Onyshko[1], O. O. Udovichenko[1] , D. D. Fugarov[2]*, V. I. Kharabadzhakhov[2]

[1]M. I. Platov South-Russian State Polytechnic University (NPI), Novocherkassk, Russia
[2]Don State Technical University, Rostov-on-Don, Russia

*ddf_1@mail.ru

Composite materials are widely used in various industries [1]. The unique properties of composites ensured their distribution in mechanical engineering, construction, optics, and other fields. An important factor determining the set of performance characteristics of composite materials, including the high sensitivity of electrical conductivity to external influences, is their structure. Impedance spectroscopy is one of the most effective methods for determining the structure and electrophysical characteristics [2]. In recent years, the possibilities of constructing impedance measuring instruments have significantly expanded due to the widespread use of digital signal processing technology [3]. For example, Analog Devices manufactures integrated impedance converters AD5933 and AD5934, on the basis of

which it is possible to implement portable frequency impedance analyzers with a measurement range from 100 Ω to 20 MΩ in the frequency range of a probing signal from 100 Hz to 100 kHz. High metrological characteristics of converters are achieved due to: (i) digital synthesis and tuning of the frequency of the sounding harmonic signal; (ii) formation of measurement results using digital processing of samples the signal of the measuring circuit according to the fast Fourier transform algorithm; (iii) digital correction of the temperature error, based on the data of the built-in temperature sensor [4]. The developed device is based on the analysis of the passage of a calibration signal of a certain frequency through a circuit with a complex resistance, followed by comparison with a reference voltage. In this case, the test signal is formed by the direct digital synthesis (DDS) method, and the value of the complex resistance is calculated through the values of the current and voltage on the measured element according to a programmable algorithm [5].

References

[1] Purchina O. A., Poluyan A. Y., Fugarov D. D., Onyshko D. A. Parallel bioinspiral search for task solutions about extremal path // *Science Prospects*. **11**(98), 31 – 34, 2017.

[2] Fugarov D. D., Solomentsev K. Yu., Onyshko D. A., Purchina O. A. Identification of parameters of control objects in the oil and gas complex // *Science and Business: Ways of Development*, **3**(81), 20 – 23, 2018.

[3] Fugarov D. D., Purchina O. A., Vovchenko D. V., Onyshko D. A. Building base blocks of imitation simulation // *Physics and Mechanics of New Materials and Their Applications. Abstracts & Schedule. Kitakyushu, Japan*, 117 – 118, 2021.

[4] Onyshko D., Fugarov D., Purchina O., Poluyan A., Rasteryaev N., Skakunova T. Synchronization system in wireless sensor networks of oil and gas complex // *E3S Web of Conferences. Topical Problems of Green Architecture, Civil and Environmental Engineering, TPACEE 2019*, 03030, 2020.

[5] Fugarov D. D., Purchina O. A., Kazimirov N. I., Onyshko D. A. Monitoring of normal operating modes of operative dc systems // *Physics and Mechanics of New Materials and Their Applications. Abstracts & Schedule. Kitakyushu, Japan*, 114 – 115, 2021.

Principles of Building Telemetry Channels for Remote Objects

D. A. Onyshko[1], D. P. Yatsenov[1], D. D. Fugarov[2]*, P. P. Solomakhin[2]

[1]M. I. Platov South-Russian State Polytechnic University (NPI), Novocherkassk, Russia
[2]Don State Technical University, Rostov-on-Don, Russia

*ddf_1@mail.ru

The report considers the principles of building a communication channel for data collection systems of remote objects [1]. An important advantage of these principles is the possibility of rapid deployment, as well as spatial movement of system elements located in the area of the radio network [2]. If the automation elements are densely located, for example, within a workshop or factory, it is more reasonable to use a corporate network that is not charged. For these purposes, various wireless communication technologies can be used in telemetry systems. When building a network, it is necessary to take into account the specialized IEEE 802.15.4 standard, which regulates the use of a wireless information network for industrial automation systems. This standard is the basis for the ZigBee, Wireless-HART, Mi-Wi, ISA-

100.11 and Thread protocols aimed at building communication systems through the implementation of upper layers [3]. The ZigBee network is a priority, it contains three types of logical devices, which include the coordinator, the router and the endpoint. The coordinator is used to scan frequency channels, determine free channels and organize the network, create a network identifier, connect new network devices, etc. The functions of the router include packet retransmission, routing, and information buffering. Terminal nodes implement only application actions, that is they are engaged in data collection and management of remote objects and do not carry out retransmission [4]. ZigBee is a promising energy-saving standard for building local wireless networks. It is convenient to use it for building self-organizing and self-repairing communication lines with a large coverage area [5].

References

[1] Fugarov D. D., Purchina O. A., Vovchenko D. V., Onyshko D. A. Building base blocks of imitation simulation // *Physics and Mechanics of New Materials and Their Applications. Abstracts & Schedule. Kitakyushu, Japan*, 117 – 118, 2021.

[2] Onyshko D., Fugarov D., Purchina O., Poluyan A., Rasteryaev N., Skakunova T. Synchronization system in wireless sensor networks of oil and gas complex // *E3S Web of Conferences. Topical Problems of Green Architecture, Civil and Environmental Engineering, TPACEE 2019*, 03030, 2020.

[3] Fugarov D. D., Purchina O. A., Kazimirov N. I., Onyshko D. A. Monitoring of normal operating modes of operative dc systems // *Physics and Mechanics of New Materials and Their Applications. Abstracts & Schedule. Kitakyushu, Japan*, 114 – 115, 2021.

[4] Fugarov D. D., Solomentsev K. Yu., Onyshko D. A., Purchina O. A. Identification of parameters of control objects in the oil and gas complex // *Science and Business: Ways of Development*, **3**(81), 20 – 23, 2018.

[5] Purchina O. A., Poluyan A. Y., Fugarov D. D., Onyshko D. A. Parallel bioinspiral search for task solutions about extremal path // *Science Prospects*. **11**(98), 31 – 34, 2017.

Influence of the Growth Temperature on the Piezoelectric Strain Coefficient of Vertically Aligned Carbon Nanotubes

O. I. Osotova, M. V. Il'ina*, M. R. Polyvianova, N. N. Rudyk, O. I. Il'in

Southern Federal University, Institute of Nanotechnologies, Electronics and Electronic Equipment Engineering, Taganrog, 347922, Russian Federation

*****mailina@sfedu.ru

In recent years, great interest has arisen in the use of carbon nanotubes (CNTs) as a basis for the creation of nanogenerators [1, 2]. This is due to the manifestation of anomalous piezoelectric properties when the centrosymmetric structure of CNTs is violated [3, 4]. However, studies in the research field of the mechanism of the piezoelectric response of CNTs and the dependence on the growth parameters are at the initial stage and require further investigations. Currently, piezoelectric force microscopy (PFM) is widely used for quantitative characterization of the piezoelectric properties of nanostructures. This method makes it possible to estimate the piezoelectric strain coefficient of a nanostructure, which reflects the dependence of its deformation on the magnitude of the applied voltage. The aim of this work is to establish the dependence of the magnitude of the piezoelectric strain coefficient of CNTs on the growth temperature by using the PFM method. The studies were

carried out on vertically aligned CNTs grown by plasma chemical vapor deposition (PECVD) at a growth temperature from 630 to 690°C. A 15 nm thick nickel film was used as the catalytic layer. A 100 nm thick TiN film was used as the bottom electrode. An NSG10/Pt AFM probe was used as the upper electrode. Measurements of the piezoelectric strain coefficient d_{33} were carried out by registering the dependence of the change in the CNTs deformation upon application of an alternating voltage $U = U_{DC} + U_{AC}(\sin \varphi t)$, where U_{DC} varied from 0 to ± 10 V, U_{AC} of ± 3 V, and a frequency φ of 5 kHz. Analysis of the obtained dependences showed that d_{33} was 15.03 ± 0.06 pm/V for CNTs grown at a temperature of 630 °C; d_{33} was 4.05 ± 0.09 pm/V for 675 °C; d_{33} was 7.29 ± 0.07 pm/V for 690 °C. It was found that a decrease in the magnitude of the piezoelectric strain coefficient is observed with an increase in the CNTs growth temperature. This dependence is associated with a decrease in the defectiveness of CNTs with an increase in the growth temperature [5]. At the same time, the defectiveness is the main source of the piezoelectric properties of CNTs as a result of violation of the centrosymmetry of the CNTs structure [3]. Thus, in this work, we calculated the magnitude of the piezoelectric strain coefficient of aligned carbon nanotubes by the PFM method. It is shown that the magnitude of the piezoelectric strain coefficient of CNTs decreases with an increase in the growth temperature. The results obtained can be used in the development of promising nanopiezotronic elements based on aligned CNTs.

Acknowledgement. This study was financially supported by a grant from RFBR (project No. 20-37-70034) and by the Ministry of Science and Higher Education of the Russian Federation; the state task in the field of scientific activity No. 0852-2020-0015.

References

[1] Gogurla N., Kim S. // *Adv. Energy Mater.*, **21**, 2100801, 2021.
[2] Khan S. A., Zhang H. L., Xie Y., Gao M., Shah M.A., Qadir A., Lin Y. // *Adv. Eng. Mater.*, **19**(3), 1–7, 2017.
[3] Il'ina M. V., Il'in O. I., Guryanov A. V., Osotova O. I., Blinov Y. F., Fedotov A. A., Ageev O. A. // *J. Mater. Chem. C*, **9**(18), 6014 – 6021, 2021.
[4] Il'ina M. V., Il'in O. I., Blinov Y. F., Konshin A. A., Konoplev B. G., Ageev O. A. // *Materials*, **11**, 638, 2018.
[5] Bulyarskiy S. V., Bogdanova D. A., Gusarov G. G., Lakalin A. V., Pavlov A. A., Ryazanov R. M. // *Diam. Relat. Mater.*, **109**, 108042, 2020.

Study of the Problem of Energy Generation by Renewable Energy Sources Based on Piezoelectric Generators

I. A. Parinov[1], A. V. Cherpakov[1,2]*

[1]Southern Federal University, Rostov-on-Don, Russia
[2]Don State Technical University, Rostov-on-Don, Russia

*alex837@yandex.ru

Energy harvesting technologies have been intensively developing since the beginning of the 21st century, representing an alternative to traditional energy sources. Mechanical vibrations are common in all media used by man. Oscillations can be fruitfully used for the operation of the mechanisms of energy converters from mechanical to electrical. To do this, various devices are used that are implemented in the environment. The main elements of the environment are wind, fluid flow, ground vibrations. One of the cyclic elements can be used by generators,

containing rotating cyclic systems. Existing sources of energy collection based on vibrations and other mechanical influences seem to be more advantageous. The collection and conversion of energy from the surrounding oscillatory processes using piezoelectric elements is usually aimed at collecting energy to power low-power electronics, ranging on a scale from a few microwatts to milliwatts. Compared to thermal and solar-powered harvesters generating hundreds of watts, piezoelectric materials typically operate at several orders of magnitude lower energy levels. Certain advantages of piezoelectric conversion compared to thermal and solar collection are due to the fact that environmental fluctuations are often continuous due to system operating conditions that do not depend on unstable environmental conditions that change in time and space. Moreover, there are a huge number of reasons why thermal and solar energy may not be available. Finally, piezoelectric harvesters are especially useful in embedded systems. This review [1] presents the latest developments in the field of piezoelectric energy collection over the past decade, largely focused on experimental, analytical and computer model solutions obtained by Russian researchers, whose research is still not well known in the scientific world. The presented review is organized as follows: (i) medical applications are considered, including piezoelectric micropumps with microneedles; (ii) an overview of the models of energy rotating combines is given; (iii) the flexoelectric effect is discussed in relation to energy collection, based on experimental and analytical approaches; (iv) the results obtained for piezoelectric generators (PEGs) of cantilever and stack types are given; (v) some variants of piezoelectric actuators used for vibration isolation of aircraft structures are presented.

Acknowledgements. The equipment of SFedU is used. The work was supported by the grant No. 21-19-00423 of the Russian Science Foundation in the Southern Federal University.

Reference

[1] Parinov, I. A., Cherpakov, A. V. Overview: State-of-the-Art in the Energy Harvesting Based on Piezoelectric Devices for Last Decade // *Symmetry*, **14**(4), 765, 2022.

Local and Macroscopic Piezoactivity and Electromechanical Response of PMN-PT Ceramics in Low-field Region

A. A. Pavelko[1]*, K. P. Andryushin[1], M. V. Il'ina[2], M. O. Moysa[1]

[1]Research Institute of Physics, Southern Federal University, Rostov-on-Don, Russia
[2]Institute of Nanotechnologies, Electronics and Equipment Engineering, Southern Federal University, Taganrog, Russia

*aapavelko@sfedu.ru

Despite more than half a century of research using the most advanced methods of measurement and calculation, the question still remains unanswered how local symmetry breaking of the long range order in relaxor ferroelectrics leads to the formation of unusual, and in many respects outstanding, macroscopic properties, such as ultra-high piezoelectric coefficients, high dielectric permeability over a wide range of temperatures, diffused phase transitions, strong frequency dependence of the dielectric response. Recently, there has been a new wave of interest to fundamental research of ferroelectrics-relaxors, which is associated both with the development of methods of experimental and theoretical analysis [1], the establishment of new records of macroscopic properties [2], and with new prospects for their practical application. Of particular interest to researchers is the amplification of piezoelectric and electromechanical

properties of such materials, the study of which at various spatial scales is devoted to this work. The macroscopic piezoelectric activity in the field of low electric fields was investigated by inducing piezoelectric resonance in non-polarized ceramic samples with a DC electric voltage from the range ± 40 V. In parallel, unipolar deformation curves, induced by the field, were obtained using the device for checking end length measures MICRON-02, nanovoltmeter/microohmmeter Agilent 34420A, and developed software for automatic control of the measurement process. Studies of the domain structure, local piezo-response and deformation were performed by force microscopy of the piezo-response using the NT-MDT Ntegra probe nanolaboratory. Scanning was carried out at a probe oscillation frequency of 5 kHz and a bias voltage up to ±50 V.

Acknowledgement. This work was financially supported by the Ministry of Science and Higher Education of the Russian Federation (State assignment in the field of scientific activity, Southern Federal University, project No. 0852-2020-0032/BAZ0110/20-3-07IF). The impedance spectroscopy measurements were performed using the equipment of the Shared Research Facility Centre of SFedU, Research Institute of Physics.

References

[1] Eremenko M., et al. Local atomic order and hierarchical polar nanoregions in a classical relaxor ferroelectric // *Nat. Commun*., **10**, 2728, 2019.

[2] Li F., et al. Giant piezoelectricity of Sm-doped $Pb(Mg_{1/3}Nb_{2/3})O_3 – PbTiO_3$ single crystals // *Science*, **364**, 264 – 268, 2019.

Low temperature dielectric properties of $Ba_2NdFeNb_4O_{15}$ multiferroic

A. V. Pavlenko[1,2]*, D. V. Stryukov[1]

[1]Federal Research Center The Southern Scientific Centre of the Russian Academy of Sciences, 41, Chekhov Street, Rostov-on-Don, 344006, Russia
[2]Research Institute of Physics, Southern Federal University, 194, Stachki, Ave., Rostov-on-Don, 344090, Russia

*antvpr@mail.ru

Lead-free multiferroics in various solid states are being intensively investigated. This is due to both the large prospects for their use as sensors and detectors, and the great interest from a fundamental viewpoint. In this work, the phase composition, structure, and dielectric characteristics of the multiferroic ceramic $Ba_2NdFeNb_4O_{15}$ (BNFNO) have been studied. X-ray diffraction studies of ceramic samples at room temperature were measured by a DRON-4-07 (CuKα radiation) and DRON-3 (CoKα radiation) X-ray diffractometers in the 20 – 110º angle range with a step of 0.02º. The calculation of the structure characteristics was carried out according to the standard procedure. Measurements of the relative complex permittivity $\varepsilon^*/\varepsilon_0 = \varepsilon'/\varepsilon_0 - i\varepsilon''/\varepsilon_0$ (ε' and ε'' are the real and imaginary parts of ε^*, respectively, ε_0 is the dielectric constant) were carried out in the $f = 20 – 2 \times 10^6$ Hz frequency range and $T = 10 – 320$ K temperature range following GSSSD ME 184 – 2011. It was found that the material is single-phase and has a tetragonal structure with $a = 12.477$ Å, $c = 3.923$ Å, V = 611 Å^3 unit cell parameters at room temperature. It is shown that the anomalies at $T = 100 – 200$ K on $\varepsilon'/\varepsilon_0(T, f)$ and $\varepsilon''/\varepsilon_0(T, f)$ dependencies are caused by a diffuse ferroelectric phase transition. With the temperature incensement of BNFNO the electrical conductivity increases, resulting in the possibility of free charges accumulation at various interfaces, when a measuring AC

field is applied to the sample. This will subsequently lead to the appearance of interlayer polarization effects (Maxwell – Wagner polarization). This, in turn, leads, from our viewpoint to the appearance of a second relaxation process, which makes a significant contribution to the paraelectric phase.

Acknowledgments. The work was financially supported by the Russian Science Foundation, grant No. 21-72-10180

Simulation of Unsteady Non-isothermal Motion of Real Gas

D. V. Petrenko, D. D. Fugarov*, Yu. S. Chudnov, R. V. Shapavalov

Don State Technical University, Rostov-on-Don, Russia

*ddf_1@mail.ru

The mathematical model of non-stationary non-isothermal motion of real gas along a section of the pipeline is built on the basis of fundamental laws of conservation of mass, energy and momentum in gas dynamics, using the general propositions of thermodynamics without simplifying restrictions [1]. The problem statement is as follows. It is necessary to determine the gas pressure and its temperature at the end of the section of the main gas pipeline at a stationary non-isothermal flow, taking into account heat exchange with the environment [2]. The length of the main gas pipeline section is l = 200 km a pipe diameter of d = 1000 mm. The gas pressure P_1 and its temperature T_1 at the beginning of the section are equal to 10 MPa and 40 °C, respectively; a gas pipeline capacity of Q = 30 million of m^3/day; a soil temperature at the pipeline laying depth of T_0 = 0 °C. The relative density of the gas transportation is Δ = 0.6. The missing parameters or the gas flow regime are set on the basis of the available experience or recommendations, after which the adopted parameters are determined and their convergence with the accepted values is checked [3]. If the deviation exceeds the desired calculation accuracy or the mode differs from the expected one, the calculations are repeated in a different mode or with different values of parameters. Taking into account the accuracy of the instruments installed on the gas pipeline, the accuracy of determining the parameters of the section operation is set [4]. In this case, the accuracy of determining the pressure: ΔP = 0.1 MPa and temperature ΔT = 1 K. According to the simulation results, the gas pressure at the end of the P_2 pipeline section will be 3.2 MPa, and its temperature at the end of the T_2 section will be 289.456 K. Thus, the gas pressure at the end of the section depends significantly on the productivity and the pressure with which the gas enters the linear section. Moreover, at a flow rate of more than 35 million of m^3/day, there is a sharp drop in pressure down to zero. The temperature decreases slowly and tends to the ambient temperature [5].

References

[1] Onyshko D., Fugarov D., Purchina O., Poluyan A., Rasteryaev N., Skakunova T. Synchronization system in wireless sensor networks of oil and gas complex // *E3S Web of Conferences. Topical Problems of Green Architecture, Civil and Environmental Engineering, TPACEE 2019*, 03030, 2020.

[2] Fugarov D. D., Purchina O. A., Poluyan A. Y., Gerasimenko A. N., Rasteryaev N. V. Magnetodielectric ac measuring transducer for automation systems in oil refineries // *Journal of Physics: Conference Series*. International Conference "Information Technologies in Business and Industry", 062020, 2019.

[3] Gerasimenko Y., Gerasimenko A., Fugarov D., Purchina O., Poluyan A. Mathematical modeling and synthesis of an electrical equivalent circuit of an electrochemical device // *Advances in Intelligent Systems and Computing*, **1259**, 471 – 480, 2021.
[4] Poluyan A. Yu., Purchina O. A., Fugarov D. D., Gerasimenko E. Yu., Skakunova T. P. Application of bionic and immune algorithms for the solution of ambiguous problems of transportation routing // *Journal of Physics: Conference Series*. International Conference "Information Technologies in Business and Industry", Mathematical Simulation and Computer Data Analysis, **2**, 032057, 2019.
[5] Poluyan A. Yu., Purchina O. A., Fugarov D. D., Golovanov A. A., Smirnova O. V. Solution of task on the minimum cost data flow based on bionic algorithm // *Journal of Physics: Conference Series*. International Conference "Information Technologies in Business and Industry", Mathematical Simulation and Computer Data Analysis, **2**, 032056, 2019.

Solution of Test Problems of Potential Theory by Boundary Element Method Using Open Source Elmer

A. N. Petrov*, A. I. Yudintseva

National Research Lobachevsky State University of Nizhny Novgorod, Nizhny Novgorod, Russia

*andrey.petrov@mech.unn.ru

The paper presents the solution of the Laplace equation by the boundary element method using the Elmer software package. Elmer implements a direct version of the BEM as a modular solution written in the Fortran language. The discrete representation of the equation is constructed using the collocation method; nodes of approximation of boundary functions are chosen as collocation nodes. The domain boundary and unknown functions are approximated by linear elements. Regular integrals are calculated using the Gauss formulas. We consider a boundary value problem as a test for the Laplace equation in the domain with a boundary in the form of an ellipse having semiaxes $a = 5$ and $b = 3$ in the Cartesian coordinate system and centered at its origin. The potential and flux values at the boundary were obtained on seven grids with uniform partitioning and containing 20, 40, 80, 160, 320, 640, and 1280 boundary elements each. The obtained results show that the error in calculating the boundary functions at the points of the coarsest grid does not exceed 8%. With increasing the number of boundary elements, the numerical solution is seen to approach the analytical one and the relative error does not exceed 1% when calculating on a grid of 160 elements, and 0.3% on a grid of 1280 elements respectively. Analytical and numerical results are in good agreement, thus the possibility of using the Elmer software for solving mixed boundary value problems for the Laplace equation by the boundary element method with sufficient accuracy in many engineering and research calculations is demonstrated.
Acknowledgement. The work was financially supported by the Strategic Academic Leadership Program "Priority 2030" (internal number H-496-99_2021-2023).

Computational Software in Julia for Studying the Motion of Viscous Incompressible Fluid in Particular Cases

A. S. Piskunov, Yu. E. Drobotov*

Southern Federal University, Rostov-on-Don, Russia

*yu.e.drobotov@yandex.ru

In this paper, the motion of viscous incompressible fluid in a limited medium is computed by applying the means of the Julia programming language. As a test mathematical problem, a non-stationary diffusion problem is considered, that is stated for a second-order differential equation with two unknowns. Julia language is used due to its high performance [1] and popularity [2]. The motion of fluid is described by the Navier–Stokes equations, which are known to be reducible from their vector form:

$$\frac{\partial U}{\partial t} + U \cdot \nabla U = -\frac{\nabla p}{\rho} + \nu \nabla^2 U$$

to the vorticity transport equation for incompressible viscous flow:

$$\frac{\partial \omega}{\partial t} + U \cdot \nabla \omega - \omega \cdot \nabla U = \nu \nabla^2 \omega,$$

where U is the flow velocity along x-axis, p is the pressure, ν is the kinematic viscosity, and ω is the vorticity in flow [3]. If viscous diffusion is considered to act independently of convection, the latter equation becomes as

$$\frac{\partial \omega}{\partial t} = \nu \nabla^2 \omega,$$

which is the subject of discussion. The report aims to demonstrate the efficiency of various approaches to the stated problem, as well as the features of the Julia programming language.

Acknowledgement. The research was financially supported by Southern Federal University, grant No. VnGr-07/2020-04-IM (Ministry of Science and Higher Education of the Russian Federation).

References

[1] *Julia Micro-Benchmarks*. Retrieved from https://julialang.org/benchmarks/

[2] *2021 Developer Survey*. Retrieved from https://insights.stackoverflow.com/survey/2021?_ga=2.9716663.340558351.1628714498-2066421306.1628167975#most-loved-dreaded-and-wanted-language-love-dread

[3] Porthouse D. T. C., Lewis R. I. Simulation of viscous diffusion for extension of the surface vorticity method to boundary layer and separated flows // *Journal of Mechanical Engineering Science*, **23**(3), 157–167, 1981, doi:10.1243/JMES_JOUR_1981_023_029_02

Crossbar Architecture Based on Memristor Structures for Neuromorphic Artificial Intelligence Systems

V. V. Polyakova*, I. N. Kots, V. A. Smirnov

Southern Federal University, Taganrog, Russia

*vik5702935@yandex.ru

The von Neumann architecture, which is still used in modern computers, has a number of narrow and technological barriers associated with the use of cache memory and the use of overheating. To overcome these barriers, it is necessary to create a new generation of artificial intelligence. This technology allows us to overcome technological barriers and create great opportunities for creating cognitive technologies, as well as to improve the Internet of things. In order to create the crossbar architecture, we developed a technology, based on the method of local anodic oxidation (LAO) under laboratory conditions. LAO was performed on a Ntegra probe microscope. At the first stage of experimental studies, oxide nanoscale structures were formed on the surface of pre-cleaned Si-substrates by the LAO method using a template. At the next stage of the studies, Ti was deposited on the formed substrate structures by magnetron sputtering using a VSE-PVD-DESK-PRO desktop magnetron sputtering vacuum unit. Then TiO_2 memristor structures were formed on the surface of Ti-film by LAO method and used in the crossbar architecture as a working layer. The formed layer of TiO_2 at −5 V showed a resistance of 1.4 ± 0.4 GΩ (high-resistance state of the membrane structure), and at +5 V the resistance was 0.2 ± 0.1 GΩ (low-resistance state of the membrane structure), which is typical for the working mechanism of the membrane structure. Thus, the results obtained can form the basis for the creation of nanoscale elements of neuromorphic artificial intelligence systems, modern computers and elements of synaptically similar electronics.

Acknowledgement. Scientific research was carried out within the framework of the project "Development and research of methods and tools for monitoring, diagnostics and forecasting of the state of engineering objects based on artificial intelligence" (task No. FENW-2020-0022, work number at SFedU No. LAB0110 / 2020-01ITs). We would like to express our gratitude to the Center for collective use of nanotechnologies of the Southern Federal University.

Building Algorithms Based on Artificial Intelligence for Solving Problems to Ensure Information Security

O. A. Purchina, A. Yu. Poluyan, D. D. Fugarov*

Don State Technical University, Rostov-on-Don, Russia

*ddf_1@mail.ru

The work is devoted to the study of intelligent methods of information protection. The report describes the ways of possible application of artificial intelligence methods in the field of information protection, and also proposes an algorithm for the information protection system from anomalous requests. Artificial intelligence (AI) is present in all areas of our activity [1].

Whether it is a household area or a commercial one. The growth in the number and variety of attacks on information systems is growing every year, and financial losses from the introduction of computer viruses and unauthorized access to the system also grow proportionally [2]. In this regard, the use of AI in the areas of information security is more often observed, which is a promising area of research. To ensure the security of network resources, a range of different specialized systems is used, such as load testing systems, network monitoring systems, management system tools, and intrusion detection systems [3]. Intrusion detection systems can be classified according to various criteria. Each of them has its own advantages and disadvantages. The report analyzes modern intrusion systems and their classification. A review of the positive and negative qualities of intelligent and traditional security systems allows one to give a clear answer to the question of more reliable and safe systems. Of course, AI-based systems are superior to traditional security systems, combining the performance of computers and emulation of the human thought process, intelligent solutions. The features of artificial immune systems, their elements and requirements for them have been studied [4]. An algorithm for detecting intrusions into information networks has been designed. It uses artificial immune systems to detect the presence of anomalies in network traffic, which makes it possible to increase the efficiency of threat detection [5].

References

[1] Poluyan A. Yu., Purchina O. A., Fugarov D. D., Gerasimenko E. Yu., Skakunova T. P. Application of bionic and immune algorithms for the solution of ambiguous problems of transportation routing // *Journal of Physics: Conference Series*. International Conference "Information Technologies in Business and Industry", Mathematical Simulation and Computer Data Analysis, **2**, 032057, 2019.

[2] Purchina O. A., Poluyan A. Yu., Fugarov D. D., Onyshko D. A. Task on data flow of minimum cost on the base of bionic algorithm. In: Physics and Mechanics of New Materials and Their Applications (PHENMA 2019), I. Parinov, B. T. Long, N. T. H. Minh, N. D. Toan, S. H. Chang (Eds.), 261, 2019.

[3] Gerasimenko Y., Gerasimenko A., Fugarov D., Purchina O., Poluyan A. Mathematical modeling and synthesis of an electrical equivalent circuit of an electrochemical device // *Advances in Intelligent Systems and Computing*, **1259**, 471 – 480, 2021.

[4] Onyshko D., Fugarov D., Purchina O., Poluyan A., Rasteryaev N., Skakunova T. Synchronization system in wireless sensor networks of oil and gas complex // *E3S Web of Conferences. Topical Problems of Green Architecture, Civil and Environmental Engineering, TPACEE 2019*, 03030, 2020.

[5] Poluyan A. Yu., Purchina O. A., Fugarov D. D., Golovanov A. A., Smirnova O. V. Solution of task on the minimum cost data flow based on bionic algorithm // *Journal of Physics: Conference Series*. International Conference "Information Technologies in Business and Industry", Mathematical Simulation and Computer Data Analysis, **2**, 032056, 2019.

Mathematical and Computer Modeling of the Drying Process of an Elastic Solid

O. G. Pustovalova[1], A. N. Soloviev[2]*, A. A. Egorova[2]

[1]*Southern Federal University, Rostov-on-Don, Russia*
[2]*Don State Technical University, Rostov-on-Don, Russia*

*solovievarc@gmail.com

The problem of drying solids is described by the diffusion equations (1), (2), therefore as the unknown we can select the relative humidity φ. At the same time, many authors [1, 2] are consider the coefficients k, c, ρ, which characterize the speed of moisture movement as constant or dependent on coordinates, but they may also depend on the humidity itself φ, what makes the problem nonlinear. In mathematical formulation of the problem, for the components u of an unknown displacement vector and relative humidity φ, the system of differential equations has the form:

$$\nabla \boldsymbol{\sigma} = 0, \tag{1}$$

$$\Delta\varphi = \frac{c\rho}{k}\frac{\partial\varphi}{\partial t}. \tag{2}$$

In the equilibrium equations (1), mass forces are not taken into account. In diffusion equation (2), c is a specific heat coefficient of the solid, ρ is the density, k is a diffusion coefficient and in this formulation of the problem these parameters are considered constant. Cauchy's equations have the form:

$$\boldsymbol{\varepsilon} = (\nabla \boldsymbol{u} + \nabla u^{\mathrm{T}})/2. \tag{3}$$

By defining the equations, we take into account the linear dependence on φ:

$$\boldsymbol{\sigma} = \lambda \mathrm{tr}\boldsymbol{\varepsilon}\boldsymbol{E} + 2\mu\boldsymbol{\varepsilon} + \varkappa(1-\varphi)\boldsymbol{E} \tag{4}$$

For the Young's modulus E, the following three-parameter dependence on relative humidity and φ is:

$$\mathrm{E} = \gamma\left(\beta\frac{e^{-\alpha(\varphi-0.5)}}{1+e^{-\alpha(\varphi-0.5)}} + 1 - \beta\right), \tag{5}$$

where α, β, γ are parameters. Mechanical boundary conditions at the boundaries define absence of displacements and stresses. Boundary conditions for relative humidity at the boundary correspond to constant humidity and drying conditions across the boundary.

As an example, we consider a two-dimensional problem for a rectangular area. Numerical simulation was carried out for the following values of physical constants and parameters from (4) and (5): $\varkappa = 1$, $k = 1$, $c = 1$, $\rho = 1$, $\alpha = 6$, $\beta = 0.8$, $\gamma = 10$. The dependence of Young 's modulus on relative humidity is shown in Fig. 1. The problem is solved by the finite element method in the FlexPDE package. Figure 2 shows the calculation schemes of the problem. Figure 3 shows a grid of triangular finite elements with cubic approximation on the deformed state of the domain for a non-stationary problem at the time when the solution goes into stationary mode. Figure 4 shows the von Mises stress distribution in the sealing area (Scheme a) at the end of the drying process. In the numerical experiment, the entire boundary of the region is stress-free and the same drying

conditions are set on it. At the same time, the shape of the region remains rectangular when entering the stationary mode, and the humidity becomes constant in all areas and is equal to the humidity of the environment.

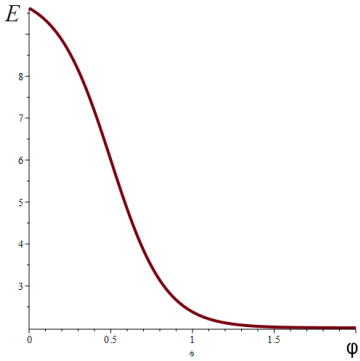

Fig. 1. Dependence of Young's modulus on relative humidity

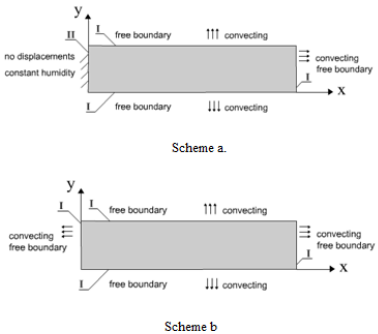

Fig. 2. Scheme *a* and *b*

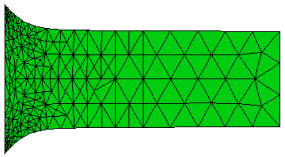

Fig. 3. Grid on deformed body

Fig. 4. Mises stress distribution

Nonstationary model of drying of a solid deformable body relative to the components of the displacement vector and relative humidity is constructed assuming a smooth dependence of Young's modulus on relative humidity, with the remaining constant physical coefficients. Numerical experiments were carried out for a rectangular area and a model material to determine the stress-strain state and relative humidity under various boundary conditions. The results of calculations qualitatively coincide with possible field experiments, which indicates the adequacy of the model.

Acknowledgments. The work was supported by the Government of the Russian Federation, contract No. 14.Z50.31.0046.

References

[1] Lan Sun, Md. Raisul Islam, Ho J. C., Mujumdar A. S. A diffusion model for drying of a heat sensitive solid under multiple heat input modes // *Bioresource Technology. J*., **96**, 1551 – 1560, 2005.

[2] Ruiz-Lópeza I. I., Ruiz-Espinosaa H., Luna-Guevaraa M. L., García-Alvaradob M. A. Modeling and simulation of heat and mass transfer during drying of solids with hemispherical shell geometry // *Computers and Chemical Engineering. J.*, **35**, 191 – 199, 2011.

Placement of Compressor Stations on the Gas Pipeline Route

A. E. Pyanov, D. D. Fugarov*, I. D. Abrosimov, Shuvailat Mohammed Yassin Joudah

Don State Technical University, Rostov-on-Don, Russia

ddf_1@mail.ru

Compressor stations (CSs) on the gas pipeline route are placed taking into account both purely technological and economic considerations [1]. In particular, it is necessary to strive to ensure that the placement of the compressor station meets the requirements for the convenience of their construction and operation. In addition, it should be remembered that the location of the compressor station along the route significantly affects the throughput capacity of individual sections and the gas pipeline as a whole, as well as the total capacity of the compressor station [2]. Using the gas pipeline throughput equation, the distance between the CSs at pressure P_1 at the beginning of the section and P_2 at the end is determined. The theoretical number of the compressor station n_0 is determined by the following relationship: $n_0 = (L - l_k)/l - 1$, where L is the length of the main gas pipeline, l is the length of the intermediate section, l_k is the length of the end section. Since it is recommended to build a gas pipeline without looping, the fractional number of compressor stations is usually rounded up [3]. If the gas pumping unit is equipped with gas turbines, the capacity of the gas pipeline will decrease by the amount of fuel gas, which will lead to an increase in the lengths of the sections, the theoretical number of the compressor station in this case can be determined from the equation [4]:

$$L = l\left(\sum_{1}^{n-1}\frac{Q}{Q - n_i \cdot Q_T} + a\frac{Q}{Q - n_0 \cdot Q_T}\right), \quad (1)$$

where n_i is the number of the compressor station operating in the i-th section; α is the lengthening of the end section. In accordance with Equation (1), the arrangement of compressor stations is carried out taking into account the conditions for the construction and operation of the main gas pipeline [5].

References

[1] Poluyan A. Yu., Purchina O. A., Fugarov D. D., Gerasimenko E. Yu., Skakunova T. P. Application of bionic and immune algorithms for the solution of ambiguous problems of transportation routing // *Journal of Physics: Conference Series*. International Conference "Information Technologies in Business and Industry", Mathematical Simulation and Computer Data Analysis, **2**, 032057, 2019.

[2] Onyshko D., Fugarov D., Purchina O., Poluyan A., Rasteryaev N., Skakunova T. Synchronization system in wireless sensor networks of oil and gas complex // *E3S Web of Conferences. Topical Problems of Green Architecture, Civil and Environmental Engineering, TPACEE 2019*, 03030, 2020.

[3] Fugarov D. D., Purchina O. A., Poluyan A. Y., Gerasimenko A. N., Rasteryaev N. V. Magnetodielectric ac measuring transducer for automation systems in oil refineries // *Journal of Physics: Conference Series*. International Conference "Information Technologies in Business and Industry", 062020, 2019.

[4] Gerasimenko Y., Gerasimenko A., Fugarov D., Purchina O., Poluyan A. Mathematical modeling and synthesis of an electrical equivalent circuit of an electrochemical device // *Advances in Intelligent Systems and Computing*, **1259**, 471 – 480, 2021.

[5] Poluyan A. Yu., Purchina O. A., Fugarov D. D., Golovanov A. A., Smirnova O. V. Solution of task on the minimum cost data flow based on bionic algorithm // *Journal of Physics:*

Conference Series. International Conference "Information Technologies in Business and Industry", Mathematical Simulation and Computer Data Analysis, **2**, 032056, 2019.

Enhancing Mode I Fracture Toughness of Adhesively Bonded Unidirectional Composite Joints Using Surfactant-Stabilized Multi-walled Carbon Nanotube and Graphene Nanoplate

Qiong Rao*, Zeyu Ouyang, Xiongqi Peng

School of Materials Science and Engineering, Shanghai Jiao Tong University, Shanghai, 200030, China

*rao_qiong@163.com

In this work, polyvinyl pyrrolidone (PVP) non-covalently functionalized multi-walled carbon nanotubes (MWCNTs), graphene nanoplates (GNPs) and MWCNTs/GNPs hybrids were respectively dispersed into epoxy adhesive to investigate their effects on mode I fracture toughness of unidirectional composite bonded joints through double cantilever beam tests. The synergy effects of MWCNTs and GNPs with different ratios were also studied. Testing results showed that 0.75wt% MWCNTs/GNPs (1:4) hybrid had the highest toughening effect of 286% improvement compared with pure adhesive. In addition, PVP was proved to have a positive effect on improving fracture toughness for single nanofillers while it declined the toughening effect of MWCNTs/GNPs hybrids. Furthermore, the fracture micromorphology of adhesive layer as well as the toughening mechanisms of MWCNTs, GNPs and MWCNTs/GNPs hybrids were analyzed.

Structural and Dielectric Studies of Pb_2BWO_6 (B = Mg, Co) Ceramics Obtained Using High-energy Mechanical Activation

S. I. Raevskaya[1], A. A. Gusev[2], N. S. Shevchenko[2], S. P. Kubrin[1], I. N. Zakharchenko[1], V. V. Titov[1], E. I. Sitalo[1], M. A. Malitskaya[1], I. P. Raevski[1]

[1]Southern Federal University, 344090, Rostov-on-Don, Russia
[2]Institute of Solid State Chemistry and Mechanochemistry SB RAS, 630128, Novosibirsk, Russia

*igorraevsky@gmail.com

Complex perovskites $Pb_2B^{2+}W^{6+}O_6$ (B = Mg, Co, Mn) are antiferroelectrics and are characterized by a high degree of ordering of B^{2+} and W^{6+} ions. For many applications, in particular for solid-state energy storage, it is desirable to reduce the strength of the electric field required to induce the ferroelectric phase and increase the smearing of the maximum of the dielectric constant. Both of these goals can be achieved by partial disordering of the B^{2+} and W^{6+} ions. Very low melting points of tungstates, however, do not allow using traditional methods of changing the degree of ordering, such as prolonged annealing at high temperatures [1, 2]. We made an attempt to use high-energy mechanical activation for partial disordering

of $Pb_2B^{2+}W^{6+}O_6$. This method previously succeeded in disordering a number of complex perovskites of the $Pb_2B^{3+}B^{5+}O_6$ type (B^{3+} = Yb, In, Sc; B^{5+} = Nb, Ta) [3 – 6]. The use for mechanical activation of a high-energy planetary-centrifugal mill - activator AGO-2 with the acceleration of steel balls 40 g made it possible to reduce the time, required for the synthesis of $Pb_2B^{2+}W^{6+}O_6$ (B = Mg, Co) from 20 – 30 hours down to 10 – 20 minutes. X-ray structural studies have shown that the $Pb_2B^{2+}W^{6+}O_6$ powders obtained by mechanochemical synthesis have a high degree of ordering S = 0.9 – 0.95. At the same time, the temperature T_m and the diffuseness degree of the dielectric constant maximum of the $Pb_2B^{2+}W^{6+}O_6$ ceramics sintered from these powders depended strongly on the sintering temperature in contrast to the degree of the B^{2+} and W^{6+} ions ordering, which varied relatively little. Samples with diffuse maxima of the dielectric constant exhibited relaxor-like properties; in particular, the dependence of T_m on frequency was well described by the Vogel-Fulcher law. T_m values changed by 50 – 150 K, when the firing temperature was varied within 600 – 1000 °C range. Since the degree of chemical (compositional) ordering S, according to X-ray diffraction data, almost does not depend on the firing temperature, possible reasons for such a strong dependence of properties on the firing temperature can be a change in the size of ceramic crystallites and/or contamination of powders with iron during high-energy mechanical activation in steel drums using steel balls, leading to the formation of a solid solution $Pb_2B^{2+}W^{6+}O_6 – Pb_3Fe_2WO_9$.

Aknowledgement. This study was supported by the Russian Foundation for Basic Research (Grant 20-03-00920_a).

References

[1] Stenger C. G. F., Scholten F. L., Burggraaf A. J. // *Solid State Commun.* **32**, 989, 1979.
[2] Bokov A. A., Rayevsky I. P. // *Ferroelectrics*, **190**(1 – 4), 125, 1989.
[3] Gao X., Xue J., Wang J. // *Mater. Sci. Eng. B*, **99**, 63, 2003.
[4] Uršič, et al. // *J. Mater. Chem. C*, **3**, 10309, 2015.
[5] Raevski I. P., et al. // *Ferroelectrics*, **525**, 54, 2018.
[6] Raevskaya S. I., et al. // *Ferroelectrics*, **542**, 28, 2019.

Dielectric Studies of $(1 – x)BiFeO_3 – xSrFe_{0.5}Sb_{0.5}O_3$ Solid Solution Ceramics Fabricated by High-pressure Synthesis

S. I. Raevskaya[1], A. V. Pushkarev[2], N. M. Olekhnovich[2], Yu. V. Radyush[2], S. P. Kubrin[1], P.A. Shishkina[1], S.I. Kolosov[1], I. P. Raevski[1], V.V. Titov[1], M. A. Malitskaya[1]

[1]Physics Research Institute and Faculty of Physics, Southern Federal University, Rostov-on-Don, Russia;
[2]Scientific-Practical Materials Research Centre of NAS of Belarus, 220072, Minsk, Belarus

*igorraevsky@gmail.com

Ceramic samples of $BiFeO_3$ (BFO) solid solution with highly-ordered complex perovskite $SrFe_{0.5}Sb_{0.5}O_3$ (SFS) were fabricated by high-pressure synthesis at 4 – 6 GPa. The temperature dependences of loss tangent tanδ and the real part ε' of the complex dielectric constant ε* were investigated in a wide range of temperatures (15 – 600 K) and frequencies (100 Hz – 1 MHz). Measurements at higher temperatures were not carried out because of the danger of transformation of the metastable perovskite phase obtained by synthesis under high pressure into the pyrochlore phase, which is stable at atmospheric pressure. All the samples studied had

substantial conductivity and showed at low frequencies very high ε' values above room temperature. In contrast to the previously investigated similar $(1-x)BiFeO_3 - xPbFe_{0.5}Sb_{0.5}O_3$ solid solution system, in which diffuse $\varepsilon'(T)$ maxima associated with the ferroelectric phase transition, appeared at high frequencies for compositions with $x > 0.6$, in the $(1-x)BiFeO_3 - xSrFe_{0.5}Sb_{0.5}O_3$ samples no such maxima were observed. The $\varepsilon'(T)$ and $\tan\delta(T)$ dependences of most of the studied $(1-x)BiFeO_3 - xSrFe_{0.5}Sb_{0.5}O_3$ samples did not show the relaxation maxima. At the same time, these dependences exhibited poorly resolved anomalies. Apparently, they correspond to maxima, which are masked due to high conductivity. For a more detailed analysis, the so-called modulus spectroscopy was used. It was found out that temperature dependences of the imaginary part M'' of the complex electrical modulus $M^* = 1/\varepsilon^*$ usually have one or two relaxation maxima. The temperature dependences of the frequencies corresponding to the maxima of both $\tan\delta(T)$ and $M''(T)$ dependences are well fitted by the Arrhenius law. The values of thus obtained relaxation activation energy fall within 0.35 – 0.4 eV range. These energies correspond to the relaxation of electrons trapped on the energy level created in the band gap by the singly-ionized oxygen vacancy (tenths of an eV) [1]. These data allow one to assume that dielectric relaxation in the compositions studied is due to the hopping of electrons captured by oxygen vacancies.

Acknowledgement. This study was supported by the Russian Foundation for Basic Research (Grant 20-52-00045) and Belarusian Republican Foundation for Fundamental Researches (Grant T20R-169).

References

[1] Prosandeev S. A., Fisenko A. V., Riabchinski A. V., et al. // *J. Phys.: Condens. Matter*, **8**, 6705, 1996.

Carbon Nanoparticles from Thermally Expanded Graphite: Effect of the Expansion Conditions on the Derived Nanoparticles Morphology

E. V. Raksha[1]*, O. N. Oskolkova[1], A. A. Davydova[1], P. V. Sukhov[1], Yu. V. Berestneva[2], V. A. Glazunova[3], M. V. Savoskin[1], I. A. Verbenko[4], Yu. I. Yurasov[4,5]**

[1]L. M. Litvinenko Institute of Physical Organic and Coal Chemistry, 283114, Donetsk, Ukraine
[2]Federal Scientific Centre of Agroecology, Complex Melioration and Protective Afforestation of the Russian Academy of Sciences, 97, Universitetsky Ave, 400062, Volgograd, Russia
[3]A. A. Galkin Donetsk Institute for Physics and Engineering, Donetsk, Ukraine
[4]Research Institute of Physics, Southern Federal University, Rostov-on-Don, Russia
[5]Southern Scientific Centre RAS, Rostov-on-Don, Russia

*elenaraksha411@gmail.com; **berestnevayuv@mail.ru

Ternary graphite nitrate co-intercalation compounds with ethyl formate, ethyl acetate, acetic acid, formic acid, acetonitrile and 1,4-dioxane were prepared and used as a source of thermally expanded graphite (TEG). Obtained cointercalates demonstrated a good thermal expansion ability: the thermal expansion coefficient, determined for considered compounds, was within 340 – 380 $cm^3 \cdot g^{-1}$. Few-layer graphenes were obtained by sonication of TEG in *tert*-butanol.

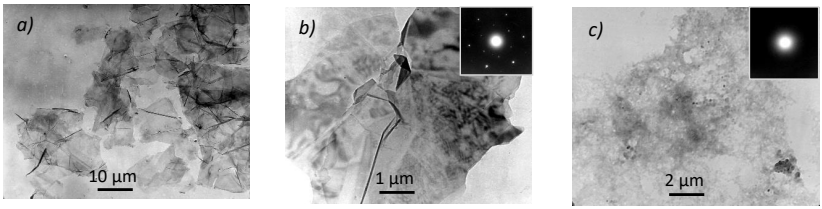

Fig. 1. Representative TEM image along with corresponded SAED patterns of carbon nanoparticles, obtained by TEG^{900} (a) and TEG^{500} (b, c) sonication in *tert*-butanol

Planar sizes of the as-prepared few-layer graphenes reached several tens of μm and the thickness was within 1 – 10 atomic layers according to TEM data (Fig. 1*a*). The co-intercalate of graphite nitrate with acetic and formic acid was expanded in different conditions at 500 °C and 900 °C, in linear and shock mode of heating. Dispersions based on TEG obtained at a lower temperature, in addition to few-layer graphenes (Fig. 1*b*), also contain a significant amount of amorphous carbon particles with planar sizes up to 100 nm (Fig. 1*c*). The influence of the conditions for obtaining the thermally expanded graphite on the morphology of resulting carbon nanoparticles is discussed.

Effect of Cr^{3+} Ions on the Chelating Ability of Natural Water

O. S. Reshetnyak

Southern Federal University, Rostov-on-Don, Russia
Hydrochemical Institute of Roshydromet, Rostov-on-Don, Russia

osreshetnyak@sfedu.ru

The chelating ability of water (CAW) is defined as a feature of natural waters that provides a buffer capacity of water to reduce the toxic effects of metal ions [1]. Determination of CAW is carried out for one metal (mostly for copper ions, Cu^{2+}). However, in real conditions several metals enter a water body simultaneously, which can significantly change the chelating ability (CA) calculated for each metal. This is due to the influence of some metals on the CA of others. Therefore, in natural waters, the effect of one metal on another can lead to both an increase and a decrease in CAW. In [2], it is shown how the mutual influence of metals in natural waters leads to an almost complete transition of their ionic forms to other forms. The behavior of certain metals in river waters (Cu^{2+}, Pb^{2+}, Zn^{2+}, Cd^{2+}, Cr^{3+}, Co^{2+}, Ni^{2+}) and their behavior in the joint presence in the water of the Seversky Donets River was studied. First, the behavior of metals in river water samples was studied, when one metal was added to the water sample. The concentration of Cd^{2+} ions nearly did not change during the experiment (more than 100 minutes) and was recorded quantitatively. The concentrations of Co^{2+} and Ni^{2+} ions in river water significantly decreased (by 55 %) as early as after 1 – 3 minutes and then stabilized. For the remaining metals (Cu^{2+}, Pb^{2+}, Zn^{2+}, Cr^{3+}), typical behavior in natural waters was revealed, namely the recorded concentrations after introduction into river water gradually decreased in time and then were established at a certain level. It should be noted that there are also differences in the behavior of the studied metals when diluting river waters. The effect of

Cr^{3+} on the behavior of metals in river and distilled water has been studied. The concentrations of metal ions (Cu^{2+}, Pb^{2+}, Zn^{2+}, Cd^{2+}, Co^{2+}, Ni^{2+}) in river waters with the presence and the absence of Cr^{3+} differs significantly although Cr^{3+} ions do not affect them in distilled water even if organic substances are added as ligands. The effects revealed are exactly typical for the Cr^{3+} ions in the waters of the Severskiy Donets River; and this is not caused by competing chelating processes (as the mutual influence of metals in natural waters is usually described) but by the ability of Cr^{3+} to facilitate the transition of other metals from ionic forms to chemically bounded ones. The results of the experiment demonstrated that in the presence of Cr^{3+}, the CA of many metals in river waters increases and Cr^{3+} promote the transition of ionic forms of metals to other ones. In other words, Cr^{3+} and several ions such as Cu^{2+}, Pb^{2+}, Zn^{2+}, Cd^{2+}, Co^{2+}, Ni^{2+} cannot simultaneously occur in ionic forms in river waters. Thus, Cr^{3+} help to reduce the toxic effects of these metal ions [2]. We used these data in a comparative assessment of the chemical composition of the water of the Seversky Donets River with data on the toxicity of river waters. In some cases, we observed discrepancies between the level of water toxicity and the concentration of metal ions [3]. There was a low level of water toxicity in some samples of river waters, where the presence of chromium ions was recorded. This is due to the fact that other metals were in a chemically bounded form.

References

[1] Linnik P. N. The chelating ability of water and methods for their determination (review) // *Hydrochemical Materials*, **106**, 78 – 101, 1989 (In Russian).

[2] Kheyfets L. Ya., Osyka V. F., Maksimovskiy S. G., Cherevik A. V., Kabanenko L. F. Behavior of metals in natural waters and chelating ability // *Hydrochemical Materials*, SPb.: Gidrometeoizdat, **115**, 47 – 59, 2000 (In Russian).

[3] Zakrutkin V. Ye., Reshetnyak O. S., Bakayeva Ye. N. Hydroecological features of the surface waters of the coal-mining territories of the Eastern Donbass // *Izvestiya RAN. Geographic Series*, **84**(3), 451 – 460, 2020, DOI:10.31857/S2587556620030139 (In Russian).

The Potential of Teak Wood as a Climate Change Resilience Furnishing Material

RA Retno Hastijanti[1]*, Briant Wiranata[2]**

[1]Architecture Department, Engineering Faculty, Universitas 17 Agustus 1945 Surabaya, Indonesia
[2]Architect, Surabaya Zoo, Indonesia

*retnohasti@untag-sby.ac.id; **briantwiranata07@gmail.com

Climate change could alter the frequency and intensity of forest disturbances such as insect outbreaks, invasive species, wildfires, and storms. These disturbances can reduce forest productivity and change the distribution of tree species. In other cases, existing species may shift their range or die out. One of the most useable woods in construction is teak wood. Teakwood is the perfect wood for many household projects because it is strong, water-resistant, and rot-resistant. A teak garden table would last for decades and age gracefully while requiring very little care. From cabinets to counters and utensils, the use of wood in kitchen design is once again gaining prominence, as it can be used in almost all styles, from rustic to modern. Teak wood is stealing the scene, besides being easy to adapt into different formats, it has a natural waterproofing which provides a strong barrier against moisture. Its composition

also guarantees protection against heat and parasite attacks. All those features bring versatility for teak wood to be present in multiple objects. Teak color allows the creation of sophisticated and eclectic pieces. In addition, it has strength and durability. It is possible to create panels of all styles and for different purposes. It will gain more durability and time before maintenance. Teak wood is also used in kitchen utensil designs, creating fine pieces. Then it is needed research for teak wood as a climate change resilience furnishing Mmaterial for identifying the potential and searching some alternatives for maintaining the product to adapt the micro climate condition.

The Method of DNA Isolation Using Magnetic Carbon Nanotubes

Y. V. Rezvantseva[1,2]*, D. I. Zybin[3], L. P. Ichkitidze[1,4], D. V. Kapustin[2]

[1]Scientific and Technological Park of Biomedicine of I. M. Sechenov First Moscow State Medical University, I. M. Sechenov University, Moscow, Russia
[2]M. M. Shemyakin & Yu. A. Ovchinnikov Institute of Bioorganic Chemistry of the Russian Academy of Sciences, Moscow, Russia
[3]Institute of Fine Chemical Technologies, Moscow Technological University, Moscow, Russia
[4]Institute of Biomedical Systems of National Research University of Electronic Technology, MIET, Zelenograd, Moscow, Russia

*genetik1997@mail.ru

The investigation of properties of innovative materials contributes to the solution of applied problems in molecular diagnostics. An isolation of DNA is often the first step in such studies. Actually, an extraction of DNA on magnetic particles has been recognized as one of the most effective methods for DNA isolation. However, this method has at least two drawbacks. Firstly, it is the high cost of the used materials (1 ml of a suspension of magnetic particles costs $ 25 – 30). Secondly, as a rule, the molecules of contaminants are retained in addition to DNA during the aggregation of the magnetic particles. These substances can inhibit subsequent reactions. In this report, it is proposed to replace the previously used magnetic particles with multi-walled carbon nanotubes (MWCNTs) of the "Taunit MD" type. Note that during CVD synthesis of MWCNTs, catalytic magnetic particles are formed mainly at the ends of nanotubes. Consequently, MWCNTs "Taunit MD" acquires properties similar to magnetic nanoparticles. It has been shown that DNA from its solution can be deposited on such MWCNTs without additional modifications, and the coating of the tubes with polydimethyldiallylammonium chloride (PDDACh) makes it possible to achieve selective binding of the sorbent to DNA from the cell lysate. It has been found that ~7.5 mg of PDDACh and 4 ng of DNA could be deposited on 1 mg of carbon nanotubes, regardless of CNT modifications. The elution of DNA into solution from the sorbent surface can be effectively carried out using 3.16×10^{-3} M aqueous solution of copper acetate. In this case, the final yield of DNA is ~67% according to both the spectrophotometry and the PCR analysis. The results of PCR, which was carried out by using DNA, isolated from the model samples by using the studied MWCNTs, confirmed the absence of inhibition of the reaction. Thus, a simple method has been developed for DNA isolation from solutions and mixtures due to reversible DNA

sorption on domestic multi-walled carbon nanotubes of the "Taunit MD" type containing catalytic magnetic nanoparticles.

Improvement of Seals of Flange Connections of Fountain Fittings and Shut-off Devices

M. I. Rodimova, H. K. Kaderov, S. O. Kireev, M. V. Korchagina*

Don State Technical University, Rostov-on-Don, Russia

*ms.korchaginamv@mail.ru

Flanged connections are widely used in fountain fittings and shut-off devices of the oil industry. One of the most important factors is their sealing. There is an extensive range of seal designs, for the manufacture of which both metallic and non-metallic materials are used, depending on the aggressiveness of the working environment and temperature fluctuations [1]. Here we will consider the design of a flange connection with a metallic ring seal. It should be noted that it is the designs with metallic ring seals that are standardized [2]. The most common are flanged joints designed for a pressure of 70 MPa with a conditional passage of Dy equal to 50, 65, 80 and 100 mm, and fastened with stud connections M20, M22, M24 and M27, respectively [2]. At the same time, the material of the sealing ring is much less durable than that of the flanges. The performed calculations for the strength of standard sealing rings, taking into account the full tightening force of the stud joints [3], showed that the ring in its entire volume passes into a plastic state and fills the annular groove associated with it. In this case, it is impossible to reuse the ring, and it is very difficult to remove it for replacement and requires considerable time. The design of a flange connection with an O-ring with the possibility of reuse is proposed by analogy with the well-known design [4]. However, unlike it, in which the sealing ring in the axial section is a rectangle with rounded edges and conjugated with the corresponding conical surfaces of the grooves on the flanges, the outer surface of the proposed ring is spherical, conjugated with the conical surfaces of both flanges according to the well-known "sphere-cone" scheme, and the inner surface contains two sealing rounded edges. The spherical surface makes it possible to reliably position the flanges relative to each other and compensate for misalignments of their axes during assembly. A mathematical model has been created that allows optimizing the shape and dimensions of the proposed O-ring design. At the same time, the necessary changes in the annular grooves in the flanges do not violate the basic dimensions of the flanges.

References

[1] Kadirov H. K., Korchagin M. V., Kireev S. O., Nikitenko S. L. The task of sealing joints of components of machines and equipment of oil and gas companies, when operating in high-temperature and low-temperature modes // *Chemical and Petroleum Engineering*, **54**(3 – 4), 188 – 192, 2018.

[2] *Flange Connection Wellhead Equipment* // GOST 28919-91, Moscow: Standards, 1991 (In Russian).

[3] Ivanov M. N. *Machine Parts: Textbook for Students of Higher Education Institutions*, V. A. Finogenov (Ed.). 6th ed., Moscow: Higher School, 383, 2000 (In Russian).

[4] Molchanov A. G. *Machinery and equipment for oil and gas production. Textbook for Universities*. 2nd ed., Moscow: Publishing house “Alliance”, 588, 2010. (In Russian).

Requirements for Sealing Existing Flange Connection Structures with Metal O-rings

M. I. Rodimova*, S. O. Kireev, M. V. Korchagina

Don State Technical University, Rostov-on-Don, Russia

*rodimova-masha@rambler.ru

Most types of oil and gas equipment are connected using flange connections. Despite the seeming unpretentiousness, such a connection performs complex and dangerous functions that oblige it to be exceptionally reliable. Accidents with this kind of equipment can lead to serious consequences, such as: emissions and fires. It is for this reason that when designing fittings, it is necessary to strive to increase its reliability [1]. The flange is used in the installation of equipment and pipelines in almost all industries. The variety of materials from which the flanges are made allows these products to be used as connecting parts of the pipeline under almost any environmental conditions (humidity, temperature) and in accordance with the environment passing through the pipeline, including aggressive. The advantages of the flange connection are strength, reliability, the possibility of repeated installation and disassembly and use in a wide temperature range, disadvantages are caused by excessive labor intensity of installation work, relatively high cost. The use of flange connections in pipelines is due to the ease of assembly. This design provides a solid connection of the pipeline parts. The flanges according to GOST 12820-80 are most often used in non-industrial fittings for flat welded parts. The element is "dressed" on the pipe with subsequent fastening by welding for butt-welded parts (collar flange) based on the GOST 12821-80, for free parts on the ring based on the GOST 12822-80. The package includes an additional element, namely a ring having a diameter equal to the flange [2]. The most important requirement for any connection of pipe fittings is tightness, to ensure it, gaskets are installed that seal the flange connection when compressed. The main requirements for sealing are: elasticity, resistance to the environment in which they work, preservation of their physical properties at the operating temperature of the medium and corrosion resistance. These properties are achieved due to the design features of the sealing element and the selection of its material [3]. Metallic gaskets are the most common: they are usually produced on the basis of plastic and soft metals, which are easily deformed during clamping and seal the joint. They can be copper, steel. Metal gaskets (including steel sealing flange gaskets and lenses) of various shapes and sizes are recommended for use at high temperatures and pressures, when non-metallic and semi-metallic gaskets cannot be used. The analysis allows us to conclude that the problem of improving the sealing of the flange connection remains relevant today.

References

[1] *Oil and Gas Field Equipment*. V. N. Ivanovsky (Ed.). Moscow: "Centrlitneftegaz", 720, 2006 (In Russian).

[2] *Limited Liability Company NPP Sistema-A.* https://systema-a.com.ua/publikatsii/flantsevye-soedineniya-chto-eto-takoe-tipy-flantsevyh-soedinenij (In Russian).

[3] *Hardware and Flange Plant* https://www.12821-80.ru/tech/83-Flancevye_prokladki_Vybor (In Russian).

Examination of Eye Tissues by Scanning Probe Microscopy

Roman V. Karotkiyan

Laboratory of Mechanics and Biocompatible Materials, Don State Technical University, Rostov-on-Don, Russia

valker94@gmail.com

One of the main tasks of ophthalmology today is the study of the mechanical characteristics of eye tissues, the knowledge of which makes it possible to predict a group of diseases directly related to degenerative diseases of the eye, primarily such diseases include keratoconus and dystrophy, which, in the absence of therapy, lead to deterioration and loss of vision [1]. Moreover, when obtaining these characteristics, it becomes possible to reduce the risks during interlayer refractive keratoplasty, namely transplanting a part of the donor's cornea between the layers of the patient's cornea. With this aim, it is required a preliminary study of the stress-strain state of the cornea under the action of intraocular pressure. In this case, it is possible to build a shell calculation scheme using several basic surfaces. The model is based on a kinematic hypothesis, according to which the spatial deformation field of the shell is determined by the deformation of several basic surfaces, as well as operations to restore individual corneal tissues. The study of the mechanical characteristics of eye tissues is also important for the development of new biocompatible materials used to create new types of implants, as well as the possibility of predicting complications, which allows choosing the method of surgery. In this report, a method is proposed for studying mechanical characteristics by considering the topological features of the layers of the cornea of the eye, as well as neighboring tissues. This technique takes into account the peculiarities of the cellular structure of the soft tissues of the eye, and also suggests the possibility of considering the cellular structure of individual layers, such as: anterior epithelium, anterior boundary membrane (Bowman's), stroma, Dua's layer, posterior boundary sheath (Descemet's membrane), posterior epithelium. Enucleated rabbit eyeballs provided by the Rostov State Medical University (RostGMU) were used as samples for testing the technique. The studies were carried out with the permission of the ethical committee of Rostov State Medical University. The topology of the corneal surface was obtained using a NanoEducator atomic force scanning microscope (NT-MDT, Russia). Guidance was carried out using positioning microscopy. Electrochemically sharpened probes with a tungsten tip were used for scanning. To process the results obtained, the Gwyddion software environment was used.

Acknowledgement. The study was supported by the Government of the Russian Federation (grant No. 14.Z50.31.0046). Scanning microscopy was carried out at the Republican Center for Collective Use of the REC "Materials" of the DSTU (https://nano.donstu.ru)

Reference

[1] Sadyrin E., Karotkiyan R., Sushentsov N., Stepanov S., Zabiyaka I., Kislyakov E., Litvinenko A. Mechanical Properties Derived by Spherical Indentation of TiN Coating Deposited by a Method Combining Magnetron Sputtering and Arc Evaporation. In: *Advanced Materials - Proceedings of the International Conference on "Physics and Mechanics of New Materials and Their Applications", PHENMA 2019*, Springer Proceedings in Materials, Ivan A. Parinov, Shun-Hsyung Chang, Banh Tien Long (Eds.). Springer Nature, Cham, Switzerland, **6**, 85 – 95, 2020.

Numerical Study of the Ballistic Performance on Soft and Hard Composite Armors

Roopendra Kumar Pathak, Shivdayal Patel*, Vijay Kumar Gupta

PDPM, Indian Institute of Information Technology Design and Manufacturing, Jabalpur, India

*shivdayal@iiitdmj.ac.in

Fiber-reinforced materials are high-performance reinforcements used in body and vehicle armors. The use of lightweight armors against ballistic plays a vital role in the aerospace and defense industry in terms of saving energy and increasing mobility. In the present study, basalt (natural) fiber and Kevlar (synthetic) fiber improves the ballistic performance with the addition of silicon carbide ceramic tile at the impacting face. The partial replacement of Kevlar/ceramic with basalt encourages the use of natural fibers for the development of eco-friendly armors. The effectiveness of three-dimensional (3D) basalt fabric hybridization with Kevlar/silicon carbide for different stacking sequences of composite armors have compared. 9 mm full metal jacket (FMJ) bullet is used with different impact velocities under ballistic impact. A constitutive model based on the concept of continuum damage mechanics is implemented based on Yen's criteria. JH-2 model is used for the damage modeling of ceramic tile. Cohesive elements are used at inter-layers for damage modeling. The damage initiation and propagation model is developed and implemented in finite element (FE) code ABAQUS as a user-defined subroutine (VUMAT). Parametric studies are performed by varying the stacking sequence of silicon carbide tile, Kevlar 3D (K3D), and basalt 3D (B3D) layers. Results revealed the panels with silicon carbide tile on the impacting face with basalt/Kevlar 3D fabric composite as backing layers in the composite laminate improved the ballistic performance among all stacking sequences impacting with 9 mm FMJ impactor.

Computational Homogenization for Determination of Porous Material Properties

Roumen Iankov[1]*, Ivan Georgiev[2], Mikhail Chebakov[3], Elena Kolosova[3], Maria Datcheva[1]

[1]Institute of Mechanics, Bulgarian Academy of Sciences, Acad. G. Bonchev St., block 4, Sofia, 1113, Bulgaria
[2]Institute of Information and Communication Technologies, Bulgarian Academy of Sciences, Acad. G. Bonchev St., block 2, Sofia, 1113, Bulgaria
[3]I. I. Vorovich Institute of Mathematics, Mechanics and Computer Sciences, Southern Federal University, 200/1, Stachki Ave. Rostov-on-Don, 344090, Russian Federation

*iankovr@abv.bg

We are presenting a 3D numerical homogenization strategy for determination of elastic material properties of porous medium with a closed pore system. The performed homogenization procedure employs micro-computed tomography (micro-CT) and

instrumented indentation testing data (IIT). The results from the micro-CT testing are used to determinate the following characteristics of the considered porous material – the volume fractions of the pores and the solid phases, the average size of the pores, the pore size distribution in a representative volume element (RVE). Using the micro-CT data, a 3D geometrical model of the closed pore material RVE is created and this geometrical model is used to generate the respective finite element model. For simplicity, the pores are considered to have a spherical form as it is depicted in Fig. 1. In order to apply the homogenization technique, proper periodic boundary conditions are imposed. The obtained within the applied homogenization procedure six boundary value problems with periodic boundary conditions are solved using the finite element software ANSYS. The employed material model in the homogenization is the linear elastic model. The elastic properties of the solid skeleton are determined based on IIT data from testing of small volumes of the porous material. In order to verify the numerical results, a parametric study is performed. The determined elastic characteristics of the porous material are analysed against data from literature in order to reveal the applicability of the homogenization procedure used in this study.

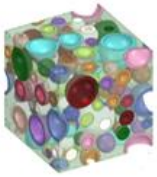

Fig. 1. RVE with spherical pores

Acknowledgement: The financial support provided by the Bulgarian National Science Fund, grants KP-06-H27/6 from 08.12.2018 (I.G.) and KP-06-Russia-1 from 27.09.2019 and by the Russian Foundation for Basic Research, project No 19-58-18011Bulg_a is gratefully acknowledged. We also acknowledge the provided access to the infrastructure of the Laboratory for 3D Digitalization and Microstructure Analysis and of the Laboratory for Nanostructure Characterization, financially supported by the Science and Education for Smart Growth Operational Program (2014-2020) and the European Structural and Investment fund through grants BG05M2OP001-1.001-0003 and BG05M2OP001-1.001-0008.

Radar-absorbing Properties of the Solid Solutions of Bismuth Ferrite – Lanthanum Manganite

A. G. Rudskaya*, E. N. Sidorenko, A. A. Babenko, I. I. Natkhin, D. I. Rudsky

Southern Federal University, Rostov-on-Don, 344006, Russia

*arudskaya@yandex.ru

At the frequency range 3.2 – 12 GHz, the absorption spectra of microwave energy for the solid solutions compositions of bismuth ferrite – lanthanum manganite $(1 - x)BiFeO_3 - xLaMnO_3$ with $x = 0.1 – 0.9$ are investigated. The samples were prepared from the pre-annealed mixtures of the simple oxides Bi_2O_3 and FeO_3 (T = 580 °C, for 4 hours) and La_2O_3 and Mn_2O_3 (T = 900 °C, for 4 hours). The final solid-phase synthesis of the samples was performed by sequential annealing at temperatures T_1 = 850 °C (for 4 hours) and T_2 = 1100 °C (for 4 hours).

To obtain the absorption spectra, a waveguide channel operating in the "transmission" mode was used. It consisted of a replaceable microwave generator, a microstrip line, a matching load, and a VSWR indicator. The synthesized compositions are non-single-phase and differ greatly in the chemical and physical properties. The obtained absorption spectra of the solid solutions with different values of x are also fundamentally different. So at the spectrum of the resonant type of the solid solution with $x = 0.1$ (rhombohedral phase $R3c$) three large absorption maxima are observed. At largest of them, located at a frequency of 8.6 GHz, the absorption reaches $L = -40$ dB. The absorption spectrum of the solid solution sample with $x = 0.2$ (tetragonal phase $P4mm$) is even more indented and has 5 maxima with the absorption $L \leq -23$ dB. For the solid solutions of the cubic phase $Pm\text{-}3m$ ($x = 0.4 – 0.6$), the spectra have a different form. In the spectra of the solid solutions with $x = 0.4 – 0.5$, where there is an impurity phase in the form of the oxide La_2O_3 and the compound $Bi_2Fe_4O_9$, apparently in a larger amount, the small oscillations of L are observed only at low frequencies ($f < 8$ GHz). The solid solutions with $x = 0.6 – 0.7$ in a wide frequency range (6 – 12 GHz) equally absorb energy at the level of 6 – 8 dB. The absorption spectra of the compositions of samples with $x = 0.7 – 0.9$ (rhombohedral phase $R\text{-}3c$) contain 2 – 3 diffuse maxima with $L \leq -15$ dB. The sharp peaks of absorption of microwave energy in the spectra are characteristic of ferroelectrics and are associated with the presence in them of the ensembles of the oscillators with frequencies close to the frequency of the measuring field [1]. The role of the oscillators, that vibrate in an electromagnetic field and absorb energy can be played by the domain walls of the mechanical twins. Exposure to a constant magnetic field with the induction up to 370 mT does not change the obtained absorption spectra.

Acknowledgements. The study was carried out with the financial support of the Ministry of Science and Higher Education of the Russian Federation (State task in the field of scientific activity, scientific project No. 0852-2020-0032), (BAZ0110/20-3-07IF).

Reference

[1] Sidorenko E. N., Chan Thi Beat Ngoc, Prikhodko G. I., Natkhin I. I., Shloma A. V., Kharchenko D. G. // *Journal of Advanced Dielectrics*, **10**, 2060020, 2020.

Controlling the Parameters of Carbon Nanotubes by the Ratio of Gas Flows in the PECVD Process

N. N. Rudyk*, O. I. Il'in, M. V. Il'ina, A. A. Fedotov

Southern Federal University, Institute of Nanotechnologies, Electronics and Equipment Engineering, Taganrog, Russia

*rudyk0918@gmail.com

Carbon nanotubes (CNTs) are a unique material that has attracted the interest of scientists over the past 30 years. The greatest success in obtaining CNTs is associated with the use of the PECVD method. However, many interrelated technological parameters affecting the properties and geometric dimensions of CNTs are still the subject of many researches. At the same time, control of the carbon-containing and hydrogen-containing gases ratio flows during the growth process allows one to manage geometric parameters of CNTs, concentration of impurities and processes of the amorphous carbon formation [1, 2]. In this work, we studied the effect of the carbon-containing (C_2H_2) and hydrogen-containing (NH_3) gases flows ratio on the geometric and structural parameters of CNTs. *p*-Si (100) wafers with a TiN buffer layer

(100 nm) and a Ni catalyst (10 nm) were used as samples. The C_2H_2 flow was 70 sccm for all experiments. The NH_3:C_2H_2 flow was varied in the ratios of 0:1, 1:1, 2:1, 3:1, 4:1 and 5:1. Scanning electron microscopy studies have shown that the presence of ammonia is critical for the formation of CNTs by the PECVD method. It was found that in the absence of ammonia, the formation of CNTs occurs with the formation of a large amount of amorphous carbon. It is deposited both on the substrate surface and on the walls of growing CNTs. In this case, the shell of amorphous carbon slows down the growth of nanotubes by reducing the rate of diffusion of carbon atoms to the catalyst surface. An increase in the NH_3:C_2H_2 ratio to 1:1 resulted in a significant decrease in the amount of amorphous carbon. In this case, carbon flakes are formed on the surface of CNTs, that reduces the growth rate of CNTs and prevents vertical alignments growth. The conical shape of CNTs can indicate both the etching of the nanotube surface by plasma ions during the growth process and the effect of ammonia on the CNT growth mechanism (top/root). With a further increase in the NH_3:C_2H_2 ratio from 2:1 to 5:1, the structure of the CNT changes. The amount of amorphous carbon on the surface of the tubes decreases, and the concentration of nitrogen impurities also changes. With an increase in the ammonia flow, the nanotube diameter decreases and the alignment of CNT growth approaches normal with respect to the substrate. The obtained data can be used in the development and creation of devices for carbon micro- and nanoelectronics.

Acknowledgement. This work was supported by the Ministry of Science and Higher Education of the Russian Federation; the state task in the field of scientific activity No. 0852-2020-0015.

References

[1] Vincent Jourdain, Christophe Bichara. Current understanding of the growth of carbon nanotubes in catalytic chemical vapour deposition // *Carbon*, **58**, 2 – 39, 2013.

[2] Pezone R., Vollebregt S., Sarro P. M., Unnikrishnan S. The influence of H_2 and NH_3 on catalyst nanoparticle formation and carbon nanotube growth // *Carbon*, **170**, 384 – 393, 2020.

Investigation of the Stress-Strain State of Enamel at the Apex of the Tooth Fissure Using Mathematical Modeling and Microtomography

E. V. Sadyrin[1]*, V. B. Zelentsov[1], M. V. Swain[1,2]

[1]Laboratory for Mechanics of Biomaterials, Don State Technical University, 1 Gagarin Square, Rostov-on-Don, 344000, Russia
[2]Faculty of Dentistry, The University of Sydney, NSW 2006, Sydney, Australia

*evgeniy.sadyrin@gmail.com

The force impact of food on the occlusal (chewing) surface of the tooth causes a stress-strain state of the enamel, characterized by natural stress concentrators, such as fissures. The concentration of stresses at the apexes of the fissures leads to the formation of areas with reduced enamel mineralization, which are areas of virtual destruction. Configuration and volume of such areas depend on the force load on the lateral surface of the fissure, on the angle at the apex of the fissure, on the location of food in the fissure, on the quality of the fissure surface and other options. In practical dentistry, the destruction of enamel is recorded using bitewing X-ray and computed tomography, and for research purposes, the state of the enamel is assessed using computed microtomography (micro-CT). In the present report from a theoretical point of view the problem of the theory of elasticity of the stress-strain state of enamel with a V-shaped notch in the form of a wedge is considered to determine the degree

of stress concentration at the apex of the fissure. The solution of the problem makes it possible to construct the boundaries of the areas of virtual destruction of the enamel at the top of the wedge. From a practical viewpoint, using micro-CT, a mineral density map is built at the apex of a real fissure, which contains an area of reduced density. Then the area of virtual enamel destruction and the density map are compared, which makes it possible to establish their approximate congruence. Thus, the researcher receives tools for recreating by theoretical means the nature and magnitude of the force load on the lateral surface of the fissure, leading to the formation of areas of demineralization. At the same time, the solution of the problem makes it possible to determine a number of parameters important in practical dentistry, primarily in the treatment and prevention of cracked tooth syndrome: critical values of bite force and the force of food impact on the side surfaces of fissures, critical angles of fissure opening at a given bite force, the influence of food location by the depth of the fissure, as well as the critical values of food adhesion on the lateral surface of the fissure. An experimental study was carried out on a human molar removed from a patient for orthodontic reasons at the dental clinic of the Rostov State Medical University (Rostov-on-Don, Russia). The local independent ethical committee of the Rostov State Medical University approved the study protocol (No. 13/20, dated September 10, 2020), informed consent was obtained from the patient. The sample under study and the calibration phantom were scanned simultaneously in Zeiss Xradia 520 micro-CT with the following parameters: X-ray tube voltage of 110 kV, power of 9.5 W, pixel size of 19.1 μm, sample rotation by 360°, exposure time of 0.9 s, X-ray tube filter HE6. During the scanning process, 1601 projections were obtained.

Acknowledgement. This work was supported by the grant of the Government of the Russian Federation, grant No. 14.Z50.31.0046.

Chemisorption of Molybdenum Atom on Carbon Nanotube using Density Functional Theory

Sangeeta A. Nirmal[1]*, M.R. Sonawane[2], R.G. Atram[3]*****

[1]Department of Physics, Patkar Varde College, Mumbai University, Mumbai, India
[2]The Institute of Science, Dr. Homi Bhabha State University, Mumbai, India
[3]The Institute of Science, Nagpur, India

*sangeetakanojia@gmail.com, **smahadev123@gmail.com, ***ramdasatram@yahoo.co.in

The effect of chemisorption of molybdenum atom (Mo) single walled (8, 0) zigzag carbon nanotube (CNT) is studied with band structure, density of state, charge transfer, charge isosurface, HOMO, LUMO molecular orbitals. The binding energy of chemisorption of molybdenum atom on carbon nanotube is found using band structure and density of state. The molybdenum is strongly chemisorbed on carbon nanotube with binding energy range 0.196 eV to 0.906 eV. The band structure and density of states clearly illustrates the creation of extra states and reduction in the band gap. The amount of charge transfer is found using Mulliken population analysis and it is in the range of 0.508 to 0.603 electron depending upon site of chemisorption. The nature of bonding between molybdenum atom and carbon atom of carbon nanotube is explained with molecular orbitals and the charge density analysis. It shows the formation of sigma bond between Mo and Carbon atoms.

Nonlinear Absorbers Based on Multi-wall Carbon Nanotubes for Protection of Sensitive Elements of Electro-optical Systems and Vision Organs

M. S. Savelyev[1,2,3]*, P. N. Vasilevsky[1,3], A. V. Kuksin[1,3], L. P. Ichkitidze[1,2], A. Yu. Tolbin[3,4], A. Yu. Gerasimenko[1,2,3]

[1]Institute of Biomedical Systems of National Research University of Electronic Technology, MIET, Zelenograd, Moscow, Russia
[2]Scientific and Technological Park of Biomedicine of I.M. Sechenov First Moscow State Medical University, I.M. Sechenov University, Moscow, Russia
[3]*Institute of Nanotechnology of Microelectronics, Russian Academy of Sciences, INME RAS, Moscow, Russia*
[4]*Institute of Physiologically Active Compounds, Russian Academy of Sciences, IPAC RAS, Chernogolovka, Russia*

*savelyev@bms.zone

To protect sensitive elements of electro-optical systems and organs of vision, active and passive optical systems are being developed, the main task of which is to limit the transmitted radiation to a safe level. Active systems do not have sufficient speed and are not able to attenuate single pulses of laser radiation in the microsecond range. For example, the minimum response time of active optical protection means, such as liquid crystal shutters, is at least 30 – 50 ns. Single pulses of shorter duration can only be attenuated using passive optical protection systems. Widespread filters based on linear attenuation of the light equally attenuate both powerful and weak non-hazardous radiation, which makes it difficult to visually control technological processes, in particular, medical operations. For these reasons, protection measures based on nonlinear optical effects are being developed. The main disadvantage of such devices is the lower degree of attenuation of laser radiation in comparison with active protective equipment. The current study is aimed to composites represented as functionally substituted monophthalocyanines adsorbed on the surface of multi-walled carbon nanotubes (MWCNTs), which have strong nonlinear optical attenuation. A nonlinear absorption coefficient of 46 cm/GW and a threshold optical fluence of 0.0260 J/cm^2 were obtained for a liquid dispersed medium with such nanoparticles in dimethyl sulfoxide (DMSO), which was confirmed by studies with nanosecond laser pulses with a duration of 17 ns. Sedimentation resistance was achieved by ultrasonic treatment with a homogenizer in a small volume of liquid (50 ml). However, in practice it is convenient to use solid materials. The preparation of the corresponding samples was carried out by mixing nanodispersions with polymethyl methacrylate (PMMA) at 80 °C. After evaporation of the solvent, thin films with high transmission (at least 78 %) were obtained in the range of 355 – 1064 nm. When studying the effect of nanosecond laser pulses on such films, it was found that the nonlinear absorption coefficient practically did not change, but the threshold optical fluence increased to 0.5496 J/cm^2. With the same transparency as liquid dispersions, the composites show less attenuation of radiation and begin to reduce the transmitted power at a higher threshold optical fluence. Despite this, film limiters are more suitable for practical use in means of protection against laser radiation. The main purpose of the obtained functional nanomaterials is the ability to attenuate high-intensity laser radiation without damaging the sensitive elements of electro-optical systems and organs of vision.

Acknowledgments. The main research concerning protection of electro-optical systems and organs of vision with using MWCNTs was supported by the Ministry of Industry and Trade of the Russian Federation (State contract No. 20411.1950192501.11.003 from 29.12.2020, identifier 17705596339200009540). The research concerning synthesis of functionally substituted monophthalocyanines adsorbed on the surface of MWCNTs was carried out with the financial support of the Russian Science Foundation (Grant 21-73-20016).

Fatigue Crack Growth Kinetics in Titanium Alloys at Different Types of Cyclic Load Surge

A. N. Savkin[1], A. A. Sedov*, K. A. Badikov, A. A. Baryshnikov, I. N. Zaharov

[1]Volgograd State Technical University (VSTU), 28, Lenin Ave, Volgograd, 400005, Russia

*sedov@vstu.ru

Many structures in operation carry variable loads, because of which fatigue cracks can occur in structural elements. The growth of fatigue cracks when they reach their critical size leads to the breakdown of the element. Operating conditions are usually associated with loads of random or variable nature. Therefore, loading history may be the main factor determining fatigue life. In order to study the influence of the character of external cyclic loading on fatigue crack growth kinetics, it is necessary to choose such methods of its change measurement that allowed to reveal the mechanisms of deformation and failure of material and to simulate crack behavior under conditions characteristic of operational loading. The aim of the present work was to study the behavior of fatigue crack growth kinetics associated with positive and negative overloads and their interaction in titanium alloys based on studying the history of its rate of advance and the manifestation of this phenomenon on fractographs of failure. Fractographic studies allow revealing on the fracture structure characteristic features associated with changes in the crack growth rate depending on the nature of the external action. To study the kinetics of fatigue crack growth, titanium alloys VT6 and 3M were used. Alloy VT6 belongs to the large group of titanium alloys based on α- and β-solid solutions containing in the stable state from 5 to 25 % of β-phase (Russian GOST 19807). Alloy VT6 refers to martensitic type alloys, has a good relationship between strength and ductility in the annealed state, can be subjected to hardening heat treatment, has a higher specific strength in comparison with α-titanium alloys. However, the alloy has a sensitivity of service properties to thermal influence, especially in insufficiently stable state. 3M is a titanium α-alloy, which occupies a dominant position in the manufacture of marine-based shipbuilding structures. It is widely used as a heat-resistant alloy, which is an α-hard solution (Russian GOST 19807-91) preserving many advantages of α- and α+β alloys. The diagrams of the loading modes are shown in Fig. 1. Table 1 shows the fatigue crack growth life in the studied VT6 and 3M titanium alloys under different types of overloading effects. Based on fatigue crack growth curves a-lg$N$, curves of fatigue fracture kinetic diagrams were plotted to determine the fatigue crack growth in titanium alloys of VT6 and 3M.

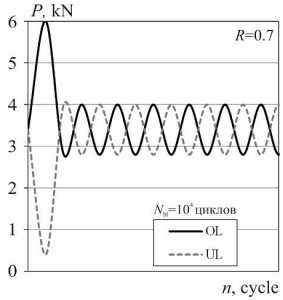

Fig. 1. Schemes of loading patterns with UL-OL and OL-UL sequences

Table 1. Influence of type of overloads on fatigue crack growth life in titanium alloys

Overload, %	Experimental crack growth life, cycles			
	VT6	VT6	3M	3M
	UL-OL	*OL-UL*	*UL-OL*	*OL-UL*
0	830167		959940	
30	1420283	920093	1820365	850086
40	7440163	1062192	8710581	1074206
50	23314663	1090110	15843169	1260127

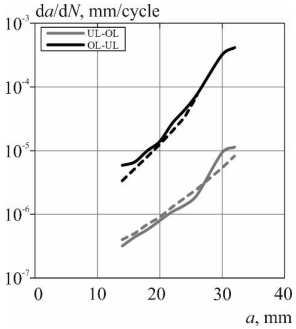

Fig. 2. Variation of crack growth rate for titanium alloy VT6 (globular structure) under UL-OL and OL-UL loading (P_{max} = 4 kN, R = 0.7, overload = 50%).

Fig. 2 shows curves of changes in the crack growth rate da/dN (mm/cycle) at control points of fatigue crack size a, mm of titanium alloy VT6 (globular microstructure) under underload – overload (UL-OL) and overload – underload (OL-UL) loading (P_{max} = 4 kN, R = 0.7, overload = 50%). The solid line is the fractography crack velocity measurement, the dashed line is the crack opening gauge measurement. A significant difference of UL-OL and OL-UL effects on the slowing down of fatigue crack growth in comparison with the regular loading has been noted for the investigated titanium alloys VT6 and 3M. UL-OL depending on the half-cycle

value of OL loading can retard fatigue crack growth by up to 27 times. For OL-UL, this retardation is negligible. For titanium alloys VT6 and 3M, which have a globular structure, a similar response of the fatugue crack growth rate curves to the identical cyclic effects of overloading and underloading is common, although for the alloy VT6, which has greater strength and ductility, this is more pronounced.

***Acknowledgments*.** The study was supported by a grant Russian Science Foundation No. 21-79-00305, https://rscf.ru/project/21-79-00305/ and within State assignment (project No. 0637-2020-0006.

Defining Characteristics of Multi-line Gas Pipelines

F. D. Savriddinov, D. D. Fugarov*, Abugharbi Ali Thamer Khalil, Ajel Mohaimen Abbas Ajel

Don State Technical University, Rostov-on-Don, Russia

*ddf_1@mail.ru

In practice, all gas pipelines are complex, because they are constructed from pipes of different wall thicknesses and have parallel pipe sections, such as loopings, reserve threads and multi-stranded gas pipelines [1]. Two methods could be used for calculating complex gas pipelines: calculating a gas pipeline by sections and replacing the calculation of a complex gas pipeline with a simple calculation. In the first method, it is required to divide the calculated area into subsections with a constant diameter [2]. Calculations are performed by alternating transitions from one section to another in the direction of the gas flow. The gas temperature and pressure at the end of the section are initial in the following [3]. When using the second method, the calculation of a complex pipeline can be replaced by the calculation of a simple one, using concepts such as equivalent diameter and flow coefficient [4]. Equivalent diameter is the diameter of a simple gas pipeline, which has a capacity equal to the capacity of a real gas pipeline under other equal conditions. The flow coefficient (k_p) is the ratio of the throughput of a real gas pipeline Q to the throughput of a reference gas pipeline Q_0 with an arbitrarily chosen reference diameter D_0 under other equal conditions: $k_p = Q/Q_0$. In this case, the capacity equation will take the form:

$$Q = k_p Q_0 = k_p \sqrt{\frac{(P_1^2 - P_2^2) D_0^5}{\lambda_0 z \pi \Delta}}.$$

Based on the convenience of calculations, the reference diameter is taken. It is most convenient to take the dominant one in a complex gas pipeline as a reference. It is best to use $D_0 = 0.7$ m or $D_0 = 1$ m, as there are flow coefficient tables for these values. Sections of a complex gas pipeline are connected in series or in parallel [5].

References

[1] Poluyan A. Yu., Purchina O. A., Fugarov D. D., Golovanov A. A., Smirnova O. V. Solution of task on the minimum cost data flow based on bionic algorithm // *Journal of Physics: Conference Series*. International Conference "Information Technologies in Business and Industry", Mathematical Simulation and Computer Data Analysis, **2**, 032056, 2019.

[2] Poluyan A. Yu., Purchina O. A., Fugarov D. D., Gerasimenko E. Yu., Skakunova T. P. Application of bionic and immune algorithms for the solution of ambiguous problems of transportation routing // *Journal of Physics: Conference Series*. International Conference

"Information Technologies in Business and Industry", Mathematical Simulation and Computer Data Analysis, **2**, 032057, 2019.
[3] Onyshko D., Fugarov D., Purchina O., Poluyan A., Rasteryaev N., Skakunova T. Synchronization system in wireless sensor networks of oil and gas complex // *E3S Web of Conferences. Topical Problems of Green Architecture, Civil and Environmental Engineering, TPACEE 2019*, 03030, 2020.
[4] Fugarov D. D., Purchina O. A., Poluyan A. Y., Gerasimenko A. N., Rasteryaev N. V. Magnetodielectric ac measuring transducer for automation systems in oil refineries // *Journal of Physics: Conference Series*. International Conference "Information Technologies in Business and Industry", 062020, 2019.
[5] Gerasimenko Y., Gerasimenko A., Fugarov D., Purchina O., Poluyan A. Mathematical modeling and synthesis of an electrical equivalent circuit of an electrochemical device // *Advances in Intelligent Systems and Computing*, **1259**, 471 – 480, 2021.

Influence of Back Contact Material on Photovoltaic Parameters of the Perovskite Solar Cells

A. V. Sayenko*, S. P. Malyukov, A. A. Rozhko, E. V. Goncharov

Institute of Nanotechnologies, Electronics and Equipment Engineering, Southern Federal University, Taganrog, Russia

*avsaenko@sfedu.ru

Currently, solar cells are actively investigated, which include organometallic compounds with a perovskite structure as a photoactive material, such as methylammonium lead halides ($CH_3NH_3PbI_{3-x}Cl_x$). The efficiency of these solar cells reaches more than 20 %, and their manufacturing technology does not require energy-intensive and complex technological processes, which makes it possible to create lightweight, inexpensive and flexible film devices [1, 2]. Despite the impressive progress in perovskite solar cells, their commercialization still requires solving several problems, including stability, when exposed to light, humidity and high temperature, as well as improved manufacturing processes and structure optimization.

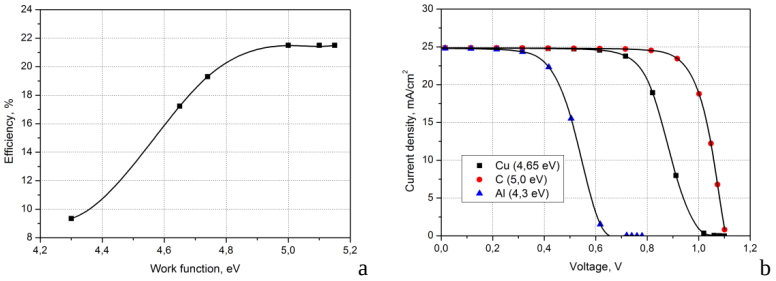

Fig. 1. Dependence of solar cell efficiency on the work function of the back contact material (a) and their current-voltage characteristics (b)

In this work, a model of a perovskite solar cell with the FTO/TiO_2/$CH_3NH_3PbI_3$/Cu_2O/Me structure has been created in the SCAPS-1D numerical simulation program. The study of the influence of the back contact material (Me) work function on the photovoltaic characteristics and parameters of the solar cell has been carried out. A gold back contact is widely used in the structure of the perovskite solar cell. Replacing this expensive material is an important task. In this structure, as a back contact, it is necessary to use a material with a certain work function to obtain an ohmic contact with the Cu_2O layer. Figure 1 shows the dependence of the solar cell efficiency on the work function of the rear contact material and their current-voltage characteristics. As a material for the back contact when modeling a solar cell with the FTO/TiO_2/$CH_3NH_3PbI_3$/Cu_2O/Me structure, we used Ni (5.15 eV), Au (5.1), C (5 eV), Ag (4.74 eV), Cu (4.65 eV) and Al (4.3 eV). It was found that an increase in the work function leads to a significant increase in the open circuit voltage from 0.76 V to 1.1 V (Fig. 1, b). In this case, the short-circuit current practically does not change (24.87 mA/cm^2). The efficiency of a solar cell increases approximately up to the work function of 5 eV (Fig. 1, a) due to a decrease in the potential Schottky barrier at the Cu_2O/Me interface, which contributes to a more efficient transfer of holes in Cu_2O to the back contact. Thus, the work function of the rear contact must be greater than or equal to 5 eV, which is necessary to obtain high characteristics of the solar cell (efficiency 21.55 %). The most suitable back contact for the FTO/TiO_2/$CH_3NH_3PbI_3$/Cu_2O/Me structure is carbon (C) with a work function of 5 eV.

References

[1] Weifu Sun, Kwang-Leong Choy, Mingqing Wang. The Role of Thickness Control and Interface Modification in Assembling Efficient Planar Perovskite Solar Cells // *Molecules*, **24**, 3466 – 3480, 2019.

[2] Sayenko A. V., Malyukov S. P., Palii A. V., Goncharov E. V. Influence of a Cu_2O hole-transport layer on perovskite solar cells characteristics // *Applied Physics*. **2**, 45 – 51, 2021.

Application of Generative Design for Calculation of Bracket of Lathe Tooling Attachment

I. V. Semenchatenko, A. A. Matrosov*

Don State Technical University, sq. Gagarina, 1, Rostov-on-Don, 344010, Russia

*amatrosov@donstu.ru

Generative design is a modern approach to the design and design of a digital or physical product, in which a person delegates part of the processes to computer technologies and platforms. This approach to creating a 3D model, including using artificial intelligence, is implemented by Autodesk and is integrated into the Autodesk Fusion 360 CAD/CAM/CAE platform and the Autodesk Netfabb Premium product. The use of this method of manufacturing models for additive production is due to a number of important factors: (i) the ability to significantly reduce the mass of the product without loss of strength; (ii) convenient subsequent sorting of generated models according to the desired characteristics; (iii) aesthetics obtained in designing products similar to natural structures; (iv) significantly reduced design time [1, 2]. To apply a generative design, you must specify: (I) Points of the generated article attachment. When designing bolted or other connections, it is necessary to specify the location for the working tool immediately with the attachment points. (II) Areas, where the generative design should not be implemented. Such areas, for example, are places where maintenance of

other units should be carried out. (III) Selection of part manufacturing method (additive manufacturing, milling). (IV) Safety criterion (margin). Software manufacturers recommend choosing it from two units or higher, or set the maximum stiffness of the designed product at all. The program creates many models of different forms at once for the selected types of production, indicating the percentage of recommendation. Models are created with no stress concentration regions, which provides a uniform load on the resulting part. All model creation operations are not performed locally on the user's computer, but on the company's cloud servers. Calculation time can take from 1 to 20 hours depending on the selected quality (the higher the quality, the smoother the product shapes are obtained) [3, 4]. In this work, using the generative design, a model of a bracket for attaching lathe tooling with numerical software was created. This model was developed specifically for additive production purposes. Ten different product variants have been obtained for different types of workpieces, designed for a given load. Several different types of materials with uniformly optimized structure are discussed.

References

[1] Semenchatenko I. V., Matrosov A. A., Nizhnik D. A. // *Status and prospects of agro-industrial complex development (INTERAGROMASH 2021)*, 2021 (In Russian).

[2] Semenchatenko I. V., Matrosov A. A. // *Intelligent Technologies and Mathematical Modeling Challenges (IT&MMC-20)*, 2020 (In Russian).

[3] Semenchatenko I. V., Matrosov A. A. // *Physics and Mechanics of New Materials and Their Applications (PHENMA 2020)*, 2021.

[4] Matrosov A. A., Semenchatenko I. V. // *Mathematical Modeling and Biomechanics at a Modern University (MMBM-21)*, 2021 (In Russian).

Formation of Nanostructures on the Surface of GaAs Using Plasma Etching

V. R. Semenov*, V. S. Klimin

Institute of Nanotechnologies, Electronics, and Electronic Equipment Engineering, Southern Federal University, Taganrog, Russia

*vlsemenov@sfedu.ru

One of the many challenges in A_3B_5 solid state electronic technology is finding efficient processing and etching methods. Such a processing technology should provide the required surface quality (minimum microroughness and defects), the invariability of the chemical composition of the surface until the formation of the next layer of the heterostructure, and the ability to control these characteristics. One of the promising directions in this area is the use of etching in a gas-discharge combined plasma. Plasma etching technology provides a structure that allows the gate of the field-effect transistor to penetrate [1, 2]. In summary, we have been formed on the GaAs surface the nanostructure with 14, 58, 234 nanometers in height. We have shown that a combination of methods of scanning probe lithography and plasma etching can be used to nano-structure surface formation in the manufacture of microwave devices. The etching rate and roughness of etched surface was installed. The combined technology of AFM lithography and plasma etching can be a competitive technology of electron-beam lithography. The results can be used in the formation of active elements of gallium arsenide.

Acknowledgement. This work was supported by the Grant of the Russian Science Foundation No. 20-69-46076. The results were obtained using the equipment of the Research and Education Center "Nanotechnologies" of Southern Federal University.

Reference

[1] Klimin V. S., Solodovnik M. S., Smirnov V. A., Eskov A. V., Tominov R. V., Ageev O. A. A study of the vertical walls and the surface roughness GaAs after the operation in the combined plasma etching // *Int. Conf. Micro- Nano-Electronics*, **10224**, 102241Z, 2016, doi: 10.1117/12.2267120.

[2] Booker K., Mayon Y. O., Jones C., Stocks M., Blakers A. Deep, vertical etching for GaAs using inductively coupled plasma/reactive ion etching // *J. Vac. Sci. Technol. B*, **38**(1), 012206, 2020, doi: 10.1116/1.5129184.

Formation of Nanostructures on the Surface of Thin Polymer Layer Using Probe Nanolithography

V. R. Semenov*, V. S. Klimin

Institute of Nanotechnologies, Electronics, and Electronic Equipment Engineering, Southern Federal University, Taganrog, Russia

*vlsemenov@sfedu.ru

In parallel to the developments of beam-based methods lithography, SPL methods are receiving renewed interest because of their flexibility to handle novel materials, and their inherent inspection and positioning capabilities [1]. The Solver P47 PRO microscope, like most modern probe microscopes, is capable not only of scanning the investigated surface, but also of modifying it due to the action of the probe. We use mechanical lithography in our experiment [2]. In summary, we have formed nanostructures on the surface of a thin polymer layer. These nanostructures can be used as a mask for plasma etching of the lower layer. The pattern of nanolithography is represented by seven stripes with a constantly decreasing distance between them. The pattern was applied in the vector mode of nanolithography, with a " HA_HR/W2C+" probe, on the surface of the photoresistive polymer layer. The parameters of the formed structures on the photoresist are also taken using a probe microscope. The average height of the structure was 20 nm, and the distance between them was 230 nm, however, if we reduce the force of impact between the probe and the surface, then we can reduce this distance in the future.

Acknowledgement. This work was supported by the Grant of the Russian Science Foundation No. 20-69-46076. The results were obtained using the equipment of the Research and Education Center "Nanotechnologies" of Southern Federal University.

Reference

[1] Garcia R., Knoll A. W., Riedo E. Advanced scanning probe lithography // *Nat. Nanotechnol.*, **9**(8), 577 – 587, 2014, doi: 10.1038/nnano.2014.157.

[2] Klimin V. S., Solodovnik M. S., Smirnov V. A., Eskov A. V., Tominov R. V., Ageev O. A. A study of the vertical walls and the surface roughness GaAs after the operation in the combined plasma etching // *Int. Conf. Micro- Nano-Electronics*, **10224**, 102241Z, 2016, doi: 10.1117/12.2267120.

Carrying Out Examination of Translucent Structures

I. A. Serebryanaya[1]*, **V. A. Chirskaia**[1], **D. S. Serebryanaya**[2]

[1]*Don State Technical University, Rostov-on-Don, 344010, Russia*
[2]*South-Russian Institute of Management - Branch of the Russian Academy of National Economy and Public Administration under the President of the Russian Federation, Rostov-on-Don, 344002, Russia*

*silveririna@mail.ru

Transparent or translucent structures are enclosing structures, used to provide thermal insulation, the necessary natural light and the possibility of visual contact with the environment. The versatility of these structures is that they can be as a stand-alone independent structure, and an element of any object. They are classified into external, enclosing and internal [1, 2]. During the construction-technical examination of these objects a number of parameters are assessed – lighting and thermal characteristics, the influence of the external and internal environment on the durability. The examination evaluates the compliance of the area of lighting apertures with the normative documents, conducts a pre-trial or forensic examination of the installation of window structures and glass units and determines the presence and causes of defects. The main complaints of users of translucent structures are mainly: the formation of condensation, frost, ice, snow deposits, leakage of rain or melt water, the presence of increased air permeability, the appearance of cracks, scratches, warping, loose or tight closing. In this case, the examination is carried out visually by external signs. Thus, the efficiency of operation of opening devices, condition of wooden elements (swelling, warping, destruction), metal bindings (deformation, corrosion and mechanical damage), seals, gaps between structural elements, loose seals, as well as moisture penetration into the adjacent areas of coatings and walls, damage to window sills on the outer sashes, etc. are determined. During the construction-technical examination of translucent structures, instrumental, such as thermal imaging, and laboratory tests are also widely used. In the course of measurements, physical and technical parameters are determined, namely resistance to heat transfer and air penetration, coefficient of light transmission, temperature field of the entire surface of the light structure. Such measurements are necessary to determine the area of condensation or frost formation. The purpose of this study was to collect, analyze, systematize the most common defects of translucent structures, to identify the causes of their occurrence and determine the possibility and ways to eliminate them [3 – 5]. This work develops a methodical approach to solving expert issues related to the establishment of compliance between the regulatory and technical documentation, on the one hand, and the technical characteristics of translucent structures, on the other hand, which are made using profiles of polyvinyl chloride alloys and metals from different companies-manufacturers.

References

[1] Serebryanaya I. A., Vinogradova E. M., Abramovskaya D. A. // *Engineering Journal of Don* **5**(56), 2019 (In Russian).
[2] Serebryanaya I. A., Egorochkina I. O., Shlyakhova E. A., Matrosov A. A., Serebryanaya D. S. // *IOP Conf. Ser.: Mater. Sci. Eng.* **913**, 022071, 2020.
[3] Nizhnik D. A., Poryadina N. A., Serebryanaya I. A. // *Mathematical Modeling and Biomechanics at a Modern University*, 2019 (In Russian).
[4] Shlyakhova E., Serebryanaya I., Serdyukova A., Pigalev D., Serebryanaya D. // *Engineering Journal of Don* **12**(72), 2020 (In Russian).

[5] Livadnaya D. B., Serebryanaya I. A. // *Engineering Journal of Don* **6**(57), 2019 (In Russian).

Dispersion Method of Measurement Quality Assessment during Construction and Technical Examination

I. A. Serebryanaya*, A. V. Nalimova, M. V. Orlov

Don State Technical University, sq. Gagarina, 1, Rostov-on-Don, 344010, Russia

*silveririna@mail.ru

Construction and technical expertise play an important role in legal proceedings. Construction and technical expertise are the complex of engineering and technical studies that includes an assessment of the compliance of documentation (design, executive, primary accounting, contractual, technical or any other) with the requirements of federal, sectoral and departmental regulatory documents [1]. An integral part of these studies is the verification of technical parameters and characteristics of construction facilities for compliance with the requirements of design documentation, the requirements of regulatory and legal acts, technical regulations in force on the territory of the Russia. The evidentiary significance of the expert's conclusion is established by such indicators as: (i) consistency of regulatory documents; (ii) accuracy of all actions and operations; (iii) a competent choice of methods and means of measurement; (iv) correct formulation of conclusions; (v) following methodological justification. Errors made by the expert lead to a decrease in the evidentiary strength of the conclusion or make its use impossible at all [2]. This clearly confirms the need to conduct competent and competent construction and technical research that meets all modern requirements. The work carried out measurements of the conditions for achieving reliability and stability of the test results carried out by the expert in the laboratory using the dispersion method. In addition, the impact of expert qualifications on these indicators was assessed [3]. Determination of strength properties of concrete carried out during technical examination of civil buildings [4] is considered as the object of research. The following were used: a device for testing the strength of concrete by the method of tear-off with chipping and a test press (destructive control method) [5]. Analysis of the results showed: (i) measurement system "object (building structures) – expert – instrument" is acceptable under conditions of simulated expert center and does not require improvement; (ii) expert qualifications do not have a significant impact on test results. The obtained statistical estimates of the variance analysis of the test results confirmed the validity of the results, their reproducibility and sufficient accuracy.

References

[1] Serebryanaya I. A., Egorochkina I. O., Shlyakhova E. A., Matrosov A. A., Serebryanaya D. S. // *IOP Conf. Ser.: Mater. Sci. Eng.* **913,** 022071, 2020.

[2] Egorochkina I. O., Serebryanaya I. A., Shlyakhova E. A., Matrosov A. A., Maltseva I. A., Lukhneva Yu. N. // *Engineering Journal of Don* **2,** 62, 2020 (In Russian).

[3] Livadnaya D. B., Serebryanaya I. A. // *Engineering Journal of Don* **6**(57), 2019 (In Russian).

[4] Serebryanaya I. A., Vinogradova E. M., Abramovskaya D. A. // *Engineering Journal of Don* **5**(56), 2019 (In Russian).

[5] Poryadina N. A., Serebryanay I. A., Matrosov A. A., Nizhnik D. A. // *Construction and Architecture*, 2017 (In Russian).

Study of Conditions for Minimization of Steel Structures Failures During the Design Phase

I. A. Serebryanaya*, E. A. Shlyakhova, I. O. Egorochkina

Don State Technical University, 1, Gagarin Sq., Rostov-on-Don, 344010, Russia

*silveririna@mail.ru

Steel structures used in the construction of buildings and structures are a popular and effective building material. However, despite favorable forecasts for the use of steel structures in construction, deformations and damage to structures occur. The main causes of accidents include: (i) redevelopment of the construction facility; (ii) natural or man-made situations; (iii) illiterate dismantling and dismantling of the facility; (iv) poor performance of construction and installation works; (v) poor quality of steel structures, etc. Based on the obtained facts, evidence reasoning is formulated because of which there was collapse, deformation and (or) damage of metal structures. On the basis of the indicated criteria, a decision is made: is it worth conducting a technical examination; check quality of project execution or construction and installation works. Factors leading to defects at various stages of the life cycle of the structure [1, 2] are studied in the work. In conducting the study, a natural examination using destructive and non-destructive testing methods was used. Simulation using software set of finite-element analysis ANSYS [3 – 5] includes metalwork design methods compared: manual design, automated 2D design, automated 3D Design. The analysis showed that the main defects of steel structures can include: (i) structural defects, arising from design errors; (ii) production and construction defects caused by the use of low-quality materials, non-compliance with construction and installation work; (iii) operational defects due to corrosion processes, changes in structural loads, etc. Since the designer-computer system acts as an executor at the design stage, the requirements for the executor are a set of requirements for its component parts. To do this, it is required: (i) to collect all the information in the form of forms, documents and technical solutions, providing the necessary and sufficient level of information support for the implementation of the selected design direction; (ii) to systematize the obtained information, ensuring the permissible level of labor costs for searching for the required information, as well as for implementing the found information in the form of newly developed technical solutions.

References

[1] Serebryanaya I. A., Vinogradova E. M., Abramovskaya D. A. // *Engineering Journal of Don*, **5**(56), 2019 (In Russian).

[2] Serebryanaya I. A., Egorochkina I. O., Shlyakhova E. A., Matrosov A. A., Serebryanaya D. S. // *IOP Conf. Ser.: Mater. Sci. Eng.* **913,** 022071, 2020.

[3] Nizhnik D., Poryadina N., Serebryanaya I. // *Mathematical Modeling and Biomechanics at a Modern University*, 2019 (In Russian).

[4] Shlyakhova E., Serebryanaya I., Serdyukova A., Pigalev D., Serebryanaya D. // *Engineering Journal of Don*, **12**(72), 2020 (In Russian).

[5] Livadnaya D. B., Serebryanaya I. A. // *Engineering Journal of Don* **6**(57), 2019 (In Russian).

Ni Matrix Composites with High Strength and Ductility

Shakti Corthay*, Magzhan Kutzhanov, Umedjon Narzulloev, Anton Konopatsky, Andrei Matveev, Dmitry Shtansky

National University of Science and Technology "MISIS", 4, Leninsky Avenue, Moscow 119049, Russia

*shakti.corthay@misis.ru

The strengthening of materials with nanoparticles (NPs) is a promising area of modern materials science. Nickel, due to its high-temperature strength, is used as a metal matrix in composite materials. NPs such as graphene, graphite, and carbon nanotubes have been studied as reinforcing phases for Ni-based composites. Hexagonal boron nitride (*h*-BN) has a high Young's modulus and lubricating properties similar to those of graphite, but has a significantly higher oxidation resistance. This can be an important advantage over carbon nanostructures. In this work, for the first time, Ni-*x*%BN composites (x = 0.001, 0.05, and 0.1 wt.%) with enhanced tensile and bending strength, as well as high ductility were obtained by a combination of ball milling (BM) and spark plasma sintering (SPS). Material with 0.05wt.% of hexagonal BN (*h*-BN) nanoflakes show an increase in tensile strength of 26% (25 °C) and 63% (750 °C) compared to additive-free Ni counterpart and high ductility. Doping with *h*-BN increases the resistance to plastic deformation at both room and high temperatures. The bending strength of Ni – 0.05%BN composite at room temperature has been increased by 121%. Small addition of *h*-BN leads to a decrease in the Ni grain size, and solid solution and grain boundary strengthening. Thus, the mechanical properties were improved by the introduction of very small amount of *h*-BN, which resulted in Ni grain refinement, and solid solution and grain boundary strengthening.

Acknowledgement. S. Corthay thanks the Russian Foundation for Basic Research (project number No. 20-33-90110).

Effect of the Dose of Si(111) Surface Ion-beam Treatment on the GaAs Nanowires Growth

N. A. Shandyba*, N. E. Chernenko, S. V. Balakirev, M. M. Eremenko, D. V. Kirichenko, M. S. Solodovnik

Institute of Nanotechnologies, Electronics and Equipment Engineering, Southern Federal University, Taganrog, 347928, Russia

*shandyba@sfedu.ru

Today, the synthesis of nanowires (NWs) is one of the actively developing technologies due to the unique electronic, optical, mechanical and magnetic properties of materials and structures based on these objects. However, the issue of effective control of various parameters of the NWs (length, diameter, density, etc.), including using pre-growth surface modification, remains relevant to this day. The use of traditional technological processes based on the operations of optical lithography, wet chemical and plasma etching either do not provide the

required parameters of the resulting structures, or are poorly compatible with growth processes, or have a high cost of pre-growth substrate processing. At the same time, the technology of focused ion beams (FIB) makes it possible to carry out technological operations of local ion-beam etching and ion-stimulated deposition of materials with high spatial resolution under high vacuum conditions, without the need for resists, masks, and chemical etchants. The aim of this work is investigation the effect of the dose of ion-beam treatment of the Si(111) surface on the growth processes of GaAs NWs. The FIB treatment of the Si(111) surface was carried out using a Nova NanoLab 600 scanning electron microscope equipped with a FIB system (with a Ga^+ ion source). The epitaxial growth of NWs was performed on a SemiTEq STE 35 molecular beam epitaxy system. Analysis of the obtained data shows a sharp difference between NWs formed on modified and non-modified regions of Si, as well as a non-linear dependence of the NW parameters on the dose of Ga^+ ion implantation into the substrate. So, in the area with an irradiation dose of 0.052 pC/μm^2, almost complete suppression of NWs growth is observed. With an increase in the dose to 0.26 pC/μm^2, active growth of NWs begins on the modified regions, which corresponds to a sharp increase in the density of NWs with a simultaneous decrease in their length and diameter relative to NWs on the unmodified surface. A further increase in the ion implantation dose first leads to an increase in the NWs density with a peak value of 7.8 pcs/μm^2, corresponding to a dose of 5.21 pC/μm^2, and then to a slight decrease to 5.76 pcs/μm^2. In the entire range of dose values (except for the first point), the NWs density is more than 2 times higher than the density on the unmodified surface. Thus, the experimental studies carried out have shown that control of various NWs parameters by the FIB method is possible by varying the dose of implantation of Ga^+ ions into the Si(111) substrate. It has been shown that a change in the Ga ion implantation dose from 0.052 to 10.4 pC/μm^2 makes it possible to adjust the NWs length in the range 1 – 6 μm, density into 0 – 7.8 pcs/μm^2, diameter into 28 – 95 nm, and verticality into 5 – 70%.
Acknowledgements. This work was supported by the Ministry of Science and Higher Education of the Russian Federation; the state task in the field of scientific activity No. 0852-2020-0015.

Synthesis and Dielectric Properties of $PbSc_{1/4}In_{1/4}Nb_{1/4}Ta_{1/4}O_3$

I. G. Sheptun[1]*, V. G. Smotrakov[1], K. A. Chebyshev[2], Yu. A. Kuprina[1], A. V. Nagaenko[1], N. V. Ter-Oganessian[1]

[1]Southern Federal University, Rostov-on-Don, Russia
[2]Donetsk National University, Donetsk, Ukraine

*sheptun.ivan@mail.ru

Perovskites $PbB'_{1/2}B''_{1/2}O_3$ (B' = Sc, In; B'' = Nb, Ta) exhibit different dielectric properties depending on the degree of ordering of B' and B'' cations, namely a relaxor-like behavior with diffuse phase transition in the case of complete disordering or experience a sharper phase transition in the ordered case [1]. An increase in the number of atoms of different sorts leads to an increase in the entropy of mixing, which, presumably, should contribute to an increase in the ordering temperature. This report describes the synthesis and study of the electrical properties of the $PbSc_{1/4}In_{1/4}Nb_{1/4}Ta_{1/4}O_3$ compound with the perovskite structure. The synthesis was carried out by the classical solid-phase method from oxides of the corresponding metals. Mixing and grinding of the starting materials was carried out in a planetary mill with a rotation speed of 400 min^{-1}, the grinding time was 4 hours. The first firing was carried out at 800 °C for 4 hours, the second one was at 900 °C for 2 hours with

intermediate grinding. To obtain the ceramics, the synthesized powder was crushed to a particle size of ≈ 1 μm, homogenized with the addition of a 5% solution of polyvinyl alcohol in an amount of 5%, and pressed into discs with a diameter of d = 12 mm and sintered at 1100 °C for 2 h.

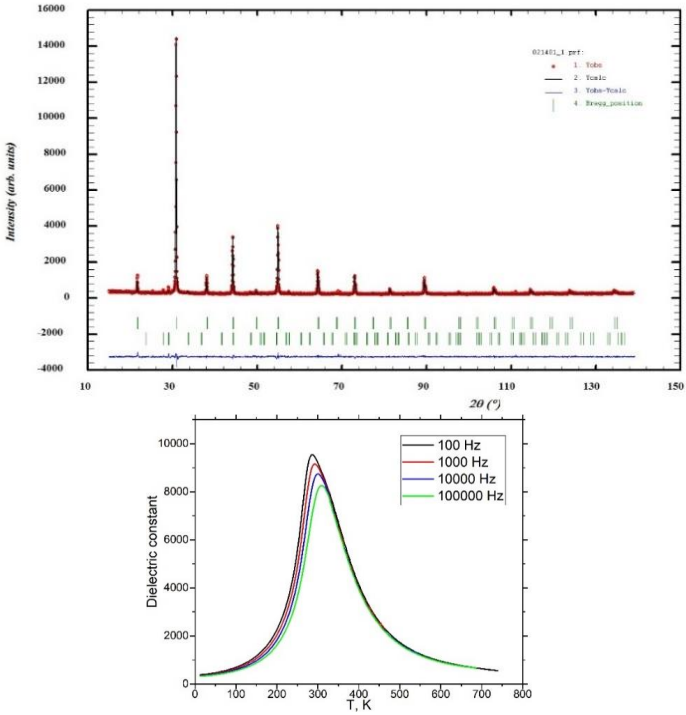

Fig. 1. (left) X-ray diffraction profile of the crushed ceramics; (right) temperature dependence of the dielectric constant

To refine the crystal structure by the Rietveld method (Fig. 1, left), an undistorted perovskite structure was used as the initial model of the crystal structure of the main phase, in which the *A*-site positions are completely occupied by lead, whereas Sc, In, Nb, and Ta are randomly distributed over the *B*-positions. The refined value of the unit cell parameter was 4.09372(9) Å. The reflections of the impurity phase with the pyrochlore structure and a volume fraction less than 3% are described by the LeBail method in the space group Fd-3m with the unit cell parameter a = 10.58448 Å. Figure 1 shows the temperature dependence of the dielectric constant, revealing the strong frequency dependence characteristic of relaxors. The resulting ceramic is characterized by a low dielectric loss tangent < 0.05.

Acknowledgement. This work was supported by the Russian Science Foundation (project No. 22-22-00678).

Reference

[1] Chu F., Setter N., Tagantsev A. K. // *J. Appl. Phys*. **74**, 5129, 1993.

Use of Fine Sands in Agricultural and Water Management Construction

E. A. Shlyakhova

Don State Technical University, Rostov-on-Don, Russia

shlyahovae@list.ru

The problem of rational use of fine sands as aggregates in concrete for various purposes has long attracted the attention of researchers. In our country, this is due to the fact that in most of its regions, deposits of such sands prevail. The main disadvantages of fine sands are their high intergranular hollowness and, often, a high content of dusty and clayey particles (DCP). Their content is often regulatory requirements for aggregates for concrete. Increased hollowness of fine sands causes significant overconsumption of cement, amounting to about 10 – 15 %. This not only worsens the economics of concrete, but can also lead to an increase in shrinkage and cracking in the hardened concrete. The latter defects reduce the strength of structures made of such concrete, their durability and operational reliability. The excessive content of DCP in excess of the regulatory requirements leads to a deterioration of adhesion of aggregate grains with the cement stone, resulting in lower concrete strength and requires a large overspending of cement. To reduce cement consumption in concretes with fine sands, the use of enlarging additives and microfillers is known. In the case of high content of DCP, washing and fractionation of aggregates is used. However, the use of these fine sand in beneficiation methods requires substantial costs to implement, especially in agricultural and water management construction environments. These types of construction, due to their considerable distance from the developed construction infrastructure, require additional investment in transportation costs, which constitute a significant part of the total costs. We have developed a resource-saving method for the preparation of concrete mixtures [1] on substandard aggregates, which does not require additional costs at the existing concrete mixing plants. The method allows the use of local substandard sands, which does not lead to an increase in transportation costs for the delivery of high-quality aggregates to the objects of agricultural and water management construction.

Reference

[1] Pitersky A. M., Shlyakhova E. A., et al. Method of preparation of concrete mixture // *Russian Patent for the invention* RU 2028279 C1, MKI C 04 B 28/04.

Ash-and-Slag Aggregate

E. A. Shlyakhova*, D.V. Bezhanov

Don State Technical University, Rostov-on-Don, Russia

*shlyahovae@list.ru

As it is well-know, the most mass in the production of concrete, the products of extraction and processing of non-solid rocks are used as aggregates. Natural raw materials for the production of building materials belong to non-renewable natural resources and a number of regions of the Russia are already experiencing a shortage of fillers. In this regard, the search for alternative types of aggregates for the production of concrete and reinforced concrete is

becoming more and more relevant. The available raw material base for this purpose is various industrial wastes, among which are sufficiently well-studied ash and slag mixtures of thermal power plants. Despite the fact that the possibility of using ash and slag mixtures as aggregates for various types of concrete is confirmed by many years of practice, for each particular plant producing this type of waste, special additional experimental studies and the development of relevant technological recommendations are required. In the present study, the possibility of using ash and slag mixtures of Novocherkassk GRES as aggregates for fine-grained concrete is evaluated. Characteristics of the Novocherkassk GPP ash mixture used in the studies are given in Table 1.

Table 1.

Fractional composition, % by weight, mm			Bulk density, kg/m^3, more than	Content, %	
less than 0.315	0.315 – 5	more than 5		SO_3, no more than	SiO_2, no less than
21.0	54.0	25.0	1400	3.0	40

Portland cement CEM I 42.5N of the Sebryakovskiy cement plant was used in the work. As a control, a composition of a fine-grained concrete mixture was taken, using quartz natural sand from the Aksai quarry in the Rostov region as a filler and screening of stone crushing from dense sandstone of a fraction of 0 – 5 mm. The consumption of cement is assumed to be constant in the control and in the composition on the ash and slag mixture. The mobility of the concrete mixture was evaluated by the standard method for the draft of the cone and amounted to 10 cm. Cubic samples with a rib of 10 cm were steamed under the regime (3 + 5 + 2) hours, at a temperature of isothermal heating equal to 80 + 5 °C. After heat and moisture treatment the strength of steamed concrete on ash-and-slag mixture was 86 %, the control composition showed 79 % of the design class of concrete B15. After curing samples of steamed concrete in the laboratory for 28 days, the strength of the control composition was 20.9 MPa or 108 % of the design class of concrete. The strength of the composition using ash-and-slag mixture as an aggregate showed 20.4 MPa or 106 %. Application of ash-and-slag mixtures for concrete production is a very promising direction, economically and technologically justified. This way, in addition to the above, allows one to solve the issues of man-made waste recycling, reduce the environmental problem of protecting the planet from pollution.

Technogenic Raw Materials in the Production of Building Materials

E. A. Shlyakhova*, V. V. Derkachev

Don State Technical University, Rostov-on-Don, Russia

*shlyahovae@list.ru

In recent years, the construction industry has experienced an increasing shortage of raw materials for the production of various building materials, products and structures. This situation has arisen, first of all, in connection with the rapidly increased rates of housing construction, which, according to analysts, have an annual growth of more than 5%. Over the past 20 years, the construction industry has shown steady dynamic growth and is one of the most stable industries in the Russian economy. This makes it possible to predict a further increase in the industry's demand for high-quality raw materials, the supply of which is

currently limited in nature. One of the ways to solve this problem may be the disposal of a variety of large-tonnage man-made wastes that have accumulated in numerous dumps in all industrially developed regions of the Russian Federation. This waste occupies areas that can be effectively used in production, or it can be agricultural land that is currently being removed from circulation. The solution of issues related to the disposal of industrial waste has both practical and environmental significance. For use in the production of building materials, industrial wastes are very promising products resulting from the combustion of solid fuel in the furnaces of thermal power plants. One of the enterprises that annually send tons of ash-and-slag waste to dumps is the Novocherkassk state district power station (SDPS) operating in the south of Russia. To date, significant experience has already been accumulated by the use of waste of power plants in construction [1, 2], summarizing which is proposed to expand the local raw materials base through the use of waste from Novocherkassk SDPS. The following ways can be attributed to the possible ways of using waste: (i) production of binders such as lime-ash, lime-slag, autoclave hardening binders, ash-slag-alkaline, gold-Portland cement and composite binders; (ii) fly ash, which contains the required amount of unburned fuel, can be used as a component of the charge in the production of clay bricks, ash gravel and agloporite; (iii) slag waste can serve as a basis for the production of slag melts for the manufacture of slag wool, slag pumice, slag casting; (iv) ash-and-slag mixtures can be used as aggregates for concrete, mortar, ash and asphalt concrete. These directions can be implemented after conducting special studies to assess the possibility of obtaining a particular building material based on fuel waste. As a result, in each particular case, rational compositions and optimal technological regimes for the production of construction materials and products, using waste from power plants, are determined and regulatory technological documentation is developed. The expansion of the raw material base of construction materials due to the use of man-made wastes will reduce the amount of natural non-renewable resources used.

References

[1] Zyryanov V. V. *Fly-ash – Man-made Raw Materials*. Moscow: Maska, 319, 2009 (In Russian).

[2] Volzhenskij A. V., Ivanov I. A., Vinogradov B. N. *Application of Ashes and Fuel Slags in the Production of Building Materials*. Moscow: Strojizdat, 255, 1984 (In Russian).

Slag-alkaline Binders with Adjustable Setting Times

E. A. Shlyakhova*, I. O. Egorochkina, A. E. Gorskikh, N. S. Iakubova

Don State Technical University, Rostov-on-Don, Russia

*shlyahovae@list.ru

Alternative to Portland cement hydraulic binders with high technical performance at a relatively low cost are clinker-free slag-alkaline binders. The undoubted advantage of alkaline activation binders is the possibility of using a wide range of man-made waste in their production, as well as the absence of an energy-intensive firing operation in the technology [1]. The technology of production of slag-alkaline binders with a hygroscopic alkaline component is based on fine grinding of blast furnace or electrothermophosphoric granular slag, followed by their mixing with aqueous solutions of alkalis [2]. Concretes based on slag-alkaline binders have high strength characteristics reaching 100 – 120 MPa. The structure of

such composites is stable over time, cement stone has high resistance, low solubility, increased density and the predominance of closed rounded gel pores and micropores. However, concretes based on slag-alkaline binders also have a number of disadvantages, the main of which are very short setting times.

Table 1. Characteristics of fly ash

Title of the hydroelectric power station	Chemical composition of fly ash, mass, %							
	SiO_2	Al_2O_3	Fe_2O_3	CaO	MgO	Na_2O	K_2O	SO_3
Novocherkasskaya	50.00	22.5	14.3	3.6	0.7	2.4	5.1	1.5

Physical and mechanical characteristics of fly ash					
pH water extract, units	Water extract, units (g) of 100 g	Mass loss during calcination, by weight, %	The content of alkaline oxides in terms of N_2O, by weight, %	The remainder on the sieve No. 008, %	Bulk density, kg/m^3
9.92	0.1	8.6	1.10	4.91	1200

This makes it excessively difficult to work in the manufacture of concrete and reinforced concrete structures, and sometimes makes it impossible. This effect is especially pronounced on freshly ground finely ground slags sealed with solutions of liquid glasses. The setting time of these binders can be characterized by a very narrow range: the beginning in 3 – 5 minutes and the end in 10 – 15 minutes. The paper investigated the possibility of replacing part of the scarce imported granulated blast furnace slag with fly ash from the Novocherkassk hydroelectric power station of the Rostov region. The aim of the work was to obtain compositions of a slag-alkaline binder with high strength indicators and technological setting times, consisting in a certain ratio of blast furnace slag, fly ash and an alkaline component. The main characteristics of fly ash of the Novocherkassk hydroelectric power station are given in Table 1.

References

[1] Shlyakhova E.A. Ways of using fuel waste of battens in building // *Building and Architecture*, 434 – 436, 2015 (In Russian).

[2] Shlyakhova E.A. Energy saving in the production of slag-alkali binders // *Science of Science*, No. **4**(13), 235, 2012.

Expansion of the Raw Material Base for the Production of Slag-Alkali Binders

E. A. Shlyakhova*, I. O. Egorochkina, A. V. Serdyukova, E. S. Bondarenko

Don State Technical University, Rostov-on-Don, Russia

*shlyahovae@list.ru

One of the urgent problems of the modern construction industry is the search for effective and relatively cheap binders that allow not only expanding the raw material base, but also to significantly reduce the environmental burden on natural mineral resources. Today, the main hydraulic binder, the most widely used in the production of concrete and reinforced concrete,

is Portland cement. The production of Portland cement depletes natural mineral resources, requires large production areas, is very metal-and energy-costly, and is accompanied by significant greenhouse gas emissions. An alternative to Portland cement can serve, developed in the twentieth century, non-clinker slag-alkaline hydraulic binders that are not inferior to Portland cement in their technical characteristics. Slag-alkali binders are obtained by mixing finely ground blast furnace or electrothermophosphoric granular slag, with a grinding fineness characterized by a specific surface area of at least 3000 cm^2/g. They are closed with aqueous solutions of alkalis of 18 – 40 % concentration by weight. The strength of compositions based on these binders can reach 120 MPa [1]. The significant disadvantages of alkaline binders include short setting times, which are influenced by the type, amount and method of introduction of the alkaline component, chemical and phase composition, as well as the fineness of the slag grinding. The recent continuous increase in the price of Portland cement contributes to an intensive search for alternative ways to reduce the cost of binders, the most acceptable of which is the use of clinker-free slag-alkali binders. In the Rostov region, the main supplier of metallurgical blast furnace slags for the needs of the construction industry for a long time was the Donbass [2]. However, due to the crisis in the ferrous metallurgy and difficult political conditions, there is a significant decrease in the production of pig iron in the industry and granulated blast furnace slag becomes a deficit. The expansion of the raw material base of slag-alkali binders at the expense of local technogenic waste of the Rostov region with the simultaneous synthesis of neoplasms that bind sodium oxide into water-resistant compounds is an urgent task and can allow solving not only economic issues, but also a number of technological ones. The report considers the possibility of using ash-slag waste of Novocherkassk hydroelectric power station as the main component of slag-alkali binders. In the studies, fly ash and ground slag were used in various combinations, five-and nine-water sodium metasilicate was used as a hardening activator. As a result, binders with an activity of 35 – 58 MPa were obtained, which differ from slag-alkali binders on blast furnace slags by extended setting times.

References

[1] Glukhovskii V.D., Pakhomov V.A. *Slag-alkali Cements and Concretes*. Kiev, Budivel'nik, 184, 1978 (In Russian).

[2] Shlyakhova E.A., Akopyan A.F. Assessment of the limits of applicability of raw materials for the production of slag binders // *Building Materials*. **11**, 28 – 29, 2010 (In Russian).

Improving the Quality of Slag-alkaline Binders

E. A. Shlyakhova*, I. O. Egorochkina, A. A. Shcherbina, A. V. Shevchenko

Don State Technical University, Rostov-on-Don, Russia

*shlyahovae@list.ru

Due to the rapid growth of prices for Portland cement observed in the last few years, the issue of the production of alternative linker-free efficient hydraulic binders is becoming more and more urgent. To the greatest extent, these requirements are met by slag binders of alkaline activation. Slag-alkaline binders are obtained on the basis of finely dispersed aluminosilicate materials of amorphous or crystalline structure, which give an alkaline reaction when mixed with alkali solutions. In the result of hydration of slags with alkali solutions, a cement stone with high physical and mechanical characteristics is formed. It is known that the activity of

the slag-alkaline binder directly depends on the optimal value of the density of the mixing solutions, the nature of the alkaline component and the value of the specific surface of the slag. The density of the solutions is in the range of 1.15 – 1.25 g/cm^3, and the specific surface area of the slag should be 320 – 350 m^2/kg [1]. The peculiarity of using aqueous silicate solutions as an alkaline component is that the setting time of cement is sometimes reduced to values that do not allow preparing and forming a concrete mixture. The setting time of the slag-alkaline binder is influenced by the type, amount, concentration and method of introduction of the alkaline component, as well as the fineness of the slag grinding, its chemical and phase composition [2]. If for binders on caustic alkalis and non-silicate salts, the setting speed is comparable to the setting speed of Portland cement, then for binders, in which the alkali metal silicate is the alkaline component, the picture changes. The setting time in this case will be determined by the value of the SiO_2/Na_2O silicate module and will vary widely. If sodium silicate with a silicate modulus of 0.5 – 4 is used, the beginning of setting can start from 5 minutes, and the end from 15 minutes. The quality of the slag is also directly related to the setting time of slag (alkaline binders): with a decrease in the basicity of the slags, they increase. The main blast furnace slag of NLMK with a basicity modulus of Mo = 1.09 was used in the work. To assess the possibility of regulating the setting time of the slag-alkaline binder, the fly ash of the Novocherkassk state district power station (SDPS) was used instead of a part of the blast furnace slag. This ash is acidic in its composition and helps to reduce the basicity of the slag component of the binder. The content of the introduced fly ash varied from 20 to 80 %, the density of the alkaline component, namely nine-water sodium metasilicate, remained constant. Due to the introduction of fly ash, the setting time increases from 15 minutes (the beginning of setting) for a composition without fly ash to 20 – 47 minutes for compositions with fly ash. The setting time increases with an increase in the dosage of fly ash, while there is a decrease in the strength parameters of the slag-alkaline binder in proportion to the proportion of ash introduced. In the result of the research, it was found that the introduction of fly ash from the Novocherkassk SDPS instead of a part of the blast furnace slag helps to prolong the setting time of the binder.

References

[1] Glukhovskii V. D., Pakhomov V. A. *Slag-alkali Cements and Concretes*. Kiev: Budivel'nik, 184, 1978 (In Russian).

[2] Shlyakhova E. A., Akopyan A. F. Assessment of the Limits of Applicability of Raw Materials for the Production of Slag Binders // *Building Materials*. **11**, 28 – 29, 2010 (In Russian).

Application of Ash-and-slag Mixtures in Production of Construction Materials

E. A. Shlyakhova*, M. E. Fufanin

Don State Technical University, Rostov-on-Don, Russia

*shlyahovae@list.ru

The use of fuel ashes and slags, which have already accumulated to date and continue to accumulate in huge quantities in the dumps of thermal power plants, is an increasing interest on the part of research organizations and industrial enterprises. This is due to the fact that the widespread use of ashes and slags for the needs of the construction industry will contribute to

saving material resources, reducing the costs of building and operating ash-and-slag dumps, provide a significant economic effect. In addition to the above, fuel waste disposal is an integral part of one of the most important problems of our time, namely protection of the environment from pollution by man-made waste. According to statistics, tens of millions of tons of ash-and-slag waste are generated annually in Russia. Only at Novocherkassk state district power station (SDPS), being the largest power plant at the south of Russia, 3.4 million tons of anthracite coal are burned annually. At the same time, about a million tons of ash-and-slag waste are formed. More than 52 million tons of ash-and-slag waste are now stored in the dumps of the Novocherkassk SDPS. Most of the ash-and-slag mixtures are sent to dumps, and only 3 – 5 % are disposed of in the construction industry. At the same time, the order of 40 – 60 % is being disposed of in the USA and Germany. By this time, a lot of positive experience has been accumulated, both foreign and domestic, of the use of fuel ashes and slags in the production of building materials. They are successfully used as a component of moulding mixtures, cellular concrete, aggloporite, mixed binders, concrete aggregates, asphalt concrete components and much more [1]. The purpose of the studies was to assess the possibility of using the waste ash-and-slag mixtures of Novocherkassk SDPS as aggregates for the production of heavy concrete. In the result of the performed studies, it was found that according to the chemical and grain composition, ash-and-slag raw materials meet the requirements of regulatory documents and are suitable for use as a component of a concrete mixture. To determine the effectiveness of ash-and-slag mixtures as aggregates, ash-slag mixtures were tested directly in concrete on a combined and single-component ash-and-slag aggregate. The combined aggregate was selected as a result of a change in the ratio between a large aggregate of natural origin from sandstone of 5 – 20 mm fraction and ash-and-slag aggregate. The composition of the ash-and-slag mixture contained at least 10 – 15 % of the slag component with a grain size of 5 – 20 mm, the rest relates sandy and dusty components. Content of sand fraction (particle size 0.315 – 5.0 mm) in ash-and-slag mixture should be within 40 – 60 %. As a result, it has been found that based on the condition of achieving the best workability of the concrete mixture with a constant water content and the maximum strength of the equally movable mixtures for concrete on a combined aggregate, a ratio between ash-and-slag aggregate and crushed stone of 0.6 can be recommended. Comparison of strength values of steamed concrete and concrete of natural hardening of similar compositions showed that steaming increases strength of ash-and-slag concrete on combined aggregate by 10 – 20 % at monthly age.

References

[1] Volzhenskij A. V., Ivanov I. A., Vinogradov B. N. *Application of Ashes and Fuel Slags in the Production of Building Materials*. Moscow: Strojizdat, 255, 1984 (In Russian).

Quality Assessment of Reinforced Concrete Products

E. A. Shlyakhova*, V. A. Kostenko, G. R. Tuminov

Don State Technical University, Rostov-on-Don, Russia

*shlyahovae@list.ru

The permeability of concrete, depending on the nature and structure of the material, characterizes the intensity of the passage of gases or liquids through its thickness. The degree of permeability can be estimated by the filtration coefficients of the liquid or gas through the

concrete. Three main varieties of liquid transfer are known. These include: (i) a viscous flow subjected to Poiseuil's law; (ii) diffusion transfer according to Fick's law and, (iii) capillary flow, described by Darcy's law. In the works of V. M. Moskvin, Yu. V. Chekhovsky and other authors, on the issues of permeability and the mechanism of transfer of gases and liquids in capillary-porous samples, it was noted that the permeability of concrete is very much influenced by its age and specific hardening conditions. Therefore, water permeability is one of the most inaccurate and difficult to determine properties of concrete. At the same time, it should be noted that the waterproof index is one of the main factors determining such a property of concrete as its durability. It is known that during the operation of reinforced concrete products there is a decrease in waterproofness due to the influence of various negative factors on them. Therefore, timely detection of an increase in water permeability will make it possible to quickly take measures to prevent further manifestation of a decrease in durability and avoid destruction of the structure. Existing standards allow many different methods of determining water permeability, which can be divided into two main types: (i) methods based on tests of samples specially prepared or drilled from the used structure, and (ii) methods when tests are carried out directly on structures or constructions. In our opinion, the most rapid and least time-consuming method is the method of assessing the waterproofness of concrete by the amount of air filtration through the same concrete. The method developed at the time by DONNII, and modernized by us in relation to the assessment of the permeability of the lining of irrigation channels, can be used both in laboratory conditions and directly at the facilities in operation. The proposed method is carried out as follows. A metal bell connected to the manual vacuum pump of the Komovsky system is installed on the surface of the tested structure, on which a layer of sealant is previously applied. In the space of the bell, a discharge of up to 96000 Pa (0.96 atm.) is created, controlled by a vacuum meter. The time during which the vacuum meter arrow drops to zero is fixed, and then the concrete waterproofness grade is determined from the calibration curve. The accuracy of the proposed method of determining the waterproofness of concrete in service structures depends mainly on the quality of the calibration curve. The calibration curve is constructed taking into account the specifics of each unit and the type of sealant used.

To Improve the Quality of Reinforced Concrete Products

E. A. Shlyakhova*, V. E. Kostylev, A. V. Serdyukova

Don State Technical University, Rostov-on-Don, Russia

*shlyahovae@list.ru

Many years of experience in the production of reinforced concrete products in the conditions of construction plants allow us to say that it is possible to identify the most common defects in production, classify them and propose ways to prevent their occurrence. Obviously, these measures will allow manufacturers of reinforced concrete products to improve the quality of their products and reduce the percentage of rejects. Reinforced concrete prestressed hollow-core slab with round voids for overlapping buildings and structures was considered as the object of research. The product is manufactured by the aggregate-flow technology with the use of a forming machine with punches for the formation of voids, with subsequent heat and moisture treatment in the pit steaming chambers. It should be noted that the analysis highlighted the most common defects of multi-hollow plates. According to the requirements

of the standard, the surface of the boards are requirements for the absence of cracks, except for shrinkage cracks on the bottom (front) and lateral surfaces, the width of the opening is not more than 0.2 mm; on the top surface, it is not more than 0.3 mm. However, this requirement does not fully reflect all the variety of types of cracks, the places of their localization, as well as the possible causes of their appearance and ways to eliminate them. The solution of the problems associated with the analysis of the causes of cracking in prestressed hollow-core slabs is of great practical importance. It must be taken into account in the development of technological charts of the manufacturing process at enterprises, in the design and modernization of heat treatment chambers, in the appointment of modes of heat and humidity treatment and cooling of products. Practical experience in manufacturing of reinforced concrete products using heat and moisture treatment allows one to say that the main reason for formation of technological cracks is, as a rule, the difference of thermal and physical characteristics of metal mold and reinforced concrete product. As a result, temperature deformations occur during heating and cooling, and to avoid cracking and loss of concrete strength, it is necessary to avoid large temperature differences between the inside and outside of the chambers. Thus, [1] recommends that the permissible rate of temperature decrease was no more than 40 °C per hour, but this recommendation cannot always be used. The following factors must be taken into account when assigning cooling modes to the products: (i) ambient temperature (summer or winter); (ii) wind speed; (iii) conditions of product retrieval, that is landfill or indoor shop; (iv) density of stacking; (v) conditions of storage, that is the heated, unheated room or open area. These factors must be accounted of to avoid disrupting the structure of the concrete, if it cools too quickly, inevitably leading to cracks.

References

[1] RajxeÍ V., Glatte R. *Concrete*. Moscow: Strojizdat, 112, 1981 (In Russian)

Prospects for the Use of Carbonate Raw Materials in Agricultural Construction

E. A. Shlyakhova*, V. N. Sukach, G. R. Tuminov

Don State Technical University, Rostov-on-Don, Russia

*shlyahovae@list.ru

Building in general and agricultural, in particular, is the most material-intensive sphere of production. This is due to the urgency of the problem of expanding the raw material base for the manufacture of building products and constructions. First of all, this applies to concrete aggregates, since they account for 80 – 85 % of the consumption of raw materials, including up to 50 % for the share of a large aggregate. In general, on the territory of the Russia, more than half of all deposits of stone materials are carbonate rocks, and in such regions of Russia as the Central, Central Chernozem, Volga-Vyatka, Volga, there are practically no other stone rocks except carbonate for construction needs. Carbonate rocks include sedimentary rocks consisting mainly of calcite $CaCO_3$ (limestones), or dolomite $CaMg(CO_3)_2$. As with other sedimentary rocks, the properties of carbonates vary in a very wide range depending on composition, origin, structure and other factors. If dense limestones and dolomites are widely studied and widely used for the preparation of concrete mixtures for various purposes, then the use of carbonates of low and medium strength (below 30 MPa) is very limited. At the same time, it should be noted that only in the Rostov region more than 100 deposits of limestone

shells and porous limestones have been explored, the total reserves of which amount to more than 10 million m^3. Such limestones with good thermal properties can be used as basic materials in the form of slab stones and large blocks, or as fillers of light concrete and products made from them. The expansion of the scope of application of the carbonate rocks under consideration is facilitated by their ability to be well machined, sawing, cutting, grinding. Denser carbonate rocks can be used as rubble stone for foundations and basement walls in low-rise agricultural construction. Carbonate sands can be used as a fine aggregate in conventional and fine-grained concrete and mortar. Crushed to a pulverized state, carbonate rocks can be used as micro-fillers in cement concretes, as components of autoclave binders in silicate concretes and as mineral powders in the production of asphalt concrete. Based on the above, it is proposed to organize the work of quarries of carbonate raw materials according to a complex scheme providing for waste-free production of products. Such production will be carried out without polluting the environment with pulverized waste, which will contribute to improving the environmental situation in the region. The technological scheme of production should be flexible and modified taking into account the specific conditions for which it is being developed.

Properties, Microstructure and Stability of Adsorption Organic Films

S. P. Shpanko[1]*, E. N. Sidorenko[1], D. A. Grineva[2]

[1]Southern Federal University, Rostov-on-Don, 344006, Russia
[2]Academy of the Higher School of Business, Katowice, 41-300, Poland

*spsha@mail.ru

The protective effect of a new organic compound and its mixtures with KBr on the corrosion of low-alloy steel in a 1 M of H_2SO_4 solution has been investigated. The inhibitor is a substituted imidazobenzimidazole derivative (SAS surfactant). The SAS concentration was kept constant at 10^{-3} mol/l. The concentration of KBr (C_{KBr}) was varied in the range of 0.01 – 0.1 mol/l, the time of film formation is t = 1 – 3 days. It was found that the use of a composite inhibitor SAS + KBr significantly reduces the rate of corrosion of steel in a sulfuric acid medium. The protective effect increases to a greater extent, the higher the KBr concentration and the longer the film formation time. However, the dependence of the degree of protection on t was determined by the concentration of KBr. The inhibitory effect increases over the entire time interval of film formation at a KBr concentration of more than 0.01 mol/l. The degree of filling the steel surface with inhibitor components θ was determined by the capacitive method. The full compliance of the capacitive measurements with the gravimetric ones has been established. For a composite inhibitor, θ is higher than for an individual compound and increases with increasing C_{KBr}. The microstructure of the coatings was studied using a scanning electron microscope. It was found that the morphology of the coatings is disordered. Extended crystal cells of various sizes were observed locally on the surface of the samples. They were completely surrounded by intercrystalline boundaries. However, most of the coatings were a collection of chaotically fused crystallites that have only locally intercrystalline boundaries. Some crystallite formations contained a large number of pores of different depths and separate segments of boundaries of different lengths. Locally extended intercrystalline boundaries of various widths had a large number of triple or even quadruple joints. Due to the large number of conjugated double bonds and delocalized π-electrons in the

inhibitor macromolecule, the conductivity of the films is high and ranges from 0.02 – 0.2 Cm for samples with an area of 1 cm^2. A slight increase in the external pressure increases the conductivity of the films by one or two orders of magnitude. In the frequency range of (25 – 3×10^6) Hz, the frequency dependences of the electrical capacity and conductivity of the films are investigated [1]. The stability of the films under study in one molar solutions of sulfuric and hydrochloric acids has been studied. It was found that films, obtained in the presence of a composite inhibitor, are more stable in acidic media [2]. Moreover, the higher the concentration of KBr in the mixed inhibitor during the preparation of the film, the more resistant the film is to acid etching. The investigated organic coatings are significantly more stable in hydrochloric acid than in sulfuric acid. The stability of adsorption films, regardless of the nature of the etching solution, is higher, the greater the protective effect of the inhibitor, when obtaining films.

References

[1] Bogatin A. S., Sidorenko E. N., Shpanko S. P., Kovrigina S. A., Abdulvakhidov K. G., Nosatschev I. O. In: *Physics and Mechanics of New Materials and Their Applications - Proceedings of the International Conference PHENMA 2020*, Springer Proceedings in Materials, Ivan A. Parinov, Shun-Hsyung Chang, Yun-Hae Kim, Nao-Aki Noda (Eds.). Springer Nature, Cham, Switzerland, **10**, 223 – 232, 2021.

[2] Shpanko S. P., Sidorenko E. N., Kuznetsova L. E., Sosin E. A. In: *Advanced Materials - Proceedings of the International Conference on "Physics and Mechanics of New Materials and Their Applications", PHENMA 2018*, Springer Proceedings in Physics, Ivan A. Parinov, Shun-Hsyung Chang, Yun-Hae Kim (Eds.). Springer Nature, Cham, Switzerland, **224**, 123 – 130, 2019.

Physico-chemical Properties of Organic Films Obtained in Saltic Acid Medium

S. P. Shpanko[1]*, E. N. Sidorenko[1], D. A. Grineva[2], M. E. Agarkova[3]

[1]Southern Federal University, Rostov-on-Don, 344006, Russia
[2]Academy of the Higher School of Business, Katowice, 41-300, Poland
[3]Hydrometeorological College, Rostov-on-Don, 344025, Russia

*spsha@mail.ru

The inhibitory effect of a new organic compound of the imidazole class (surfactant, SAS) and its mixture with KBr on the corrosion of steel St3 in a 1M HCl solution was studied. The investigated organic compound is a salt consisting of a bulky organic cation and an anion of chlorine. The surfactant concentration was kept constant (10^{-3} mol/l). The KBr concentration (C_{KBr}) in the mixture was varied in the range of 0.1 – 0.3 mol/l. The time of obtaining organic films is t = 0.5 – 3 days. This work is a continuation of the studies of the physico-chemical properties of adsorption films, obtained from electrolytes, inhibited by various organic and inorganic compounds [1, 2]. It was found that the degree of protection of the composite inhibitor Z is higher than that of the organic compound and increases with an increase in C_{KBr} and the time of formation of a protective film t. The microstructure of the films was studied using a scanning electron microscope. Films obtained in electrolytes at low values of C_{KBr} and t (especially at C_{KBr} = 0) have a disordered structure. It is a chaotically arranged fine-crystalline formations with numerous pores and separate sections of intercrystalline boundaries. All

studied films have a negative electrical capacity due to the jumping mechanism of their electrical conductivity and/or a negative contribution to the polarization of the film from the relaxation process in an inverse electric field. Two dielectric dispersions are observed on the frequency dependence of the electrical capacity $C(f)$ in the frequency range $(25 – 3\times10^6)$ Hz. The deepest low-frequency dispersion is characteristic of films, obtained without potassium bromide. The electrical capacity and conductivity of the films are sensitive to mechanical stress. A decrease in the capacity of the double electric layer (DEL) in the presence of inhibitors, compared to the background, indicates the adsorption of inhibitors on the steel surface. The degree of filling the steel surface with surfactant cations θ is calculated. It is higher for a composite inhibitor and increases with an increase in C_{KBr}. The isotherm of adsorption in θ – lg$C$ coordinates is *S*-shaped, which is realized in the presence of interacting particles in the adsorption layer. It is known that this isotherm is realized in the presence of interaction of particles in the adsorption layer [3]. Indeed, for the HCl + SAS + KBr system under study, the adsorption of organic cations occurs over the surface, on which there are already adsorbed chlorine anions. An electrostatic attraction is realized between surfactant cations and chlorine anions. It increases with additional adsorption of bromine anions, the greater the higher the C_{KBr}. Comparison of gravimetric and capacitive measurements ($Z > \theta > 0$) allowed us to determine a mixed blocking-activation mechanism of inhibition of steel corrosion in HCl.

References

[1] Shpanko S. P., Sidorenko E. N., Semenchev A. F., Lyanguzov N. V., Anisimova V. A. // *Physicochemistry of the Surface and Protection of Materials*. **53**(2), 210 – 217, 2017 (In Russian).

[2] Sidorenko E. N., Shpanko S. P., Prikhodko G. I. // *Izvestiya RAS. Ser. Fiz*., **80**(11), 1547 – 1549, 2016 (In Russian).

[3] Damaskin B. B., Petri O. A., Batrakov V. V. *Adsorption of Organic Compounds on Electrodes*. Moscow, Science, 1 – 332, 1968 (In Russian).

Crystal Textures and Anisotropic Electromechanical Properties of Layered Piezoceramics Based on Bismuth-Sodium Titanate System

I. A. Shvetsov*, N. A. Shvetsova, E. I. Petrova, M. A. Lugovaya, O. A. Bunina, M. A. Marakhovsky, A. N. Rybyanets

Southern Federal University, Rostov-on-Don, 344090, Russia

*wbeg@mail.ru

Ferroelectrics based on bismuth-containing compounds with a perovskite-like structure (BCPS) are characterized by high values of the Curie point temperature, but low electromechanical and piezoelectric activity, associated with two-dimensional limitation of possible rotations of the spontaneous polarization vector of crystallites. To improve the piezoelectric and electromechanical properties, it was proposed to use textured piezoelectric BCPS ceramics with a controlled degree of preferred orientation of crystallites. The aim of this work was to reveal the regularities of the formation of crystal textures and anisotropic electromechanical properties of layered bismuth-containing piezoceramics. Piezoceramics based on solid solutions of the bismuth-sodium titanate system (NBT) was chosen as the object

of the study. Textured piezoelectric ceramics were obtained by uniaxial hot pressing at the optimal sintering mode. The degree of crystallite orientation was evaluated using X-ray diffraction analysis (XRD) using DRON-7 diffractometer (Co-Kα radiation) and scanning electron microscopy (JEOL JSM-6390LA). Diffraction patterns obtained for textured samples from surfaces, the normal $\boldsymbol{n}$ to which is parallel ($\boldsymbol{n} \parallel \boldsymbol{P}$) and perpendicular ($\boldsymbol{n} \perp \boldsymbol{P}$) to the pressure axis $\boldsymbol{P}$, were compared with the diffractogram of a reference, namely an untextured powder of the same composition. To study the anisotropy of electromechanical properties, experimental disk-shaped samples were cut from the hot-pressed blocks and polarized parallel ($\boldsymbol{E} \parallel \boldsymbol{P}$) and perpendicular ($\boldsymbol{E} \perp \boldsymbol{P}$) to the hot-pressing axis ($\boldsymbol{P}$). The measurements of the dielectric, piezoelectric, and electromechanical parameters of the samples were carried out at the radial and thickness modes of oscillations of piezoceramic discs in accordance with the IEEE standard, as well as using the method of analysis of resonance spectra (PRAP). It was found that textured NBT piezoceramics of the cut ($E \perp P$) is characterized by high piezo- and electromechanical characteristics $d_{33} = 35\times10^{-12}$ C/N, $k_t = 0.35$, along with a high anisotropy of the indicated properties $d_{31} = -2.28\times10^{-12}$ C/N, $k_p = 0.03$, as well as low elastic losses and dispersion of ultrasonic waves over a wide frequency range. The Curie point temperature of NBT- based piezoceramics, found from the temperature dependence of the dielectric constant, is 920 K. It was shown that the features of the domain structure and the degree of crystallite orientation determine the anisotropy of the piezoelectric and electromechanical properties of NBT piezoceramics. The textured NBT piezoceramics with a unique combination of high and essentially anisotropic electromechanical and piezoelectric characteristics and high Curie point temperature can be used in high-frequency ultrasonic transducers for medical equipment and non-destructive testing.

Acknowledgement. The study was financially supported by the Ministry of Science and Higher Education of the Russian Federation (scientific project No. 0852-2020-0032 (BAS0110/20-3-08IF)).

A New Method of Spatial and Temporal Localization of Ultrasonic Therapeutic Effects Using Cylindrical Transducers of Ultrasonic Standing Waves

N.A. Shvetsova[1]*, N.A. Kolpacheva[2], I.A. Shvetsov[1], A.N. Reznichenko[1], A.N. Rybyanets[1]

[1]Southern Federal University, Rostov-on-Don, 344090, Russia
[2]Don State Technical University, Rostov-on-Don, 344000, Russia

*yfnfif_71@bk.ru

Currently, ultrasound methods are used in almost all areas of medical practice and are among the most important modern methods of diagnosis and treatment. Ultrasound is used both for diseases diagnosis and for the effect of high-intensity focused ultrasound (HIFU) on blood vessels for the purpose of hemostasis, vein obliteration and local tissue ablation in the treatment of cancer and some cardiovascular diseases. The main advantages of HIFU therapy in comparison with other surgical methods of treatment are: non-invasiveness, no blood loss, no harmful chemical and radiation factors, the ability to control the processes occurring in the

area of the tumor focus during the procedure, and rapid patient recovery. One of the disadvantages of the HIFU method in the treatment of superficial and nearby organs of the patient is the small size of the area of ultrasound exposure and the large focal length. Thus, there is a need for biological tissue processing methods and devices, in which ultrasonic energy is applied to a patient in a safer, more efficient and more productive manner. The aim of this work is to develop new alternative methods of focused ultrasound for spatial and temporal localization of ultrasonic therapeutic effects using cylindrical standing waves for ultrasonic therapy of the superficial tissues of patients. In the result of the research and development carried out, the following results were obtained: (i) finite element and finite difference models of ultrasonic transducers and processes of formation of ultrasonic standing waves in biological tissues; (ii) results of theoretical calculations and numerical simulation of fields of ultrasonic standing waves in viscoelastic media; (iii) designs and prototype samples of ultrasonic transducers of cylindrical standing waves; (iv) results of physical modeling of the impact of ultrasonic standing waves on biological tissues, measurement techniques, ultrasonic and therapeutic phantoms (tissue or organ-substituting objects for visualization and measurement of ultrasonic exposure) and test benches; (v) results of ultrasonic transducers parameters and ultrasonic fields measurements in a 3D acoustic bath; (vi) results of experimental testing of the developed methods for spatial and temporal localization of ultrasonic exposure using ultrasonic transducers of cylindrical standing waves on therapeutic phantoms and *ex vivo* biological tissue samples. The results of the work will be used to create a new generation of ultrasound equipment, which will make it possible to widely apply modern methods of diagnostics and treatment of patients with non-invasive methods, promote the introduction of new competitive scientific and technical products to the market, develop world-class technologies, and develop new therapeutic standards.

Acknowledgement. The study was financially supported by the Russian Science Foundation grant No. 22-22-00710, https://rscf.ru/project/22-22-00710/ at the Southern Federal University.

A New Method of Spatial and Temporal Localization of Ultrasonic Therapeutic Effects Using Flat Ultrasonic Transducers with a Cooled Surface

N.A. Shvetsova[1]*, N.A. Kolpacheva[2], I.A. Shvetsov[1], A.N. Reznichenko[1], A.N. Rybyanets[1]

[1]Southern Federal University, Rostov-on-Don, 344090, Russia
[2]Don State Technical University, Rostov-on-Don, 344000, Russia

*yfnfif_71@bk.ru

HIFU therapy, based on the principles of local heating or mechanical destruction of biological tissues under the influence of high intensity focused ultrasound, has been successfully used to remove solid tumors in various areas of the body, as well as to stop bleeding, dissolve blood clots, treat joints, block nerve conduction and non-invasive liposuction. One of the disadvantages of the HIFU method in the treatment of the surface tissues of the patient and nearby organs is the small size of the area of ultrasound exposure and the large focal length. Realization of the potential of new ultrasound technologies requires the development of new,

more effective and safe methods for diagnosing the condition and effects on biological tissues, as well as ultrasound hardware for ultrasound therapy. The aim of this work is to develop new methods of spatial and temporal localization of the therapeutic effect, alternative to focused ultrasound, using various combinations of ultrasonic and thermal fields for complex ultrasound therapy of superficial tissues or nearby organs. The development is based on new designs of flat ultrasonic transducers with a controlled temperature of the radiating surface. As a result of the research and development carried out, the following results were obtained: (i) finite element and finite difference models of ultrasonic transducers and ultrasonic wave propagation processes in biological tissues; (ii) the results of theoretical calculations and numerical modeling of various combinations of ultrasonic and thermal fields of flat ultrasonic transducers with a cooled surface; (iii) designs and mock-up samples of flat ultrasonic transducers with a controlled temperature of the radiating surface; (iv) The results of physical modeling of ultrasonic impact on biological tissues, measurement methods, ultrasonic and therapeutic phantoms (tissue or organ replacing objects for visualization and measurement of ultrasonic impact) and test benches; (v) parameters of ultrasonic transducers and ultrasonic fields measured in a 3D acoustic bath; (vi) the results of experimental approbation of the developed methods of spatial and temporal localization of ultrasonic exposure using the superposition of thermal fields of flat ultrasonic transducers with a cooled surface on therapeutic phantoms and *ex vivo* biological tissue samples. The results of the work will be used to create a new generation of ultrasound equipment, which will make it possible to widely apply modern methods of diagnostics and treatment of patients with non-invasive methods, promote the introduction of new competitive scientific and technical products to the market, develop world-class technologies, and develop new therapeutic standards.

Acknowledgement. The study was financially supported by the Russian Science Foundation grant No. 22-22-00710, https://rscf.ru/project/22-22-00710/ at the Southern Federal University

The Relaxation Polarization Processes in Protective Organic Films

E. N. Sidorenko*, A. S. Bogatin, S. P. Shpanko, A. V. Shloma

Southern Federal University, Rostov-on-Don, 344006, Russia

*si-do-re@mail.ru

Organic materials have recently been of great interest, as they are the basis for the elemental base of various electronic devices of molecular electronics. We have obtained and studied protective films on the steel surfaces of a new organic compound and its mixtures with potassium bromide (KBr). Films with a new inhibitor differ in KBr concentration within C_{KBr} = (0.01 – 0.1) mol/l and formation time (t = 1 – 3 days). All investigated films, regardless of C_{KBr} and t, have a negative value of the real part of the complex electrical capacity C'. An experimental proof of this fact has been carried out. Measurements of parallel-connected measuring film with capacitors of different capacitance C_C were performed at different frequencies with the help of immitance meter E7-30. A family of curves $\lg|C_R| = f(\lg C_C)$ was obtained. At the intersection points of these curves with the abscissa axis, the resulting capacity C_R is zero. It is established that the studied films have a large through electrical conductivity G'. The value of electrical conductivity, as well as the C' modulus at low frequencies (LF), increase by more than an order of magnitude with an increase in uniaxial

compression of samples. The imaginary part of the complex electrical conductivity G'' is negative. The frequency dependence $G''(F)$ has a maximum, the modulus of which also increases with an increase in pressure. In the frequency dependences of the capacitance C' obtained at different pressures, there are two regions of dielectric dispersion. The first dispersion is located at the LF ($F < 10^2$ Hz), and the second is in the high frequency region. The start of high frequency dispersion observed for films, measured at low pressure at frequencies $F \geq 10^5$ Hz is shifted by an order of magnitude to the LF region as the pressure rises to 3×10^5 Pa. The specific frequency dependence of the electrical capacity C', as well as the presence of a maximum in the frequency dependence of the imaginary part of the electrical conductivity G'', suggest that the cause of the negative capacitance in the films under study is the process of relaxation polarization development with an inverse vector of the electric field strength. However, the real part of the electrical conductivity G' in these films decreases with decreasing frequency and reaches saturation. An additional factor affecting the occurrence of negative capacitance is the hopping mechanism of charge carrier transfer in the studied films. This is indicated by the areas of volt-ampere characteristics with negative differential resistances in anticorrosive organic films [1]. When voltage is applied to the sample, charges are accumulated on numerous traps of the organic compound with their subsequent emptying. The resulting current flowing through the sample lags behind the applied voltage in phase, which is a sign of the inductive nature of the film reactive resistances or negative C' values.

Reference

[1] Shpanko S. P., Sidorenko E. N., Semenchev A. F., Lyanguzov N. V., Anisimova V. A. // *Physicochemistry of the Surface and Protection of Materials*. **53**(2), 210 – 217, 2017.

The Relationship of Morphology and Protective Properties of Organic Film Coatings

E. N. Sidorenko, M. A. Bunin, S. P. Shpanko

Southern Federal University, Rostov-on-Don, 344006, Russia

*si-do-re@mail.ru

The surface morphology of organic protective films was studied by atomic force microscopy (AFM) using a Veeco Multimode VS scanning probe microscope. The images were processed using the built-in software. 2D and 3D AFM images of the films surface and histograms of the height distribution of structural formations were obtained. The values of the arithmetic and geometric roughness of the coatings, as well as the distribution of the heights of structural formations in the sections of the scan surface are determined. Fourier filtering of images was used to highlight small-sized details of the surface relief. The films on the surface of the St-3 steel samples were obtained from an inhibited sulfuric acid solution. The composite inhibitor based on an organic compound of the imidazole class and thiocyanate anions was used. The concentration (C_{KCNS}) of thiocyanate anions varied within (0.01 – 0.09) mol/l, and the time of formation of the protective layer t was from 1 to 3 days. 1M H_2SO_4 was used as a medium. The concentration of the organic inhibitor was equal to 10^{-3} mol/l. The protective properties of the inhibitor, expressed by a corrosion inhibition coefficient K, for various values of C_{KCNS} and t, were studied. It was found that the protective effect of the organic compound significantly increases with the introduction of thiocyanate anions and an increase in the time t. The extreme nature of the $K - C_{KCNS}$ dependence was found. This fact is associated with

different mechanisms of the interaction of KCNS with the steel surface, depending on its concentration. The study of the surface morphology of the films indicates the islet mechanism of their growth. Schematically, the process of their growth can be represented as follows. Small islands (critical nuclei) are formed from metastable clusters of organic molecules. Subsequently, their three-dimensional growth and coalescence occurs. Crystalline cone-shaped globules are formed, the number, size and shape of which depend on C_{KCNS} and t. The globules cover the entire surface of the steel substrate and have a great protective effect. The surfaces of the films with high values of C_{KCNS} and t are covered with conglomerates of intergrown crystalline 3D formations of a globular structure. In photos of a scanning electron microscope, crystalline conglomerates look like cells separated by boundaries. The dimensions of the cells, as well as their depth, width, and the presence or absence of boundaries breaks, depend on the experimental conditions. Thus, an increase in t contributes to the formation of large cells separated by clear boundaries. On the contrary, with an increase in C_{KNCS}, films with smaller cell sizes and local discontinuities of shallow boundaries are deposited. Thus, the protective properties of organic coatings are determined by the morphology of the formed precipitation. A high degree of protection is provided by thickened, multilayer coatings of large intergrown crystal globules forming big cells with clear outlines of the boundaries.

Research of the Microwave Properties of the PZTL Relaxor Piezoceramics

E. N. Sidorenko[1]*, A. G. Rudskaya[1], M. E. Agarkova[2], D. I. Rudsky[1], A. V. Panova[1]

[1]Southern Federal University, Rostov-on-Don, 344006, Russia
[2]Hydrometeorological college, Rostov-on-Don, 344025, Russia

* spsha@mail.ru

PLZT ceramic compounds with different lanthanum content are of particular interest for applied and fundamental research. They exhibit a number of abnormal properties due to the relaxor state. PLZT ceramic compounds are characterized by a wide frequency-dependent maximum of the imaginary part of the complex permittivity and a complex phase diagram. They are characterized by a morphotropic phase boundary between high-temperature (R_{HT}) and low-temperature (R_{LT}) rhombohedral phases. This variety of properties of PLZT ceramics is attributed to the presence of polar nanoparticles in them, which are the cause of spontaneous polarization. In this work, X-ray diffraction studies were performed and lattice parameters of PLZT (8/65/35) were determined. AFM images of the surface of ceramic samples were obtained. The energy absorption spectra in the electromagnetic field of the microstrip line were taken in the frequency range of 3.2 – 12 GHz for PLZT piezoceramic samples. The samples under study were plane-parallel plates with an area of 1 – 0.8 cm^2 and a thickness of 400 μm. The spectrum contains two huge ($L \geq -40$ dB) sharp resonance-type maxima in the region of lower 4 – 5 GHz and higher 10 – 11 GHz frequencies. These maxima shift significantly to higher frequencies during aging of piezoceramic samples. These changes in the absorption spectrum in the range 3.2 – 5.6 GHz when heating PLZT samples were investigated. It was found that with increasing temperature from room temperature to 90 °C, the absorption maximum observed at a frequency of 5 GHz shifts to a lower frequency range by 0.6 GHz, and absorption decreases by 15 dB. When further heating the sample, the position of the maximum in the spectrum and its magnitude did not change. At the same time, it was

found that at a frequency of 4 GHz at t = 90 °C a new maximum is born and with increasing temperature to 160 90 °C reaches an absorption level of 35 dB. The microstrip line with the PLZT sample under study on its surface forms a dielectric resonator antenna capable of radiating electromagnetic energy. We obtained energy emission spectra of electric and magnetic fields at different heights from the surface of the sample. The presence of large maxima in the microwave absorption spectra, changes in their frequencies and absorption levels depending on external factors are interpreted in terms of resonance processes. PLZT piezoceramics crystallites contain ensembles of elements of the domain structure (twin domain walls) capable of making forced oscillations in the electromagnetic field and selectively absorbing energy, converting it into heat. This view is confirmed by the visually observed dynamic nature of the spectra when we examine the maxima in a narrow frequency band in more detail.

Acknowledgement. The study was carried out with the financial support of the Ministry of Science and Higher Education of the Russian Federation (State task in the field of scientific activity, scientific project No. 0852-2020-0032), (BAZ0110/20-3-07IF).

Resonance Absorption Spectra of Multiferroic Ceramics of Lead Ferrotungsten

E. N. Sidorenko*, V. G. Smotrakov, M. A. Marakhovskiy, I. I. Natkhin, A. V. Shloma, V. S. Saburova

Southern Federal University, Rostov-on-Don, 344006, Russia

*spsha@mail.ru

$PbFe_{2/3}W_{1/3}O_3$ (PFW) is the multiferroic ferrovoltaframate of lead exhibits relaxor with antiferromagnetic properties. Multiferroics have high dielectric permittivity values and increased dielectric and magnetic losses. Therefore, they are promising for use as radio-absorbing materials (RAMs). The RAMs are widely used to protect radio equipment and people from electromagnetic radiation, to reduce the radar visibility of objects, and to protect computer information processing systems from unauthorized access. We obtained ceramic samples of PFW by the method of spark plasma sintering at 700 °C. Their domain structure was studied using an electron microscope. These ceramics are characterized by a fine-grained porous structure. The grains are well faceted and have a size of 1 – 2 μm. The irregularly distributed large pores, which significantly affect the strength of the ceramic samples, are observed. The absorption and emission spectra of electromagnetic energy of the PFW multiferroic in the frequency range 3.2 – 12 GHz were studied using a microstrip line as a measuring cell. The same measurement technique was used as in earlier works [1, 2]. The measured samples without electrodes had a cylindrical shape with a diameter of 1 cm and a height of 0.1 cm. The average level of microwave energy absorption is (15 – 20) dB. The absorption spectra $L(f)$ have a resonant character. They, as a rule, along with a large number of small maxima, contain 3 – 4 large (up to 30 – 40 dB) maxima with bandwidths of (1 – 0.5) GHz. Uniaxial compression of samples up to 3×10^5 Pa contributes to the disappearance of previously existing maxima and the appearance of new ones with higher resonance frequencies. Heating samples to 150 °C causes the appearance of a large number of narrowband maxima with absorption levels of (15 – 20) dB. As the temperature increases, the

large maxima (35 – 40) dB shift to the high frequency region and new lower frequency maxima are formed. Three-mode spectra of integral emission of electric field strength and magnetic field induction at different heights from the sample surface were obtained. When probing the field with a pin-type antenna, the detected signal measured by a digital voltmeter B7-38 without an additional amplifier was fixed at heights up to 60 mm. At room temperature, a constant magnetic field did not change the PFW absorption spectra either because of the weak magnetoelectric effect in the studied multiferroics or because of the small value of the field induction (B = 0.375 T). The absorption spectra of PFW with a large number of resonance-type maxima, sensitive to external influences, indicate the existence in this multiferroic groups of oscillators with different natural frequencies. Domain walls of mechanical twins of PFW polar nanoregions (clusters) can be considered as oscillators. They are capable of making elastic vibrations and absorbing energy while in an electromagnetic field when their natural frequency coincides with the frequency of the field.

References

[1] Sidorenko E. N., Chan Thi Beat Ngoc, Prikhodko G. I., Natkhin I. I., Shloma A. V., Kharchenko D. G. // *Journal of Advanced Dielectrics*, **10**(01n02), 2060020, 2020, DOI: 10.1142/S2010135X20600206.

[2] Sidorenko E. N., Kabirov Yu. V., Nathin I. I., Privalova T. Y., Belokobylskiy M. V., Klochnev A. M. // *Radiation and Scattering of Electromagnetic Waves (RSEMW)*, 269 – 272, 2021, https://ieeexplore.ieee.org/xpl/conhome/9493854/proceeding

Composite Materials Ferropiezoelectric Ceramics - Polymer for Hydroacoustic Receivers

V. G. Smotrakov, V. V. Eremkin, E. I. Sitalo, N. V. Malomyzheva

Research Institute of Physics Southern Federal University, Rostov-on-Don, 344090, Russia

*sitalo@sfedu.ru

The object of research is composite materials of ferropiezoelectric ceramics, namely a polymer with a connectivity type of 0-3, which is a ceramic powder uniformly distributed in a polymer matrix. The purpose of the work is to study the processes of interfacial interactions, their influence on the piezoelectric properties in highly elastic composite structures, to establish the patterns that determine the volume-sensitive piezoelectric characteristics of composites, and to create effective piezoelectric materials for hydroacoustic receiving devices. In the process of work, the development of a method for obtaining anisotropic ferropiezoelectric ceramics, the development of methods for the preparation of perfect ceramic powders and composite materials based on thermoplastic fluoropolymers, and the study of composite materials based on lead-calcium titanate were carried out. In the result of the study, the dependences of the hydrostatic parameters of the composites on the degree of filling, particle size distribution, piezoelectric anisotropy of the active phase, and the elastic properties of the polymer matrix were established. Composite materials are based on ceramics of the TS-TK system and thermoplastic fluoropolymers F-2ME, F-62, F-2N (JSC Plastpolimer, St. Petersburg) with a degree of filling with a ceramic phase from 30 to 60 % vol. The dependences of the hydrostatic piezoelectric moduli g_h and d_h, and the quality factor $g_h d_h$ on the degree of filling of the composite for polymers F-62 and F-2ME with different average sizes of ceramic particles are plotted. It has been established that the maximum values $g_h = 119.1 \times 10^{-3}$ V·m/N and the

quality factor $g_h d_h$ = 6074×10^{-15} m^2/N are achieved for a polymer with a higher elastic compliance (F-62) at a degree of filling of 60 % vol. and the use of granular filler. These results correspond to the best foreign literature data [1, 2] for composite materials "ceramic-polymer" with the type of connectivity 0-3.

Acknowledgement. The work was supported by the Ministry of Science and Higher Education of the Russian Federation [State task in the field of scientific activity, scientific project No. 0852-2020-0032 (BAZ0110/20-3-08IF)].

References

[1] Han K., Safari A., Riman R. E. Colloidal processing for improved piezoelectric properties of flexible 0-3 ceramic-polymer composites // *J. Amer. Ceram. Soc*. **74**(7), 1699 – 1702, 1991.
[2] Gui C., Baughman R. H., Iqbal Z., et al. Improved piezoelectrics for hydrophone applications based on calcium-modified lead titanate/poly(vinylidene fluoride) composites // *Sensors and Actuators A*. **65**, 76 – 85, 1998.

Investigation of Oscillations of a Bimorph Plate Taking into Account the Inhomogeneous Distribution of Mechanical Properties over the Thickness

A. N. Soloviev[1,2]*, V. A. Chebanenko[3]**

[1]Don State Technical University, Rostov-on-Don, Russia
[2]Vorovich Mathematics, Mechanics and Computer Science Institute, Southern Federal University, Rostov-on-Don, Russia
[3]Federal Research Center "Southern Scientific Center of the Russian Academy of Sciences", Rostov-on-Don, Russia

*solovievarc@gmail.com; **valera.chebanenko@yandex.ru

An applied theory of vibrations of a bimorph plate is developed, which takes into account the inhomogeneous distribution of mechanical properties over the thickness in piezoelectric layers. A similar distribution can occur during the manufacturing process when the electrode is burned into the surface. This inhomogeneity was modeled as a linear or quadratic dependence of the components of the tensor of elastic constants on the thickness. Based on the developed theory, a plane problem of harmonic vibrations of a three-layer plate was studied, the outer layers of which have electroelastic properties and a non-uniform distribution of the values of elastic coefficients, and the inner layer is purely elastic. Within the framework of the problem, it was assumed that the electric potentials at the external and internal electrodes are known, and the distribution of the electric potential along the length in the middle of the layer is an unknown function. To simplify the problem, Kirchhoff's hypotheses were adopted. Based on the variational principle and the quadratic potential distribution adopted in the work, a system of differential equations and boundary conditions was obtained. COMSOL Multiphysics provides the ability to solve general partial differential equations. This made it possible to develop a two-dimensional finite element model, which takes into account the inhomogeneity of the thickness distribution. On the basis of the model obtained, comparisons were made between the obtained applied theory and the results of finite element analysis.

Acknowledgement. The study was supported by a grant from the Russian Science Foundation No. 22-11-00265 at the Southern Federal University.

Modeling Flexoelectric Bimorph Oscillations in the COMSOL Multiphysics Package

A.N. Soloviev[1,2]*, V.A. Chebanenko[2,3]*, A.N. Yudin[2,3,4]****, I.A. Parinov[2]****

[1]Don State Technical University, Rostov-on-Don, Russia
[2]Vorovich Mathematics, Mechanics and Computer Science Institute, Southern Federal University, Rostov-on-Don, Russia
[3]Federal Research Center "Southern Scientific Center of the Russian Academy of Sciences", Rostov-on-Don, Russia
[4]Platov Southern Russian State Polytechnic University, Novocherkassk, Russia

*solovievarc@gmail.com; **parinov_ia@mail.ru; ***valera.chebanenko@yandex.ru; ****andryudin1997@gmail.com

The flexoelectric effect is the occurrence of electric polarization in solids during their bending or any other form of inhomogeneous deformation. Unlike piezoelectricity, which occurs in a material with a certain symmetry, the flexoelectric effect appears in all dielectrics. However, the values of flexoelectric potentials are much lower than piezoelectric ones. Nevertheless, this effect is of research interest due to the fact that it is observed not only in solids, but also in polymers, liquid crystals, and biological tissues. The plane problem of steady bending vibrations of a cantilever consisting of two identical dielectric layers with flexoelectric properties is considered. Large surfaces of the layers were electroplated, one of the ends of the beam was clamped, while the other was free. A distributed mechanical load acted on the upper boundary of the beam. All other surfaces were free from mechanical stresses. The electric potential was equal to zero at the inner electrode, while at the outer electrode it was unknown. The side surfaces were considered isolated from the electric field. COMSOL Multiphysics does not support the flexoelectric effect, but it is possible to solve partial differential equations written in general form. Therefore, using the Cauchy equation of motion, which takes into account the stress tensor of a higher order, the electrostatics equation, as well as the constitutive relations for the material with the flexoelectric effect, a model of cantilever bending vibrations was built. On the basis of this model, the distributions of electric and mechanical fields were obtained, and a modal analysis was also carried out.
Acknowledgement. The study was supported by a grant from the Russian Science Foundation No. 21-19-00423 at the Southern Federal University.

Modeling of a Piezoelectric Generator with Porous Properties of Piezoelements

A. N. Soloviev[1,2], A. V. Cherpakov[1,2], I. A. Parinov[1]

[1]Southern Federal University, Rostov-on-Don, Russia
[2]Don State Technical University, Rostov-on-Don, Russia

*alex837@yandex.ru

When operating piezoelectric generators (PEGs), it is possible to use piezoelectric elements having different porosity. The question remains how much the output power of such a

generator can be changed. Using the example of [1], the simulation of vibrations of a cantilever-type PEG with active fixing, which has piezoelectric elements with the effective properties of piezoceramics with a certain porosity, is considered. The simulation was carried out in the FE ANSYS software. As part of the simulation, it is possible to consider variations in porosity ranging from 0 to 80%. A modal harmonic analysis of the calculations was carried out. When modeling, calculations of 10 vibration modes were carried out. The most effective were modes 1 and 3 of vibrations, which had bending modes of vibration in the plane of least rigidity. The analysis showed that when comparing the output characteristics of ceramic material with 0% and 80% porosity, the output voltage of the structure decreased by 31 times, and the output power under load decreased by more than 1000 times. Cylindrical piezoelectric elements are proved to be more effective in comparison, located by pinching the PEG. When comparing the output characteristics of these ceramic structures to a structure with porosity 0% and 80%, the voltage changed by a factor of 6.8, while the power changed by a factor of 47, respectively.

Acknowledgement. This research was funded by the grant No. VnGr-07/2020-04-IM from the Southern Federal University (Ministry of Science and Higher Education of Russian Federation).

Reference

[1] Soloviev A., Parinov I., Cherpakov A. Modeling the Cantilever Type PEG with Proof Mass and Active Pinching by Using the Porous Piezoceramics with Effective Properties. In: *Physics and Mechanics of New Materials and Their Applications - Proceedings of the International Conference PHENMA 2020*, Springer Proceedings in Materials, Ivan A. Parinov, Shun-Hsyung Chang, Yun-Hae Kim, Nao-Aki Noda (Eds.). Springer Nature, Cham, Switzerland, **10**, 481– 493, 2021.

Applied Theory of Bending Vibrations of a Piezomagnetoelectric Bimorph in an Alternating Magnetic Field

A. N. Soloviev[1,2]*, Do Thanh Binh[2], V. A. Chebanenko[3], E. V. Kirillova[4]*****

[1]Don State Technical University, Rostov-on-Don, Russia
[3]Federal Research Center "Southern Scientific Center of the Russian Academy of Sciences", Rostov-on-Don, Russia
[4]RheinMain University of Applied Sciences, Wiesbaden, Germany

*solovievarc@gmail.com; **valera.chebanenko@yandex.ru;
***Evgenia.Kirillova@hs-rm.de

This work is devoted to the study of transverse vibrations of a bimorph, consisting of two piezomagnetoelectric layers, located in an alternating magnetic field. On the basis of the applied theory of oscillations of a multilayer plate, taking into account the nonlinear distribution of the electric and magnetic potential in the piezoactive layers, both in the longitudinal and transverse directions, the stress-strain state, electric and magnetic fields of the cantilever bimorph have been studied. The electric potential is assumed to be zero at all electrodes, while the magnetic potential is equal to zero at the inner boundary and is unknown at the outer ones. Therefore, the distributions of the electric and magnetic potentials in the middle of the layer are assumed to be unknown functions, and in the case of a magnetic potential, the distribution at the outer boundary is also a function to be found. In the problem,

Kirchhoff's hypotheses for mechanical characteristics were accepted. Using the variational principle and the quadratic dependence of the electric and magnetic potentials over the thickness of the piezoactive layers accepted in the work, a system of differential equations and boundary conditions was obtained. The resulting boundary-value problem was solved by numerical methods. Comparison of the calculation results according to the proposed theory with the plane problem solved in the finite element (FE) package Comsol Multiphysics in the low-frequency region showed that the error in finding the characteristics of the mechanical and magnetic fields is less than 1%. In turn, when determining the electric field, the difference was of the order of 5%, with the exception of the clamping area. The study of the size of the area of this discrepancy depending on the relative thickness of the bimorph showed that its size is of the order of the thickness of the bimorph. In this case, the value of the output potential, calculated according to the proposed theory and FE, differs by 1.7%. It was found that this discrepancy is due to the fact that in applied theory, due to the introduction of Kirchhoff's hypotheses, tangential stresses disappear, while they are present in the FE model. The shear stress distribution diagram indicates that these stresses are negligibly small everywhere except for the ends of the cantilever, where their extrema are observed. Thus, the proposed applied theory makes it possible to determine the output characteristics of the considered bimorph with a sufficient degree of accuracy. On the basis of the conducted numerical experiments, it was shown that the developed applied theory of oscillations of piezomagnetoelectric bimorphs is described with a high degree of accuracy due to the introduced hypotheses.

Acknowledgement. The study was supported by a grant from the Russian Science Foundation No. 22-11-00302 at the Southern Federal University.

Analysis of the Frequency Response of an Electromagnetoelastic Bimorph with Regard to Damping

A. N. Soloviev[1,2]*, Do Thanh Binh[2], V. A. Chebanenko[3]*, I. A. Parinov[2]****

[1]Don State Technical University, Rostov-on-Don, Russia
[2]Vorovich Mathematics, Mechanics and Computer Science Institute, Southern Federal University, Rostov-on-Don, Russia
[3]Federal Research Center "Southern Scientific Center of the Russian Academy of Sciences", Rostov-on-Don, Russia

*solovievarc@gmail.com; **parinov_ia@mail.ru; ***valera.chebanenko@yandex.ru

A layered composite consisting of alternating piezoelectric and piezomagnetic layers is considered. Such a layered package can be used as a piezoactive layer in a bimorph structure, in which these layers are glued to the middle passive layer, that is to the substrate. The presented piezoelectric element can be used as a piezoelectric generator (PEG) for an energy harvesting device operating in an external alternating magnetic field. An alternating magnetic field is associated with some electromagnetic device or may be artificial due to the rotation of some mechanism on which permanent magnets are located. Damping must be taken into account in order to calculate the actual characteristics of the PEG, such as the beam displacement and the output electric potential, as well as to plot their frequency response characteristics. The theory is based on the plane problem of steady bending vibrations of a plate. The plate consists of two piezoactive elements, which are two identical layers made of

a composite electromagnetoelastic material. It is assumed that the considered composite material is a package consisting of alternating piezoelectric and piezomagnetic layers. Therefore, to simplify the problem, when describing the layers of a piezoactive bimorph, we will use the effective physical constants of a multilayer package. The presented problem is solved within the framework of the linear theory of electromagnetoelasticity. Applied theory is based on hypotheses about the distribution of mechanical, electric and magnetic fields using the variational principle. Damping is introduced by taking into account mechanical losses associated with the elasticity tensor. All unknown variables are assumed to be complex-valued. The resulting system of equations and boundary conditions consists of real and imaginary parts. Within the framework of the constructed theory, the problem of finding the frequencies of the plate resonances is solved, the values of the mechanical, electrical and magnetic characteristics of the field, as well as their frequency response characteristics, are calculated.

Acknowledgement. The study was supported by a grant from the Russian Science Foundation No. 21-19-00423 at the Southern Federal University.

Modeling of the Interaction of Elastic Haptic Parts of an Intraocular Lens with a Capsular Lens Sac

A. N. Soloviev[1]* A. N. Epikhin[2], D. V. Krasnov[1]

[1]*Don State Technical University, Rostov-on-Don*
[2]*Rostov State Medical University, Rostov-on-Don*

*solovievarc@gmail.com

Cataract is a clouding of the lens of the eye, which leads to a decrease in vision. Cataracts often develop slowly and can affect one or both eyes. Signs of cataracts include faded colors, blurry or double vision, halos around a light source, vision problems at night, as well as with intense lights. This can cause problems with driving, reading, and face recognition. This type of visual impairment causes half of all cases of blindness and 33 % of visual impairments worldwide. Approximately twenty million people have gone blind due to cataracts. This is the cause of approximately 5 % of blindness in the world. Cataract blindness occurs in approximately 10 – 40 per 100,000 children in developing countries and 1 – 4 per 100,000 children in developed countries. An intraocular lens implanted into the eye for the treatment of diseases such as cataracts or myopia. Most often, lenses consist of a small plastic plate with side posts called haptics, which serve to hold the lens in place in the capsule bag of the eye. The aim of the work is to develop a project of a bioptic complex that simulates the natural accommodative properties of the lens of the eye using a computer simulation method. Computer modeling was performed using the ANSYS software package. The models were created using SpaceClaim CAD. polymethylmethacrylate was chosen as the material, because unlike silicone lenses, in cases of turbidity, they often become cloudy at the edges, without violating the optical properties of the lens. Mathematical modeling was performed using the finite element method, which is essentially a method of approximate numerical solution of physical problems. Which is based on two main ideas: discretization of the object under study into a finite set of elements and piecewise-element approximation of the functions under study. The finite element method leads to a ribbon sparse structure of the matrix of coefficients of the resolving system of equations. The body subject to deformation is divided into finite

elements. In the result of the breakdown, a grid is formed from the borders of the elements. The intersections of these boundaries form nodes. Additional nodal points can be created on the borders and inside the elements. The discrete model should cover the area of the object under study well enough. Loads were applied to which the lens would presumably be subjected in the lens equal to 0.4 MPa and boundary conditions were set limiting movement along the edges of the lens and contacts between the lens and the lens. The solution of the problem consists of three stages. The first stage is pressing the haptic parts to the lens, which is located inside the capsular sac of the lens (Fig. 1).

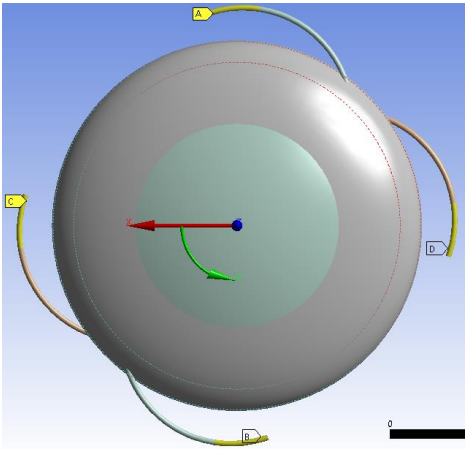

Fig. 1

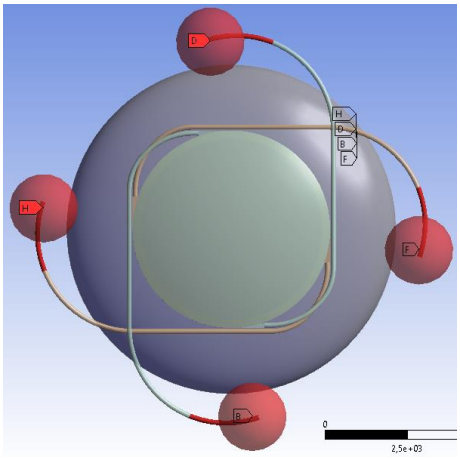

Fig. 2

The second stage is the implementation of internal contact of the haptic parts with the lens bag (Fig. 2). The third stage is the application of loads to the outer surface of the capsule sac of the lens, which simulate the action of the muscles of the eye. (Fig. 3). The result of this study confirm that it is possible to create an accommodating complex simulating the natural accommodation of the eye. The models are deformed according to the assumptions and their optimal preliminary shape has been established. The obtained models are suitable for further work on their optimization, the maximum displacements do not exceed the maximum displacements specified biologically.

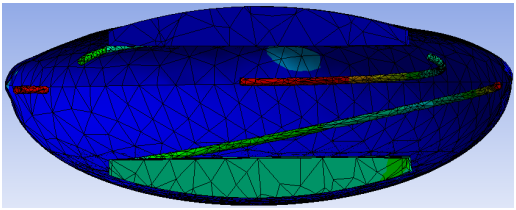

Fig. 3

Acknowledgements. This research was supported by the Government of Russia grant No. 14.Z50.31.0046.

Simulation of the Keratoprosthesis with a Functionally Gradient Layer in FEM Package FlexPDE

A. N. Soloviev[1]*, N. I. Glushko[1] A. D. Alekseeva[1] A. N. Epikhin[2]

[1]*Don State Technical University, Rostov-on-Don*
[2]*Rostov State Medical University, Rostov-on-Don*

*solovievarc@gmail.com

In our time, the number of blind people is constantly growing according to WHO, their number worldwide is approximately 39 million, and people with poor eyesight are about 246 million, moreover, they quickly lose it completely as a result of diseases, poor healing or unsuccessful surgical interventions. In Russia, the number of registered visually impaired and blind patients exceeds 218 thousand people. Of these, about 22% are young people of working age, respectively, almost every fifth inhabitant of Russia suffers as a result of the progression of one or another ophthalmic disease. This leads to a constant increase in the number of blind citizens in our country. Corneal ulcer is one of the most common causes of this. This disease is often caused by the herpes simplex virus, as well as fungi and bacteria. With a rapid, acute course of this disease, the only method of restoring vision is corneal transplantation. Transplantation of donor cornea and artificial keratoprostheses is currently widely used and is the most effective method for treating ophthalmic diseases leading to the formation of leukomas. The use of donor grafts in the treatment is often quite problematic, because may cause rejection of the donor material. This postoperative complication will cause tissue necrosis (complete or partial rejection), which is fraught with repeated surgical intervention

or a long implantation time. In addition, in the result of the growth of such patients, the demand for transplanted tissues is constantly growing, that is eye transplant banks cannot keep up with the growing demand for donor tissue. This is provoked by the age restrictions of the population. The shortage of donor tissue is a continuing concern for shortages in the global medical community. This gives rise to the need to develop alternative developments that can replace the donor cornea. That is why the interest of the scientific and medical world community in the development of artificial structures has recently been growing. Now such structures are made from various synthetic, biocompatible artificial materials that can replace living biological tissues functionally. Gradually, structures appear and are used that can replace the cornea without compromising the visual function of the eye [1, 2]. The human eye has a rather complex structure. The cornea is the transparent front part of the eye, covering the iris, the anterior chamber, and the pupil. Quite often, in the result of complications after ophthalmic diseases, mechanical damage, clouding of the cornea is possible, which contributes to a significant decrease in vision. The most common method of treatment in this case of damaged layers of the cornea is surgical intervention, namely keratoprosthetics. This explains the great interest in the development of tissue engineering products. Currently, attempts are being made to develop and improve keratoprostheses, which are necessary, when replacing the cornea or part of it with artificial tissues consisting of biocompatible materials. In the process of research, it was revealed that the corneal tissues have a multilayer structure, which causes anisotropy in the meridional, circumferential and perpendicular directions to its surface. Also, its mechanical properties are affected by the stroma, formed from many parallel plates (lamellae), which are woven from collagen fibers that is a transparent layer that makes up the main part of the cornea of the eye. The thickness of the stoma is almost 90 % of the entire thickness of the cornea. Therefore, when modeling the contact interaction of a keratoprosthesis with the natural tissues of the eye, the cornea should be considered as a multilayer shell, since its geometric parameters ($h/R < 0.1$) make it possible to represent the layers of the cornea as a shell. When creating a model, it is necessary to take into account that the cornea is uneven in thickness, and its outer surface is non-spherical. End-to-end keratoprosthetics, presenting implantation of the keratoprosthesis structure into the layers of the patient's cornea, requires a preliminary study of the stress-strain state of the contact of the cornea with the implant structure under the action of intraocular pressure. To do this, it is required to create a shell model based on several base surfaces. Such a model should be based on a kinematic hypothesis, according to which the spatial deformations of the shell will be determined by the deformations of several basic surfaces. Such a model will allow one to study deformations of the shell, taking into account shear, as well as changes in the thickness of the multilayer shell, depending on the conditions of interaction between the layers of the cornea and the keratoprosthesis. A keratoprosthesis is an artificial cell-free implant, the design feature of which is an optical element (lens) fixed in a frame, which is a thin-walled cylinder [3]. The bulk of modern keratoprostheses consists of an optical lens with a base. Which structurally can be made in the form of a ring with holes, ears, perforated crossed plates, amoeba-like legs, a wheel with spokes, etc. [4]. Keratoprostheses are being developed to replace the opaque part of the cornea. This replacement is necessary in case of irreversible damage to the cornea, which occurs as a result of mechanical injuries, burns, diseases or unsuccessful surgical intervention, complications in the healing process (rehabilitation) and as a result of the lack of a subsequent possibility of another method of recovery. For successful operation of a combined keratoprosthesis, its supporting part must withstand DVZh, while minimizing the deformation of the natural tissues of the eye. Also, it should be made a biocompatible material, structured in such a way that the fusion of the super- and underlying layers of the cornea occurs, which are separated during the indentation of the structure. The supporting part of

keratoprostheses can be made of the following materials: polyethylene, PTFE, nonreactive polymer, titanium or metal. Each material has its own advantages and disadvantages. Titanium and metal injure tissues much more, such prostheses more often than others cause the death of biological tissues. In turn, structures made of PTEF or polyethylene due to excessive flexibility and low mechanical strength are short-lived in operation and less reliable in fixing and holding a large optical structure. The operation to install a keratoprosthesis consists in excising a burr hole, through which the affected fragments of the cornea are removed. A keratoprosthesis support (haptic element) is inserted into the resulting hole, after healing, a lens is screwed into it (optical part of the structure) [3]. Rejection of an artificial implant (the most common complication after surgery) may occur in the result of the impact of design of the keratoprosthesis on the living tissues of the cornea, namely aseptic necrosis of biological tissues. Since the corneal tissues are subjected to deformation, which in the result makes it difficult or completely blocks the movement of vital substances in the layers in contact with the implant support [4]. Taking into account the data of the study, in this work we will assume that the biocompatibility of the material from which the supporting part of the keratoprosthesis is made. Its structure ensures the fusion of the layers of the cornea, separated during the introduction into the burr hole of the base of the keratoprosthesis. This study is conducted to consider the causes that affect the minimization of exposure, deformation of the natural tissues of the eye. It will contribute to the development of an implant model with a functionally gradient layer. This layer will be the connection of the hard part with the soft biological tissue, functionally preventing traumatization of the corneal layers by the artificial implant. Such a constructive connection is necessary due to the large discrepancy between the elasticity moduli of the corneal tissue and the materials from which the haptics and the optical element of the keratoprosthesis are made. The difference between them is three orders of magnitude. Based on the above reasons, it is important to carry out modeling and calculation of a keratoprosthesis with an intermediate functionally gradient layer, which will have heterogeneous, functionally gradient mechanical properties. In order to be able to produce artificial implants with a similar design, a study of the stress-strain state of the contact interaction of a keratoprosthesis with the boundary layers of the cornea is performed.

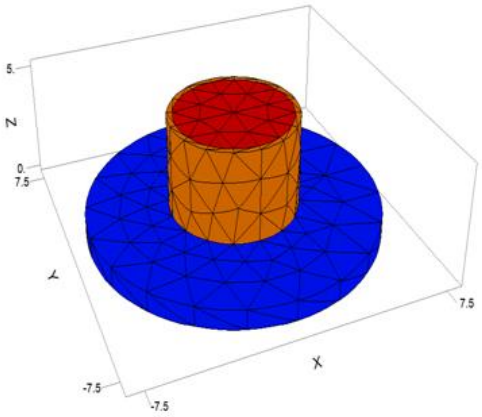

Fig. 1. Finite element 3D model of keratorothesis with a buffer layer

For the calculation, a 3D finite element model of keratorothesis was used, created in the finite element model constructor for partial differential equations FlexPDE (Fig. 1). The figure shows an artificial implant, whose optical part is of 6 mm in diameter and 5 mm in height; support disk, has an outer diameter of 15 mm and a thickness of 0.9 mm with a functionally gradient layer of 5 mm in height and 0.3 mm in thickness, which has non-uniform mechanical properties. Next, we plan to calculate the displacements, the components of the stress tensor and the strain tensor. To obtain the dependences of the distribution of displacements and stresses at different values of IOP in the area under study, which will make it possible to create a more convenient and efficient design of the keratoprosthesis.

Acknowledgements. This research was supported by the Government of Russia, grant No. 14.Z50.31.0046.

References

[1] Glushko N. I., Epikhin A. N., Svein M., Solovyov A. N. Mathematical and computer modeling of the eye implant // *Mathematical Modeling and Biomechanics at the Modern University*, Divnomorskoye, May 27-31, 2019, Southern Federal University Press, 32, 2019.

[2] Solovyov A. N., Glushko N. I., Epikhin A. N., et al. Mechanical and finite element models of keratoprostheses of the cornea of the eye // *Advanced Engineering Research*. **20**(4), 350 – 359, 2020. https://doi.org/10.23947/2687-1653-2020-20-4-350-359

[3] Sooraj Hussain Nandyala. Collagen-Chitosan-Glycerol-HPMC Composite as Cornea Artificial Candidate // *Journal of Biomimetics, Biomaterials and Biomedical Engineering*, **42**,14 – 21, 2019.

[4] Soloviev A., Glushko N., Vasiliev A., Matrosov A., Swain M. To Determining the Mechanical Properties of the Eye Corne Based on the Contact Problem of Consolidation // *2nd Scientific-Practical Conference of Russian and Croatian Scientists in Dubrovnik*. Moscow: NUST "MISIS", 49 – 50, 2020.

Mathematical Modeling of Indentation of the Eye Cornea with a Flat Punch, Taking into Account the Pore Pressure

A. N. Soloviev[1]*, A. S. Lednov[1], C.-Y. Jenny Lee[2], Y.-M. Liu[3]

[1]Don State Technical University, Rostov-on-Don
[2]Department of Microelectronics Engineering, National Kaohsiung University of Science and Technology, Kaohsiung, Taiwan (R.O.C.)
[3]Department of Electric Communication Engineering, National Kaohsiung University of Science and Technology, Kaohsiung, Taiwan (R.O.C.)

*solovievarc@gmail.com

When developing prostheses of biological tissues based on preliminary mathematical modeling, it is necessary to know their mechanical properties; one of the ways to determine them is indentation. In the result of this process, the relationship between the force and the penetration depth can be established, the shape of the deformed surface can be determined, and in the case of inelastic deformation, the size of the imprint after the load is removed. These data can serve as additional information for solving the inverse coefficient problem, to which the described problem is reduced. As a model of soft biological materials, which are the prototype of the cornea of the eye, here we consider a poroelastic water-saturated medium, known in the literature as a model of consolidation or Biot. Within the framework of plane

deformation, a mathematical model of indentation of the cornea of the human eye is studied, in the form of a rectangular area with a total thickness of h = 543 μm, a length of L = 3000 μm, with a flat stamp of 500 μm long. Two different models were considered: a layered model that takes into account Young's modulus and Poisson's ratio, which are different for layers, and a model of a homogeneous water-saturated medium. Four types of boundary conditions for pore pressure under a flat die are considered. Moreover, three types of different mechanical conditions under the stamp during indentation were considered: (i) contact without friction, (ii) conditions, taking into account Coulomb friction, and (iii) rigid adhesion. Their influence on the relationship between the depth of its penetration and the contact force is studied. 12 problem statements were considered for different boundary conditions under the die for a model with different mechanical properties in the layers of the cornea of the eye (shear modulus and Poisson's ratio). Moreover, similar 12 settings were considered, but for a homogeneous model close to a porous sponge. The calculation was carried out in the FlexPDE finite element analysis complex. Graphs of the distribution of pore pressure in the layers during indentation and the dependence "force – depth of penetration of the stamp" were obtained, the forms of the deformed surface and their difference for a certain set of boundary conditions were determined. The calculation results for a model homogeneous poroelastic water-saturated medium can be compared with a natural experiment. In the result of this comparison, the most adequate set of boundary conditions will be selected. This set of boundary conditions will be used to solve the inverse coefficient problem based on the results of a natural experiment on the cornea.

Acknowledgements: This research was supported by the Government of Russia grant No. 14.Z50.31.0046

Numerical Simulation of Relative Humidity in a Vehicle Cabin

A. N. Soloviev[1]*, I. A. Panfilov[1], O. N. Lesnyak[1], C.-Y. Jenny Lee[2], Y.-M. Liu[3]

[1]Don State Technical University, Rostov-on-Don
[2]Department of Microelectronics Engineering, National Kaohsiung University of Science and Technology, Kaohsiung, Taiwan (R.O.C.)
[3]Department of Electric Communication Engineering, National Kaohsiung University of Science and Technology, Kaohsiung, Taiwan (R.O.C.)

*solovievarc@gmail.com

In the work, numerical simulation of the thermal state in the vehicle cabin is carried out, taking into account air humidity, based on the equations of convection-diffusion. This model allows one to find the "dew point" on car windows and optimize the process of no fogging windows. One of the urgent problems of thermal comfort and maintenance of safe operating conditions of transport (HVAC) is the problem of window fogging. This phenomenon is commonly called the "dew point", and it consists in reaching the state of saturation of the steam on the surface, in particular, the window due to the temperature difference. Water vapor can enter the cabin both from the ventilation system from the ambient air and from the breathing of passengers. To unambiguously determine the "dew point", it is necessary to determine the amount of water vapor in the air, the temperature and pressure at the desired points. To obtain the fields of these quantities, an algorithm based on the numerical solution of the Navier-Stokes equations and the energy equation together with the convection-diffusion equations is proposed. For the

numerical implementation of the model, the Ansys Fluent computer fluid dynamics complex is used. When modeling, the initial data are, among other things, the proportions of wet steam and air in the deflectors of the climate system. The problem is solved in the formulation of a steady state, and the fields of pressure, velocities, temperature, density and relative humidity inside the cabin are calculated. The implemented numerical method for determining the relative humidity inside the cabin allows one to effectively determine the formation of a "dew point" on the inner surface of the vehicle window and provides opportunities to minimize this phenomenon by controlling the parameters of temperature, direction, speed and humidity of the incoming air from the transport climate system.

Determination of Heat Transfer Coefficients in Vehicle Cabins by Numerical Methods of Heat and Mass Transfer and Aerodynamics

A. N. Soloviev[1]*, I. A. Panfilov[1], E. I. Shpraizer[1], J.-P. Wang[2]

[1]Don State Technical University, Rostov-on-Don
[1]Department of Naval Architecture Engineering, National Kaohsiung University of Science and Technology, Kaohsiung, Taiwan (R.O.C.)

*solovievarc@gmail.com

The paper implements a method for calculating the heat transfer coefficients of a multilayer wall of a vehicle cabin with internal and external air during convective heat transfer. A stationary case is considered, taking into account the movement of air, the solution is constructed using the methods of computer hydroaerodynamics. At the moment, the materials of the cabin of vehicles and mobile technological machines, including those for special purposes, are, as a rule, a complex multilayer composition of heat-insulating, decorative, protective and other layers. Increasingly complex cabin materials, additional heat-loaded equipment, and increasing requirements for thermal comfort (HVAC) require the development of refined approaches to modeling the thermal state of vehicles. When modeling the problem of thermal comfort, determining the coefficient of convective heat transfer with internal and external air is one of the key tasks of heat and mass transfer and applied hydroaerodynamics. Due to the impossibility of obtaining an analytical solution of the Navier-Stokes equations for such problems, the main way to find the heat transfer coefficients is the experiment and the Nusselt criterion based on dimensionless complexes and similarity theory. In this way, experimental values were obtained, in particular, for vertical and horizontal walls and pipes under natural and forced convection for a constant air velocity. However, the vehicle cabin may be a structure with a rather complex geometric shape with significantly non-uniform air flows inside and outside the cabin. This paper discusses the calculation of the cabin heat transfer coefficients based on the Navier-Stokes equations using turbulence models, and the energy equation. The internal and external domains of cabin air are considered. Ansys Fluent is used as a numerical implementation of the computer fluid dynamics model. This method makes it possible to obtain the most accurate values of the heat transfer coefficients and evaluate the applicability of applied theories, including those depending on air velocities. In the study, the values of heat transfer coefficients for vehicle cabins were obtained, a comparison was made with existing applied formulas. This method can be used to simulate the thermal state of cabins of any complexity and high air flow rates. The proposed numerical

implementation can be considered as the most optimal alternative for obtaining values based on experimental data.

Numerical Study of the Propagation of Harmonic Surface Waves Generated by Two Types of Piezoelectric Actuators

A.N. Soloviev[1,2]*, A.V. Yudin[2,3,4], V.A. Chebanenko[3]*****

[1]Don State Technical University, Rostov-on-Don, Russia
[2]Vorovich Mathematics, Mechanics and Computer Science Institute, Southern Federal University, Rostov-on-Don, Russia
[3]Federal Research Center "Southern Scientific Center of the Russian Academy of Sciences", Rostov-on-Don, Russia
[4]Platov Southern Russian State Polytechnic University, Novocherkassk, Russia

*solovievarc@gmail.com, **andryudin1997@gmail.com,
***valera.chebanenko@yandex.ru

In this study, a three-dimensional coupled stationary problem of elastic waves propagation for a system of bodies made of various elastic materials by the finite element method is considered and solved. The aim of the study is to analyze and compare wave processes that are generated in a large thin plate by piezoceramic transducers for isotropic and orthotropic materials. An aluminum alloy, widely used in aircraft construction, is regarded as an isotropic analogue of the selected composite. The choice of computational frequencies is based on the data of numerical experiments. Harmonic analysis was chosen because of its low computational cost and ease of measuring wave attenuation. Analysis of the data for isotropic media allows us to conclude that the obtained distributions of the amplitudes of harmonic waves for a directed transducer strictly depend on the normal displacements of the actuator footprint surface. Comparisons of the investigated values for both types of transducers show the best amplitude characteristics for directed transducer. For an orthotropic material, the wavefront is elliptical. Amplitude distributions are measured for points located on the same waveform. The results obtained showed that there is a deviation of the directivity peak from the main direction of the transducer orientation towards the direction of the main axis of anisotropy. An approach to damage detection for harmonic analysis by the finite element method has been developed. It is shown that the presented technique can interact with structural defects. Further development of the method is associated with the formation of a database of structural responses to various types of damage and their localization. The presented approach is economical in time and allows one to reduce the computation time in comparison with the non-stationary problem. Despite the low level of accuracy of the developed method, the high speed of calculations makes it an effective tool for fast calculations in the first assumption and the choice of frequency ranges for further calculations in nonstationary problems.

Acknowledgement. The study was prepared within the framework of the state task of the SSC RAS, project AAAA-A16-116012610052-3. The work of the first co-author was supported by a grant from the Russian Science Foundation, contract No. 22-11-00302.

Dielectric Properties of Heteroepitaxial Barium – Strontium Niobate Films at f = 0.1 – 2.5 THz

D. V. Stryukov[1], A. A. Mamrashev[2], V. D. Antsygin[2], A. V. Pavlenko[1,3]*

[1]Federal Research Center Southern Scientific Center of the Russian Academy of Sciences, 41, Chekhov Ave, Rostov-on-Don, 344006, Russia
[2]Institute of Automation and Electrometry of the Siberian Branch of the Russian Academy of Sciences, 1, Akad. Coptyug Ave, Novosibirsk, 630090, Russia
[3]Research Institute of Physics of the Southern Federal University, 194, Stachki Ave., Rostov-on-Don, 344090, Russia

*antvpr@mail.ru

In this work, we present the results of studying the structure and dielectric properties in the terahertz frequency range of heteroepitaxial barium-strontium niobate SBN50 films, grown on a magnesium oxide substrate of the (001) cut. The parameters of the unit cell of the film (c = 0.3961 ± 0.0001 nm and $a = b$ = 1.241 ± 0.001 nm) were determined from the data of X-ray diffraction analysis. The deformation in the conjugation plane of the film and the substrate was – 4.3 × 10^{-3}; in the perpendicular direction, it was 4.6 × 10^{-3}, and the relative change in the volume of the tetragonal unit cell was 0.996. The calculations of the terahertz properties of the heterostructure shown in Fig. 1 were performed for an MgO substrate thickness of 560 μm and an SBN50 film thickness from 2.41 μm to 2.55 μm (the inaccuracy in determining the film thickness determined the main error in the calculations).

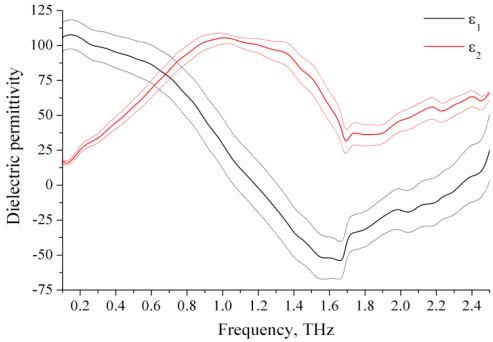

Fig. 1. $\varepsilon_1(f)$ and $\varepsilon_2(f)$ dependence of an SBN film at room temperature; the error range is indicated by thin lines

The measured dielectric terahertz properties of the SBN50 films in terms of the magnitude and nature of the dispersion are in good qualitative agreement with the calculations of the dielectric constant, obtained for SBN35 and SBN61 single crystals by analyzing the IR reflection data. In single crystals, phonon modes were observed at frequencies of ~ 45 cm^{-1}, ~ 72 cm^{-1}, and ~ 100 cm^{-1}. In the films, in the spectrum of the imaginary part of the permittivity ε_2, a more diffuse maximum at a frequency of 1.1 THz (37 cm^{-1}) and an increase in ε_2 at high frequencies up to 2.5 THz (83 cm^{-1}) are observed. Most likely, it is advisable to study the effect of external influences on the dielectric properties in the terahertz region in the vicinity of these

frequencies, which is planned to be implemented in further research. The reasons for the revealed patterns are discussed.

Acknowledgement. The work was carried out as part of the implementation of the state assignment of the SSC RAS (theme of state registration No. 01201354247) and the President of the Russian Federation grant No. MK-678.2020.2. Measurements of terahertz dielectric properties were carried out with the support of the Ministry of Education and Science of the Russian Federation as part of the project state assignment No. 121032400052-6 using the equipment of the Center for Collective Use "Optics and Spectroscopy" of the IAE SB RAS.

Plasmonic Properties upon Aggregation of Size-Selective Ultrasmall Gold Nanospheres

Sudip Kumar Pal[a]*, Anton A. Scrjabin[a], Alexey T. Kozakov[a], Sujit Kumar Ghosh[b]

[a]Research Institute of Physics, Southern Federal University, 194, Stachki Avenue, Rostov-on-Don, 344090, Russia
[b]Department of Chemistry, Assam University, Silchar, Assam-788011, India

*skpalchem@gmail.com

Monolayer-protected metal nanoparticles have received immense attention since the past decade because of their unusual electronic properties and potential applications in plasmonic sensing. Gold nanoparticles exhibit size-dependent the localized surface plasmon resonance when their conducting electrons in both the ground and excited states become confined to dimensions smaller than the electronic mean free path (*ca.* 20 nm). These electrodynamic theories predict observed spectra of gold nanoparticles with diameters larger than 2.3 nm, but fail for smaller particles (Fig. 1).

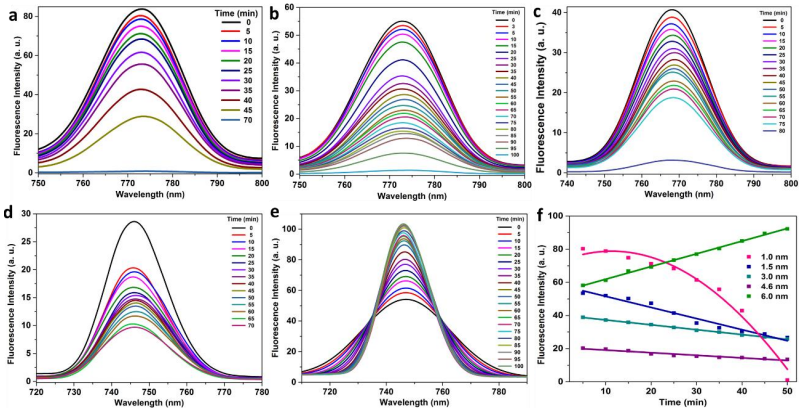

Fig. 1. (a-e) Fluorescence emission spectra of 1, 1.5, 3.0, 4.6 and 6.0 nm gold nanospheres during aggregation taken at an interval of 5 minutes upon addition of CTAB; and (f) temporal change in fluorescence response of gold nano-aggregates for five different sizes

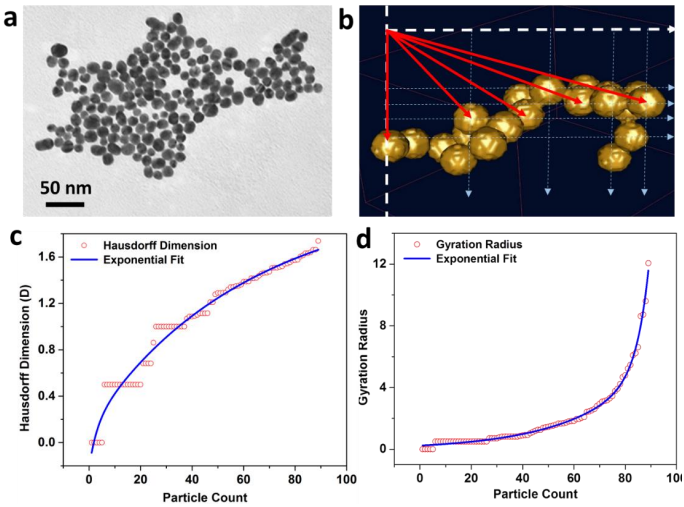

Fig. 2. (a) Vectorized transmission electron micrograph; (b) schematic representation of the assignment of r_0 coordinate; (c & d) the fractal dimension and the radius of gyration as a function of particle count, respectively.

Confinement of electrons within metallic nanostructures, particularly, at sizes comparable to the Fermi wavelength of the electrons (*ca.* 0.7 nm) results in electronic energy states, which show molecule-like transitions as the density of states is, too, low to reproduce the properties of bulk metals. The photoluminescence quantum yields of monolayer-protected gold clusters can be enhanced up to eight orders of magnitude compared to that of bulk gold (10^{-10}). Alkanethiol-protected gold nanoclusters possessing several atoms to small particles (less than 1.2 nm), exhibit fluorescence (quantum yield $\approx 10^{-5} – 10^{-2}$) in the blue to near-infrared region. Decreasing the size of the homologous ligand-protected gold nanoclusters, the emission wavelength exhibits a blue shift (Fig. 2).

Acknowledgement. The study was carried out with the financial support of the Southern Federal University (SFedU grants No. VNGr-07/2020-01-IF and No. P-VNGr/21-07-IF).

Localized Surface Plasmon Resonance of 'Normal' and 'Inverted' Core-Shell Nanostructures

Sudip Kumar Pal[a]*, Anton A. Scrjabin[a], Alexey T. Kozakov[a], Sujit Kumar Ghosh[b]

[a]Research Institute of Physics, Southern Federal University, 194, Stachki Avenue, Rostov-on-Don, 344090, Russia
[b]Department of Chemistry, Assam University, Silchar, Assam-788011, India

*skpalchem@gmail.com

The bimetallic core-shell nanoparticles are of greater interest than the monometallic ones from both technological and scientific points of view [1 – 3] and this can be well-attributed to the fact that in such bimetallic nanoparticles, one of the metals (the shell) determines the surface properties while the specific functional properties (optical, catalytic, magnetic, etc.) of the system may be characterized by the other metal (the core) [4]. These physical and chemical properties of core-shell nanoparticles strongly depend on the structure of the core, the shell and the interface. The properties can also be modified by changing the constituent materials or the core-to-shell ratio. Such core-shell particles have a varied number of applications, such as, in drug-delivery, providing chemical stability to colloids, enhancing luminescence properties.

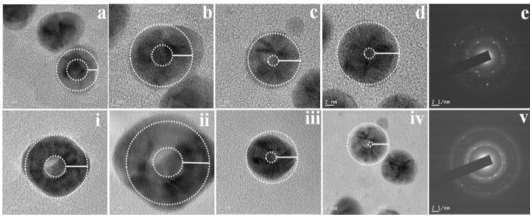

Fig. 1. TEM image of core-shell of different shell thickness

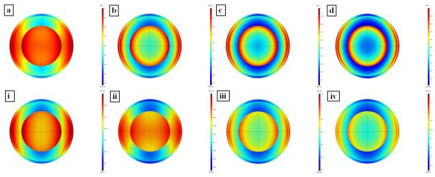

Fig. 2. FEM simulation of core-shell of different shell thickness

In this work, we have focused on the synthesis of 'normal' and 'inverted' gold-silver core-shell nanostructures following the method of Pal group [5]. The 'normal' and 'inverted' core-shell so formed was characterized using transmission electron microscopy (see Fig. 1) and UV-visible spectroscopic techniques. Then, we have simulated the electric field generated using finite element method (FEM) (see Fig. 2) and validated the experimental results with theoretical calculations.

Acknowledgement. The study was carried out with the financial support of the Southern Federal University (SFedU grants No. VNGr-07/2020-01-IF and No. P-VNGr/21-07-IF).

References

[1] Norman T. J., Grant C. D., Magana D., Zhang J. Z., Liu J., Cao D., Bridges F., van Buuren A. // *J. Phys. Chem. B*, **106**, 7005, 2002.

[2] Treguer M., de Cointet C., Remita H., Khatouri J., Mostafavi M., Amblard J., Belloni J., de Keyzer R. // *J. Phys. Chem. B*, **102**, 4310, **1998**.

[3] Anandan S., Grieser F., Ashokkumar M. // *J. Phys. Chem. C*, **112**, 15102, **2008**.

[4] Pande S., Ghosh S. K., Praharaj S., Panigrahi S., Basu S., Jana S., Pal A., Tsukuda T., Pal T. // *J. Phys. Chem. C*, **111**, 10806, 2007.
[5] Ghosh S. K., Pal T. // *Chem. Rev.*, **107**, 4797, 2007.

Testing Procedures to Characterize Variable-Amplitude Fatigue Crack Growth

R. Sunder

BISS Division, ITW-India Pvt Ltd, Bangalore, India

rs@biss.in

Most practical applications of fatigue crack growth rate data involve service loading that is variable-amplitude by nature. Prevailing standard testing practice prescribes constant amplitude testing to characterize fatigue crack growth rate properties of a material. Crack growth behaviour under spectrum loading can be vastly different from estimates based on constant amplitude behaviour [1, 2]. The difference tends to grow under near-threshold conditions and smaller crack sizes, associated with the early stages of fatigue. This assumes particular importance, given growing requirements of extended service life between inspections and larger inherent defect size as in the case of additive manufactured components. Prevailing engineering practice for estimating residual fatigue life involves the use of one of several load interaction models that rely on constants derived from constant amplitude crack growth rate data coupled with other constants iteratively selected to model load interaction effects [3, 4]. The proposed report is a review of work in progress targeting laboratory testing to characterize material properties associated with different known mechanisms of load interaction. The effort is based on the assumption that individual load interaction effects can be characterized in isolation, by a suitably designed reproducible and standardizable laboratory testing practice. The hope is that properties characterized in this manner can be incorporated into analytical estimates of crack growth for any given spectrum loading. The first project in the ongoing research is an encouraging example of progress in the development of standard practices for testing to target engineering application. It involved the development and validation on more than half a dozen different materials of a fully automated and therefore reproducible testing practice to characterize the unique relationship between intrinsic (closure free) threshold stress intensity range and a certain computed near-tip residual stress, σ^* [5 – 7]. σ^* is sensitive to K_{max} under constant amplitude loading and extremely sensitive to load history under variable amplitude loading. The $\Delta K_{th,i}$ versus σ^* relationship was established for an Al-Cu alloy, an Al-Li alloy, a stainless steel and an automotive steel, a titanium alloy and two additive manufactured steels, one stainless and the other from maraging steel powder. Obviously, these materials may be expected to exhibit vastly different sensitivity to variable-amplitude loading. This was brought out by testing under extremely different but statistically identical load sequence variations of an extended duration load spectrum in the HCF/VHCF range of residual life. For all materials studied, the $\Delta K_{th,i}$ versus σ^* relationship was able to model observed variations in crack growth response, suggesting the success of an emergent standard practice for laboratory characterization of a new material property vital to engineering application [8, 9]. The focus of ongoing effort is on an Inter Laboratory Study to confirm satisfactory reproducibility of test results obtained from the test procedure to

characterize the $\Delta K_{th,i}$ versus σ^* relationship. Work is also in progress on methods to account for the isolated effect of other mechanisms that are bound to affect crack growth under service loading. It is proposed to report progress in these activities at the forthcoming symposium.

References

[1] Schijve J. Effect of Load Sequences on Crack Propagation Under Random and Program Loading // *Eng. Fracture Mech*., **5**, 269 – 280, 1973.

[2] Sunder R. In: *Fatigue and Fracture Mechanics*: ASTM STP, S. R. Daniewicz, C. A. Belsick, E. E. Gdoutos (Eds.), **38**, 1546, 2012.

[3] *Advances in Fatigue Lifetime Predictive Techniques*, ASTM STP, M. R. Mitchell, R. W. Landgraf (Eds.), 1122, 1992.

[4] *Advances in Fatigue Lifetime Predictive Techniques*, ASTM STP, M. R. Mitchell, R.W. Landgraf (Eds.), 1192, 1996.

[5] Sunder R., Characterization of Threshold Stress Intensity as a Function of Near-Tip Residual Stress: Theory, Experiment, and Applications, Materials Performance and Characterization // *An ASTM Journal*, **4**(2), 105 – 130, 2015.

[6] Sunder R., Ramesh K., Gorunov A., *Intrinsic Threshold Stress Intensity of Additive Manufactured Metals*, in ASTM STP 1631, American Society for Testing and Materials, 188 – 202, 2020, http://doi.org/10.1520/STP163120190114

[7] Sunder R., Ramesh K., Vishwas C., Threshold Characterization to Support Residual Life Estimates Under Variable-Amplitude Loading // *Materials Performance and Characterization*, Journal of the American Society for Testing and Materials, 2020, DOI: 10.1520/MPC20190223.

[8] Sunder R., Cycle Sequence Sensitivity of Near Threshold Fatigue under Programmed Loading – a Fractographic Study, International // *J. Fatigue*, **135**, 105537, June 2020,

[9] https://myastm.astm.org/KEY_DOCUMENTS/PDF_FILES/e080000sunder.pdf

Colossal Dielectric Response, Conductivity and Complex Impedance Analysis of $LaFeO_3$ Ceramics

Sushrisangita Sahoo[1*], K. P. Andryushin[1], P. K. Mahapatra[2], R. N. P. Choudhary[2]

[1]Research Institute of Physics, Southern Federal University, 344090, Rostov-on-Don, Russia
[2]Department of Physics, Siksha O Anusandhan (Deemed to be University), Bhubaneswar, 751030, India

The present investigations mainly focused on the colossal dielectric response, temperature and frequency dependent studies of electrical conductivity and complex impedance analysis of $LaFeO_3$ ceramics. The studied sample was prepared by a chemical method. Structural and microstructural properties are analyzed from the XRD pattern and SEM micrograph. The anomalies in the dielectric constant *vs* temperature plots are analyzed on the basis of polarization induced by the Maxwell-Wagner mechanisms and ferromagnetic interaction between the Fe^{3+} ions driven by the oxygen vacancy mediated $Fe^{3+} – Vo – Fe^{3+}$ exchange interaction. A giant dielectric permittivity of 225392 was observed in the sample even at the room temperature for 100 Hz. The colossal dielectric constant in $LaFeO_3$ is mainly driven by the internal barrier layer capacitor (IBLC) formation. The formation of IBLC was explained on the basis of highly insulating grain boundary and less resistive/semiconducting grain, which was confirmed from both the activation energy and capacitance of grain and grain boundary from the impedance analysis. The non-Debye type relaxation process, associated with the

grain and grain boundary effect, was investigated from the broad and asymmetric relaxation peak. The relaxation time for both the grain and grain boundary effect was also calculated. In addition to this, we have also analyzed the normalized bode plot of imaginary part of impedance and electrical modulus, which suggests the relaxation process, dominated by the short-range movement of charge carriers. The frequency and temperature dependent studies of conductivity are analyzed by the Jonscher's power law and Arrhenius relation (see Fig. 1).

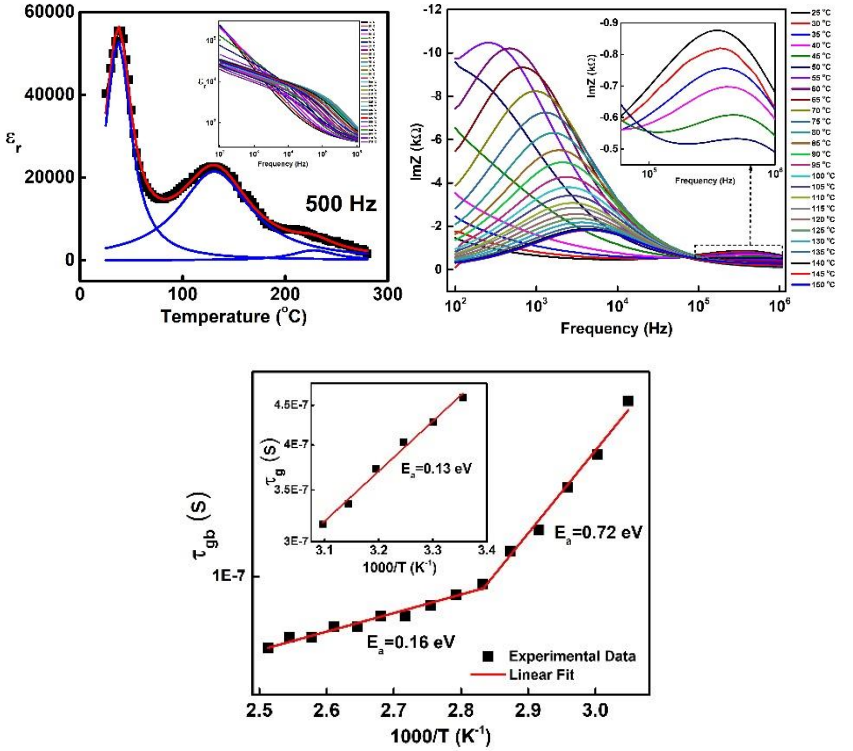

Fig. 1

Dielectric Relaxation and Electromechanical Resonance in Ferroelectric $Cd_2Nb_2O_7$ Single Crystal

M. V. Talanov[1]*, A. A. Pavelko[1], L. S. Kamzina[2]

[1]*Research Institute of Physics, Southern Federal University, Rostov-on-Don, 344090, Russia*
[2]*Ioffe Institute, St. Petersburg, 194021, Russia*

*mvtalanov@sfedu.ru

Among the whole plethora of pyrochlore-like structures, there are only several reliably confirmed examples of the bulk ferroelectrics [1]. All of them are related to the cadmium niobate (pyroniobate) $Cd_2Nb_2O_7$ family of materials [2, 3]. In spite of more than half-century history of studying $Cd_2Nb_2O_7$, the nature of its ferroelectric behavior remains practically unknown that is largely due to the extremely complex phase diagram including paraelectric, improper ferroelectric-ferroelastic, proper ferroelectric, relaxor, incommensurate and glassy phases [4, 5]. The aim of this work was to define the main features of the ferroelectric state as well as the origins of the relaxor-like behavior in $Cd_2Nb_2O_7$. The objects of the study were (111)-oriented single crystals of $Cd_2Nb_2O_7$ grown by a fluxed melt technique using cadmium borate as a flux. Dielectric and electromechanical properties were studied with a help of setup, which includes a nitrogen cryostat with a RTD temperature sensor, Cryotel TC-77 temperature controller, Wayne Kerr 6505B impedance meter, and a personal computer. It was shown that the temperature-frequency behavior of the dielectric permittivity in these crystals demonstrates all the typical features for the systems with domain-walls "freezing" dynamics such as the characteristic "kink" of the temperature behavior of the dielectric permittivity and the corresponding asymmetric dielectric loss maximum as well as following the temperature dependence of the mean relaxation time on the Vogel-Tammann-Fulcher with the fitting parameters close to other systems with domain-walls "freezing" dynamics [6].

Acknowledgement. The reported study was funded by the Russian Science Foundation (projects No. 20-72-00086). The dielectric spectroscopy measurements were performed using the equipment of the Shared Research Facility Centre of SFedU, Research Institute of Physics.

References

[1] Talanov M. V., Talanov V. M. // *Chem. Mater*. **33**, 2706 – 2725, 2021.
[2] Cook W. R., Jaffe H. // *Phys. Rev*., **89**, 1426, 1953.
[3] Jona F., Shirane G., Pepinsky R. // *Phys. Rev*., **92**, 903 – 909, 1953.
[4] Kolpakova N. N., Shulpina I. L., Shcheglov M. P., Waplak S., Bednarski W., Nawrocik W., Wiesner M. // *Ferroelectrics*, **240**, 1531 – 1538, 2000.
[5] Salaev F. M., Kamzina L. S., Krainik N. N. // *Soviet Phys. Solid State*, **34**, 982 – 985, 1992.
[6] Talanov M. V., Pavelko A. A., Kamzina L. S. // *Mater. Res. Bull*., **145**, 111548, 2022.

Multi-order States and Emergent Phenomena on the Pyrochlore Lattice

M. V. Talanov[1,2]*, V. B. Shirokov[1,2,3], E. A. Muratova[2], V. M. Talanov[2]

[1]Southern Federal University, Rostov-on-Don, 344090, Russia
[2]South-Russian State Polytechnic University, Novocherkassk, 346428, Russia
[3]South Scientific Center, Russian Academy of Sciences, Rostov-on-Don, 344006, Russia

*mvtalanov@sfedu.ru

Pyrochlore lattice allows competition between different interactions giving rise to a geometrical frustration and highly degenerate ground states, as well as it acts as a playground for theoretical models for quantum and electronic materials. Crystals with a pyrochlore sublattice (including pyrochlores, spinels and Laves phases C15) also have attracted great attention because their unique physical properties: superconductivity, metal-insulator transitions, quantum spin liquid state, radiation resistance, anomalous Hall effect, heavy fermion behavior and many others [1 – 5]. In many ways unprecedented diversity of crystal and magnetic structures as well as intriguing physical behavior are the results of interplay between spin, lattice, charge and orbital degrees of freedom giving rise to the multi-ordered states. In this work, we considered the problem of the multi-ordered states formation on the pyrochlore lattice in the framework of the Landau theory. Using the order parameter concept for the magnetic crystals with the pyrochlore sublattice allowed us to describe in a uniform manner the possible magnetic structure derivatives of the high-symmetrical aristotype phase, features of magnetic crystallography of the low-symmetrical phases, symmetrical hierarchy of magnetic structures and interactions, the improper degrees of freedom and symmetry-permitted spin-induced properties, as well possible phase diagrams. Special attention has been paid to the emergent phenomena and, in particular, to possible multiferroic and magnetoelectric phases. Based on the results of group-theoretical analysis the multi-ordered classes of low-symmetrical phases were distinguished that open new prospects to the design of quantum materials.

Acknowledgement. The reported study was funded by Russian Science Foundation (projects No. 22-22-00183).

References

[1] Talanov M. V., Talanov V. M. // *Chem. Mater*., **33**, 2706, 2021.
[2] Gingras M. J. P., McClarty P. A. // *Rep. Prog. Phys*., **77**, 056501, 2014.
[3] Tsurkan V., et al. // *Physics Reports*, **926**, 1, 2021.
[4] Taguchi Y., et al. // *Science*, **291**, 2573, 2001.
[5] Gardner J. S., Gingras M. J. P., Greedan J. E. // *Rev. Mod. Phys*., **83**, 53, 2010.

Design and Analysis of Leverage Based Shear Mode Rotary Piezoelectric Energy Harvester

Tejkaran Narolia*, Vijay K. Gupta

PDPM IIITDM Jabalpur, India,

*tejkaran.narolia@iiitdmj.ac.in

Day-to-day expended traditional energy sources and their noxious effects on environment have attracted the scientists to alternative. Energy harvesting from the kinetic energy of blowing wind or flowing water through piezoelectric material is one of the better alternatives. Various small-power based sensors, wireless communications devices and actuators, implantable medical devices and structural health monitoring system depend on batteries to operate [1]. The replacement of batteries in such devices have become a tough and tedious task [2]. Rezaei-Hosseinabadi et al. [3] developed a topology for lift-based wind turbine piezoelectric harvester without contact vibration mechanism. Xie et al. [4] designed a ring piezoelectric energy harvester having inner and outer concentric ring. The results show that a power of 5274.8 W has been generated at radius 0.5 m of the harvester. Wang and Liu [5] fabricated a shear mode piezoelectric energy harvester for harnessing the power from pressurized water flow. FEM simulation and experimental results show that the open circuit peak-to-peak voltage varies from −72 mV to +72 mV. Zhou et al. [6] combined shear mode (d_{15}) piezoelectric constitutive equations and single degree of freedom vibration system to harvest the energy from cantilever. Frequency dependent peak-to-peak voltage and power has been found out. Assembly of 'shear mode (d_{15}) rotary energy harvester' is shown in Fig. 1. For extracting power from rotating object, shaft is coupled to the rotary object. The main components of harvester are a rotating hub of radius R_1, a leverage system (see Fig. 2) to magnify the shear force at the PZTpatches, 12 magnets are mounted on the rotary hub while the same number of magnets with same pole in front of faces, mounted on the end of the levers. The rotation of the hub produces a repulsive magnetic force on the lever end and magnifies at the PZT. The piezoelectric patches of length, l_p, width, w_p, and thickness, t_p, are mounted on the support as shown in Fig.1. A mathematical model has been developed to calculate RMS of the output electric power. Electrical power is plotted against various physical and geometrical parameters of the harvester. The maximum power (see Fig. 3) is calculated as 160 W at $l_m = w_m$ = 10 mm, t_m = 10 − 20 mm, $l_p = w_p = t_p$ = 10 mm, d = 10 mm, d_{15} = 5.84×10^{-10} C/N, and rotation of shaft varies from 1160 RPM to 1391 RPM. Depending on the available ambient energy more and more power can be harvested by increasing dimension and size of the harvester. The analytical results are compared with FEM results and better agreement has been found.

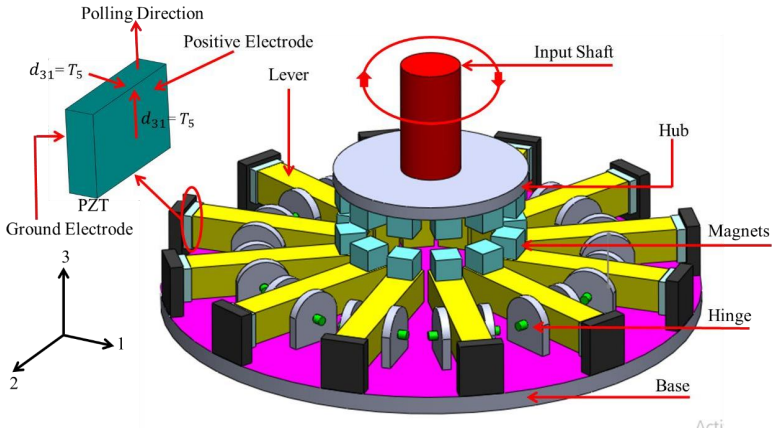

Fig. 1. Simple configuration of energy harvester

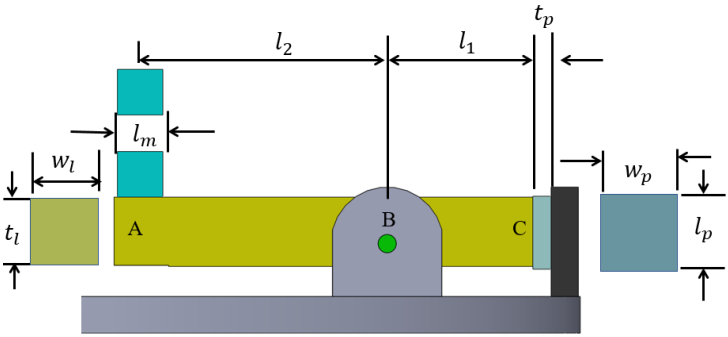

Fig. 2. Leverage system

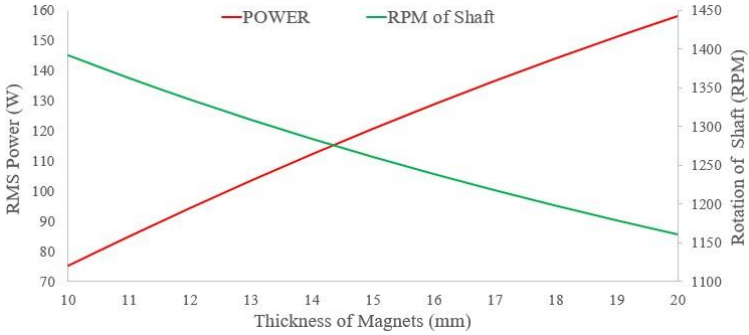

Fig. 3. Variation in power and rotation of shaft with thickness of magnets

References
[1] Wang W., Ismail F., Golnaraghi F. A neuro-fuzzy approach to gear system monitoring // *IEEE Trans. Fuzzy Syst*., **12**, 710 – 723, 2004.
[2] Bhardwaj M., Garnett T., Chandrakasan A. P. Upper Bounds on the Lifetime // *Commun. 2001 ICC 2001 IEEE Int. Conf*. **3**, 785 – 790, 2001.
[3] Rezaei-Hosseinabadi N., Tabesh A., Dehghani R., Aghili A. An efficient piezoelectric windmill topology for energy harvesting from low-speed air flows // *IEEE Trans. Ind. Electron*., **6**2, 3576 – 3583, 2015. doi:10.1109/TIE.2014.2370933.
[4] Xie X. D., Wang Q., Wu N. A ring piezoelectric energy harvester excited by magnetic forces // *Int. J. Eng. Sci*., **77**, 71 – 78, 2014, doi:10.1016/j.ijengsci.2014.01.001.
[5] Wang D.-A., Liu N.-Z. A shear mode piezoelectric energy harvester based on a pressurized water flow // *Sensors Actuators A. Phys.*, **167**, 449 – 458, 2011, doi:10.1016/j.sna.2011.03.003.
[6] Zhou L., Sun J., Zheng X. J., Deng S. F., Zhao J. H., Peng S. T., et al. A model for the energy harvesting performance of shear mode piezoelectric cantilever // *Sensors Actuators A. Phys.*, **179**, 185 – 192, 2012, doi:10.1016/j.sna.2012.02.041.

Efficiency of Bridges between Main Gas Pipelines

V. A. Temnenko, D. D. Fugarov*, Alchganbe Ahmed Abed Tuama, Albelame Amir Basim Kadim

Don State Technical University, Rostov-on-Don, Russia

*ddf_1@mail.ru

All strings of a multi-line gas pipeline are interconnected by jumpers [1]. The use of jumpers allows one to solve two main problems: increasing the reliability of the gas pipeline and reducing the hydraulic resistance of the gas pipeline [2]. Moreove, the advantage of the jumpers available on the main line is that in case of an accident on one of the lines, only the section between the jumpers is turned off. This function allows one to keep the performance of the gas pipeline at a higher level [3]. If the gas flows are optimally distributed along the lines between the bridges, then it is possible to achieve a decrease in hydraulic resistance. Gas flow from one line to another is possible only if there is a pressure drop in the lines [4]. Different pressure can be caused with different clogging of the threads, with different lengths and positions of loopings, as well as with different layouts of pipes along the length of the section. According to the change in the throughput of the gas pipeline, the effectiveness of opening the bulkhead is estimated: $X = Q^{+}/Q^{-}$, where X is the effectiveness of the bulkhead; $Q+$ is the throughput of the section with an open bulkhead; Q^{-} is the capacity of the section, when the bulkhead is closed. Taking into account the flow rate: $X=k_p{}^{+}/k_p{}^{-}$, where $k_p{}^{+}$ is the flow rate with an open bulkhead; $k_p{}^{-}$ is the flow coefficient with a closed bulkhead [5].

References
[1] Onyshko D., Fugarov D., Purchina O., Poluyan A., Rasteryaev N., Skakunova T. Synchronization system in wireless sensor networks of oil and gas complex // *E3S Web of Conferences. Topical Problems of Green Architecture, Civil and Environmental Engineering, TPACEE 2019*, 03030, 2020.
[2] Poluyan A. Yu., Purchina O. A., Fugarov D. D., Golovanov A. A., Smirnova O. V. Solution of task on the minimum cost data flow based on bionic algorithm // *Journal of Physics:*

Conference Series. International Conference "Information Technologies in Business and Industry", Mathematical Simulation and Computer Data Analysis, **2**, 032056, 2019.
[3] Poluyan A. Yu., Purchina O. A., Fugarov D. D., Gerasimenko E. Yu., Skakunova T. P. Application of bionic and immune algorithms for the solution of ambiguous problems of transportation routing // *Journal of Physics: Conference Series*. International Conference "Information Technologies in Business and Industry", Mathematical Simulation and Computer Data Analysis, **2**, 032057, 2019.
[4] Fugarov D. D., Purchina O. A., Poluyan A. Y., Gerasimenko A. N., Rasteryaev N. V. Magnetodielectric ac measuring transducer for automation systems in oil refineries // *Journal of Physics: Conference Series*. International Conference "Information Technologies in Business and Industry", 062020, 2019.
[5] Gerasimenko Y., Gerasimenko A., Fugarov D., Purchina O., Poluyan A. Mathematical modeling and synthesis of an electrical equivalent circuit of an electrochemical device // *Advances in Intelligent Systems and Computing*, **1259**, 471 – 480, 2021.

Relaxor Behavior in Multiferroic $PbFe_{1/2}Nb_{1/2}O_3$ Ceramics Induced by Ba-doping

V. V. Titov, S. I. Raevskaya, S. P. Kubrin, M. A. Evstigneeva, I. N. Zakharchenko, S. I. Kolosov, I. P. Raevski*

Physics Research Institute and Faculty of Physics, Southern Federal University, Rostov-on-Don, Russia

*igorraevsky@gmail.com

Complex perovskite $PbFe_{1/2}Nb_{1/2}O_3$ (PFN) is a multiferroic, that is it combines ferroelectric and magnetic properties [1]. Dielectric permittivity ε dependences on temperature for the $Pb_{1-x}Ba_xFe_{1/2}Nb_{1/2}O_3$ solid solution compositions in the $0 \le x \le 0.5$ compositional range were found to change, as x grows, from relatively sharp frequency-independent maxima typical of usual ferroelectrics to the diffused and frequency-dependent maxima typical of relaxors and then to the saturated at low temperatures and frequency-independent $\varepsilon(T)$ curves typical of incipient ferroelectrics [2] At the same time, Ba-doping leads to the drastic change of magnetic properties of PFN, namely to the drop down of the temperature of the antiferromagnetic phase transition (Néel temperature) in the vicinity of the $x \approx 0.15 – 0.20$ compositional threshold [3]. The scope of the present work is to compare the compositional ranges, where the relaxor properties appear with that, where the drastic change of magnetic properties of PFN is observed. To evaluated the degree of the relaxor behavior, we used a theoretical framework for $PbB_nNb_mO_3$ relaxors suggested in [4] which takes into account the contributions made by individual NbO_6 octahedra, which are believed to be polar units and are said to be "ferroelectrically active". Later it was shown [5] that the probability, w, of the situation when the Nb ion is surrounded by only the Pb-ions for $Pb_{1-x}A_xB_nNb_mO_3$ solid solutions is given by a simple analytical expression: $w = (1 – x)^{\alpha}$, where $\alpha = 8$. In order to check this model, the fall-off in the dielectric permittivity maximum, ε_{max}, with the concentration x for the $Pb_{1-x}Ba_xFe_{1/2}Nb_{1/2}O_3$ solid solution was compared with the computed values of w. In contrast to the model [4], for which $\alpha = 8$ and should not depend on x, the α-values are estimated from the experimental □ □ □$_{max}(x)$/□$_{max}(x = 0)$ ratio dependence on composition, vary crucially with

x at small x-values. It seems that this decrease of α with x corresponds to the decrease of the polar volume, where the substitutions in the A-sites (near the Nb-ions) are absent. This implies that the $w = (1 - x)^{\alpha}$ dependence is not true at very small x, where α exceeds the polar region of the composition with $x = 0$. On the other hand, in the $0.15 < x < 0.4$ compositional range the α- values are close to 8, implying that the polar volume reduces to eight-unit cells. These data correlate well with the compositional dependence of the activation energy ΔW in the Vogel-Fulcher relation, which shows an abrupt increase at $x \approx 0.15$ up to the values typical of the textbook relaxor $PbMg_{1/3}Nb_{2/3}O_3$. Thus, the classic relaxor behavior in the $Pb_{1-x}Ba_xFe_{1/2}Nb_{1/2}O_3$ solid solution starts above $x \approx 0.15$ and is stable up to $x \approx 0.4$.

Acknowledgement. This study was partially supported by the Ministry of Science and Higher Education of the Russian Federation (State assignment in the field of scientific activity, Southern Federal University, 2020). (State task in the field of scientific activity, scientific project No. 0852-2020-0032 (BAS0110/20-3-07IF).

References

[1] Raevski I. P., Kubrin S. P., Raevskaya S. I., Prosandeev S. A., Malitskaya M. A., Titov V. V., Sarychev D. A., Blazhevich A. V., Zakharchenko I. N. // *IEEE Trans. Ultrason. Ferroelect. Freq. Contr*. **59**, 1872–1878, 2012.

[2] Raevski I. P., Titov V. V., Chen H., Zakharchenko I. N., Raevskaya S. I., Shevtsova S. I. // *J. Mater. Sci*. **54**,10984, 2019.

[3] Raevski I. P., Kubrin S. P., Raevskaya S. I., Titov V. V., Sarychev D. A., Malitskaya M. A., Zakharchenko I. N., Prosandeev S. A. // *Phys. Rev. B*, **80**, 024108, 2009.

[4] Butcher J., Thomas N. W. // *J. Phys. Chem. Solids*, **52**, 595 – 601, 1991.

[5] Raevski I. P., Prosandeev S. A. *J. Phys.: Condens. Matter*., **13**, L299 – L303, 2001.

Resistive Switching in Thin ZnO Nanorods for Neuromorphic Systems

R. V. Tominov*, I. A. Shikhovtsov, I. S. Ugrumov, Z. E. Vakulov, V. A. Smirnov

Southern Federal University, Institute of Nanotechnology, Electronics and Electronic Equipment Engineering, 2, Schevchenko Str., Taganrog, 347928, Russia

*roman.tominov@gmail.com

The development of memristor memory is one of the priority areas of the electronics industry. In particular, the scientific community is focused on the manufacturing and research of elements of non-volatile memory (ReRAM), the principle of operation of which is to change the electrical resistance between low-resistance states (LRSs) and high-resistance states (HRSs) under the electric field (resistive switching effect) [1, 2]. Much attention is currently being paid to the study of resistive switching in various nanostructures, such as zinc oxide nanorods grown by pulsed laser deposition. However, the fabrication of ReRAM elements based on zinc oxide nanorods requires systematic regimes of the resistive switching effect and the study of the effect of the control voltage amplitude on the HRSs and LRSs resistances, which is the purpose of this work. The zinc oxide rods were produced by pulsed laser deposition on a Pioneer 180 system (Neocera Co, USA) at the following modes: substrate temperature 400 °C, target-substrate distance 50 mm, O_2 pressure 1 mTorr, pulse energy at 300 mJ, number of pulses 1000. An Al_2O_3 plate with a TiN film bottom electrode 50.6 ± 4.2 nm thick was used as a substrate. The geometrical and electrical parameters of the ZnO

nanorods were investigated using the Ntegra probe nanolaboratory (NT-MDT, Russia) with W_2C probes. The results were processed using Image Analysis 2.0 software. As a result, current-voltage characteristics were obtained with the amplitude of the control voltage in the range from 1 to 6 V. The HRSs and LRSs, as well as the HRSs/LRSs ratio, were derived from the results. The analysis of the results showed that the ZnO nanorods have a diameter of 421.3 ± 87.1 nm. It was also shown that increasing the amplitude of the control voltage (U_0) from 1 to 6 V leads to a decrease in HRSs resistance from 25.32 ± 1.64 GΩ to 0.36 ± 0.07 GΩ, and a decrease in LRSs resistance from 0.32 ± 0.05 GΩ to 0.06 ± 0.01 GΩ. The result obtained can be explained by an increase in the concentration of oxygen vacancies in the zinc oxide nanorods with an increase in voltage U_0 and, therefore, an increase in the electric current flowing through the zinc oxide rods. The maximum HRSs/LRSs ratio was 78. The results obtained can be used in the formation of ReRAM elements based on ZnO nanorods for neuromorphic systems of artificial intelligence.

Acknowledgement. The study was supported by a grant from the Russian Science Foundation № 21-79-00216, https://rscf.ru/project/21-79-00216/

References

[1] Shandyba N. A., Panchenko I. V., Tominov R. V., Smirnov V. A., Pelipenko M. I., Zamburg E. G., Chu Y. H. Size effect on memristive properties of nanocrystalline ZnO film for resistive synaptic devices // *Journal of Physics: Conference Series*, **1124**, 081036, 2018.

[2] Tominov R. V., Vakulov Z. E., Avilov V. I., Khakhulin D. A., Fedotov A. A., Zamburg E. G., Ageev, O. A. Synthesis and memristor effect of a forming-free ZnO nanocrystalline films. *Nanomaterials*, **10**(5), 1007, 2020.

Multilevel Resistive Switching in Nanocrystalline ZnO Films for Neuromorphic Devices

R.V. Tominov*, I.A. Shikhovtsov, Z.E. Vakulov, V.A. Smirnov

Southern Federal University, Institute of Nanotechnology, Electronics and Electronic Equipment Engineering, Taganrog, Russia

*roman.tominov@gmail.com

In recent years, the relevance of technology development and the creation of artificial intelligence systems is increasing, due to the low efficiency of processors based on the von Neumann architecture in solving problems associated with machine learning algorithms [1]. To solve this problem, it is necessary to eliminate the movement of data between the processor and memory, which causes increased power consumption and a significant decrease in the performance of computing systems. To create neuromorphic systems, CMOS technology has serious limitations, so there is a need to develop and research a new element base, which would meet several requirements for energy efficiency, layout density, nonvolatile, etc. Nonvolatile resistive memory (ReRAM) is considered one of the most promising candidates for neuromorphic applications because of its high switching speed, low operating voltage, and high degree of scalability. Resistive switching is observed in many metal-oxide systems, the most popular of which are TiO_2, Ta_2O_5, ZnO, etc. Also, the analysis of the literature data showed that one of the most promising materials for the fabrication of ReRAM elements of neuromorphic systems is a forming-free nanocrystalline zinc oxide (ZnO) film, which can be obtained under certain growth modes of the pulse-laser deposition method [2]. However, the

use of forming-free ZnO nanocrystalline films for neuromorphic applications is currently limited by the insufficient study of resistive switching and by the insufficient study of the patterns of occurrence of multilevel resistive switching. To experimentally study the effect of multilevel resistive switching on the Si/TiN substrate, forming-free nanocrystalline ZnO films were obtained by pulsed laser deposition at the Pioneer 180 unit (Neocera LCC, USA) under the following conditions: substrate temperature was 300 °C, distance between the target and the plate was 50 mm, O_2 pressure was 1 mTorr, pulse energy was 250 mJ. Electrical measurements were made using the Keithley 4200-SCS semiconductor measurement system (Keithley, USA). The top and bottom contacts were a tungsten probe and a TiN film, respectively. Analysis of the experimental results obtained showed that increasing the film thickness of forming-free nanocrystalline ZnO from 12.3 ± 2.7 nm to 42.2 ± 4.6 nm leads to an increase in the HRS/LRS ratio from 76 to 912 and an increase in the stable resistive states from 4 to 9. Also, analysis of the experimental results showed that increasing the resistivity of the forming-free nanocrystalline ZnO film from 0.38×10^{-2} to 0.67×10^{-2} Ω·cm leads to an increase in the HRS/LRS ratio from 435 to 1871 and an increase in the stable resistive states from 6 to 11. The results obtained can be used in the fabrication of neuromorphic systems based on forming-free nanocrystalline zinc oxide films.

Acknowledgement. The study was supported by the Russian Science Foundation Grant No. 21-79-00216, https://rscf.ru/project/21-79-00216/, Southern Federal University.

References

[1] Upadhyay N. K., Jiang H., Wang Z., Asapu S., Xia Q., Joshua Yang J. Emerging memory devices for neuromorphic computing // *Advanced Materials Technologies*, **4**(4), 1800589, 2019.

[2] Tominov R. V., Vakulov Z. E., Avilov V. I., Khakhulin D. A., Fedotov A. A., Zamburg E. G., Ageev, O. A. Synthesis and memristor effect of a forming-free ZnO nanocrystalline films // *Nanomaterials*, **10**(5), 1007, 2020.

Comparative Analysis of Hydrostatic Parameters of 1–3-type Composites with One or Two Piezoelectric Components

V. Yu. Topolov[1], A. O. Denisova[1,2]*

[1]*Department of Physics, Southern Federal University, Rostov-on-Don, 344090, Russia*
[2]*I.I. Vorovich Institute of Mathematics, Mechanics and Computer Science, Southern Federal University, Rostov-on-Don, 344090, Russia*

*alifived193@mail.ru

Piezo-active 1–3-type composites based on domain-engineered single crystals (SCs) [1, 2] are of interest due to high piezoelectric sensitivity and anisotropy, large electromechanical coupling factors and other parameters. Among them, the hydrostatic parameters exhibit numerous examples of a non-monotonic volume-fraction behaviour. The aim of the present report is to compare the hydrostatic parameters of the lead-free 1–0–3 composites with 0–3 matrices where either piezo-passive or piezoelectric inclusions are surrounded by polymer media. The main piezoelectric component is a [001]-poled domain-engineered $[Li_x(K_{1-y}Na_y)_{1-x}](Nb_{1-z}Ta_z)O_3$:Mn (KNNTL-Mn) SC with the perovskite-type structure, where $x = 0.06$, $y = 0.1 – 0.3$, $z = 0.07 – 0.17$, and the level of Mn doping is 0.25 mol. %. Our study is carried out within the framework of the model of the 1–0–3 composite [1, 2]. In this composite a system

of the parallelepiped-shaped SC rods is surrounded by the 0 – 3 matrix with the spheroidal inclusions. A regular arrangement of the rods and inclusions is assumed. A shape of the inclusion is characterised by its aspect ratio ρ_i that is varied from 0.01 (the heavily prolate inclusion along the poling axis) to 100 (the heavily oblate inclusion). The matrix method [3] and effective field method [3] are applied to evaluate effective electromechanical properties of the 1–0–3 composite and its following hydrostatic parameters: piezoelectric coefficients d_h^* and g_h^*, related figure of merit $(Q_h^*)^2 = d_h^* g_h^*$, and electromechanical coupling factor k_h^*. Hereby we consider the performance of the following 1–0–3 composites: KNNTL-Mn SC/corundum ceramic/polyethylene and KNNTL-Mn SC/$Li_2B_4O_7$ SC/polyethylene. The hydrostatic parameters of the 1–0–3 composites are compared at fixed volume fractions m (SC rods in the composite) and m_i (inclusions in the matrix), and the aspect ratio ρ_i. A presence of the isolated piezoelectric $Li_2B_4O_7$ SC inclusions in the 0–3 matrix does not lead to an appreciable increase of maxima of the aforementioned hydrostatic parameters in comparison to their maxima related to the corundum-containing composite with the piezo-passive matrix. Maxima of the piezoelectric coefficient d_h^* of both the studied composites at $\rho_i = 1 – 100$ and $m_i = 0.05 – 0.20$ are in the range of 188 – 282 pC/N, and these values are by an order-of-magnitude larger than the piezoelectric coefficient $d_h^{(1)}$ of the KNNTL-Mn SC. The hydrostatic electromechanical coupling factor k_h^* of both the composites at $\rho_i = 100$ is characterised by max $k_h^* \approx 0.6–0.7$, and these max k_h^* values are ca. 4.7 – 5.4 times larger than the hydrostatic electromechanical coupling factor $k_h^{(1)}$ of the KNNTL-Mn SC. Our results on the hydrostatic parameters of the lead-free 1–0–3 composites are compared to literature data. Due to the large hydrostatic parameters, the studied piezo-active composites can be applied as active elements of hydroacoustic devices and systems.

Acknowledgement. The authors are grateful to Prof. Dr. I. A. Parinov (Southern Federal University, Russia) for his constant interest in the research field of modern piezoelectric materials and their applications. Research was financially supported by Southern Federal University, grant No. VnGr-07/2020-04-IM (Ministry of Science and Higher Education of the Russian Federation).

References

[1] Topolov V. Yu., Isaeva A. N. // *Ferroelectrics Lett. Sec*. **44**, 73, 2017.

[2] Topolov V. Yu., Bowen C. R., Isaeva A. N. // *IEEE Trans. Ultrason., Ferroelec., a. Freq. Cont.* **65**, 1278, 2018.

[3] Topolov V. Yu., Bowen C. R., Bisegna P., *Piezo-active Composites. Microgeometry – Sensitivity Relations*. Cham: Springer Internat. Publ., 2018.

Piezoelectric Properties, Anisotropy Factors and Energy-harvesting Characteristics of Novel 1–2–2 composites Based on Domain-engineered Single Crystals

V. Yu. Topolov[1], A. N. Isaeva[1]*, C. R. Bowen[2], B. O. Protsenko[1]

[1]*Department of Physics, Southern Federal University, Rostov-on-Don, 344090, Russia*
[2]*Department of Mechanical Engineering, University of Bath, BA2 7AY Bath, UK*

*isaeva.ashura@yandex.ru

A study on novel piezo-active 1–2–2 composites [1] based on [001]-poled domain-engineered single crystals (SCs) points an effect of the laminar 2–2 matrix on electromechanical properties

and many parameters of these composites. The aim of the present report is to analyse a high piezoelectric performance, large piezoelectric anisotropy and large figures of merit of the 1–2–2 composites in the context of sensor and energy-harvesting applications [2]. In the 1–2–2 composite, a system of long ferroelectric domain-engineered SC rods is surrounded by a laminar matrix (see Fig. 1), and this matrix contains two types of polymer layer that are arranged regularly [3]. The SC rods with a spontaneous polarisation $\boldsymbol{P}_s^{(1)} \uparrow\uparrow OX_3$ are poled along [001] of the perovskite unit cell (see inset 1 in Fig. 1) and are arranged in a regular square in the (X_1OX_2) plane. The crystallographic axes $X^{(1)}$, $Y^{(1)}$ and $Z^{(1)}$ of each SC rod obey conditions $X^{(1)} \parallel OX_1$, $Y^{(1)} \parallel OX_2$ and $Z^{(1)} \parallel OX_3$. Two shapes of the SC rod are considered, see insets 2 and 3 in Fig. 1. The main components are domain-engineered perovskite-type $0.92Pb(Zn_{1/3}Nb_{2/3})O_3 – 0.08PbTiO_3$, $0.67Pb(Mg_{1/3}Nb_{2/3})O_3 – 0.33PbTiO_3$ and $[Li_x(K_{1-y}Na_y)_{1-x}](Nb_{1-z}Ta_z)O_3$:Mn SCs, where $x = 0.06$, $y = 0.1 – 0.3$, $z = 0.07 – 0.17$, and the level of Mn doping is 0.25 mol. %.

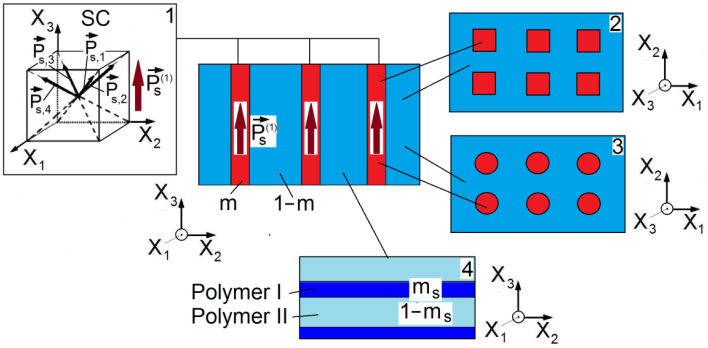

Fig. 1

Non-monotonic volume – fraction dependences of the piezoelectric properties, anisotropy factors and figures of merit are studied. New diagrams are put forward [3] to demonstrate the volume-fraction regions where a large anisotropy of the piezoelectric coefficients d_{3j}^* and electromechanical coupling factors k_{3j}^* is achieved, and where energy-harvesting figures of merit of the composite are at least five times larger than analogous parameters of the SC component. The studied 1–2–2 composites are of interest as anisotropic materials with high piezoelectric sensitivity, large piezoelectric anisotropy and large figures of merit, which are important for sensor, energy-harvesting and related applications.

Acknowledgement. This study was supported by the Russian Foundation for Basic Research (project No. 20-38-90163).

References

[1] Topolov V. Yu., Bowen C. R., Isaeva A. N., Panich A. A. // *Phys. Stat. Solidi A*, **215**, 1700548, 2018.

[2] Bowen C. R., Topolov V. Yu., Kim H. A., *Modern Piezoelectric Energy-Harvesting Materials.* Cham: Springer Internat. Publ., 2016.

[3] Topolov V. Yu., Isaeva A. N., Bowen C. R., Protsenko B. O. // *Ferroelectrics*, **583**, 230 – 242, 2021.

Effect of the Matrix Subsystem on Piezoelectric Properties and Related Parameters of Lead-free 1–3-type Composites

V. Yu. Topolov[1], A. N. Isaeva[1], A. O. Denisova[1], C. R. Bowen[2]

[1]*Department of Physics, Southern Federal University, Rostov-on-Don, 344090, Russia*
[2]*Department of Mechanical Engineering, University of Bath, BA2 7AY Bath, UK*

*vutopolov@sfedu.ru

Among the piezoelectric materials that attract much attention in the recent years, composites based on ferroelectric domain-engineered single crystals (SCs) occupy one of the important positions. This is concerned with a high performance of the 1–3- and 2–2-type composites and with opportunities to vary their effective electromechanical properties, anisotropy factors, energy-harvesting parameters, and other characteristics in wide ranges. In the present study novel 1–3-type composites based on lead-free perovskite-type alkali niobate – alkali tantalate SCs poled along [001] are in the focus of our attention. The main microgeometrical feature of the studied 1–3-type composites is a system of long parallel SC rods surrounded by a large matrix being heterogeneous [1, 2]. The aim of the present report is to highlight the active role of the matrix subsystem in forming the piezoelectric performance and energy-harvesting parameters of the 1–3-type composites. The main connectivity patterns of the studied composites are 1–0–3 and 1–3–0, and the matrix is characterised by 0–3 or 3–0 connectivity, respectively. We study an effect of the anisotropic elastic and/or piezoelectric properties of the heterogeneous polymer-based matrix on the following parameters of lead-free composites:
(i) piezoelectric coefficients d_{3j}^* and g_{3j}^*, where j = 1 and 3;
(ii) energy-harvesting (voltage or squared) figures of merit: $(Q_{3j}^*)^2 = d_{3j}^* g_{3j}^*$;
(iii) modified figure of merit [3, 4] at the applied mechanical stress: $F_{ij}^{*\sigma} = \lambda_{max} (d_{ij}^*)^2/[(k_{ij}^*)^2 \varepsilon_{ii}^{*\sigma}]$, where $\lambda_{max} = \{(k_{ij}^*)^{-1} - [(k_{ij}^*)^{-2} - 1]^{1/2}\}^2$ is the maximum transmission coefficient, k_{ij}^* is the electromechanical coupling factor, and $\varepsilon_{ii}^{*\sigma}$ is the dielectric permittivity at stress σ = const;
(iv) modified figure of merit at the applied mechanical strain $F_{ij}^{*\xi} = \lambda_{max}(d_{ij}^*)^2/[(k_{ij}^*)^2 \varepsilon_{ii}^{*\sigma} s_{jj}^{*E} s_{jj}^{*D}]$, where s_{jj}^{*E} and s_{jj}^{*D} are elastic compliances at the electric field E = const and electric displacement D = const, respectively.
An influence of the piezoelectric anisotropy of the composite on the anisotropy of figures of merit (ii) – (iv) is considered depending on the anisotropic properties and contents of the heterogeneous matrix. Large figures of merit [for instance, $(Q_{33}^*)^2 \sim 10^{-10}$ Pa^{-1} and $F_{33}^{*\sigma} \sim 10^{-10}$ Pa^{-1} at the longitudinal piezoelectric effect] and a large anisotropy of figures of merit [$(Q_{33}^*)^2 / (Q_{31}^*)^2 \sim 10^2$] are achieved in specific volume-fraction ranges and in the presence of the heterogeneous matrix with a large elastic anisotropy. New diagrams that link figures of merit of the composite and volume fractions of its components [4] are put forward to show advantages of the studied lead-free composites over traditional 1–3 composites based on ferroelectric PZT-type ceramics. The large parameters of the studied lead-free composites are compared to the similar parameters of piezo-active composites known from earlier studies, see for example monograph [2].

Acknowledgement. Research was financially supported by Southern Federal University, grant No. VnGr-07/2020-04-IM (Ministry of Science and Higher Education of the Russian Federation).

References

[1] Topolov V. Yu., Bowen C. R., Isaeva A. N. // *IEEE Trans. Ultrason., Ferroelec., a. Freq. Cont.* **65**, 1278, 2018.
[2] Topolov V. Yu., Bowen C. R., Bisegna P., *Piezo-active Composites. Microgeometry – Sensitivity Relations*. Cham: Springer Internat. Publ., 2018.
[3] Roscow J. I., Pearce H., Khanbareh H., et al. // *Eur. Phys. J. Special Topics* **228**, 1537, 2019.
[4] Topolov V. Yu., Isaeva A. N. // *J. Adv. Dielec.* **11**, 2160003, 2021.

Orientation Effects in 2–2 Composites Based on [011]-poled Domain-engineered Single Crystals

V. Yu. Topolov[1], A. N. Isaeva[1], A. V. Krivoruchko[2]

[1]*Department of Physics, Southern Federal University, Rostov-on-Don, 344090, Russia*
[2]*Don State Technical University, Rostov-on-Don, 344000, Russia*

*isaeva.ashura@yandex.ru

Piezo-active 2–2 composites based on domain-engineered single crystals (SCs) are advanced piezoelectric materials with large piezoelectric coefficients, electromechanical coupling factors, hydrostatic parameters, and other characteristics. Orientation effects in these composites [1] are mainly concerned with rotations of crystallographic axes in the SC component. This component is represented by relaxor-ferroelectric SCs, for example (1 – *x*)Pb($Mg_{1/3}Nb_{2/3}$)O_3 – *x*$PbTiO_3$ (PMN – *x*PT) or (1 – *x*)Pb($Zn_{1/3}Nb_{2/3}$)O_3 – *x*$PbTiO_3$ (PZN – *x*PT) with perovskite-type structures and compositions near the morphotropic phase boundary.

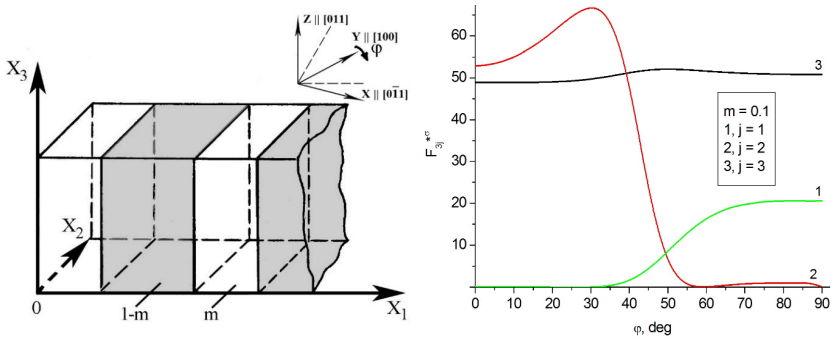

Fig. 1.(a) Schematic of parallel-connected 2–2 composite [2]; (b) orientation dependence of modified FOMs $F_{3j}^{*\sigma}$(in 10^{-12} Pa^{-1}) of the 2–2 PZN–0.07PT SC/polyurethane composite at the volume fraction of SC *m* = 0.1.

The aforementioned rotations influence the electromechanical properties and many parameters of the 2–2 composites [1, 2]. In the present report we show an influence of the rotation of the main crystallographic axes in the [011]-poled SC component on some energy-harvesting and

modified figures of merit (FOMs) of the 2–2 SC/polymer composites. In the 2–2 composite shown in Fig. 1, a, the SC (volume fraction m) and polymer layers (volume fraction $1 - m$) are arranged regularly along the OX_1 axis. Irrespective of the rotation angle φ, the poling axis of the composite is OX_3. The effective electromechanical properties are found by means of the matrix method [1]. Non-monotonic orientation dependences of energy-harvesting FOMs $(Q_{3j}^*)^2 = d_{3j}^* g_{3j}^*$ and modified FOMs $F_{3j}^{*\sigma} = L_{3j}^* (Q_{3j}^*)^2$ at stress σ = const (see Fig. 1, b) are analysed for the 2–2 composites based on SCs (either PMN – xPT or PZN – xPT). Highlighted is the active role of the elastic and piezoelectric properties of the [011]-poled SC in forming the non-monotonic dependences of $(Q_{3j}^*)^2$ and $F_{3j}^{*\sigma}$ on m and φ, and the large anisotropy of some FOMs.

Acknowledgement. Research was financially supported by Southern Federal University, grant No. VnGr-07/2020-04-IM (Ministry of Science and Higher Education of the Russian Federation).

References

[1] Topolov V. Yu., Bisegna P., Bowen C. R., *Piezo-active Composites. Orientation Effects and Anisotropy Factors*. Berlin, Heidelberg: Springer, 2014.

[2] Krivoruchko A. V., Topolov V. Yu. // *J. Phys. D: Appl. Phys*. **40,** 7113, 2007.

The Importance of Technical Inspections in Building Construction

E. S. Tsygankova*, I. O. Egorochkina, R. E. Zatona

Don State Technical University, Rostov-on-Don, Russia

*tsugankova@bk.ru

Every year the expansion of the sphere of construction industry has both positive and negative factors of impact on society, associated with increased risk of work process, in the result of the workplace traumas and deaths, increase in defects and low-quality houses that do not respond to the requirements of quality standards. The main problem of disturbance in construction is the abuse of authority of the builder, or his carelessness [1]. Construction of buildings and structures is the sphere of ensuring the safety and comfort of human life. Construction is characterized by the following functions: sale, operation of construction projects, social one, connected with improving the quality of life of the population, juridical one, connected with protection of rights and interests of consumers, the guarantee of safe and comfortable use of building facilities. Safety and quality of construction processes depend on a large number of external factors and, to a large extent, on the human factor [2]. However, in spite of rather effectively organized activity of author's and technical supervision services, a number of defects take place and tend to multiply and develop during the exploitation of construction objects. These are not only invisible defects due to the complexity of accounting of internal processes in the structure of building materials, these are also the types of defects that are visually detected during the inspection of building structures. Cases of carelessness in construction and montage, finishing, roofing and other works are widespread enough in the construction sphere, which is the most frequent reason of unsatisfactory quality of buildings, occurrence of uncontrolled condition of constructions, reason of independent rearrangement, insulation and other violations that create potential risk of causing harm to life, health of citizens, material damage personal, municipal, state [3]. Prevention, detection, elimination, continuous monitoring in order to reduce and eliminate the consequences of nonconformities

and defects in the course of production, construction and operation of buildings and structures is the most important state task directly related to the safety of life of citizens. Therefore, considerable attention is paid to the issues of supervision in construction. Construction inspection (author's design organization, construction and technical inspection services) prevents non-compliance with design requirements, increases the level of construction culture, reveals and eliminates theft, irresponsible attitude to work.

References

[1] Egorochkina I. O., Serebryanay I. A., Shlyakhova E. A. Monitoring the condition of structures of an existing building near new construction. In: *Physics and Mechanics of New Materials and Their Applications*. Abstracts & Schedule. Kitakyushu, Japan, 2021, 99 – 100.

[2] Egorochkina I. O., Serebryanaya I. A., Shlyakhova E. A., Matrosov A. A. *Enginneering Vestnik of Don*. **2**(62), 40, 2020, ivdon.ru/magazine/archive/n2y2020/6330 (In Russian).

[3] Egorochkina I. O., Buzanova A. V., Dergousov P. A., Voloshina V. V. Construction-technical examination of the external wall structures of a dwelling house. In: *Actual Problems of Science and Technology-2021*. Materials of All-Russian (National) Scientific and Practical Conference. Rostov-on-Don, 948 – 949, 2021 (In Russian).

Improvement of Methodological Approaches to the Implementation of Forensic Construction-technical Expertise

E. S. Tsygankova*, R. E. Zatona, I. O. Egorochkina

Don State Technical University, Rostov-on-Don, Russia

*tsugankova@bk.ru

Currently there are several tens of various types of expertise. One of the most demanded is construction-technical expertise. The purpose of forensic construction-technical expertise is to prevent irregularities in construction. In its essence, the construction technical expertise is a kind of guarantee of the safety of the result, as the research is aimed at identifying mistakes and negative consequences of construction. The expertise becomes judicial, when the parties refer the case to the court. Conditions for the development of expert practice and theory in the field of forensic examination are issues of methodological support and science-based methods. Currently, more than three hundred methodologies are passported. However, the analysis of research papers [1 – 3] allows us to conclude that there are no unified expert methodologies. In this aspect is the disadvantage of methodological support of forensic examination, namely the lack of certified, scientifically based techniques, which does not allow one to carry out qualitative research, generates numerous expert and investigative errors. The general order of methodology of construction expertise includes the following stages: (i) statement of the goal of the study and the choice of necessary method; (ii) study of related regulatory and legal documentation, identifying relevant standards and regulations; (iii) implementation of the necessary measurements and their fixation; (iv) performance of calculations, drawing conclusions and recommendations. Methods of forensic construction expertise includes the use of such techniques as: (i) technical and legal monitoring of available documentation; (ii) detailed examination of facilities for obvious defects; (iii) implementation of the required measurements; (iv) methods of nondestructive testing; (v) laboratory examination of samples that are collected at the facility; (vi) field tests by means of mechanical impact on certain areas

of the construction; (vii) observation of cracks appeared by placing lighthouses in areas with problems; (viii) examination of specific building elements. Development of a common algorithm of forensic construction expertise, program of procedures for its implementation with the use of modern technical means and devices, development of express methods of rapid obtaining information about the object are timely relevant research objectives. The purpose of the present research work is improvement of methodical approaches to execution of forensic construction-technical expert examination of residential buildings and development of express methods of building and construction examination for solving tasks of investigation; quick, operative and reliable revealing and prevention of crimes in construction.

References

[1] Egorochkina I. O., Serebryanay I. A., Shlyakhova E. A. Monitoring the condition of structures of an existing building near new construction. In: *Physics and Mechanics of New Materials and Their Applications*. Abstracts & Schedule. Kitakyushu, Japan, 2021, 99 – 100.
[2] Egorochkina I. O., Serebryanaya I. A., Shlyakhova E. A., Matrosov A. A. *Enginneering Vestnik of Don*. **2**(62), 40, 2020, ivdon.ru/magazine/archive/n2y2020/6330 (In Russian).
[3] Butyrin A. Y. *Theory and Practice of Forensic Construction-technical Expertise*. Moscow; Gorodets Publishing House, 544, 2006.

Hydrodynamic Characteristics of Oil Reservoirs and Wells

K. M. Ugrovatov, D. D. Fugarov*, Al-Saedi Ali Abdulzahra Hassan, V. V. Aseev

Don State Technical University, Rostov-on-Don, Russia

*ddf_1@mail.ru

Hydrodynamic well survey methods are a system of special works that are carried out to determine the general characteristics of productive formations and wells by establishing links between pressure drops in the formation and well flow rates [1]. Among the parameters characterizing the hydrodynamic properties of formations and wells, the permeability coefficient and well efficiency are taken into account [2]. The piezo-conductivity coefficient of layer, *c*, characterizes the rate of pressure distribution in the layer, under elastic conditions, or the ability of the layer to transmit disturbances, caused by a change in the operating mode [3]. For a homogeneous reservoir: $c=k/\mu$, where μ is an effective porosity [4], k is a reservoir permeability coefficient. This is the most important hydrodynamic characteristic of a porous medium; it characterizes own ability to pass liquids and gases through the medium at pressure drops. In accordance with the laboratory determination method, the reservoir permeability coefficient is equal to:

$$k = \frac{Q \cdot \mu \cdot l}{F \cdot (P_1 - P_2)},$$

where Q is the volumetric flow rate of the well, F is the cross-section area, μ is the coefficient of fluid viscosity, P_1, P_2 are the pressures at the input and output of the channel of the porous medium, l is the length of the porous medium. These parameters allow solving numerous practical problems, when planning the process of developing oil and gas fields [5].

References

[1] Fugarov D. D., Purchina O. A., Poluyan A. Y., Gerasimenko A. N., Rasteryaev N. V. Magnetodielectric ac measuring transducer for automation systems in oil refineries // *Journal of Physics: Conference Series*. International Conference "Information Technologies in Business and Industry", 062020, 2019.
[2] Onyshko D., Fugarov D., Purchina O., Poluyan A., Rasteryaev N., Skakunova T. Synchronization system in wireless sensor networks of oil and gas complex // *E3S Web of Conferences. Topical Problems of Green Architecture, Civil and Environmental Engineering, TPACEE 2019*, 03030, 2020.
[3] Poluyan A. Yu., Purchina O. A., Fugarov D. D., Golovanov A. A., Smirnova O. V. Solution of task on the minimum cost data flow based on bionic algorithm // *Journal of Physics: Conference Series*. International Conference "Information Technologies in Business and Industry", Mathematical Simulation and Computer Data Analysis, **2**, 032056, 2019.
[4] Poluyan A. Yu., Purchina O. A., Fugarov D. D., Gerasimenko E. Yu., Skakunova T. P. Application of bionic and immune algorithms for the solution of ambiguous problems of transportation routing // *Journal of Physics: Conference Series*. International Conference "Information Technologies in Business and Industry", Mathematical Simulation and Computer Data Analysis, **2**, 032057, 2019.
[5] Gerasimenko Y., Gerasimenko A., Fugarov D., Purchina O., Poluyan A. Mathematical modeling and synthesis of an electrical equivalent circuit of an electrochemical device // *Advances in Intelligent Systems and Computing*, **1259**, 471 – 480, 2021.

Hypersingular Integrals on Sets of Metrical Spaces and Their Smoothness Properties

B. G. Vakulov, Yu. E. Drobotov*

Southern Federal University, Rostov-on-Don, Russia

*yu.e.drobotov@yandex.ru

Let Ω denote an open bounded set in the metrical space (X,d), such that the balls $B(x,r)=\{y\in X: d(x,y)<r\}$ are measurable with their measures satisfying the growing condition with not necessarily integer exponent $N>0$:

$$\mu\big[B(x,r)\big]\le K r^N, \quad r\to 0, \quad K>0.$$

In this report, hypersingular integrals are defined on Ω in the form of the following operator:

$$D^{\alpha(\cdot)} f(x)=\lim_{\varepsilon\to 0}\int\limits_{y\in M: d(x,y)>\varepsilon}\frac{f(y)-f(x)}{d^{N+\alpha(x)}(x,y)}\,d\mu(y), \quad x\in\Omega.$$

The smoothness properties of $D^{\alpha(\cdot)}$ are studied, considered in terms of the generalized variable Hölder spaces $H^{\omega(\cdot)}(\Omega,w)$ with the weight function $w(x)$. These function spaces are defined by the condition on the local continuity modulus of their elements, i.e., $f\in H^{\omega(\cdot)}(\Omega,w)$ if

$$\Omega_d(wf,x,t):=\sup_{y\in\Omega: d(x,y)\le t}\big|(wf)(x)-(wf)(y)\big|\le A\omega(x,t), \quad A,t>0.$$

Previously, $D^{\alpha(\cdot)}$ was considered in [1] for a constant α and classical Hölder spaces $H^{\lambda}(\Omega)$. The case of a special weight $\mathrm{Re}\,\alpha(x)$ was presented in [2], while variable order hypersingular integrals were shown to be bounded from the variable exponent Hölder space $H^{\lambda(x)}(\Omega)$ into the space with "worse" exponent $\lambda(x)-\alpha(x)$, $\alpha(x)<\lambda(x)$. The purpose of the presented paper is to generalize the problem under consideration and discuss the possibilities of using the theoretical results obtained in a number of disciplines, such as those related to machine learning.

Acknowledgement. The research was financially supported by Southern Federal University, grant No. VnGr-07/2020-04-IM (Ministry of Science and Higher Education of the Russian Federation).

References

[1] Garcia-Cuerva J., Gatto A. E. Boundedness properties of fractional integral operators associated to non-doubling measures // Studia Math., **162**, 245-261, 2004.

[2] Vakulov B. G. Spherical operators of potential type in weighted Hölder spaces of variable order // Vladikavkaz. Mat. Zh., **7**(2), 26-40, 2005.

[3] Samko N. G., Samko S. G., Vakulov B. G. Fractional integrals and hypersingular integrals in variable order Hölder spaces on homogeneous spaces // *Journal of Function Spaces and Applications*, **8**(2), 215 – 244, 2010.

On Smoothness of Spherical Riesz Potential Type Operator with Mild Singularities on Poles

B. G. Vakulov, Yu. E. Drobotov*

Southern Federal University, Rostov-on-Don, Russia

*yu.e.drobotov@yandex.ru

When determining the solvability and stability of solutions to multidimensional integral equations of the first kind, an essential role is played by the study of the relationship between the smoothness of the image of an integral operator and the analytical properties of its preimage. The presented study is devoted to solving this problem in the case of the integral operator:

$$K^{\alpha,\beta} f(x) = \frac{1}{\gamma_{n-1}(\alpha,\beta)} \int\limits_{S^{n-1}} \frac{f(\sigma)}{|x-\sigma|^{n-1-\alpha} |x+\sigma|^{n-1-\beta}} d\sigma, \quad x \in S^{n-1}, \tag{1}$$

that is of the Riesz potential type and has weak singularities at the poles of the unit sphere $S^{n-1} := \{x \in R^n : |x| = 1\}$ embedded into the n-dimensional Euclidean space R^n. In (1), $\gamma_{n-1}(\alpha,\beta)$ is, with α and β fixed, a numeric constant whose value is determined by the spectral properties of the operator (1). When (1) is decomposed into spherical harmonics, its spectrum is called the Fourier–Laplace multiplier. By analyzing the multiplier, the properties of reflection by (1) and similar integral operators can be researched [1, 2]. The smoothness of functions defined on S^{n-1} is understood in terms of the generalized Hölder space H^{ω} that is defined by a condition on the continuity modulus of its elements. Conditions under which

$K^{\alpha,\beta} f \in H^{\omega}$ are found by representing (1) as a classical Riesz potential that is contained in the definition (1) with $\beta = n-1$ [3]. The smoothness properties of the Riesz potential can be investigated through applying the Zygmund type estimates for the continuity moduli of specific integral constructions, related to (1) [4]. The objectives of this study include the proof of isomorphisms in H^{ω} of a spatial operator corresponding to (1) due to the stereographic projection. Also, general theorems on action of this operator in the spaces $H^{\omega}(w)$ with radial weights $w(\cdot)$ are formulated.

Acknowledgement. Research was financially supported by Southern Federal University, grant No. VnGr-07/2020-04-IM (Ministry of Science and Higher Education of the Russian Federation).

References

[1] Samko S. G. *Hypersingular Integrals and Their Applications*. London and New York: Taylor & Francis, 2002.

[2] Samko S. G., Kilbas A. A., Marichev O. I. *Fractional Integrals and Derivatives. Theory and Applications*. Gordon and Breach Science Publishers, 1993.

[3] Vakulov B. G., Karapetyants N. K. // *Dokl. Russ. Akad. Nauk*. **392**(2), 151—154, 2003.

[4] Vakulov B. G., Kostetskaya G. S., Drobotov Y. E. In: *Fractal Approaches for Modeling Financial Assets and Predicting Crises*. IGI Global, 249-273, 2018, http://doi:10.4018/978-1-5225-3767-0.ch013

Regularization of a Variable Order Abel Equation in the Generalized Variable Hölder Spaces and Its Applications

B. G. Vakulov[1], Yu. E. Drobotov[1]*, E. S. Kochurov[2]

[1]Southern Federal University, Rostov-on-Don, Russia
[2]Sberbank, Rostov-on-Don, Russia

*yu.e.drobotov@yandex.ru

In this report, a variable order Abel equation of the first kind is considered in the form:

$$\frac{1}{\Gamma\left[\alpha(x)\right]}\int_a^x \frac{\varphi(t)\,dt}{(x-t)^{1-\alpha(x)}} = f(x), \quad x > a, \tag{2}$$

where a is real, and the function $\alpha(x)$ satisfies the following conditions:

$$\alpha \in \mathrm{Lip}\left(\left[a,b\right]\right), \quad 0 < \inf_{x\in[a,b]} \alpha(x) \le \sup_{x\in[a,b]} \alpha(x) < 1. \tag{3}$$

By $\mathrm{Lip}(\Omega)$ the set of functions, for which the Lipschitz condition holds, is denoted as

$$\forall x, x+h \in \Omega \quad \left|f(x+h) - f(x)\right| \le c|h|, \quad c > 0,$$

Regularization of equation (1) under conditions (2) is carried out in the generalized variable Hölder spaces $H^{\omega(\cdot)}$ with a characteristic $\omega(\cdot)$ dependent on a parameter. This space of functions continuous on the segment $[a,b]$ of the real line is defined by the condition:

$$\forall x \in [a,b] \quad \omega_f(t,x) \le c\,\omega(t,x),$$

where the constant $c > 0$ is independent of x and t, while the left side functional is the local continuity modulus of the function $f(x)$:

$$\omega_f(t,x) = \sup_{|h|<t} |f(x+h) - f(x)|, \quad t \in [0, b-a], \quad x \in [a,b].$$

The spaces $H^{\omega(\cdot)}$ are of interest because of their role in generalizing the concept of smoothness. They contain as particular cases both classical Hölder spaces with a constant exponent and their most common generalizations for the case of a variable exponent or specific characteristics. Numerous natural science problems lead to Equation (1), making it relevant to research conditions for smooth solutions in the broadest formulation of this problem. Previously, the regularization of (1) was considered in [1] for the L^p spaces, as well as in the prior studies [2, 3]. In the present report, the applications of these theoretical results are discussed.

Acknowledgement. The study was financially supported by the Grant No. 21-19-00423 of the Russian Science Foundation in the Southern Federal University.

References

[1] Samko S. G. *Analysis Mathematica*, **21**, 213–236, 1995.

[2] Vakulov B. G., Kochurov E. S., Samko N.G. Russian Mathematics // *Izvestiya VUZov. Matematika*, **55**(6), 20–28, 2011.

[3] Vakulov B. G., Kochurov E. S. // *Vladikavkaz. Mat. Zh.*, **12**(4), 3–11, 2010.

Plasma Micromachining of Nanocrystalline $LiNbO_3$ Films

Z. E. Vakulov[1]*, V. S. Klimin[2], R. V. Tominov[2], V. A. Smirnov[2], O. A. Ageev[2]

[1]Federal Research Centre The Southern Scientific Centre of the Russian Academy of Sciences (SSC RAS), Rostov-on-Don, Russia

[2]Southern Federal University, Research and Education Centre «Nanotechnology», Taganrog, Russia

*zakhar.vakulov@gmail.com

Formation of nanocrystalline ferroelectric films with controlled surface parameters is challenging and significantly limits the abilities of the films integration with the silicon technology of micro- and nanoelectronics. One of the ways for controlled modification of the ferroelectric films surface morphology is plasma micromachining. Thus, the purpose of this work to determine the influence of capacitive and inductively coupled plasma power on the morphological parameters of nanocrystalline ferroelectric $LiNbO_3$ films. The combined plasma-chemical etching technique used in an atmosphere of fluoride plasma with two types of discharge (capacitive and inductively coupled). It is possible to combine two modes of plasma-chemical etching: (i) reactive ion etching and (ii) plasma-chemical etching in inductively coupled plasma. $Si/LiNbO_3$ structures, fabricated by pulsed laser deposition, were used as experimental samples. Protective layer of a plasma-resistant layer was applied to the samples for correctly determination of the etching depth. The morphological parameters of the samples after plasma micromachining were investigated using the atomic force microscope (AFM) study in the semicontact mode. The samples were processed in plasma at a pressure of 2 Pa, the flow rate of process gases was Ar = 100 cm^3/min, SF_6 = 10 cm^3/min. The power of the inductively coupled and capacitive plasma sources varied from 200 to 600 W and from 10

to 40 W, respectively. It was found that increasing in the power of the inductively coupled plasma source from 200 to 600 W results in increasing in the etching depth of $LiNbO_3$ films from (0.4 ± 0.03) nm to (1.9 ± 0.17) nm. The etching depth of $LiNbO_3$ films increased from (1.1 ± 0.1) nm to (3.1 ± 0.3) nm, with a change in the capacitive plasma power from 10 to 40 W. Increasing in the etching rate of the films can be associated with strong influence of the physical component in the etching process with increasing in the power of the capacitive plasma source. In the result of AFM images analysis, it was found that with an increase in the power of the inductively coupled plasma source from 200 to 400 W, the surface roughness of nanocrystalline $LiNbO_3$ films decreases from (3.8 ± 0.3) nm to (2.4 ± 0.2) nm. Two points can be highlighted, which describe the surface roughness on plasma source power: (i) there is a decrease in the surface roughness of the films (up to 400 W for inductively coupled plasma and up to 20 W for capacitive plasma), which corresponds to the polishing mode; (ii) a gradual increase in the surface roughness of the films is observed (etching mode), with an increase in the power of plasma sources (more than 400 W for inductively coupled plasma and more than 20 W for capacitive plasma). Thus, using the obtained regularities, it is possible to form $LiNbO_3$ nanocrystalline films with controlled morphological parameters. Obtained results are promising and opens new ways to the fabrication of MEMS, new generation of energy conversion devices, and the sensors for the Internet of Things devices based on lead-free ferroelectric films.

Acknowldgements. The reported study was funded by the Russian Foundation for Basic Research, projects numbers 19-38-60052, 19-29-03041 mk, and partially supported by Grant of the President of the Russian Federation MK-6252.2021.4.

Tubular Fiber-reinforced Dielectric Actuator

Valeriy M. Anesyan[1], Alexey M. Kolesnikov[1,2]*, Daria A. Letunova[1]

[1]Southern Federal University, Rostov-on-Don, Russia
[2]Don State Technical University, Rostov-on-Don, Russia

*Alexey.M.Kolesnikov@gmail.com

Currently, polymeric materials called electroactive (EAP), which can undergo large deformations under the influence of an electric field, are being actively researched. Two classes of electroactive polymers are distinguished: ionic and dielectric. Ionic polymers are deformed due to the movement of ions within the polymer. Deformation of dielectric polymers is caused by electrostatic forces between two electrodes that compress the body. Ionic EAPs require low voltage to operate, but require a constant energy input to maintain the deformed state of the body. Dielectric EAPs can be classified as capacitors with variable capacitance due to compression in the direction of electrostatic forces and expansion in the perpendicular direction. Their operation requires high voltage (up to several kilovolts), but no energy is required to hold the deformed state of the body. Devices based on EAP offer new opportunities for the development of soft robots, actuators, artificial muscles, etc. [1 – 4]. In this work, a large deformation problem of a single layer and a double layer dielectric reinforced tube, which is a prototype of a linear and rotary actuator, is considered. In the problem of a single-layered tube reinforced with two families of fibers, dependence between tube deformation (elongation, twisting angle, radial expansion) and electric charge induced on compliant electrodes on its side surfaces are constructed. It is shown that we can controlled the response

of the tube to electrical action by selecting the reinforcement angles. For the two-layer tube problem, an approach to the description of its deformation under the action of electric charges on its lateral surfaces and on the surface between the layers is proposed. It is supposed, that the choice of reinforcing parameters of each layer will allow regulate a response of the tube on an electrical action in wider limits.

References

[1] Tongqing Lu, Cheng Ma, Tiejun Wang. Mechanics of dielectric elastomer structures: A review // *Extreme Mechanics Letters*, **38**, 100752, 2020.

[2] Jiaqing Xiong, Jian Chen, Pooi See Lee. Functional fibers and fabrics for soft robotics, wearables, and human–robot interface // *Advanced Materials*, **33**(19), 2002640, 2021.

[3] Philipp Rothemund, Nicholas Kellaris, Shane K Mitchell, Eric Acome, Christoph Keplinger. Hasel artificial muscles for a new generation of lifelike robots-recent progress and future opportunities // *Advanced Materials*, **33**(19), 2003375, 2021.

[4] Yaguang Guo, Liwu Liu, Yanju Liu, Jinsong Leng. Review of dielectric elastomer actuators and their applications in soft robots // *Advanced Intelligent Systems*, **10**, 2000282, 2021.

Defect Imaging Technique Using Acoustic Nondestructive Model and Convolutional Neural Network

P. V. Vasiliev*, A. V. Senichev

Don State Technical University, Rostov-on-Don, Russia

*lyftzeigen@mail.ru

In this report, we explore and develop nondestructive testing techniques in combination with advanced developments in neural network architectures. We propose an approach to identify and visualize internal defects based on an ultrasonic nondestructive testing model. By conducting a series of numerical experiments, we have analyzed the results and trained a neural network model. The neural network can reconstruct the shape, position, and orientation of the defect based on ultrasonic vibrations obtained from the external surface of the test object. In contrast to previous works [1], the convolutional neural network does not allow one to carry out additional transformations of the information before its training. This set of methods shows the promising application of neural network technologies in solving inverse problems of mechanics and in the problem of visualization of internal defects in general [2 – 4]. The input of the convolutional neural network is the ultrasonic signal received at the internal points of the control object. The output generates an image, visualizing the internal defect. The inner part of the steel plate is chosen as the object of study. Inside the strip, there may be a defect marked by a lack of material. The shape, size, and orientation of the defect are randomly set. The approach consists of a series of numerical experiments from which it is possible to train a deep neural network model. By varying the geometric parameters of the defect and modeling the acoustic ultrasonic wave propagation, a training set is created for each case. Based on the collected data the optimal structure of the neural network model and its training are constructed. Modeling of ultrasonic wave propagation is carried out by the finite difference method in the time domain [5]. It belongs to a class of grid methods of differential equations solution. In this method, the velocity and acoustic pressure of particles of the simulated object are placed one-by-one at grid nodes. Then their values are calculated

sequentially, which makes it possible to calculate the sound field propagation in time. The inner part of the steel plate containing the defect is chosen as a model of nondestructive testing. The size of the investigated area is 20 × 20 mm^2. Physical parameters of the defects vary concerning the modeled area in the following limits. Defect position from 0.3 to 0.7, defect size from 0.1 to 0.35, defect inclination angle from 0° to 360°. The probing pulse frequency is 10 MHz. After several numerical experiments, the neural network model is trained and tested. Based on the results obtained, it is revealed that the proposed model shows high accuracy in the cases, when the wavelength of the probing pulse is tens of times smaller than the defect size. We believe that the combination of the proposed methods in this approach can serve as a good starting point for future research in the field of nondestructive testing problems and inverse problems in general.

Acknowledgement. This work was supported by the RFBR in the framework of the project 20-31-90026.

References

[1] Solov'ev A. N., Sobol' B. V., Vasil'ev P. V. Ultrasonic Location of Inner Crack Defects in a Compound Elastic Cylinder Using an Artificial Neural-Network Apparatus // *Russian Journal of Nondestructive Testing*. **52**(3), 119 – 124, 2016.

[2] Vladimir Puzyrev. Deep learning electromagnetic inversion with convolutional neural networks // *Geophysical Journal International*, **218**(2), 817 – 832, August 2019, https://doi.org/10.1093/gji/ggz204.

[3] Nagatani Y., Okumura S., Wu S., Matsuda T. Two-dimensional Ultrasound Imaging Technique based on Neural Network using Acoustic Simulation // *arXiv preprint*, arXiv:2004.08775, 2020.

[4] Soloviev A., Sobol B., Vasiliev P., Senichev A. Generative Artificial Neural Network Model for Visualization of Internal Defects of Structural Elements. In: Parinov I., Chang S.H., Long B. (Eds.) *Advanced Materials. Springer Proceedings in Materials*, Springer, Cham, **6**, 587 – 595, 2020. https://doi.org/10.1007/978-3-030-45120-2_48.

[5] Yee K. Numerical solution of initial boundary value problems involving Maxwell's equations in isotropic media // *IEEE Transactions on Antennas and Propagation*, **14**, 302 – 307, 1966.

Size-dependent Models of Deformation of Layered Electroelastic Bodies

A. O. Vatulyan[1], S. A. Nesterov[2]*

[1]Southern Federal University, Rostov-on-Don, Russia
[2]Southern Mathematical Institute - branch of the VSC RAS, Vladikavkaz, Russia

*1079@list.ru

In connection with the development of microelectronics and micro-electromechanical systems, much attention of scientists is drawn to the study of the stress-strain state of small-sized layered bodies. In such structures, the dimensions of the elements under study can become commensurate with the characteristic dimensions of the microstructure of the material and, therefore, scale effects may arise. Scale effects for homogeneous bodies are usually taken into account on the basis of gradient mechanics models, which contain gradient parameters of the length dimension. However, at the moment there are no works on the study of the stress-

strain state of layered electroelastic bodies. In this report, based on the gradient theory of electroelasticity, we study the stress-strain state that occurs during the deformation of layered electroelastic bodies. Based on the variational principle of gradient electroelasticity, equilibrium equations, boundary conditions and conjugation conditions for a composite rod, micro-beam, micro-cylinder are obtained. Analytical expressions are obtained for finding the stress-strain state of electroelastic bodies. Specific examples show the difference between the distributions of displacements, potential and stresses found on the basis of solutions to the problem in the classical formulation and in the gradient formulation, scale effects are estimated.

Acknowledgement. This work was supported by the Southern Mathematical Institute, a Branch of the VSC RAS, Vladikavkaz.

Investigation of the Problem for a Plane Waveguide with Local Inhomogeneity in the Framework of the Gradient Theory of Elasticity

A. O. Vatulyan, O. V. Yavruyan*, D. V. Zhukov

Southern Mathematical Institute VSC RSA, Southern Federal University

*yavruyan@mail.ru

Inhomogeneous planar waveguides are widely used in many areas of industry. The heterogeneity considered in this study is represented by local heterogeneity (delamination from the base). This kind of inhomogeneity are found very often in practice and arise as a result of not gluing or not welding. As a result, areas of stress concentration form, presenting itself the area around the delamination tips. That is why the problems, connected with the search for mathematical models, allow us to clarify the behavior of mechanical fields in the area of the tips. The problems deal with study and estimate of the stress-strain state in their vicinity are especially actual. Such mathematical models include models of the nonclassical theory of elasticity, that is the gradient theory of elasticity and the generalized theory of elasticity. The problem of oscillations for the plane isotropic waveguide with delamination is considered. The Aifantis single-parameter gradient model is used as a mathematical model, which takes into account the first-order gradients of the strain tensor in the expression for the strain energy density. The boundary problem is represented by the fourth-order differential equations and completed by boundary conditions in terms of moment stresses. A system of boundary integral equations (BIEs) is formulated with respect to the components of the strain tensor at the delamination edge, which are represented by integrals with cubic singularity. Numerical investigation of BIEs was realized using approximating Chebyshev polynomials and corresponding spectral relations. The specific character of gradient models in the study of crack theory problems is the possibility to obtain regular solution for components of the deformation tensors and Cauchy stress tensors, which makes it possible to estimate the stress-strain state in the vicinity of the delamination tips, with the stress components having a pronounced maximum, the estimation of which makes it possible to formulate a new strength criterion. An asymptotic investigation of the problem depending on the correlation between the parameters, namely the gradient model parameter and the delamination length, was also carried out. A numerical study of the problem was realized and a comparative analysis of the results of the gradient and linear theory of elasticity was performed.

Acknowledgement. The research was supported by Russian Science Foundation (No. 22-11-00265).

Investigation of Waves in FGM Waveguide with Attenuation

A. O. Vatulyan, V. O. Yurov*

Department of Elasticity Theory, I.I. Vorovich Institute of Mathematics, Mechanics and Computer Sciences, Southern Federal University, 8a, Milchakov Str., Rostov-on-Don, 344090, Russia

***vyurov@sfedu.ru**

In recent years, functionally graded materials (FGMs) have become important in the design of structural elements and replaced layered structures in many practically important situations. The problem of forced oscillations of a cylindrical FGM waveguide is solved taking into account the rheological properties of the material. Wave propagation is studied on the basis of a model of a cylindrical waveguide inhomogeneous in the radial direction. Damping was taken into account within the concept of complex modules using the standard viscoelastic solid model for shear components. The rheological properties of the material are determined in terms of the functions of the instantaneous and long-term moduli of elasticity, which depend on the radial coordinate, and the constant relaxation time. To construct the wave fields, we used a combination of the integral Fourier transform along the axial coordinate of the waveguide and a complex version of the shooting method, which was used to numerically construct the displacement transforms and find residues in simple poles. The problem of reconstructing the properties of a waveguide from information about the displacement field on the final part of the outer boundary of the waveguide in a certain frequency range is considered. The inverse problem is reduced to a sequential (iterative) finding of corrections for the restored functions. At each iteration, using the A. N. Tikhonov regularization method, the system of Fredholm integral equations of the first kind with smooth kernels is solved. The implementation of the computational scheme showed a high efficiency of the reconstruction of the shear modulus and density in the elastic version using additional information in the frequency range up to the first radial resonance. In experiments with attenuation, it was possible to restore the long-term elastic moduli and density. In the low-frequency range, the influence of instantaneous moduli on displacement fields is rather weak, which manifests itself in the small norm of some kernels of integral operators. A technique for determining the relaxation time for a cylinder made of an inhomogeneous viscoelastic material is proposed from the points of the dispersion set using a formula derived from the perturbation theory method. Computational experiments have been carried out.

Acknowledgement. This work is supported by the Russian Science Foundation under grant 22-11-00265.

Phase Formation and the Effect of Phase Formation on the Dielectric and Magnetic Properties of Solid Solutions $(Bi_{0.5}La_{0.5})_{1-x}R_xMnO_3$

D. V. Volkov[a], L. A. Shilkina[a], A. V. Nagaenko[b], A. A. Pavelko[a]

[a]Research Institute of Physics, Southern Federal University
[b]Institute of High Technologies and Piezotechnics, Southern Federal University
Rostov-on-Don, 344090, Russia

*dvvolkov@sfedu.ru

In recent years, the attention of many researchers has focused on a group of solid-state media called multiferroics. Multiferroics are substances in which at least two of the possible orders coexist simultaneously, namely ferromagnetic, ferroelectric or ferroelectric. They have a wide range of possible applications. Bismuth manganite, and its solid solutions of multicomponent systems using BaO, La_2O_3 and PbO, are representatives of this class of materials. Currently, they are considered as the basis for the creation of various magnetoelectric devices. However, the widespread use of these solid solutions is limited by several reasons. Thus, the presence in these compounds of ions of variable valence (Mn^{3+}/Mn^{4+}) and oxygen vacancies are one of the reasons for the high electrical conductivity. The effects associated with interlayer polarization make it difficult to describe dielectric and magnetic properties. However, the creation of solid solutions based on bismuth manganite using the above compounds makes it possible to stabilize the structure of perovskite and improve the properties of materials. Thus, the purpose of this work was to establish the influence on the structural, dielectric and magnetic properties of the cationic composition of ceramics of solid solutions $(La_{0.5}Bi_{0.5})_{1-x}Pb_xMnO_3$ and $(La_{0.5}Bi_{0.5})_{1-x}Ba_xMnO_3$. In the course of the work solid solutions $La_{0.5}Bi_{0.5})_{1-x}Pb_xMnO_3$ and $(La_{0.5}Bi_{0.5})_{1-x}Ba_xMnO_3$ with x = 0.03, 0.05 were prepared. For their manufacture, $BaCO_3$ (99%), La_2O_3 (99%), Mn_2O_3 (99%), Bi_2O_3 (99%), and PbO (98%) compounds were used. The solid solutions were prepared using a two-stage solid-state synthesis at T_1 = 1073 K, τ_1 = 10 h. and T_2 = 1223 K, τ_2 = 10 h. The sintering was carried out using conventional ceramic technology at (T_{sint} = 1293 K, τ_{sint} = 2.5 h). At each stage of the technological process, a phase optimization of the conditions for the formation of solid solutions was carried out. The phase composition and completeness of the synthesis were controlled using X-ray diffraction on the DRON-3 diffractometer. In the course of the work, information was obtained on the structural characteristics of the studied samples of ceramics, phase analysis was carried out, their dielectric and magnetic properties were investigated. Based on the data obtained, a conclusion was made about the possibility of using the considered solid solutions as a basis for the development of new functional materials.

Acknowledgement. The study was carried out with the financial support of the Ministry of Science and Higher Education of the Russian Federation, State task in the field of scientific activity, scientific project No (0852-2020-0032)/(BAZ0110/20-3-07IF), using the equipment of the Collective Use Center "Electromagnetic, Electromechanical and Thermal Properties of Solids" of the Research Institute of Physics.

Preparation and Characterization of Sn – ZnO Nanorod Array

M. G. Volkova[1]*, V. V. Petrov[2], E. M. Bayan[1]

[1]Southern Federal University, Faculty of Chemistry, Rostov-on-Don, Russia
[2]Southern Federal University, Institute of Nanotechnologies, Electronics, and Equipment Engineering, Taganrog, Russia

*mvol@sfedu.ru

Nanostructures based on zinc oxide, containing small amount of other oxide materials, are widely used in various fields of modern industry. Due to the combination of low cost and promising physicochemical characteristics, film materials can be used in solar cells, various sensors, energy converters, etc. The two-step synthesis of zinc oxide nanorods with a tin dioxide content of 0.5 – 5 mol.% was the main aim of this study. The seed layer was formed by the sol-gel method using $SnCl_4 \cdot 5H_2O$, $Zn(NO_3)_2 \cdot 6H_2O$ and isopropanol as a solvent. The required quantity of salts was dissolved in the organic solvent. The resulting solution was applied once on the pre-prepared soda-lime glass, silicon and polycore substrates, after that all of substrates were calcined in a muffle furnace at 550 °C for two hours. The obtained substrates were cooled with muffle furnace at the room temperature for homogeneous coating without cracks. The second step of synthesis was hydrothermal treatment, while the concentration of substances in the solution was 25 mmol/l of tin and zinc salts and 25 mmol/l of hexamethylenetetramine. The substrates obtained at the first synthesis step were placed in a hydrothermal cell and kept for 2 hours at a temperature of 100 °C. At the end of the synthesis, the samples were washed with distilled water and dried. Obtained materials were studied by XRD (diffractometer Thermo ARL, Switzerland) in CuKα radiation and scanning electron microscopy methods (SEM, scanning electron microscope Nova Nanolab 600). According to XRD analysis results, the obtained samples are amorphous, this fact indirectly confirms the nanostructures. According to SEM analysis data, during the hydrothermal synthesis arrays of nanorods with an average length of about 240 nm and inner diameter of 85 nm were obtained (for a sample containing 1 mol.% SnO_2 and 99 mol.% ZnO). Thus, during the two-step synthesis, arrays of zinc oxide nanorods with a small content of tin dioxide were obtained. The obtained materials are nanoscale and homogeneous, which makes it possible to recommend this material for further study of optical, gas-sensitive and electrophysical properties.

Acknowledgements. This work was financially supported by the RFBR, project 20-07-00653 A. SEM measurements were carried out with the technical support of the Research Laboratory of Functional Nanomaterials Technology, Institute of Nanotechnologies, Electronics and Equipment Engineering, Southern Federal University (scientific project No. 0852-2020-0015 within the framework of the state assignment of the Ministry of Education and Science of Russia in the field of scientific activity).

Modelling the Controlled Electromagnetic Field Diffraction in Analog and Digital Integrated Circuits in the Giga- and Terahertz Bands

P. Yu. Voloshchenko, Yu. P. Voloshchenko*

Engineering Technological Academy, Southern Federal University, 2, Shevchenko Str., Taganrog, 347900, Russia

*yvoloshchenko@yandex.ru

The report presents an algorithm for engineering modelling the amplitude-dependent diffraction of electromagnetic waves propagating in the material of analog and digital integrated circuits. For example, the dielectric in integrated circuits surrounds feeding wires and over-emitting vacuum or semiconductor electronic devices with electrostatic control. It is shown that multiparameter symbolic analysis of the composition of influences and coherent responses in any type of integrated circuits in the giga- and terahertz ranges should be carried out by methods known in electrical and radio engineering, microelectronics and technical microwave electronics – equivalent circuits and sinusoids, complex amplitudes and harmonic linearization. In this case, analytical calculation of collective amplification and signal recuperation by dependent sources of electromotive forces, instantaneous coordination of conduction currents, displacement, and transfer in ambient space are performed using Kirchhoff laws and Tellegen's theorem without the superposition principle. Graphical and analytical operators of the wave nonlinear element, which describe the phenomena of nonlinear diffraction and interference of the electromagnetic field as a function of transmission inertia and regeneration of electric disturbances of different intensity based on the theory of electronic wave circuit, are proposed. Determination of changes in flux density and redistribution of oscillatory energy between its common parts is based on the study of impedance and traveling wave coefficient of nonreciprocal four-terminal network equivalent to a long line shunted by a concentrated resistor and negatron (Fig. 1) [1, 2].

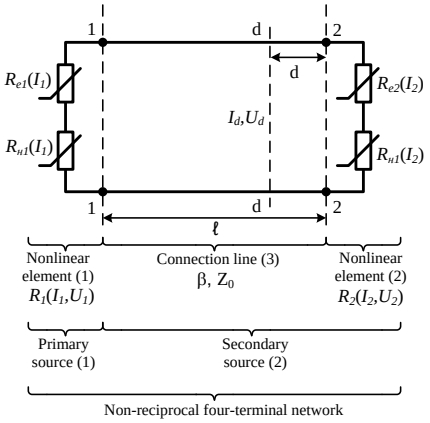

Fig. 1. Nonreciprocal four-terminal network

This theoretical study of mixed current wave mode in analog and digital giga- and terahertz-band integrated circuits substantiates and specifies a way to increase energy efficiency and reduce heating of a single set of one-dimensional metal junctions and discrete microwave electronic devices by joint design of conductive and wireless connections using the non-autonomous block method.

References

[1] Voloshchenko P. Yu., Voloshchenko Yu. P. Researching the phenomenon of nonlinear diffraction in structure of microwave integrated circuits // *International Conference on "Physics and Mechanics of New Materials and Their Applications": Abstracts & Schedule*. 298 – 299, 2021.

[2] Voloshchenko P. Yu., Voloshchenko Yu. P. Topology synthesis of integrated circuits of the giga and terahertz range by the method of non-autonomous blocks // *Physics and Mechanics of New Materials and Their Applications": Abstracts & Schedule*. 300 – 301, 2021.

Modeling the Impedance Characteristics of Microwave Integrated Circuits in Wireless Data Networks

P. Yu. Voloshchenko, Yu. P. Voloshchenko*

Engineering Technological Academy, Southern Federal University, 2, Shevchenko Str., Taganrog, 347900, Russia

*yvoloshchenko@yandex.ru

At the initial stage of mathematical modeling of telemetry and information, communication or energy network modes (for example, LPWAN or Wi-Fi, IoT or WPT), it is necessary to estimate the limitations for modern energy-saving methodology, which requires short-term power on and off of wireless microwave integrated circuits systems. This determines the circulation directions of convection and induced current, coherent superposition and redistribution of electromagnetic field energy in space and time. At present, the above-mentioned energy saving method for inertially interacting electronic microwave devices is intended to increase the autonomous operation time of " open" analog-digital equipment and providing stable signal regeneration in giga- and terahertz ranges in it. However, such a realization of receiving and transmitting blocks stationary state in wireless network is always accompanied by spontaneous amplification and recuperation of the current and voltage thermal oscillations, self-excitation and spontaneous generation of electrical impacts, uncontrolled diffraction and multipath interference in transporting electromagnetic disturbances. At present, there are no engineering mathematical models of electromagnetic field scattering, which take into account the manufacturing technology and material (Si, GaAs, etc) of integrated circuits, can objectively predict oscillatory and wave processes, assess thermal breakdown conditions and reliability of integrated electronic devices in air and space. The study proposes to use the theory of forced mode electron wave circuit for preliminary estimation of amplitude-dependent steady-state adjustment criteria of a set of integrated circuits in the giga- and terahertz bands in monochromatic approximation to solve the described problem. The developed single-frequency phenomenological model of the wireless network reliably determines the correlated operation of electronic devices and controlled microwave power regeneration under composition and instantaneous variation of electromagnetic flows in its any reflecting fragment [1, 2]. Nonlinear impedance of branches

and circuits in electron wave circuit depends on signal intensity and power of electric sources and is estimated by analytical method based on the method of complex amplitudes and harmonic linearization of receiving and transmitting unit parameters, which excludes the use of the superposition principle. When formalizing the initial and boundary conditions, it uses an impedance approach based on the Helmholtz equations and electron mobility, the laws of energy and charge conservation. To minimize energy consumption and heating of analog-digital equipment, correlated variation of "working" points on the DC and AC current and voltage of the volt-ampere characteristics of electronic components, and modification of the existing component design are used. In this case, commensurability and "complex-conjugate" adjustment of input impedance of electronic devices systems and free space is achieved. Maximum acceptable power factor and efficiency of integrated circuit is obtained by losses recuperation and oscillatory energy amplification in the course of purposeful parameters control of the surrounding electromagnetic field in giga- and terahertz ranges.

References

[1] Voloshchenko P. Yu., Voloshchenko Yu. P. An experimental study of a regenerative secondary source of microwave energy // *Izvestiya Vysshikh Uchebnykh Zavedenii. Elektromekhanika (Russian Electromechanics)*, **63**(4), 84 – 89, 2020. (In Russian)

[2] Voloshchenko P. Yu., Voloshchenko Yu. P. Topology synthesis of integrated circuits of the giga and terahertz range by the method of non-autonomous blocks // *International Conference on "Physics and Mechanics of New Materials and Their Applications": Abstracts & Schedule*. 300 – 301, 2021.

Control of Sliding Contact Parameters during Abrasive Treatment of Functionally Graded Material

Y.-C. Wang[a], V. B. Zelentsov[b], P. A. Lapina[b]*, A. L. Nikolaev[b], A. S. Vasiliev[b]

[a]National Cheng Kung University, NCKU, Department of Civil Engineering, Tainan City, 701, Taiwan
[b]Don State Technical University, 1, Gagarin Square, Rostov-on-Don, 344000, Russia

*polina_azarova86@mail.ru

Significant technological limitations are imposed on the sliding contact parameters when processing products from functionally graded materials by grinding. These limitations are related to contact heating temperature, contact wear, abrasive wear rate, contact pressures, abrasive movement speed, etc. For this purpose, the problem of wear of an elastic strip of a functionally graded material by an abrasive is considered. The speed of sliding of the abrasive over the upper surface of the strip is constant, the abrasive has a flat shape at the point of contact. The surface of the strip is heated by friction at the point of contact. The lower surface of the functionally graded strip is rigidly linked to the non-deformable base. In the result of solving the problem, the sliding contact parameters (temperature, pressure, wear on the contact and in the strip) are represented as Laplace convolutions from the abrasive upset in the strip and the corresponding kernels from the difference in time variables. The stability of the obtained solutions is studied. A scheme for solving the problem with restrictions on the parameters of the sliding contact is developed. Examples of calculations for grinding functionally graded materials under conditions of restrictions on the sliding contact parameters are given.

Acknowledgement. This work was supported by the Russian Science Foundation grant 22-49-08014.

Construction of Technique for Identifying the Parameters of Rod Construction during the Propagation of Longitudinal Waves

V. E. Yakovlev[2], A. V. Cherpakov[1,2]*, S.-H. Chang[3], C.-F. Lin[4]

[1]Don State Technical University, Rostov-on-Don, Russia
[2]Southern Federal University, Rostov-on-Don, Russia
[3]Department of Microelectronics Engineering, National Kaohsiung University of Science and Technology, Kaohsiung, Taiwan (R.O.C.)
[4]Departmen. of Electrical Engineering, National Taiwan Ocean University, Taiwan (R.O.C.)

*alex837@yandex.ru

An inverse coefficient problem is considered for a one-dimensional wave equation that describes the propagation of longitudinal waves in an inhomogeneous elastic solid. Based on known data on displacement, velocity, and acceleration at a given point of the solid, such parameters as density and Young's modulus are identified. The solution is based on minimizing the misfit between recorded and modeled data, using various regularization methods. The numerical solution of the wave equation is carried out using the method of lines. Based on the solution of the forward and conjugate problems, the sensitivity or Fréchet derivative matrix is constructed, that is partial derivative of measured data with respect to model parameters. This operator is used as the Jacobian matrix in the Newton's method and the Levenberg-Marquardt's algorithm. It is used to calculate the residual functional gradient and the Hessian matrix in Trust-Region methods. The resulting algorithm was used in a full-scale experiment to study the characteristics of a metal beam.
Acknowledgement. The study was supported by the Russian Science Foundation, grant No. 22-29-01259, https://rscf.ru/project/22-29-01259/.

A 3D Finite Strain Viscoelastic Model with Uncoupled Structural and Stress Relaxations for Shape Memory Polymers

Yingyu Wang

Shanghai Jiao Tong University, Shanghai, China

Wong-Sjtu@sjtu.edu.cn

In this study, a 3D finite strain viscoelastic model with uncoupled structural and stress relaxations is proposed to characterize the thermomechanical behaviors of amorphous shape memory polymers (SMPs). The temperature- and rate-dependent viscoelastic behaviors and stress relaxation are described by the modified Eyring model and nonlinear Adam-Gibbs model based on molecular mechanism. A modified weight function analogous to frozen

fraction in phase transition theory is proposed to improve accuracy of the model on predicting the stress-strain response before yielding when temperature is below glass transition temperature. The developed model is implemented with MATLAB to simulate shape recovery experiments of amorphous SMPs under constraints or free in the literature. Good consistency between simulation results and experimental data is obtained.

Constructive Anisotropy and Shape Parametrization of Non-axisymmetric Shells

A. S. Yudin

I. I. Vorovich Institute of Mathematics, Mechanics and Computer Sciences, Southern Federal University, Rostov-on-Don, Russia

ayudin@sfedu.ru

To increase the rigidity of the shells, as a rule, they are supported by a grid of ribs. This is characteristic of the designs of aircraft fuselages and ship hulls. The grid of edges is easy to take into account for axisymmetric shells having an orthogonal coordinate system. In the case of skew-angle grids, it is necessary to work according to the rules of tensor algebra and analysis. Here, the elasticity relations for non-axisymmetric shells supported by a grid of edges are derived, which are taken into account according to the scheme of constructive anisotropy. We assume that the grid lines coincide with the directions of the coordinate lines that can be selected for the grid configuration of the reinforcing set. We consider the edges spaced with a sufficiently small step so that at least two edges fall on the half-wave in the expected waveforms. Then we can apply the scheme of constructive anisotropy by the method of "smearing" the energy of each edge at the placement step. In general, the placement step will be discretely variable. However, the smearing scheme essentially moves away from a more complex scheme with discrete edges to a scheme of an anisotropic shell with continuously changing properties. Therefore, in cases of non-sharp variability of the placement of edges, we can take their averaged values within the section (module-element) as steps in each of the two directions. For more accurate modeling, we can introduce functions that approximate the distribution of steps in each of the coordinate directions. In general, we assume that the sections of the grid edges are in a stress-strain state of the same type as the shell, that is, they are determined by the same set of components of stress and strain tensors. According to the scheme of energy smearing, the contribution of the edges to the specific potential energy of the system is determined by the sum of integrals over the sections of the edges of two directions. Integration is performed over the areas of the oblique section of the edges by a plane passing through the normal of the shell and tangent to the coordinate line intersecting the edge at the point of attachment of the edge. The attachment point is understood as the projection of the center of gravity of the section on the skin. The energy components for the edges and the potential energy of the shell are summed up. After performing the integration, a quadratic form is obtained from the deformation components of the median surface. The derivatives of the total potential energy of the shell with respect to the deformation components give the relations of elasticity in forces and moments. Formulas are presented and on their basis the construction of the main surface of non-axisymmetric shells closed in the circumferential direction is carried out. Parameterization of such shells is performed in the class of framed shells with linear surfaces of the constituent sections (module elements). The

module-element is built on two guiding plane contours, defined in local coordinate systems. The contour equations are translated into a polar coordinate system and given by analytical or piecewise analytical functions. The contours can have different angles of inclination to the local axis of the module element. The plane passing through the axis intersects the guiding contours at two points. When this plane rotates, the segment between the points forms a ruled surface. The shell of a composite structure is assembled from a chain of module elements. The main line of a composite structure can be a multi-link flat polyline, on which the centers of the contours of the frame are located. The surface of a composite structure is constructed in a global Cartesian coordinate system under the assumption that the diametrical planes of all contours are in the same plane. The ability to control the angles of inclination of the planes of the guide contours allows one to combine them with the configuration of the ends, the docking lines of the sections and the external borders of the frames. Examples of constructing the main surfaces in a grid form are shown.

Acknowledgement. Research was financially supported by Southern Federal University, grant No. VnGr-07/2020-04-IM (Ministry of Science and Higher Education of the Russian Federation).

Plastic Forming of an Axisymmetric Shell with a Given Critical Load

A. S. Yudin

I. I. Vorovich Institute of Mathematics, Mechanics and Computer Sciences, Southern Federal University, Rostov-on-Don, Russia

ayudin@sfedu.ru

Many types of equipment that operate under the influence of increased pressure of liquid and gaseous media are used in the chemical and oil refining industries, in thermal and nuclear power. The destruction of such equipment leads to catastrophic results, namely leakage of aggressive liquids, explosions and fires. To prevent such consequences, appropriate protection devices against abnormal pressure increase are necessary. In the beginning, these were valves. Then bursting membranes appeared. But the most effective were flapping membranes, which lose stability and collapse at the required pressure [1]. At the same time, ensuring high-precision actuation pressure proved to be a difficult task. The technology of free drawing by pressure from round plates does not allow ensuring the stability of critical loads. This is due to the influence of a number of random factors, which are called initial imperfections. These include, first of all, geometric imperfections such as small loss and features of the edge support in the area of bends from the dome part of the membrane to the support surfaces of the holder. There are other deviations from the calculated models. The difference in the physical and mechanical properties of the sheet material along and across the direction of rolling and the thickness difference in the area of the sheet significantly affect. Ideas about the real nature of the support of membranes under conditions of their clamping in the elements of the holders to the stages ensuring the achievement of the required tightness, as a rule, are not identical with the usual concepts such as "rigid pinching", "plastic hinge" or "free support". Microstructural analysis of the marginal zone of membranes obtained by plastic molding showed that the membrane material has a pronounced heterogeneity in thickness in the form of microstructure grains and local zones of compaction and loosening in the inflection zone. This leads to instability of critical loads and their significant dispersion. On the basis of numerous

experiments, a technology was found for influencing the shape of the shell with additional force influences, which allows creating membranes with high actuation accuracy. Having the experimental results, we set the task of mathematical modeling of the dome extraction process by pressure combined with the force in the apex. Equations were derived and a theoretical method was developed, which gave a good agreement with the experiment on the ratio of exhaust pressure and lifting height. However, when compared with the load of loss of stability, coordination failed. In this report, the reasons for the discrepancy are analyzed and a possible correction of the shape is given, leading to a given critical load. It also gives an idea of the technology actually used for manufacturing high-precision membranes. The molding of the shell is carried out by free extraction by pressure from a flat round plate, pinched along the contour, with additional force action. This is a concentrated force in the apex, which is created by the load on the rod. Thus, by the method of mathematical modeling, the problem of plastic molding of a domed shell providing a given critical load of loss of stability is considered. A semi-inverse method is used to solve the physically and geometrically nonlinear molding problem [2]. In the method, a functional for the molding load is constructed based on a differential system of equations, which is brought to a stationary value. The buckling load is estimated for a uniform pressure applied from the side of the bulge. The stability problem is solved using a geometrically nonlinear system of second-order precision equations in the elastic domain of the material.

Acknowledgement. The research was financially supported by the Southern Federal University, grant No. VnGr/2020-04-IM (Ministry of Science and Higher Education of the Russian Federation).

Reference

[1] Yudin A. S., Belikov N. V. Protection of Equipment from Destruction by Excessive Pressure. In: *Advanced Materials - Studies and Applications*, I. A. Parinov, S. H. Chang, S. Theerakulpisut (Eds.). Nova Science Publishers: New York, 499 – 509, 2015.

[2] Anatoly S. Yudin, Dmitry V. Shchitov. *Semi-inverse Method in Nonlinear Problems of Axisymmetric Shells Forming*. World Scientific Publishing, Europe Ltd., 230, 2021.

Obtaining, Dielectric and Piezoelectric Properties of Modified Lead-free $NaNbO_3$ – $KNbO_3$/White – Cement Composite Ceramics

Yu. I. Yurasov[1,2]*, M. I. Tolstunov[2], A. V. Nazarenko[1], A. V. Yudin[1,3], E. V. Glazunova[2], V. V. Likhatsky[1,2], I. A. Verbenko[2], L. A. Reznitchenko[2]

[1]Southern Scientific Center, Russian Academy of Sciences, Rostov- on-Don, 344006, Russia
[2]Southern Federal University, Rostov- on-Don, 344090, Russia
[3]YRSPU (NPI) named after M. I. Platov, Novocherkassk, 346428, Russia

*yucomp@ya.ru

For many years, many researchers have been searching for optimal methods for obtaining piezo materials, including those with reduced sintering temperatures. Reducing the sintering temperature is one of the main tasks in the production of piezo materials in large batches to reduce the cost of final products. The transition to lead-free piezoceramics is also a priority to exclude toxic elements from production. The solution of these two tasks can be realized through the creation of lead-free piezocomposites, that is piezoceramic/polymer or piezoceramic/cement. In [1] we have shown that a lead-free piezocomposite

piezoceramic/polymer based on potassium-sodium niobate using 25 vols.% polyvinyldenafluoride (KNN-LSTN/PVDF) has a piezo module $|d_{33}|$ = 30 pC/N at a production temperature of 180 °C and a pressure of 20 MPa for 10 min. If cement is used as a binder, the sintering stage leaves the production method, which will reduce the cost of production many times and increase its energy efficiency. Work on the study of piezocomposites with cement is underway, but mainly in interaction with PZT [2], lead-free ceramics have been used very rarely. The paper [3] shows a connection diagram of 2-2 unleaded piezoelectric ceramic composites $Bi_{0.5}Na_{0.5}TiO_3$/Portland cement with a content of about 30 – 70 vol.% At the same time, cement was not a binder, but was used as interlayers between parts of piezoceramics, besides, less bismuth oxide is also a dangerous component. Accordingly, the paper presents the preparation and study of dielectric [4] and piezoelectric properties of modified lead-free $NaNbO_3$ – $KNbO_3$/White-cement composite ceramics. The choice of white cement is due to the minimum content of manganese, chromium and iron compounds, as well as almost identical strength characteristics compared to cement of other brands. A composite material of 3-0 type is obtained, where the connectivity of the structure is provided by a three-dimensional cement matrix. When using sodium-containing materials, ion exchange occurs on the surface of the material due to the almost identical ionic radius of Na^+ and Ca^{2+} cations. For example, for the material: $Na_{0.495}K_{0.495}Cu_{0.005}NbO_3 + Ca(OH)_2 = Na_{0.495-2x}K_{0.495}Cu_{0.005}NbO_3 + 2x$NaOH. The materials obtained are thermally stable and can withstand heating over 400 °C. At temperatures of about 700 °C, another endothermic effect occurs associated with the decomposition of the cement matrix. When the electric field strength exceeds 4 kV/mm, an electrical breakdown occurs. At the maximum achieved intensity, the value of d_{33} was 34 pkCl/N. Storage of the polarized sample for a month led to a decrease in this value to 15 pcCl/N. At the same time, the dispersion of the dielectric permittivity was studied using a new model to describe the complex electrical conductivity [4].

Acknowledgement. This study was supported financially by the Ministry of Education and Science of the Russian Federation SFEDU [0852-2020-0032 (BAZ0110/20-3-07IF)], SSC-RAS (122020100254-3, 121100500084-2), CKP No. 1483136, CKP No. 501994.

References

[1] Yurasov Yu. I., Tolstunov M. I. et al. Dielectric and piezoelectric properties of modified lead-free $NaNbO_3$ – $KNbO_3$/PVDF composite ceramics // *Journal of Advanced Dielectrics*, **11**(4, 5), 2160015, 2021.

[2] Nesterov A. A., Topolov V. Yu., et al. Longitudinal piezoelectric effect and hydrostatic response in novel laminar composites based on ferroelectric ceramics // *Ceramics International*. **45**(17), 22241, 2019, doi:10.1016/j.ceramint.2019.07.248

[3] Rianyoi R. et al, Dielectric and piezoelectric properties of 2-2 connectivity lead-free piezoelectric ceramic $Bi_{0.5}Na_{0.5}TiO_3$/Portland cement composites // *Ceramics International*. **44**(1), S220 – S223, 2018.

[4] Yurasov Yu. I., Nazarenko A. V Temperature-frequency parameter of dielectric losses distribution in nonlinear dielectrics // *Science of the South of Russia*, **15**(1), 31 – 41, 2019.

Synthesis of High-pressure Pump Drive Reducer for Service of Oil and Gas Wells

V. V. Zaitsev*, A. V. Biel, S. O. Kireev, M. V. Korchagina

Don State Technical University, Rostov-on-Don, Russia

*zaytsev18061999@mail.ru

Due to the deterioration of the environmental situation in the world, technologies for the rational use of subsoil are becoming more and more relevant. Oil recovery enhancement technologies significantly extend the service life of oil and gas wells, which generally increases production efficiency. The most common method of intensification of production is hydraulic fracturing (HF) [1]. The efficiency of HF is primarily dependent on the pump equipment used [2]. As a rule, the pump unit consists of the following units: electric motor, reduction gear box and pump. The most efficient in such units are single-stage cylindrical gearboxes with oblique engagement. In most cases, it is necessary for each pump to design a gear box with the required torque and gear ratio. During the design of the reduction gearbox for the three-plunger high pressure pump NP-720 [3], certain calculations were made. The requirements for the reduction gear of the pump in question are high, since the torque on the output shaft is 47,677 N·m, at a gear ratio of 5. These values are provided by single-stage cylindrical transmission. The choice of high-strength alloy steel for the gear pair of the reduction gear was made, the axial distance was calculated according to the design formula for contact endurance. It is known that with other equal values of transmission parameters, helical gears are able to transmit more torque. The estimated angle of inclination of the teeth was 10°. The engagement modulus was 6 mm. The number of gear and wheel teeth was calculated, after which the remaining necessary geometric parameters of gear engagement were determined. All calculations were made according to the method [4]. According to the calculations, the design of the gear box was developed. Moreover, the pump layout diagram is made using the developed design of the reduction gear box. The overall layout showed that the promising direction of improvement of the pump unit is to reduce its weight and dimensions by combining the designed reduction gear and pump NP-720 into a single unit.

References

[1] *Prud'homme A. Hydrofracking: What Everyone Needs to Know*. Oxford University Press, 208, 2013.

[2] Dautov T. M., Gazarov R. E. *New Generation of High-pressure Plunger Pumps. Izhneftemash*. Izhevsk: Oil Production Equipment, 2003 (In Russian).

[3] Popov V., Kireev S. O. *Three-plunger High Pressure Pumps. Trust-Engineering*. Rostov-on-Don: Fuel Market, 6, 2010 (In Russian).

[4] Menkova N. M. *Design of a Single-stage Cylindrical Reduction Gear Box. Tutorial*. Moscow: Sergo Ordzhonikidze Russian State Geological Exploration University Press, 2013 (In Russian).

Electric-field Induced Phase Transformation in Relaxor-based Multicomponent Ceramics

I. N. Zakharchenko, M. V. Talanov

Research Institute of Physics, Southern Federal University, Rostov-on-Don, 344090, Russia

*mvtalanov@sfedu.ru

Relaxor ferroelectrics are of promising interest for science and technology due to their intriguing physical properties. One interesting feature of the relaxor ferroelectrics is the occurrence of the electric-field induced phase transition into a normal ferroelectric state [1]. Such transition can activate the polarization rotation mechanism in the compositions of the relaxor-based solid solutions with the initial rhombohedral or monoclinic structures [2]. It is believed that polarization rotation is the structural origin of high values of the piezoelectric and dielectric response of the ferroelectric solid solutions near the morphotropic phase boundary [3]. In the case of relaxor ferroelectrics, the presence of the polar nano regions can facilitate the electric-field induced polarization rotation leading to ultra-high electromechanical properties [4]. In this work we perform X-ray diffraction study of the multicomponent ceramics based on the typical relaxor ferroelectrics $PbMg_{1/3}Nb_{2/3}O_3$, $PbZn_{1/3}Nb_{2/3}O_3$ and $PbNi_{1/3}Nb_{2/3}O_3$ with ultra-high values of electric-field induced strain (large-signal piezoelectric coefficient d_{33} is more than 2000 pm/V) [5]. Our investigation shows visible changes in the X-ray diffraction patterns starting with relatively small values of electric field (~200 V/cm). The results are discussed in terms of the polarization rotation mechanism and its influence on the macroscopical strain of the ceramics studied.

Acknowledgement. This work was financially supported by the Ministry of Science and Higher Education of the Russian Federation (State assignment in the field of scientific activity, Southern Federal University, 2020, scientific project No. 0852-2020-0032), (BAZ0110/20-3-08IF).

References

[1] Bokov A. A., Ye Z.-G. // *J. Materials Sci*., **41**, 31 – 52, 2006.
[2] Noheda B., Cox D. E., Shirane G., Park S.-E., Cross L. E., Zhong Z. // *Phys. Rev. Lett*., **86**, 3891 – 3894, 2001.
[3] Fu H., Cohen R. E. // *Nature*, **403**, 281 – 283, 2000.
[4] Li F., et al. // *Nature Commun*., **7**, 13807, 2016.
[5] Talanov M. V., Bokov A. A., Marakhovsky M. A. // *Acta Materialia*, **193**, 40 – 50, 2020.

Dielectric and Optical Properties of Polycrystalline $SrTiO_3$ Thin Films

K. M. Zhidel[1,2]*, A. V. Pavlenko[1,2]

[1]Research Institute of Physics, Southern Federal University, 194, Stachki Ave., Rostov-on-Don, 344090, Russia
[2]Federal Research Centre The Southern Scientific Centre of the Russian Academy of Sciences, 41, Chekhov Str., Rostov-on-Don, 344006, Russia

*karinagidele@gmail.com

In recent years, it has been noted in physical materials science that transition metal oxides, in particular $SrTiO_3$ (STO), would open a new path for heterogeneous new functions in inexpensive silicon technology. In this work, the results of studying the structure, dielectric, and optical properties of STO thin films, grown by RF cathode sputtering in an oxygen atmosphere on Si (001) substrates, are presented. Preliminary XRD studies of the $SrTiO_3$ film indicate the absence of impurity phases and its polycrystallinity, as well as the presence of unit cell deformation. The revealed effects affected the dielectric and optical characteristics of the STO film. According to dielectric measurements, polycrystalline $SrTiO_3$ films on silicon substrates are in the ferroelectric phase. It was shown by spectral ellipsometry that the film, obtained by RF cathode sputtering in an oxygen atmosphere, contains a small amount of silicon oxide. The picked-up structure optical model (rough layer – film – buffer layer – substrate) allowed one to reach good coincidence to experimental data in spectral parameters ψ and Δ and to define layers' optical characteristics of STO/SiO_2/Si (001) structure. Thus, the films have weak absorption, a normal dispersion of the refractive index, and interdiffusion layers at the interfaces. The resulting films have a high refractive index (n = 2.4) compared to conventional planar materials (n = 1.46 for SiO_2), which is beneficial for miniaturization of devices.

Acknowledgements. The study was carried out with the financial support of the Ministry of Science and Higher Education of the Russian Federation (State task in the field of scientific activity, project No. (0852-2020-0032)/(BAZ0110/20-3-07IF)). The work was performed with the use of equipment of the Center for Collective Use "Integrated Centre of Scientific-Technological Equipment SSC RAS (Research, Development, Approval)", the Southern Scientific Centre of the Russian Academy of Sciences (No. 501994).

(1 – x)BFO – xPFN Ceramics System: Features of Dielectric Properties

K. M. Zhidel[1,2]*, A. V. Pavlenko[1,2]

[1]Research Institute of Physics, Southern Federal University, 194, Stachki Ave., Rostov-on-Don, 344090, Russia
[2]Federal Research Centre The Southern Scientific Centre of the Russian Academy of Sciences, 41, Chekhov Str., Rostov-on-Don, 344006, Russia

*karinagidele@gmail.com

Currently, multiferroics based on bismuth ferrite ($BiFeO_3$, BFO) and lead ferroniobate ($PbFe_{0.5}Nb_{0.5}O_3$, PFN) are being actively investigated. This is due to the prospects for their

application in functional electronics devices. In this work, we investigated the dielectric characteristics of $(1 - x)$BFO – xPFN system. The $\varepsilon'/\varepsilon_0(T)$ dependences of the $(1 - x)$BFO – xPFN solid solution (SS) in the range $T = (300 - 1000)$ K at $f = 10^6$ Hz are shown as an example in the Fig. 1. The regularities, obtained in the study of the dielectric characteristics, indicate the existence on the system phase diagram of boundaries separating compositions with different manifestations of ferroelectric properties: ferroelectrics with a diffuse phase transition ($FDPT_1$) at $0.00 \le x < 0.40$; ferroelectrics-relaxors (FRs) at $0.40 \le x \le 0.90$ and ferroelectrics with a diffuse phase transition ($FDPT_2$) at $0.90 < x \le 1.00$. It is interesting, in this case, the fact of localization of SS related to the FDTP, near the extreme components of the system. At the same time, we note the large extent of the FDPT near BFO. From our viewpoint, this is associated with the inherent dielectric instability of BFO and pronounced structural instability. The reasons for the revealed patterns are discussed in the work.

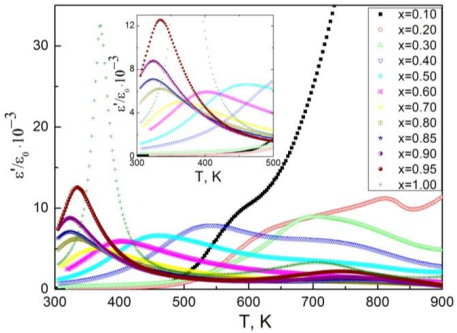

Fig. 1. $\varepsilon'/\varepsilon_0(T)$ dependences for ceramics of the $(1 - x)$BFO – xPFN SS system ($f = 1$ MHz)

Acknowledgements. The study was carried out with the financial support of the Ministry of Science and Higher Education of the Russian Federation (State task in the field of scientific activity, project No. (0852-2020-0032)/(BAZ0110/20-3-07IF)). The work was performed with the use of equipment of the Center for Collective Use "Integrated Centre of Scientific-Technological Equipment SSC RAS (Research, Development, Approval)", the Southern Scientific Centre of the Russian Academy of Sciences (No. 501994).

Explaining the Inconsistency of Solutions to the Contact Problem on the Convergence of Two Elastic Cylinders

G. A. Zhuravlev[1]*, T. M. Andreeva, Yu. E. Drobotov[2]**

Southern Federal University, Rostov-on-Don, Russia

*zhur.okp@yandex.ru; **yu.e.drobotov@yandex.ru

Analysis of the more than a century-old inconsistency of methods to calculate the axial approach of elastic circular cylinders in the initially linear contact usually begins with the works of Hertz. Hertz, however, did not provide the solution to this problem, which had led to

the creation (and, moreover, widespread use) of various methods: fewer incorrect as [1, 2] (nevertheless, sufficiently accurate for a number of theoretical and practical fields), as well as misleading ones like [3]. This conclusion became fully justified only after the selective independence of the contact approach in the smaller radius was revealed. The mechanical effect, called here 'EA' for short, has its place only when the difference between the cylinder radii is large enough, which has been demonstrated applying the results of [4, 5]. In the report presented, it is stated that studying this effect can explain the reasons for the traditional inconsistency of the known solutions to the problem on the contact approach. To prove EA, a theoretical investigation is carried out for various combinations of material parameters, and the experimental data are considered in the framework of the theoretical models developed. It is shown that, for a large difference in the radii of the contacting cylinders, varying the radius of the smaller cylinder selectively leads to the same absolute value but different sign of the displacements in the contacting cylinders. The well-known methods, which were based on the classical Hertz solution, such as [1], and on the solution of N. I. Muskhelishvili [6], such as the method [2], completely denied the absence of the influence of radii on the approach. At the same time, other methods (for example, [3]) fundamentally denied its presence, being based on theory, which was proven to be false in [4].

Acknowledgement. The research was financially supported by Southern Federal University, grant No. VnGr/2020-04-IM (Ministry of Science and Higher Education of the Russian Federation).

References

[1] Kovalsky B. S. *Calculation of details on local compression.* Kharkov, HVKIU, 1967 (In Russian).

[2] Loo T. T. Effect of curvature on the Hertz theory for two cylindrical rings in contact // *J. Appl. Mech.*, **25**, 122 – 124, 1958.

[3] Ajrapetov E. L. Contact strain of cylinders with parallel axes // *Vestnik Mashinostroeniya*, **6**, 6–10, 1988 (In Russian).

[4] Zhuravlev G. A., Karpenko V. A. Approaching elastic solids, modeled by circular cylinders // *Tekhnika Mashinostroeniya*, **6** (28), 51–55, 2008.

[5] Zhuravlev G. A. In: *Mixed Problems of Solid Mechanics. Materials of the V Russian Conference with International Participation, 23 – 25 August 2005*. Saratov, Saratov State University Press, 148–151, 2005 (In Russian)

[6] Muskhelishvili N. I. *Some Basic Problems of the Mathematical Theory of Elasticity*. Springer Netherlands, 1977

Maximum Tangential Stresses Due to Contact of Two Elastic Parallel Circular Cylinders and Their Depth

G. A. Zhuravlev*, Yu. E. Drobotov**

Southern Federal University, Rostov-on-Don, Russia

*****zhur.okp@yandex.ru, ******yu.e.drobotov@yandex.ru

Analytical and numerical methods for calculating maximal shear stresses and their depth in the contact area of two parallel elastic circular cylinders are considered. The presented research aims to discuss the reasons for the contradictory nature of these methods and to argue for the statement that the most important is in the misstatement of the role played by the

curvature of the contact elements by the solutions treated as exact ones. Hertzian contact theories have been being the common basis of standards in mechanical engineering for decades. The Boussinesq–Cerruti solution of the Hertz problem assumes substituting one of the cylinders with an elastic half-space [1]. In this case, the relative values $\tau_{\max}/\sigma_{z\max}$ and $h_{\tau\max}/b$ of the maximal shear stress $\tau_{\max}$, the maximal contact stress $\sigma_{z\max}$, the depth $h_{\tau\max}$ of $\tau_{\max}$, and the minor b-axis of the elliptical contact area appear to be independent of the curvature of the cylinders. However, the solution [2] has shown that, with varying one of the radii, these values correspond to those of the classical theory only for a particular range of geometric parameters [3, 4]. In this report, the solution [2] is compared with the finite element modelling for the contact problem. The Hertzian solution is assumed as a criterion, and the contradictions between the results are studied. An approach to a reliable assessment of the accuracy of classical and numerical solutions to contact problems is provided by calculating the maximal shear stresses and the depth of their occurrence.

Acknowledgement. The research was financially supported by Southern Federal University, grant No. VnGr/2020-04-IM (Ministry of Science and Higher Education of the Russian Federation).

References

[1] Johnson K. L. *Contact Mechanics*. Cambridge University Press. 1987.

[2] Zhuravlev G. A., Azarov A. D., Babenko I. S. To definition of depth stresses in contact area of elastic cylinders // News of Univesities. North-Caucasus Region. Natural Sciences, **1**(173), 26–30, 2013.

[3] Zhuravlev G.A., Drobotov Yu. E., Piskunov A. S. On the contradictory values of stresses in the area of contact of two parallel rollers // *International Journal for Research in Applied Science & Engineering*, **4**(VII), 410–416, 2016.

[4] Zhuravlev G. A., Drobotov Yu. E., Piskunov A. S., Maksimets S. V. The comparative evaluation of precision of classical and numerical solutions of contact problems // *Material Physics and Mechanics*, **37**, 84–91, 2018.

On the Structural Strength of Machine Elements with Loaded Projections

G. A. Zhuravlev*, Yu. E. Drobotov**

Southern Federal University, Rostov-on-Don, Russia

*zhur.okp@yandex.ru, **yu.e.drobotov@yandex.ru

The presented report shows the possibilities of using structural strength techniques to propose an original technology (in the development of the method [1]) for the hardening of machine elements with loaded projections. Such elements are complex shaped and loaded by bending with compression of the projections on their stressed base. The position of the calculated section depends on various factors and generally does not match the minimum thickness section of a rod. However, the stress concentration values are usually provided for the minimum thickness section in the recess zone of the rod, whereas information on the base of a projection is limited and relates to specific cases only. In this report, the stress-strain state of machine elements with a geometric concentrator is carried out based on “elastic” solutions, particularly with the application of widely used S. P. Timoshenko’s hypothesis on deformation

distribution law's being independent of the way in which material is strained and hardened [2, 3]:

$$\tilde{\varepsilon}_x(y) = \varepsilon_x(y)\frac{\varepsilon_T}{\varepsilon_I(y_T)}.$$

Here, $\varepsilon_x(y)$ and $\tilde{\varepsilon}_x(y)$ are relative linear deformations at the current point y for a specific cross-section at $x = \text{const}$ for an ideal absolutely elastic material and the real one, respectively; ε_T is the relative deformation, corresponding to the material yield stress; $\varepsilon_I(y_T)$ is the criterion value, characterizing transition from elastic deforming to the nonelastic one at the boundary point $y = y_T$ of the section for ideally elastic material. To calculate the stresses in the elastic part, the analytical solution of Heinz Neuber [4] is used, which is generalized to model various geometric characteristics of a loaded rod, specifically to vary its thickness and the orientation of the hyperbolic recesses. The precision of the constructed elastic-plastic model is compared with the results provided by the finite element method.

Acknowledgement. The study was financially supported by the Grant No. 21-19-00423 of the Russian Science Foundation in the Southern Federal University.

References

[1] Zhuravlev G.A. et al. Method of and device for gear teeth hardening. *United States Patent*, US3851512A.

[2] Del' G.D.; Chebaevskii B.P., Pronkin A.F. Engineering method of calculating the stress concentration factor with consideration of ductility and creep // *Strength Mater.* **3,** 80–83, 1971, https://doi.org/10.1007/BF01530378

[3] Troshchenko V.T., Getman A.F. Study of the effect of small elastoplastic deformations on the load-bearing capacity of specimens with stress concentrators under repeated variable loading // *Strength Mater.* **4,** 140–144, 1972, https://doi.org/10.1007/BF01527567

[4] Neuber H. *Kerbspannungslehre. Theorie der Spannungskonzentration Genaue Berechnung der Festigkeit*. Springer-Verlag Berlin Heidelberg, 2001.

Crystal Structure and Ferroelectrics Properties of Mixed-layer $Bi_{7-x}Y_xTi_4TaO_{21}$ (x = 0, 0.2, 0.4, 0.6, 0.8, 1.0) Ceramics

S. V. Zubkov[1], I.A. Parinov[2]

[1]Research Institute of Physics, Southern Federal University, Rostov-on-Don, Russia
[2]I. I. Vorovich Mathematics, Mechanics and Computer Science Institute, Southern Federal University, Rostov-on-Don, Russia

*svzubkov61@mail.ru

Layered perovskite-like bismuth oxides with the Aurivillius phase (AP) structure have been known for several decades [1, 2], but interest to them has been growing due to their potential practical applications. APs are promising materials for fabricating high-temperature piezoelectric transducers operating in extreme conditions and are considered as elements of ferroelectric memory devices (FeRAM), as multifunctional materials exhibiting magnetic properties (multiferroics), photoluminescence etc. At the present time, the number of known APs is several hundred, and this continues to increase. A number of solid solutions $Bi_{7-x}Y_xTi_4TaO_{21}$ (x = 0.0, 0.2, 0.4, 0.6, 0.8, 1.0) have been synthesized from oxides by solid-

phase reaction. The crystal structure, the electrophysical characteristics (see Fig. 1) and the microstructure of the prepared ceramic samples have been studied. According to X-ray powder diffraction, all the compounds are single-phase with the structure of mixed-layer Aurivillius phases ($m = 2.5$) with the orthorhombic crystal lattice (space group I2cm, $Z = 2$). The activation energies of charge carriers have been found in different temperature ranges.

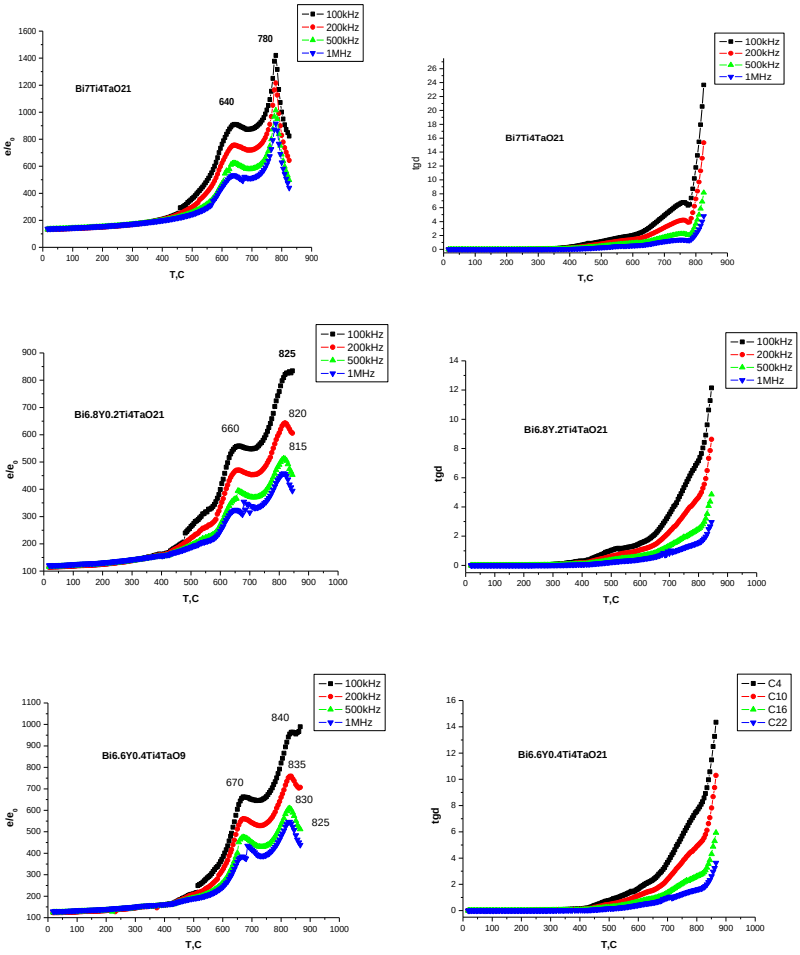

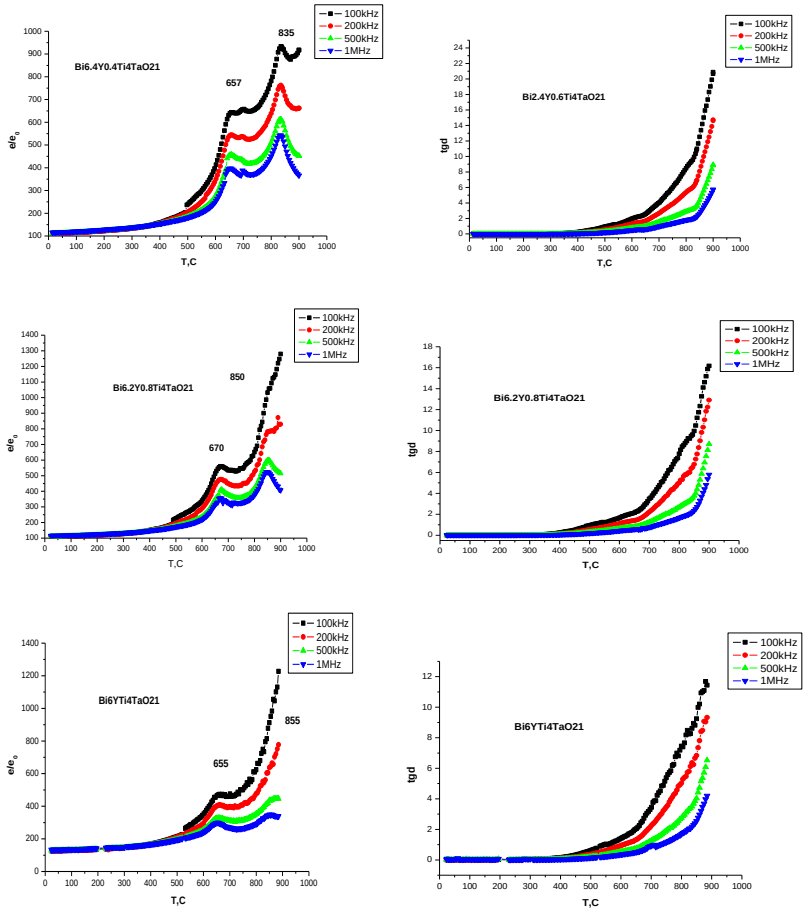

Fig. 1

Acknowledgement. The study was financially supported by the Russian Science Foundation (Grant No. 21-19-00423) in the Southern Federal Univesity.

References

[1] Zubkov S. V., Vlasenko V. G., Shuvaeva V. A., Shevtsova S. I. Structure and dielectric properties of solid solutions $Bi_7Ti_{4+x}W_xTa_{1-2x}O_{21}$ (x = 0 – 0.5) // *Phys. Solid State*, **58**(1), 42, 2016.

[2] Mercurio D., Trolliard G., Hansen T., Mercurio J.P., Crystal structure of the ferroelectric mixed Aurivillius phase $Bi_7Ti_4NbO_{21}$ // *International Journal of Inorganic Materials*, **2**(5), 397 – 406, 2000.

New Mixed-layer Compound of the Aurivillius Family of Phases with the Highest Phase Transition Temperature

S. V. Zubkov[1], I. A. Parinov[2]

[1]Research Institute of Physics, Southern Federal University, 194, Stachki Ave., Rostov-on- Don, 344090, Russia
[2]I. I. Vorovich Mathematics, Mechanics and Computer Science Institute, Southern Federal University, Rostov-on-Don, Russia

*svzubkov61@mail.ru

The perovskite-like layer of the phase Aurivillius (APs) unit cell has a structural fragment in which six X = O ions form a crystallographic polyhedron in the form of an octahedron around the smaller *B*-cation, and eight large *A*-cations can form a cube. Twelve oxygen ions form a cuboctahedron. For each X = O, the nearest neighbors will be both *A* and *B*, located in the form of a tetragonal bipyramid and having different sizes and properties. Four *A*-cations form the base of the bipyramid with sides equal to the unit cell parameter *a*. Two *B*-cations ($R_B < R_A$) are located perpendicular to the center of the base of the bipyramid on both sides at distances *a*/2. Cations *A* in positions with a cuboctahedral environment can be one-, two-, and trivalent large-radius cations (Na^+, K^+, Ca^{2+}, Sr^{2+}, Ba^{2+}, Pb^{2+}, Bi^{3+}, Ln^{3+} (lanthanides) and Ac (actinides)), and positions *B* inside oxygen octahedra are occupied by highly charged ($\geq 3+$) cations with small radii (Ti^{4+}, Cr^{3+}, Ga^{3+}, Mn^{4+}, Fe^{3+}, Nb^{5+}, Mo^{6+}, Co^{3+}, Ta^{4+}, W^{6+}, Ir^{4+}, etc.). The value of *m* is determined by the number of perovskite layers $[A_{m-1}B_mO_{3m+1}]^{2-}$ located between the fluorite-like layers $[Bi_2O_2]^{2+}$ and can take integer or half-integer values in the range $m = 1 – 5$. If *m* is a half-integer number, then there is an alternation of perovskite layers with *m*, differing by 1 in the lattice. Figure 1 shows the APs structures with $m = 2, 3, 4$. The AP structure above the Curie point is tetragonal and belongs to the space group I4/mmm. Positions *A* and *B* can be occupied by the same or by several different atoms. Atomic substitutions in positions *A* and *B* have a significant effect on the electrophysical characteristics of the AP.

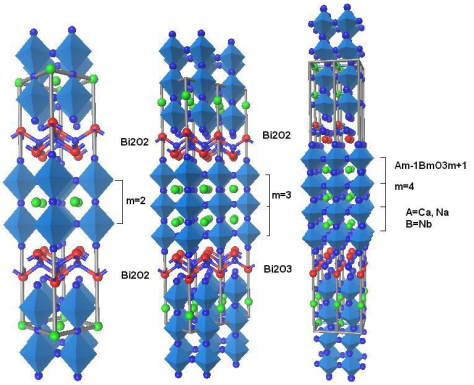

Fig. 1. APs structures with $m = 2, 3, 4$

Polycrystalline AP samples were synthesized by solid-phase reaction of the corresponding oxides Bi_2O_3, TiO_2, Nb_2O_3, $CaCO_3$. The oxide powders weighed in accordance with the stoichiometric composition of the synthesized compound were pressed into a tablet after prolonged grinding and mixing. The samples were fired in a laboratory muffle furnace in air. The sample was preheated to temperatures T = 770 °C, after which intermediate grinding and mixing were performed. The final firing was carried out at a temperature of T = 1100 – 1150 °C [1]. It was found that all the obtained APs crystallize in the orthorhombic system with the space group of the unit cell B2cb. For electrical measurements, Ag-Pd electrodes were applied to the flat surfaces of ceramic samples. The measurements were carried out using an E7-20 immitance meter in the frequency range of 100 kHz – 1 MHz in the temperature range from room temperature to 960 °C (see Fig. 2).

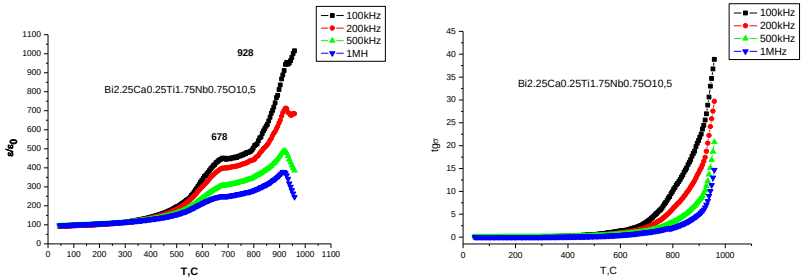

Fig. 2. Temperature dependence of the relative permittivity $\varepsilon/\varepsilon_0$ and the loss tangent tgσ for $Bi_{3.25}Ca_{0.25}Ti_{1.75}Nb_{0.75}O_{10.5}$

It is generally accepted for mixed-layer PA that the first peak $\varepsilon/\varepsilon_0(T)$ at T_1 corresponds to a phase transition from the polar to the polar phase (ferroelectric – ferroelectric), while the temperature T_2 corresponds to the transition from the polar to the nonpolar phase (ferroelectric – paraelectric), that is the Curie temperature T_C. Table 1 shows the values of the phase transition temperature T_1 and T_2, the values of $\varepsilon/\varepsilon_0$ (T_1, T_2) at a frequency of 100 kHz. The $Bi_{3.25}Ca_{0.25}Ti_{1.75}Nb_{0.75}O_{10.5}$ compound can be represented as a combination of a two-layer Bi_3TiNbO_9 compound and a three-layer $B_4T_3O_9$ compound doped with calcium Ca. It is a well-known fact that doping in a mixed layer compound occurs in a perovskite layer with fewer layers. Calcium ions Ca^{2+} replace bismuth ions Bi^{3+} in Bi_3TiNbO (m = 2) [2]. An increase of the Curie temperature T_C is associated with the difference in ionic radii in positions A of perovskite-like layers, where Bi^{3+}-ions are replaced by ions of a smaller radius Ca^{2+} (R_{Bi4+} = 1.38 Å, R_{Ca2+} = 1.34 Å) [3].

Table 1. Curie temperature T_{C1}, T_{C2}, $\varepsilon/\varepsilon_0(T_1, T_2)$

Compound	T_{C1}, °C	T_{C2}, °C	$\varepsilon/\varepsilon_0$ (T_1) at 100 kHz	$\varepsilon/\varepsilon_0$ (T_2) at 100 kH
$Bi_{3.25}Ca_{0.25}Ti_{1.75}Nb_{0.75}O_{10.5}$	678	928	450	1100

A layered perovskite-like oxide of the Aurivillius family of phases $Bi_{3.25}Ca_{0.25}Ti_{1.75}Nb_{0.75}O_{10.5}$ was synthesized by the method of high-temperature solid-state reaction. The synthesized mixed-layer compound with m = 2.5 has a high-temperature ferroelectric-paraelectric transition with a Curie temperature T_C = 928 °C at a frequency of 100 kHz. This is the highest

phase transition temperature for mixed-layer compounds of the Aurivillius family of phases in the world!

Acknowledgement. The study was financially supported by the Russian Science Foundation (Grant No. 21-19-00423) in the Southern Federal University.

References

[1] Zubkov S. V., Vlasenko V. G., Shuvaeva V. A. Shevsova C. I. Ferrelectric properties and crystal structure of mixed-layer $Bi_7Ti_{4+x}W_xTa_{1-2x}O_{21}$ (x = 0 – 0.5) // *J. Physics of the Solid State*, **58**(1), 44 – 50, 2016.

[2] Kikuchi, T., Watanabe, A., Uchida, K. A family of mixed layer type bismuth compounds // *Mat. Res. Bull*. **12**, 299 – 304, 1977.

[3] Shannon R. D. // *Acta Crystallogr. A: Cryst. Phys., Diffr., Theor. Gen. Crystallogr*. **32**, 75, 1976.

Crystal Structure and Dielectric Properties of Layered Perovskite-Like Solid Solutions $Bi_{3-x}Nd_xTi_{1.5}W_{0.5}O_9$ (x = 0.25, 0.5, 0.75, 1.0)

S. V. Zubkov[1]*, U. A. Kuprina[1], I. A. Parinov[2]

[1]Research Institute of Physics, Southern Federal University, 194, Stachki Ave., Rostov-on Don, 344090, Russia

[2]I.I. Vorovich Institute of Mathematics, Mechanics and Computer Science Southern Federal University, Rostov-on-Don, Russia

*svzubkov61@mail.ru

The Aurivillius phases $[Bi_2O_2][A_{n-1}B_nO_{3n+1}]$ are well-known ferroelectrics with high Curie temperatures. High-temperature piezoceramics $Bi_{3-x}Nd_xTiWO_9$ (BNdTW, x = 0.25, 0.5, 0.75, 1.0) were prepared by a solid-state reaction method [1]. The structural and electrophysical characteristics of BNdTW-ceramics have been studied.

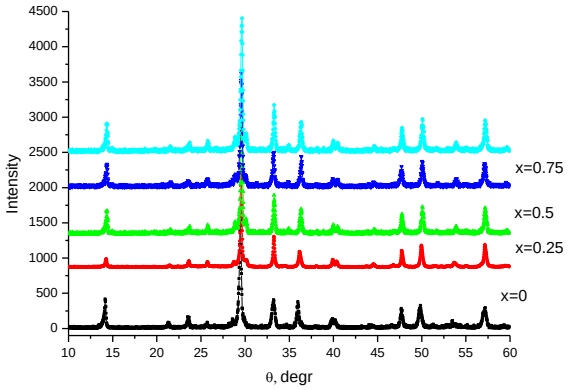

Fig. 1. X-ray diffraction patterns $Bi_{3-x}Nd_xTi_{1.5}W_{0.5}O_9$(BNdTW, x = 0.25, 0.5,0.75,1.0)

According to the data of powder X-ray diffraction (Fig. 1), all the compounds are single-phase with the structures of two-layer Aurivillius phases ($m = 2$) with the orthorhombic crystal lattice (space group $A2_1am$). Figure 2 shows the temperature dependences of the relative permittivity and dielectric loss tangent at frequencies from 100 kHz to 1 MHz. The temperature dependence of the relative permittivity $\varepsilon/\varepsilon_0(T)$ of the compounds was measured and showed that the Curie temperature of perovskite-like oxides $Bi_{3-x}Nd_xTi_{1.5}W_{0.5}O_9$ decreases linearly with a decrease in the substitution parameter x to T_C = 165 °C. Table 1 presents Curie temperature, piezomodule and tolerance factor for $Bi_{3-x}Nd_xTi_{1.5}W_{0.5}O_9$ (x = 0.25, 0.5, 0.75, 1.0) compounds.

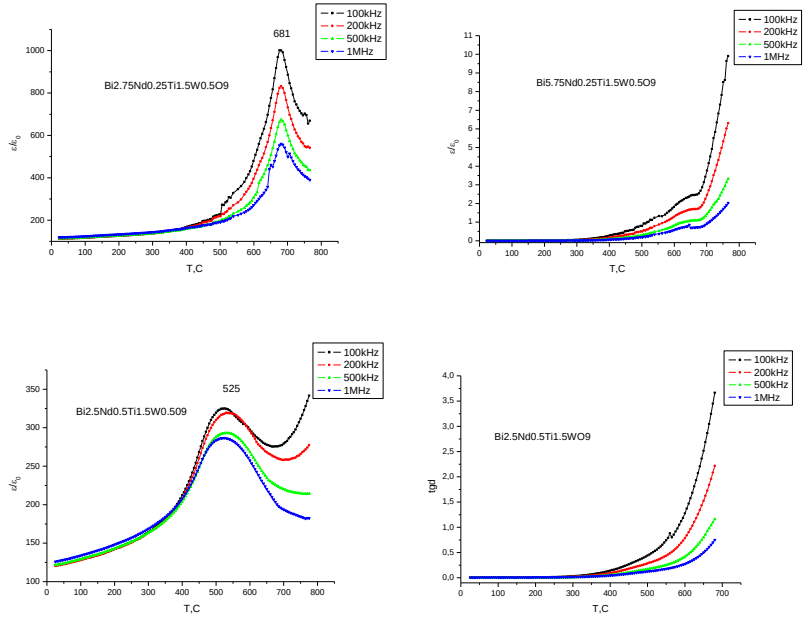

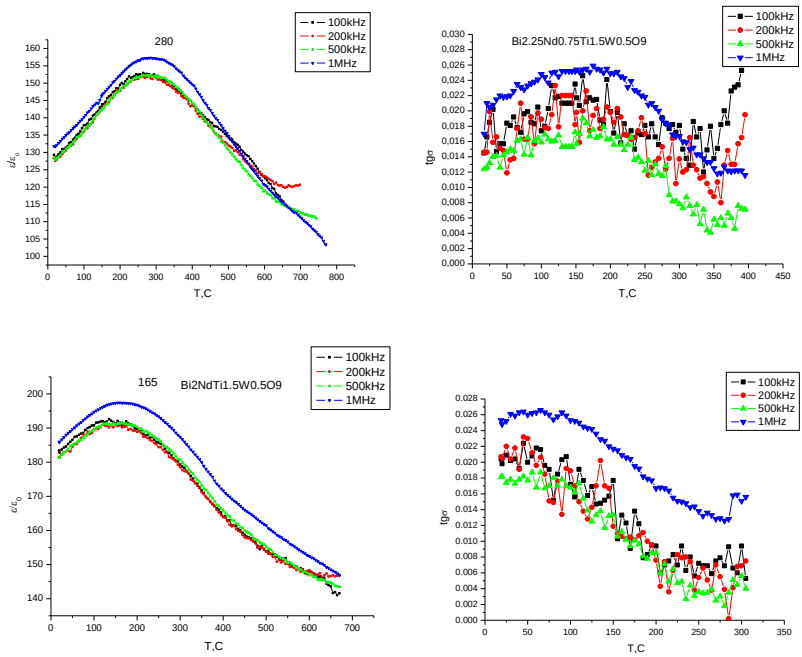

Fig. 2. Temperature dependences of the relative permittivity $\varepsilon/\varepsilon_0$ for APs $Bi_{3-x}Nd_xTi_{1.5}W_{0.5}O_9$ (x = 0.25, 0.5, 0.75, 1.0) at a frequency from 100 kHz to 1 MHz: $Bi_{2.75}Nd_{0.25}Ti_{1.5}W_{0.5}O_9$, $Bi_{2.5}Nd_{0.5}Ti_{1.5}W_{0.5}O_9$, $Bi_{2.25}Nd_{0.75}Ti_{1.5}W_{0.5}O_9$, $Bi_2NdTi_{1.5}W_{0.5}O_9$

Table 1. Curie temperature, piezomodule and tolerance factor for $Bi_{3-x}Nd_xTi_{1.5}W_{0.5}O_9$ (x = 0.25, 0.5, 0.75, 1.0) compounds

Compounds	T_C	d_{33}, pC/N	t
$Bi_{2.75}Nd_{0.25}Ti_{1.5}W_{0.5}O_9$	681	4	0.9615
$Bi_{2.5}Nd_{0.5}Ti_{1.5}W_{0.5}O_9$	525	5	0.9577
$Bi_{2.25}Nd_{0.75}Ti_{1.5}W_{0.5}O_9$	280	3.5	0.9581
$Bi_2NdTi_{1.5}W_{0.5}O_9$	165	0	0.9563

Acknowledgement. The study was financially supported by the Russian Science Foundation (Grant No. 21-19-00423) in the Southern Federal University.

Reference

[1] Zubkov S. V., Crystal Structure and Dielectric Properties of Layered Perovskite-Like Solid Solutions $Bi_{3-x}Nd_xTiNbO_9$ (x = 0, 0.2, 0.4, 0.6, 0.8, 1.0), In: *Physics and Mechanics of New Materials and Their Applications - Proceedings of the International Conference PHENMA 2020*, Springer Proceedings in Materials, Ivan A. Parinov, Shun-Hsyung Chang, Yun-Hae Kim, Nao-Aki Noda (Eds.). Springer Nature, Cham, Switzerland, **10**, 177 – 184, 2021, doi:10.1007/978-3-030-76481-4_15

Crystal Structure and Dielectric Properties of $Bi_3Ti_{1.5}W_{0.5}O_9$

S. V. Zubkov[1]*, I.A. Parinov[2], U. A. Kuprina[1]

[1]Research Institute of Physics, Southern Federal University, Rostov-on- Don, Russia
[2]I. I. Vorovich Mathematics, Mechanics and Computer Science Institute, Southern Federal University, Rostov-on-Don, Russia

*svzubkov61@mail.ru

Layered perovskite-like oxide $Bi_3Ti_{1.5}W_{0.5}O_9$ was synthesized by high-temperature solid-state reaction. X-ray diffraction studies (see Fig.1) have shown that the compound is single-phase and has the structure of the Aurivillius phase corresponding to the space group $A2_1am$. The temperature dependences of the relative permittivity $\varepsilon/\varepsilon_0$ and the tangent of the dielectric loss angle $\tan\sigma$ were measured at different frequencies. The piezomodule was measured and a hysteresis loop was obtained, and the Curie temperature T_C was determined. Aurivillius phases (APs) form a large family of bismuth-containing layered perovskite type compounds, with the chemical composition described by the general formula $A_{m-1}Bi_2B_mO_{3m+3}$. The crystal structure of APs consists of alternating layers $[Bi_2O_2]^{2+}$, which are separated by m perovskite-like layers $[A_{m-1}B_mO_{3m+1}]^{2}$. Layered perovskite-like oxide (AP) $Bi_3Ti_{1.5}W_{0.5}O_9$ was described in work [1]. The purpose of our study was to refine the dielectric characteristics and refine the technology for the synthesis of $Bi_3Ti_{1.5}W_{0.5}O_9$. Polycrystalline samples of APs were synthesized by the solid-phase reaction described in work [2]. It was found that synthesized APs crystallize in an orthorhombic system with a unit cell space group $A2_1am(36)$. Figure 2 shows the temperature dependences of the relative permittivity and dielectric loss tangent at frequencies from 100 kHz to 1 MHz (see Fig. 2). The piezomodule was measured and a hysteresis loop was obtained. The values of the piezomodule d_{33} and the phase transition (ferroelectric – paraelectric) temperature are given in Table 1. In the result, it has been obtained a high Curie temperature T_C = 760 °C for the manufactured $Bi_3Ti_{1.5}W_{0.5}O_9$ and its piezomodule was equal to d_{33}= 8 pC/H.

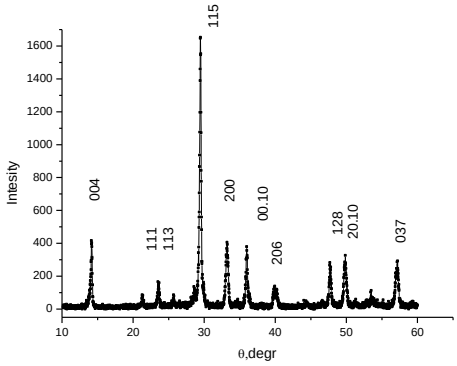

Fig. 1. Diffraction data for pure $Bi_3Ti_{1.5}W_{0.5}O_9$

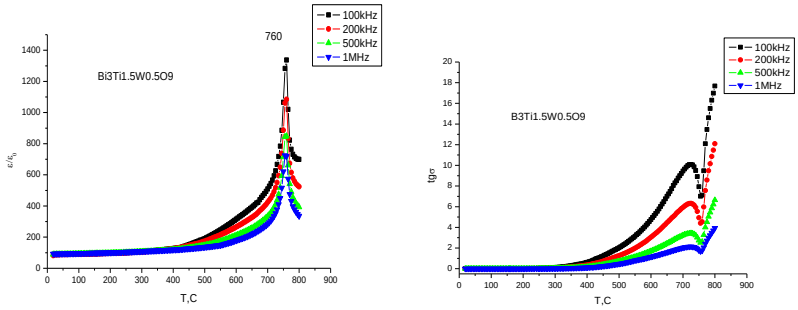

Fig. 2. Temperature dependences of the relative permittivity $\varepsilon/\varepsilon_0$ and loss tangent tgσ for APs $Bi_3Ti_{1.5}W_{0.5}O_9$ at a frequency from 100 kHz to 1 MHz

Table 1. Curie temperature, piezomodule, tolerance factor of $Bi_3Ti_{1.5}W_{0.5}O_9$

Compound	T_C	T_C (1)	d_{33}, pC/H	t
$Bi_3Ti_{1.5}W_{0.5}O_9$	760	730	8	0.9634

Acknowledgement. **The study was financially supported by the Russian Science Foundation (Grant No. 21-19-00423) in the Southern Federal University.**

References

[1] Neil C. Hyatt, Ian M. Reaney. Ferroelectric-paraelectric phase transition in the n = 2 Aurivillius phase $Bi_3Ti_{1.5}W_{0.5}O_9$: A neutron powder diffraction study // *Physical Review B*, **71**, 024119, 2005.

[2] Zubkov S. V. Crystal Structure and Dielectric Properties of Layered Perovskite-Like Solid Solutions $Bi_{3-x}Nd_xTiNbO_9$ (x = 0, 0.2, 0.4, 0.6, 0.8, 1.0). In: *Physics and Mechanics of New Materials and Their Applications - Proceedings of the International Conference PHENMA 2020*, Springer Proceedings in Materials, Ivan A. Parinov, Shun-Hsyung Chang, Yun-Hae Kim, Nao-Aki Noda (Eds.). Springer Nature, Cham, Switzerland, **10**, 177 – 184, 2021.

AUTHOR INDEX

PARTICIPARING COUNTRIES AND ORGANIZATIONS

Australia

- Faculty of Dentistry, The University of Sydney, Sydney

Belarus

- Scientific-Practical Materials Research Centre of NAS of Belarus, Minsk

Bulgaria

- Institute of Mechanics, Bulgarian Academy of Sciences, Sofia
- Institute of Information and Communication Technologies, Bulgarian Academy of Sciences, Sofia

China

- School of Materials Science and Engineering, Shanghai Jiao Tong University, Shanghai

Egypt

- Department of Mathematics, Faculty of Science, South Valley University, Qena
- Faculty of Electronic Engineering, Menoufia University, Menouf

Germany

- Chair of Structural Mechanics, Department of Civil Engineering, University of Siegen, Siegen
- Fraunhofer SIT, Darmstadt
- Gottfried Wilhelm Leibniz University, Hannover
- RheinMain University of Applied Sciences, Wiesbaden

India

- Banasthali Vidyapith, Rajasthan
- BISS Division, ITW-India Pvt Ltd, Bangalore
- Department of Chemistry, Assam University, Silchar, Assam
- Department of Mechanical Engineering, G H Raisoni College of Engineering, Nagpur, Maharashtra
- Department of Physics, Mumbai University, Mumbai
- Department of Physics, Siksha O Anusandhan (Deemed to be University), Bhubaneswar
- Maulana Azad National Institute of Technology, Bhopal

- PDPM, Indian Institute of Information Technology Design and Manufacturing, Jabalpur
- School of Automation, Banasthali Vidyapith University, Rajasthan
- The Institute of Science, Dr. Homi Bhabha State University, Mumbai
- The Institute of Science, Nagpur

Indonesia

- Architect, Surabaya Zoo
- Architecture Department, Engineering Faculty, Universitas 17 Agustus 1945 Surabaya
- Department of Industrial Engineering, University of 17 Agustus 1945, Surabaya
- Informatics Engineering Department, University of 17 Agustus 1945 Surabaya
- Mechanical Engineering, University of 17 Agustus 1945 Surabaya

Japan

- Magnesium Research Center, Kumamoto University, Kumamoto
- Research Center for Structural Materials, National Institute for Materials Science, Tsukuba

Kazakhstan

- Al Farabi Kazakh National University, National Nanotechnology Laboratory of Open Type, Almaty

Latvia

- Riga Technical University, Riga

Poland

- Academy of the Higher School of Business, Katowice

Republic of Korea

- Department of Materials Science and Engineering, Pusan National University
- Department of Nano Fusion Technology, Pusan National University, Busan
- Department of Nanomechatronics Engineering, Pusan National University, Busan
- Division of Mechanical Engineering, Korea Maritime and Ocean University, Busan,
- Division of Refrigeration & Air-conditioning Engineering, Korea Maritime and Ocean University, Busan
- Energy and Environmental Division, Korea Institute of Ceramic Engineering and Technology, Jinju

Russia

- Academician N. V. Melnikov Institute of Comprehensive Exploitation of Mineral Resources – IPKON, Russian Academy of Sciences, Moscow
- Advanced Data Transfer Systems Institute, ITMO University, Saint-Petersburg

- Aircraft Systems and Technologies Laboratory at the South Center of Russian Academy of Science, Rostov-on-Don
- Astrakhan State University, Astrakhan
- N. E. Bauman Moscow State Technical University, Moscow
- G. K. Boreskov Institute of Catalysis SB RAS, Novosibirsk
- Chechen State University, Grozny
- Dagestan State University, Makhachkala
- Department of Applied Mathematics, Don State Technical University, Rostov-on-Don
- Department of Mechanics and Control Processes, Moscow Institute of Physics and Technology (National Research University), Moscow
- Department of Physics, Southern Federal University, Rostov-on-Don
- Digital Agriculture Laboratory, Skolkovo Institute of Science and Technology, Moscow
- Don State Technical University, Rostov-on-Don
- Engineering Technological Academy, Southern Federal University, Taganrog
- Faculty of Chemistry, Southern Federal University, Rostov-on-Don
- Federal Scientific Centre of Agroecology, Complex Melioration and Protective Afforestation of the Russian Academy of Sciences, Volgograd
- Hydrochemical Institute of Roshydromet, Rostov-on-Don
- Hydrometeorological college, Rostov-on-Don
- Institute of Automation and Electrometry of the Siberian Branch of the Russian Academy of Sciences, Novosibirsk
- Institute of Biomedical Systems of National Research University of Electronic Technology, MIET, Zelenograd, Moscow
- Institute for Bionic Technologies and Engineering of I.M. Sechenov First Moscow State Medical University, Moscow
- Institute of Fine Chemical Technologies, Moscow Technological University, Moscow
- Institute of High Technology and Piezo Technic, Southern Federal University, Rostov-on-Don
- Institute for Mathematics, Mechanics, and Informatics, Kuban State University, Krasnodar
- Institute of Nanotechnologies, Electronics, and Electronic Equipment Engineering, Southern Federal University, Taganrog
- Institute of Nanotechnology of Microelectronics, Russian Academy of Sciences, INME RAS, Moscow
- Institute for Physics, Southern Federal University, Rostov-on-Don
- Institute of Physiologically Active Compounds, Russian Academy of Sciences, IPAC RAS, Chernogolovka
- Institute of Solid-State Chemistry and Mechanochemistry SB RAS, Novosibirsk
- International Department, Don Technical University, Rostov-on-Don
- A. F. Ioffe Institute, St. Petersburg
- Laboratory of Mechanics and Biocompatible Materials, Don State Technical University, Rostov-on-Don
- Laboratory of Nanomaterials, Southern Federal University, Rostov-on-Don
- Membrane Institute, Kuban State University, Krasnodar
- Moscow Aviation Institute, Moscow
- Municipal autonomous educational institution Lyceum No.4 (TMGL), Taganrog
- National Research N. I. Lobachevsky State University of Nizhny Novgorod, Nizhny Novgorod

- National Research University of Electronic Technology, MIET, Zelenograd, Moscow
- National University of Science and Technology, MISIS, Moscow
- OOO "Parametrica", Taganrog
- M. I. Platov South-Russian State Polytechnic University (NPI), Novocherkassk
- Premium Consulting, Moscow
- PROMETHEUS R&D Ltd., Rostov-on-Don
- Research and Education Center “Materials”, Don State Technical University, Rostov-on-Don
- Research and Education Centre “Microsystem Techniques and Multisensor Monitoring Systems”, Southern Federal University, Taganrog
- Research and Education Centre “Nanotechnology”, Southern Federal University, Rostov-on-Don
- Rostov State Transport University, Rostov-on-Don
- Scientific-Manufacturing Complex "Technological Centre", Zelenograd, Moscow
- Scientific and Technological Park of Biomedicine of I. M. Sechenov First Moscow State Medical University, I. M. Sechenov University, Moscow
- M. M. Shemyakin & Yu. A. Ovchinnikov Institute of Bioorganic Chemistry of the Russian Academy of Sciences, Moscow
- South-Russian Institute of Management – Branch of the Russian Academy of National Economy and Public Administration under the President of the Russian Federation, Rostov-on-Don
- Southern Mathematical Institute - Branch of the VSC RAS, Vladikavkaz
- Sberbank, Rostov-on-Don
- I.M. Sechenov First Moscow State Medical University, Moscow
- Smart Materials Research Institute, Southern Federal University, Rostov-on-Don
- Southern Federal University, Rostov-on-Don, Taganrog
- Southern Scientific Center of the Russian Academy of Sciences, Rostov-on-Don,
- Volgograd State Technical University (VSTU), Volgograd
- I. I. Vorovich Mathematics, Mechanics, and Computer Science Institute, Southern Federal University, Rostov-on-Don

Taiwan

- Department of Electrical Engineering, National Taiwan Ocean University, Keelung
- Department of Electronics Engineering, National Kaohsiung University of Science and Technology, Kaohsiung
- Department of Hematology and Oncology, Kaohsiung Chang Gung Memorial Hospital and Chang Gung University College of Medicine, Kaohsiung
- Department of Marine Engineering, National Kaohsiung University of Science and Technology, Kaohsiung
- Department of Marine Environmental Engineering, National Kaohsiung University of Science and Technology, Kaohsiung
- Departments of Medical Imaging and Radiological Sciences, I-Shou University, Kaohsiung
- Department of Microelectronic Engineering, National Kaohsiung University of Science and Technology, Kaohsiung
- Department of Radiation Oncology, Kaohsiung Chang Gung Memorial Hospital and Chang Gung University College of Medicine, Kaohsiung

- Department of Shipping Technology, National Kaohsiung University of Science and Technology, Kaohsiung
- Medical Physics and Informatics Laboratory of Electronics Engineering, National Kaohsiung University of Science and Technology, Kaohsiung
- National Cheng Kung University, NCKU, Department of Civil Engineering, Tainan
- Ph.D. Program in Biomedical Engineering, Kaohsiung Medical University, Kaohsiung
- Ph.D. Program in Maritime Science and Technology, College of Maritime, National Kaohsiung University of Science and Technology, Kaohsiung

Ukraine

- A.A. Galkin Institute for Physics and Engineering, Donetsk
- Donetsk National University, Donetsk
- Institute of Physical Organic and Coal Chemistry, Donetsk
- L.M. Litvinenko Institute of Physical Organic and Coal Chemistry, Donetsk
- Lugansk State Pedagogical University, Lugansk

United Kingdom

- Department of Mechanical Engineering, University of Bath, Bath

Vietnam

- Cao Thang Technical College, Ho Chi Minh City
- Faculty of Environment, Hanoi University of Mining and Geology, Hanoi
- Faculty of Environment and Natural Resources, Nong Lam University, Ho Chi Minh Ciy
- Faculty of Mechanical Engineering, Ho Chi Minh City University of Technology and Education, Ho Chi Minh City
- Hanoi Industrial Textile Garment University, Hanoi
- Hanoi University of Science and Technology, Hanoi
- Ho Chi Minh City University of Technology and Education, Ho Chi Minh City
- Ly Tu Trong College, Ho Chi Minh City
- Nam Sai Gon Polytechnic College, Nam Sai Gon
- Nong Lam University, Ho Chi Minh City
- Phenikaa University, Hanoi
- Van Lang University, Ho Chi Minh City
- Vinh Long University of Technology Education, Vinh Long City

SCHEDULE OF 10th Anniversary International Conference on "Physics and Mechanics of New Materials and Their Applications" (PHENMA 2021 - 2022), May 23 – 27, 2022

23 May 2022 (Monday)

Arrival and registration of the PHENMA 2021 – 2022 participants in Divnomorsk

24 May 2012 (Tuesday)

8:30 – 9:30 ***Breakfast***

8:30 – 9:50 ***Registration of the PHENMA 2021 – 2022 participants at REGISTRATION DESK***

OPENING CEREMONY 10:00

Greetings of the PMNM-2012 Co-Chairmen:

Arkady N. Soloviev 10:00 - 10:10

Shun-Hsyung Chang 10:10 - 10:20

Ivan A. Parinov 10:20 - 10:30

Plenary Report: **Ivan A. Parinov[1], Shun-Hsyung Chang[2]**. The way to success: PHENMA for the last decade. *[1]I.I. Vorovich Institute of Mathematics, Mechanics and Computer Sciences, Southern Federal University, Rostov on Don, Russia; [2]National Kaohsiung University of Science and Technology, Kaohsiung, Taiwan* **10:30 - 10:50** (the report duration is 15 min + questions and discussion during 5 min)

Plenary Report**: Rakesh Kumaar Haldkar**. Design Modeling and Analysis of Axial-type Piezoelectric Energy Generator. ***I. I. Vorovich Mathematics, Mechanics and Computer Sciences Institute, Southern Federal University, Rostov-on-Don, Russia;*** *G H Raisoni college of Engineering Nagpur, India* **10:50 - 11:15** (the report duration is 20 min + questions and discussion during 5 min)

Plenary Report: **President Tai-Wen Hsu**, National Taiwan Ocean University, *Keelung, Taiwan*

11:15 - 11:40 (the report duration is 20 min + questions and discussion during 5 min)

***Coffee-Break* 11:40 - 12:10**

On-line/video Sessions:

"Technologies of New Materials" (T1) 12:10 - 13:00 (a report duration is 10 min) ***(Chairman – Dr. A. V. Cherpakov)***

E.M. Bayan[1], L.E. Pustovaya[2], Yu.A. Bayan[1], T.G. Lupeiko[1]. Optimization of the synthesis conditions of N-doped TiO_2 nanoparticles wastewater treatment. *[1]Southern Federal University, Faculty of chemistry, Rostov-on-Don, Russia; [2]Don State Technical University, Rostov-on-Don, Russia* **12:10 - 12:20**

M.G. Volkova[1], V.V. Petrov[2], E.M. Bayan[1]. Preparation and Characterization of Sn-ZnO Nanorod Array. [1]Southern Federal University, Faculty of Chemistry, Rostov-on-Don, Russia; [2]Southern Federal University, Institute of Nanotechnologies, Electronics, and Equipment Engineering, Taganrog, Russia **12:20 - 12:30**

Sangeeta A. Nirmal[1], M.R. Sonawane[2], R.G. Atram[3]. Chemisorption of Molybdenum Atom on Carbon Nanotube using Density Functional Theory. [1]Department of Physics, Patkar Varde College, Mumbai University, Mumbai, India; [2]The Institute of Science, Dr. Homi Bhabha State University, Mumbai, India; [3]The Institute of Science, Nagpur, India **12:30 - 12:40**

Chu Dieu Huong, Nguyen Thi Tu Trinh. Fragrance Durability depending on compression of Knitted Fabric bandage coated by Microcapsule Contained Cinnamon Essential Oil. *Hanoi University of Science and Technology, Hanoi, Vietnam* **12:40 - 12:50**

Chu Dieu Huong, Nguyen Thi Tu Trinh. Investigation of the creep relaxation behavior in use of single jersey fabric depending on the elastic yarn ratio. *Hanoi University of Science and Technology, Hanoi, Vietnam*12:50 - 13:00

***Dinner* 13:00 - 14:00**

"Physics of New Materials" (P1) 14:00 - 14:50 (a report duration is 10 min) ***(Chairman – Dr. A. V. Chebanenko)***

V.O. Dmitriev, M. Khalil, A.P. Budnik, E.S. Bogoslavskaya, V.A. Shmatko, G.E. Yalovega. Features of the Electronic Structure of Some MeOx/MWCNTs *Faculty of Physics, Southern Federal University, Rostov-on-Don, Russia* **14:00 -14:10**

Abhinav Yadav[1], E.A. Bikyashev[2], S.P. Kubrin[1], N. V. Ter-Oganessian[1], I. P. Raevski[1], Systematic investigation of dielectric characteristics of $BaFe_{1/2}Sn_{1/2}O_{3-\delta}$ ceramic. *[1]Institute of Physics, Southern Federal University, Rostov-on-Don, Russia; [2]Faculty of Chemistry, Southern Federal University, Rostov-on-Don, Russia* **14:10 - 14:20**

Sudip Kumar Pal[a], Anton A. Scrjabin[a], Alexey T. Kozakov[a], Sujit Kumar Ghosh[b]. Localized Surface Plasmon Resonance of 'Normal' and 'Inverted' Core-Shell Nanostructures. *[a]Research Institute of Physics, Southern Federal University, Rostov-on-Don, Russia; [b]Department of Chemistry, Assam University, Silchar, Assam, India* **14:20 -14:30**

Sudip Kumar Pal[a], Anton A. Scrjabin[a], Alexey T. Kozakov[a], Sujit Kumar Ghosh[b]. Plasmonic Properties upon Aggregation of Size-Selective Ultrasmall Gold Nanospheres. *[a]Research Institute of Physics, Southern Federal University, Rostov-on-Don, Russia; [b]Department of Chemistry, Assam University, Silchar, Assam, India* **14:30 -14:40**

L.P. Ichkitidze[1,2], M.V. Belodedov[3], A.Yu. Gerasimenko[1,2], D.V. Telyshev[1,2], S.V. Selishchev[1]. Registration of Magnetic Particles in a Biological Medium with Using Magnetometers.*[1]Institute of Biomedical Systems of National Research University of Electronic Technology, MIET, Zelenograd, Moscow, Russia; [2]Scientific and Technological Park of Biomedicine of I.M. Sechenov First Moscow State Medical University, I.M. Sechenov University, Moscow, Russia; [3]Bauman Moscow State Technical University, Russia* **14:40 - 14:50**

"Mechanics of New Materials (M1) 14:50 - 16:00 (a report duration is 10 min)
(Chairman – Dr. R. K. Haldkar)

Roumen Iankov[1], Ivan Georgiev[2], Mikhail Chebakov[3], Elena Kolosova[3], Maria Datcheva[1]. Computational Homogenization for Determination of Porous Material Properties. *[1]Institute of Mechanics, Bulgarian Academy of Sciences, Sofia, Bulgaria; [2]Institute of Information and Communication Technologies, Bulgarian Academy of Sciences, Sofia, Bulgaria; [3]Vorovich Institute for Mathematics, Mechanics and Computer Sciences, Southern Federal University, Rostov-on-Don, Russia* **14:50 - 15:00**

G. A. Zhuravlev, Yu. E. Drobotov. Maximum Tangential Stresses Due to Contact of Two Elastic Parallel Circular Cylinders and Their Depth *Southern Federal University, Rostov-on-Don, Russia* **15:00 - 15:10**

G. A. Zhuravlev, T. M. Andreeva, Yu. E. Drobotov. Explaining the Inconsistency of Solutions to the Contact Problem on the Convergence of Two Elastic Cylinders **15:10 - 15:20**

Yu. E. Drobotov. On the Stress State of Details with Projections of Complex Shape. *Southern Federal University, Rostov-on-Don, Russia* **15:20 - 15:30**

Yu. E. Drobotov, R. K. Haldkar. On Numerical and Analytical Approaches to the Problem on the Stress-Strain State of a Cantilever Plate *Southern Federal University, Rostov-on-Don, Russia* **15:30 - 15:40**

D.A. Kalganov, V.V. Kaminskii. Influence of ternary intermetallic inclusions on the mechanical properties of aluminum alloys in Al-Ti-Zn system. *Advanced Data Transfer Systems Institute, ITMO University, Saint-Petersburg, Russia* **15:40 - 15:50**

D.A. Kalganov[1], V.V. Kaminskii[1], A.E. Romanov[1], E. Abe[2], Y. Kawamura[3]. Investigations of magnesium alloys containing LPSO phase by composite oscillator method. *[1]Advanced Data Transfer Systems Institute, ITMO University, Saint-Petersburg, Russia; [2]Research Center for Structural Materials, National Institute for Materials Science, Tsukuba, Japan; [3]Magnesium Research Center, Kumamoto University, Kumamoto, Japan* **15:50 - 16:00**

Coffee-Break **16:10 - 16:40**

"Applications of New Materials" (A1) 16:40 - 17:50 (a report duration is 10 min)
(Chairman – Yu. E. Drobotov)

M.S. Savelyev, P.N. Vasilevsky, A.V. Kuksin, L.P. Ichkitidze, A.Yu. Tolbin, A.Yu. Gerasimenko. Nonlinear Absorbers Based on Multi-wall Carbon Nanotubes for Protection of Sensitive Elements of Electro-optical Systems and Vision Organs **16:40 - 16:50**

L. P. Ichkitidze[1,2], G. Yu. Galechian[1], A. Yu. Gerasimenko[1,2], D. V. Telyshev[1,2]. The role of magnetic particles and nanoparticles in cancer hyperthermia. *[1]Institute of Biomedical Systems of National Research University of Electronic Technology, MIET, Zelenograd, Moscow, Russia;*
[2]Scientific and Technological Park of Biomedicine of I.M. Sechenov First Moscow State Medical University, I.M. Sechenov University, Moscow, Russia **16:50 - 17:00**
G.M. Glebova, G.A. Zhbankov, O.A. Maltseva. Prospects of the Vector Scalar Arrays Usage for Underwater Communications. *Institute for Physics, Southern Federal University, Rostov-on-Don, Russia* **17:00 - 17:10**
L. P. Ichkitidze[1,2], V. A. Petukhov[1], N. A. Demidenko[1], E. P. Kitsyuk[3], A. Y. Gerasimenko[1,2], D. V. Telyshev[1,2]. Films of biological nanomaterials as a prototype of a tactile sensor. [1]Institute of Biomedical Systems of National Research University of Electronic Technology, MIET, Zelenograd, Moscow, Russia; [2]Scientific and Technological Park of Biomedicine of I.M. Sechenov First Moscow State Medical University, Sechenov University, Moscow, Russia; [3]*Scientific-Manufacturing Complex "Technological Centre", Zelenograd, Moscow, Russia* **17:10 - 17:20**
Nguyen Thanh Tung and Luong Van Van. A study on the effect of the grip coefficient on the slip coefficient when braking of the tractor semi-trailer on a straight road at a speed of 80 km/h. *Vinh Long University of Technology Education, Vinh Long City, Vietnam* **17:20 - 17:30**
Artem M. Kharakhashyan. Comparative analysis of the efficiency of scalar and vector-scalar antennas for onboard receiving systems. *Department of Applied Mathematics, Don State Technical University, Rostov-on-Don, Russia* **17:30 - 17:40**
Jeong Wan Kim[1], Tae Gyu Kim[2]. Mold core DSLR camera tool mark analysis according to the surface roughness of the aspherical lens. *[1]Department of Nano Fusion Technology, Pusan National University, Busan, Korea; [2]Department of Nanomechatronics Engineering, Pusan National University, Busan, Korea* **17:40 - 17:50**

Supper 18:00 - 19:00

25 May 2022 (Wednesday)

8:30 – 9:30 ***Breakfast***

Poster Session **10:00 - 18:00** ***(Co-Chairmen – N. I. Glushko)***

Oral Sessions

"Physics of New Materials" (P2) 10:00 - 11:10 (a report duration is 10 min + questions and discussion during 5 min) ***(Chairman – Dr. S.V. Zubkov)***

Yu. E. Drobotov. On analytical approaches in mathematical modelling of ferroelectric switching kinetics in injection mode **10:00 - 10:15**
V. Yu. Topolov,[1] A. N. Isaeva,[1] C. R. Bowen,[2] B. O. Protsenko[1]. Piezoelectric Properties, Anisotropy Factors and Energy-harvesting Characteristics of Novel 1–2–2 composites Based on Domain-engineered Single Crystals. [1]*Department of Physics, Southern Federal University, Rostov-on-Don, Russia; [2]Department of Mechanical Engineering, University of Bath, Bath, UK.* **10:15 - 10:30**

V. Yu. Topolov,[1] A. N. Isaeva,[1] A. O. Denisova,[1] C. R. Bowen[2]. Effect of the Matrix Subsystem on Piezoelectric Properties and Related Parameters of Lead-free 1–3-type Composites. [1]*Department of Physics, Southern Federal University, Rostov-on-Don, Russia;* [2]*Department of Mechanical Engineering, University of Bath, Bath, UK* **10:30 - 10:45**

M.V. Talanov[1], A.A. Pavelko[1], L.S. Kamzina[2]. Dielectric Relaxation and Electromechanical Resonance in Ferroelectric $Cd_2Nb_2O_7$ Single Crystal. [1]*Research Institute of Physics, Southern Federal University, Rostov-on-Don, Russia;* [2]*Ioffe Institute, St. Petersburg, Russia* **10:45 - 11:00**

***Coffee-Break* 11:10 - 11:40**

"Mechanics of New Materials (M2) 11:40 - 13:00 (a report duration is 10 min + questions and discussion during 5 min) (*Chairman – Dr. V.A. Chebanenko*)

M.V. Golub[1], S.I. Fomenko[1], O.V. Doroshenko[1], I. Moroz[2], E. Okoneshnikova[1], Y. Wang[3], C. Zhang[3]. Multi-layered acoustic/elastic metamaterials with arrays of strip-like cracks: modelling and manufacturing. [1]*Institute for Mathematics, Mechanics and Informatics, Kuban State University, Krasnodar, Russia;* [2]*Membrane Institute, Kuban State University, Krasnodar, Russia;* [2]*Chair of Structural Mechanics, Department of Civil Engineering, University of Siegen, Siegen, Germany* **11:40 - 11:55**

S.I. Fomenko[1], R.B. Jana[2], M.V. Golub[1]. Theoretical estimation of porosity and fluid saturation by ultrasound methods based on surface waves. [1]*Institute for Mathematics, Mechanics and Informatics, Kuban State University, Krasnodar, Russia;* [2]*Digital Agriculture Laboratory, Skolkovo Institute of Science and Technology, Moscow, Russia* **11:55 - 12:10**

V.E. Yakovlev, A. V. Cherpakov, Construction of a technique for identifying the parameters of a stubble structure during the propagation of longitudinal waves **12:10 - 12:35**

A.N. Soloviev[1,2], A.V. Yudin[2,3,4], V.A. Chebanenko[3]. Numerical study of the propagation of harmonic surface waves generated by two types of piezoelectric actuators. [1]*Don State Technical University, Rostov-on-Don, Russia;* [2]*Vorovich Mathematics, Mechanics and Computer Science Institute, Southern Federal University, Rostov-on-Don, Russia;* [3]*Federal Research Center "Southern Scientific Center of the Russian Academy of Sciences", Rostov-on-Don, Russia;* [4]*Platov Southern Russian State Polytechnic University, Novocherkassk, Russia* **12:35 - 12:50**

***Dinner* 13:00 - 14:00**

On-line/video Sessions:

"Applications of New Materials" (A1) 14:00 - 16:10 (a report duration is 10 min) *(Chairman – Dr. A. V. Cherpakov)*

Chin-Shiuh Shieh[1], Chin-Dar Tseng[1,2], Chen-Lin Kang[3], Hsuan-Chih Hsu[3], Liyun Chang[4], Chin-Hsueh Lin[1], Yu-Jie Huang[5], Tsair-Fwu Lee[1,2,6]. Using convolutional neural networks to recognize randomly generated images and visualize the results. [1]*Department of Electronics Engineering, National Kaohsiung University of Science and Technology, Kaohsiung, Taiwan, R.O.C.;* [2]*Medical Physics and Informatics Laboratory of Electronics Engineering, National Kaohsiung University of Science and Technology, Kaohsiung, Taiwan, R.O.C.;* [3]*Department of Hematology and Oncology, Kaohsiung Chang Gung*

Memorial Hospital and Chang Gung University College of Medicine, Kaohsiung, Taiwan, R.O.C.; [4]Departments of Medical Imaging and Radiological Sciences, I-Shou University, Kaohsiung, Taiwan, R.O.C.; [5]Department of Radiation Oncology, Kaohsiung Chang Gung Memorial Hospital and Chang Gung University College of Medicine, Kaohsiung 83342, Taiwan, ROC; [6]Ph.D. program in Biomedical Engineering, Kaohsiung Medical University, Kaohsiung, Taiwan, ROC **14:00 - 14:10**

Chin-Feng Lin[1], Yu-Chi Wei[1], Chai-Sheng, Wen[1], Chan-Chung Wen[2], Shun-Hsyung Chang[3], Ivan A. Parinov[4], Sergey Shevtsov[5], DM-MIMO Based GFDM Advanced Underwater Image Transmission Scheme. *[1]Department of Electrical Engineering, National Taiwan Ocean University, Taiwan, ROC; [2]Department of Shipping Technology, National Kaohsiung University of Science and Technology, Taiwan, ROC; [3]Department of Microelectronic Engineering, National Kaohsiung University of Science and Technology, Taiwan, ROC; [4]I. I. Vorovich Mathematics, Mechanics, and Computer Science Institute, Southern Federal University, Russia; [5]Aircraft Systems and Technologies Laboratory at the South Center of Russian Academy of Science, Russia* **14:10 - 14:20**

Nguyen Minh Ky[1,3], Chitsan Lin[2], Nguyen Duy Hieu[1], Nguyen Cong Manh[3], Nguyen Tuan Anh[3]. Evaluating the efficiency of organic matter treatment using Vetiver grass (*Vetiveria Zizanioides* L.) - A pilot-scale. *[1]Ph.D. Program in Maritime Science and Technology, College of Maritime, National Kaohsiung University of Science and Technology, Kaohsiung, Taiwan; [2]Department of Marine Environmental Engineering, National Kaohsiung University of Science and Technology, Kaohsiung, Taiwan; [3]Faculty of Environment and Natural Resources, Nong Lam University, Ho Chi Minh Ciy, Vietnam* **14:20 - 14:30**

Ankit Nayak. On design considerations of In-Pipe Inspection Robot. *School of Automation, Banasthali Vidyapith University, Rajasthan, India* **14:30 - 14:40**

V.I. Korotkin, E.M. Kolosova. A New Approach to Assessing and Improving the Load-bearing Capacity of Novikov Gears. Southern Federal University, *I.I. Vorovich Mathematics, Mechanics and Computer Science Institute, Rostov-on-Don, Russia* **14:40 - 14:50**

D.V. Karabanov, V.V. Zaitsev, S.O. Kireev, M.V. Korchagina. Advantages of the Novikov transmission on the slow-speed stage of the cylindrical gearbox transmission **14:50 - 15:00**

Yu.A. Akopyan, S.O. Kireev, A.R. Lebedev, M. V. Korchagina. A new design of the surface drive of the screw pump for the extraction of high-viscosity oil. *Don State Technical University, Rostov-on-Don, Russia* **15:00 - 15:10**

V.V. Zaitsev, A.V. Biel, S.O. Kireev, M.V. Korchagina. Synthesis of high-pressure pump drive reducer for service of oil and gas wells **15:10 - 15:20**

A.V. Bil, D.V. Karabanov, S.O. Kireev, M.V. Korchagina. Design and principle of operation of the pneumatic wedge gripper **15:20 - 15:30**

A.V. Bil, M. V. Korchagina, S. O. Kireev, V.N. Stepanov. Research tension and deformations in the elastic element of the universal spherical preventer seal **15:30 - 15:40**

K.P. Matsneva, M.V. Korchagina, S.O. Kireev. Features of the choice of construction materials for downhole equipment **15:40 - 15:50**

M.I. Rodimova, H.K. Kaderov, S. O. Kireev, M. V. Korchagina. Improvement of seals of flange connections of fountain fittings and shut-off devices **15:50 - 16:00**

M.I. Rodimova, S.O. Kireev, M.V. Korchagina. Requirements for sealing existing flange connection structures with metal O-rings **16:00 - 16:10**

***Coffee-Break* 16:20 - 16:50**

"Industry and Management (MIM1) 16:50 - 17:30 (a report duration is 10 min)
(Chairman – Yu. E. Drobotov)

Erni Puspanantasari Putri. Development Strategy of MSMEs Based on Creative Economy in Indonesia. *Department of Industrial Engineering, Universitas 17 Agustus 1945 Surabaya, Indonesia* **16:50 - 17:00**

Erni Puspanantasari Putri. Development Strategy of the Local Village Economy in Indonesia. *Department of Industrial Engineering, Universitas 17 Agustus 1945 Surabaya, Indonesia* **17:00 - 17:10**

Erni Puspanantasari Putri, Zainal Arief, Istantyo Yuwono. Performance Evaluation Using Input-oriented Envelopment DEA Method: A Case Study of Micro and Small Industry in Indonesia. *Department of Industrial Engineering, Universitas 17 Agustus 1945 Surabaya, Indonesia* **17:10 - 17:20**

RA Retno Hastijanti[1], Briant Wiranata[2]. The Potential of Teak Wood as a Climate Change Resilience Furnishing Material. [1]*Architecture Department, Engineering Faculty, Universitas 17 Agustus 1945 Surabaya, Indonesia;* [2]*Architect, Surabaya Zoo, Indonesia* **17:20 - 17:30**

Supper 18:00 - 19:00

26 May 2022 (Thursday)

8:30 – 9:30 ***Breakfast***

Oral Sessions

"Physics of New Materials" (P2) 10:00 - 11:00 (a report duration is 10 min + questions and discussion during 5 min) ***(Chairman – Dr. S.V. Zubkov)***

I.A. Gulyaeva[1], A.V. Nesterenko[1], A.V. Petrov[2], V.V. Petrov[1]. Research of the photoconductivity characteristics of ZnO–SnO_2 sol-gel thin films. [1]*Southern Federal University, Institute of Nanotechnologies, Electronics, and Equipment Engineering, Taganrog, Russia;* [2]*Municipal autonomous educational institution Lyceum No.4 (TMGL), Taganrog, Russia* **10:00 - 10:15**

V. Yu. Topolov[1], A. O. Denisova[1,2]. Comparative Analysis of Hydrostatic Parameters of 1–3-type Composites with One or Two Piezoelectric Components. 1*Department of Physics, Southern Federal University, Rostov-on-Don, Russia;* 2*I.I. Vorovich Institute of Mathematics, Mechanics and Computer Science, Southern Federal University, Rostov-on-Don, Russia* **10:15 - 10:30**

I.N. Zakharchenko, M.V. Talanov. Electric-field Induced Phase Transformation in Relaxor-based Multicomponent Ceramics *Research Institute of Physics, Southern Federal University, Rostov-on-Don, Russia* **10:30 - 10:45**

M.V. Talanov[1,2], V.B. Shirokov[1,2,3], E.A. Muratova[2], V.M. Talanov[2]. Multi-order states and emergent phenomena on the pyrochlore lattice. [1]*Southern Federal University, Rostov-on-Don, Russia;* [2]*South-Russian State Polytechnic University, Novocherkassk, Russia;* [3]*South Scientific Center, Russian Academy of Sciences, Rostov-on-Don, Russia* **10:45 - 11:00**

Coffee-Break **11:10 - 11:40**

"Mechanics of New Materials (M2) 11:40 - 12:40 (a report duration is 10 min + questions and discussion during 5 min) (*Chairman – Dr. I.V. Bogachev*)

I.V. Bogachev. Identification of prestress in round inhomogeneous solid and annular plates for the Timoshenko's theory. *Southern Federal University, Rostov-on-Don, Russia* **11:40-11:55**
I.V. Bogachev, R.D. Nedin. Modeling of solid and holed 2D FGM plates with prestress. *Southern Federal University, Rostov-on-Don, Russia* **11:55 - 12:10**
R. Sunder, Testing Procedures to Characterize Variable-Amplitude Fatigue Crack Growth. *BISS Division, ITW-India Pvt Ltd, Bangalore, India* **12:10 - 12:25**
V.V. Dudarev, R.M. Mnukhin. On vibrations of two inhomogeneous elastic objects. *Department of Theory of Elasticity, I.I. Vorovich Institute of Mathematics, Mechanics and Computer Sciences, Southern Federal University, Rostov-on-Don, Russia* **12:25 - 12:40**

***Dinner* 13:00 - 14:00**

"Mechanics of New Materials (M2) 14:00 - 14:30 (a report duration is 10 min + questions and discussion during 5 min) (*Chairman – Prof. A.S. Skaliukh*)

Alexander Skaliukh. Modeling the Hysteresis Response of Ferroelectric Ceramics Subjected to High and Low Intensity Electric and Mechanical Fields. *I.I. Vorovich Institute of Mathematics, Mechanics and Computer Sciences, Southern Federal University, Rostov on Don, Russia* **14:00 - 14:15**
A.N. Soloviev[1,2], Do Thanh Binh[2], V.A. Chebanenko[3], E.V. Kirillova[4]. Applied theory of bending vibrations of a piezomagnetoelectric bimorph in an alternating magnetic field. *Don State Technical University, Rostov-on-Don, Russia; [2]Vorovich Mathematics, Mechanics and Computer Science Institute, Southern Federal University, Rostov-on-Don, Russia; [3]Federal Research Center "Southern Scientific Center of the Russian Academy of Sciences", Rostov-on-Don, Russia; [4]RheinMain University of Applied Sciences, Wiesbaden, Germany* **14:15 - 14:30**
A.V. Cherpakov, Parinov I.A., Haldkar R.K. Carrying out a simulation of an axial-type piezoelectric power generator with an active base **14:30 - 14:45**

"Mathematics 14:45 - 15:15 (a report duration is 10 min + questions and discussion during 5 min) *(Chairman – Yu. E. Drobotov)*

Yu. E. Drobotov. Hypersingular integral operators on weighted generalized Hölder spaces. *Southern Federal University, Rostov-on-Don, Russia* **14:45 - 15:00**
Yu. E. Drobotov. The Riesz potentials on the generalized grand Lebesgue spaces. *Southern Federal University, Rostov-on-Don, Russia* **15:00 - 15:15**

On-line/video Sessions:

"Mathematics 15:20 - 14:30 (a report duration is 10 min) *(Chairman – Yu. E. Drobotov)*

B. G. Vakulov, Yu. E. Drobotov. On Smoothness of Spherical Riesz Potential Type Operator with Mild Singularities on Poles. *Southern Federal University, Rostov-on-Don, Russia* **15:20 - 15:30**
G**. S. Kostetskaya, Yu. E. Drobotov, B. G. Vakulov**. On an Integrodifferential Equation and Its Solutions in Terms of the Riesz Potential Type Operator with a Difference Characteristic *Southern Federal University, Rostov-on-Don, Russia* **15:30 - 15:40**

Yu. E. Drobotov, K. A. Egiazaryan. Hypersingular Integral Equations with Specific Characteristics and Their Applications. *Southern Federal University, Rostov-on-Don, Russia* **15:40 - 15:50**
B. G. Vakulov, Yu. E. Drobotov, E. S. Kochurov. Regularization of a Variable Order Abel Equation in the Generalized Variable Hölder Spaces and Its Applications. *Southern Federal University, Rostov-on-Don, Russia* **15:50 - 16:00**
Yu. E. Drobotov, D. S. Baraeva. The Spherical Fractional Poisson Equation and the Characteristics of Conditioning. *Southern Federal University, Rostov-on-Don, Russia* **16:00 - 16:10**

***Coffee-Break* 16:20 - 16:50**

CLOSING CEREMONY 17:00 - 17:30

BANQUET 17:30 - 20:00

27 May 2022 (Friday)

8:30 – 9:30 *Breakfast*

Departure of participants after breakfast

Scientific publication

10th Anniversary International Conference on "Physics and Mechanics of New Materials and Their Applications"
(PHENMA 2021 – 2022)

Divnomorsk, Russia, May 23 – 27, 2022

http://phenma2021.sfedu.ru/

Abstracts & Schedule

Подписано в печать 16.05.2022 г.
Бумага офсетная. Формат 60×84 1/16. Тираж 100 экз.
Усл. печ. лист. 21,97. Уч.-изд. л. 26,5. Заказ № 8512.

Отпечатано в отделе полиграфической, корпоративной и сувенирной продукции
Издательско-полиграфического комплекса КИБИ МЕДИА ЦЕНТРА ЮФУ.
344090, г. Ростов-на-Дону, пр. Стачки, 200/1, тел (863) 243-41-66.